

UC Santa Barbara

UC Santa Barbara Electronic Theses and Dissertations

Title

Expanding the Toolbox of Green Chemistry for Constructing Bioactive Compounds

Permalink

<https://escholarship.org/uc/item/03q8c55b>

Author

Yu, Julie

Publication Date

2022

Peer reviewed|Thesis/dissertation

UNIVERSITY OF CALIFORNIA

Santa Barbara

Expanding the Toolbox of Green Chemistry for Constructing Bioactive Compounds

A dissertation submitted in partial satisfaction of the
requirements for the degree Doctor of Philosophy
in Chemistry

by

Julie Yu

Committee in charge:

Professor Bruce H. Lipshutz, Chair

Professor Armen Zakarian

Professor Liming Zhang

Professor Mahdi Abu-Omar

June 2022

The dissertation of Julie Yu is approved.

Armen Zakarian

Liming Zhang

Mahdi Abu-Omar

Bruce Lipshutz, Committee Chair

June 2022

Expanding the Toolbox of Green Chemistry for Constructing Bioactive Compounds

Copyright © 2022

by

Julie Yu

ACKNOWLEDGEMENTS

I am very lucky to complete this PhD program at this beautiful UC Santa Barbara campus. The experiences in the past four years have been the most gratifying years of my life. First and foremost, I would like to give my deepest thanks to Prof. Bruce H. Lipshutz for being an understanding and open-minded PI with abundant resources and lab spaces to work on my research projects. You are someone I respect and admire.

To all past and present Lipshutz group members, without them, my experience wouldn't have been the same. I have met many great people and I want to thank you all. Drs. Bala and Ruchi, for providing guidance when I first joined the group. My first lab mate, Jerry Jin, for his valuable advice to thrive in grad school, and his buddy Haobo Pang, for always motivating me to perform quality research. My first close friend in lab, Dr. Elham Etemadi-Davan, for encouraging me when grad life got difficult. My cohort, Joseph, Vani, and Yuting, for working together to finish Pettus' homework and getting through candidacy with all the craziness of the COVID pandemic that happened in 2020. Dr. Margery and Nnamdi, for being the coolest people with endless fun ideas for lab and for life. Drs. David and Jade, two post-docs who always brought me joy. Maddy J. Wong, for being my favorite person during my entire time here; I love the times that we laugh at stupid things and match the same hairstyle. Juan and Erfan, the baristas in lab, are also very great and friendly people. Xiaohan, a smart and productive girl in lab with a kind heart and talents. And Dr. Rahul, Katie, Karthik, Alex, Chandler, thank you all for the advice and fun times that we shared.

Zakarian group: Joon Lee, Josh Gladfelder, Yang Li, Kai Yu...

My Thesis Committee: Prof. Armen Zakarian, Prof. Mahdi Abu-Omar, Prof. Liming Zhang as well as Prof. Thomas Pettus, Prof. Daniel Little.

My past professors at NTU and NTNU, for their warm encouragement and honest criticism, and most importantly, for providing me with sufficient training to become a chemist.

My family, for their enduring support.

Thank you to everyone who has motivated me to work harder to reach the finish line finally.

VITA OF JULIE YU

June 2022

EDUCATION

Doctor of Philosophy in Chemistry, University of California, Santa Barbara, June 2022

Master of Science in Chemistry and Biochemistry, National Taiwan Normal University,
July 2018

Bachelor of Science in Chemistry, National Taiwan Normal University, January 2016

PROFESSIONAL EMPLOYMENT

- Teaching Assistant, Department of Chemistry, University of California, Santa Barbara
 - General Chemistry Laboratory: Fall 2018 (Chem 1AL), Winter 2019 and Spring 2019 (Chem 1BL)
 - Physical Chemistry Laboratory: Fall 2021 (Chem 113AL), Winter 2022 (Chem 116AL) and Spring 2022 (Chem 116BL)
- Research Assistant, Department of Chemistry, National Taiwan University, Summer 2018
- Teaching Assistant, Department of Chemistry, National Taiwan University
 - General Chemistry Laboratory: Fall 2016
 - Organic Chemistry Laboratory: Spring 2017

PUBLICATIONS

1. Dussart-Gautheret, J.*; **Yu, J.**; Ganesh, K.; Rajendra, G.; Gallou, F.; Lipshutz, B. H.* “Impact of Aqueous Micellar Media on Biocatalytic Transformations Involving Transaminase (ATA); Applications to Chemoenzymatic Catalysis” (*Submitted to Green Chem.*)
2. **Yu, J.**; Iyer, K. S.; Lipshutz, B. H.* “An Environmentally Responsible Synthesis of the Antitumor Agent Lapatinib (Tykerb)” *Green Chem.* **2022**, *24*, 3640.

3. **Yu, J.**; Chou, P.; Ko, M.; Chi, P. H.*; C. Chen.* “Discovery of COOH-SW as a novel DNA alkylator for tumor treatment” (*In preparation*)
4. Singhanian, V.; Cortes-Clerget, M.; Akkachairin, B.; Dussart-Gautheret, J.; **Yu, J.**; Akporji, N.; Lipshutz, B. H.* “Lipase-catalyzed esterification in water enabled by nanomicelles. Applications to 1-pot multi-step sequences” *Chem. Sci.* **2022**, *13*, 1440.
5. Cortes-Clerget, M.; **Yu, J.**; Kincaid, J. R. A.; Walde, P.; Gallou, F.; Lipshutz, B. H.* “Water as the reaction medium in organic chemistry: from our worst enemy to our best friend” *Chem. Sci.* **2021**, *12*, 4237.
6. Pang, H.; Hu, Y.; **Yu, J.**, Gallou, F.; Lipshutz, B. H.* “Water-Sculpting of a Heterogeneous Nanoparticle Pre- catalyst for Mizoroki-Heck Couplings Under Aqueous Micellar Catalysis Conditions” *J. Am. Chem. Soc.* **2021**, *143*, 3373.
7. **Yu, T.**; Pang, H.; Cao, Y.; Gallou, F.; Lipshutz, B. H.* “Safe, Scalable, Inexpensive, and Mild Nickel-Catalyzed Migita-like C–S Cross-Couplings in Recyclable Water” *Angew. Chem. Int. Ed.* **2021**, *60*, 3708.
8. Yeh, M. P.*; Shiue, Y.; Lin, H.; **Yu, T.**; Hu, T.; Hong, J. “Iron(II) Halide Promoted Cyclization of Cyclic 2- Enynamides: Stereoselective Synthesis of Halogenated Bicyclic γ -Lactames.” *Org. Lett.*, **2016**, *18*, 2407.

*Corresponding author.

ABSTRACT

Expanding the Toolbox of Green Chemistry for Constructing Bioactive Compounds

by

Julie Yu

I. A mild and affordable method for C–S couplings under environmentally responsible micellar aqueous conditions with low nickel loadings is presented. The scope includes various heterocycles and API-related structures. Moreover, the practicability was demonstrated by a gram-scale synthesis with low residual nickel in the products detected after standard purification. Opportunities to use the aqueous medium for tandem, 1-pot applications are also demonstrated.

II. Introducing the use of nanomicelles in transaminase-catalyzed chemoenzymatic reactions enables a faster reaction rate and minimizes enzymatic inhibition. Furthermore, it allows chem- and bio-catalytic reactions to run in a single reaction vessel without switching solvents. An anti-dementia drug (*S*)-rivastigmine is synthesized efficiently with this new technology.

III. A green chemistry-based synthesis of lapatinib was developed. A streamlined 5-step synthesis in 3 pots was carried out in water and ethanol as the only solvents. This unprecedented method represents an opportunity for shifting from petroleum-based

solvents to green solvents. Additionally, a less precious metal catalyst was involved using mild reaction conditions with less reaction time.

IV. Fluorinated compounds are one of the most important categories in pharmaceuticals. A convenient method has been developed for the synthesis of difluorocyclopropenes and difluorocyclopropanes using commercially available TMSCF_2Br in the absence of solvents. Complex alkenes and alkynes can readily undergo [2+1] cycloaddition to difluorocarbene with extraordinarily low E Factors.

TABLE OF CONTENT

1. Safe, Scalable, Inexpensive, and Mild Nickel-Catalyzed Migita-like C–S Cross-Couplings in Recyclable Water	1
1.1. Background and introduction.....	2
1.2. Results and discussion	4
1.3. Proposed mechanism	22
1.4. Conclusions.....	23
1.5. References.....	23
1.6. General experimental information	27
1.7. Supplementary tables and figures	32
1.8. Experimental procedures and characterizations data for thioether products	32
1.9. Recycling procedures and E Factor calculations	64
1.10. One-pot sequence: procedures and characterizations	67
1.11. ICP-MS data for residual Ni level detection.....	69
1.12. NMR spectra	70
2. Impact of Aqueous Micellar Media on Biocatalytic Transformations Involving Transaminase; Applications to Chemoenzymatic Catalysis.....	113
2.1. Background and introduction.....	114
2.2. Reaction mechanism of ATA.....	117

2.3.	Results and discussion	118
2.4.	Conclusions.....	140
2.5.	References.....	141
2.6.	General experimental information	144
2.7.	Experimental procedures	146
2.8.	Product characterization (NMR, HRMS, and chirality assessment).....	161
2.9.	NMR spectra	173
2.10.	HPLC traces	194
2.11.	SI References	212
3.	An Environmentally Responsible 5-step, 3-pot Synthesis of the Antitumor Agent Lapatinib (Tykerb).....	213
3.1.	Background and introduction.....	214
3.2.	Literature on the synthesis of lapatinib.....	216
3.3.	Green chemistry: telescoping synthetic sequences.....	218
3.4.	Results and discussion	219
3.5.	Conclusions.....	230
3.6.	References.....	231
3.7.	General experimental information	234
3.8.	Procedures for the synthesis of lapatinib	236

3.9.	E Factor calculations.....	246
3.10.	Compound characterization data and spectra	247
4.	Difluorocarbene addition to alkenes and alkynes using TMSCF_2Br under neat conditions.....	253
4.1.	Background and introduction.....	253
4.2.	Literature on the synthesis of difluorocyclopropanes and difluorocyclopropenes	256
4.3.	Results and discussion	261
4.4.	Conclusions and future work	272
4.5.	References.....	272
4.6.	General experimental information	275
4.7.	General procedures	277
4.8.	E Factor calculations.....	280
4.9.	Compound characterization data.....	284
4.10.	NMR spectra	292

1. Safe, Scalable, Inexpensive, and Mild Nickel-Catalyzed Migita-like C–S Cross-Couplings in Recyclable Water

Reproduced with permission from

Yu, T.-Y.; Pang, H.; Cao, Y.; Gallou, F.; Lipshutz, B. H. Safe, Scalable, Inexpensive, and Mild Nickel-Catalyzed Migita-like C–S Cross-Couplings in Recyclable Water. *Angew. Chem. Int. Ed.* **2021**, *60*, 3708.

Copyright 2021 John Wiley and Sons

1.1. Background and introduction

Thioethers are abundant in nature and can be found in a variety of physiologically active chemicals (**Figure 1**). A general approach for Migita cross-couplings that lead to thioethers relies on the use of transition metal-catalyzed carbon-sulfur (C–S) bond formation between organic halides and thiols under basic conditions. These transformations remain challenging in several ways, including the typically high loadings of endangered Pd catalysts attributed to strong coordination of thiolates to the metal,¹ oftentimes leading to catalyst deactivation and thus overall low efficiency.^{2,3} Perhaps not surprisingly, the development of methodologies aimed at building C–S bonds remains a topic of considerable interest.⁴

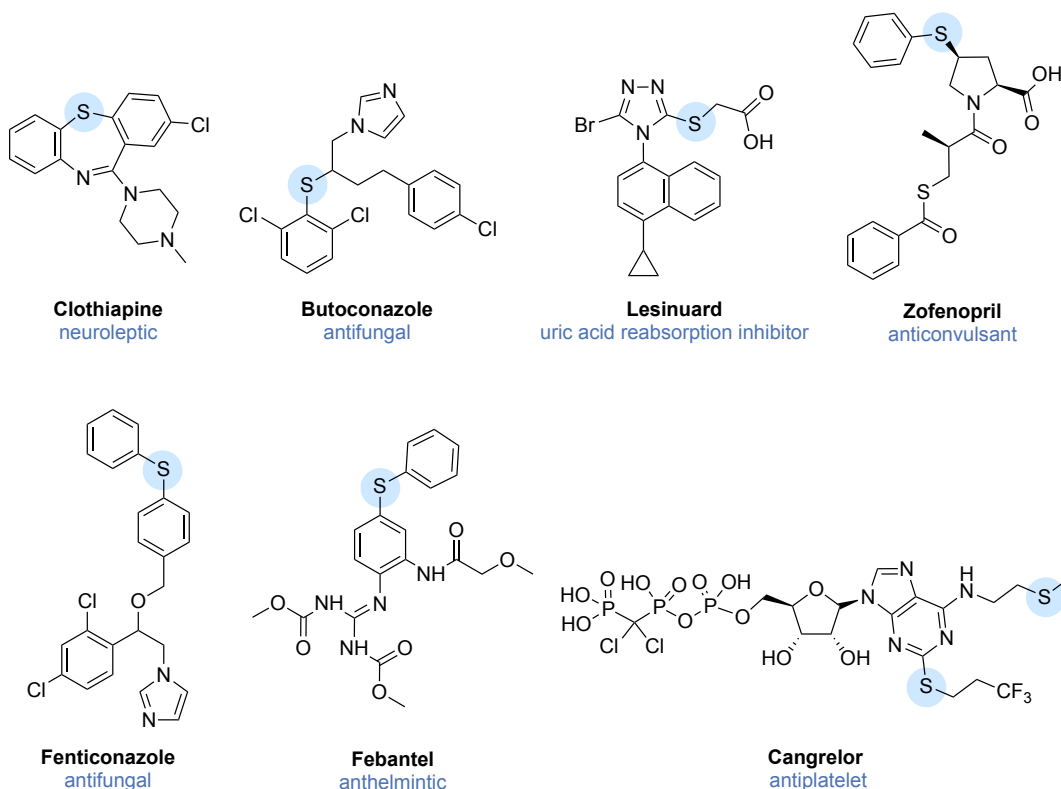


Figure 1. Selected examples of therapeutic agents bearing aromatic/heteroaromatic thioethers

Migita *et al.* first reported the C–S cross-coupling of aryl halides with thiols using [Pd(PPh₃)₄] as the catalyst in polar solvents (*e.g.* DMSO).⁵ Since then, however, much of the effort has focused on the use of precious and expensive metals, such as palladium,^{6–13} iridium,¹⁴ rhodium,¹⁵ and ruthenium,¹⁶ while high temperatures are typically needed in waste-generating organic solvents. Lately, alternative routes have emerged that call for milder conditions using photoredox catalysis and less costly metals such as copper, cobalt,^[11] or nickel.^{1–6,16,17} Nonetheless, they often rely on the presence of additional expensive metals (*e.g.*, Ir),¹⁴ can involve forcing conditions, and always require organic solvents sometimes to the strict exclusion of moisture.¹⁶ Moreover, most rarely include direct applications to highly functionalized products, especially those characteristics of pharmaceuticals.

Recently, Fleischer and coworkers reported a mild method to couple alkyl thiols (1°, 2°, and 3°) with aryl chlorides at room temperature using (Xantphos)Ni^{II}(*o*-tolyl)Cl as a precatalyst; even complex drug molecules achieved high yield in only two hours.¹⁸ In addition, discoveries involving electrochemical approaches look enticing. For example, Molander *et al* developed a Ni/Ru photoredox catalytic cycle that can be used on peptides and biomolecules, such as biotin, coumarin, and unprotected glycoside derivatives.¹⁶ However, they tend to involve high loadings of metal catalyst and are run in polar aprotic media (DMF and THF).¹⁹

A few reports have been published on C–S cross-couplings in water. For example, Bhaumik *et al* described a nanoparticle formed from nickel oxide and zirconia that can catalyze C–S cross-coupling reaction in water at room temperature. The nanoparticle can easily be reused by simple filtration, water/acetone wash, and finally dried and activated

by heating at 673 K, with no change in the crystallographic structure and no significant decrease in yield in the second cycle.¹ Another recent study by Bhattacharjee used a water-soluble Ni-Schiff base complex in water with heating to 60 °C. However, the substrate scope in both methods mentioned above is limited to a few aryl iodides with *para*-monosubstituted thiophenols formed in moderate to good yields.²¹

Clearly, an extensive study on Migita-type cross-couplings in pursuit of a convenient, sustainable, and reliable method remains in need. An alternative protocol that replaces dangerously flammable and toxic organic solvents with safe, recyclable water while minimizing the investment in both energy and metal catalyst would be extremely beneficial in working toward an environmentally responsible solution to the majority of these difficult issues. In this report, we describe such a process that relies on low levels of base metal (nickel) catalysis enabled by aqueous micellar catalysis. This new technology involves a readily available catalyst, is used under mild conditions, and is scalable; hence, it is both environmentally responsible as well as available for immediate use.

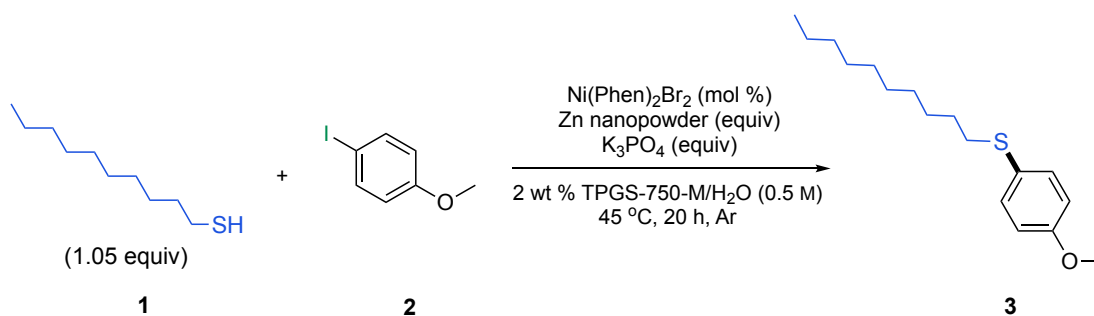
1.2. Results and discussion

1.2.1. Optimization and substrate scope

The study began with a pre-ligated nickel, Ni(Phen)₂Br₂, prepared by mixing NiBr₂ and phenanthroline in a 1:2 molar ratio in acetonitrile and heating at 45 °C overnight to afford a fully ligated complex. The choice of zinc as the reductant was based on established nickel

chemistry, inspired by an earlier report from Cheng *et al.* using a related pre-ligated Ni/Zn catalytic cycle to synthesize ketones from aryl iodides and aldehydes.²²

Initially, a lipophilic decanethiol and 4-methoxyiodobenzene were chosen as the model reaction for these aqueous micellar conditions; optimization of the conditions is shown in **Table 1**. Remarkably, the desired C–S cross-coupling occurred smoothly using only a 5% molar excess of thiol. Complete conversion occurred in the presence of only 2 mol % of this Ni(II) species, in the presence of zinc nanopowder (particle size 40–60 nm; 2 equiv) and anhydrous K₃PO₄ (2 equiv; entry 1). Reducing the amount of pre-catalyst to 0.35 mol % or 0.07 mol % (or 700 ppm) decreased the extent of conversion to 77% and 79%, respectively (entries 2–3). When only 0.0035 mol % (350 ppm) of this same pre-catalyst was utilized, a much inferior result: 53%, was noted (entry 4). Fortunately, reducing the base to 1.2 equivalents had no effect on conversion (entry 5), but the necessity of its presence for presumably activation of the nucleophile was established (entry 6; see mechanistic details in **Section 3**). Running this coupling at room temperature (22 °C) significantly reduced the yield to only 6% over the same period of time at 45 °C (entry 7). Notably, screening the Zn loading in the 0.1–1.0 equivalent range revealed that only 0.25 equivalents are necessary (entries 8–11). Previous literature, on the other hand, has used super-stoichiometric amounts of zinc.²³ When air remained within the reaction vessel (entry 12), reaction efficiency was lowered as the thiols are oxidized to disulfides under these slightly basic conditions (pH = 7–9).²⁴

Table 1. Optimization of equivalents of catalyst and base^[a]

Entry	Ni(Phen) ₂ Br ₂	Zn (equiv)	K ₃ PO ₄ (equiv)	Conv. [%] ^[b]
1	2 mol %	2	2	100
2	0.35 mol %	2	2	77
3	0.07 mol %	2	2	79
4	0.0035 mol %	2	2	53
5	2 mol %	2	1.2	100
6	2 mol %	2	0	0
7	2 mol %	2	2	6 ^[c]
8	0.7 mol %	1	1.2	100
9	0.7 mol %	0.5	1.2	99
10	0.7 mol %	0.25	1.2	94 (96)
11	0.7 mol %	0.1	1.2	83
12	0.7 mol %	0.5	1.2	62 ^[d]

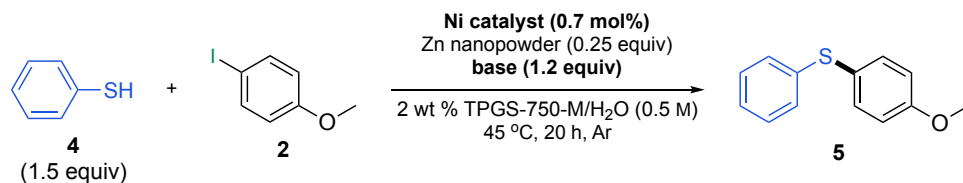
[a] Scale of reaction: 0.25 mmol of 4-iodoanisole and 2 wt % TPGS-750-M/H₂O (0.5 mL).

[b] Conversion determined by ¹H NMR. Isolated yields in parenthesis. [c] Run at rt (22 °C).

[d] Disulfide formed when run in air.

Only a modest yield was obtained, however, when the above-mentioned optimal conditions were applied to thioarenes (**Table 1**, entry 1). Changing the ligand to bipyridyl had no effect on the reaction result (entry 2). A more sterically demanding ligand, neocuproine,

which bears two methyl groups on phenanthroline, also failed to catalyze the reaction (entry 3). Phosphine ligands were also tested, such as DPPF, DPPE, and DPPB, but only resulted in much lower yields (entries 4–6). Moreover, the nature of the counterion in the initial nickel salt was found to be crucial, as switching from bromide to chloride, iodide, or acetate afforded inferior results (entries 7–9). Altering the bases, including both Cs₂CO₃ and KO*t*-Bu, was found to give better results (entries 10–11); see **Table S1** for more base screenings. Control experiments indicated that the nickel catalyst and zinc powder were both required (entries 12–13). The reaction failed completely when Zn was replaced by manganese,¹⁷ or other weak reducing agents²⁵ (e.g., ascorbic acid or polymethylhydrosiloxane (PMHS); entry 14).

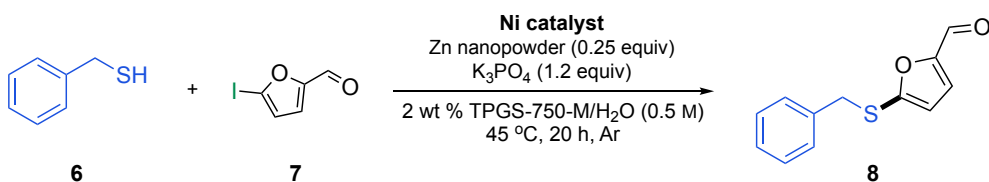
Table 2. Screening of pre-catalyst and base^[a]

Entry	Base	Source of Ni	Ligand	Yield [%] ^[b]
1	K ₃ PO ₄	NiBr ₂	Phen	57 (66)
2	K ₃ PO ₄	NiBr ₂	bpy	59
3	K ₃ PO ₄	NiBr ₂	neocuproine	0
4	K ₃ PO ₄	NiBr ₂	DPPF	19
5	K ₃ PO ₄	NiBr ₂	DPPB	5
6	K ₃ PO ₄	NiBr ₂	DPPE	5
7	K ₃ PO ₄	Ni(OAc) ₂	Phen	18
8	K ₃ PO ₄	NiCl ₂	Phen	8
9	K ₃ PO ₄	NiI ₂	Phen	7
10	KO ^{<i>t</i>} -Bu	NiBr ₂	Phen	94 (82)
11	Cs ₂ CO ₃	NiBr ₂	Phen	74 (71)
12	K ₃ PO ₄	NiBr ₂	Phen	0 ^[c]
13	K ₃ PO ₄	–	–	0
14	K ₃ PO ₄	NiBr ₂	Phen	0 ^[d]

[a] Scale of reaction: 0.25 mmol of 4-iodoanisole and 2 wt % TPGS-750-M/H₂O (0.5 mL), Ni: ligand = 1 : 2 molar ratio. [b] Yield determined by ¹H NMR using 1,3,5-trimethylbenzene as internal standard. Isolated yields in parenthesis. [c] Run without Zn. [d] Mn, ascorbic acid, or PMHS used instead of Zn.

Further investigation of reaction conditions using benzyl mercaptan and iodofurfural as coupling partners revealed that pre-ligation of Ni gave the desired coupling product in 87–88% yield (**Table 3**, entries 1–2). Adding NiBr₂ and phenanthroline directly, but separately, into the reaction flask resulted in a slightly lower yield (81%; entry 3). The use of recrystallized catalyst had a significant impact on the loading, which could be further reduced to only 0.70 mol %, while the isolated yield jumped to 95% (entries 4–5). An X-ray crystal structure of this octahedrally configured Ni(II) pre-catalyst Ni(Phen)₂Br₂ is shown in **Figure 2**.

Table 3. Catalyst screening^[a]



Entry	[Ni]	Catalyst	Conv. [%] ^[b]
1	1 mol %	Pre-mixed NiBr ₂ : Phen = 1 : 1 ^[c]	87
2	1 mol %	Pre-mixed NiBr ₂ : Phen = 1 : 2 ^[c]	88
3	1 mol %	NiBr ₂ : Phen = 1 : 2 ^[d]	81
4	1 mol %	recrystallized Ni(Phen) ₂ Br ₂ ^[e]	94
5	0.7 mol %	recrystallized Ni(Phen) ₂ Br ₂ ^[e]	95 (95)

[a] Scale of reaction: 0.25 mmol of 5-iodo-2-furaldehyde and 0.5 mL of 2 wt % TPGS-750-M/H₂O. [b] Conversion determined by ¹H NMR. [c] NiBr₂ and phenanthroline were

pre-ligated in acetonitrile and then dried. [d] NiBr₂ and phenanthroline were used as received. [e] Ni(Phen)₂Br₂ was recrystallized from EtOAc/hexane.

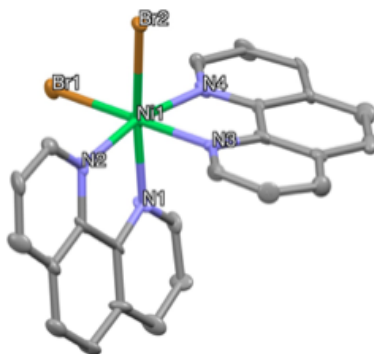
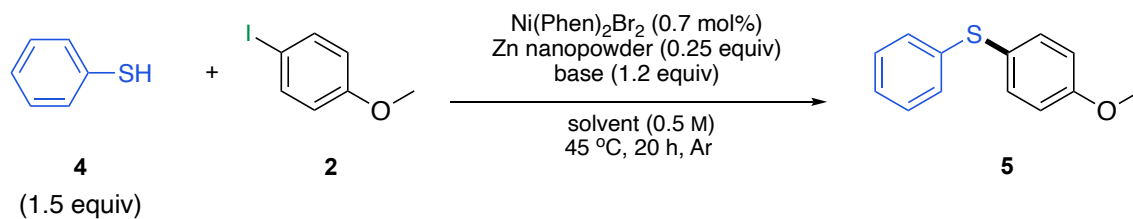


Figure 2. X-ray structure of Ni(Phen)₂Br₂ (CCDC 1993760)

Hydrogen atoms are omitted for clarity. Refined formula: C₂₄H₁₆Br₂N₄Ni, formula weight *M_r*: 578.90. Selected bond lengths (Å): Ni1–Br1, 2.530; Ni1–Br2, 2.596; Ni1–N1, 2.105; Ni1–N2 2.063; Ni1–N3 2.092; Ni1–N 2.061.

To demonstrate the crucial role played by the nanoreactors formed by the surfactant in water, comparison reactions in organic solvents (**Table 4**) were studied. Under optimized conditions, nanoreactors present in an aqueous solution performed competitively with commonly used, dipolar organic solvents. When KO*t*-Bu was used as the base, 2 wt % TPGS-750-M gave a 30% higher yield than acetonitrile, and a comparable yield to DMF. Notably, when K₃PO₄ was used, a considerable decrease in the yields was observed in both DMF and acetonitrile (32% and 6% yield respectively).

Table 4. Evaluation of the reaction medium^a



Entry	Solvent	Yield [%] ^[b]	
		base = KO ^t -Bu	base = K ₃ PO ₄
1	DMF	99	32
2	acetonitrile	59	6
3	2 wt % TPGS-750-M	90	58

[a] Scale of reaction: 0.25 mmol of 4-iodoanisole (**2**) in the designated medium (0.5 mL).

[b] Yield determined by ¹H NMR using 1,3,5-trimethylbenzene as internal standard. Isolated yield in parentheses.

Several commercially available nonionic surfactants were also examined. Lower conversions were seen when water alone or 2 wt % PEG 2000 in water was used, mainly due to substrate polarity (i.e., insolubility) leading to adherence to the stirrer, especially for more challenging reaction partners (**Figure 3**). The presence of surfactants emulsified these materials in reaction 1, raising the overall conversion from 56% to *ca.* 95%, as shown in **Table 5**. A control experiment using this electron-deficient pyridinyl bromide showed that in the absence of metals, the reactivity is significantly reduced (**Scheme 1**). In the case of reaction 2 in **Table 5**, designer surfactant TPGS-750-M led to superior results compared to other amphiphiles, although the background reaction in its absence (i.e., “on water”)²⁶ was somewhat competitive in this particular case (entry 1).

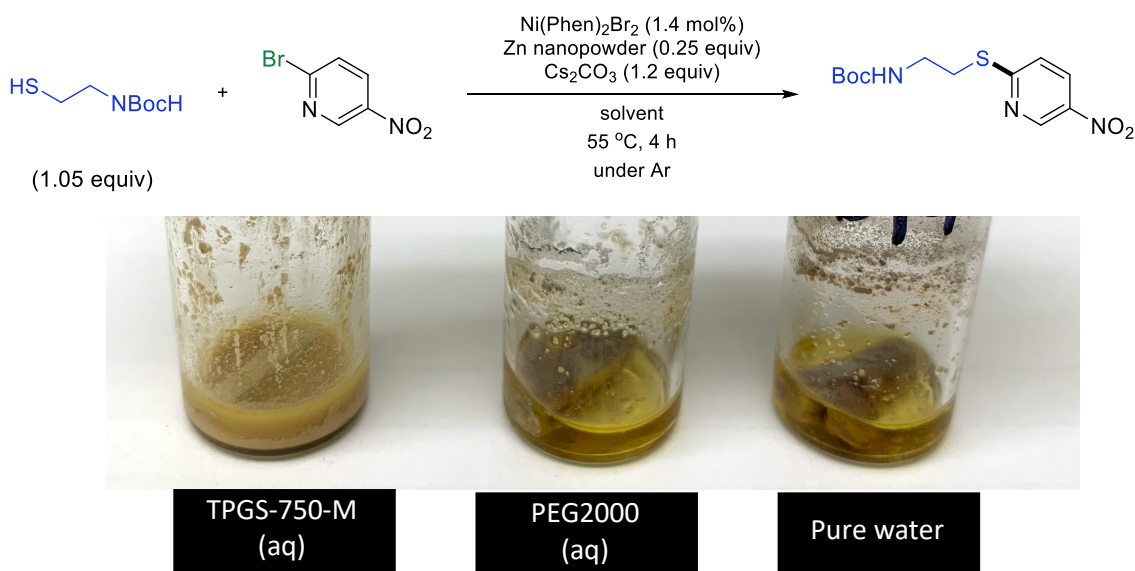
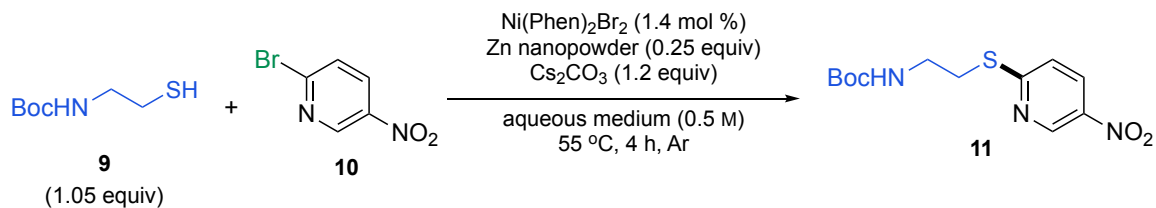


Figure 3. Reaction appearance after 4 h

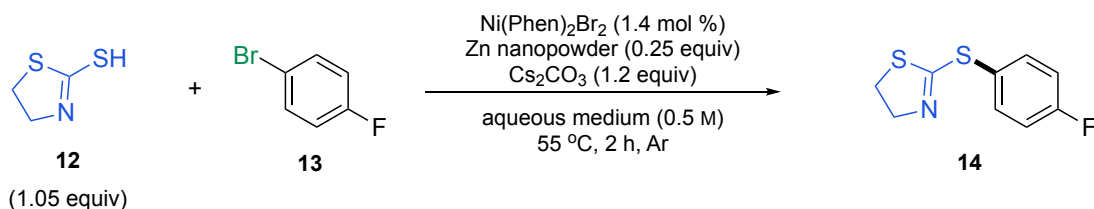
From left to right: TPGS-750-M/H₂O appeared as powdery granules in water; PEG-2000/H₂O and pure water appeared as a clear yellow aqueous solution with solids adhering to the stir bar

Table 5. Evaluation of the reaction medium^a

reaction 1:

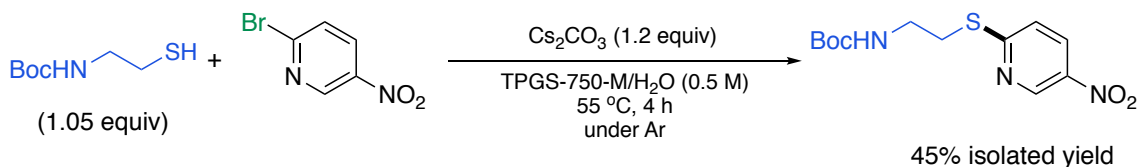


reaction 2:



Entry	Aqueous medium	Conversion [%] ^[b]	
		reaction 1	reaction 2
1	pure water	56	61
2	2 wt % PEG 2000/H ₂ O	55	20
3	2 wt % Brij 30/H ₂ O	96	6
4	2 wt % Triton X 100/H ₂ O	95	15
5	2 wt % PTS 600/H ₂ O	95	19
6	2 wt % Tween 60/H ₂ O	94	13
7	2 wt % TPGS-750-M/H₂O	95	66

[a] 0.125 mmol 5-nitro-2-bromopyridine or 4-fluoroiodobenzene in the designated aqueous medium (0.25 mL). [b] Conversion¹ determined by proton NMR.



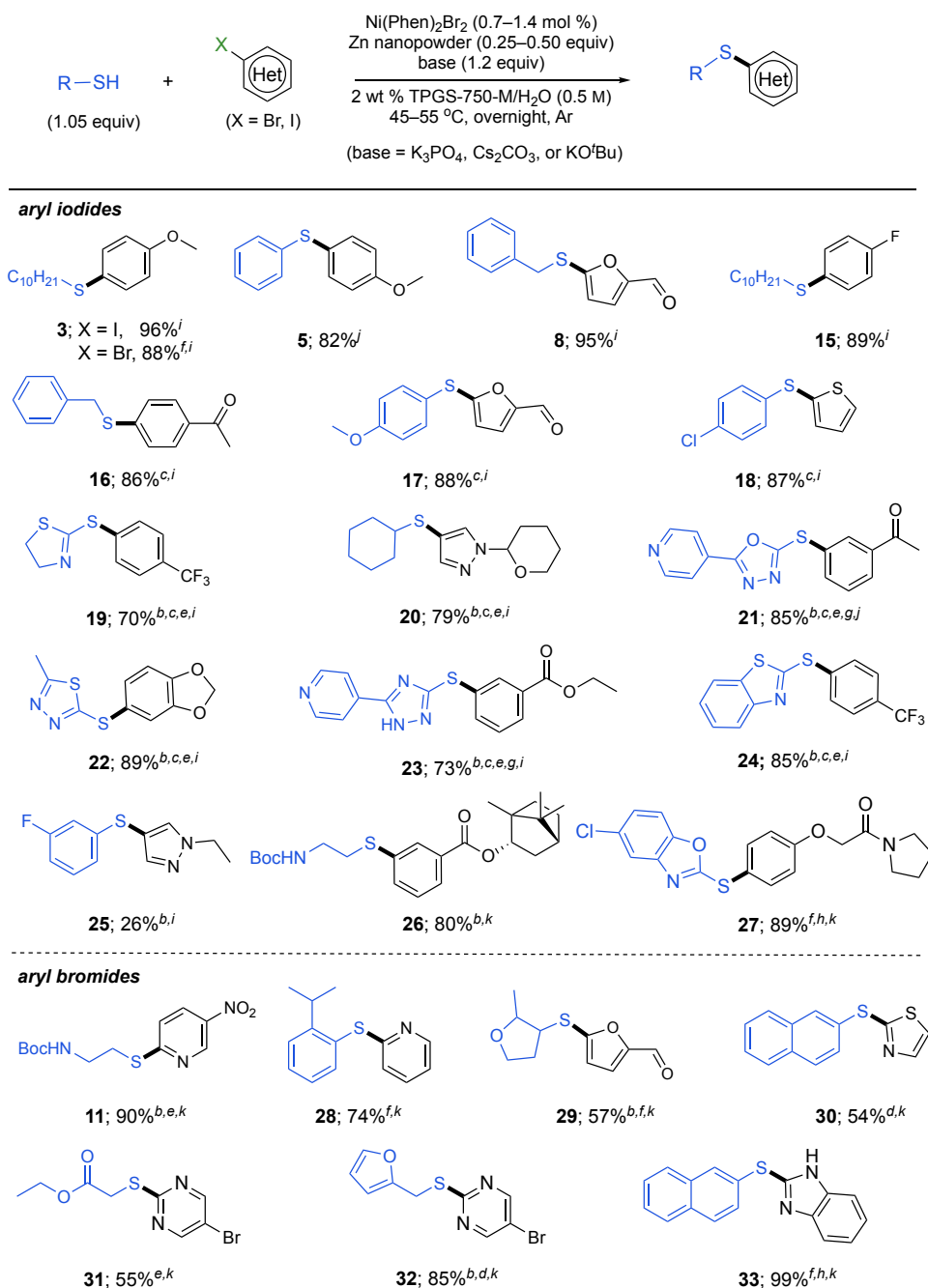
Scheme 1. Control reaction: an activated aryl bromide run in the absence of metals

Under optimized conditions, the scope of these C–S couplings was extensively explored. As summarized in **Table 6**, most combinations of thiols and aryl iodides/bromides afforded coupled products in good-to-excellent yields.²⁷ Although alkylthiols have previously been problematic in such cross-couplings due to their strong nucleophilicity that can compete with a ligand on palladium,^{28,29} both primary (leading to products **3**, **8**, **11**, **15**, **16**, **26**, **31**, **32**) and secondary alkyl (affording products **20**, **29**) thiols gave the desired thioethers to the extent of 55–96%. The reaction also took place smoothly when more complex heterocyclic thiols were involved, including use of a thiazoline giving **19**, an oxadiazole leading to **21**, a thiadiazole producing **22**, a triazole arriving at **23**, a benzothiazole yielding **24**), and a furan generating **32**.

Insofar as the aryl halide coupling partner is concerned, aryl iodides, either electron-donating (*e.g.*, containing methoxy; see products **3** and **5**), or electron-withdrawing (*e.g.*, bearing fluoro, as in **15** and trifluoromethyl, as in **19**), delivered the corresponding thioethers in good-to-excellent yields (70–96%). Perhaps more importantly, aryl iodides bearing reducible functional groups, such as ketone (in **16** and **21**), aldehyde (see thioethers **8**, **17**, and **29**), and ester (in **26** and **31**), were tolerated notwithstanding the presence of zinc nanopowder.^[21] Aryl bromides, whether activated (*e.g.*, leading to products **11** and **28-33**) or not (see product **3**) appear to undergo coupling under otherwise identical conditions.

Nickel-based catalysts have been known to lose activity due to metal chelation by the presence of heteroatoms within either or both reaction partners, as well as by the products formed.³⁰ Hence, it is noteworthy that heterocyclic aryl iodides, such as those containing a furan (see **8**), thiophene (as in **18**), methylenedioxybenzenepyrazole (product **22**), or pyrazole ring (products **20** and **25**), all participated with similar efficiency. Moreover, a variety of heteroaryl bromides leading to products **28** to **33**, likewise, can be used when the loading of nickel pre-catalyst was increased from 0.7 to 1.4 mol % (or to 3 mol % in rare cases).

Table 6. Substrate scope



[a] Reaction conditions unless otherwise noted: 0.25 mmol aryl bromide/iodide, 0.263 mmol thiol, 0.70 mol % Ni(Phen)₂Br₂, 0.25 equiv Zn, 1.2 equiv base, stirred in 2 wt % TPGS-750-M/H₂O (0.5 mL), 45 °C. Isolated yields; see SI for details. [b] Run at 55 °C. [c] 0.5 equiv Zn. [d] 1 mol % Ni(Phen)₂Br₂. [e] 1.4 mol % Ni(Phen)₂Br₂. [f] 3 mol % Ni(Phen)₂Br₂. [g] 10 v/v % DMSO added. [h] 10 v/v % EtOAc added. [i] K₃PO₄. [j] KO*t*-Bu. [k] Cs₂CO₃.

Particularly instructive were side-by-side comparison studies involving the preparation of problematic sulfides chosen from prior art. Examples included cases leading to pyrazoles **34** and **35**, as well as *ortho*-substituted aromatics **36** and **37**, which are common components in therapeutic agents (see **Figure 4**). As summarized in Figure 3, photocatalysis conditions lead to compounds **34** and **35**, calling for 2 mol % of an *iridium* catalyst together with 10 mol % nickel(II), in addition to being run in organic solvents with a costly catalyst.¹⁴ Conditions associated with the formation of **36** involved 10 mol % CuI,³¹ while super-stoichiometric zinc at high temperature (80 °C) was needed to synthesize compound **37**,³² neither of which is synthetically competitive.

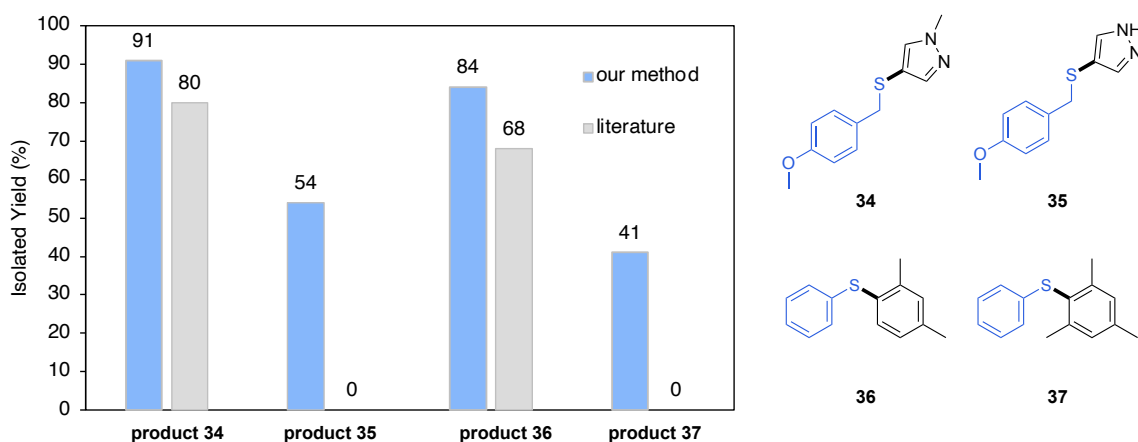


Figure 3. Selected examples of therapeutic agents bearing aromatic thioethers

Direct comparison with literature conditions. Prior art conditions: For **34** and **35**: [Ir] (2 mol %), NiCl₂ glyme (10 mol %), dtbbpy (15 mol %), pyridine (2 equiv), 34 W blue-LED, MeCN (0.1 M).¹⁴ For **36**: CuI (10 mol %), NaOt-Bu (1 equiv), 100-watt Hg lamp, MeCN (0.3 M), 0 °C, 5 h.³¹ For **37**: CoI₂(dppe) (1 mol %), Zn (1.5 equiv), pyridine (1 equiv), MeCN (0.25 M), 80 °C, 10 h.³² Current conditions: 1.4 mol % Ni(Phen)₂Br₂, 0.25 equiv

Zn, 1.2 equiv base, stirred in 2 wt % TPGS-750-M/H₂O (0.5 mL), 55 °C, 23 h. For **36** and **37**: 0.7 mol % Ni(Phen)₂Br₂ was used, stirred at 45 °C, 18 h. Isolated yields.

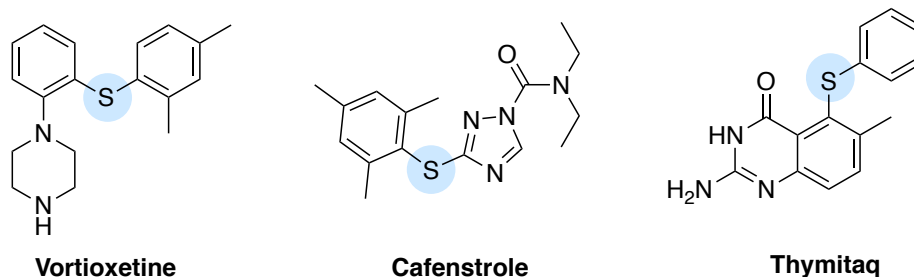


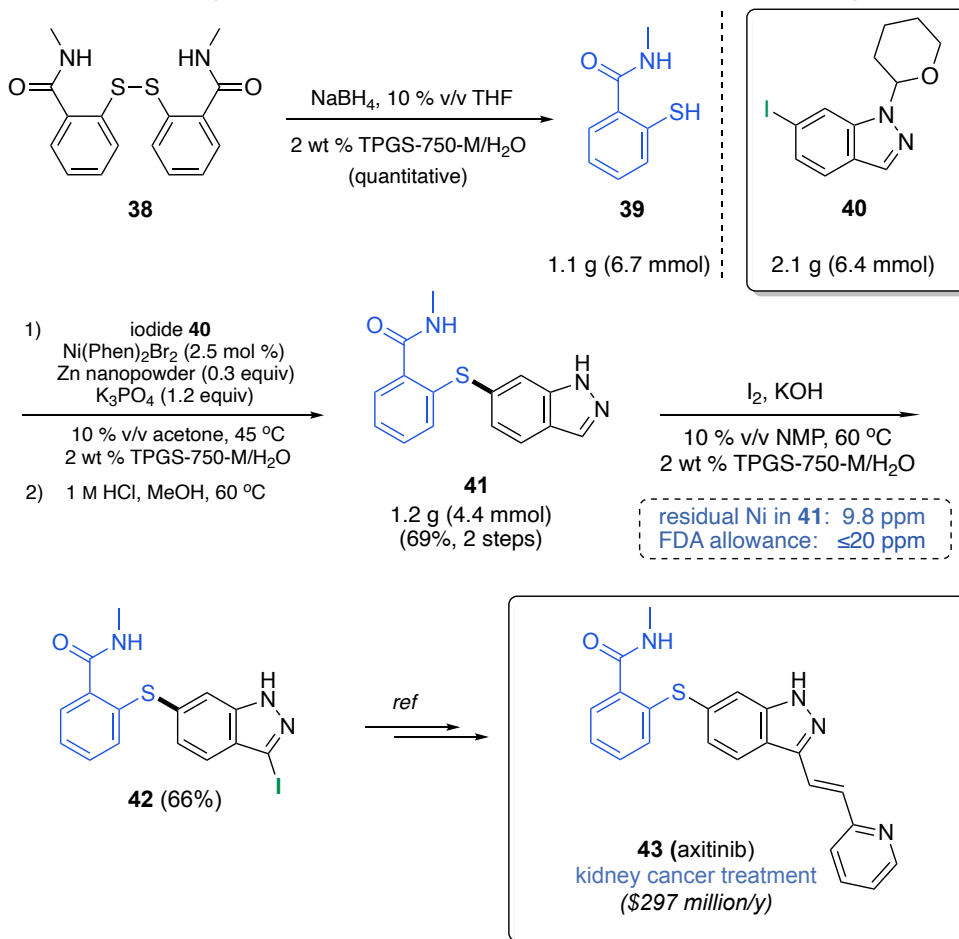
Figure 4. Selected examples of therapeutic agents bearing methyl groups *ortho* to thiophenols

1.2.2. Application: synthesis of APIs and one-pot sequence

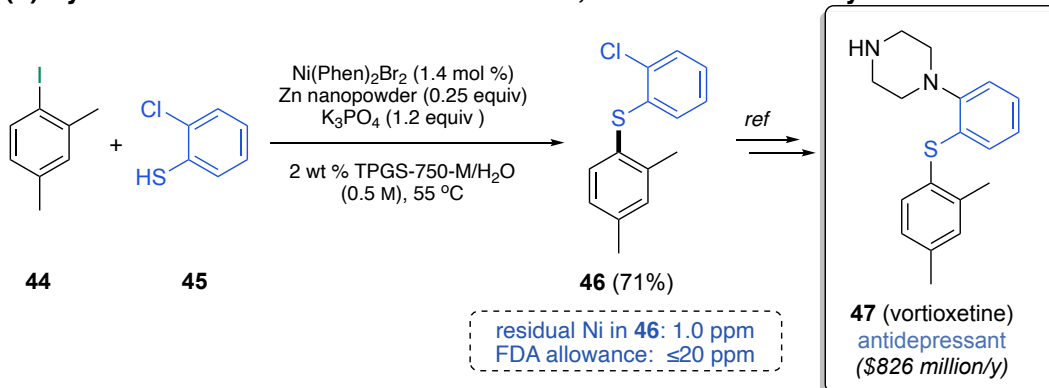
As a meaningful application of this chemistry in water, the penultimate intermediate to Pfizer's antitumor agent axitinib (**43**) was prepared using aqueous micellar catalysis technology (**Scheme 2a**). Commercially available disulfide **38** was reduced with NaBH₄ in aqueous TPGS-750-M forming thiol **39**, generated in gram quantities. Subsequent coupling with aryl iodide **40** led to the benzopyrazole-protected sulfide, taking place in water under very mild conditions rather than the traditional use of harmful solvents at the reported high temperatures using high loadings of palladium.^{7,33,34} Without isolation, methanolic HCl was added to remove the THP group to afford **41** in 69% isolated yield over both steps. Importantly, based on ICP-MS results, residual nickel found in axitinib precursor **41** was 9.8 ppm, which is well under the limit permitted under FDA guidelines (≤ 20 ppm). Iodination could also be achieved under aqueous surfactant conditions, thereby reducing the amount of NMP by 90% relative to the literature route.³³ Further extension to

key precursor **46** of the antidepressant vortioxetine³⁵ (**47**; **Scheme 2b**) could also be realized in 71% yield. Similar analysis of this product indicated only 1.0 ppm residual nickel.

(a) Gram-scale synthesis en route to axitinib; residual metal analysis

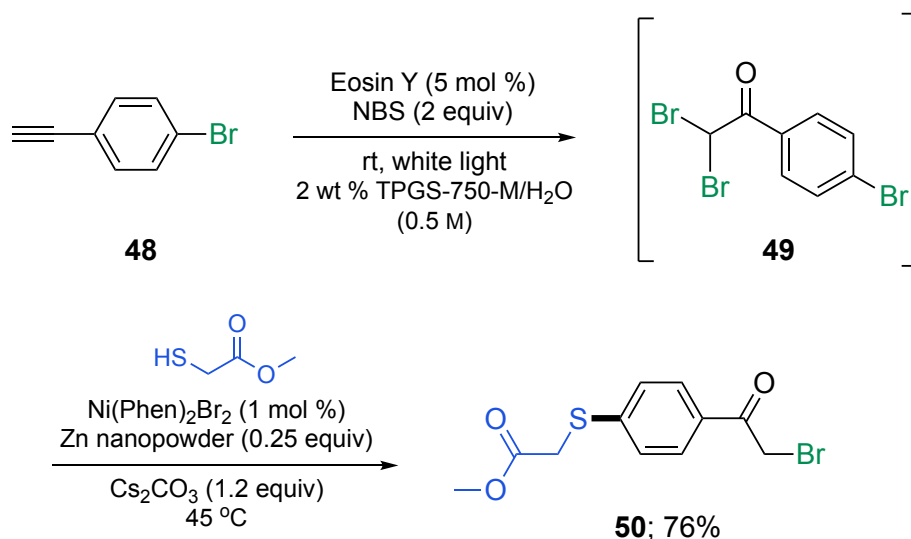


(b) Synthesis of a vortioxetine intermediate; residual metal analysis

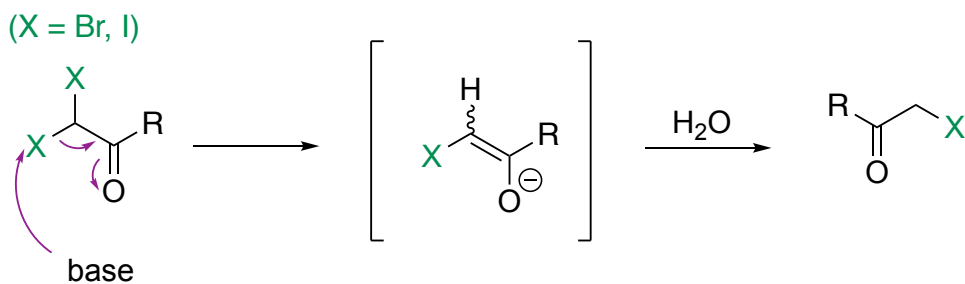


Scheme 2. Synthetic routes towards intermediates en route to axitinib and vortioxetine

Thioether formation can be demonstrated in tandem with photocatalysis in aqueous solution (**Scheme 3**). Initially, 4-bromophenylacetylene was converted to α,α -dibromoketone **49** under visible light irradiation, following the method recently disclosed by Handa and co-workers.³⁶ Subsequent nickel-catalyzed thioetherification could then take place concurrent with monodebromination, via enolate formation in the presence of base; see the mechanism in **Scheme 4**.^{37,38} Noteworthy is the observation that the α -bromoketone product **50** remained intact under these aqueous micellar conditions.

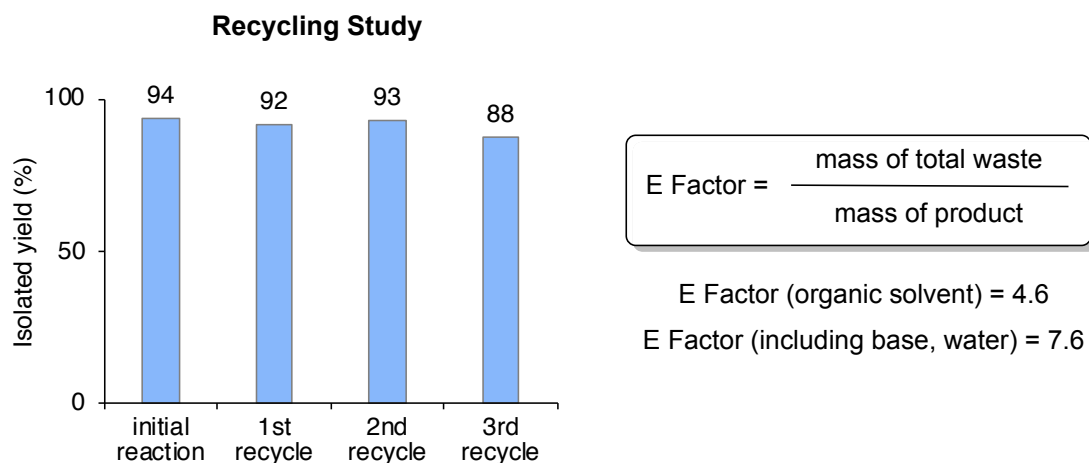
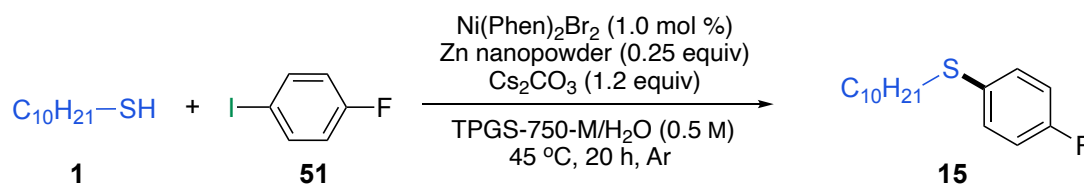


Scheme 3. 1-Pot, 2-reaction sequence



Scheme 4. Mechanism of mono-dehalogenation.

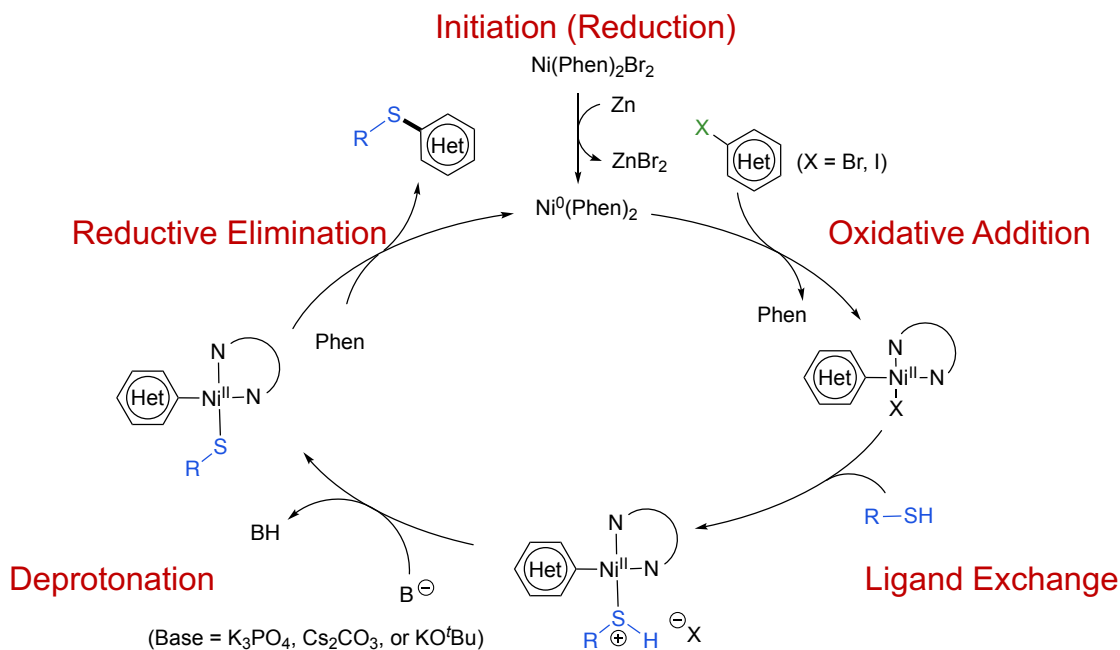
Recycling of the aqueous reaction mixture, which was employed at a global substrate concentration of 0.50 M containing 2 wt % TPGS-750-M, is straightforward and routine, as is characteristic of designer surfactant technology in water, leading to reduced effluent discharges. By virtue of the sub-stoichiometric amount of zinc required, reaction mixtures stirred easily, and “in-flask” extraction with minimal and recoverable MTBE allowed for the isolation of the desired product. The remaining medium could be re-used in three subsequent cycles (**Scheme 5**). The E Factor³⁹ based on the organic solvent employed was only 4.6, suggesting, overall, a sustainable process is in hand for thioether bond formation.



Scheme 5. Recycling study and determination of E Factors

1.3. Proposed mechanism

Based on reported literature on Ni-catalyzed C–S cross-coupling, a possible mechanism for this presented reaction is proposed in Scheme 6.^{40,41} The catalytic cycle begins with generation of the active catalyst $\text{Ni}^0(\text{Phen})_2$ that derives from reduction of $\text{Ni}^{\text{II}}(\text{Phen})_2\text{Br}_2$ with Zn^0 . Next, the nickel⁰ complex undergoes oxidative addition into the C–X bond (X = Br, I), forming $\text{Ar–Ni}^{\text{II}}\text{–X}$. Ligand exchange of the nitrogen ligand and thiol forms a cross-product of the aryl and the thiol; the proton was rapidly removed by the base. Subsequent reductive elimination of the diorganonickel^{II} intermediate generates the cross-coupled sulfide. Meanwhile, the Ni^0 species was regenerated for participation in subsequent catalytic cycles.



Scheme 6. Proposed reaction mechanism for Ni-catalyzed Migita-type reaction

1.4. Conclusions

In summary, a mild and recyclable Ni-catalyzed C–S cross-coupling reaction has been developed in recyclable water under environmentally responsible micellar aqueous conditions. The process effectively promotes thioetherification at sp^2 carbon centers with both aryl and alkyl thiols that is not only general but is also tolerant of a variety of functionality in either or both reaction partners. Opportunities to use the aqueous medium for tandem, 1-pot applications are also demonstrated. Overall, this new technology offers an inexpensive, safe, scalable, and reliable route to aryl/heteroaryl sulfides that may find, in particular, applications to active pharmaceutical ingredients (APIs).

1.5. References

- (1) Scattolin, T.; Senol, E.; Yin, G.; Guo, Q.; Schoenebeck, F. Site-Selective C–S Bond Formation at C–Br over C–OTf and C–Cl Enabled by an Air-Stable, Easily Recoverable, and Recyclable Palladium(I) Catalyst. *Angew. Chem., Int. Ed.* **2018**, *57*, 12425–12429.
- (2) Oudar, J. Sulfur Adsorption and Poisoning of Metallic Catalysts. *Catal. Rev.* **1980**, *22*, 171–195.
- (3) Kolpin, A.; Jones, G.; Jones, S.; Zheng, W.; Cookson, J.; York, A. P. E.; Collier, P. J.; Tsang, S. C. E. Quantitative Differences in Sulfur Poisoning Phenomena over Ruthenium and Palladium: An Attempt To Deconvolute Geometric and Electronic Poisoning Effects Using Model Catalysts. *ACS Catal.* **2017**, *7*, 592–605.
- (4) Beletskaya, I. P.; Ananikov, V. P. Transition-Metal-Catalyzed C–S, C–Se, and C–Te Bond Formation via Cross-Coupling and Atom-Economic Addition Reactions. *Chem. Rev.* **2011**, *111*, 1596–1636.
- (5) Kosugi, M.; Shimizu, T.; Migita, T. Reactions of Aryl Halides with Thiolate Anions in the Presence of Catalytic Amounts of Tetrakis(Triphenylphosphine)Palladium Preparation of Aryl Sulfides. *Chem. Lett.* **1978**, *7*, 13–14.
- (6) Norris, T.; Leeman, K. Development of a New Variant of the Migita Reaction for Carbon–Sulfur Bond Formation Used in the Manufacture of Tetrahydro-4-[3-[4-(2-

Methyl-1H-Imidazol-1-yl)Phenyl]Thio]Phenyl-2H-Pyran-4-Carboxamide. *Org. Process Res. Dev.* **2008**, *12*, 869–876.

- (7) Ganley, J. M.; Yeung, C. S. Unprotected Indazoles Are Resilient to Ring-Opening Isomerization: A Case Study on Catalytic C–S Couplings in the Presence of Strong Base. *J. Org. Chem.* **2017**, *82*, 13557–13562.
- (8) Bandaru, S. S. M.; Bhilare, S.; Cardozo, J.; Chrysochos, N.; Schulzke, C.; Sanghvi, Y. S.; Gunturu, K. C.; Kapdi, A. R. Pd/PTABS: Low-Temperature Thioetherification of Chloro(Hetero)Arenes. *J. Org. Chem.* **2019**, *84*, 8921–8940.
- (9) Hartwig, J. F. Evolution of a Fourth Generation Catalyst for the Amination and Thioetherification of Aryl Halides. *Acc. Chem. Res.* **2008**, *41*, 1534–1544.
- (10) Fernández-Rodríguez, M. A.; Shen, Q.; Hartwig, J. F. A General and Long-Lived Catalyst for the Palladium-Catalyzed Coupling of Aryl Halides with Thiols. *J. Am. Chem. Soc.* **2006**, *128*, 2180–2181.
- (11) Xu, J.; Liu, R. Y.; Yeung, C. S.; Buchwald, S. L. Monophosphine Ligands Promote Pd-Catalyzed C–S Cross-Coupling Reactions at Room Temperature with Soluble Bases. *ACS Catal.* **2019**, *9*, 6461–6466.
- (12) Cong, M.; Fan, Y.; Raimundo, J.-M.; Xia, Y.; Liu, Y.; Quéléver, G.; Qu, F.; Peng, L. C–S Coupling Using a Mixed-Ligand Pd Catalyst: A Highly Effective Strategy for Synthesizing Arylthio-Substituted Heterocycles. *Chem. Eur. J.* **2013**, *19*, 17267–17272.
- (13) Jones, A. C.; Nicholson, W. I.; Smallman, H. R.; Browne, D. L. A Robust Pd-Catalyzed C–S Cross-Coupling Process Enabled by Ball-Milling. *Org. Lett.* **2020**, *19*, 7433.
- (14) Oderinde, M. S.; Frenette, M.; Robbins, D. W.; Aquila, B.; Johannes, J. W. Photoredox Mediated Nickel Catalyzed Cross-Coupling of Thiols With Aryl and Heteroaryl Iodides via Thiyl Radicals. *J. Am. Chem. Soc.* **2016**, *138*, 1760–1763.
- (15) Timpa, S. D.; Pell, C. J.; Ozerov, O. V. A Well-Defined (POCOP)Rh Catalyst for the Coupling of Aryl Halides with Thiols. *J. Am. Chem. Soc.* **2014**, *136*, 14772–14779.
- (16) Vara, B. A.; Li, X.; Berritt, S.; Walters, C. R.; Petersson, E. J.; Molander, G. A. Scalable Thioarylation of Unprotected Peptides and Biomolecules under Ni/Photoredox Catalysis. *Chem. Sci.* **2018**, *9*, 336–344.
- (17) Lee, S.-C.; Liao, H.-H.; Chatupheeraphat, A.; Rueping, M. Nickel-Catalyzed C–S Bond Formation via Decarbonylative Thioetherification of Esters, Amides and Intramolecular Recombination Fragment Coupling of Thioesters. *Chem. Eur. J.* **2018**, *24*, 3608–3612.
- (18) Oechsner, R. M.; Wagner, J. P.; Fleischer, I. Acetate Facilitated Nickel Catalyzed Coupling of Aryl Chlorides and Alkyl Thiols. *ACS Catal.* **2022**, *12*, 2233–2243.

- (19) Substance Information - ECHA <https://echa.europa.eu/substance-information/-/substanceinfo/100.000.617> (accessed 2022-04-19).
- (20) Pal, N.; Bhaumik, A. Self-Assembled NiO–ZrO₂ Nanocrystals with Mesoscopic Void Space: An Efficient and Green Catalyst for C–S Cross-Coupling Reaction in Water. *Dalton Trans.* **2012**, *41*, 9161–9169.
- (21) Biswas, B.; Choudhury, P.; Ghosh, A.; Kumar Dubey, S.; Rizzoli, C.; Saha, R.; Bhattacharjee, S. A Water Soluble Ni-Schiff Base Complex for Homogeneous Green Catalytic CS Cross-Coupling Reactions. *Inorg. Chim. Acta* **2022**, *532*, 120755.
- (22) Huang, Y.-C.; Majumdar, K. K.; Cheng, C.-H. Nickel-Catalyzed Coupling of Aryl Iodides with Aromatic Aldehydes: Chemoselective Synthesis of Ketones. *J. Org. Chem.* **2002**, *67*, 1682–1684.
- (23) Kim, S.; Goldfogel, M. J.; Gilbert, M. M.; Weix, D. J. Nickel-Catalyzed Cross-Electrophile Coupling of Aryl Chlorides with Primary Alkyl Chlorides. *J. Am. Chem. Soc.* **2020**, *142*, 9902–9907.
- (24) Bagiyan, G. A.; Koroleva, I. K.; Soroka, N. V.; Ufimtsev, A. V. Oxidation of Thiol Compounds by Molecular Oxygen in Aqueous Solutions. *Russ. Chem. Bull.* **2003**, *52*, 1135–1141.
- (25) Wang, P.-Z.; Chen, J.-R.; Xiao, W.-J. Hantzsch Esters: An Emerging Versatile Class of Reagents in Photoredox Catalyzed Organic Synthesis. *Org. Biomol. Chem.* **2019**, *17*, 6936–6951.
- (26) La Sorella, G.; Strukul, G.; Scarso, A. Recent Advances in Catalysis in Micellar Media. *Green Chem.* **2015**, *17*, 644–683.
- (27) The only limitation observed thus far concerns aryl nitro-containing pyridines. That is, for those that contain a bromide, competing for coupling at the nitro group (i.e., via loss of the NO₂ moiety) appears to take place, leading to a mixture of products.
- (28) Jones, K. D.; Power, D. J.; Bierer, D.; Gericke, K. M.; Stewart, S. G. Nickel Phosphite/Phosphine-Catalyzed C–S Cross-Coupling of Aryl Chlorides and Thiols. *Org. Lett.* **2018**, *20*, 208–211.
- (29) Stambuli, J. P. CHAPTER 6. Transition Metal-Catalyzed Formation of C–O and C–S Bonds. In *Catalysis Series*; Colacot, T., Ed.; Royal Society of Chemistry: Cambridge, 2014; pp 254–275.
- (30) Wilkinson, G.; Gillard, R. D.; McCleverty, J. A. *Comprehensive Coordination Chemistry. the Synthesis, Reactions, Properties & Applications of Coordination Compounds Vol. 6*; Pergamon: Oxford, 1987.
- (31) Schwab, R. S.; Singh, D.; Alberto, E. E.; Piquini, P.; Rodrigues, O. E. D.; Braga, A. L. C–S Cross-Coupling of Thiols with Aryl Iodides under Ligand-Free Conditions Using Nano Copper Oxide as a Recyclable Catalyst in Ionic Liquid. *Catal. Sci. Technol.* **2011**, *1*, 569.

- (32) Wong, Y.-C.; Jayanth, T. T.; Cheng, C.-H. Cobalt-Catalyzed Aryl–Sulfur Bond Formation. *Org. Lett.* **2006**, *8*, 5613–5616.
- (33) Zhai, L.-H.; Guo, L.-H.; Luo, Y.-H.; Ling, Y.; Sun, B.-W. Effective Laboratory-Scale Preparation of Axitinib by Two CuI-Catalyzed Coupling Reactions. *Org. Process Res. Dev.* **2015**, *19*, 849–857.
- (34) Chekal, B. P.; Guinness, S. M.; Lillie, B. M.; McLaughlin, R. W.; Palmer, C. W.; Post, R. J.; Sieser, J. E.; Singer, R. A.; Sluggett, G. W.; Vaidyanathan, R.; Withbroe, G. J. Development of an Efficient Pd-Catalyzed Coupling Process for Axitinib. *Org. Process Res. Dev.* **2014**, *18*, 266–274.
- (35) Boros, Z.; Nagy-Győr, L.; Kátai-Fadgyas, K.; Kőhegyi, I.; Ling, I.; Nagy, T.; Iványi, Z.; Oláh, M.; Ruzsics, G.; Temesi, O.; Volk, B. Continuous Flow Production in the Final Step of Vortioxetine Synthesis. Piperazine Ring Formation on a Flow Platform with a Focus on Productivity and Scalability. *J. Flow. Chem.* **2019**, *9*, 101–113.
- (36) Finck, L.; Brals, J.; Pavuluri, B.; Gallou, F.; Handa, S. Micelle-Enabled Photoassisted Selective Oxyhalogenation of Alkynes in Water under Mild Conditions. *J. Org. Chem.* **2018**, *83*, 7366–7372.
- (37) Sadhukhan, S.; Baire, B. Lewis Basicity of Water for a Selective Monodehalogenation of α,α -Dihalo Ketones to α -Halo Ketones and Mechanistic Study. *Adv. Synth. Catal.* **2018**, *360*, 298–304.
- (38) Rajbongshi, K. K.; Hazarika, D.; Phukan, P. TsNBr₂ Mediated Oxidative Functionalization of Alkynes. *Tetrahedron* **2016**, *72*, 4151–4158.
- (39) Sheldon, R. A. The E Factor 25 Years on: The Rise of Green Chemistry and Sustainability. *Green Chem.* **2017**, *19*, 18–43.
- (40) Rosen, B. M.; Quasdorf, K. W.; Wilson, D. A.; Zhang, N.; Resmerita, A.-M.; Garg, N. K.; Percec, V. Nickel-Catalyzed Cross-Couplings Involving Carbon–Oxygen Bonds. *Chem. Rev.* **2011**, *111*, 1346–1416.
- (41) Xu, X.-B.; Liu, J.; Zhang, J.-J.; Wang, Y.-W.; Peng, Y. Nickel-Mediated Inter- and Intramolecular C–S Coupling of Thiols and Thioacetates with Aryl Iodides at Room Temperature. *Org. Lett.* **2013**, *15*, 550–553.
- (42) Lipshutz, B. H.; Ghorai, S.; Abela, A. R.; Moser, R.; Nishikata, T.; Duplais, C.; Krasovskiy, A.; Gaston, R. D.; Gadwood, R. C. TPGS-750-M: A Second-Generation Amphiphile for Metal-Catalyzed Cross-Couplings in Water at Room Temperature. *J. Org. Chem.* **2011**, *76*, 4379–4391.
- (43) Meng, Y.; Wang, M.; Jiang, X. Multicomponent Reductive Cross-Coupling of an Inorganic Sulfur Dioxide Surrogate: Straightforward Construction of Diversely Functionalized Sulfones. *Angew. Chem., Int. Ed.* **2020**, *59*, 1346–1353.

1.6. General experimental information

a. Surfactant solution preparation

TPGS-750-M was synthesized according to the published procedure and is also commercially available from Sigma-Aldrich (catalog number 733857) [*J. Org. Chem.* **2011**, *76*, 4379]. HPLC grade water was purged by argon before use to prepare surfactant solution. The 2 wt % TPGS-750-M aqueous solution was prepared by dissolving 2 g of TPGS-750-M solid into 98 g of HPLC water and stored under argon.

b. TLC

Thin-layer chromatography (TLC) was performed using Silica Gel 60 F254 plates (Merck, 0.25 mm thick). Flash chromatography was done in glass columns using Silica Gel 60 (EMD, 40-63 μm).

c. NMR

^1H and ^{13}C NMR spectra were recorded on either a Varian Unity Inova 400 MHz (400 MHz for ^1H , 100 MHz for ^{13}C), a Varian Unity Inova 500 MHz (500 MHz for ^1H , 125 MHz for ^{13}C), a Varian Unity Inova 600 MHz (600 MHz for ^1H), or Bruker (500 MHz for ^1H , 125 MHz for ^{13}C).

Deuterated NMR solvents were purchased from Cambridge Isotopes Laboratories. DMSO-*d*₆, CD₃OD, and CDCl₃ were used as solvents. Residual peaks for CHCl₃ in CDCl₃ (^1H = 7.24 ppm, ^{13}C = 77.00 ppm), (CH₃)₂SO in (CD₃)₂SO (^1H = 2.50 ppm, ^{13}C = 39.52 ppm) or MeOH in MeOD (^1H = 3.31 ppm, ^{13}C = 49.00 ppm) have been assigned as internal standards. The chemical shifts are reported in ppm. The coupling constants

J values are given in Hz. Data are reported as follows: chemical shift, multiplicity (s = singlet, bs = broad singlet, d = doublet, bd = broad doublet, t = triplet, q = quartet, quin = quintet, m = multiplet), coupling constant (if applicable) and integration.

d. HRMS

Mass spectra were obtained from the UC Santa Barbara Mass Spectrometry Facility.

LCT-Premier (ESI)

Mass spectra were acquired via ESI-MS using a Waters LCT Premier mass spectrometer equipped with an Alliance 2695 Separations module. Samples dissolved in methanol were directly infused into the mass spectrometer with no chromatography performed. Accurate mass data was calibrated using sodiated polyethylene glycol or sodiated polyethylene glycol monomethyl ether as an internal standard for positive ions and using clusters of sodium formate as an internal standard for negative ions.

GCT-Premier (GC-EI and GC-CI)

Mass spectra were acquired via GC-MS using a Waters GCT Premier mass spectrometer equipped with an Agilent 7890A GC oven and J&W Scientific DB-5ms+DG narrow bore column using helium carrier gas. Samples dissolved in DCM were injected into the GC injector port which was maintained at 260 °C. GC oven temperature was held at 50 °C for one minute, then raised to 290 °C at a rate of 10 °C per minute to elute the sample. Accurate mass data was calibrated using perfluorotributylamine or 2,4,6-tris(trifluoromethyl)-1,3,5-triazine as a co-injected

standard. Where applicable, methane reagent gas was used to perform chemical ionization (CI) experiments.

e. ICP-MS

ICP-MS data were obtained from the UC Los Angeles ICP-MS facility within the UC Center for Environmental Implications of Nanotechnology in CNSI. Inductively coupled plasma mass spectrometry (ICP-MS, NexION 2000, PerkinElmer) analysis was performed to detect nickel. Each sample was transferred to clean Teflon vessel for acid digestion. Digestion was carried out with a mixture of concentrated HNO₃ (65-70%, Trace Metal Grade, Fisher Scientific) and H₂O₂ (30%, Certified ACS, Fisher Scientific) at 200 °C for 50 min in a microwave digestion system (Titan MPS, PerkinElmer). Once the sample was cooled to room temperature, it was subsequently diluted to make a final volume of 50 mL by adding filtered DI water for analysis. The calibration curve was established using a standard solution, and each sample and standard was analyzed in triplicate with background correction.

f. Reagents

Organic reagents were purchased from Sigma-Aldrich, Combi-Blocks, Alfa Aesar, TCI, or Acros Organics and used without further purification. NiBr₂ was purchased from Sigma Aldrich and stored in a dessicator. Zinc nanopowder (40-60 nm avg. part. size, ≥99% trace metals basis) was purchased from Sigma Aldrich and stored in a dessicator.

g. Pre-catalyst Ni(Phen)₂Br₂ preparation

To a 1 dram microwave reaction vial with magnetic stir bar was added NiBr₂ (0.5 mmol), phenanthroline (1.0 mmol) and acetonitrile (1 mL). The vial was placed in a 45 °C metal heating block. This resulted a rapid color change to pink, then to green. It was allowed to stirred overnight. The vial was centrifuged, and the supernatant was removed. The pellet was washed by EtOAc (1 x 1 mL) and then pentane (2 x 1 mL). The green solid was dried under vacuum for 24 h.

Crystallization: The crude pellet was placed in a 5 mL test tube and dissolved with a minimum amount of methanol. The test tube was placed in a 25 mL jar with cap containing EtOAc at rt overnight. The deposition of green, crystalline Ni(Phen)₂Br₂, was isolated by decanting off the colorless supernatant, after which the crystalline material was dried under vacuum.



**Ni(Phen)₂Br₂
After Precipitation**



**Ni(Phen)₂Br₂
After Crystallization**

Figure S1. Appearance of the Ni(Phen)₂Br₂. Left: before crystallization; right: after crystallization.

h. Preparation of pre-catalysts used in Table 2

To a 1 dram microwave reaction vial with magnetic stir bar was added NiBr₂ (0.5 mmol), ligand (1.0 mmol) and acetonitrile (1 mL). The vial was placed in a 45 °C metal heating block. It was allowed to stir overnight. The vial was then centrifuged, and the supernatant was removed. The pellet was washed by EtOAc (1 x 1 mL) and then pentane (2 x 1 mL). The precipitated solid was dried under vacuum for 24 h.

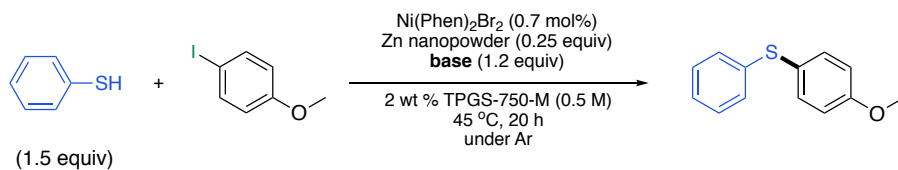
i. X-ray data collection

X-ray data were obtained from the UC Santa Barbara X-ray Facility. The crystal was mounted on a nylon loop and transferred to a Bruker Kappa APEX II diffractometer with Mo K-alpha Radiation. The APEX2 program was used to determine the unit cell parameters and data collection (10 sec / frame, 0.5 deg. /frame Omega scan). The data were collected at 110k. The raw frame data were processed using SAINT program. The absorption correction was applied using program SADABS. Subsequent calculations were carried out using SHELXTL program. The structure was solved by direct methods and refined on F by full-matrix least-squares techniques. (CCDC number of Ni(Phen)₂Br₂ is 1993760. These data can be obtained free of charge from The Cambridge Crystallographic Data Centre via

<https://www.ccdc.cam.ac.uk/structures/Search?access=referee&ccdc=1993760&Author=Tzu-Yu+Yu>)

1.7. Supplementary tables and figures

Table S1. Screening of base^a



entry	base	yield (%) ^b
1	KOH	31
2	NaOH	39
3	K ₃ PO ₄	58
4	NaO <i>t</i> -Bu	68
5	Et ₃ N	69
6	Cs ₂ CO ₃	74 (71)
7	KO <i>t</i> -Bu	94 (82)

^a Scale of reaction: 0.25 mmol of 4-iodoanisole and 2 wt % TPGS-750-M/H₂O (0.5 mL).

^b Yield determined by ¹H NMR using 1,3,5-trimethylbenzene as internal standard. Isolated yields in parenthesis.

1.8. Experimental procedures and characterizations data for thioether products

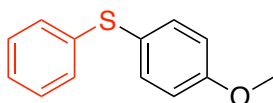
Decyl(4-methoxyphenyl)sulfane (3)



To a 1 dram microwave reaction vial with a magnetic stir bar was added Ni(Phen)₂Br₂ (1.0 mg, 0.002 mmol, 0.007 equiv), Zn nanopowder (4.1 mg, 0.063 mmol, 0.25 equiv), K₃PO₄ (63.7 mg, 0.3 mmol, 1.2 equiv), and 4-methoxyiodobenzene (58.5 mg, 0.25 mmol, 1 equiv). The vial was capped with a rubber septum and then evacuated and backfilled with argon three times. Next, 1-decanethiol (45.8 mg, 0.2625 mmol, 1.05 equiv) and 2 wt % TPGS-750-M aqueous solution (0.5 mL) was added via a syringe through the septum. The solution was heated at 45 °C and stirred vigorously for 16 h. After the reaction, to the vial was added approximately 1 mL of EtOAc and silica gel. The mixture was concentrated under reduced pressure to obtain product-loaded silica, which was then used for flash chromatography using 0-15% EtOAc/hexanes as eluent.

Off-white solid, yield 66.9 mg (96%) R_f = 0.32 (hexanes). ¹H NMR (600 MHz, CDCl₃) δ 7.35 – 7.28 (m, 2H), 6.86 – 6.78 (m, 2H), 3.77 (s, 3H), 2.79 (t, *J* = 7.4 Hz, 2H), 1.56 (p, *J* = 7.4 Hz, 2H), 1.36 (p, *J* = 6.9 Hz, 2H), 1.23 (m, 12H), 0.86 (t, *J* = 7.0 Hz, 3H). ¹³C NMR (151 MHz, CDCl₃) δ 158.67, 132.85, 126.96, 114.44, 55.26, 35.79, 31.86, 29.51, 29.49, 29.32, 29.27, 29.15, 28.68, 22.65, 14.08. HRMS TOF MS EI⁺ *m/z* calcd for C₁₇H₂₈OS [M]⁺: 216.1861; found: 280.1859.

(4-Methoxyphenyl)(phenyl)sulfane (5)

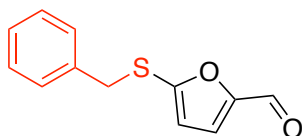


To a 1 dram microwave reaction vial with a magnetic stir bar was added Ni(Phen)₂Br₂ (1.0 mg, 0.002 mmol, 0.007 equiv), Zn nanopowder (4.1 mg, 0.063 mmol, 0.25 equiv) and KO^t-Bu (33.6 mg, 0.3 mmol, 1.2 equiv). The vial was capped with a rubber septum and then

evacuated and backfilled with argon three times. Next, 4-methoxyiodobenzene (58.5 mg, 0.25 mmol, 1 equiv), thiophenol (28.9 mg, 0.2625 mmol, 1.05 equiv) and 2 wt % TPGS-750-M aqueous solution (0.5 mL) was added via a syringe through the septum. The solution was heated at 45 °C and stirred vigorously for 16 h. After the reaction, to the vial was added approximately 1 mL of EtOAc and silica gel. The mixture was concentrated under reduced pressure to obtain product-loaded silica, which was then used for flash chromatography using EtOAc/hexanes as eluent.

Colorless oil, yield 44.3 mg (82%) $R_f = 0.59$ (hexanes). $^1\text{H NMR}$ (500 MHz, CDCl_3) δ 7.41 (d, $J = 8.2$ Hz, 2H), 7.22 (d, $J = 7.6$ Hz, 2H), 7.19 – 7.08 (m, 3H), 6.89 (d, $J = 8.2$ Hz, 2H), 3.81 (s, 3H). $^{13}\text{C NMR}$ (126 MHz, CDCl_3) δ 159.82, 138.57, 135.32, 128.90, 128.23, 125.75, 124.35, 114.97, 55.34. **HRMS** TOF MS EI^+ m/z calcd for $\text{C}_{13}\text{H}_{12}\text{OS}$ $[\text{M}]^+$: 216.0608; found: 216.0609.

5-(Benzylthio)furan-2-carbaldehyde (8)

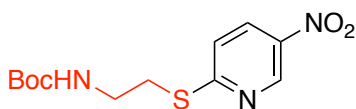


To a 1 dram microwave reaction vial with a magnetic stir bar was added $\text{Ni}(\text{Phen})_2\text{Br}_2$ (1.0 mg, 0.002 mmol, 0.007 equiv), Zn nanopowder (4.1 mg, 0.063 mmol, 0.25 equiv), K_3PO_4 (63.7 mg, 0.3 mmol, 1.2 equiv) and 5-iodofuran-2-carbaldehyde (55.5 mg, 0.25 mmol, 1 equiv). The vial was capped with a rubber septum and then evacuated and backfilled with argon three times. Next, benzyl mercaptan (77.6 mg, 0.2625 mmol, 1.05 equiv) and 0.5 mL 2 wt % TPGS-750-M aqueous solution was added via a syringe through the septum. The

solution was heated at 45 °C and stirred vigorously for 20 h. After the reaction, to the vial was added approximately 1 mL of EtOAc and silica gel. The mixture was concentrated under reduced pressure to obtain product-loaded silica, which was then used for flash chromatography using EtOAc/hexanes as eluent.

Brown oil, yield 51.8 mg (95%) $R_f = 0.26$ (10% EtOAc/hexanes). $^1\text{H NMR}$ (500 MHz, CDCl_3) δ 9.51 (s, 1H), 7.31 – 7.24 (m, 3H), 7.24 – 7.21 (m, 2H), 7.13 (d, $J = 3.6$ Hz, 1H), 6.35 (d, $J = 3.6$ Hz, 1H), 4.18 (s, 2H). $^{13}\text{C NMR}$ (126 MHz, CDCl_3) δ 176.40, 154.77, 154.11, 136.36, 128.78, 128.63, 127.65, 122.66, 115.45, 38.52. **HRMS** TOF MS EI^+ m/z calcd for $\text{C}_{12}\text{H}_{10}\text{O}_2\text{S Na}$ $[\text{M}+\text{Na}]^+$: 241.0299; found: 241.0301.

***t*-Butyl (2-((5-nitropyridin-2-yl)thio)ethyl)carbamate (11)**



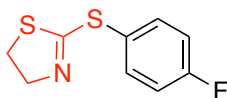
To a 1 dram microwave reaction vial with a magnetic stir bar was added $\text{Ni}(\text{Phen})_2\text{Br}_2$ (2.0 mg, 0.0034 mmol, 0.014 equiv), Zn nanopowder (4.1 mg, 0.063 mmol, 0.25 equiv), Cs_2CO_3 (97.8 mg, 0.3 mmol, 1.2 equiv) and 2-bromo-5-nitropyridine (50.8 mg, 0.25 mmol, 1 equiv). The vial was capped with a rubber septum and then evacuated and backfilled with argon three times. Next, 2-(Boc-amino)ethanethiol (46.5 mg, 0.2625 mmol, 1.05 equiv) and 0.5 mL 2 wt % TPGS-750-M aqueous solution was added via a syringe through the septum. The solution was heated at 55 °C and stirred vigorously for 20 h. After the reaction, to the vial was added approximately 1 mL of EtOAc and silica gel. The mixture was concentrated under reduced pressure to obtain product-loaded silica, which was then used for flash chromatography using 20% EtOAc/hexanes as eluent.

Light yellow solid, yield 66.8 mg (90%) $R_f = 0.45$ (20% EtOAc/hexanes).

*When KO^tBu was used as base, yield 49.1 mg (66%).

¹H NMR (500 MHz, CDCl₃) δ 9.19 (s, 1H), 8.20 (d, $J = 8.9$ Hz, 1H), 7.29 (d, $J = 8.8$ Hz, 1H), 4.98 (s, 1H), 3.43 (t, $J = 6.4$ Hz, 2H), 3.37 (d, $J = 6.4$ Hz, 2H), 1.40 (s, 9H). ¹³C NMR (126 MHz, CDCl₃) δ 167.02, 155.76, 144.94, 141.68, 141.22, 130.43, 121.64, 79.53, 40.01, 30.49, 28.32. HRMS TOF MS m/z calcd for C₁₂H₁₇N₃O₄S Na [M+Na]⁺: 322.0837; found: 322.0836.

2-((4-Fluorophenyl)thio)-4,5-dihydrothiazole (14)



To a 1 dram microwave reaction vial with a magnetic stir bar was added Ni(Phen)₂Br₂ (1.0 mg, 0.0018 mmol, 0.014 equiv), Zn nanopowder (2.0 mg, 0.031 mmol, 0.25 equiv), Cs₂CO₃ (48.9 mg, 0.15 mmol, 1.2 equiv) and 4,5-dihydrothiazole-2-thiol (15.7 mg, 0.125 mmol, 1 equiv). The vial was capped with a rubber septum and then evacuated and backfilled with argon three times. Next, 4-fluoriodobenzene (27.8 mg, 0.131 mmol, 1.05 equiv) and 0.25 mL 2 wt % TPGS-750-M aqueous solution was added via a syringe through the septum. The solution was heated at 55 °C and stirred vigorously for 2 h. After the reaction, to the vial was added approximately 1 mL of EtOAc and silica gel. The mixture was concentrated under reduced pressure to obtain product-loaded silica, which was then used for flash chromatography using 20% EtOAc/hexanes as eluent.

Colorless oil, yield 17.0 mg (64%) $R_f = 0.44$ (30% EtOAc/hexanes). $^1\text{H NMR}$ (500 MHz, CDCl_3) δ 7.63 – 7.56 (m, 2H), 7.11 – 7.03 (m, 2H), 4.24 (t, $J = 8.1$ Hz, 2H), 3.30 (t, $J = 8.1$ Hz, 2H). $^{13}\text{C NMR}$ (126 MHz, CDCl_3) δ 167.49, 164.83, 162.84, 137.56, 124.75, 124.73, 116.51, 116.33, 77.26, 77.00, 76.75, 65.43, 35.09. $^{19}\text{F NMR}$ (471 MHz, CDCl_3) δ 47.70, -109.97. **HRMS** TOF MS Cl^+ m/z calcd for $\text{C}_9\text{H}_8\text{FNS}_2$ H $[\text{M}+\text{H}]^+$: 214.0161; found: 241.0162.

Decyl(4-fluorophenyl)sulfane (15)

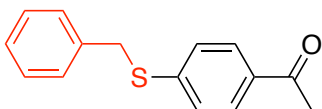


To a 1 dram microwave reaction vial with a magnetic stir bar was added $\text{Ni}(\text{Phen})_2\text{Br}_2$ (1.0 mg, 0.002 mmol, 0.007 equiv), Zn nanopowder (4.1 mg, 0.063 mmol, 0.25 equiv), and K_3PO_4 (63.7 mg, 0.30 mmol, 1.2 equiv). The vial was capped with a rubber septum and then evacuated and backfilled with argon three times. Next, 4-fluoroiodobenzene (55.5 mg, 0.25 mmol, 1 equiv), 1-decanethiol (45.8 mg, 0.2625 mmol, 1.05 equiv) and 0.5 mL 2 wt % TPGS-750-M aqueous solution was added via a syringe through the septum. The solution was heated at 45 °C and stirred vigorously for 20 h. After the reaction, to the vial was added approximately 1 mL of EtOAc and silica gel. The mixture was concentrated under reduced pressure to obtain product-loaded silica, which was then used for flash chromatography using hexanes as eluent.

Light brown liquid, yield 59.3 mg (89%) $R_f = 0.60$ (hexanes). $^1\text{H NMR}$ (600 MHz, CDCl_3) δ 7.34 – 7.28 (m, 2H), 7.00 – 6.93 (m, 2H), 2.86 – 2.82 (m, 2H), 1.62 – 1.56 (m, 2H), 1.38 (p, $J = 7.0$ Hz, 2H), 1.30 – 1.22 (m, 12H), 0.86 (t, $J = 7.0$ Hz, 3H). $^{13}\text{C NMR}$ (151 MHz,

CDCl₃) δ 161.6 (d, J_{C-F} = 245.3 Hz), 131.90 (d, J_{C-F} = 75.2 Hz), 131.73 (d, J_{C-F} = 3.0 Hz), 115.85 (d, J_{C-F} = 22.7 Hz), 34.97, 31.87, 29.51, 29.48, 29.28, 29.22, 29.15, 29.13, 28.70, 22.65, 14.08. ¹⁹F NMR (376 MHz, CDCl₃) δ -116.19 (tt, J_{F-H} = 8.6, 5.2 Hz). HRMS TOF MS EI⁺ m/z calcd for C₁₆H₂₅FS [M]⁺: 266.1661; found: 266.1662.

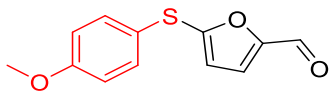
1-(4-(Benzylthio)phenyl)ethan-1-one (16)



To a 1 dram microwave reaction vial with a magnetic stir bar was added Ni(Phen)₂Br₂ (1.0 mg, 0.002 mmol, 0.007 equiv), Zn nanopowder (8.2 mg, 0.125 mmol, 0.5 equiv), K₃PO₄ (63.7 mg, 0.3 mmol, 1.2 equiv) and 4'-iodoacetophenone (61.5 mg, 0.25 mmol, 1 equiv). The vial was capped with a rubber septum and then evacuated and backfilled with argon three times. Next, benzyl mercaptan (77.6 mg, 0.2625 mmol, 1.05 equiv) and 0.5 mL 2 wt % TPGS-750-M aqueous solution was added via a syringe through the septum. The solution was heated at 45 °C and stirred vigorously for 19 h. After the reaction, to the vial was added approximately 1 mL of EtOAc and silica gel. The mixture was concentrated under reduced pressure to obtain product-loaded silica, which was then used for flash chromatography using EtOAc/hexanes as eluent.

White solid, yield 52.1 mg (86%) R_f = 0.44 (10% EtOAc/hexanes). ¹H NMR (500 MHz, CDCl₃) δ 7.82 (d, J = 8.3 Hz, 2H), 7.36 (d, J = 7.5 Hz, 2H), 7.31 (m, 4H), 7.26 (d, J = 7.5 Hz, 1H), 4.20 (s, 2H), 2.54 (s, 3H). ¹³C NMR (126 MHz, CDCl₃) δ 197.07, 144.13, 136.19, 134.12, 128.68, 128.63, 127.46, 126.83, 37.11, 26.37. HRMS TOF MS CI⁺ m/z calcd for C₁₅H₁₄OS H [M+H]⁺: 243.0844; found: 243.0844.

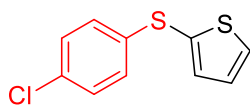
5-((4-Methoxyphenyl)thio)furan-2-carbaldehyde (17)



To a 1 dram microwave reaction vial with a magnetic stir bar was added Ni(Phen)₂Br₂ (1.0 mg, 0.002 mmol, 0.007 equiv), Zn nanopowder (8.2 mg, 0.125 mmol, 0.5 equiv), K₃PO₄ (63.7 mg, 0.3 mmol, 1.2 equiv) and 5-iodofuran-2-carbaldehyde (55.5 mg, 0.25 mmol, 1 equiv). The vial was capped with a rubber septum and then evacuated and backfilled with argon three times. Next, 4-methoxybenzenethiol (140.2 mg, 0.2625 mmol, 1.05 equiv) and 0.5 mL 2 wt % TPGS-750-M aqueous solution was added via a syringe through the septum. The solution was heated at 45 °C and stirred vigorously for 16 h. After the reaction, to the vial was added approximately 1 mL of EtOAc and silica gel. The mixture was concentrated under reduced pressure to obtain product-loaded silica, which was then used for flash chromatography using EtOAc/hexanes as eluent.

Faint yellow solid, yield 51.3 mg (88%) $R_f = 0.36$ (10% EtOAc/hexanes). ¹H NMR (500 MHz, CDCl₃) δ 9.47 (s, 1H), 7.42 (d, $J = 8.8$ Hz, 2H), 7.13 (d, $J = 3.6$ Hz, 1H), 6.86 (d, $J = 8.7$ Hz, 2H), 6.31 (d, $J = 3.6$ Hz, 1H), 3.77 (s, 3H). ¹³C NMR (126 MHz, CDCl₃) δ 176.55, 160.44, 156.58, 153.96, 134.82, 122.42, 120.64, 115.13, 114.26, 55.32. HRMS TOF MS CI⁺ m/z calcd for C₁₂H₁₀O₃S H [M+H]⁺: 235.0429; found: 235.0435.

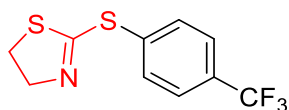
2-((4-Chlorophenyl)thio)thiophene (18)



To a 1 dram microwave reaction vial with a magnetic stir bar was added Ni(Phen)₂Br₂ (2.0 mg, 0.0034 mmol, 0.014 equiv), Zn nanopowder (8.2 mg, 0.125 mmol, 0.5 equiv), K₃PO₄ (63.7 mg, 0.3 mmol, 1.2 equiv) and 4-chlorobenzenethiol (46.8 mg, 0.263 mmol, 1.05 equiv). The vial was capped with a rubber septum and then evacuated and backfilled with argon three times. Next, 2-iodothiophene (52.5 mg, 0.25 mmol, 1 equiv) and 0.5 mL 2 wt % TPGS-750-M aqueous solution was added via a syringe through the septum. The solution was heated at 55 °C and stirred vigorously for 20 h. After the reaction, to the vial was added approximately 1 mL of EtOAc and silica gel. The mixture was concentrated under reduced pressure to obtain product-loaded silica, which was then used for flash chromatography using EtOAc/hexanes as eluent.

Faint yellow oil, yield 49.5 mg (87%) R_f = 0.6 (10% EtOAc/hexanes). ¹H NMR (500 MHz, CDCl₃) δ 7.47 (d, *J* = 5.3 Hz, 1H), 7.28 (d, *J* = 2.8 Hz, 1H), 7.20 (d, *J* = 8.6 Hz, 2H), 7.10 (d, *J* = 8.6 Hz, 2H), 7.07 (dd, *J* = 5.3, 3.6 Hz, 1H). ¹³C NMR (126 MHz, Chloroform-*d*) δ 137.19, 136.24, 131.97, 131.59, 130.55, 129.02, 128.37, 127.99. HRMS TOF MS CI⁺ *m/z* calcd for C₁₀H₇ClS₂ H [M+H]⁺: 226.9756; found: 226.9767.

2-((4-(Trifluoromethyl)phenyl)thio)-4,5-dihydrothiazole (19)



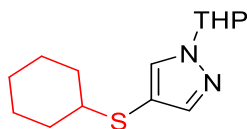
To a 1 dram microwave reaction vial with a magnetic stir bar was added Ni(Phen)₂Br₂ (2.0 mg, 0.0034 mmol, 0.014 equiv), Zn nanopowder (8.2 mg, 0.125 mmol, 0.5 equiv), K₃PO₄ (63.7 mg, 0.3 mmol, 1.2 equiv) and 4,5-dihydrothiazole-2-thiol (31.3 mg, 0.2625 mmol, 1.05 equiv). The vial was capped with a rubber septum and then evacuated and backfilled

with argon three times. Next, 1-iodo-4-(trifluoromethyl)benzene (68 mg, 0.25 mmol, 1 equiv) and 0.5 mL 2 wt % TPGS-750-M aqueous solution was added via a syringe through the septum. The solution was heated at 55 °C and stirred vigorously for 20 h. After the reaction, to the vial was added approximately 1 mL of EtOAc and silica gel. The mixture was concentrated under reduced pressure to obtain product-loaded silica, which was then used for flash chromatography using EtOAc/hexanes as eluent.

Yellow oil, yield 46.2 mg (70%) $R_f = 0.40$ (20% EtOAc/hexanes).

¹H NMR (500 MHz, CDCl₃) δ 7.73 (d, $J = 8.2$ Hz, 2H), 7.62 (d, $J = 8.2$ Hz, 2H), 4.24 (t, $J = 8.1$ Hz, 2H), 3.35 (t, $J = 8.1$ Hz, 2H). **¹³C NMR** (126 MHz, CDCl₃) δ 165.28, 134.68, 134.20, 131.47 (q, $^1J_{(C-F)} = 32.7$ Hz), 125.91 (q, $^1J_{(C-F)} = 3.7$ Hz), 123.68 (q, $^1J_{(C-F)} = 272.5$ Hz), 65.12, 35.30. **¹⁹F NMR** (376 MHz, CDCl₃) δ -62.93. **HRMS** TOF MS CI⁺ m/z calcd for C₁₀H₈F₃NS₂ H [M+H]⁺: 264.0128; found: 264.0121.

4-(Cyclohexylthio)-1-(tetrahydro-2H-pyran-2-yl)-1H-pyrazole (20)



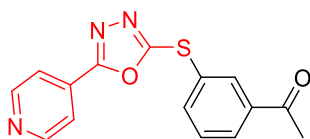
To a 1 dram microwave reaction vial with a magnetic stir bar was added Ni(Phen)₂Br₂ (2.0 mg, 0.0034 mmol, 0.014 equiv), Zn nanopowder (8.2 mg, 0.125 mmol, 0.5 equiv), K₃PO₄ (63.7 mg, 0.3 mmol, 1.2 equiv) and 4-iodo-1-(tetrahydro-2H-pyran-2-yl)-1H-pyrazole (69.5 mg, 0.25 mmol, 1 equiv). The vial was capped with a rubber septum and then evacuated and backfilled with argon three times. Next, cyclohexanethiol (30.5 mg, 0.2625 mmol, 1.05 equiv) and 0.5 mL 2 wt % TPGS-750-M aqueous solution was added via a

syringe through the septum. The solution was heated at 55 °C and stirred vigorously for 20 h. After the reaction, to the vial was added approximately 1 mL of EtOAc and silica gel. The mixture was concentrated under reduced pressure to obtain product-loaded silica, which was then used for flash chromatography using EtOAc/hexanes as eluent.

*When 0.7% Ni(Phen)₂Br₂ were used, yield = 49%.

Yellow solid, yield 52.5 mg (79%) R_f = 0.38 (20% EtOAc/hexanes). ¹H NMR (500 MHz, CDCl₃) δ 7.58 (s, 1H), 7.46 (s, 1H), 5.29 (dd, *J* = 9.0, 2.4 Hz, 1H), 4.00 (d, *J* = 10.4 Hz, 1H), 3.64 (t, *J* = 9.9 Hz, 1H), 2.59 (t, *J* = 8.0 Hz, 1H), 2.10 – 1.93 (m, 3H), 1.92 – 1.82 (m, 2H), 1.74 – 1.49 (m, 6H), 1.25 – 1.07 (m, 5H). ¹³C NMR (126 MHz, CDCl₃) δ 144.57, 132.40, 109.21, 87.59, 67.66, 47.57, 33.24, 30.27, 25.99, 25.46, 24.77, 22.20. HRMS TOF MS CI⁺ *m/z* calcd for C₁₄H₂₂N₂OS H [M+H]⁺: 267.1531; found: 267.1537.

1-(3-((5-(Pyridin-4-yl)-1,3,4-oxadiazol-2-yl)thio)phenyl)ethan-1-one (21)

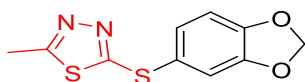


To a 1 dram microwave reaction vial with a magnetic stir bar was added Ni(Phen)₂Br₂ (2.0 mg, 0.0034 mmol, 0.014 equiv), Zn nanopowder (8.2 mg, 0.125 mmol, 0.5 equiv), ^tBuOK (33.7 mg, 0.3 mmol, 1.2 equiv) and 5-(pyridin-4-yl)-1,3,4-oxadiazole-2-thiol (47.1 mg, 0.263 mmol, 1.05 equiv). The vial was capped with a rubber septum and then evacuated and backfilled with argon three times. Next, 1-(3-iodophenyl)ethan-1-one (61.5 mg, 0.25 mmol, 1 equiv) 0.2 mL DMSO and 1 mL 2 wt % TPGS-750-M aqueous solution was added via a syringe through the septum. The solution was heated at 55 °C and stirred vigorously

for 20 h. After the reaction, to the vial was added approximately 1 mL of EtOAc and silica gel. The mixture was concentrated under reduced pressure to obtain product-loaded silica, which was then used for flash chromatography using EtOAc/hexanes as eluent.

White solid, yield 62.9 mg (85%) $R_f = 0.45$ (100% EtOAc). $^1\text{H NMR}$ (500 MHz, DMSO- d_6) δ 8.79 (d, $J = 5.9$ Hz, 2H), 8.25 (s, 1H), 8.06 (d, $J = 7.8$ Hz, 1H), 7.98 (d, $J = 7.9$ Hz, 1H), 7.83 (d, $J = 6.0$ Hz, 2H), 7.66 (t, $J = 7.8$ Hz, 1H), 2.61 (s, 3H). $^{13}\text{C NMR}$ (126 MHz, DMSO- d_6) δ 197.04, 164.23, 163.28, 150.96, 138.10, 137.46, 132.47, 130.40, 129.99, 129.60, 127.48, 120.02, 26.85. **HRMS** TOF MS Cl^+ m/z calcd for $\text{C}_{15}\text{H}_{11}\text{N}_3\text{O}_2\text{S H}$ $[\text{M}+\text{H}]^+$: 298.0650; found: 298.0650.

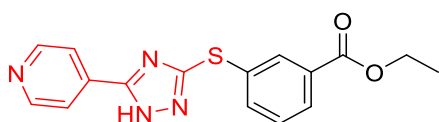
2-(Benzo[d][1,3]dioxol-5-ylthio)-5-methyl-1,3,4-thiadiazole (22)



To a 1 dram microwave reaction vial with a magnetic stir bar was added $\text{Ni}(\text{Phen})_2\text{Br}_2$ (2.0 mg, 0.0034 mmol, 0.014 equiv), Zn nanopowder (8.2 mg, 0.125 mmol, 0.5 equiv), K_3PO_4 (63.7 mg, 0.3 mmol, 1.2 equiv) and 5-methyl-1,3,4-thiadiazole-2-thiol (34.7 mg, 0.2625 mmol, 1.05 equiv). The vial was capped with a rubber septum and then evacuated and backfilled with argon three times. Next, 5-iodobenzo[d][1,3]-dioxole (62 mg, 0.25 mmol, 1 equiv) and 0.5 mL 2 wt % TPGS-750-M aqueous solution was added via a syringe through the septum. The solution was heated at 55 °C and stirred vigorously for 20 h. After the reaction, to the vial was added approximately 1 mL of EtOAc and silica gel. The mixture was concentrated under reduced pressure to obtain product-loaded silica, which was then used for flash chromatography using EtOAc/hexanes as eluent.

White solid, yield 56.3 mg (89%) $R_f = 0.13$ (20% EtOAc/hexanes). $^1\text{H NMR}$ (500 MHz, CDCl_3) δ 7.12 (d, $J = 7.9$ Hz, 1H), 7.02 (s, 1H), 6.78 (d, $J = 8.0$ Hz, 1H), 5.98 (s, 2H), 2.60 (s, 3H). $^{13}\text{C NMR}$ (126 MHz, CDCl_3) δ 169.29, 165.65, 149.63, 148.55, 129.14, 122.36, 114.39, 109.28, 101.83, 15.55. **HRMS** TOF MS Cl^+ m/z calcd for $\text{C}_{10}\text{H}_8\text{N}_2\text{O}_2\text{S}_2\text{H}$ $[\text{M}+\text{H}]^+$: 253.0105; found: 253.0114.

Ethyl 3-((5-(pyridin-4-yl)-1H-1,2,4-triazol-3-yl)thio)benzoate (23)



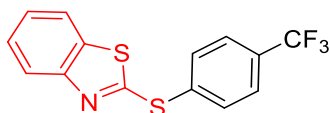
To a 1 dram microwave reaction vial with a magnetic stir bar was added $\text{Ni}(\text{Phen})_2\text{Br}_2$ (2.0 mg, 0.0034 mmol, 0.014 equiv), Zn nanopowder (8.2 mg, 0.125 mmol, 0.5 equiv), $t\text{BuOK}$ (33.7 mg, 0.3 mmol, 1.2 equiv) and 5-(pyridin-4-yl)-1H-1,2,4-triazole-3-thiol (46.8 mg, 0.2625 mmol, 1.05 equiv). The vial was capped with a rubber septum and then evacuated and backfilled with argon three times. Next, ethyl 3-iodobenzoate (69 mg, 0.25 mmol, 1 equiv) 0.2 mL DMSO and 1 mL 2 wt % TPGS-750-M aqueous solution was added via a syringe through the septum. The solution was heated at 55 °C and stirred vigorously for 20 h. After the reaction, to the vial was added approximately 1 mL of EtOAc and silica gel. The mixture was concentrated under reduced pressure to obtain product-loaded silica, which was then used for flash chromatography using EtOAc/hexanes as eluent.

White solid, yield 59.4 mg (73%) $R_f = 0.25$ (EtOAc).

$^1\text{H NMR}$ (500 MHz, $\text{DMSO}-d_6$) δ 15.02 (s, 1H), 8.70 (d, $J = 5.3$ Hz, 2H), 8.05 (s, 1H), 7.88 (t, $J = 6.6$ Hz, 3H), 7.73 (d, $J = 7.7$ Hz, 1H), 7.52 (t, $J = 7.8$ Hz, 1H), 4.27 (q, $J = 7.0$

Hz, 2H), 1.26 (t, $J = 7.1$ Hz, 3H). ^{13}C NMR (126 MHz, DMSO- d_6) δ 164.87, 157.27, 153.36, 150.54, 135.52, 134.88, 132.55, 131.06, 130.66, 129.92, 128.50, 119.97, 61.07, 14.03. HRMS TOF MS Cl^+ m/z calcd for $\text{C}_{16}\text{H}_{14}\text{N}_4\text{O}_2\text{S H}$ $[\text{M}+\text{H}]^+$: 327.0916; found: 327.0927.

2-((4-(Trifluoromethyl)phenyl)thio)benzo[d]thiazole (24)

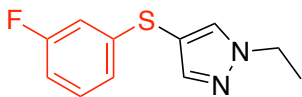


To a 1 dram microwave reaction vial with a magnetic stir bar was added $\text{Ni}(\text{Phen})_2\text{Br}_2$ (2.0 mg, 0.0034 mmol, 0.014 equiv), Zn nanopowder (8.2 mg, 0.125 mmol, 0.5 equiv), K_3PO_4 (63.7 mg, 0.3 mmol, 1.2 equiv) and 4,5-dihydrothiazole-2-thiol (43.9 mg, 0.2625 mmol, 1.05 equiv). The vial was capped with a rubber septum and then evacuated and backfilled with argon three times. Next, 1-iodo-4-(trifluoromethyl)-benzene (68 mg, 0.25 mmol, 1 equiv) and 0.5 mL 2 wt % TPGS-750-M aqueous solution was added via a syringe through the septum. The solution was heated at 55 °C and stirred vigorously for 20 h. After the reaction, to the vial was added approximately 1 mL of EtOAc and silica gel. The mixture was concentrated under reduced pressure to obtain product-loaded silica, which was then used for flash chromatography using EtOAc/hexanes as eluent.

White solid, yield 54.5 mg (70%) $R_f = 0.58$ (20% EtOAc/hexanes). ^1H NMR (500 MHz, CDCl_3) δ 7.91 (d, $J = 8.2$ Hz, 1H), 7.79 (d, $J = 8.1$ Hz, 2H), 7.72 – 7.64 (m, 3H), 7.42 (t, $J = 7.7$ Hz, 1H), 7.31 (t, $J = 7.6$ Hz, 1H). ^{13}C NMR (126 MHz, CDCl_3) δ 165.67, 153.53, 135.79, 135.23, 134.05, 131.69 (q, $^1J_{(\text{C-F})} = 32.9$ Hz), 126.51 (q, $^1J_{(\text{C-F})} = 3.7$ Hz), 126.38, 124.93, 123.63 (q, $^1J_{(\text{C-F})} = 272.5$ Hz), 122.36, 120.93. ^{19}F NMR (376 MHz, CDCl_3) δ -

62.89. **HRMS** TOF MS Cl^+ m/z calcd for $\text{C}_{14}\text{H}_8\text{F}_3\text{NS}_2$ H $[\text{M}+\text{H}]^+$: 312.0128; found: 312.0137.

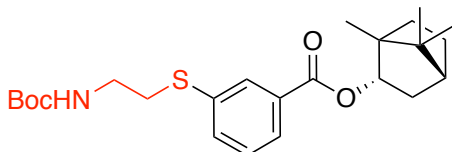
1-Ethyl-4-((3-fluorophenyl)thio)-1H-pyrazole (25)



To a 1 dram microwave reaction vial with a magnetic stir bar was added $\text{Ni}(\text{Phen})_2\text{Br}_2$ (2.0 mg, 0.0034 mmol, 0.014 equiv), Zn nanopowder (8.2 mg, 0.125 mmol, 0.5 equiv), K_3PO_4 (63.7 mg, 0.3 mmol, 1.2 equiv) and 1-ethyl-4-iodo-1H-pyrazole (52.0 mg, 0.25 mmol, 1.0 equiv). The vial was capped with a rubber septum and then evacuated and backfilled with argon three times. Next, 3-fluorobenzenethiol (33.6 mg, 0.2625 mmol, 1.05 equiv) and 0.5 mL 2 wt % TPGS-750-M aqueous solution was added via a syringe through the septum. The solution was heated at 45 °C and stirred vigorously for 20 h. After the reaction, to the vial was added approximately 1 mL of EtOAc and silica gel. The mixture was concentrated under reduced pressure to obtain product-loaded silica, which was then used for flash chromatography using EtOAc/hexanes as eluent.

White solid, yield 14.5 mg (26%) $R_f = 0.29$ (20% EtOAc/hexanes). **^1H NMR** (500 MHz, CDCl_3) δ 7.57 (d, $J = 13.6$ Hz, 2H), 7.15 (td, $J = 8.0, 5.9$ Hz, 1H), 6.86 (d, $J = 8.0$ Hz, 1H), 6.75 (ddd, $J = 18.6, 9.0, 2.2$ Hz, 2H), 4.21 (q, $J = 7.4$ Hz, 2H), 1.51 (t, $J = 7.4$ Hz, 3H). **^{13}C NMR** (126 MHz, CDCl_3) δ 164.07, 162.10, 144.60, 141.81 (d, $J_{\text{C-F}} = 7.5$ Hz), 133.85, 130.00 (d, $J_{\text{C-F}} = 8.6$ Hz), 121.33, 121.31, 112.86 – 111.87 (m), 105.85, 47.58, 15.32. **^{19}F NMR** (471 MHz, CDCl_3) δ -112.37 – -112.44 (m). **HRMS** TOF MS Cl^+ m/z calcd for $\text{C}_{11}\text{H}_{11}\text{FN}_2\text{S}$ H $[\text{M}+\text{H}]^+$: 223.0705; found: 223.0709.

(2*S*,4*R*)-1,7,7-Trimethylbicyclo[2.2.1]heptan-2-yl-3-((2-((*t*-butoxycarbonyl)amino)ethyl)-thio)benzoate (26)

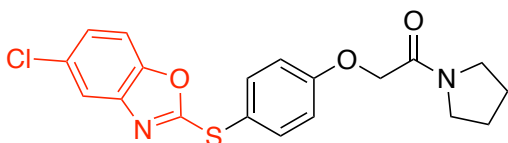


To a 1 dram microwave reaction vial with a magnetic stir bar was added Ni(Phen)₂Br₂ (0.5 mg, 0.0009 mmol, 0.007 equiv), Zn nanopowder (2.0 mg, 0.031 mmol, 0.25 equiv), Cs₂CO₃ (48.9 mg, 0.15 mmol, 1.2 equiv) and (2*S*,4*R*)-1,7,7-trimethylbicyclo[2.2.1]heptan-2-yl-3-iodobenzoate (48.0 mg, 0.125 mmol, 1 equiv). The vial was capped with a rubber septum and then evacuated and backfilled with argon three times. Next, 2-(Boc-amino)ethanethiol (23.3 mg, 0.131 mmol, 1.05 equiv) and 0.25 mL 2 wt % TPGS-750-M aqueous solution was added via a syringe through the septum. The solution was heated at 55 °C and stirred vigorously for 20 h. After the reaction, to the vial was added approximately 1 mL of EtOAc and silica gel. The mixture was concentrated under reduced pressure to obtain product-loaded silica, which was then used for flash chromatography using EtOAc/hexanes as eluent.

Colorless oil, yield 43.2 mg (80%), R_f = 0.33 (10% EtOAc/hexanes). ¹H NMR (500 MHz, CDCl₃) δ 7.99 (t, *J* = 1.8 Hz, 1H), 7.85 (dt, *J* = 7.7, 1.4 Hz, 1H), 7.52 (dt, *J* = 7.9, 1.5 Hz, 1H), 7.36 (t, *J* = 7.8 Hz, 1H), 5.09 (ddd, *J* = 9.9, 3.5, 2.1 Hz, 1H), 4.88 (s, br, 1H), 3.33 (q, *J* = 6.4 Hz, 2H), 3.07 (t, *J* = 6.4 Hz, 2H), 2.50 – 2.40 (m, 1H), 2.08 (ddd, *J* = 13.3, 9.4, 4.5 Hz, 1H), 1.79 (tq, *J* = 12.2, 4.2 Hz, 1H), 1.72 (t, *J* = 4.5 Hz, 1H), 1.62 (dd, *J* = 4.3, 2.1 Hz, 1H), 1.41 (s, 9H), 1.29 (ddd, *J* = 12.2, 9.5, 4.4 Hz, 1H), 1.09 (dd, *J* = 13.8, 3.5 Hz, 1H),

0.94 (s, 3H), 0.89 (d, $J = 3.3$ Hz, 6H). ^{13}C NMR (126 MHz, CDCl_3) δ 166.18, 155.66, 136.05, 133.46, 131.72, 130.24, 129.03, 127.36, 80.86, 79.55, 49.09, 47.89, 44.94, 39.48, 36.85, 34.00, 28.34, 28.07, 27.39, 19.70, 18.90, 13.62. HRMS TOF MS ES^+ m/z calcd for $\text{C}_{24}\text{H}_{35}\text{NO}_4\text{S Na}$ $[\text{M}+\text{Na}]^+$: 456.2184; found: 456.2180.

2-(4-((5-Chlorobenzo[d]oxazol-2-yl)thio)phenoxy)-1-cyclopentylethan-1-one (27)

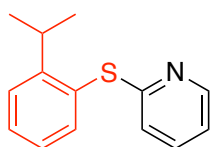


To a 1 dram microwave reaction vial with a magnetic stir bar was added $\text{Ni}(\text{Phen})_2\text{Br}_2$ (2.2 mg, 0.0038 mmol, 0.03 equiv), Zn nanopowder (2.0 mg, 0.0313 mmol, 0.25 equiv), Cs_2CO_3 (48.9 mg, 0.15 mmol, 1.2 equiv) 5-chlorobenzo[d]oxazole-2-thiol (24.4 mg, 0.1313 mmol, 1.05 equiv) and 1-cyclopentyl-2-(4-iodophenoxy)ethan-1-one (41.3 mg, 0.125 mmol, 1 equiv). The vial was capped with a rubber septum and then evacuated and backfilled with argon three times. Next, 0.25 mL 2 wt % TPGS-750-M aqueous solution and 25 μL EtOAc were added via a syringe through the septum. The solution was heated at 45 $^\circ\text{C}$ and stirred vigorously for 15 h. After the reaction, to the vial was added approximately 1 mL of EtOAc and silica gel. The mixture was concentrated under reduced pressure to obtain product-loaded silica, which was then used for flash chromatography using EtOAc/hexanes as eluent.

White solid, yield 42.9 mg (89%) $R_f = 0.21$ (50% EtOAc/hexanes). ^1H NMR (500 MHz, CDCl_3) δ 7.84 – 7.77 (m, 2H), 7.72 (d, $J = 2.3$ Hz, 1H), 7.52 – 7.42 (m, 2H), 7.37 (dt, $J = 8.7, 2.3$ Hz, 1H), 7.25 – 7.19 (m, 2H), 4.85 (d, $J = 2.1$ Hz, 2H), 3.71 (qd, $J = 6.6, 2.0$ Hz,

4H), 2.18 (dq, $J = 13.6, 7.9, 6.8, 2.2$ Hz, 2H), 2.06 (pd, $J = 6.8, 2.1$ Hz, 2H), 1.82 (d, $J = 2.3$ Hz, 1H). ^{13}C NMR (126 MHz, CDCl_3) δ 165.97, 165.81, 159.82, 150.43, 143.11, 136.80, 129.83, 124.23, 118.91, 117.59, 116.05, 110.60, 67.86, 46.24, 45.98, 26.24, 23.80. HRMS TOF MS ES⁺ m/z calcd for $\text{C}_{19}\text{H}_{17}\text{N}_2\text{O}_3\text{S Na}$ $[\text{M}+\text{Na}]^+$: 411.0546; found: 411.0537.

2-((2-Isopropylphenyl)thio)pyridine (28)

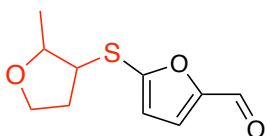


To a 1 dram microwave reaction vial with a magnetic stir bar was added $\text{Ni}(\text{Phen})_2\text{Br}_2$ (4.3 mg, 0.0075 mmol, 0.03 equiv), Zn nanopowder (4.1 mg, 0.063 mmol, 0.25 equiv) and Cs_2CO_3 (97.8 mg, 0.3 mmol, 1.2 equiv). The vial was capped with a rubber septum and then evacuated and backfilled with argon three times. Next, 2-bromopyridine (39.5 mg, 0.25 mmol, 1 equiv), 2-isopropylthiophenol (40.0 mg, 0.2625 mmol, 1.05 equiv) and 0.5 mL 2 wt % TPGS-750-M aqueous solution were added via a syringe through the septum. The solution was heated at 55 °C and stirred vigorously for 24 h. After the reaction, to the vial was added approximately 1 mL of EtOAc and silica gel. The mixture was concentrated under reduced pressure to obtain product-loaded silica, which was then used for flash chromatography using EtOAc/hexanes as eluent.

*When KO^tBu was used as base, and with 1.4 mol % $\text{Ni}(\text{Phen})_2\text{Br}_2$, yield was 24.1 mg (42%).

Colorless oil, yield 42.2 mg (74%) $R_f = 0.43$ (20% EtOAc/hexanes). $^1\text{H NMR}$ (500 MHz, CDCl_3) δ 8.43 (d, $J = 4.9$ Hz, 1H), 7.62 (d, $J = 7.7$ Hz, 1H), 7.46 (s, 1H), 7.44 (d, $J = 13.6$ Hz, 2H), 7.29 – 7.24 (m, 1H), 6.98 (dd, $J = 7.4, 4.9$ Hz, 1H), 6.71 (d, $J = 8.1$ Hz, 1H), 3.61 (hept, $J = 7.0$ Hz, 1H), 1.20 (d, $J = 6.9$ Hz, 6H). $^{13}\text{C NMR}$ (126 MHz, CDCl_3) δ 162.35, 152.86, 149.43, 137.11, 136.61, 130.33, 128.79, 126.91, 126.68, 120.49, 119.43, 30.97, 23.73. **HRMS** TOF MS Cl^+ m/z calcd for $\text{C}_{14}\text{H}_{15}\text{NS}$ H $[\text{M}+\text{H}]^+$: 230.1003; found: 230.1001.

(±)5-((2-Methyltetrahydrofuran-3-yl)thio)furan-2-carbaldehyde (29)



To a 1 dram microwave reaction vial with a magnetic stir bar was added added $\text{Ni}(\text{Phen})_2\text{Br}_2$ (4.3 mg, 0.0075 mmol, 0.03 equiv), Zn nanopowder (4.1 mg, 0.063 mmol, 0.25 equiv), Cs_2CO_3 (97.8 mg, 0.3 mmol, 1.2 equiv) and 5-bromo-2-furaldehyde (43.8 mg, 0.25 mmol, 1 equiv). The vial was capped with a rubber septum and then evacuated and backfilled with argon three times. Next, 2-methyl-3-tetrahydrofuranthiol (mixture of *cis* and *trans*) (31.0 mg, 0.263 mmol, 1.05 equiv) and 0.5 mL 2 wt % TPGS-750-M aqueous solution was added via a syringe through the septum. The solution was heated at 45 °C and stirred vigorously for 24 h. After the reaction, to the vial was added approximately 1 mL of EtOAc and silica gel. The mixture was concentrated under reduced pressure to obtain product-loaded silica, which was then used for flash chromatography using 20%-40% EtOAc/hexanes as eluent. Two products, *cis* and *trans* were yielded (42.2 mg, 74%).

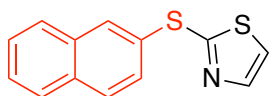
Yellow oil, $R_f = 0.47$ (50% EtOAc/hexanes).

$^1\text{H NMR}$ (500 MHz, CDCl_3) δ 9.55 (s, 1H), 7.19 (d, $J = 3.5$ Hz, 1H), 6.58 (d, $J = 3.6$ Hz, 1H), 3.95 (ddd, $J = 8.7, 7.7, 5.0$ Hz, 1H), 3.85 – 3.77 (m, 2H), 3.34 (dt, $J = 8.5, 6.5$ Hz, 1H), 2.42 (dq, $J = 13.1, 7.8$ Hz, 1H), 2.02 – 1.92 (m, 1H), 1.25 (d, $J = 6.2$ Hz, 3H). $^{13}\text{C NMR}$ (126 MHz, CDCl_3) δ 176.58, 154.47, 153.76, 121.77, 116.74, 80.53, 66.50, 51.16, 33.79, 19.35. **HRMS** TOF MS ES^+ m/z calcd for $\text{C}_{10}\text{H}_{12}\text{O}_3\text{S}$ $[\text{M}+\text{Na}]^+$: 235.0405; found: 235.0406.

Yellow oil, $R_f = 0.37$ (50% EtOAc/hexanes).

$^1\text{H NMR}$ (500 MHz, CDCl_3) δ 9.51 (s, 1H), 7.19 (d, $J = 3.6$ Hz, 1H), 6.52 (d, $J = 3.6$ Hz, 1H), 4.15 (qd, $J = 6.3, 5.0$ Hz, 1H), 4.04 – 3.95 (m, 2H), 3.76 (td, $J = 8.5, 6.1$ Hz, 1H), 2.43 (dddd, $J = 13.3, 8.4, 7.3, 6.1$ Hz, 1H), 2.05 (dddd, $J = 13.9, 8.1, 6.1, 4.5$ Hz, 1H), 1.30 (d, $J = 6.3$ Hz, 3H), 0.86 (t, $J = 7.0$ Hz, 1H). $^{13}\text{C NMR}$ (126 MHz, CDCl_3) δ 175.23, 155.01, 154.19, 123.87, 115.12, 77.09, 65.85, 50.43, 33.92, 16.57. **HRMS** TOF MS ES^+ m/z calcd for $\text{C}_{10}\text{H}_{12}\text{O}_3\text{S}$ $[\text{M}]^+$: 212.0507; found: 212.0515.

2-(Naphthalen-2-ylthio)thiazole (30)

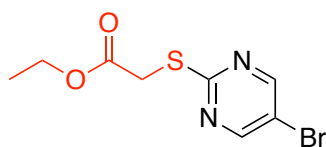


To a 1 dram microwave reaction vial with a magnetic stir bar was added $\text{Ni}(\text{Phen})_2\text{Br}_2$ (1.5 mg, 0.003 mmol, 0.01 equiv), Zn nanopowder (4.1 mg, 0.063 mmol, 0.25 equiv) Cs_2CO_3 (97.8 mg, 0.3 mmol, 1.2 equiv) and naphthalene-2-thiol (42.1 mg, 0.263 mmol, 1.05 equiv). The vial was capped with a rubber septum and then evacuated and backfilled with argon

three times. Next, 2-bromothiazole (20.5 mg, 0.25 mmol, 1 equiv), and 0.25 mL 2 wt % TPGS-750-M aqueous solution and 25 μ L EtOAc were added via a syringe through the septum. The solution was heated at 45 $^{\circ}$ C and stirred vigorously for 24 h. After the reaction, to the vial was added approximately 1 mL of EtOAc and silica gel. The mixture was concentrated under reduced pressure to obtain product-loaded silica, which was then used for flash chromatography using EtOAc/hexanes as eluent.

Brown crystalline solid, yield 32.9 mg (54%), $R_f = 0.33$ (10% EtOAc/hexanes). $^1\text{H NMR}$ (500 MHz, CDCl_3) δ 8.13 (d, $J = 2.0$ Hz, 1H), 7.84 (ddd, $J = 11.8, 9.1, 4.5$ Hz, 3H), 7.71 (d, $J = 3.2$ Hz, 1H), 7.61 (dd, $J = 8.6, 1.9$ Hz, 1H), 7.52 (dd, $J = 6.6, 2.9$ Hz, 2H), 7.20 (d, $J = 3.3$ Hz, 1H). $^{13}\text{C NMR}$ (126 MHz, CDCl_3) δ 165.93, 143.44, 133.73, 133.44, 133.31, 130.07, 129.55, 128.97, 127.95, 127.82, 127.29, 126.87, 120.47. **HRMS** TOF MS EI^+ m/z calcd for $\text{C}_{13}\text{H}_8\text{NS}_2$ $[\text{M}-\text{H}]^+$: 242.0098; found: 242.0099; m/z calcd for $\text{C}_{13}\text{H}_9\text{NS}_2$ $(\text{M})^+$: 243.0176; found: 243.0164.

Ethyl 2-((5-bromopyrimidin-2-yl)thio)acetate (31)

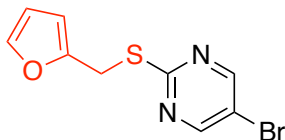


To a 1 dram microwave reaction vial with a magnetic stir bar was added added $\text{Ni}(\text{Phen})_2\text{Br}_2$ (1.16 mg, 0.002 mmol, 0.01 equiv), Zn nanopowder (3.3 mg, 0.05 mmol, 0.25 equiv), Cs_2CO_3 (78.2 mg, 0.24 mmol, 1.2 equiv) and 2,5-dibromopyrimidine (47.6 mg, 0.2 mmol, 1 equiv). The vial was capped with a rubber septum and then evacuated and backfilled with argon three times. Next, ethyl 2-mercaptoacetate (25.2 mg, 0.21 mmol, 1.05

equiv) and 0.4 mL 2 wt % TPGS-750-M aqueous solution was added via a syringe through the septum. The solution was heated at 45 °C and stirred vigorously for 17 h. After the reaction, to the vial was added approximately 1 mL of EtOAc and silica gel. The mixture was concentrated under reduced pressure to obtain product-loaded silica, which was then used for flash chromatography using 0-20% EtOAc/hexanes as eluent.

Colorless liquid, yield 30.2 mg (55%), $R_f = 0.33$ (20% EtOAc/hexanes). $^1\text{H NMR}$ (500 MHz, CDCl_3) δ 8.53 (s, 1H), 4.19 (q, $J = 7.1$ Hz, 1H), 3.88 (s, 1H), 1.25 (t, $J = 7.1$ Hz, 2H). $^{13}\text{C NMR}$ (126 MHz, CDCl_3) δ 169.06, 168.80, 157.77, 115.46, 61.77, 33.72, 14.14. **HRMS** TOF MS ES^+ m/z calcd for $\text{C}_8\text{H}_9\text{BrN}_2\text{O}_2\text{S Na}$ $[\text{M}+\text{Na}]^+$: 298.9466; found: 298.9469.

5-Bromo-2-((furan-2-ylmethyl)thio)pyrimidine (32)

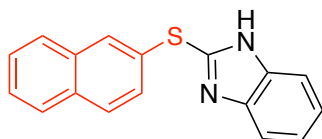


To a 1 dram microwave reaction vial with a magnetic stir bar was added added $\text{Ni}(\text{Phen})_2\text{Br}_2$ (1.45 mg, 0.003 mmol, 0.01 equiv), Zn nanopowder (4.1 mg, 0.063 mmol, 0.25 equiv), Cs_2CO_3 (97.8 mg, 0.3 mmol, 1.2 equiv) and 2,5-dibromopyrimidine (59.5 mg, 0.25 mmol, 1 equiv). The vial was capped with a rubber septum and then evacuated and backfilled with argon three times. Next, furan-2-ylmethanethiol (30.0 mg, 0.2625 mmol, 1.05 equiv) and 0.25 mL 2 wt % TPGS-750-M aqueous solution were added via a syringe through the septum. The solution was heated at 55 °C and stirred vigorously for 24 h. After the reaction, to the vial was added approximately 1 mL of EtOAc and silica gel. The

mixture was concentrated under reduced pressure to obtain product-loaded silica, which was then used for flash chromatography using 0-20% EtOAc/hexanes as eluent.

Yellow oil, yield 57.4 mg (85%), $R_f = 0.12$ (hexanes). $^1\text{H NMR}$ (500 MHz, CDCl_3) δ 8.55 (s, 2H), 7.36 – 7.28 (m, 1H), 6.30 – 6.23 (m, 2H), 4.39 (s, 2H). $^{13}\text{C NMR}$ (126 MHz, CDCl_3) δ 169.65, 157.74, 150.37, 142.22, 115.16, 110.49, 108.05, 28.02. **HRMS** TOF MS EI^+ m/z calcd for $\text{C}_9\text{H}_7\text{BrN}_2\text{OS}$ $[\text{M}]^+$: 269.9463; found: 269.9462.

2-(Naphthalen-2-ylthio)-1H-benzo[d]imidazole (33)

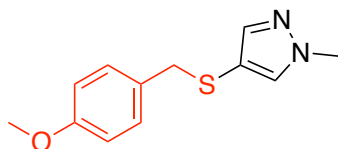


To a 1 dram microwave reaction vial with a magnetic stir bar was added added $\text{Ni}(\text{Phen})_2\text{Br}_2$ (2.17 mg, 0.004 mmol, 0.03 equiv), Zn nanopowder (2.0 mg, 0.031 mmol, 0.25 equiv), Cs_2CO_3 (48.9 mg, 0.15 mmol, 1.2 equiv) and 2-bromo-1H-benzimidazole (20.5 mg, 0.125 mmol, 1 equiv). The vial was capped with a rubber septum and then evacuated and backfilled with argon three times. Next, 2-naphthalenethiol (21.0 mg, 0.13 mmol, 1.05 equiv) and 0.25 mL 2 wt % TPGS-750-M aqueous solution was added via a syringe through the septum. The solution was heated at 45 °C and stirred vigorously for 24 h. After the reaction, to the vial was added approximately 1 mL of EtOAc and silica gel. The mixture was concentrated under reduced pressure to obtain product-loaded silica, which was then used for flash chromatography using EtOAc/hexanes as eluent.

White solid, yield 30.1 mg (99%), $R_f = 0.33$ (30% EtOAc/hexanes). $^1\text{H NMR}$ (500 MHz, CDCl_3) δ 9.15 (s, 1H), 8.10 (d, $J = 1.8$ Hz, 1H), 7.82 (d, $J = 8.4$ Hz, 2H), 7.79 – 7.75 (m,

1H), 7.66 (s, 1H), 7.53 (dtd, $J = 14.8, 7.9, 7.3, 3.7$ Hz, 3H), 7.26 (s, 1H), 7.20 – 7.15 (m, 2H). ^{13}C NMR (126 MHz, CDCl_3) δ 148.74, 133.72, 133.15, 133.13, 129.82, 129.79, 127.83, 127.80, 127.34, 127.09, 126.94. HRMS TOF MS ES^+ m/z calcd for $\text{C}_{17}\text{H}_{12}\text{N}_2\text{S Na}$ $[\text{M}+\text{Na}]^+$: 299.0610; found: 299.0622.

4-((4-Methoxybenzyl)thio)-1-methyl-1H-pyrazole (34)

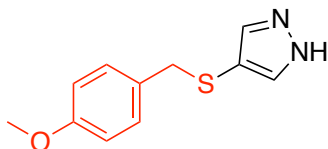


To a 1 dram microwave reaction vial with a magnetic stir bar was added $\text{Ni}(\text{Phen})_2\text{Br}_2$ (2.0 mg, 0.0034 mmol, 0.014 equiv), Zn nanopowder (4.1 mg, 0.063 mmol, 0.25 equiv), Cs_2CO_3 (97.8 mg, 0.3 mmol, 1.2 equiv) and 4-iodo-1-methyl-1H-pyrazole (48.5 mg, 0.25 mmol, 1 equiv). The vial was capped with a rubber septum and then evacuated and backfilled with argon three times. Next, 4-methoxybenzylthiol (40.5 mg, 0.2625 mmol, 1.05 equiv) and 0.5 mL 2 wt % TPGS-750-M aqueous solution was added via a syringe through the septum. The solution was heated at 55 °C and stirred vigorously for 23 h. After the reaction, to the vial was added approximately 1 mL of EtOAc and silica gel. The mixture was concentrated under reduced pressure to obtain product-loaded silica, which was then used for flash chromatography using EtOAc /hexanes as eluent.

Brown crystalline solid, yield 53.6 mg (91%), $R_f = 0.35$ (50% EtOAc/hexanes). ^1H NMR (500 MHz, CDCl_3) δ 7.32 (s, 1H), 7.17 (s, 1H), 7.04 (d, $J = 8.1$ Hz, 2H), 6.78 (d, $J = 8.0$ Hz, 2H), 3.80 (s, 3H), 3.77 (s, 3H), 3.72 (s, 2H). ^{13}C NMR (126 MHz, CDCl_3) δ 158.63, 143.96, 134.63, 130.45, 130.06, 113.67, 110.10, 55.22, 41.56, 39.06. HRMS TOF MS ES^+

m/z calcd for $C_{12}H_{14}N_2OS$ H $[M+H]^+$: 235.0905; found: 235.0912. The spectral data matched that from a previous report.¹⁴

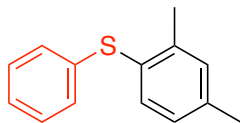
4-((4-Methoxybenzyl)thio)-1*H*-pyrazole (35)



To a 1 dram microwave reaction vial with a magnetic stir bar was added $Ni(Phen)_2Br_2$ (2.0 mg, 0.0034 mmol, 0.014 equiv), Zn nanopowder (4.1 mg, 0.063 mmol, 0.25 equiv), Cs_2CO_3 (97.8 mg, 0.3 mmol, 1.2 equiv) and 4-iodo-1*H*-pyrazole (48.5 mg, 0.25 mmol, 1 equiv). The vial was capped with a rubber septum and then evacuated and backfilled with argon three times. Next, 4-methoxybenzylthiol (40.5 mg, 0.263 mmol, 1.05 equiv) and 0.5 mL 2 wt % TPGS-750-M aqueous solution was added via a syringe through the septum. The solution was heated at 55 °C and stirred vigorously for 23 h. After the reaction, to the vial was added approximately 1 mL of EtOAc and silica gel. The mixture was concentrated under reduced pressure to obtain product-loaded silica, which was then used for flash chromatography using EtOAc/hexanes as eluent.

White solid, yield 29.6 mg (54%), $R_f = 0.29$ (20% EtOAc/hexanes). **1H NMR** (500 MHz, $CDCl_3$) δ 7.37 (s, 2H), 7.03 (d, $J = 8.1$ Hz, 2H), 6.78 (d, $J = 8.1$ Hz, 2H), 6.44 (s, 1H), 3.77 (s, 3H), 3.74 (s, 2H). **^{13}C NMR** (126 MHz, $CDCl_3$) δ 158.69, 138.31, 130.28, 130.11, 113.73, 109.75, 55.24, 41.29. **HRMS** TOF MS ES^+ m/z calcd for $C_{11}H_{12}N_2OS$ H $[M+H]^+$: 221.0749; found: 299.0752.

(2,4-Dimethylphenyl)(phenyl)sulfane (36)

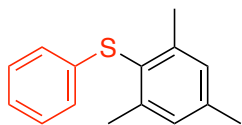


To a 1 dram microwave reaction vial with a magnetic stir bar was added Ni(Phen)₂Br₂ (1.0 mg, 0.002 mmol, 0.007 equiv), Zn nanopowder (4.1 mg, 0.063 mmol, 0.25 equiv) and Cs₂CO₃ (97.8 mg, 0.3 mmol, 1.2 equiv). The vial was capped with a rubber septum and then evacuated and backfilled with argon three times. Next, 2,4-dimethyliodobenzene (58.1 mg, 0.25 mmol, 1 equiv), thiophenol (41.3 mg, 0.375 mmol, 1.5 equiv) and 0.5 mL 2 wt % TPGS-750-M aqueous solution were added via a syringe through the septum. The solution was heated at 45 °C and stirred vigorously for 18 h. After the reaction, to the vial was added approximately 1 mL of EtOAc and silica gel. The mixture was concentrated under reduced pressure to obtain product-loaded silica, which was then used for flash chromatography using hexanes as eluent.

*When K₃PO₄ was used as base, the yield is also 84%.

Colorless liquid, yield 45.1 mg (84%) R_f = 0.49 (hexanes). ¹H NMR (500 MHz, CDCl₃) δ 7.28 (d, *J* = 7.8 Hz, 1H), 7.26 – 7.19 (m, 2H), 7.12 (dddd, *J* = 11.0, 9.6, 8.1, 1.6 Hz, 4H), 6.98 (dd, *J* = 7.9, 2.0 Hz, 1H), 2.33 (d, *J* = 4.7 Hz, 6H). ¹³C NMR (126 MHz, CDCl₃) δ 140.83, 138.54, 137.34, 134.42, 131.57, 131.32, 129.26, 128.96, 128.28, 127.56, 127.14, 125.67, 21.08, 20.57. HRMS TOF MS EI⁺ *m/z* calcd for C₁₄H₁₄S [M]⁺: 214.0816; found: 214.0820.

Mesityl(phenyl)sulfane (37)

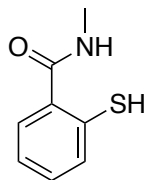


To a 1 dram microwave reaction vial with a magnetic stir bar was added Ni(Phen)₂Br₂ (1.0 mg, 0.002 mmol, 0.007 equiv), Zn nanopowder (4.1 mg, 0.063 mmol, 0.25 equiv) and K₃PO₄ (63.7 mg, 0.3 mmol, 1.2 equiv) and 2,4,6-trimethyliodobenzene (61.5 mg, 0.25 mmol, 1 equiv). The vial was capped with a rubber septum and then evacuated and backfilled with argon three times. Next, thiophenol (41.3 mg, 0.38 mmol, 1.5 equiv) and 0.5 mL 2 wt % TPGS-750-M aqueous solution were added via a syringe through the septum. The solution was heated at 45 °C and stirred vigorously for 18 h. After the reaction, to the vial was added approximately 1 mL of EtOAc and silica gel. The mixture was concentrated under reduced pressure to obtain product-loaded silica, which was then used for flash chromatography using EtOAc/hexanes as eluent.

*When Cs₂CO₃ was used as base, no reaction took place.

Colorless liquid, yield 23.3 mg (41%) R_f = 0.83 (hexanes). ¹H NMR (500 MHz, CDCl₃) δ 7.18 – 7.12 (m, 2H), 7.05 – 7.01 (m, 1H), 6.99 (s, 2H), 6.93 – 6.88 (m, 2H), 2.37 (s, 6H), 2.31 (s, 3H). ¹³C NMR (126 MHz, CDCl₃) δ 143.71, 139.25, 138.38, 129.51, 129.30, 129.05, 128.83, 127.50, 127.14, 126.93, 125.44, 124.44, 21.68, 21.11. HRMS TOF MS CI⁺ *m/z* calcd for C₁₅H₁₆S H [M+H]⁺: 229.1051; found: 218.9856.

2-Mercapto-*N*-methylbenzamide (39)*

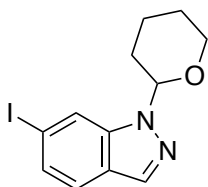


To a 25 mL round bottom flask with a magnetic stir bar was added 2,2'-disulfanediylbis(*N*-methylbenzamide) (100.0 mg, 0.3 mmol, 1.0 equiv) and THF (3 mL). Then, NaBH₄ (34.0 mg, 0.9 mmol, 3 equiv) was added and stirred at rt, under Ar. The reaction was monitored by TLC. After the reaction is finished, 1% CH₃COOH/THF was added to quench residual NaBH₄. Then the reaction was evaporated to dryness and purified by flash chromatography using a 40-100% EtOAc/hexanes gradient.

*This product must be stored under Ar.

White solid, yield 89.4 mg (89%), R_f = 0.50 (80% EtOAc/hexanes). ¹H NMR (500 MHz, CDCl₃) δ 7.41 (dd, *J* = 7.6, 1.5 Hz, 1H), 7.31 (dd, *J* = 7.8, 1.3 Hz, 1H), 7.25 – 7.21 (m, 2H), 7.12 (td, *J* = 7.5, 1.3 Hz, 1H), 4.76 (s, 1H), 3.00 (d, *J* = 4.9 Hz, 3H). ¹³C NMR (126 MHz, CDCl₃) δ 130.99, 130.55, 127.79, 125.15, 26.78. The NMR data match that reported previously.³³

6-Iodo-1-(tetrahydro-2*H*-pyran-2-yl)-1*H*-indazole (40)

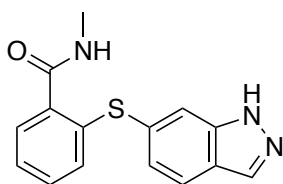


To a 25 mL round bottom flask with a magnetic stir bar was added 6-iodoindazole (927.4 mg, 3.8 mmol, 1.0 equiv), DCM (4.5 mL), and THF (3.4 mL). Then, dihydropyran (799.1

mg, 0.9 mmol, 3 equiv) was added. MsOH (54.7 mg, 0.57 mmol, 0.15 equiv) was added slowly at 0 °C. After addition, the reaction was allowed to warm to rt. The reaction was monitored by TLC. After the reaction was complete, the solvents were evaporated to dryness. The crude material was purified by flash chromatography using 10–20% EtOAc/hexanes as eluent.

White solid, yield 0.9513 g (76%), $R_f = 0.29$ (10% EtOAc/hexanes). $^1\text{H NMR}$ (500 MHz, CDCl_3) δ 7.99 (q, $J = 1.0$ Hz, 1H), 7.95 (d, $J = 0.9$ Hz, 1H), 7.43 (t, $J = 1.3$ Hz, 2H), 5.64 (dd, $J = 9.4, 2.8$ Hz, 1H), 4.01 (ddd, $J = 11.6, 4.0, 2.0$ Hz, 1H), 3.73 (ddd, $J = 11.6, 10.4, 2.8$ Hz, 1H), 2.51 (ddd, $J = 11.2, 4.1, 1.9$ Hz, 1H), 2.13 (ddd, $J = 9.2, 4.4, 1.6$ Hz, 1H), 2.08 – 2.00 (m, 1H), 1.74 (ddt, $J = 12.8, 9.6, 3.6$ Hz, 2H), 1.65 (ddt, $J = 6.8, 3.4, 1.6$ Hz, 1H). $^{13}\text{C NMR}$ (126 MHz, CDCl_3) δ 140.58, 133.99, 130.16, 123.94, 122.26, 119.38, 92.45, 85.46, 67.49, 29.36, 25.03, 22.47. **HRMS** TOF MS Cl^+ m/z calcd for $\text{C}_{12}\text{H}_{13}\text{IN}_2\text{O Na}$ $[\text{M}+\text{Na}]^+$: 350.9970; found: 350.9971.

2-((1*H*-Indazol-6-yl)thio)-*N*-methylbenzamide (41)



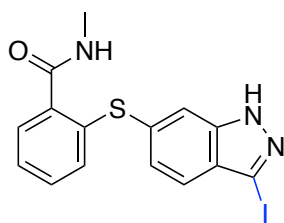
To a 25 mL round bottom flask with a magnetic stir bar was added added $\text{Ni}(\text{Phen})_2\text{Br}_2$ (127.0 mg, 0.219 mmol, 0.034 equiv), Zn nanopowder (2.0 mg, 0.031 mmol, 0.25 equiv), K_3PO_4 (1.6200 g, 7.63 mmol, 1.2 equiv), 2-mercapto-*N*-methylbenzamide (1.1168 g, 6.678 mmol, 1.05 equiv) and 6-iodo-1-(tetrahydro-2*H*-pyran-2-yl)-1*H*-indazole (2.0870 g, 6.678 mmol, 1 equiv). The flask was capped with a rubber septum and then evacuated and

backfilled with argon three times. Next, acetone (3.1 mL) and 31.8 mL 2 wt % TPGS-750-M aqueous solution were added via a syringe through the septum. The solution was heated at 55 °C and stirred vigorously for 24 h. The reaction progress was checked by TLC (product $R_f = 0.39$; 80% EtOAc/hexanes).

After the reaction was complete, the vial was extracted with DCM (20 mL x 3; the product is not very soluble in EtOAc.) The DCM layers were collected and the solvent evaporated under reduced pressure. Methanol (50 mL) and 1 M HCl (50 mL) were then added. The reaction was heated to 60 °C. After the reaction was complete the mixture was concentrated under reduced pressure. The reaction was extracted with DCM (30 mL x 3). The collected organic phases were dried over anhydrous Na_2SO_4 and then purified via flash chromatography using 70–80% EtOAc/hexanes as eluent.

White solid, yield 1.3233 g (70%), $R_f = 0.21$ (80% EtOAc/hexanes). $^1\text{H NMR}$ (500 MHz, CDCl_3) δ 8.01 (s, 1H), 7.68 – 7.61 (m, 2H), 7.56 (dd, $J = 7.0, 2.2$ Hz, 1H), 7.20 (td, $J = 7.7, 4.2$ Hz, 2H), 7.11 (t, $J = 8.1$ Hz, 2H), 6.41 (d, $J = 6.4$ Hz, 1H), 2.94 (d, $J = 4.8$ Hz, 3H). $^{13}\text{C NMR}$ (126 MHz, CDCl_3) δ 168.91, 140.66, 136.06, 135.05, 134.40, 132.75, 131.34, 130.82, 128.53, 126.79, 124.75, 122.58, 121.59, 113.96, 26.83. **HRMS** TOF MS Cl^+ m/z calcd for $\text{C}_{15}\text{H}_{13}\text{N}_3\text{OS Na}$ $[\text{M}+\text{Na}]^+$: 306.0677; found: 306.0681.

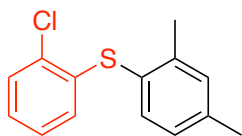
2-((3-Iodo-1*H*-indazol-6-yl)thio)-*N*-methylbenzamide (42)



To a 1 dram vial containing a magnetic stir bar was added added 2-((1*H*-indazol-6-yl)thio)-*N*-methylbenzamide (10.8 mg, 0.038 mmol, 1 equiv), KOH (6.4 g, 0.196 mmol, 5.2 equiv), iodine (38.6 mg, 0.152 mmol, 4 equiv), 15.2 μ L *N*-methyl-2-pyrrolidone (NMP), and 0.15 mL 2 wt % TPGS-750-M aqueous solution. The solution was heated at 60 °C and stirred vigorously overnight. The reaction progress was checked by TLC. Once complete. the reaction was quenched with Na₂S₂O₃ (aq) until the solution turned light yellow. It was then purified via flash chromatography using 60-90% EtOAc/hexanes as eluent.

Yellow solid, 10.3 mg (66%), $R_f = 0.39$ (80% EtOAc/hexanes). ¹H NMR (400 MHz, DMSO-*d*₆) δ 13.56 (s, 1H), 8.38 (d, $J = 8.1$ Hz, 1H), 7.56 (s, 1H), 7.51 – 7.41 (m, 2H), 7.30 (dt, $J = 8.6, 4.3$ Hz, 2H), 7.13 (d, $J = 8.0$ Hz, 1H), 7.05 – 6.98 (m, 1H), 2.75 (d, $J = 4.5$ Hz, 3H). ¹³C NMR (126 MHz, DMSO-*d*₆) δ 167.83, 140.87, 137.27, 135.15, 134.00, 130.35, 127.81, 126.39, 126.33, 125.45, 121.55, 114.24, 93.71, 28.10, 26.09. HRMS TOF MS CI⁺ m/z calcd for C₁₅H₁₂IN₃OS Na [M+Na]⁺: 431.9644; found: 431.9649.

(2-Chlorophenyl)(2,4-dimethylphenyl)sulfane (46)



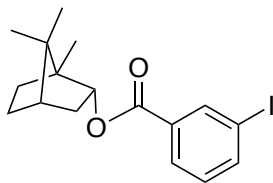
To a 1 dram microwave reaction vial with a magnetic stir bar was added Ni(Phen)₂Br₂ (1.0 mg, 0.002 mmol, 0.007 equiv), Zn nanopowder (4.1 mg, 0.063 mmol, 0.25 equiv), and Cs₂CO₃ (97.8 mg, 0.3 mmol, 1.2 equiv). The vial was capped with a rubber septum and then evacuated and backfilled with argon three times. Next, 4-iodo-*m*-xylene (58.0 mg, 0.25 mmol, 1 equiv), 2-chlorothiophenol (38.0 mg, 0.263 mmol, 1.05 equiv) and 0.5 mL 2

wt % TPGS-750-M aqueous solution was added via a syringe through the septum. The solution was heated at 55 °C and stirred vigorously for 20 h. After the reaction, the vial was added approximately 3 mL of MTBE to extract the product (repeated 3x), followed by the addition of silica gel to the extracts. The mixture was concentrated under reduced pressure to obtain product-loaded silica, which was then used for flash chromatography using hexanes as eluent.

Yellow oil, yield 44.2 mg (71%), $R_f = 0.63$ (10% EtOAc/hexanes).

$^1\text{H NMR}$ (500 MHz, CDCl_3) δ 7.37 (d, $J = 7.8$ Hz, 1H), 7.34-7.32 (m, 1H), 7.15 (m, 1H), 7.04- 6.99 (m, 3H), 6.60-6.58 (m, 1 H), 2.35 (s, 3H), 2.32 (s, 3H). **$^{13}\text{C NMR}$** (126 MHz, CDCl_3) δ 142.31, 139.80, 137.41, 136.08, 131.88, 131.39, 129.49, 127.97, 127.20, 127.04, 126.87, 125.92, 21.18, 20.47. **HRMS** TOF MS CI^+ m/z calcd for $\text{C}_{14}\text{H}_{13}\text{ClS H}$ $[\text{M}+\text{H}]^+$: 249.0505; found: 249.0509.

(1S,2R,4S)-1,7,7-Trimethylbicyclo[2.2.1]heptan-2-yl 3-iodobenzoate

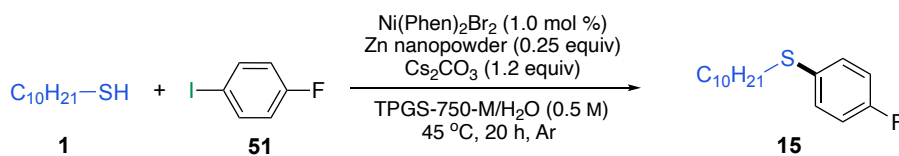


[(1S)-endo]-(-)-Borneol (277.7 mg, 1.8 mmol), DCC (557.1 mg, 2.7 mmol), TsOH (62.0 mg, 0.36 mmol), and DMAP (44.0 mg, 2.0 mmol) were dissolved in 25 mL of dry DCM in a 50 mL, two-necked flask under an atmosphere of dry argon. The solution was cooled to 0-5 °C with an ice-water bath, to which 446.5 mg of phenylpropionic acid (1.8 mmol) dissolved in 9 mL of DCM was added under stirring through a syringe. The reaction

mixture was stirred overnight. After filtering out the formed urea solid, the solution was concentrated using a rotary evaporator. The product was purified by silica gel column chromatography using 7% EtOAc/hexane as eluent.

Yield 527.0 mg (76%) $R_f = 0.56$ (10% EtOAc/hexanes). $^1\text{H NMR}$ (500 MHz, CDCl_3) δ 8.34 (s, 1H), 8.00 (d, $J = 7.8$ Hz, 1H), 7.87 (d, $J = 7.9$ Hz, 1H), 7.17 (t, $J = 7.9$ Hz, 1H), 5.09 (d, $J = 9.9$ Hz, 1H), 2.49 – 2.41 (m, 1H), 2.11 – 2.02 (m, 1H), 1.84 – 1.75 (m, 1H), 1.52 (s, 3H), 1.45 – 1.35 (m, 1H), 1.34 – 1.26 (m, 1H), 1.23 (s, 1H), 1.08 (dd, $J = 13.9, 3.4$ Hz, 1H), 0.96 – 0.87 (m, 6H). $^{13}\text{C NMR}$ (126 MHz, CDCl_3) δ 165.30, 141.59, 138.35, 132.79, 130.02, 128.67, 93.81, 81.08, 49.11, 47.92, 44.94, 36.83, 28.07, 27.38, 19.71, 18.90, 13.61. The spectral data matched that from a previous report.⁴³

1.9. Recycling procedures and E Factor calculations



	initial reaction	first recycle	second recycle	third recycle
isolated yield (%)	94	92	93	88
E Factor (organic solvent)	4.5	4.6	4.5	4.8
E Factor (including base and water)	5.4	5.5	5.5	13.8

Recycle procedures

Initial reaction. To a 1 dram microwave reaction vial with a magnetic stir bar was added $\text{Ni}(\text{Phen})_2\text{Br}_2$ (1.0 mg, 0.002 mmol, 0.007 equiv), Zn nanopowder (4.1 mg, 0.063 mmol, 0.25 equiv), and K_3PO_4 (63.7 mg, 0.6 mmol, 1.2 equiv). The vial was capped with a rubber

septum and then evacuated and backfilled with argon three times. Next, 1-decanethiol (45.8 mg, 0.2625 mmol, 1.05 equiv) and *p*-fluoroiodobenzene (55.5 mg, 0.25 mmol, 1 equiv) and 1 mL 2 wt % TPGS-750-M aqueous solution was added via a syringe through the septum. The solution was heated at 45 °C and stirred vigorously for 20 h. After the reaction, to the vial was added 0.4 mL of MTBE. With the aid of a centrifuge, the organic layer was separated. The organic layer was then evaporated to dryness and to yield the desired product (66.0 mg, 94%).

The 1st recycle. To a *new* 1 dram microwave reaction vial with a magnetic stir bar was added Ni(Phen)₂Br₂ (1.0 mg, 0.002 mmol, 0.007 equiv), Zn nanopowder (4.1 mg, 0.063 mmol, 0.25 equiv), and K₃PO₄ (63.7 mg, 0.6 mmol, 1.2 equiv). The vial was capped with a rubber septum and then evacuated and backfilled with argon three times. Next, 1-decanethiol (45.8 mg, 0.2625 mmol, 1.05 equiv) and *p*-fluoroiodobenzene (55.5 mg, 0.25 mmol, 1 equiv) and *the recovered* 0.5 mL 2 wt % TPGS-750-M aqueous solution *from the prior reaction* was added via a syringe through the septum. The solution was heated at 45 °C and stirred vigorously for 20 h. After the reaction, to the vial was added 0.4 mL of MTBE. With the aid of a centrifuge, the organic layer was separated. The organic layer was then evaporated to dryness and yield the desired product (65.0 mg, 92%).

Further recycling. The same procedure from the **1st recycle** was repeated for the **2nd recycle** (yield 65.6 mg, 93%) and the **3rd recycle** (yield 62.1 mg, 88%).

E Factor calculation

initial reaction calculations

extracted with MTBE 0.40 mL MTBE

66.0 mg product was isolated

Density of MTBE = 0.74 g/mL \rightarrow 0.40 mL = 296.0 mg MTBE

$(296.0 \text{ mg MTBE}) / 66.0 \text{ mg product} = 4.5$ E Factor counting only organic solvent.

$(296.0 \text{ mg MTBE} + 63.7 \text{ mg mg K}_3\text{PO}_4) / 66.0 \text{ mg product} = 5.4$ E Factor considering **base** as waste; **water was recycled**.

1st recycle calculations

$(296.0 \text{ mg MTBE}) / 65.0 \text{ mg product} = 4.6$ E Factor counting only organic solvent.

$(296.0 \text{ mg MTBE} + 63.7 \text{ mg K}_3\text{PO}_4) / 65.0 \text{ mg product} = 5.5$ E Factor considering **base** as waste; **water was recycled**.

2nd recycle calculations

$(296.0 \text{ mg MTBE}) / 65.6 \text{ mg product} = 4.5$ E Factor counting only organic solvent.

$(296.0 \text{ mg MTBE} + 63.7 \text{ mg K}_3\text{PO}_4) / 65.6 \text{ mg product} = 5.5$ E Factor considering **base** as waste; **water was recycled**.

3rd recycle calculations

$(296.0 \text{ mg MTBE}) / 62.1 \text{ mg product} = 4.8$ E Factor counting only organic solvent.

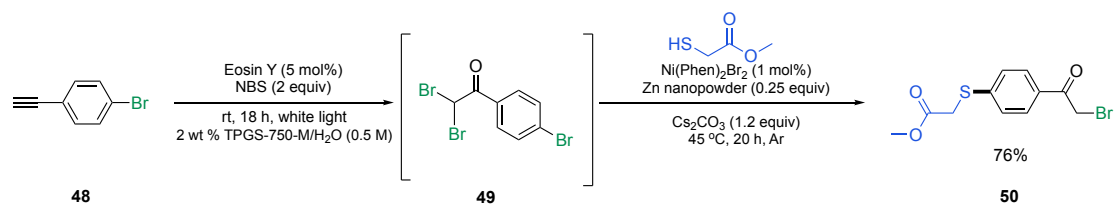
(296.0 mg MTBE + 500 mg TPGS-750-M solution + 63.7 mg K₃PO₄)/ 62.1 mg product
= 13.8 E Factor considering **base** and **water** as waste.

Average E Factor

(4.5+4.6+4.5+4.8)/4 = 4.6 avg. E Factor counting only organic solvent.

(6.4+6.5+6.4+13.8)/4 = 7.6 avg. E Factor considering **base** and **water** as waste.

1.10. One-pot sequence: procedures and characterizations

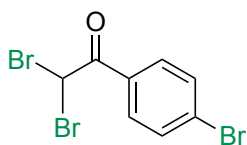


To a 1 dram microwave reaction vial with a magnetic stir bar was added NBS (2.0 equiv, 0.5 mmol, 99.0 mg), Eosin Y (5.0 mol %, 0.0125 mmol, 8.1 mg), and 4-bromophenylacetylene (1.0 equiv, 0.25 mmol, 45.3 mg) were sequentially added. The reaction vial was closed with a rubber septum and subsequently evacuated and backfilled with argon. Then, 0.5 mL 2 wt % TPGS-750-M aqueous solution was added via a syringe through the septum. The septum was wrapped with PTFE tape and black electrical tape. The reaction mixture was irradiated under a 13 W compact fluorescent bulb and allowed to stir at rt overnight.

Ni(Phen)₂Br₂ (1.5 mg, 0.002 mmol, 0.01 equiv), Zn nanopowder (4.1 mg, 0.063 mmol, 0.25 equiv), and Cs₂CO₃ (97.8 mg, 0.3 mmol, 1.2 equiv) were then added. The vial was capped with a rubber septum and then evacuated and backfilled with argon three times.

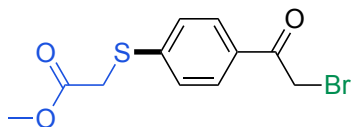
Next, methyl thioglycolate (27.9 mg, 0.2625 mmol, 1.05 equiv) and 0.5 mL 2 wt % TPGS-750-M aqueous solution was added via a syringe through the septum. The solution was heated at 45 °C and stirred vigorously for 20 h. After the reaction, the vial was added approximately 1 mL of EtOAc and silica gel. The mixture was concentrated under reduced pressure to obtain product-loaded silica, which was then used for flash chromatography using 5-25% EtOAc/hexanes as eluent.

2,2-Dibromo-1-(4-bromophenyl)ethan-1-one (49)



White solid, $R_f = 0.33$ (hexanes). $^1\text{H NMR}$ (600 MHz, CDCl_3) δ 7.99 – 7.95 (m, 2H), 7.68 – 7.63 (m, 2H), 6.60 (s, 1H). $^{13}\text{C NMR}$ (126 MHz, CDCl_3) δ 185.07, 133.24, 132.26, 131.20, 130.08, 129.87, 129.46, 65.82, 39.18. **HRMS** TOF MS ES^+ m/z calcd for $\text{C}_{17}\text{H}_{12}\text{N}_2\text{S Na [M+Na]}^+$: 299.0610; found: 299.0622.

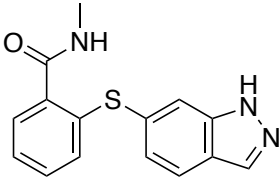
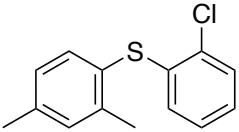
Methyl 2-((4-(2-bromoacetyl)phenyl)thio)acetate (50)



Yellow solid, yield 49.5 mg (76%), $R_f = 0.29$ (30% EtOAc/hexanes). $^1\text{H NMR}$ (500 MHz, CDCl_3) δ 7.81 (d, $J = 8.2$ Hz, 2H), 7.61 (d, $J = 7.8$ Hz, 2H), 3.96 (s, 2H), 3.71 (s, 3H), 3.31 (s, 2H). $^{13}\text{C NMR}$ (126 MHz, CDCl_3) δ 193.03, 170.17, 133.99, 132.08, 130.13, 128.85,

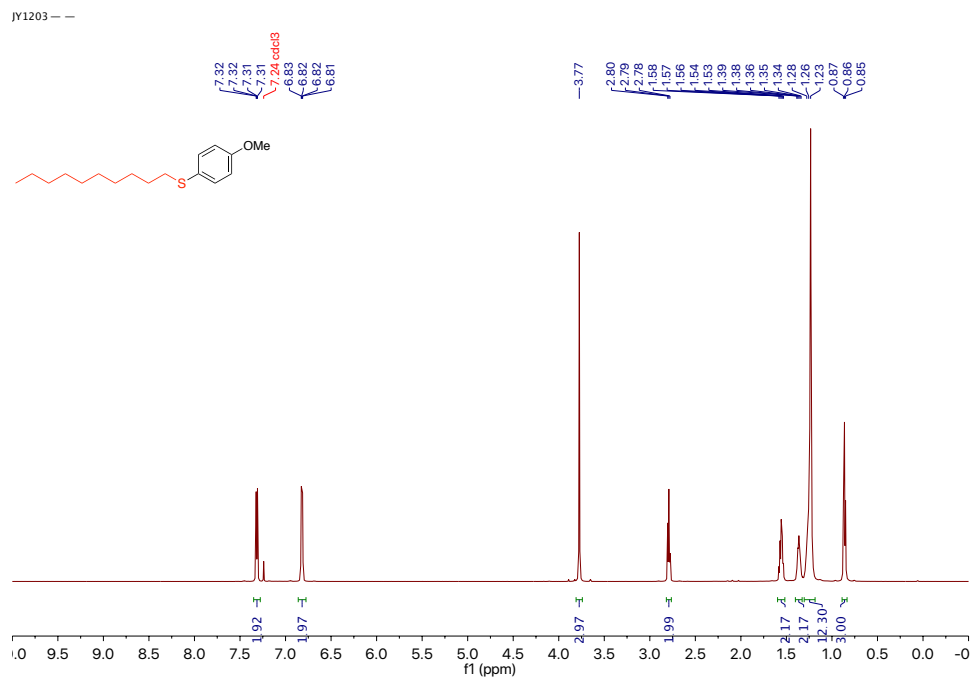
52.53, 37.55, 33.12. **HRMS** TOF MS ES⁺ *m/z* calcd for C₁₁H₁₁BrO₃S Na [M+Na]⁺:
324.9510; found: 324.9515.

1.11. ICP-MS data for residual Ni level detection

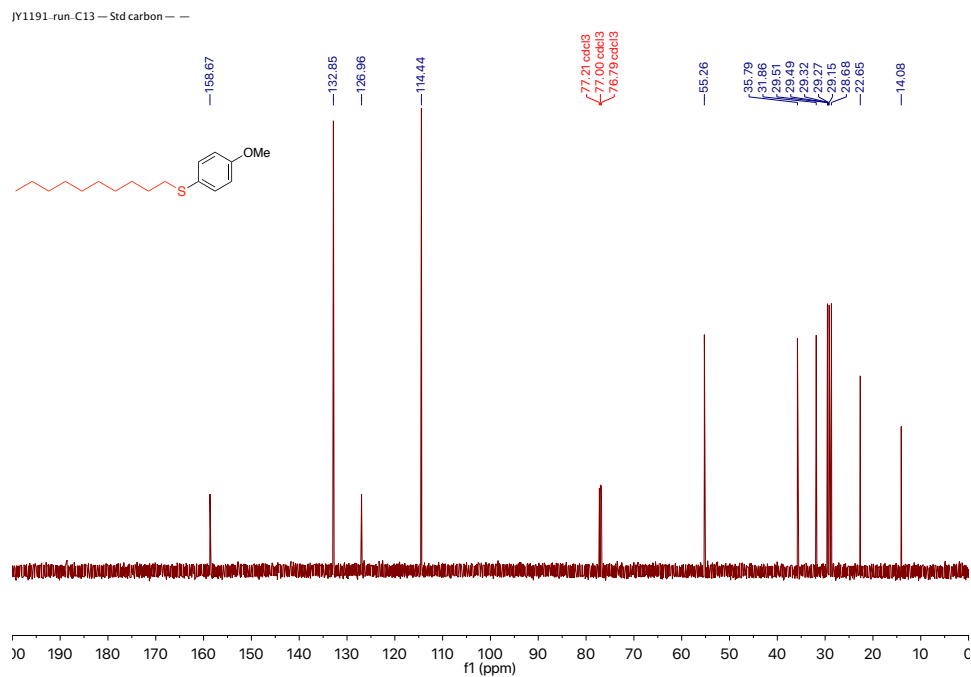
	average residual Ni in the product*	[Ni] used in the reaction
	9.82±0.13 µg/g	3.4 mol%
	1.03±0.10 µg/g	1.4 mol%

*Each measurement was done in triplicate, with background correction.

1.12. NMR spectra

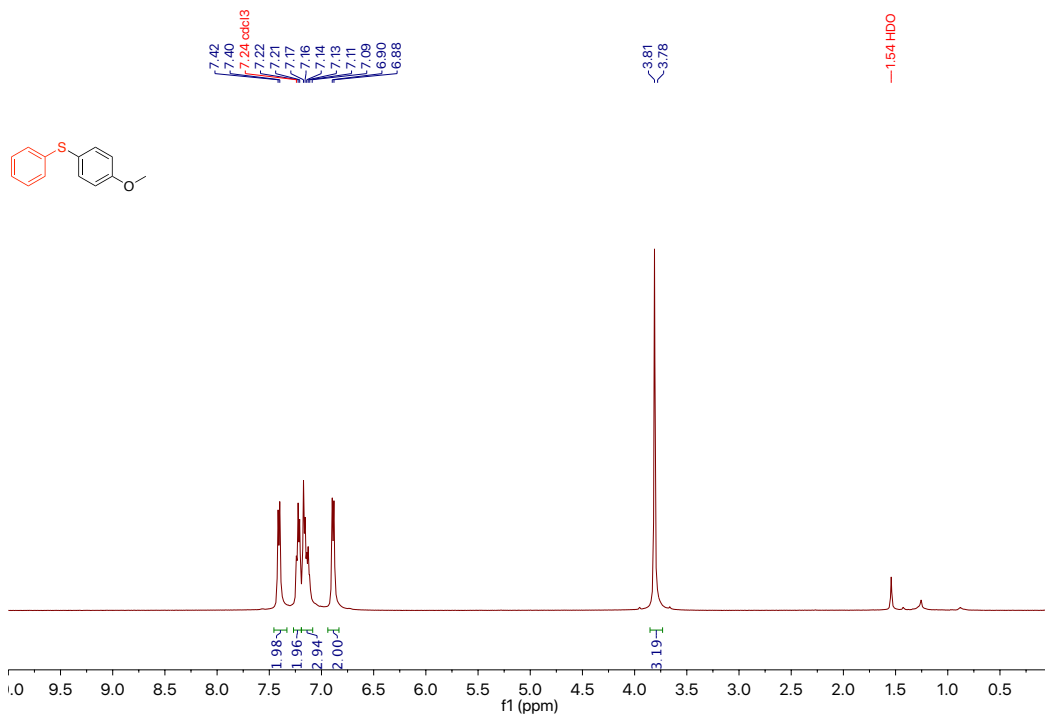


¹H NMR spectrum of decyl(4-methoxyphenyl)sulfane (3)



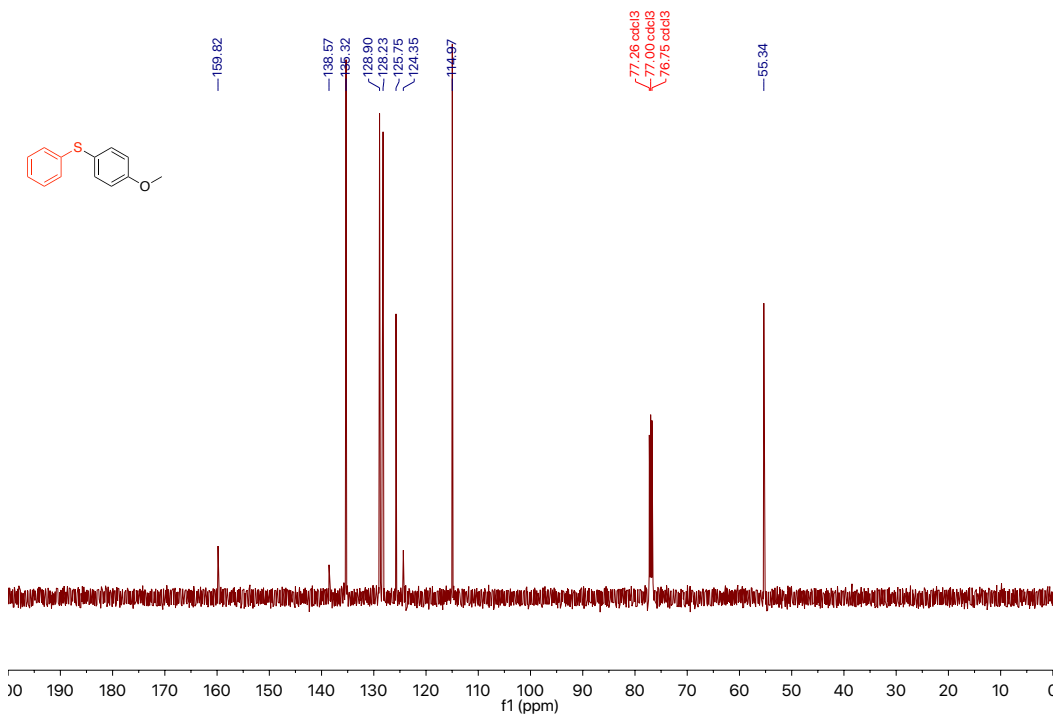
¹³C NMR spectrum of decyl(4-methoxyphenyl)sulfane (3)

JY1176-run8-10 --

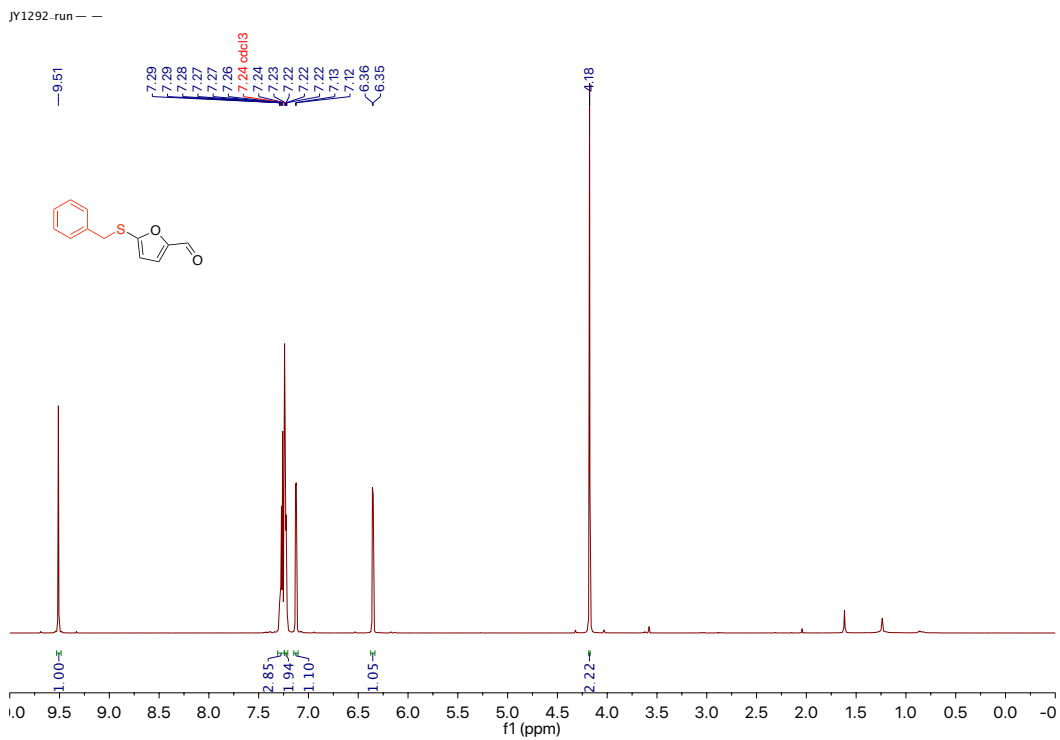


¹H NMR spectrum of (4-methoxyphenyl)(phenyl)sulfane (5)

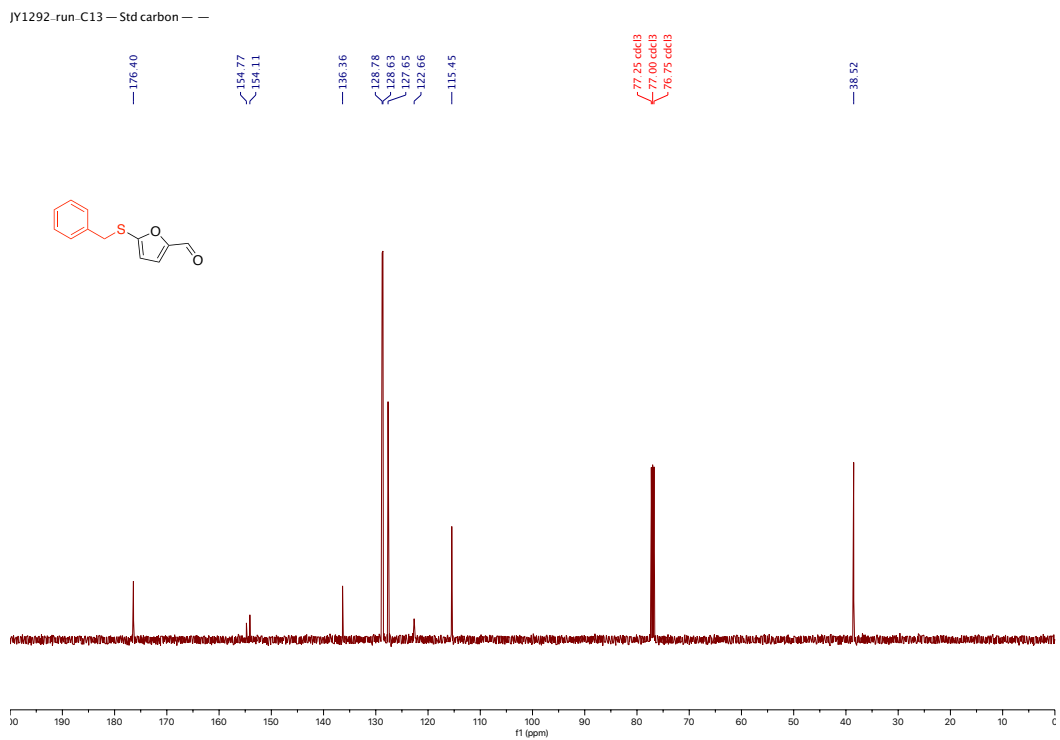
JY1176-run8-10.C13 -- Std carbon --



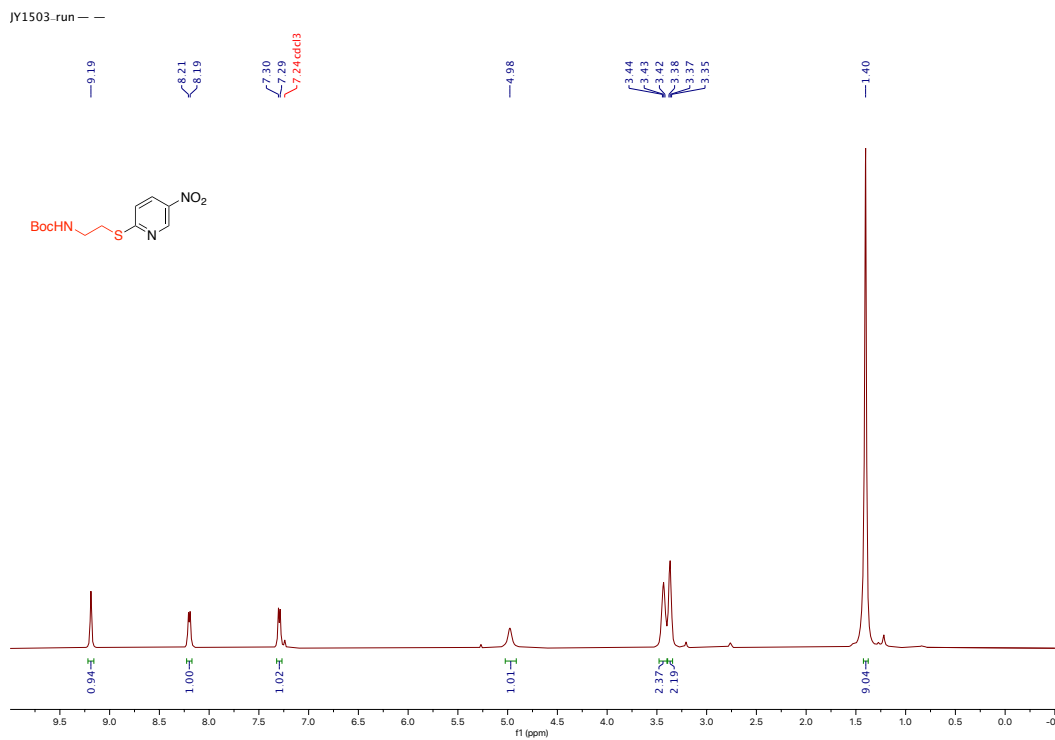
¹³C NMR spectrum of (4-methoxyphenyl)(phenyl)sulfane (5)



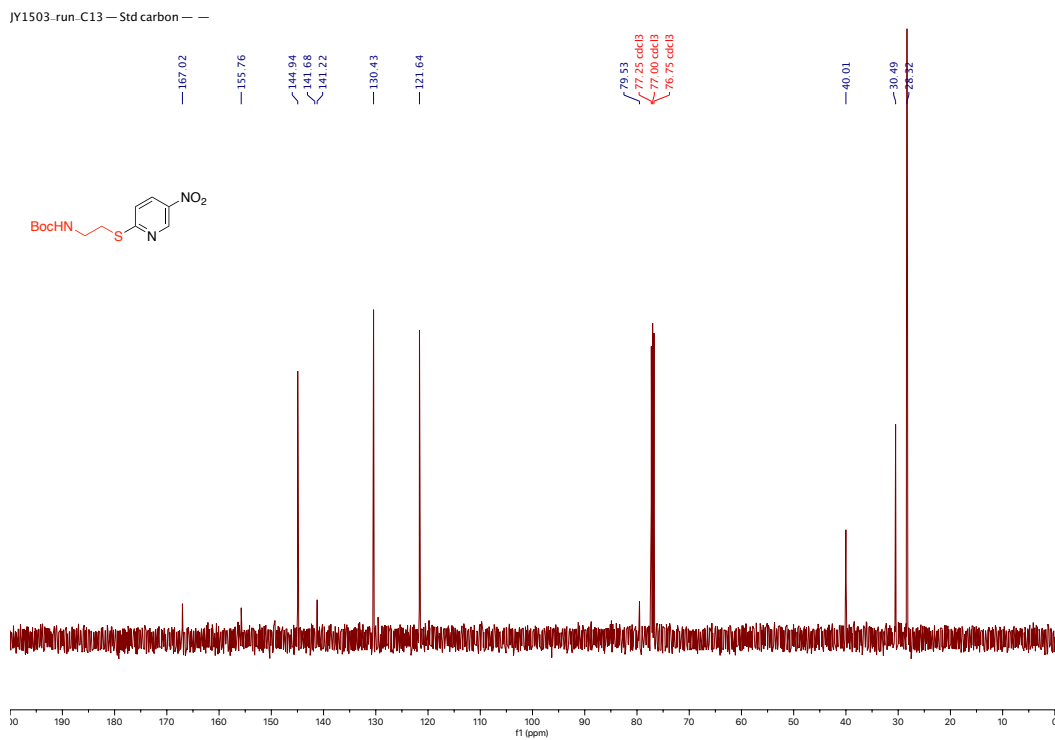
^1H NMR spectrum of 5-(benzylthio)furan-2-carbaldehyde (8)



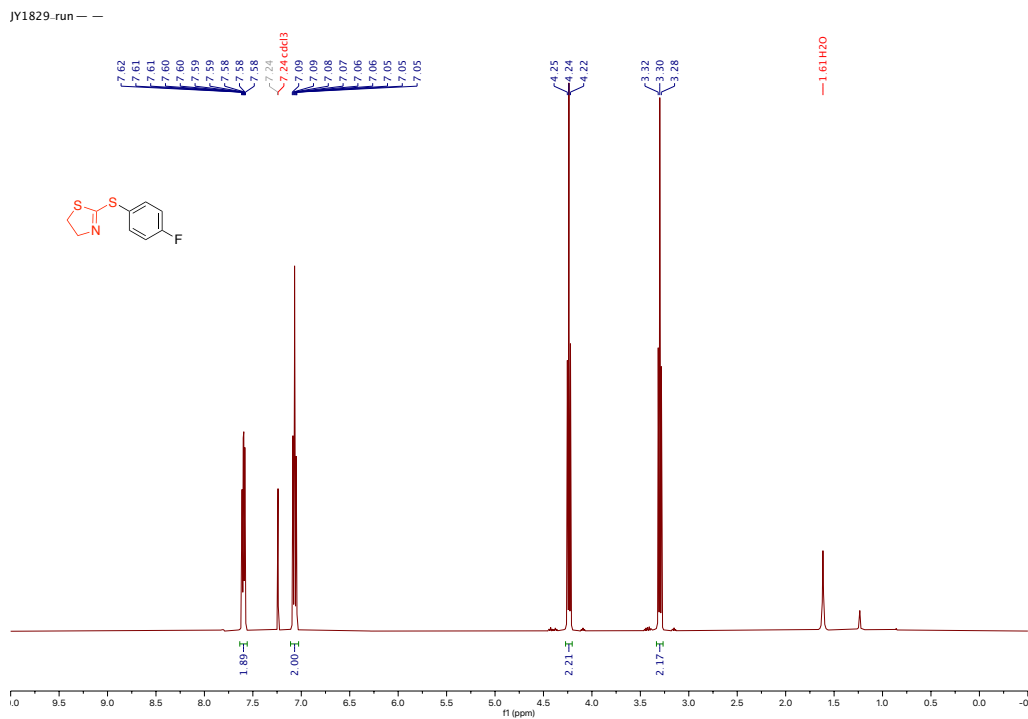
^{13}C NMR spectrum of 5-(benzylthio)furan-2-carbaldehyde (8)



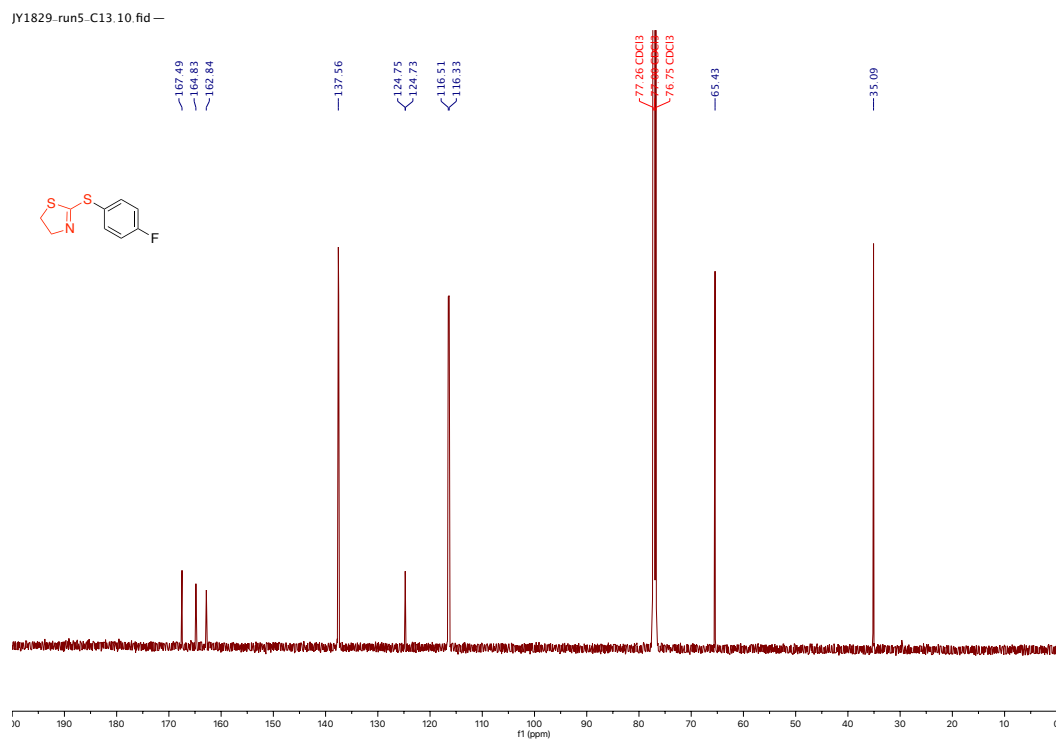
¹H NMR spectrum of *tert*-butyl (2-((5-nitropyridin-2-yl)thio)ethyl)carbamate (11)



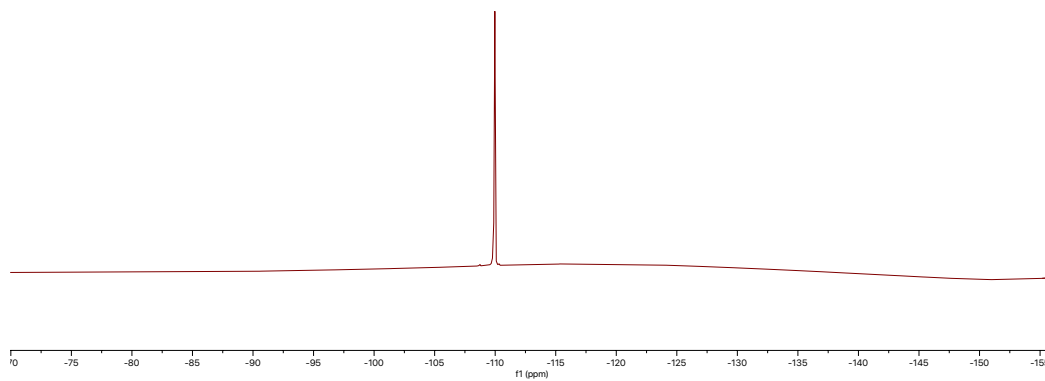
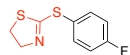
¹³C NMR spectrum of *tert*-butyl (2-((5-nitropyridin-2-yl)thio)ethyl)carbamate (11)



¹H NMR spectrum of 2-((4-fluorophenyl)thio)-4,5-dihydrothiazole (14)

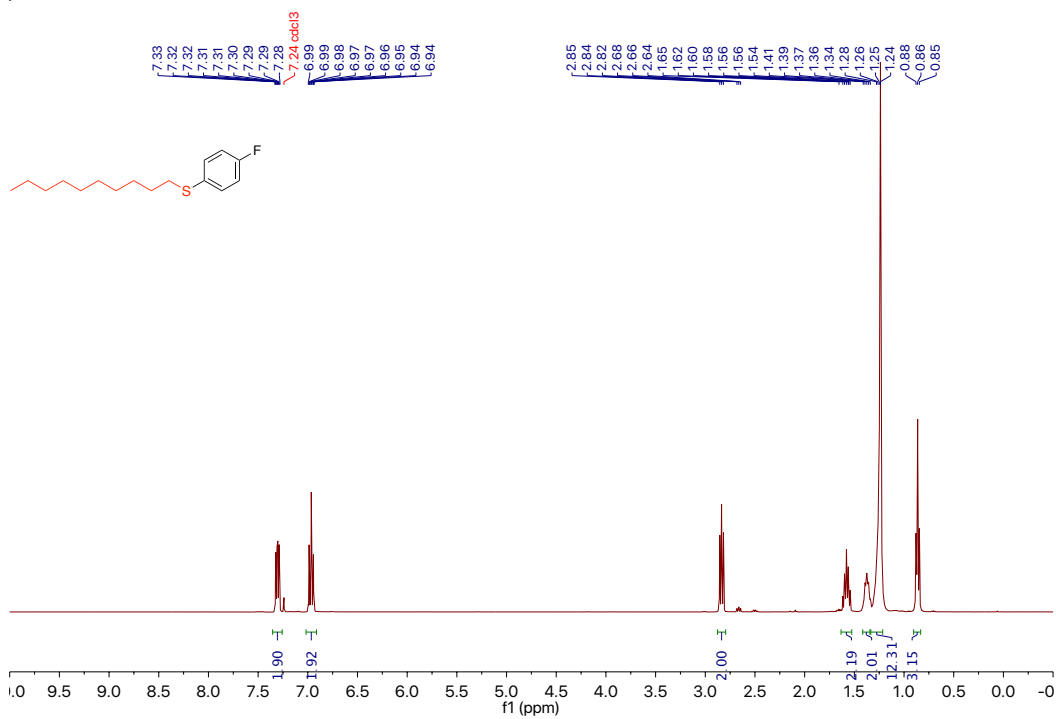


¹³C NMR spectrum of 2-((4-fluorophenyl)thio)-4,5-dihydrothiazole (14)



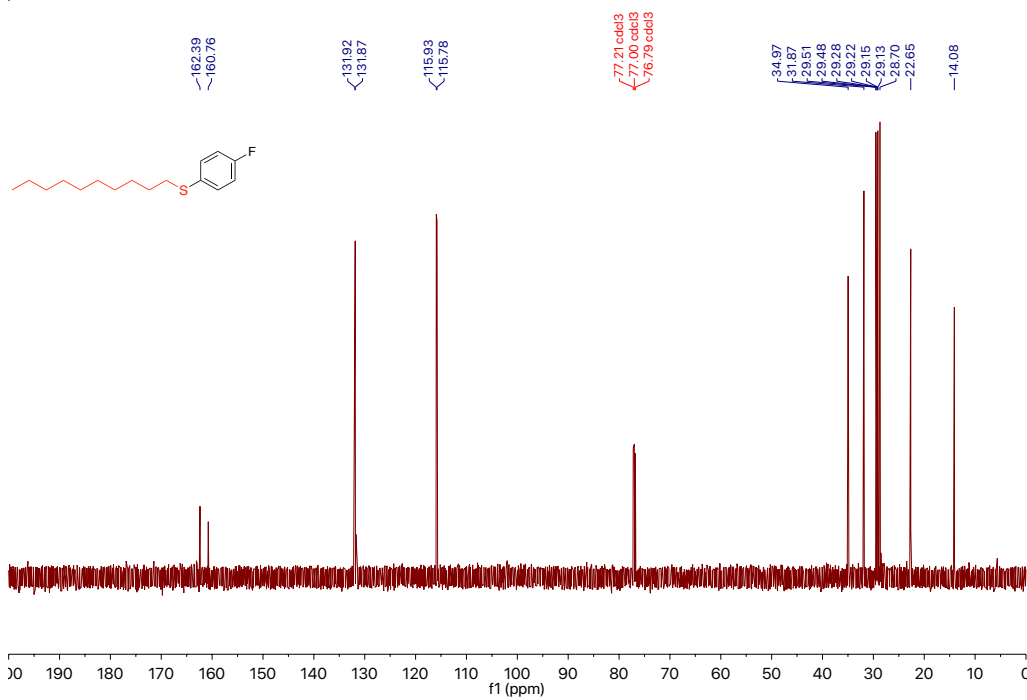
^{19}F NMR spectrum of 2-((4-fluorophenyl)thio)-4,5-dihydrothiazole (14)

JY1239.run.H1 --

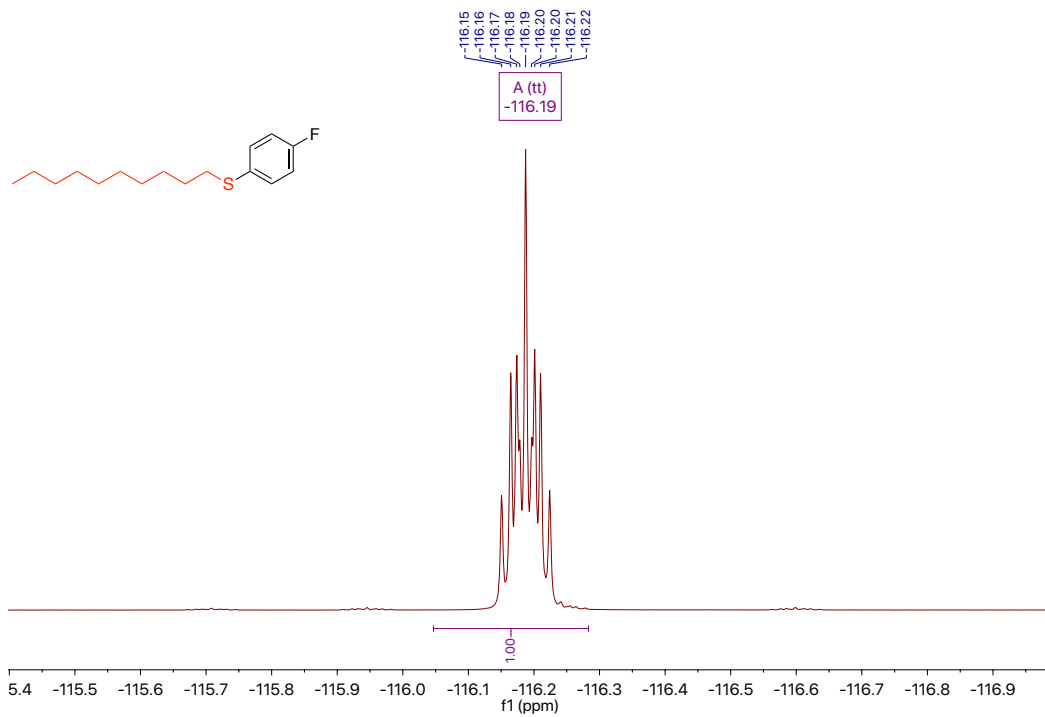


¹H NMR spectrum of decyl(4-fluorophenyl)sulfane (15)

JY1236.crude.C13 -- Std carbon --

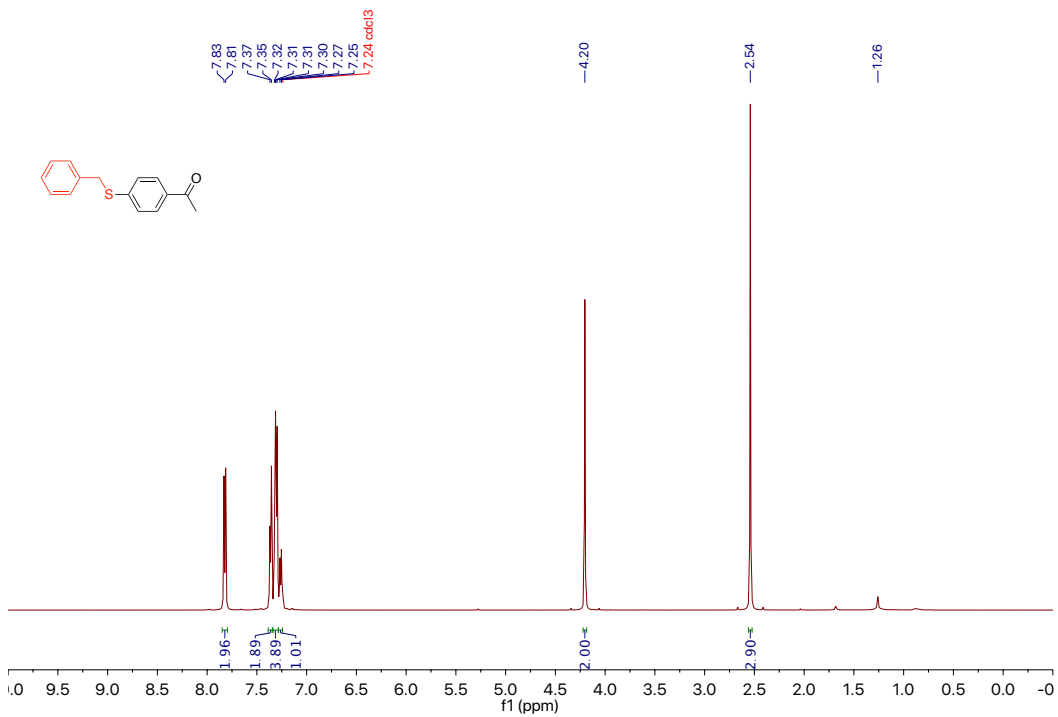


¹³C NMR spectrum of decyl(4-fluorophenyl)sulfane (15)



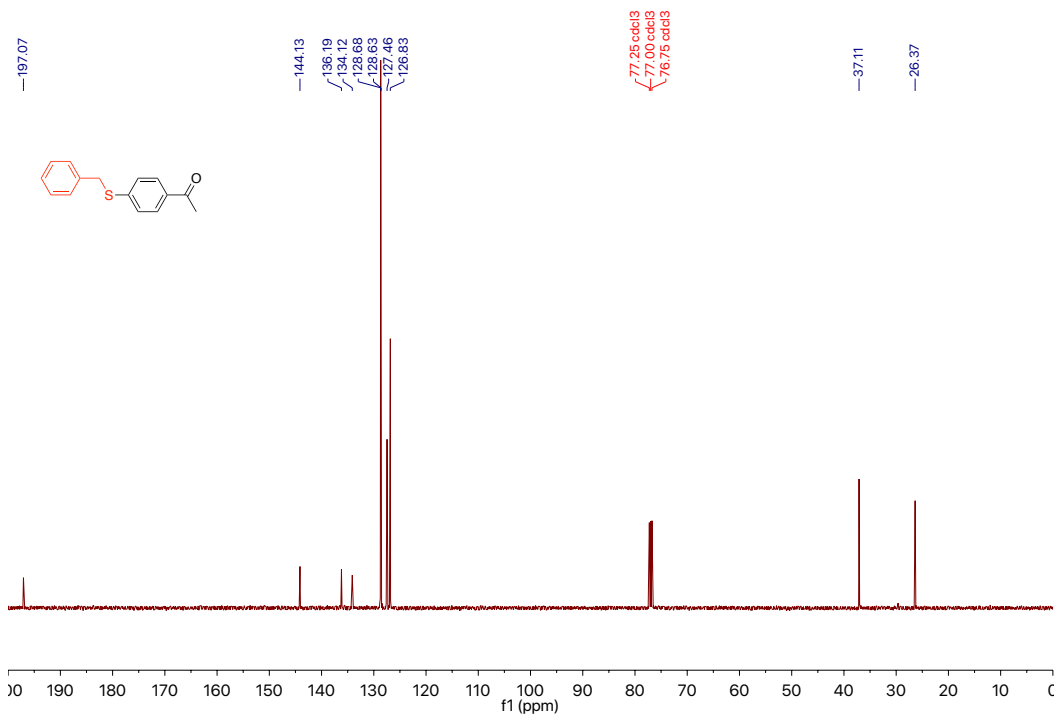
^{19}F NMR spectrum of decyl(4-fluorophenyl)sulfane (15)

JY1267.run --

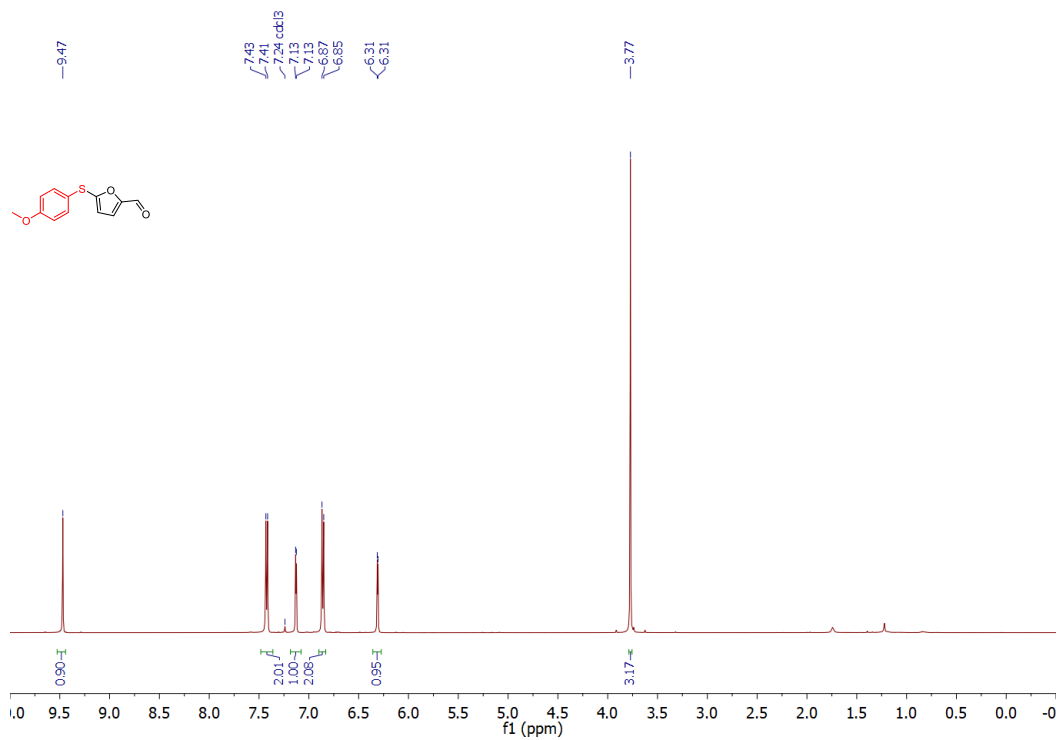


¹H NMR spectrum of 1-(4-(benzylthio)phenyl)ethan-1-one (16)

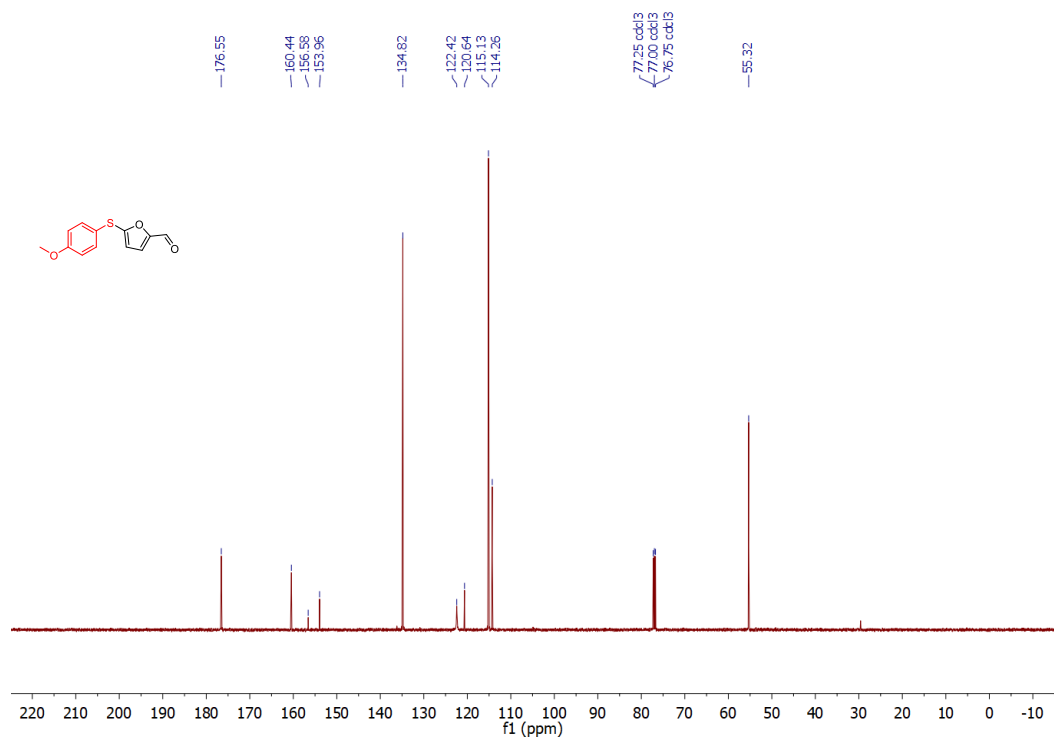
JY1267.run.C13—Std carbon --



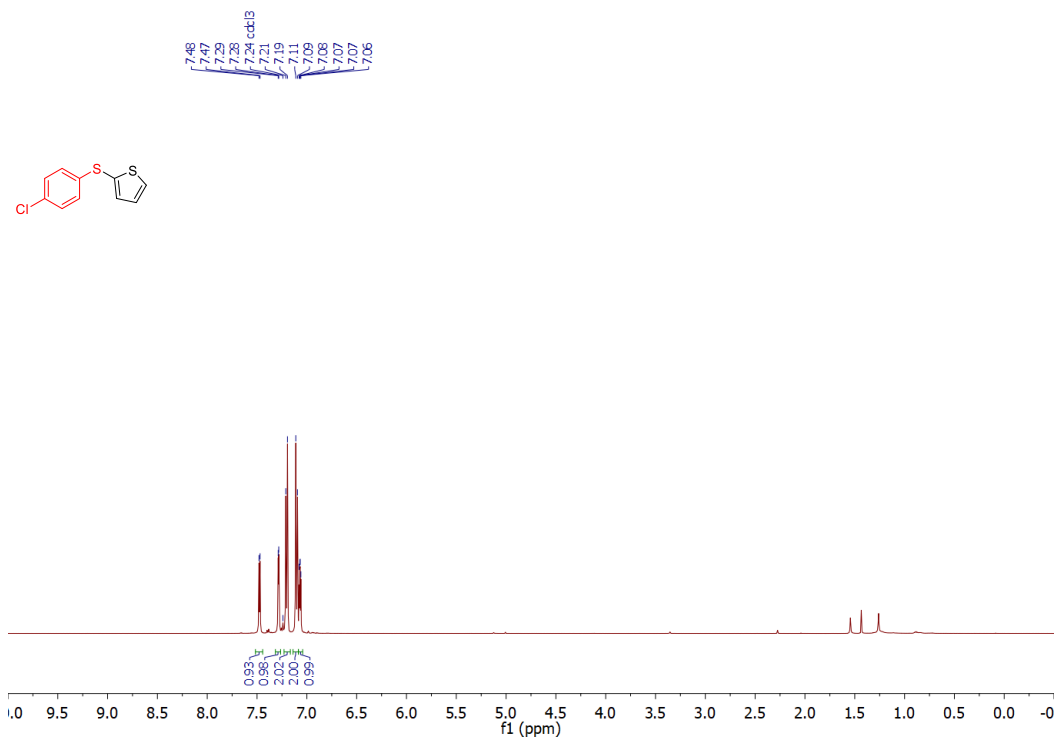
¹³C NMR spectrum of 1-(4-(benzylthio)phenyl)ethan-1-one (16)



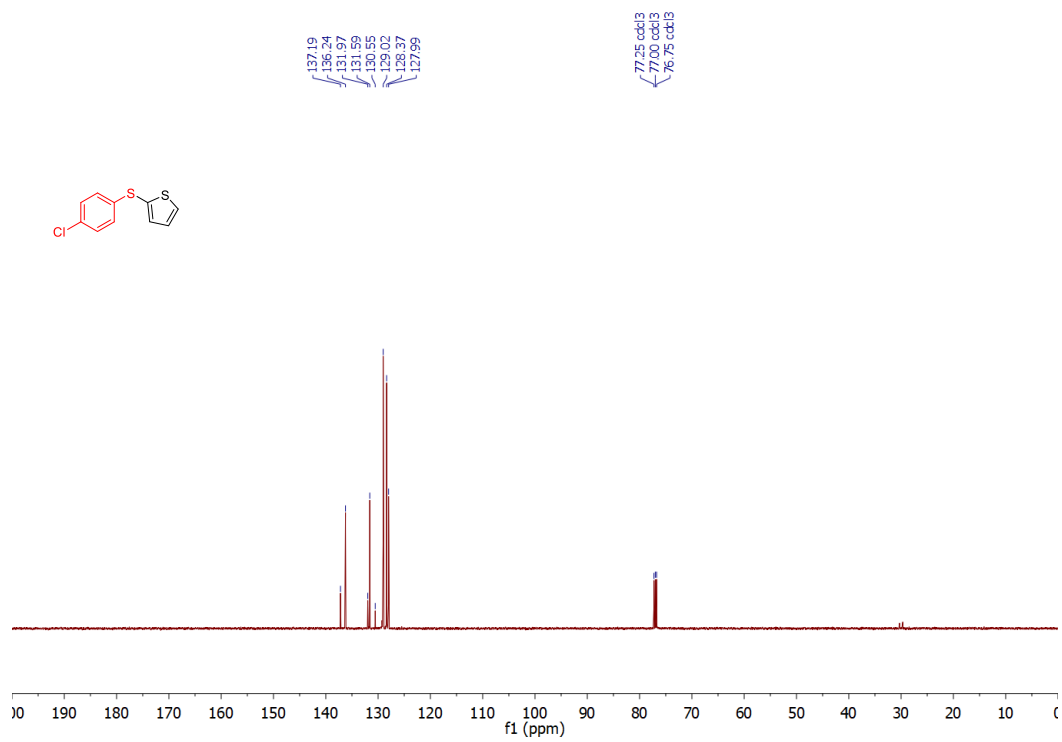
¹H NMR spectrum of 5-((4-methoxyphenyl)thio)furan-2-carbaldehyde (17)



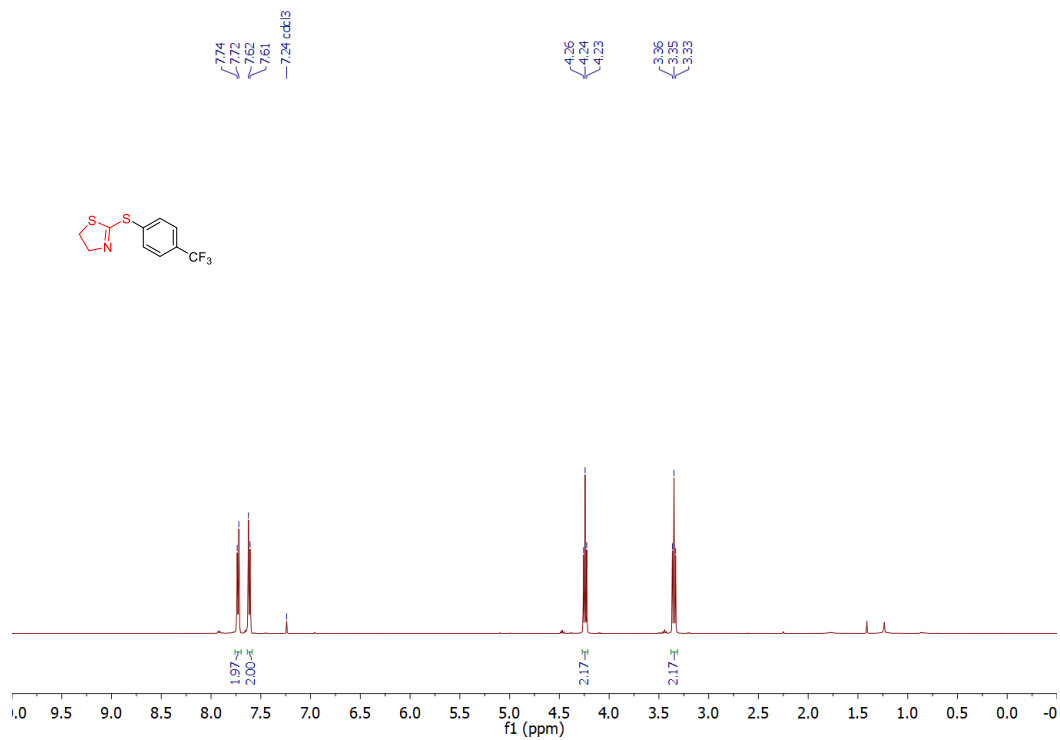
¹³C NMR spectrum of 5-((4-methoxyphenyl)thio)furan-2-carbaldehyde (17)



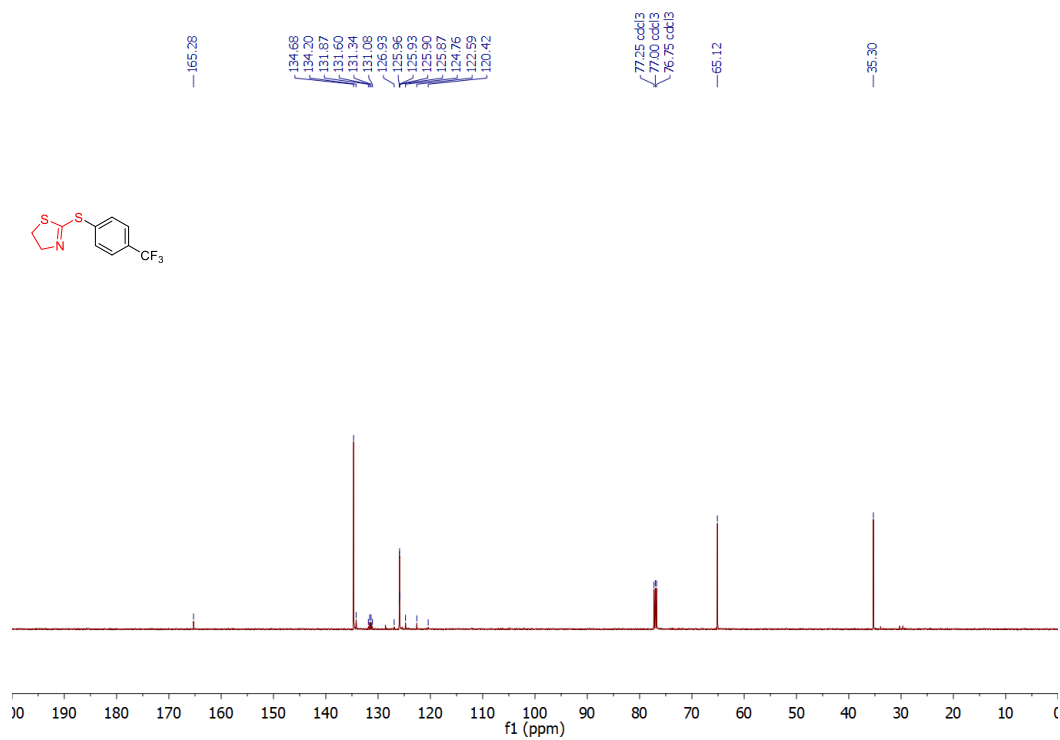
¹H NMR spectrum of 2-((4-chlorophenyl)thio)thiophene (18)



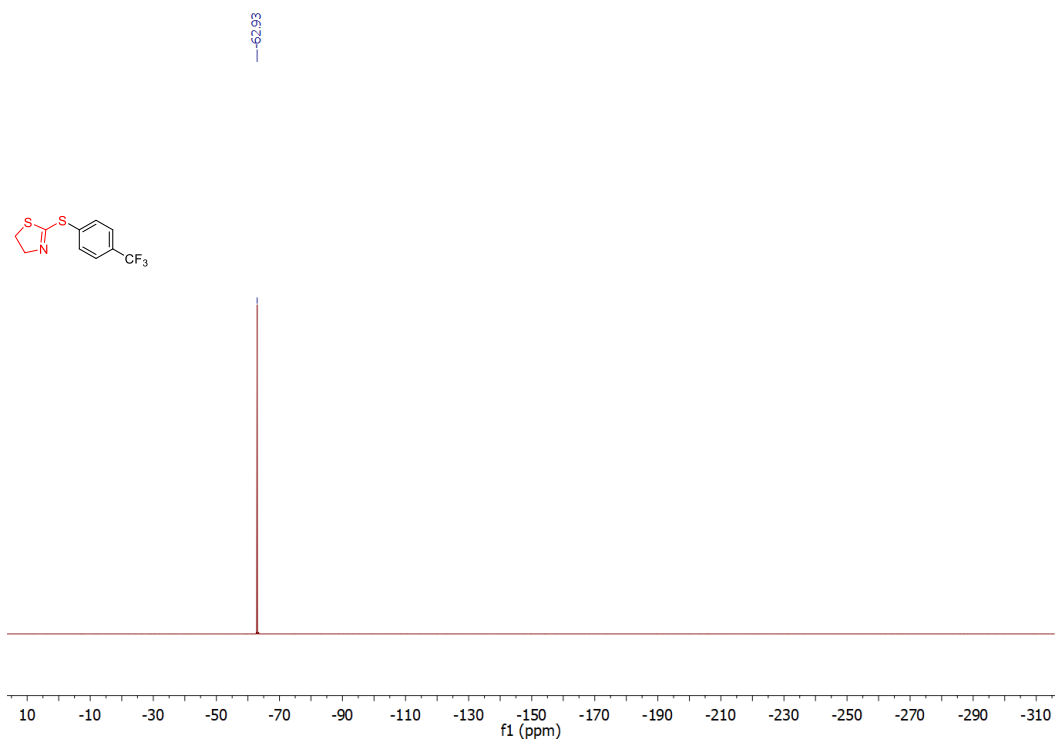
¹³C NMR spectrum of 2-((4-chlorophenyl)thio)thiophene (18)



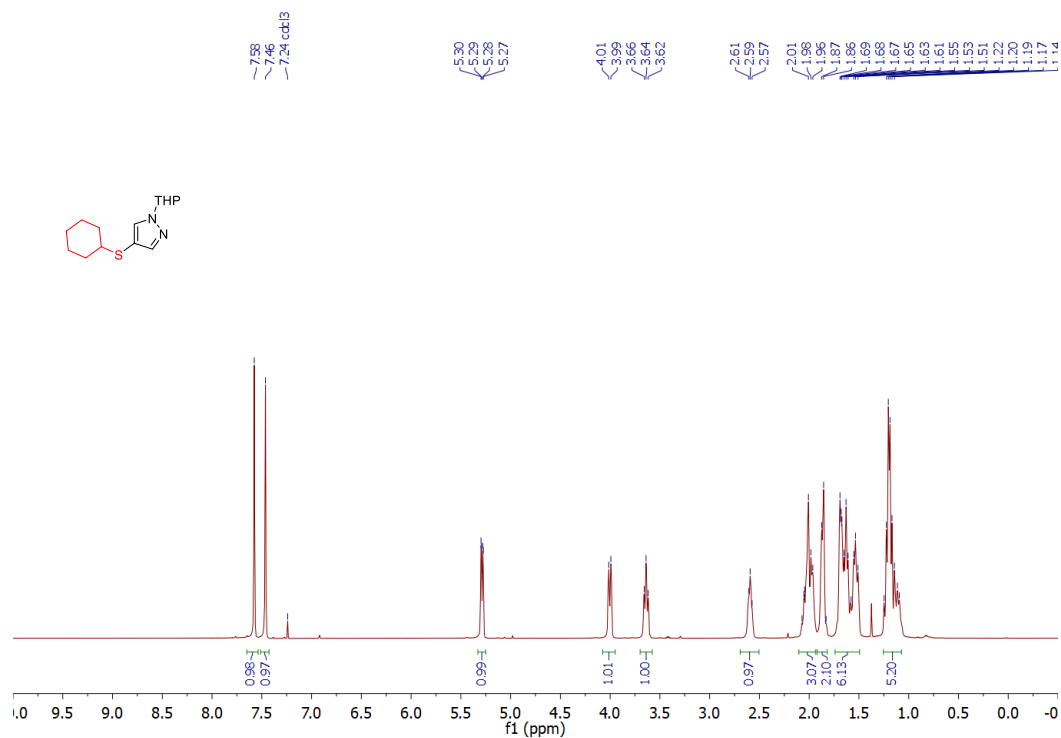
¹H NMR spectrum of 2-((4-(trifluoromethyl)phenyl)thio)-4,5-dihydrothiazole (19)



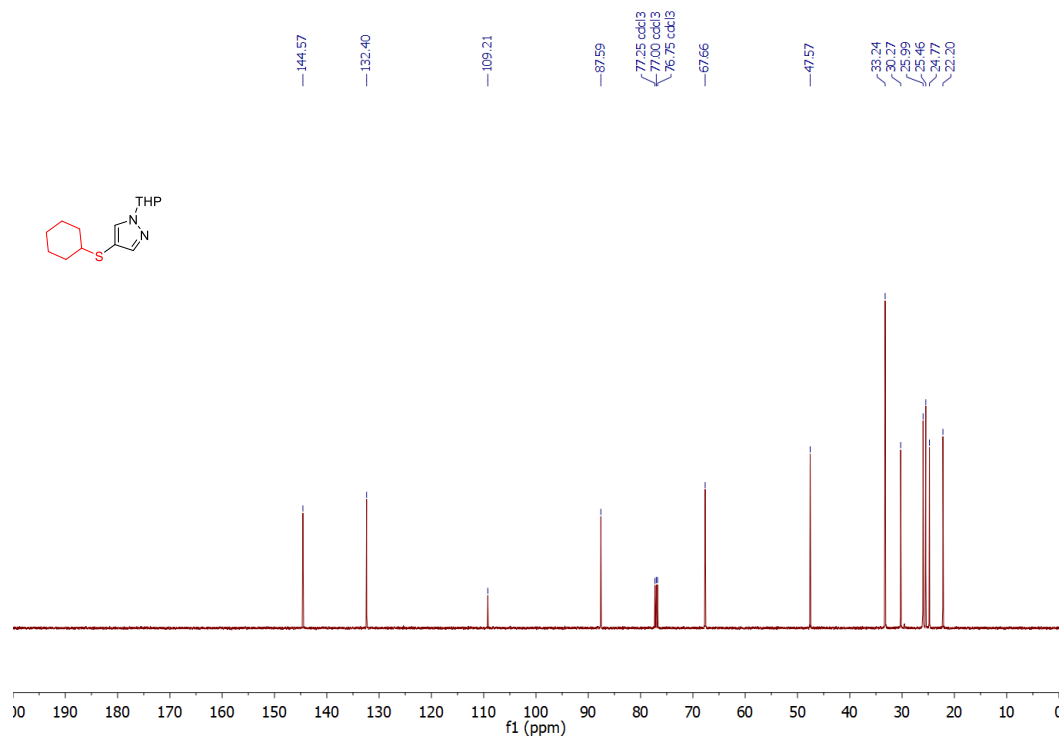
¹³C NMR spectrum of 2-((4-(trifluoromethyl)phenyl)thio)-4,5-dihydrothiazole (19)



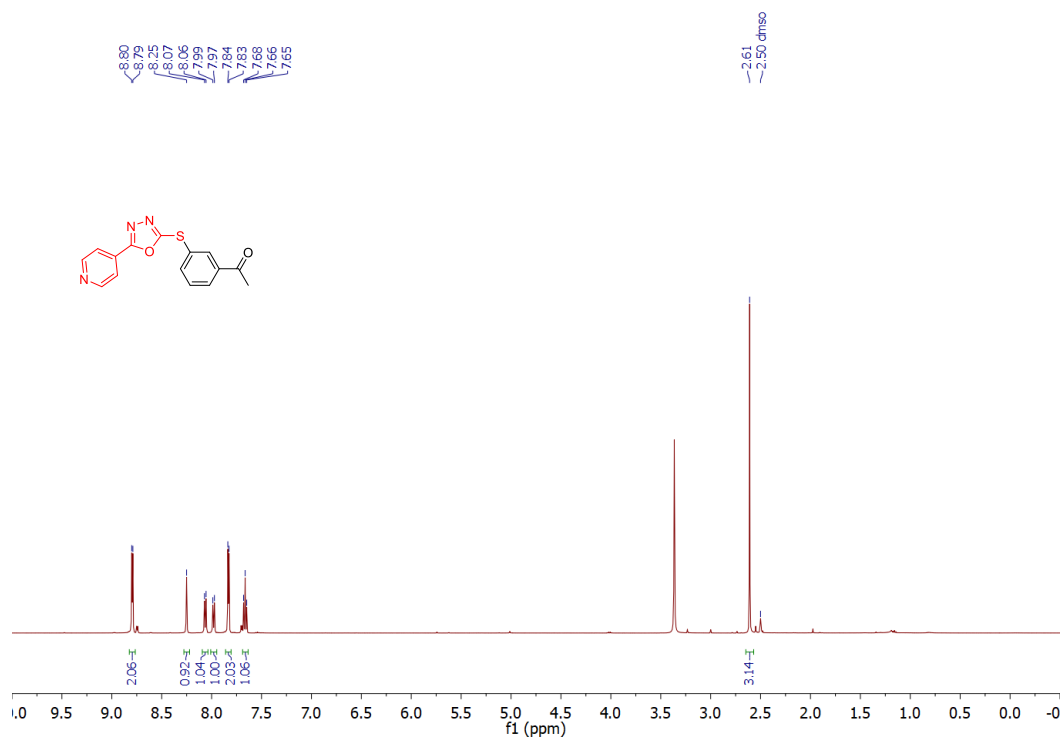
^{19}F NMR spectrum of 2-((4-(trifluoromethyl)phenyl)thio)-4,5-dihydrothiazole (19)



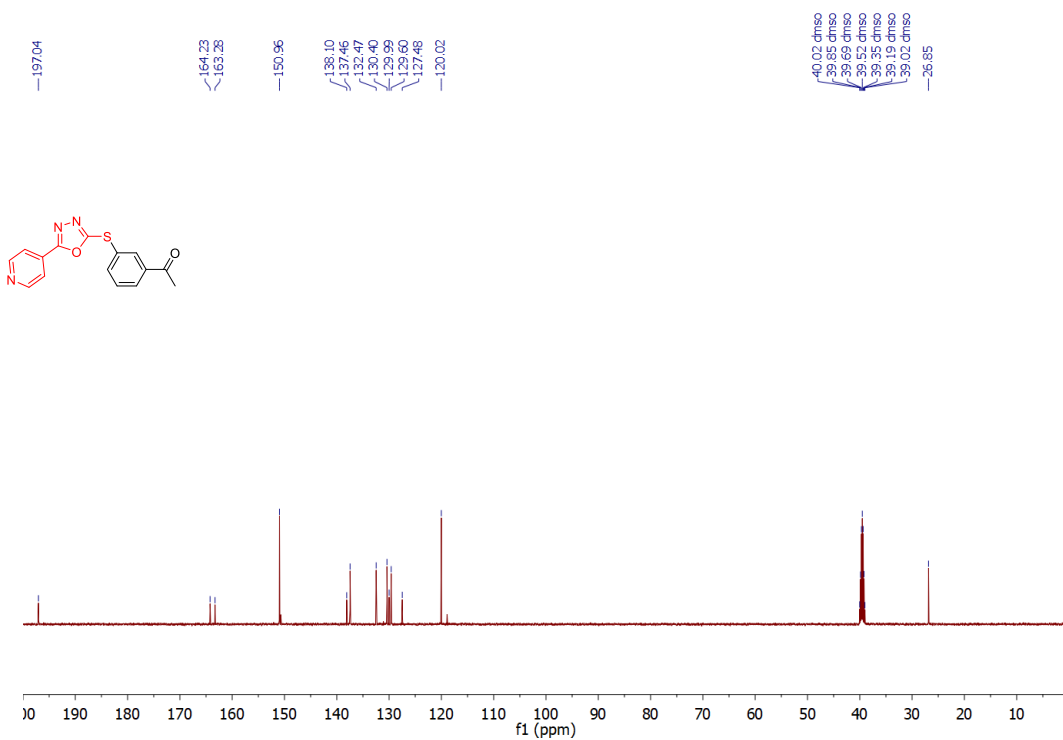
¹H NMR spectrum of 4-(cyclohexylthio)-1-(tetrahydro-2H-pyran-2-yl)-1H-pyrazole (20)



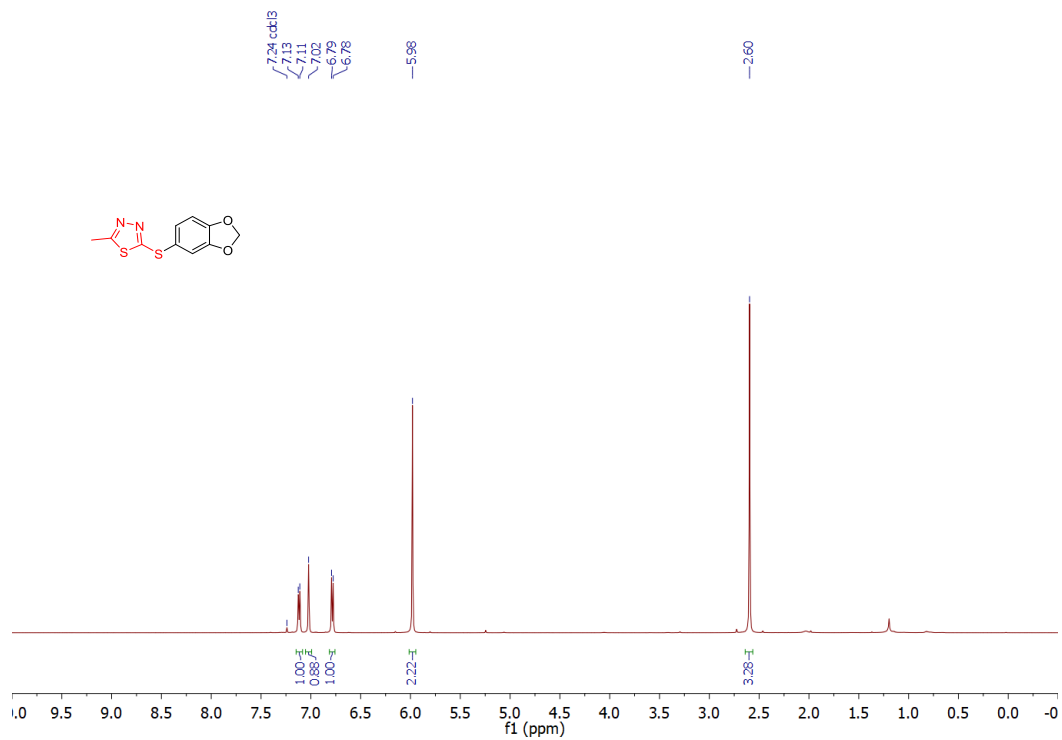
¹³C NMR spectrum of 4-(cyclohexylthio)-1-(tetrahydro-2H-pyran-2-yl)-1H-pyrazole (20)



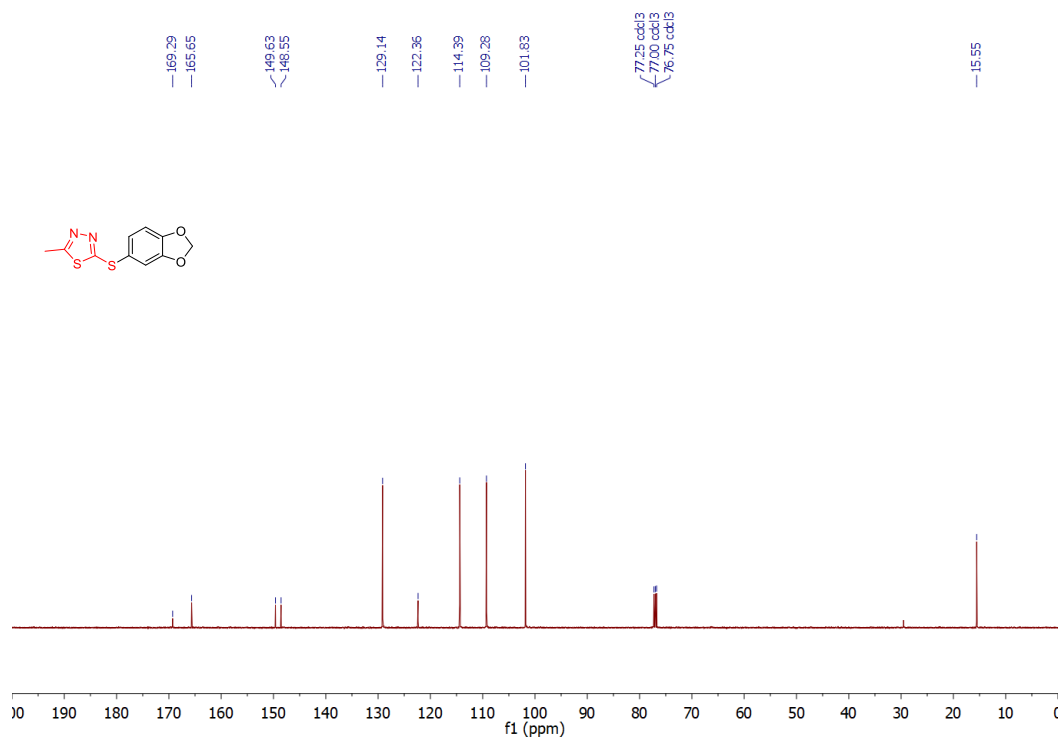
¹H NMR spectrum of 1-(3-((5-(pyridin-4-yl)-1,3,4-oxadiazol-2-yl)thio)phenyl)ethan-1-one (21)



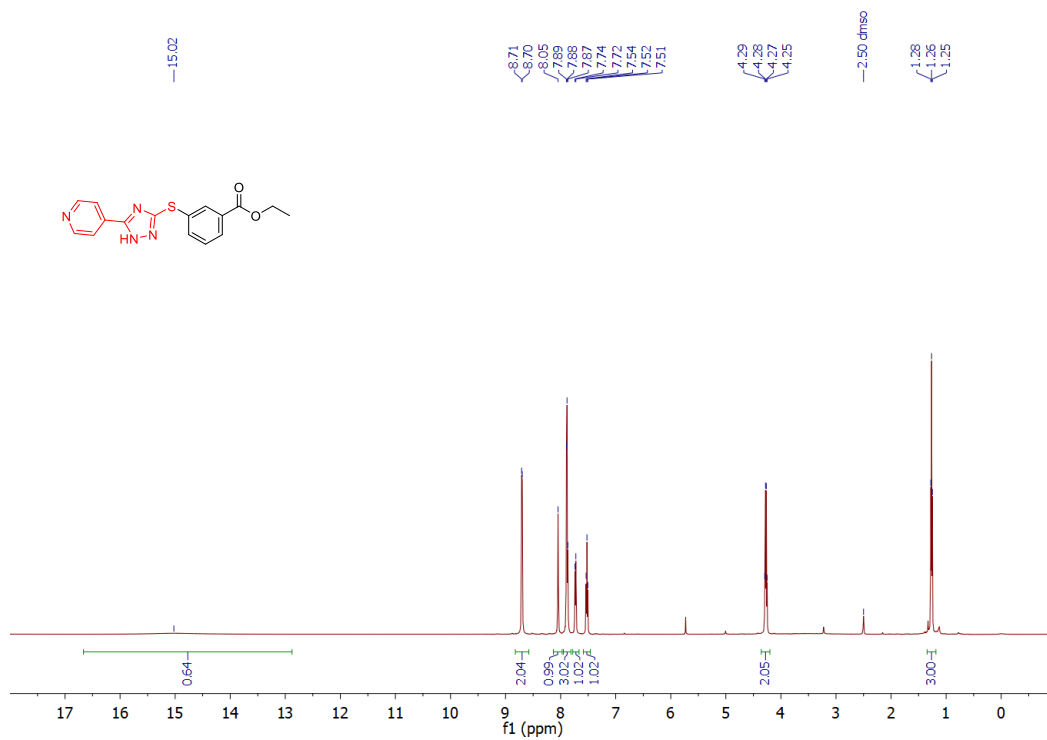
¹³C NMR spectrum of 1-(3-((5-(pyridin-4-yl)-1,3,4-oxadiazol-2-yl)thio)phenyl)ethan-1-one (21)



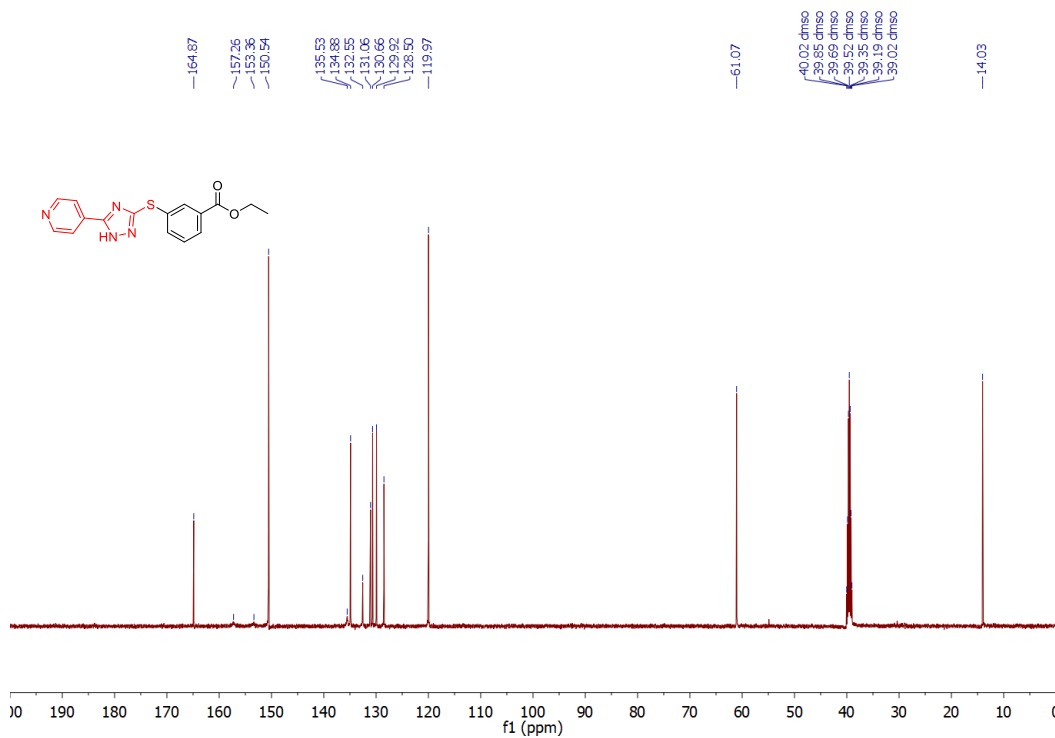
¹H NMR spectrum of 2-(benzo[d][1,3]dioxol-5-ylthio)-5-methyl-1,3,4-thiadiazole (22)



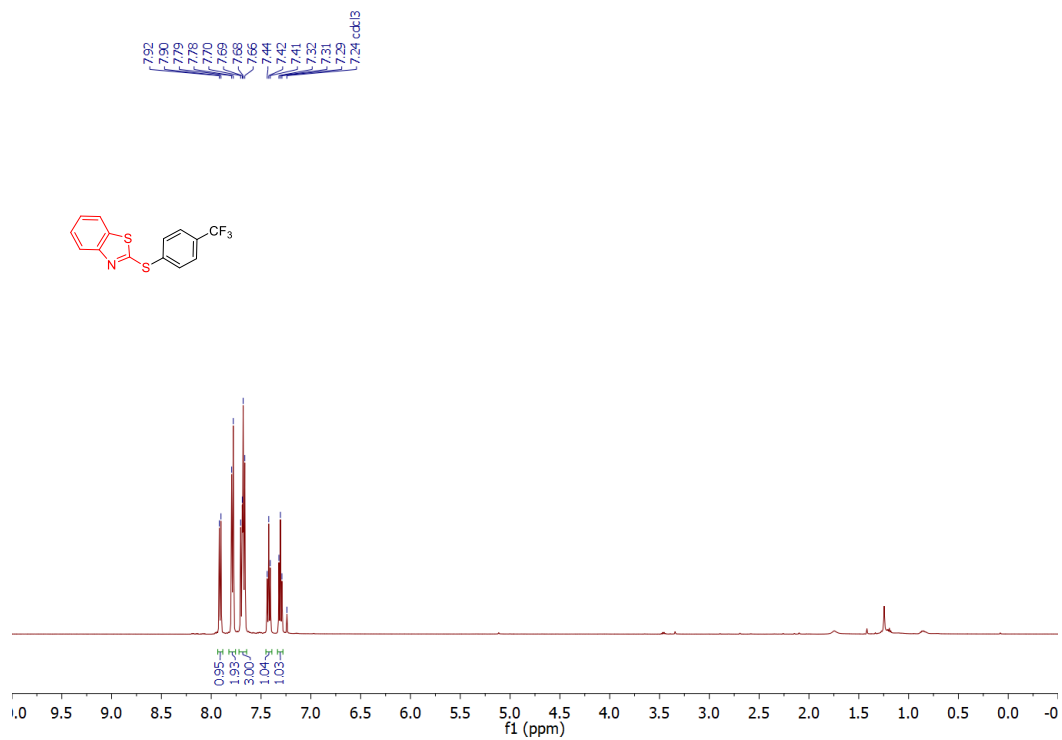
¹³C NMR spectrum of 2-(benzo[d][1,3]dioxol-5-ylthio)-5-methyl-1,3,4-thiadiazole (22)



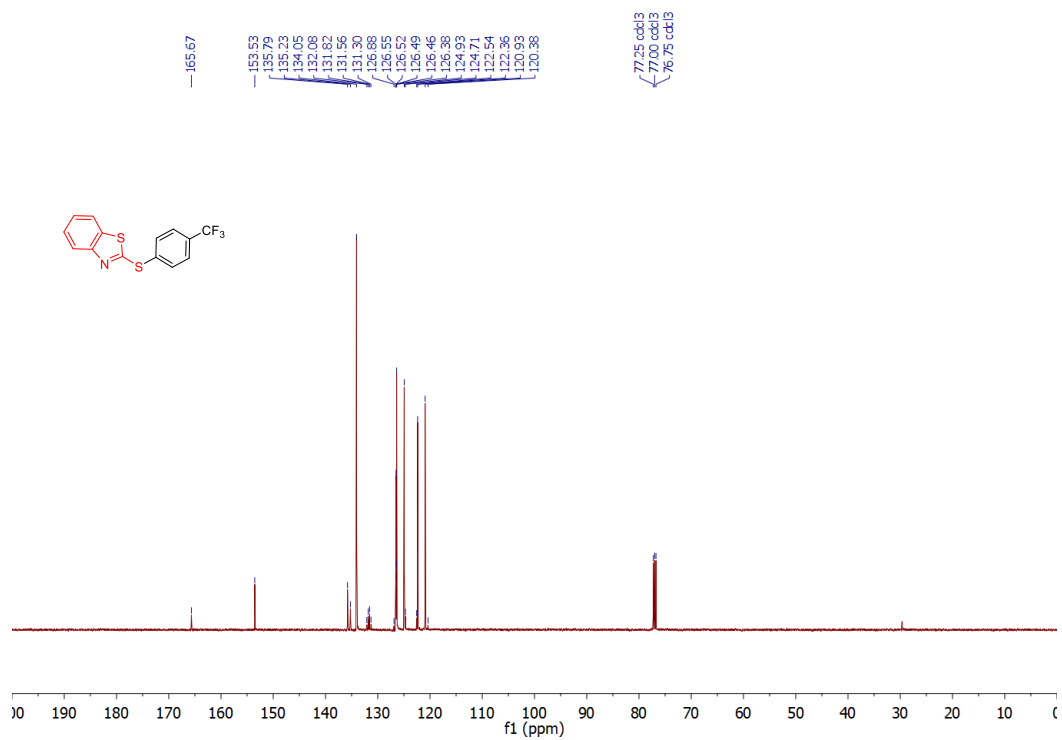
¹H NMR spectrum of ethyl 3-((5-(pyridin-4-yl)-1H-1,2,4-triazol-3-yl)thio)benzoate (23)



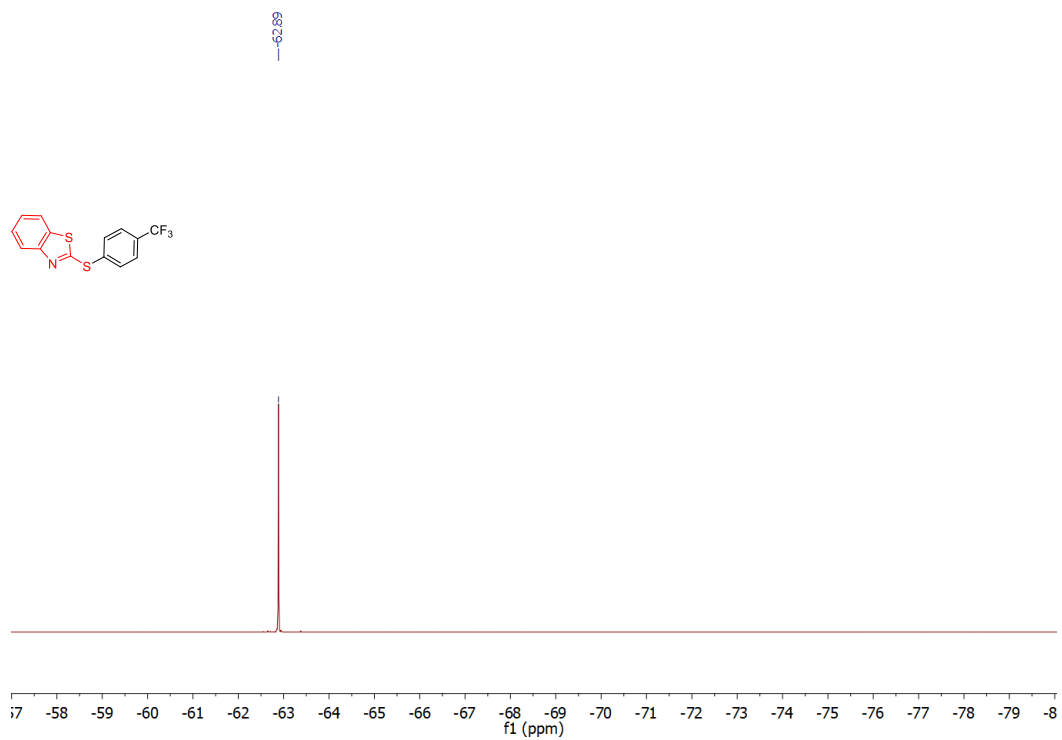
¹³C NMR spectrum of ethyl 3-((5-(pyridin-4-yl)-1H-1,2,4-triazol-3-yl)thio)benzoate (23)



¹H NMR spectrum of 2-((4-(trifluoromethyl)phenyl)thio)benzo[d]thiazole (24)

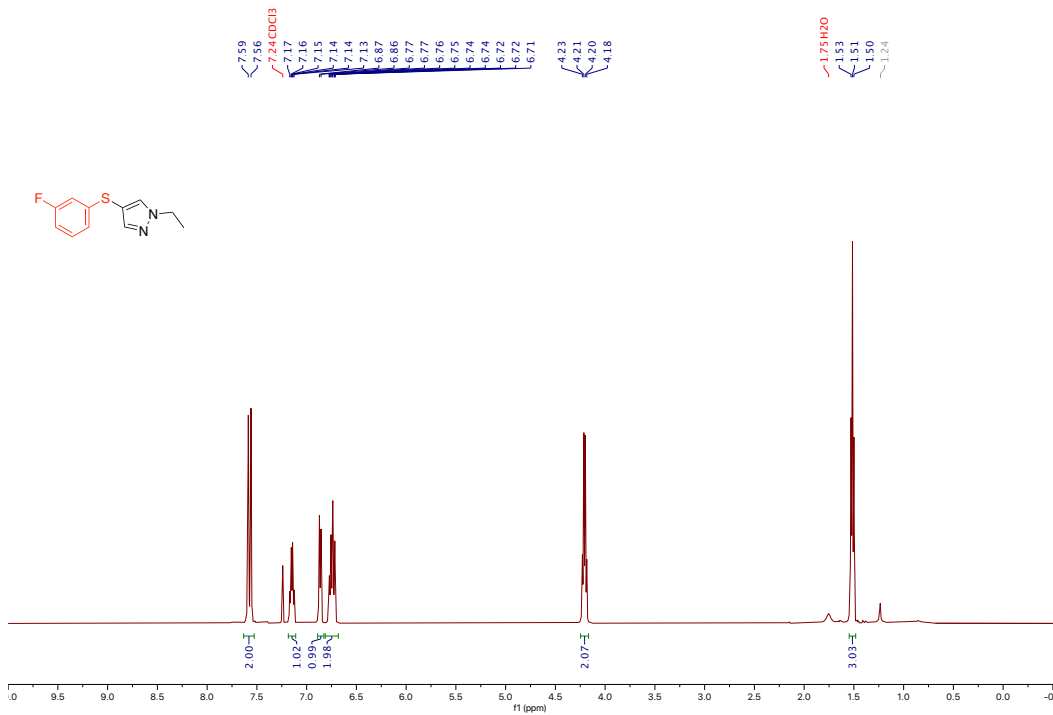


¹³C NMR spectrum of 2-((4-(trifluoromethyl)phenyl)thio)benzo[d]thiazole (24)



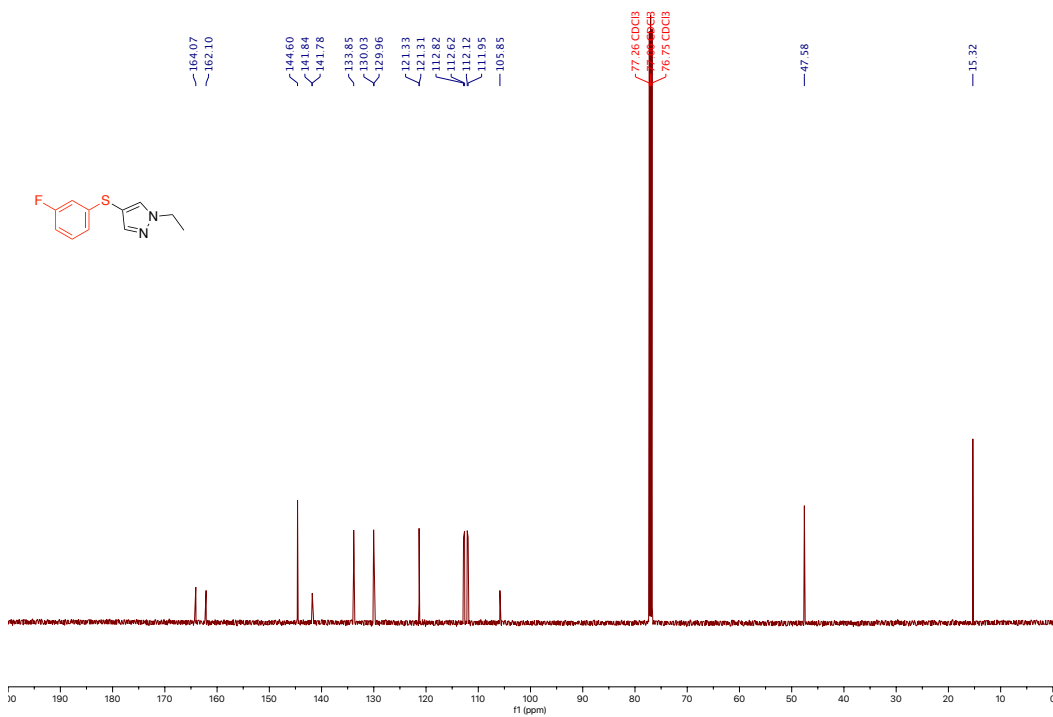
^{19}F NMR spectrum of **2-((4-(trifluoromethyl)phenyl)thio)benzo[d]thiazole (24)**

JY1538-run.10.fid—



¹H NMR spectrum of 1-ethyl-4-((3-fluorophenyl)thio)-1H-pyrazole (25)

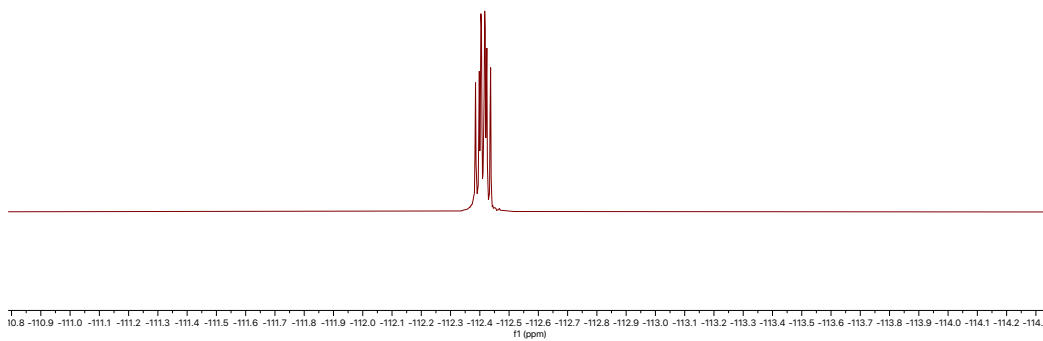
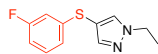
JY1538-run.C13.20.fid—



¹³C NMR spectrum of 1-ethyl-4-((3-fluorophenyl)thio)-1H-pyrazole (25)

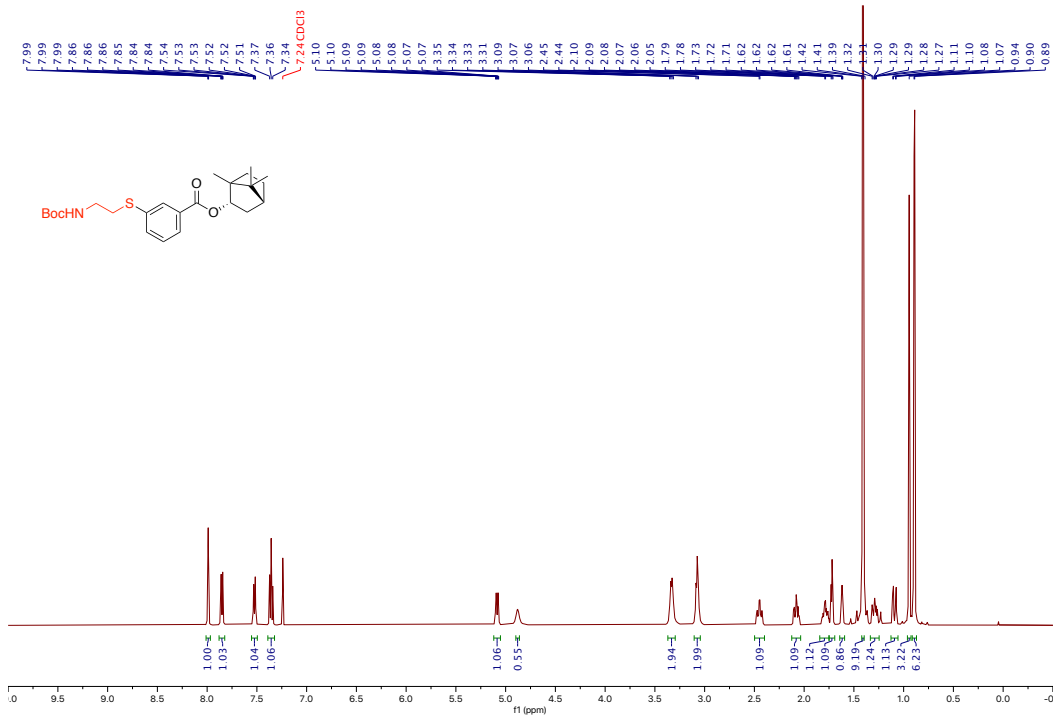
JY1538-run-F19 10 fid

112.39
112.40
112.42
112.44



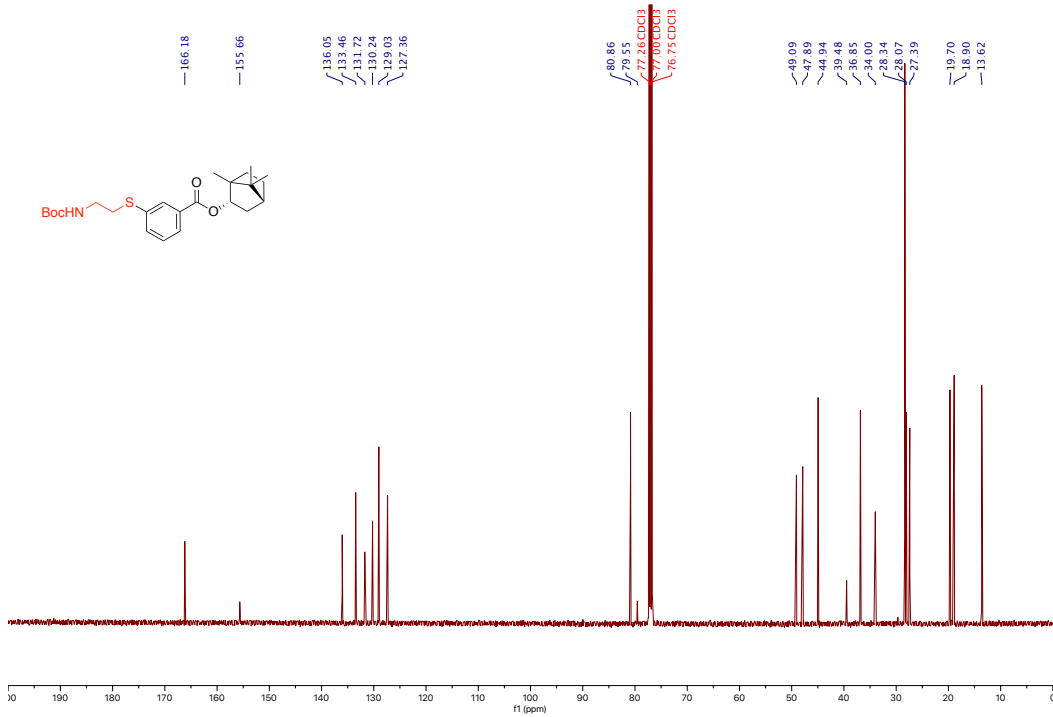
^{19}F NMR spectrum of **1-ethyl-4-((3-fluorophenyl)thio)-1H-pyrazole (25)**

JY1588-run.10.fid—



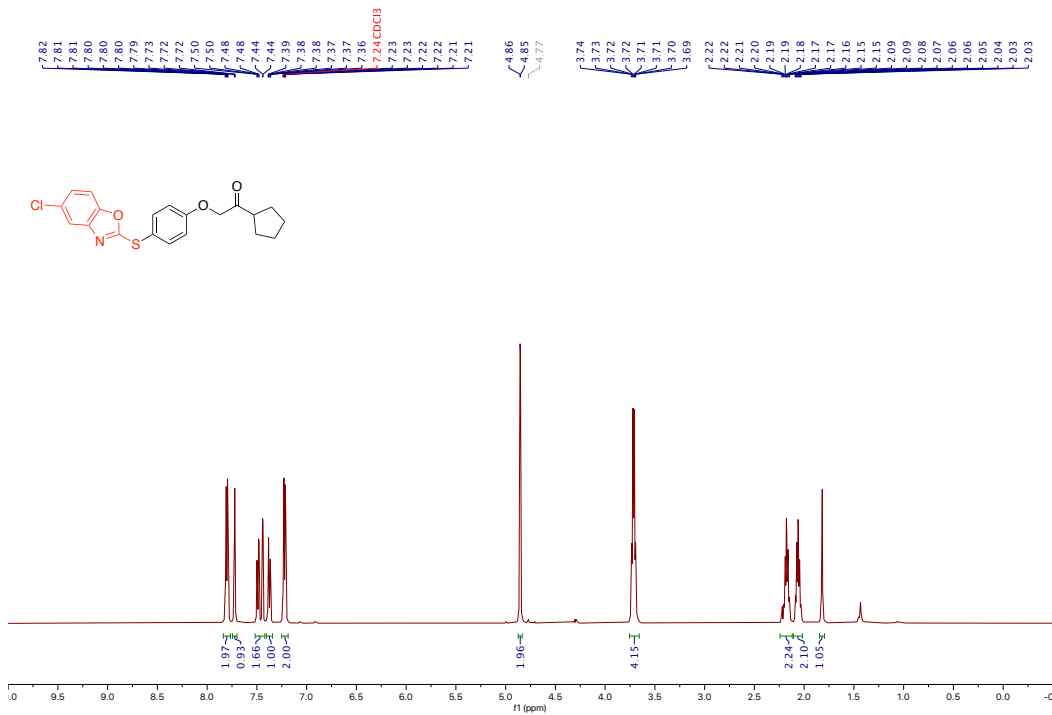
¹H NMR spectrum of (2*S*,4*R*)-1,7,7-trimethylbicyclo[2.2.1]heptan-2-yl-3-((2-((*tert*-butoxycarbonyl)amino)ethyl)thio)benzoate (26)

JY1588-run.C13.10.fid—



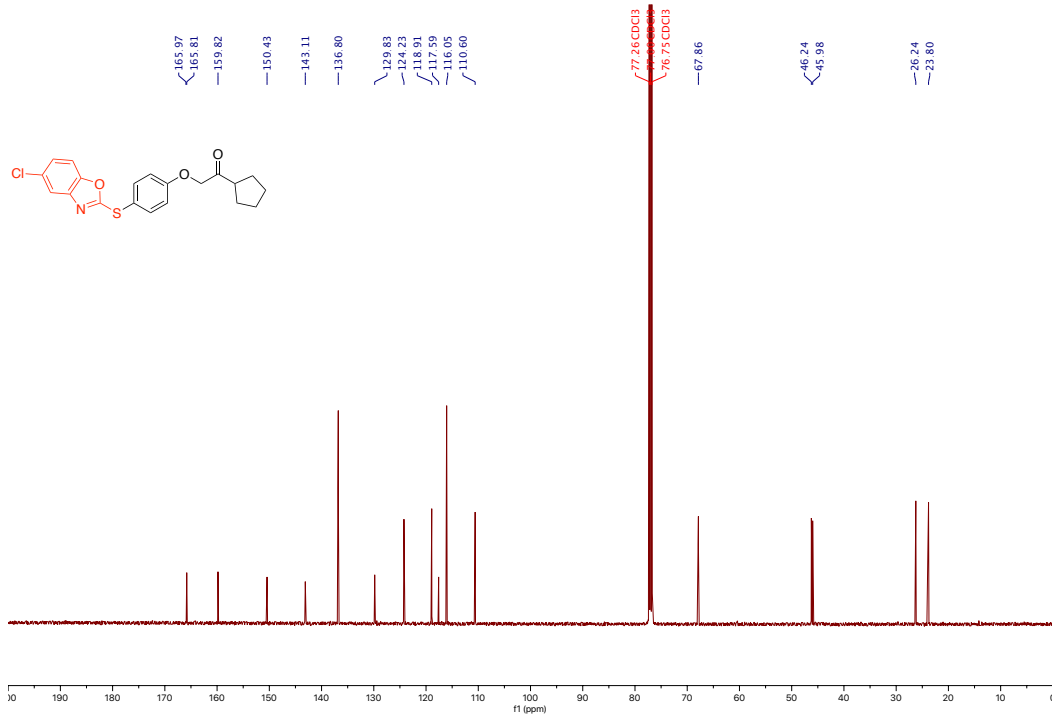
¹³C NMR spectrum of (2*S*,4*R*)-1,7,7-trimethylbicyclo[2.2.1]heptan-2-yl-3-((2-((*tert*-butoxycarbonyl)amino)ethyl)thio)benzoate (26)

JY1686.run10.10.fid—



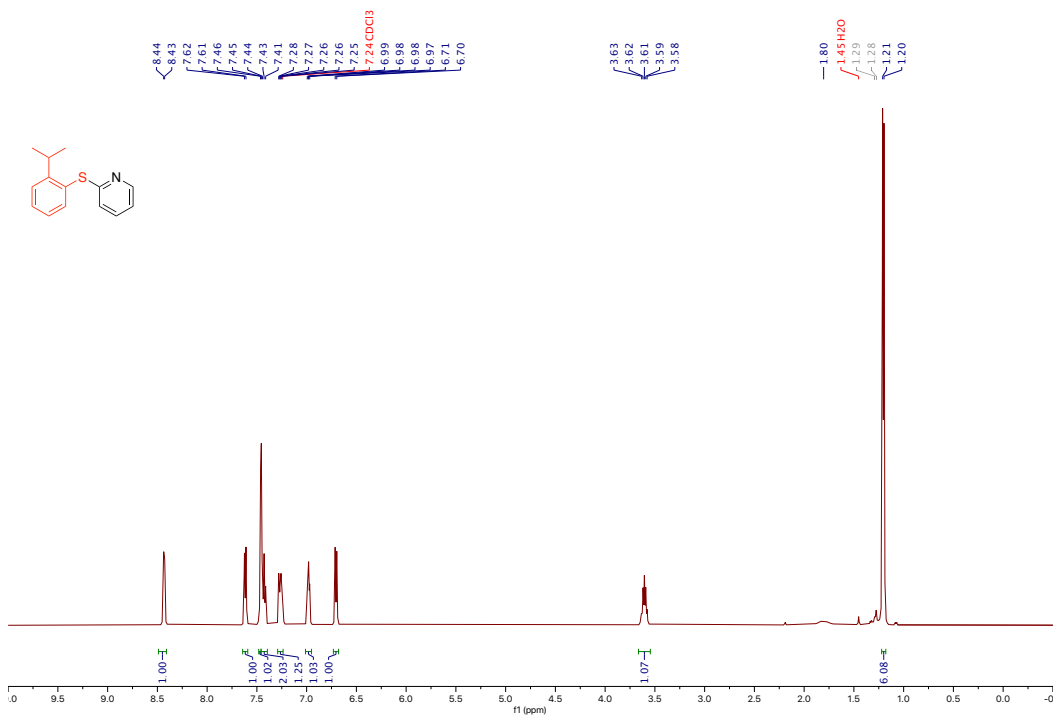
¹H NMR spectrum of 2-(4-((5-chlorobenzo[d]oxazol-2-yl)thio)phenoxy)-1-cyclopentylethan-1-one (27)

JY1686.run10.C13.10.fid—



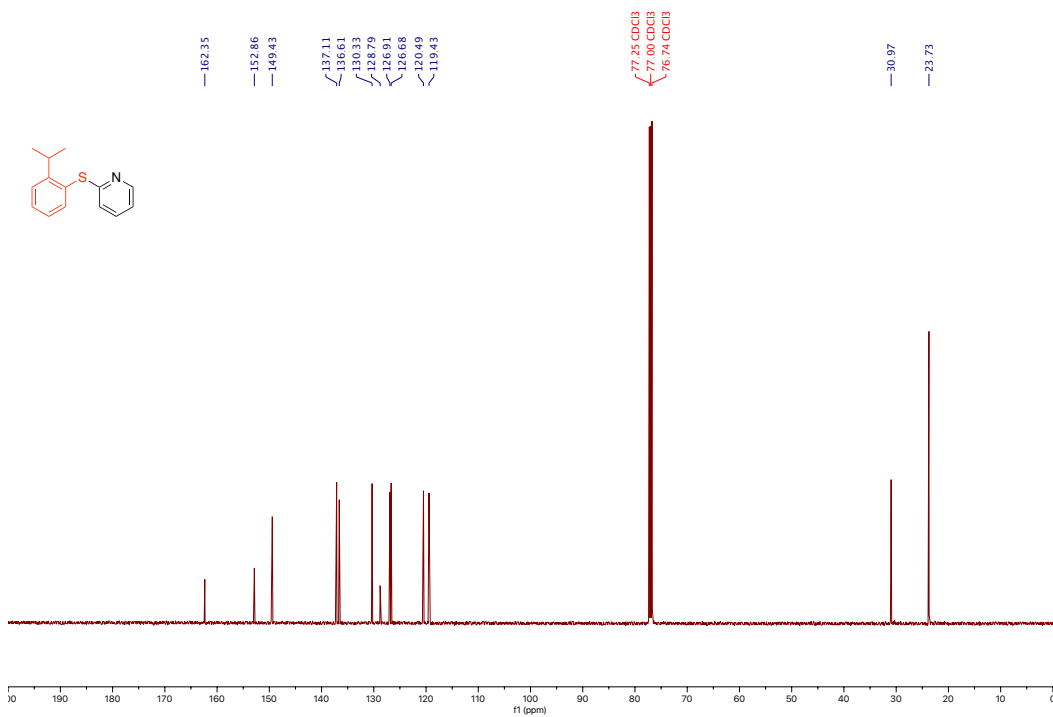
¹³C NMR spectrum of 2-(4-((5-chlorobenzo[d]oxazol-2-yl)thio)phenoxy)-1-cyclopentylethan-1-one (27)

BHL_JY1521.10.fid



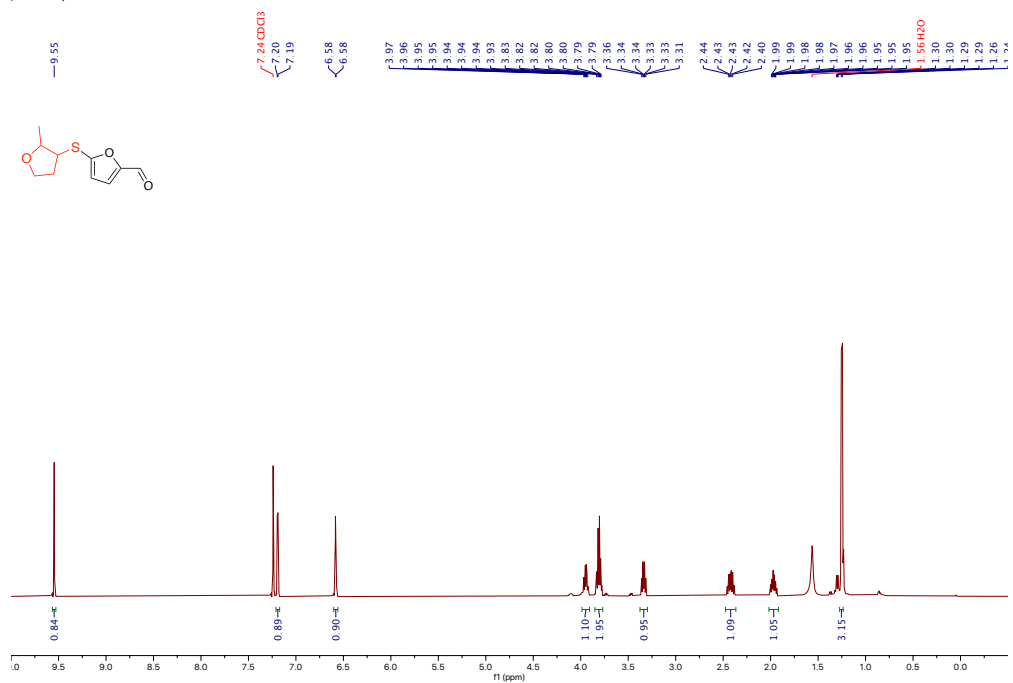
¹H NMR spectrum of 2-((2-isopropylphenyl)thio)pyridine (28)

BHL_JY1521.11.fid



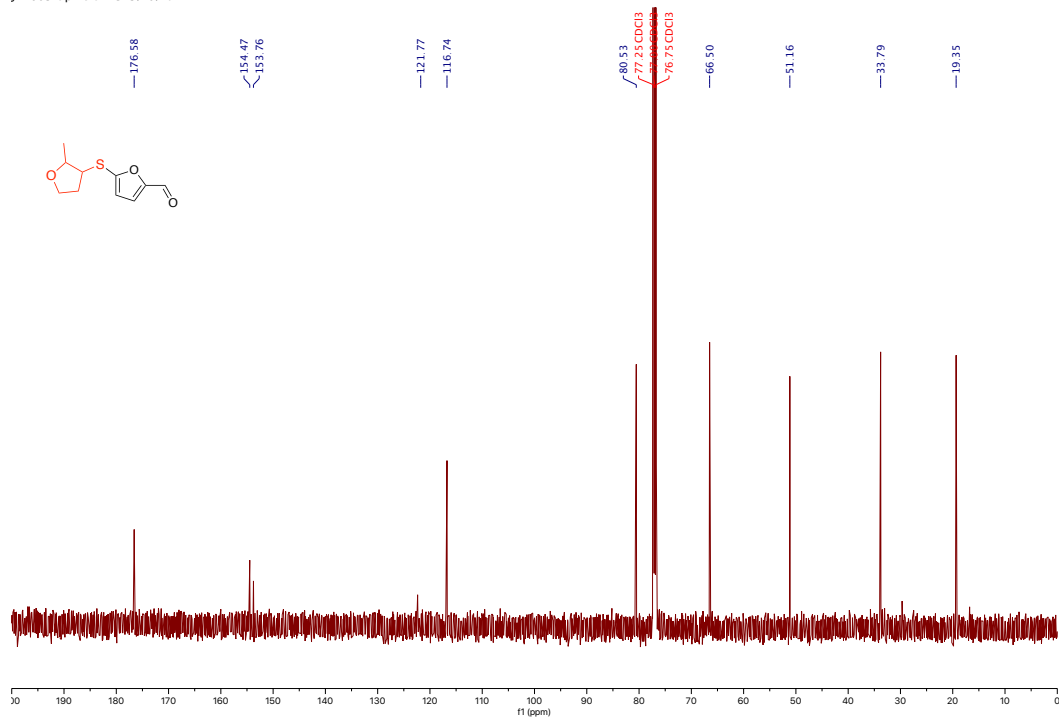
¹³C NMR spectrum of 2-((2-isopropylphenyl)thio)pyridine (28)

JY1603-up-rerun.10.fid



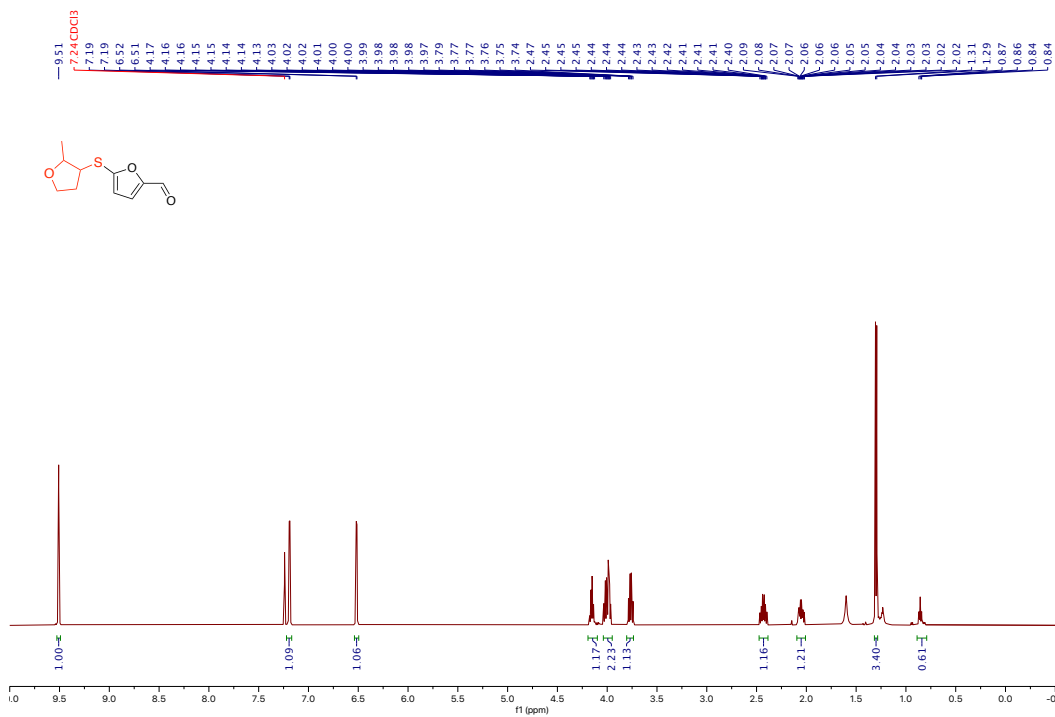
¹H NMR spectrum of 5-((2-methyltetrahydrofuran-3-yl)thio)furan-2-carbaldehyde (29)

JY1603-up-rerun.C13.10.fid



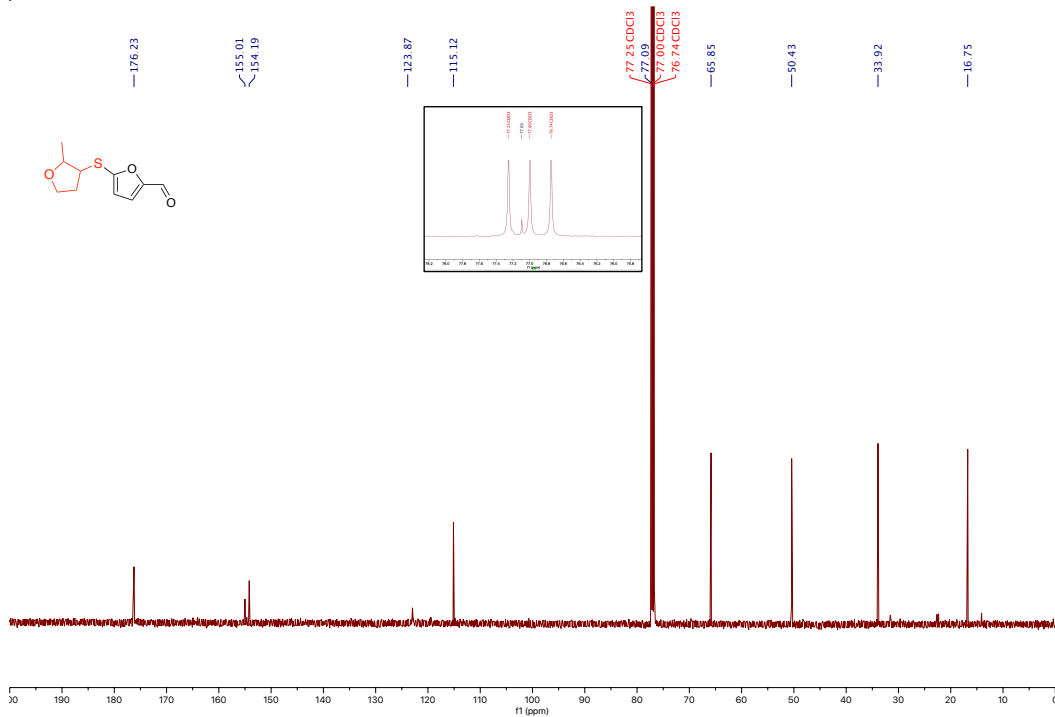
¹³C NMR spectrum of 5-((2-methyltetrahydrofuran-3-yl)thio)furan-2-carbaldehyde (29)

JY1603.rerun_low.10.fid



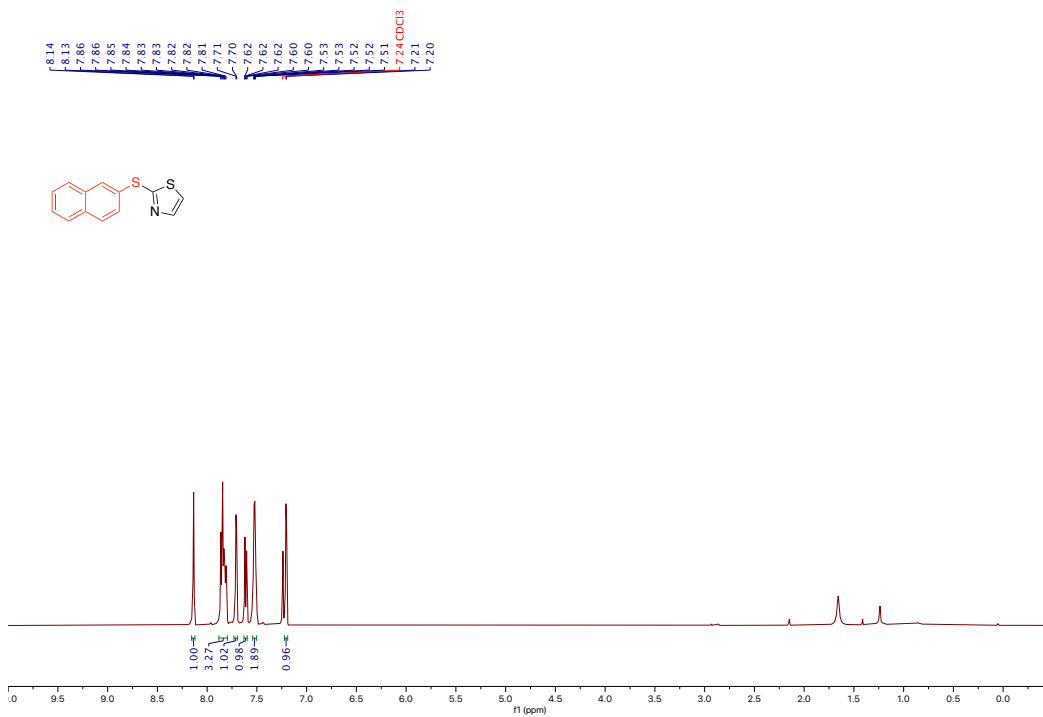
¹H NMR spectrum of 5-((2-methyltetrahydrofuran-3-yl)thio)furan-2-carbaldehyde (29)

JY1603.rerun_low.C13.10.fid



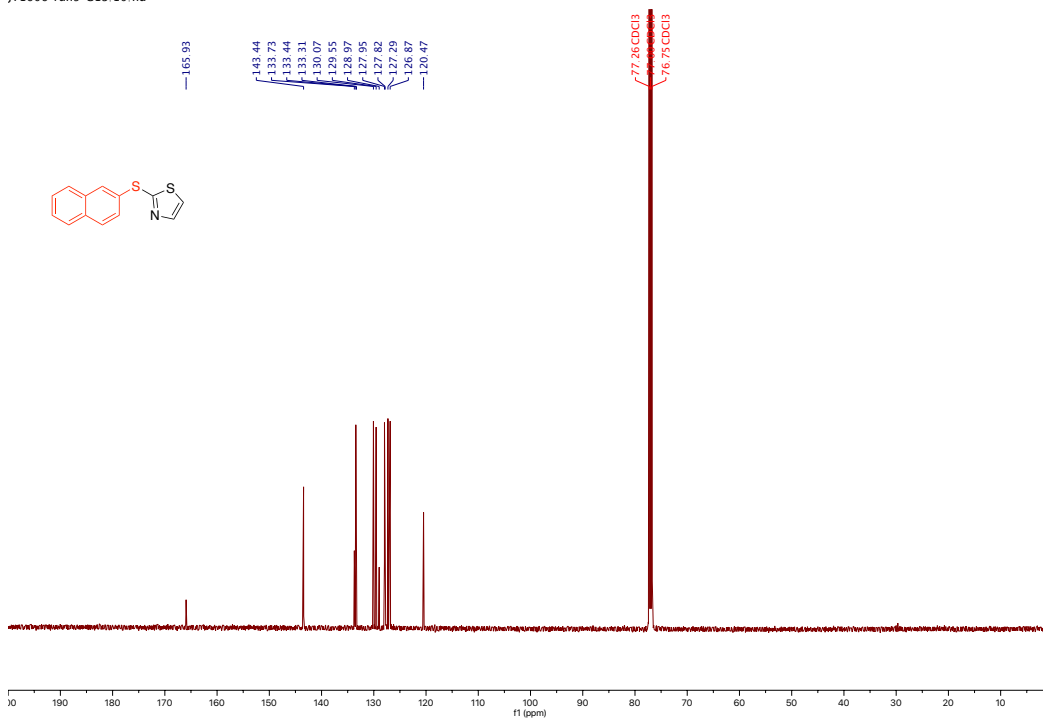
¹³C NMR spectrum of 5-((2-methyltetrahydrofuran-3-yl)thio)furan-2-carbaldehyde (29)

JY1606-run9.10.fid —



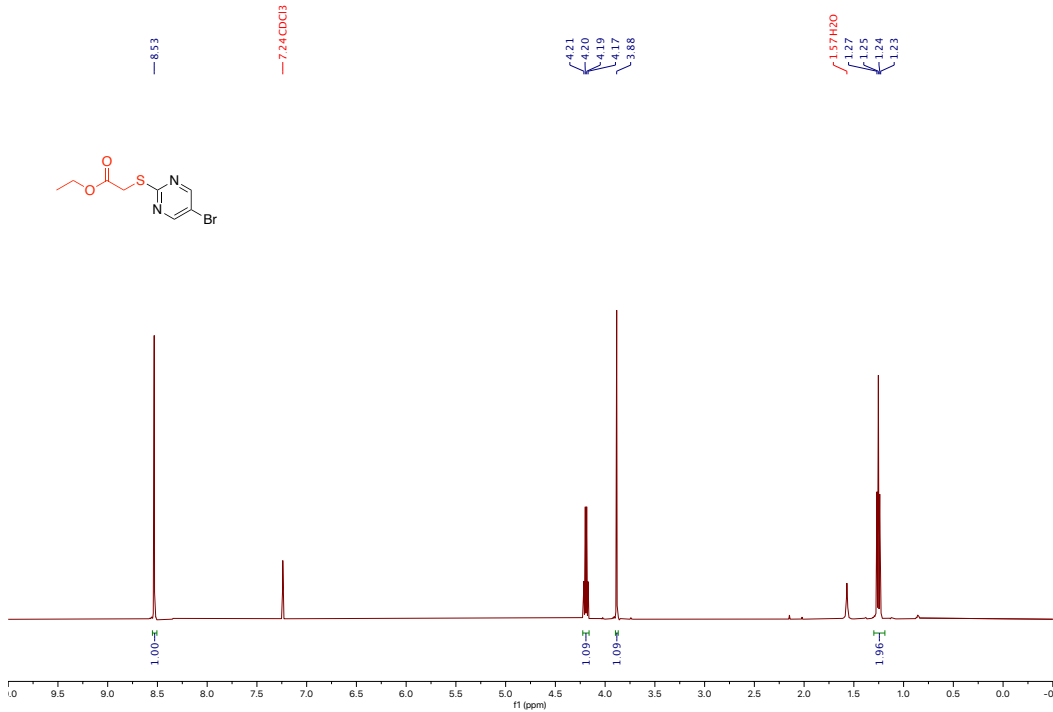
¹H NMR spectrum of 2-(naphthalen-2-ylthio)thiazole (30)

JY1606-run9.C13.10.fid —



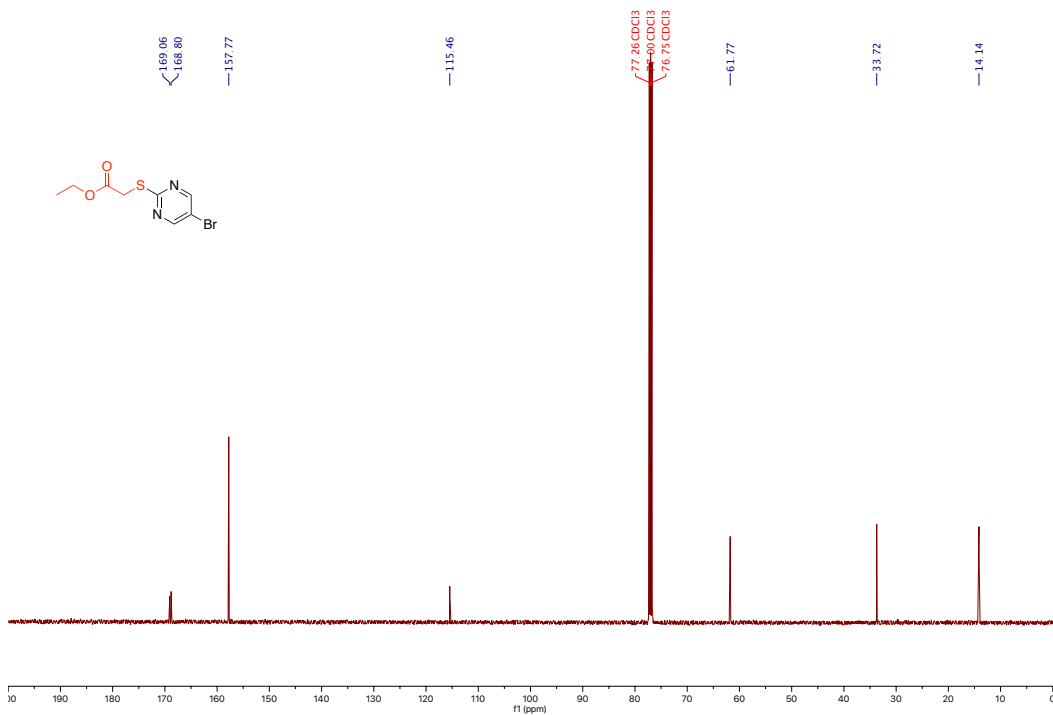
¹³C NMR spectrum of 2-(naphthalen-2-ylthio)thiazole (30)

JY1610-run.10.fid -



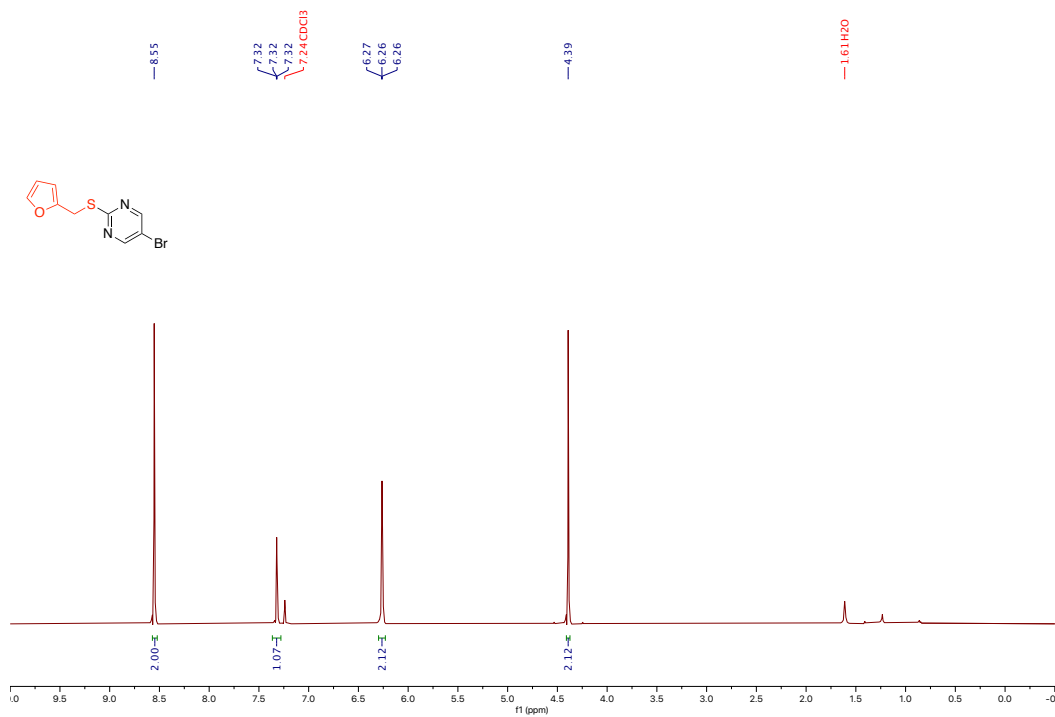
¹H NMR spectrum of ethyl 2-((2-bromopyrimidin-5-yl)thio)acetate (31)

JY1610-run.C13.10.fid -



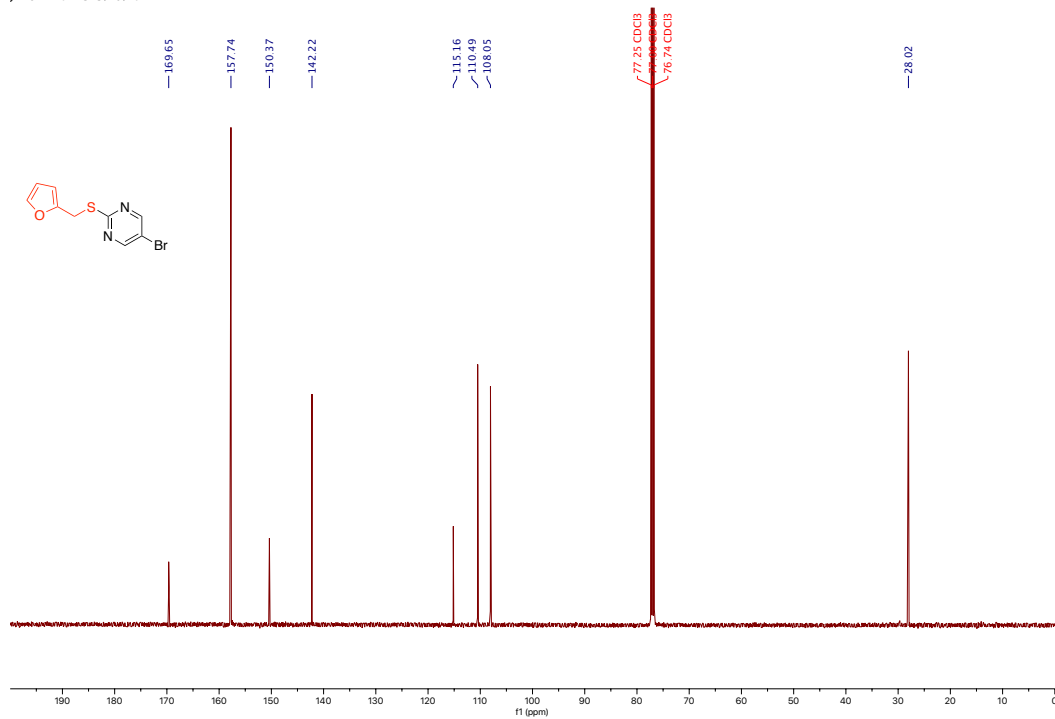
¹³C NMR spectrum of ethyl 2-((2-bromopyrimidin-5-yl)thio)acetate (31)

JY1611-run.10.fid—



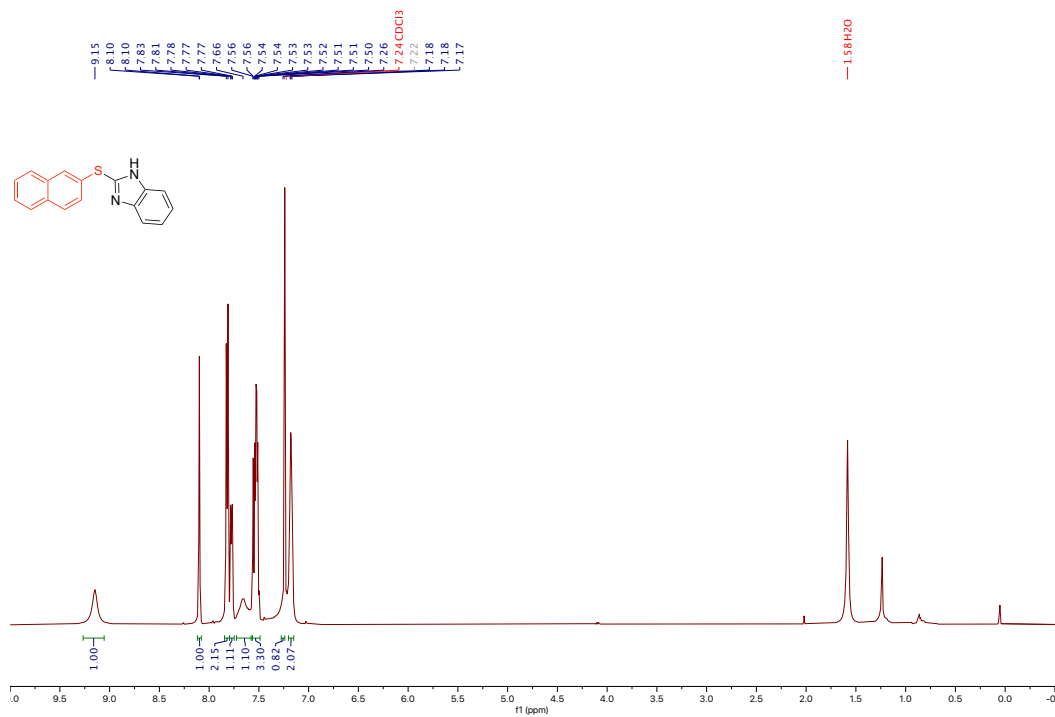
¹H NMR spectrum of 2-bromo-5-((furan-2-ylmethyl)thio)pyrimidine (32)

JY1611-run.C13.10.fid—



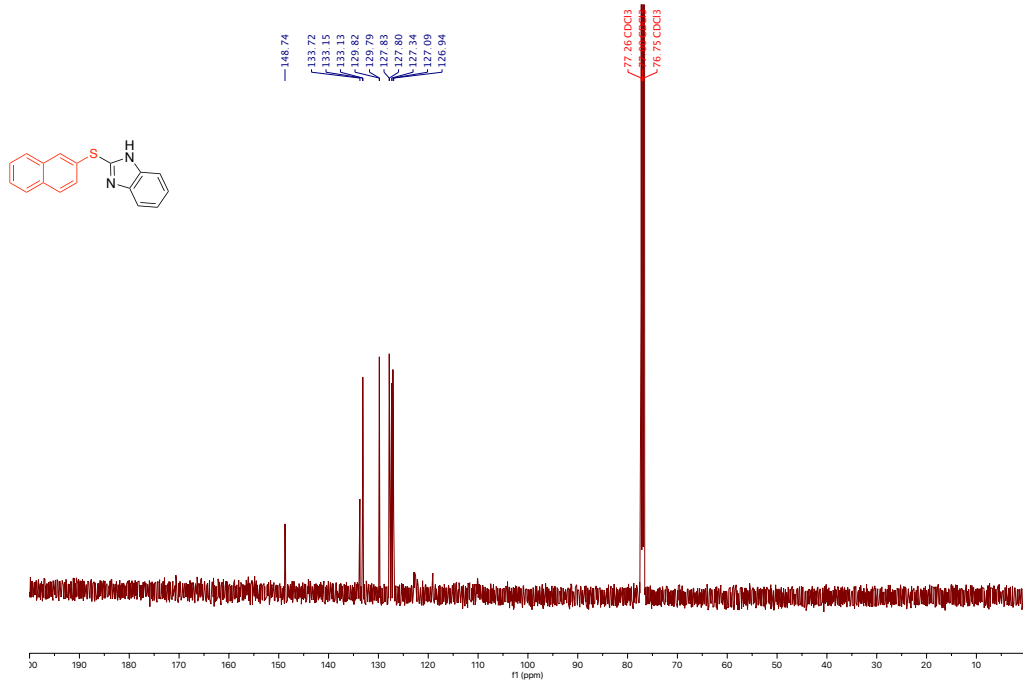
¹³C NMR spectrum of 2-bromo-5-((furan-2-ylmethyl)thio)pyrimidine (32)

JY1678-run.10.fid



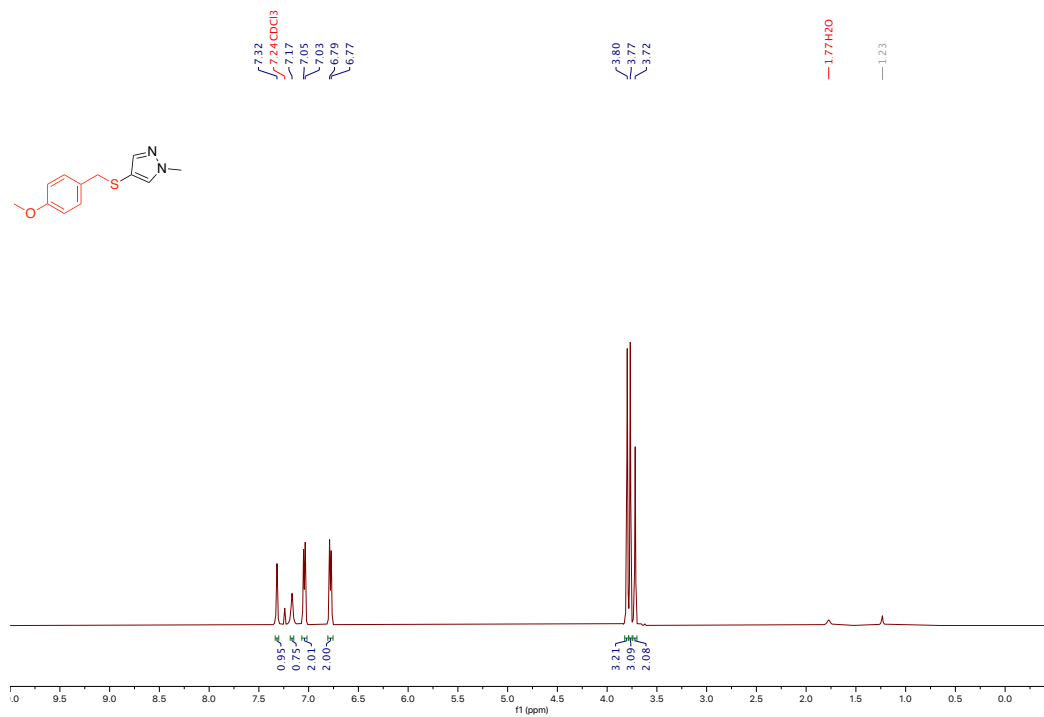
¹H NMR spectrum of 2-(naphthalen-2-ylthio)-1H-benzo[d]imidazole (33)

JY1678-run.C13.11.fid



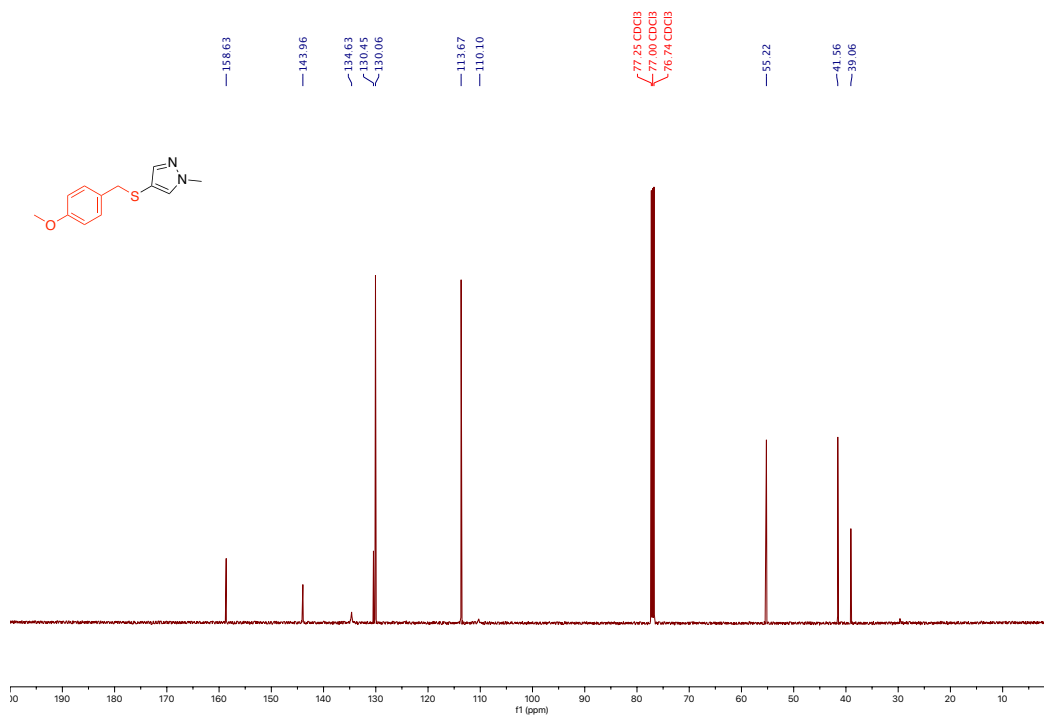
¹³C NMR spectrum of 2-(naphthalen-2-ylthio)-1H-benzo[d]imidazole (33)

JY1542-run.11.fid—



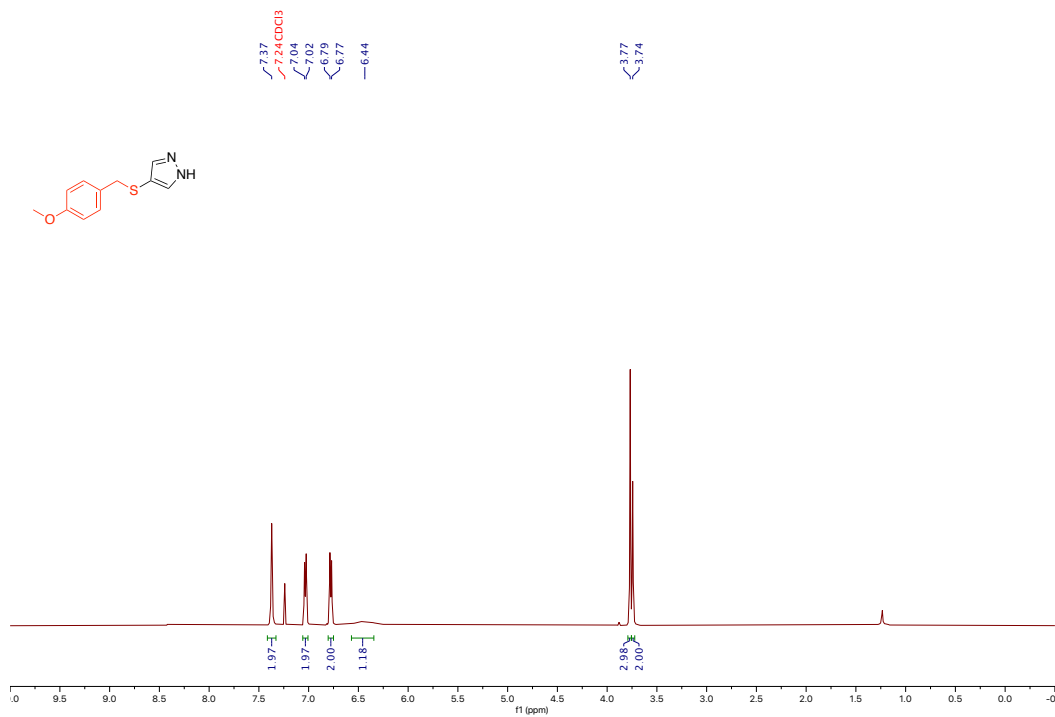
¹H NMR spectrum of 4-((4-methoxybenzyl)thio)-1-methyl-1H-pyrazole (34)

JY1542-run.12.fid—



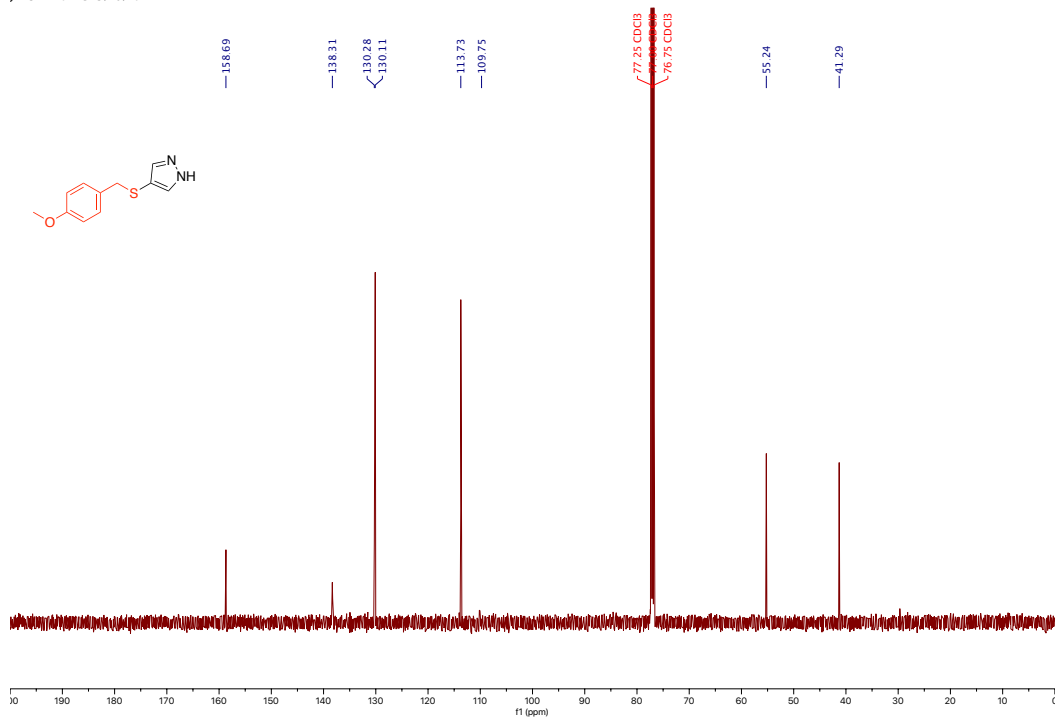
¹³C NMR spectrum of 4-((4-methoxybenzyl)thio)-1-methyl-1H-pyrazole (34)

JY1541-run.10.fid —

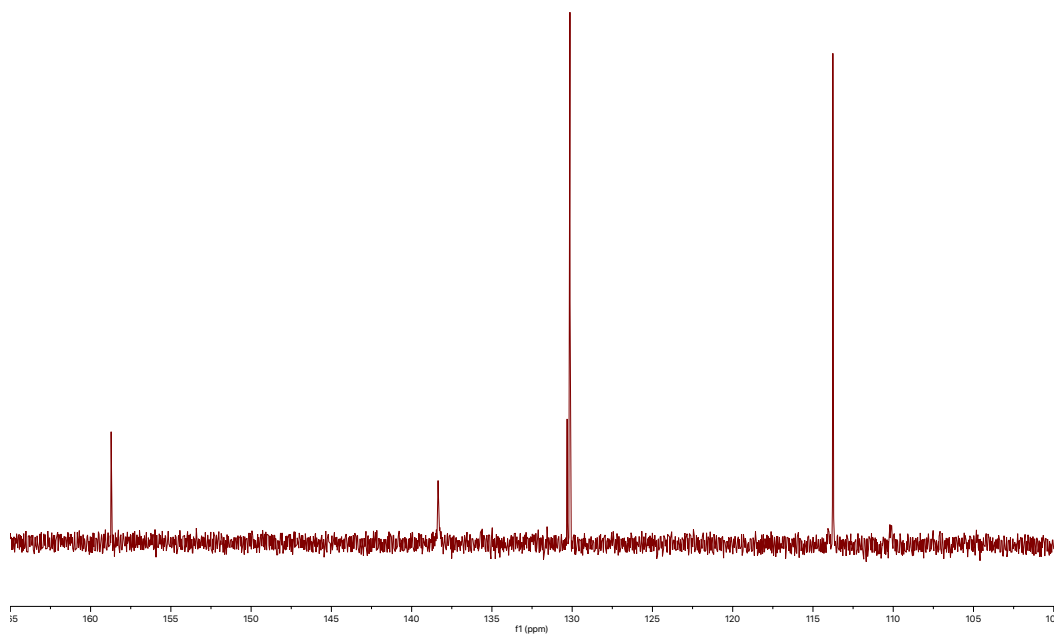


¹H NMR spectrum of 4-((4-methoxybenzyl)thio)-1H-pyrazole (35)

JY1541-run.C13.10.fid —

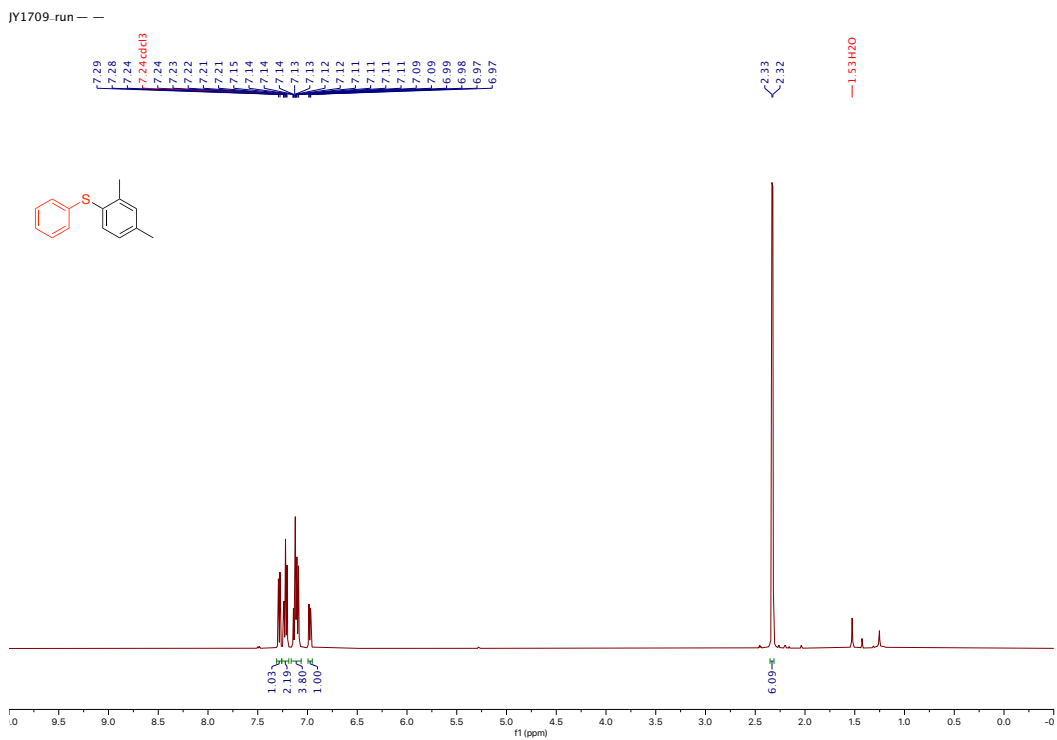


¹³C NMR spectrum of 4-((4-methoxybenzyl)thio)-1H-pyrazole (35)

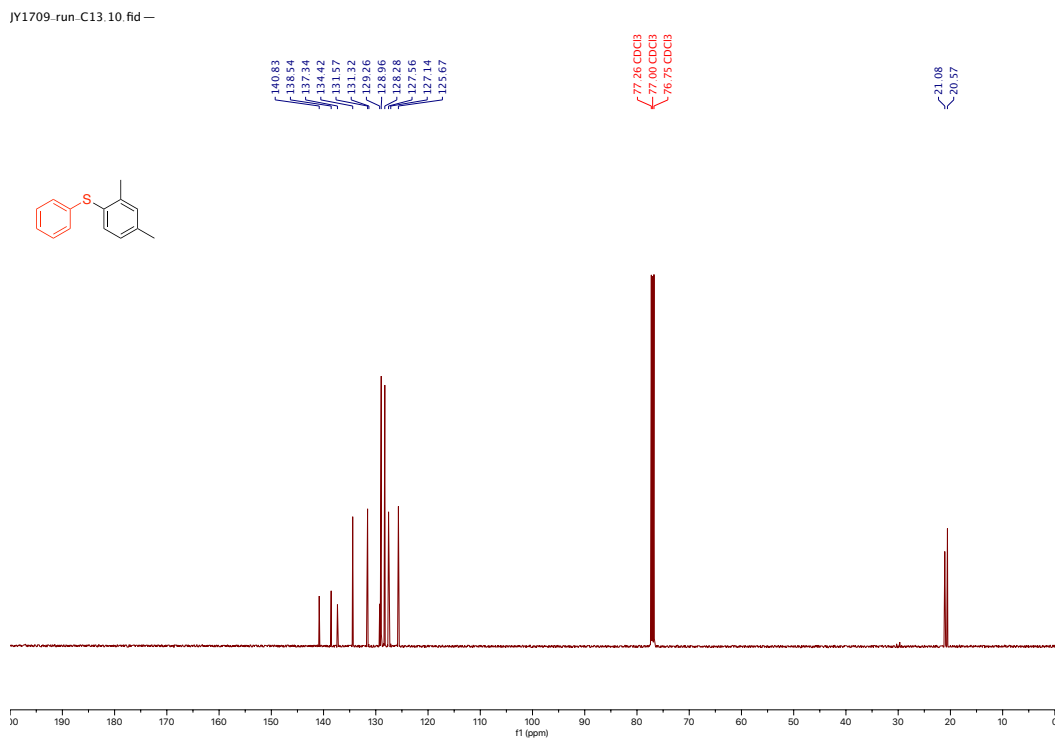


¹³C NMR spectrum of **4-((4-methoxybenzyl)thio)-1H-pyrazole (35)** zoom in 165-100

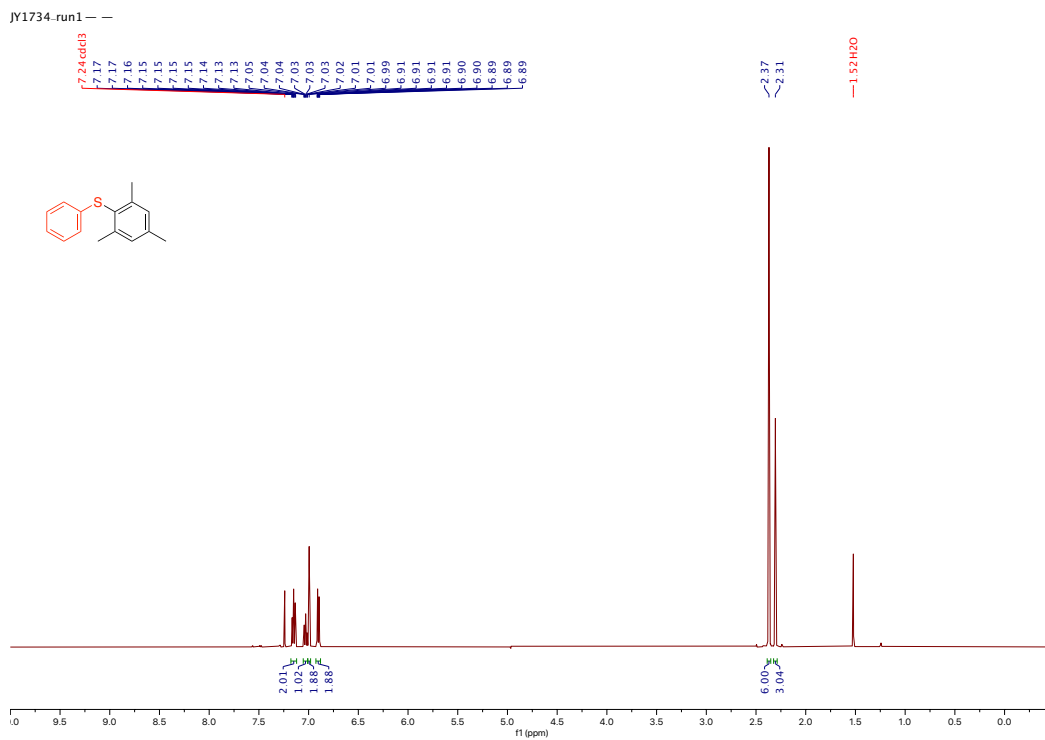
ppm



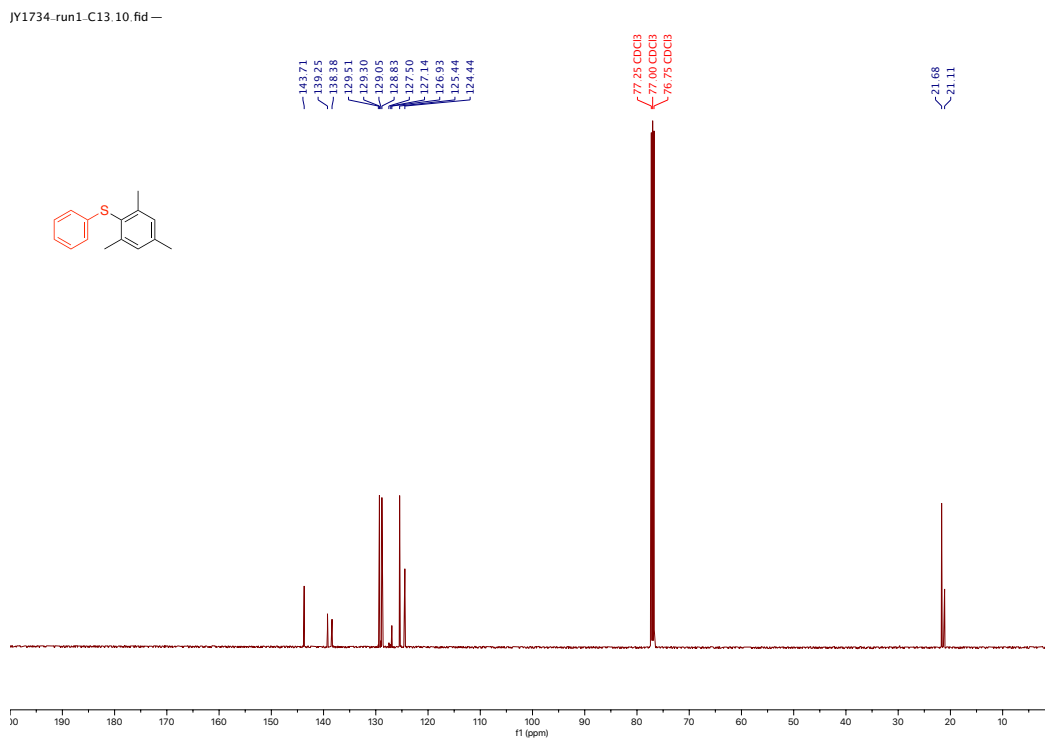
^1H NMR spectrum of (2,4-dimethylphenyl)(phenyl)sulfane (36)



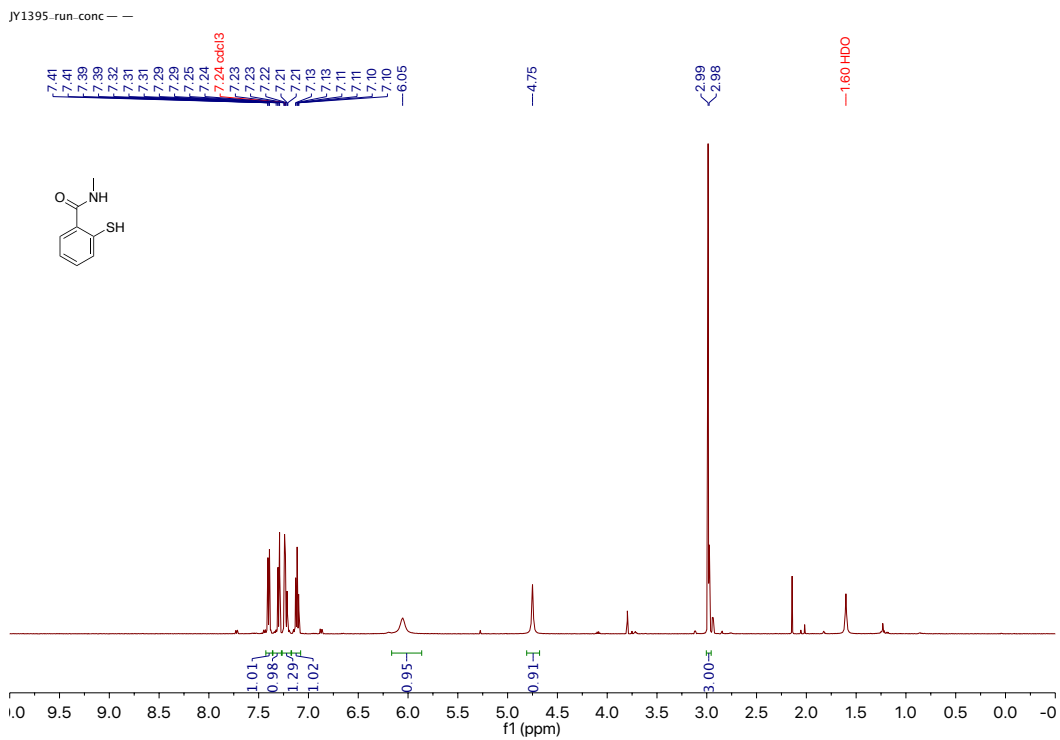
^{13}C NMR spectrum of (2,4-dimethylphenyl)(phenyl)sulfane (36)



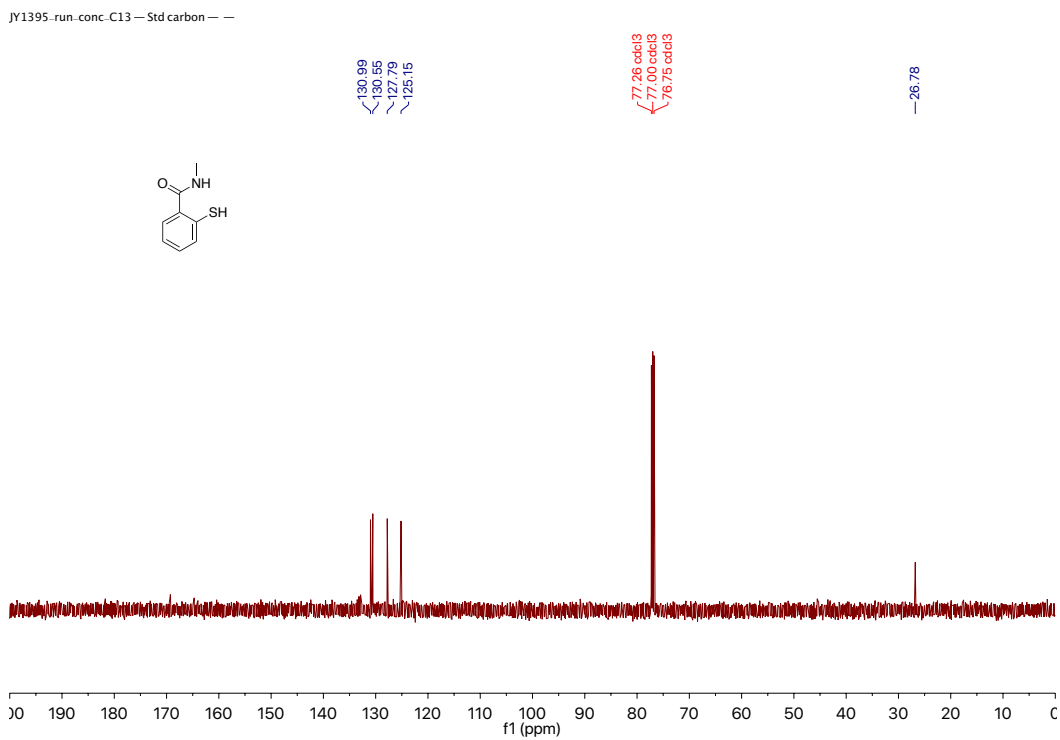
¹H NMR spectrum of mesityl(phenyl)sulfane (36)



¹³C NMR spectrum of mesityl(phenyl)sulfane (36)

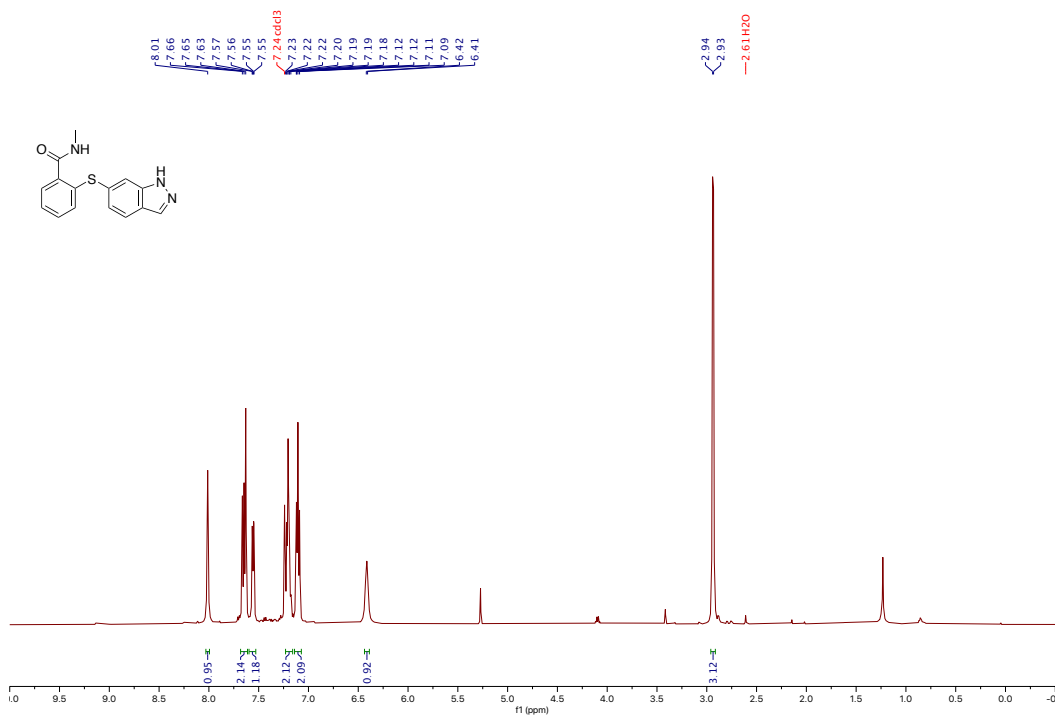


¹H NMR spectrum of 2-mercapto-*N*-methylbenzamide (39)



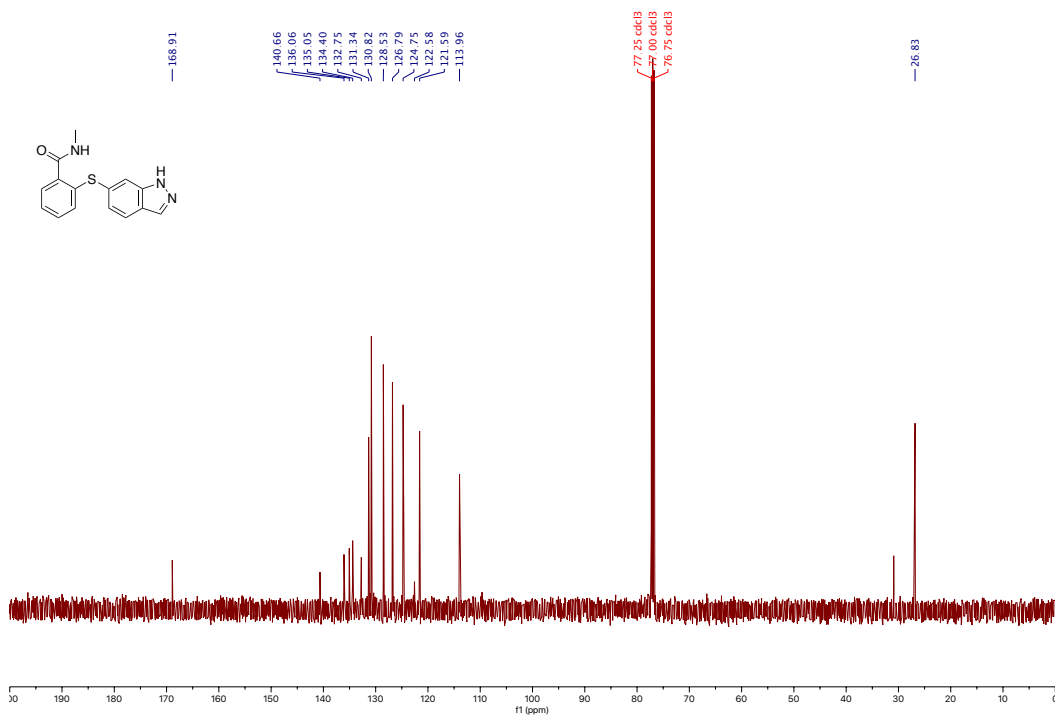
¹³C NMR spectrum of 2-mercapto-*N*-methylbenzamide (39)

JY1445-run --



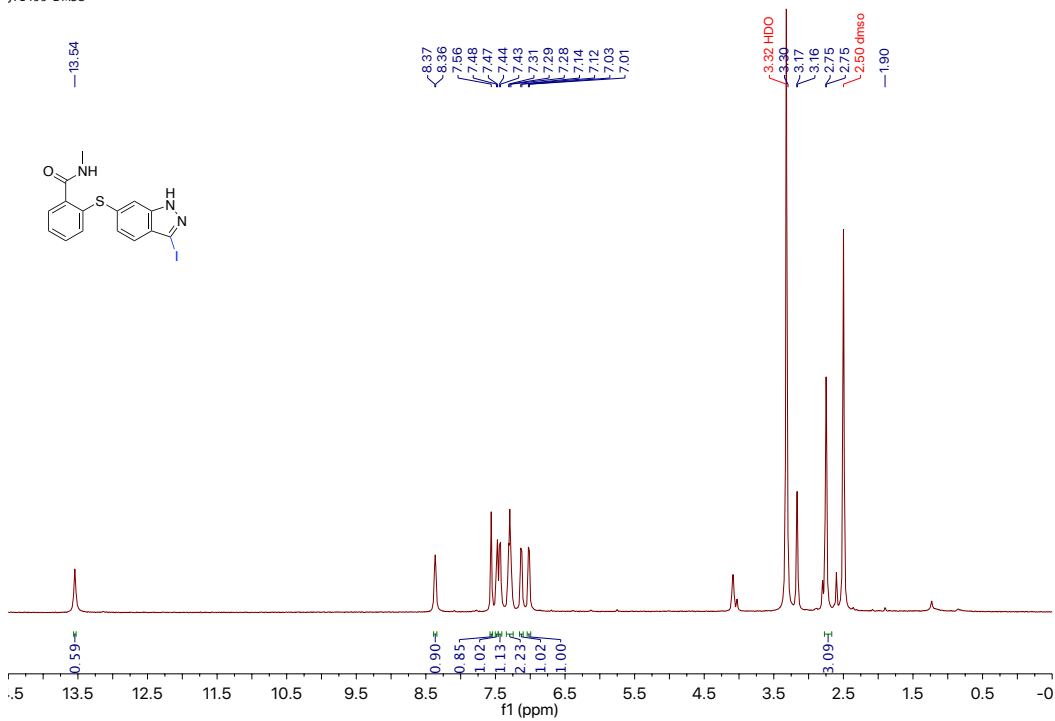
¹H NMR spectrum of 2-((1H-indazol-6-yl)thio)-N-methylbenzamide (41)

JY1445-run.C13—Std carbon --



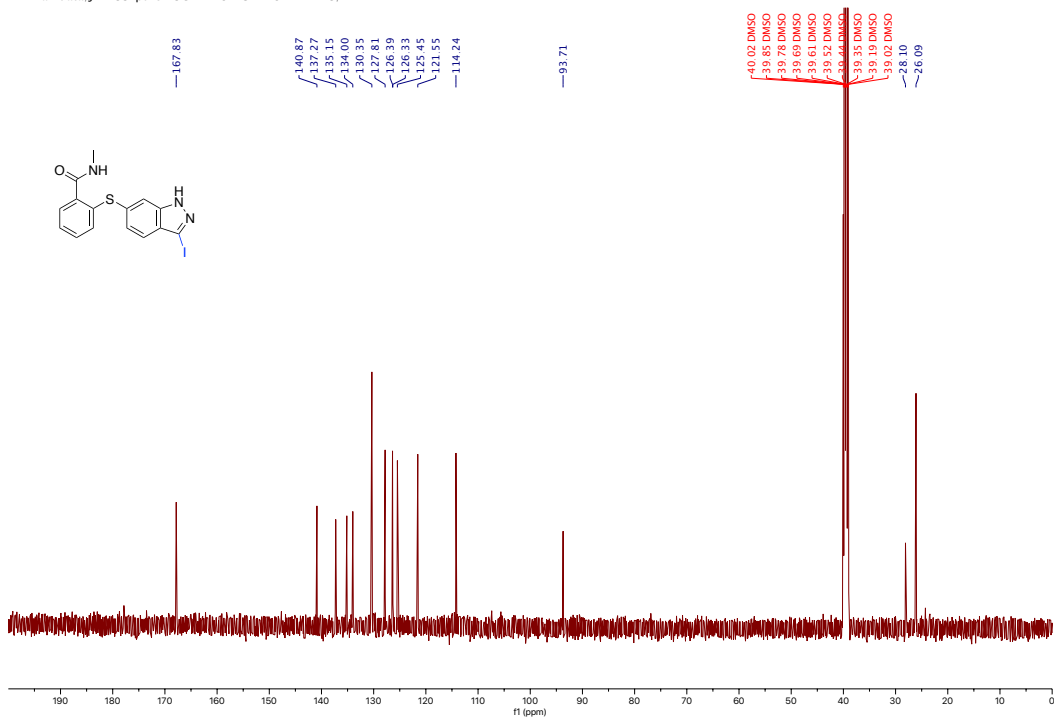
¹³C NMR spectrum of 2-((1H-indazol-6-yl)thio)-N-methylbenzamide (41)

JY1455.DMSO --

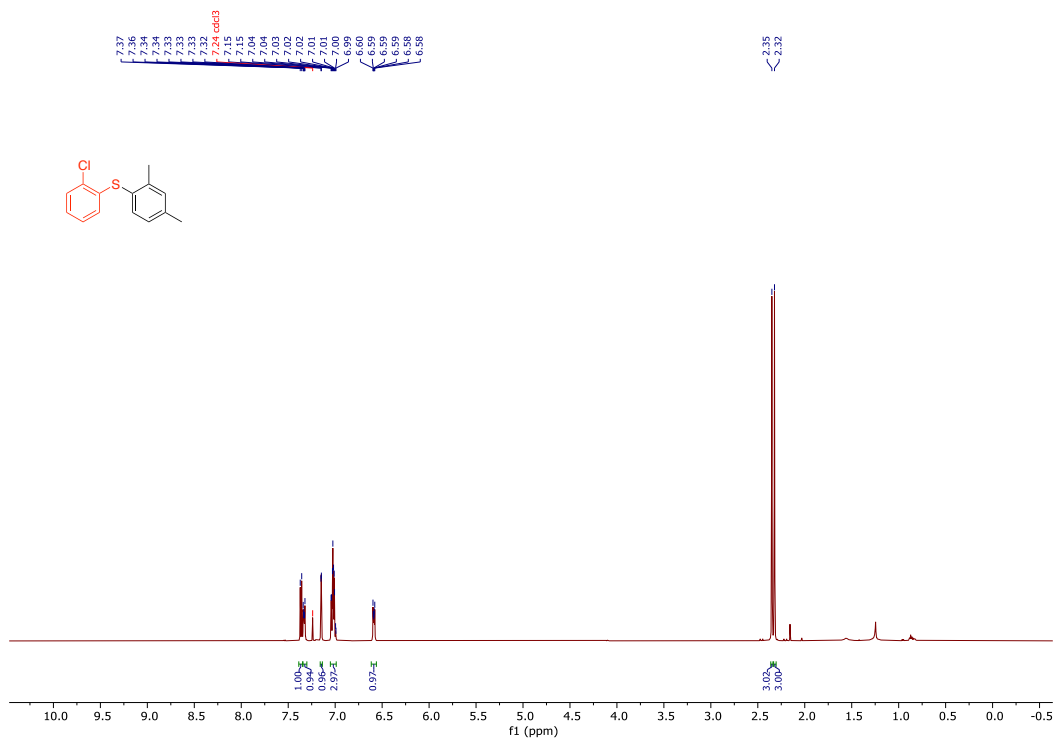


¹H NMR spectrum of 2-((3-iodo-1H-indazol-6-yl)thio)-N-methylbenzamide (42)

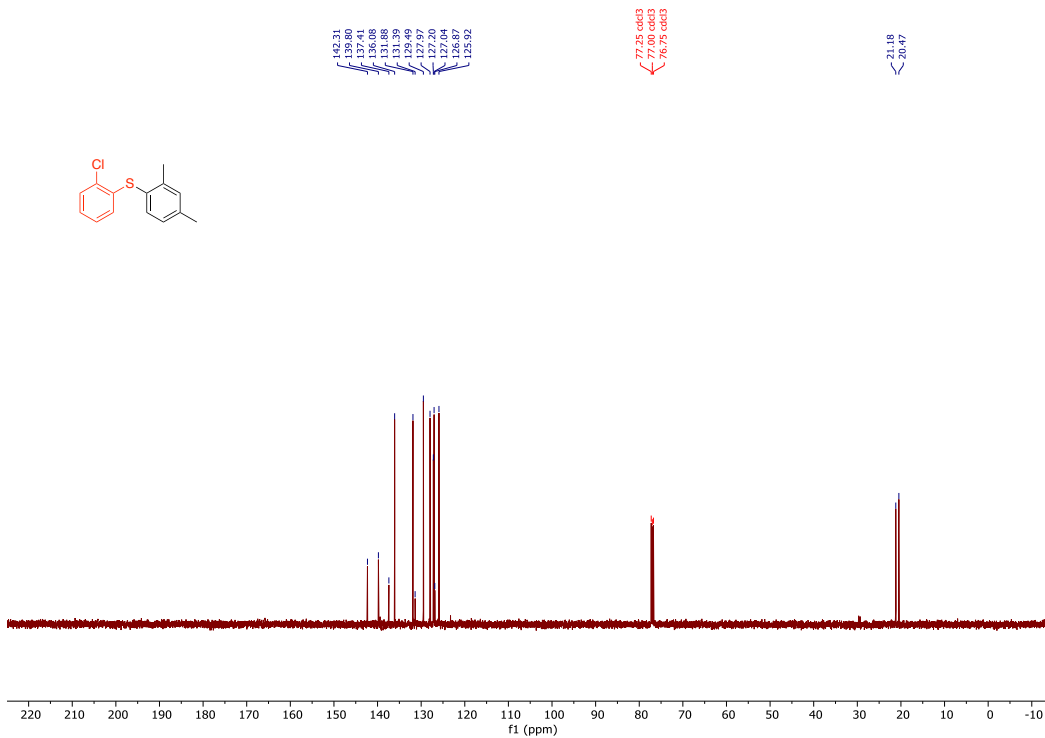
NMR raw data /JY1455.pure.13C -- PRODIGY PROBE -- 1H S/N



¹³C NMR spectrum of 2-((3-iodo-1H-indazol-6-yl)thio)-N-methylbenzamide (42)

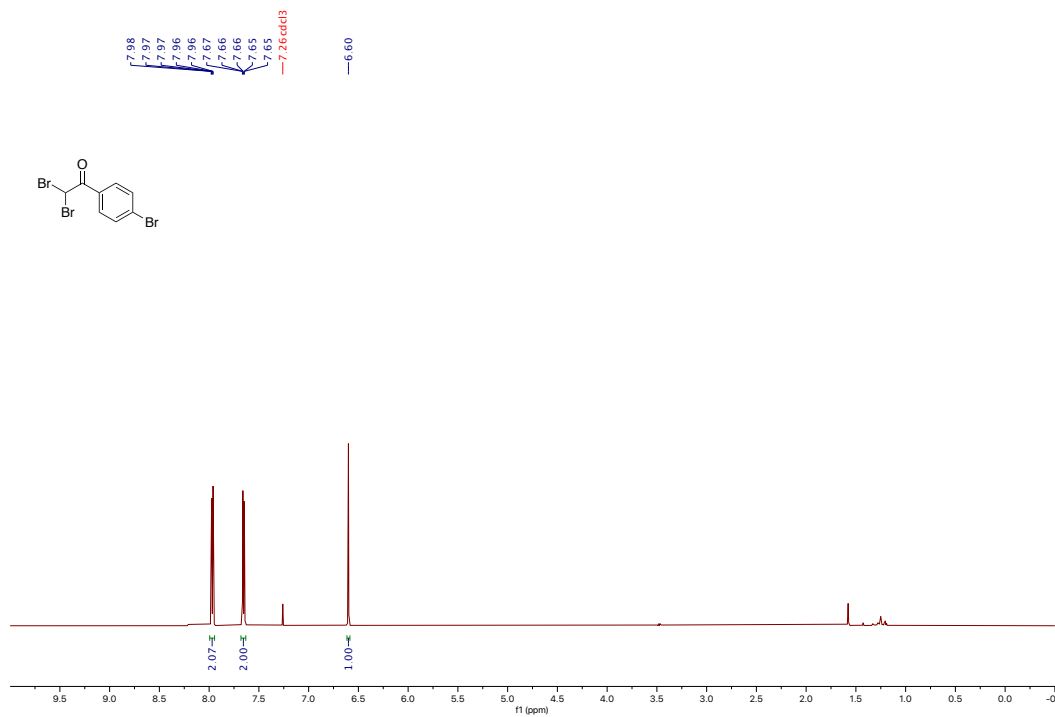


¹H NMR spectrum of (2-chlorophenyl)(2,4-dimethylphenyl)sulfane (46)



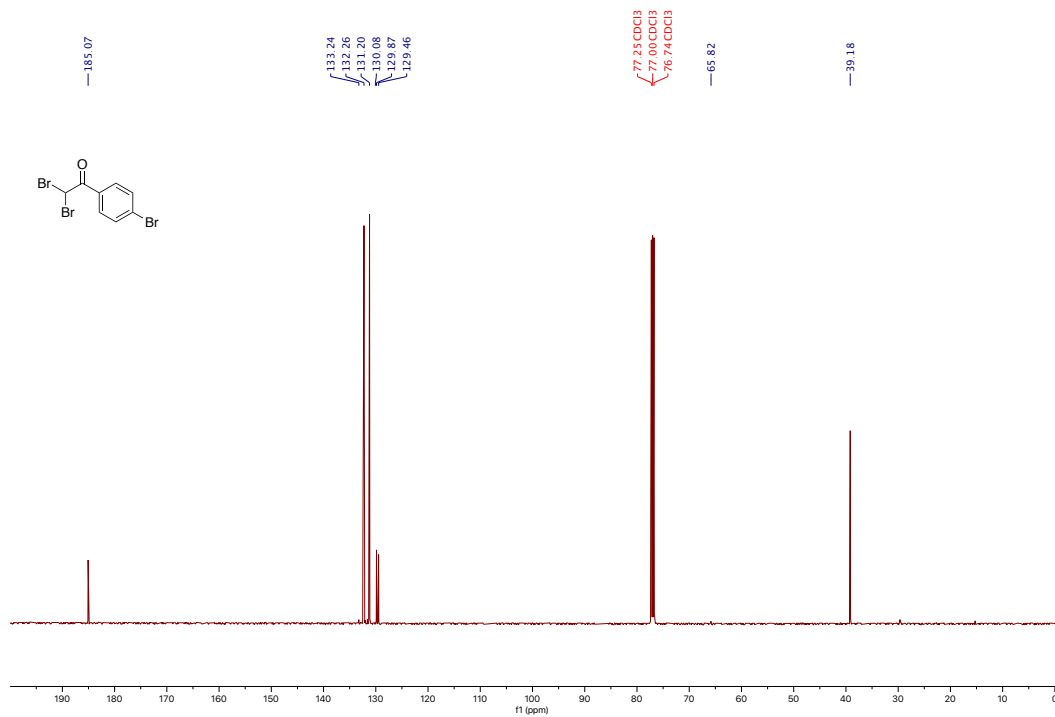
¹³C NMR spectrum of (2-chlorophenyl)(2,4-dimethylphenyl)sulfane (46)

JY1725-run3 --



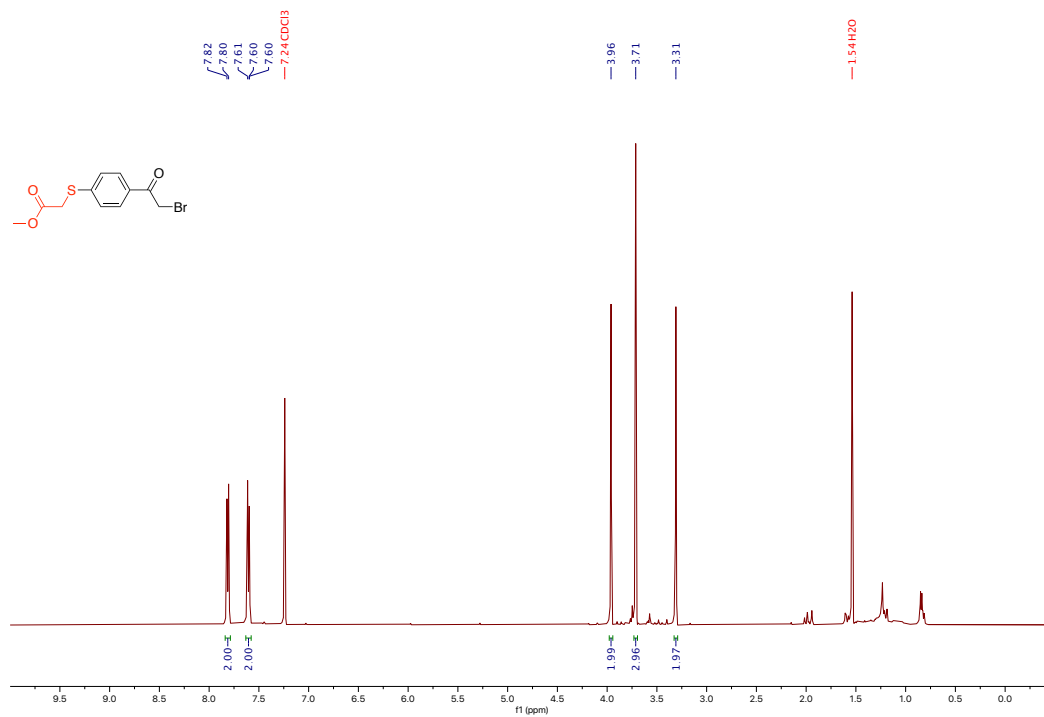
¹H NMR spectrum of **2,2-dibromo-1-(4-bromophenyl)ethan-1-one (49)**

JY1725-run3.C13.11.fid --



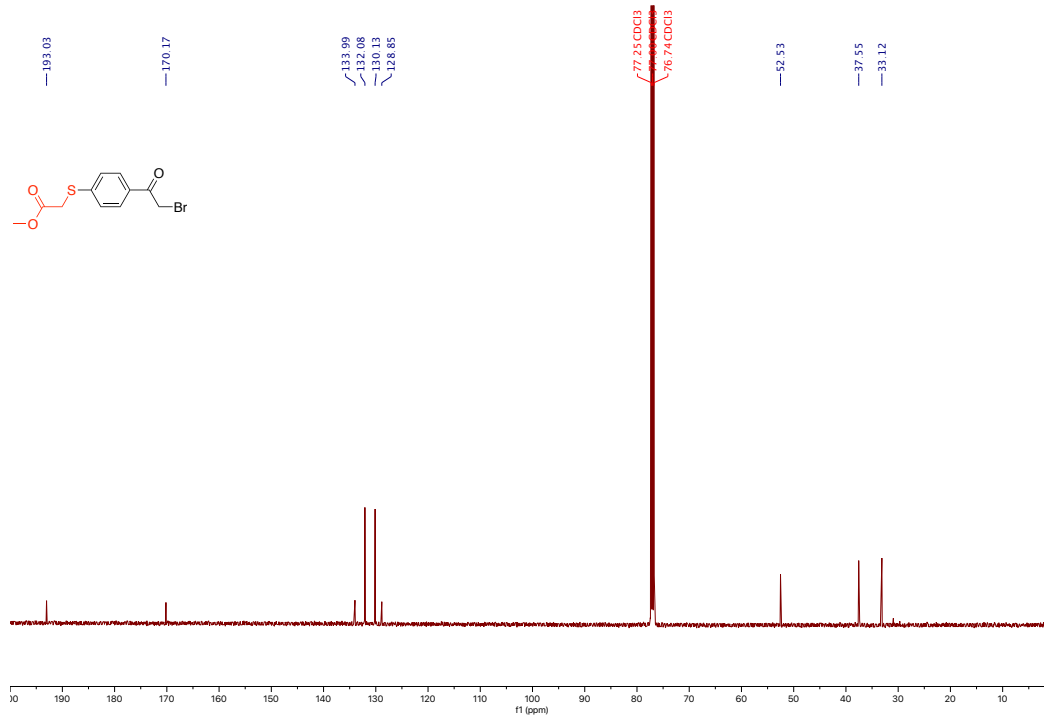
¹³C NMR spectrum of **2,2-dibromo-1-(4-bromophenyl)ethan-1-one (49)**

JY1711-run11 10.fid



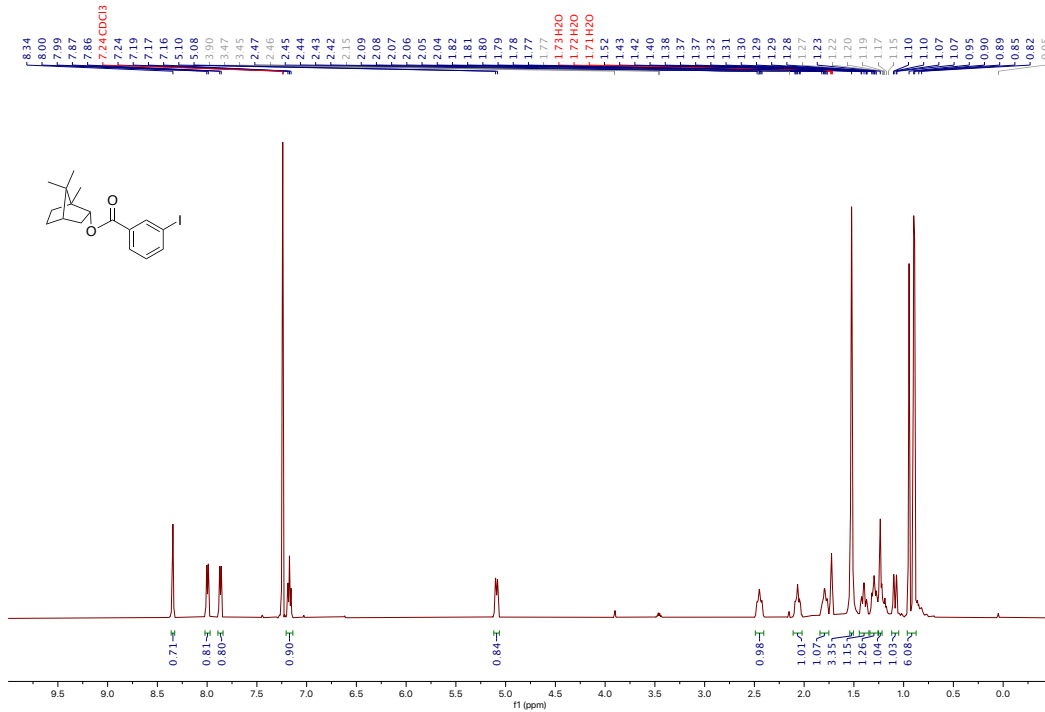
¹H NMR spectrum of methyl 2-((4-(2-bromoacetyl)phenyl)thio)acetate (50)

JY1711-run11.C13 10.fid



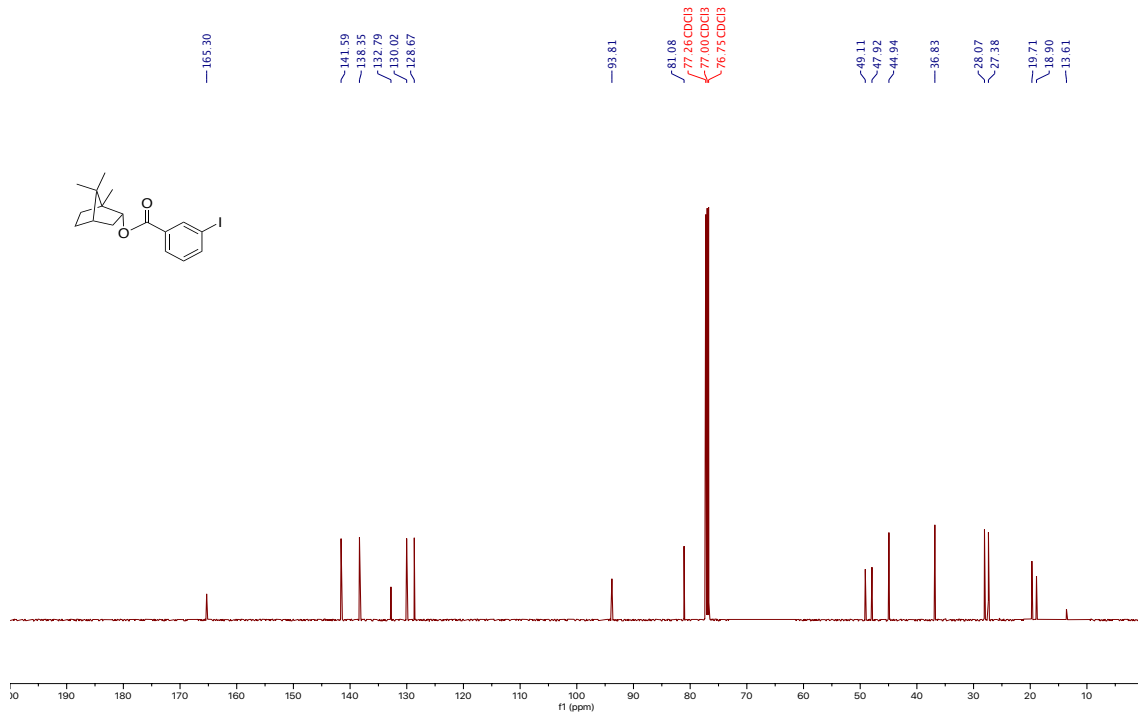
¹³C NMR spectrum of methyl 2-((4-(2-bromoacetyl)phenyl)thio)acetate (50)

JY1546-run.10.fid



¹H NMR spectrum of (1*S*,2*R*,4*S*)-1,7,7-trimethylbicyclo[2.2.1]heptan-2-yl 3-iodobenzoate

JY1549-run.C13.10.fid



¹³C NMR spectrum of (1*S*,2*R*,4*S*)-1,7,7-trimethylbicyclo[2.2.1]heptan-2-yl 3-iodobenzoate

2. Impact of Aqueous Micellar Media on Biocatalytic Transformations Involving Transaminase; Applications to Chemoenzymatic Catalysis

Reproduced with permission from Dussart-Gautheret, J.; Yu, J.; Ganesh, K.; Rajendra, G.; Gallou, F.; Lipshutz, B. H. Impact of Aqueous Micellar Media on Biocatalytic Transformations Involving Transaminase (ATA); Applications to Chemoenzymatic Catalysis. Preprint at <https://doi.org/10.21203/rs.3.rs-1409444/v1> (accessed 2022-05-26)

2.1. Background and introduction

The predominance of chiral amines in today's pharmaceutical market and pipeline is a driving force for developing chemocatalysis and biocatalysis to manufacture chiral intermediates using stereocontrolled asymmetric processes at a lower cost. The value of chiral molecule synthesis was boosted after the US Food and Drug Administration (FDA) announced a policy to govern the development of new stereoisomeric drugs in 1992 since disclosing that different interactions between the enantiomers with bioreceptors could result in distinctive biological responses.¹ According to statistics, at least one chiral amine component was found in almost 20% of the top 200 small molecule medications marketed in 2020; examples are shown in **Figure 1**.

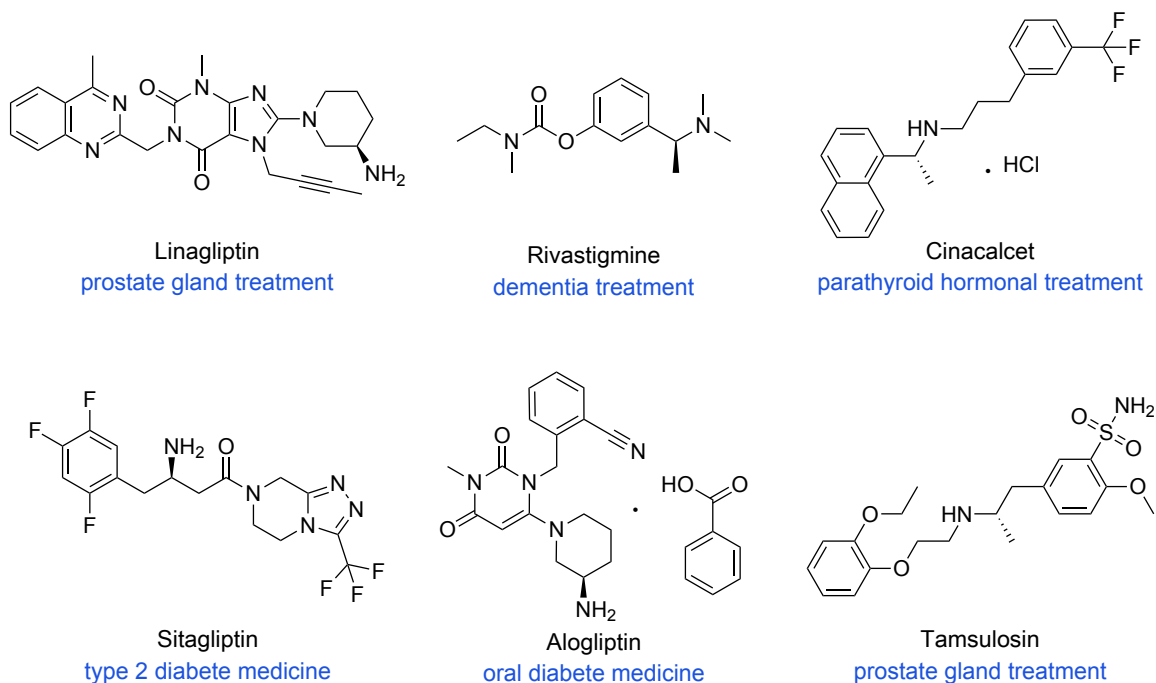


Figure 1. Selected common pharmaceuticals bearing a nonracemic amine

There are numerous well-established methods for amine synthesis, most of which involve the coupling of a carbonyl group with an amine. Chemocatalytic approaches commonly rely on metal-catalyzed asymmetric transfer hydrogenation (ATH) of a pre-formed imine from a ketone (**Figure 2**, top).^{2,3} In the past 30 years, several effective catalytic systems have been reported utilizing transition metals, such as Ir, Ti, Rh, Pd, Ru, and Au.⁴ This approach, however, is often hampered by the instability of particular imines, poor enantiocontrol caused by imine-enamine tautomerization, and *E/Z* acyclic imine interconversion.⁵ Alternatively, direct asymmetric reductive amination (DARA) of carbonyl compounds with transition metal hydrides has emerged as a simple way to obtain enantiomerically enriched amines, but it remains difficult, especially for heteroaryl ketones (**Figure 2**, bottom).^{6,7,8} Moreover, both methods require moderate-to-high pressure of hydrogen gas and hazardous organic solvents, while use of rare-earth transition metals might contaminate the targeted product(s) owing to the high loadings oftentimes used, which requires further product purification.

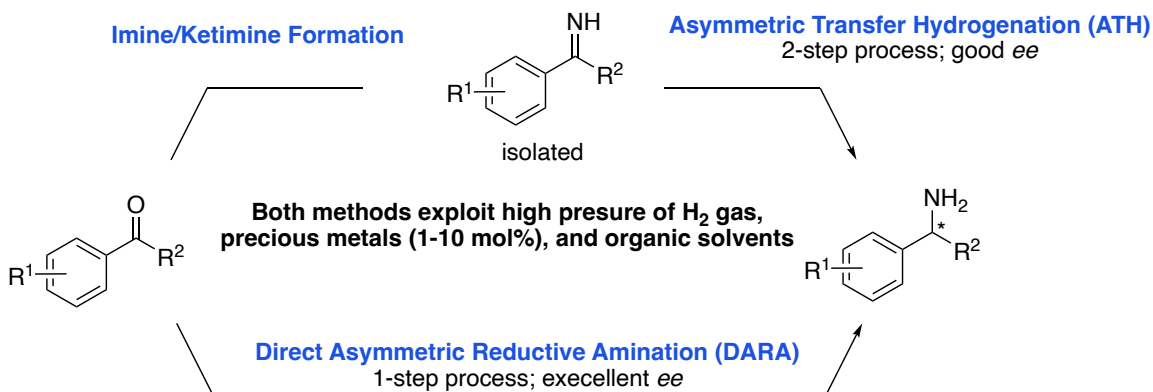


Figure 2. Comparison of ATH and DARA

ee: enantiomeric excess.

Over the past ten years, scientific advancements have established biocatalysis as a practical and environmentally friendly substitute to traditional metallo- and organo-catalysis in chemical synthesis.⁹ Not surprisingly, considering the Nobel Prize in this area having been awarded in 2018, biocatalysis (along with chemocatalysis; *i.e.*, chemoenzymatic catalysis) *en route* to various chiral compounds has grown in popularity.^{10,11} Among the many enzymes in use, transaminases have been identified as suitable and convenient green catalysts for producing amines. The most prominent example utilizing a transaminase in an industrial application was demonstrated in the production of the antidiabetic sitagliptin (Januvia/Janumets; see **Figure 3**), where scientists from Merck and Codexis evolved ATA-117 through multiple rounds of mutagenesis.¹² The enzymatic route led to an improved yield, greater enantioselectivity, and favorable green metrics compared to the traditional Rh-catalyzed asymmetric hydrogenation.¹³

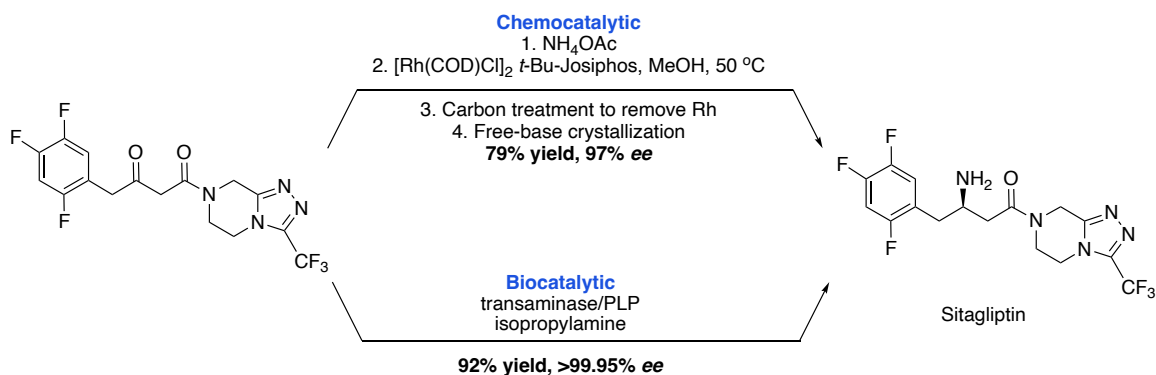


Figure 3. Comparison of chemocatalytic and biocatalytic processes en route to sitagliptin

While directed evolution has been recognized as one of the main ways for improving enzyme performance, investigation of the enhanced activities of readily available enzymes in aqueous micellar solutions is well-worth pursuing, providing a more facile way to

increase the extent of conversion. Previous research had shown that amphiphiles induce a “reservoir effect”, in which the presence of the micelles positively influenced the result of enzymatic processes involving enzymes such as KRED, ERED, and lipase.^{14,15,16} The micelles function as a solubilizing medium and an alternative location for water-insoluble products from enzymatic catalysis, resulting in faster reaction rates and less pronounced enzymatic inhibition. Anticipating the additional role of the reservoir effect, exploration of such an effect in the transamination of ketones in the presence of isopropylamine was studied.

2.2. Reaction mechanism of ATA

Transaminases, also known as aminotransferases (ATA), are PLP (pyridoxal 5'-phosphate)-dependent enzymes. PLP, a cofactor employed by enzymes that catalyze the synthesis of amine derivatives, acts as the transient reservoir of the amino group.¹⁷ The transaminase catalyzed reaction consists of two half-reactions, as depicted in **Figure 4**. In the first half-reaction, the ϵ -amino group of the lysine residue active site forms a Schiff base with PLP and results in a stable enzyme–PLP complex generally called the internal aldimine. Subsequently, the amine donor, isopropylamine, replaces the lysine residue in the internal aldimine, forming an external aldimine that resides in the enzyme pocket. Following proton shifts, PMP results along with acetone as a byproduct. In the second half-reaction, the amino group present in PMP (pyridoxamine 5'-phosphate) is transferred to an amine acceptor (*i.e.* ketone substrate), yielding a ketimine intermediate which is finally hydrolyzed to the corresponding amine and PLP, completing the catalytic cycle.¹⁸

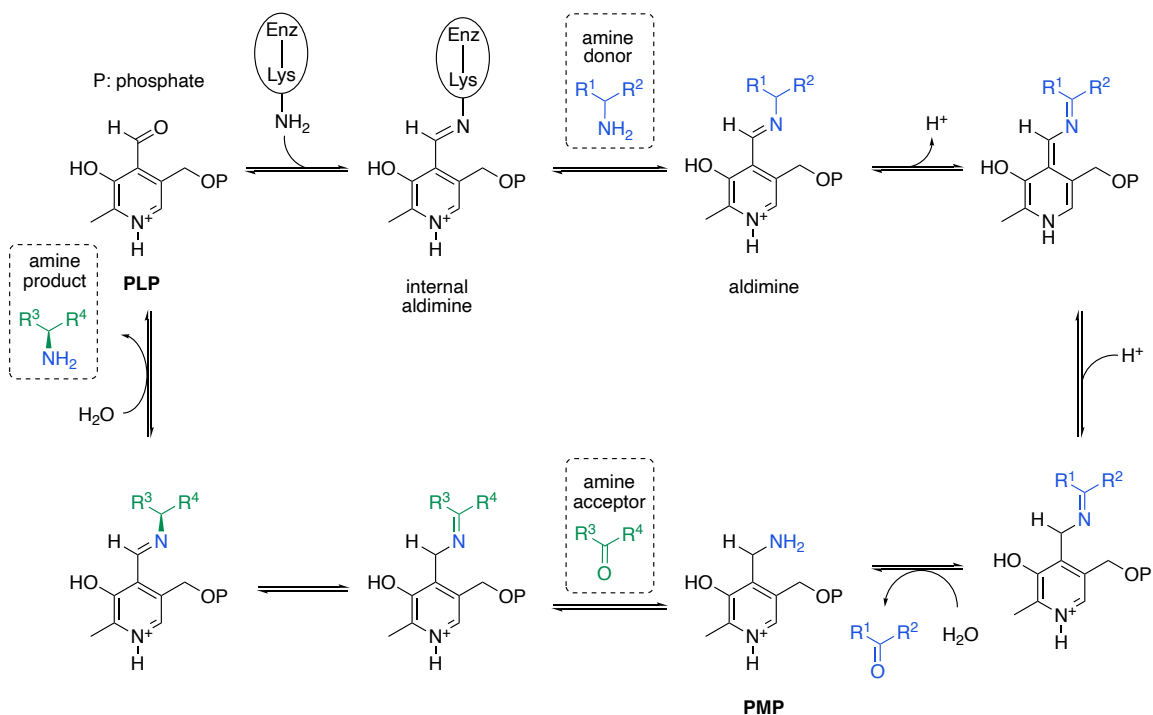


Figure 4. A representation of the transaminase mechanism showing key intermediates

2.3. Results and discussion

2.3.1. Screening of transaminase

The initial screening consisted of a survey of various ATAs as well as suitable pH and reaction temperature. According to the results from these tests, ATA-025, ATA-254, ATA-256, and ATA-260 outperformed all other ATAs present in the kit from Codexis (**Figure 5**). Over the course of ATA evaluation, these four ATAs were found to be the most responsive to a variety of substrate types.

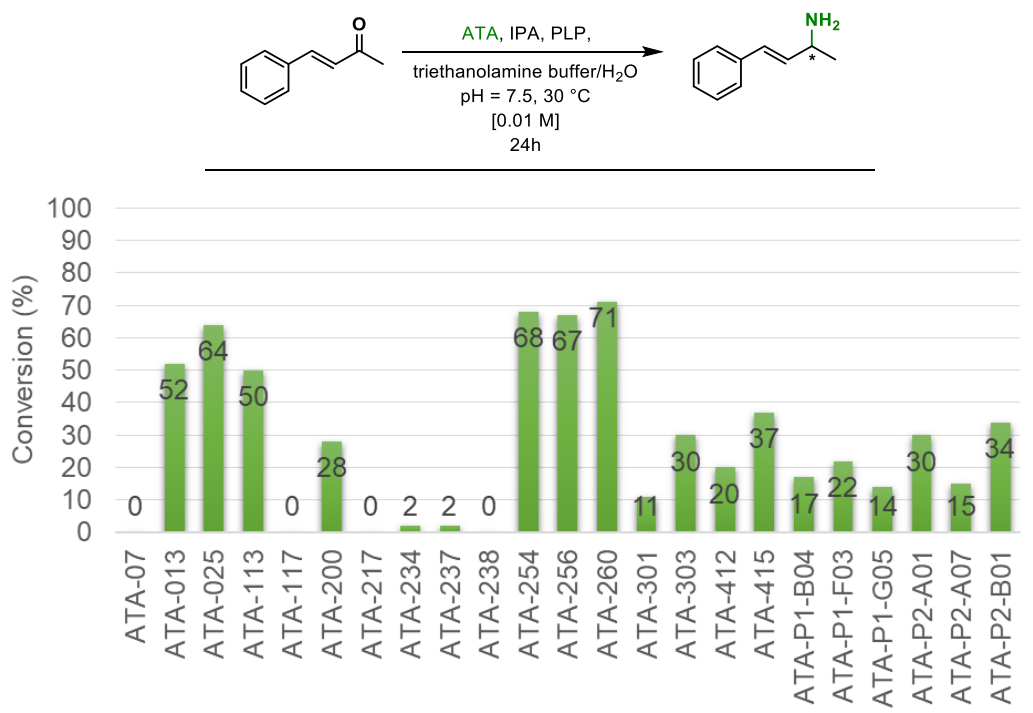
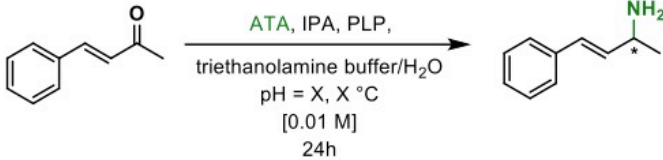


Figure 5. ATA screening with (*E*)-4-phenylbut-3-en-2-one. Reaction conditions: ketone substrate (0.01 mmol), isopropyl amine (IPA) (1.3 M), PLP (1.0 mM), ATA (1 mg), triethanolamine (TEA) buffer (pH = 7.5) was used. Conversions were determined by ¹H NMR.

Once the most effective ATAs were identified, screening of physiological temperature and pH was carried out to determine the optimum reaction conditions. Using a vial containing a magnetic stir bar, reactions were done on a millimole scale, rather than using the conventional Eppendorf and shaker on a micromole scale. It was observed that raising both temperature and pH favored ATA-025 and ATA-254. Furthermore, ATA-260 requires a higher temperature, whereas ATA-256 is not affected by temperature or change in pH (see **Table 1**). Overall, the best results were obtained when the temperature was set to 50 °C, and the pH was set to 8.5.



pH	Temp. (°C)	ATA-025	ATA-254	ATA-256	ATA-260
7.5	30	64%	68%	67%	71%
	40	64%	70%	69%	70%
	50	69%	70%	69%	75%
8.5	30	64%	70%	71%	61%
	40	72%	74%	70%	67%
	50	75%	76%	71%	75%

Table 1. Temperature and pH screening with ATAs

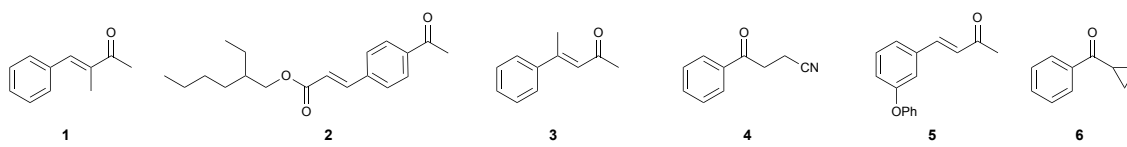
Reaction conditions: ketone substrate (0.01 mmol), isopropylamine (IPA) (1.3 M), PLP (1.0 mM), ATA (1 mg), triethanolamine (TEA) buffer was used. Conversions were determined by ^1H NMR.

The optimized conditions (in early screenings) examined for several representative ketones are listed in **Table 2**. Several surfactants were evaluated, including TPGS-750-M, solutol, PTS-600, Brij 30, Tween 60, and Triton X-100, leading to a number of unprecedented observations. First, as seen with educt **1**, TPGS-750-M, Solutol, Brij 30, and Triton X-100 gave comparable results, with each improving conversion by *ca.* 20% relative to that observed in buffer alone. However, considering the similarity of TPGS-750-M to others, it was surprising that PTS-600 *reduced* conversion by 13%. For substrates **2**, **3**, and **4**, 2 wt % *solutol* consistently provided the greatest extent of conversion. Conversely, unlike with KRED, increasing the amount of solutol from 2 wt % to 4 wt % and 6 wt % did not improve the reaction outcome. Similarly, in the case of enone **5**, solutol was the most effective, albeit in this case, 4 wt % percent yielded the best results. A comparable level of conversion was also achieved with 2 wt % TPGS-750-M. The behavior of cyclopropyl ketone **6** proved

to be striking; the addition of any surfactant into the buffered medium led to a *decrease* in the extent of conversion from 63% to *ca.* 35%, with no clear explanation at this time.

Previously, TPGS-750-M was the surfactant of choice in all cases (*i.e.*, KREDs, EREDs, and lipases). However, the effectiveness of ATAs appears to be surfactant-dependent, indicative of the need to screen various types in anticipation of finding a “match” that maximizes levels of educt-to-product conversion.

Table 2. Screening of the aqueous reaction medium involving various ATAs



Substrate	Enzyme	Buffer only	2 wt % TPGS-750-M/buffer	2 wt % Solutol/buffer	4 wt % Solutol/buffer	6 wt % Solutol/buffer	2 wt % PTS600/buffer	2 wt % Brij30/buffer	2 wt % Triton X-100/buffer
1	ATA-256	26	46 (56) ^a	45	48	45	13	48	44
2	ATA-256	46	52 (55) ^a	68	59	54	52	38	59
3	ATA-260	75	82	83	80	80	79	79	70
4	ATA-256	75	72	84	72	72	70	70	71
5	ATA-260	19	35	27	38	29	25	28	24
6	ATA-025	63	38	40	38	39	37	35	32

Reaction conditions: ketone substrate (0.01 mmol), isopropyl amine (IPA) (1.3 M), PLP (1.0 mM), ATA (1 mg), triethanolamine (TEA) buffer (pH = 8.5) at 50 °C was used. Conversions were determined by ¹H NMR. ^a TPGS-750-M (6 wt %)/triethanolamine (TEA) buffer was used.

2.3.2. Time course study of transaminase in micellar solution

Consistent with previously reported enzymatic reactions the reaction profile of six methyl ketones, each with structurally unique features, showed a greater extent of conversion in the presence of small amounts of surfactant than in buffer alone (**Figure 6**). However, the impact was not as dramatic as that found with other enzymes (*i.e.*, sometimes up to >60%).¹⁶

The highly functionalized biaryl **8** shown in **Figure 6A** raised the conversion from 67% to 87% simply due to the presence of 2 wt % TPGS-750-M in the aqueous buffered medium. In the case of *p*-CF₃-substituted acetophenone **9**, as illustrated in **Figure 6B**, the reaction in 2 wt % TPGS-750-M gave *ca.* 10% improvement throughout the course of reaction. For enone **11** in **Figure 6C**, relatively little difference (3-5%) was seen between the buffer alone and in 2 wt % TPGS-750-M, whereas Tween 60 boosted this difference to 7–10%, culminating at 85% conversion *vs.* 75% in buffer alone. The addition of a methyl group to the α -position of this enone (as shown in **Figure 6D**) resulted in drastically changed catalysis, with the differential increasing to 20% after only one hour. In this case, 2 wt % solutol provided the most significant outcome.¹⁹

Similar to the effect reported with KRED, the highly lipophilic ketone **2** shown in **Figure 6E** was most receptive to the presence of TPGS-750-M in the aqueous medium. Accordingly, 2 wt % TPGS-750-M afforded an enhancement of 19% over 24 hours (*i.e.*, from 22 to 41%), increasing the surfactant concentration to 6 wt %, further raising to 56% in the extent of conversion. In the case of *p*-iodoacetophenone (**Figure 6F**) without any surfactant, the reaction peaks after *ca.* three hours and then begins to reverse over the 24-hour time frame dropping the conversion from 78 to 26%. However, in the presence of

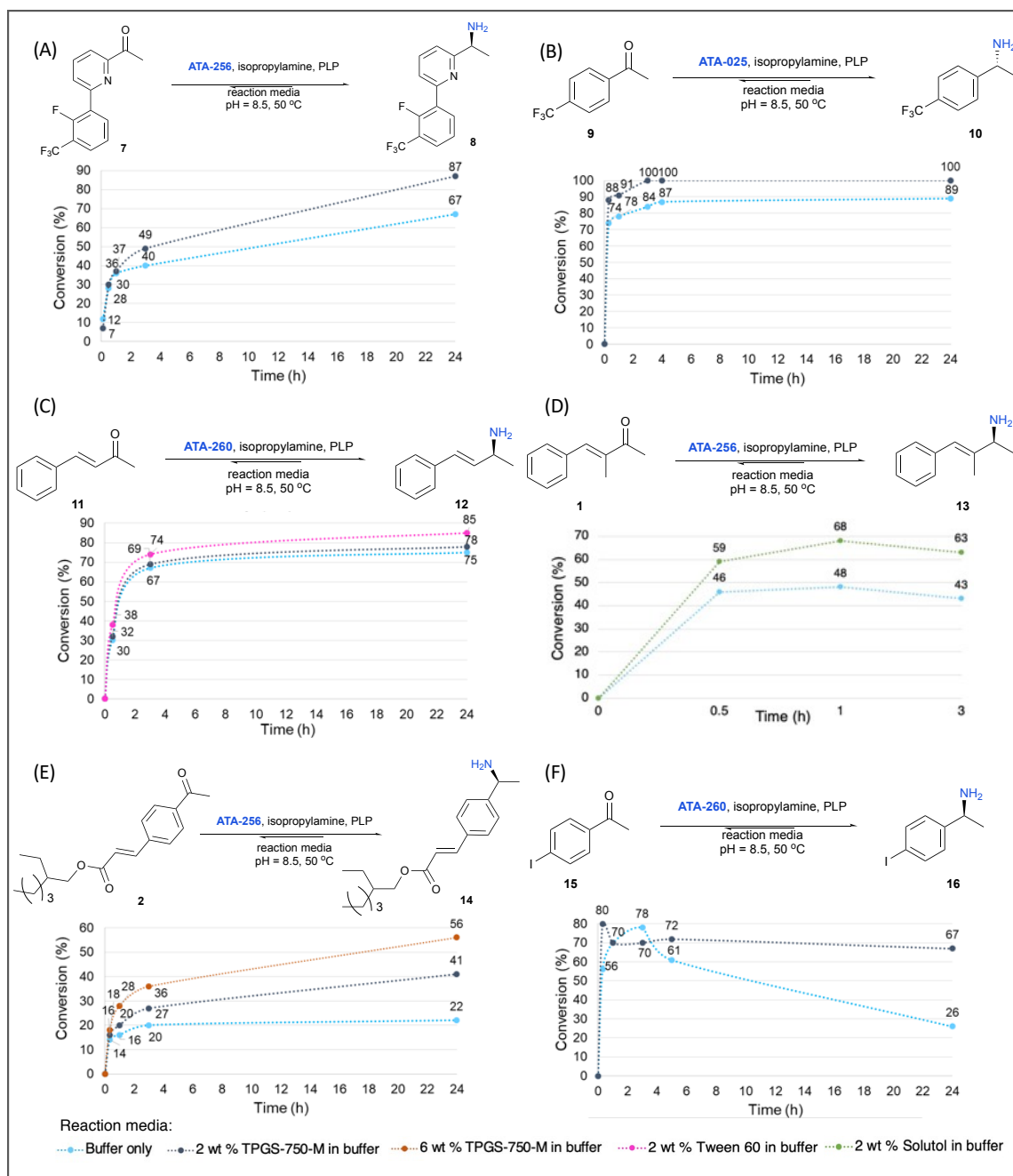


Figure 6. Time-course study of reductive aminations using an ATA. Reaction conditions: ketone substrate (0.01 mmol), isopropyl amine (IPA) (1.3 M), PLP (1.0 mM), ATA (1 mg), triethanolamine (TEA) buffer (pH = 8.5) at 50 °C was used. Conversions were determined by ^1H NMR.

TPGS-750-M, the initial rapid conversion (80%) only drops to 70% over the same 24-hour period. Since the enzymes are water-soluble, the product amine may localize within the micellar array, and thereby is unavailable for the enzyme to convert back to the starting ketone.

2.3.3. Substrate scope of transamination in aqueous micellar media

Representative examples of asymmetric transamination associated with various ATAs benefiting from micellar buffered media were explored, as shown in **Figure 7**. Rather than screening surfactants for every substrate, and since the differences between other surfactants and 2 wt % TPGS-750-M were not huge (*i.e.*, *ca.* 20%), TPGS-750-M was selected. Acetophenone-containing substrates were all readily accommodated to form nonracemic primary amine products regardless of the substituent and location on the ring (**10**, **14**, **16–20**), including highly lipophilic cases (**14** and **19**) and for one case bearing *ortho*-substitution (**20**). Nitrogen-containing cyclic compounds bearing a carbonyl group, such as a Cbz-protected 4-oxoazepane (**21**), *N*-Boc (**22**) and *N*-Cbz-protected (**23**) 3-pyrrolidinones, afforded the corresponding amines in reasonable yields and, except for **21**, high *ee*'s. Enones proceeded smoothly in this asymmetric reductive amination to yield allylic amines **12** and **13**. Propiophenone appeared to be no obstacle to this asymmetric reductive amination, giving the expected nonracemic amine **24**. Moreover, an array of heteroaromatic ring-containing substrates, such as acetylated furan (**25**) and substituted acylpyridines (**8** and **26**), led to good yields of the anticipated products. As compared to a Ru/BINAP catalyst described in recent literature, acylated 2-bromopyridine can be

converted to the same nonracemic primary amine **26** under high pressures (8 atm H₂), organic solvents (THF), and high temperatures (90 °C), and high temperatures (90 °C), and may require further processing due to residual metal in the products given the amounts of Ru-containing catalyst being used.²⁰ The results suggest that biocatalysts provide a more environmentally friendly option to access these valuable amine building blocks.

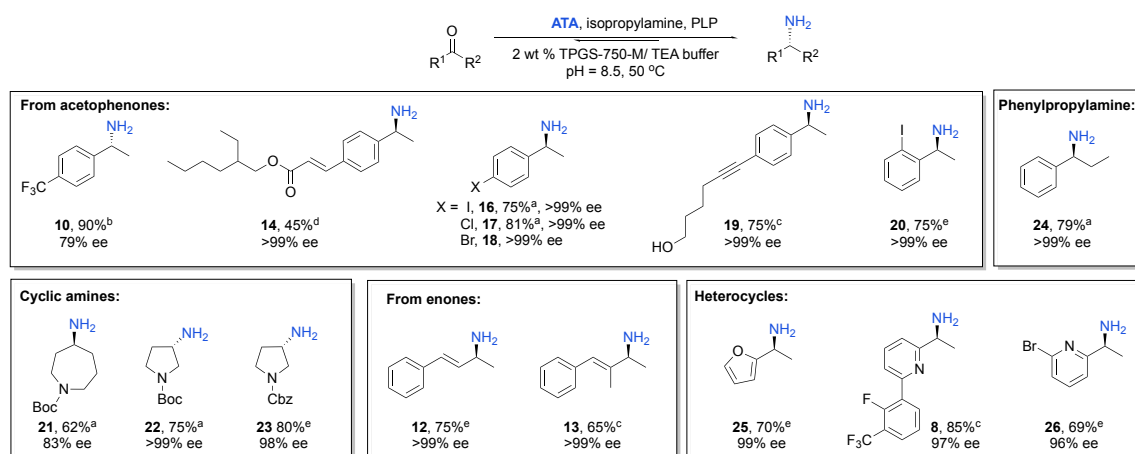


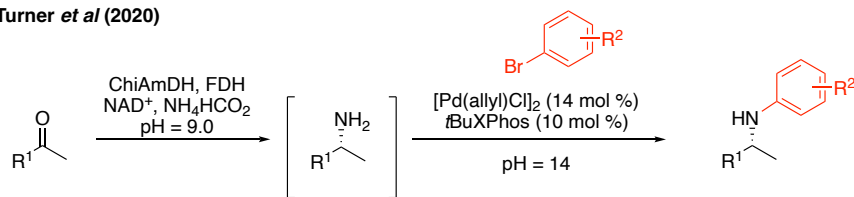
Figure 7. Substrate scope: ATA-catalyzed reductive aminations in TEA buffer (0.142 M) containing TPGS-750-M. Reactions were performed with 10.0 mM ketone substrate (0.1 mmol) in a 20 mL vial equipped with a magnetic stirrer. Isolated yields are shown. PLP: pyridoxal 5'-phosphate (co-factor). % ee was determined by chiral HPLC. ^aATA-260 was used; the product was isolated as a Cbz-protected (*S*)-amine; ^bATA-025 was used; the product was isolated as a Cbz-protected (*R*)-amine; ^cATA-256 was used; the product was isolated as a Cbz-protected (*S*)-amine; use of 6 wt % surfactant led to the same conversion. ^dATA-256 was used; the product was isolated as an Ac-protected (*S*)-amine; ^eATA-260 was used; the product was isolated as the (*S*)-amine.

2.3.4. Application: multistep transformations in one pot

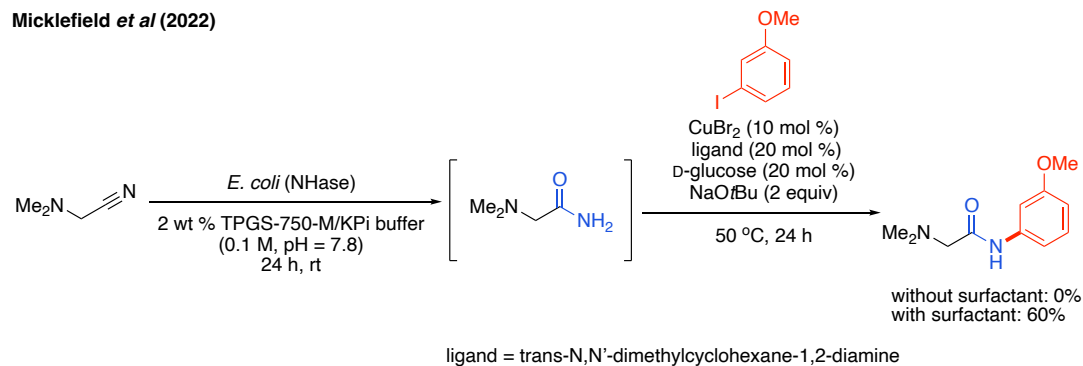
Producing a target molecule in a single reaction vessel represents one of the hallmarks of contemporary synthetic chemistry. Given that TPGS-750-M can now enable chemocatalysis as well as biocatalysis in water, telescoping both reactions in aqueous surfactant solutions will minimize the need for solvent exchange. As is characteristic of designer surfactant technology in water, a typical in-flask extraction of the aqueous reaction mixture to obtain the product is straightforward and routine.

Several recent literature successes in telescoping enzymatic processes using TPGS-750-M under aqueous micellar conditions have been shown; selected examples are shown in **Figure 8**. Turner *et al.* combined a variety of enantioselective biocatalysis processes leading to amine products (*e.g.*, using ChiAmDH, IRED, ATA) followed by Buchwald-Hartwig aminations²¹; Micklefield *et al.* also revealed TPGS-750-M led to a drastic enhancement in isolated yields of an initial NHase (*i.e.*, nitrile hydratase)-catalyzed reaction, followed by Cu-catalyzed *N*-arylation for aliphatic nitriles in the aqueous medium.²² Another example from Hastings *et al* showed that TPGS-750-M-aided 1-pot cascades were viable, coupling various classes of chemocatalysis (*e.g.*, Mizoroki-Heck cross-coupling, ring-closing metathesis, and olefin metathesis) with biocatalysis (*e.g.*, lipase and esterase).²³

Turner *et al* (2020)



Micklefield *et al* (2022)



Hastings *et al* (2022)

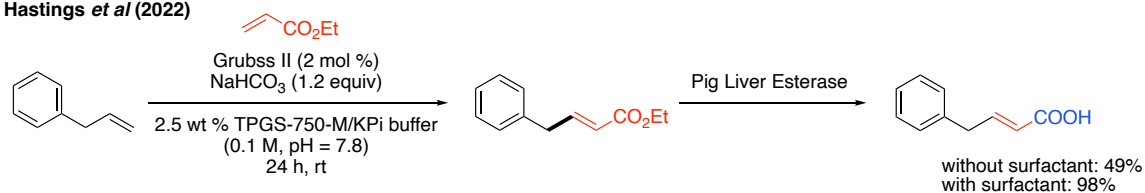


Figure 8. Selected examples from reported chemoenzymatic reactions in TPGS-750-M aqueous solution^{21,22,23}

2.3.5. Deracemization of racemic secondary alcohols to nonracemic primary amines

2.3.6. Literature on the synthesis of nonracemic primary amines from secondary alcohols with ammonia

As mentioned in the Introduction, nonracemic primary amines are remarkably useful intermediates for further derivatization in pharmaceuticals and agrochemicals. Preparing them from inexpensive alcohols is of particular interest to the industry. Popular ways for synthesizing primary amines from alcohols include the “borrowing hydrogen” (BH) methodology, also known as “hydrogen auto-transfer.”²⁴ The mechanism is described in **Figure 9a**. The alcohol is first dehydrogenated *in situ* to yield the corresponding ketone or aldehyde, then condensed with the amine. Subsequent metal-catalyzed hydrogenation of the resulting imine with the initially generated hydrogen produces the desired amine. Beller’s group developed an atom efficient BH process employing a Ru/CataCXiumPcy catalytic system to generate the racemic amine from secondary alcohols with ammonia, as shown in **Figure 9b**. This process was conducted under super-heated *t*-amyl alcohol with volatile ruthenium carbonyl, which implies a potential poison inhalation hazard.²⁵ And yet, several BH methods are available for amine synthesis, surprisingly, an enantioselective alcohol amination has not been reported, leaving the non-green options of chiral preparative HPLC as alternatives.

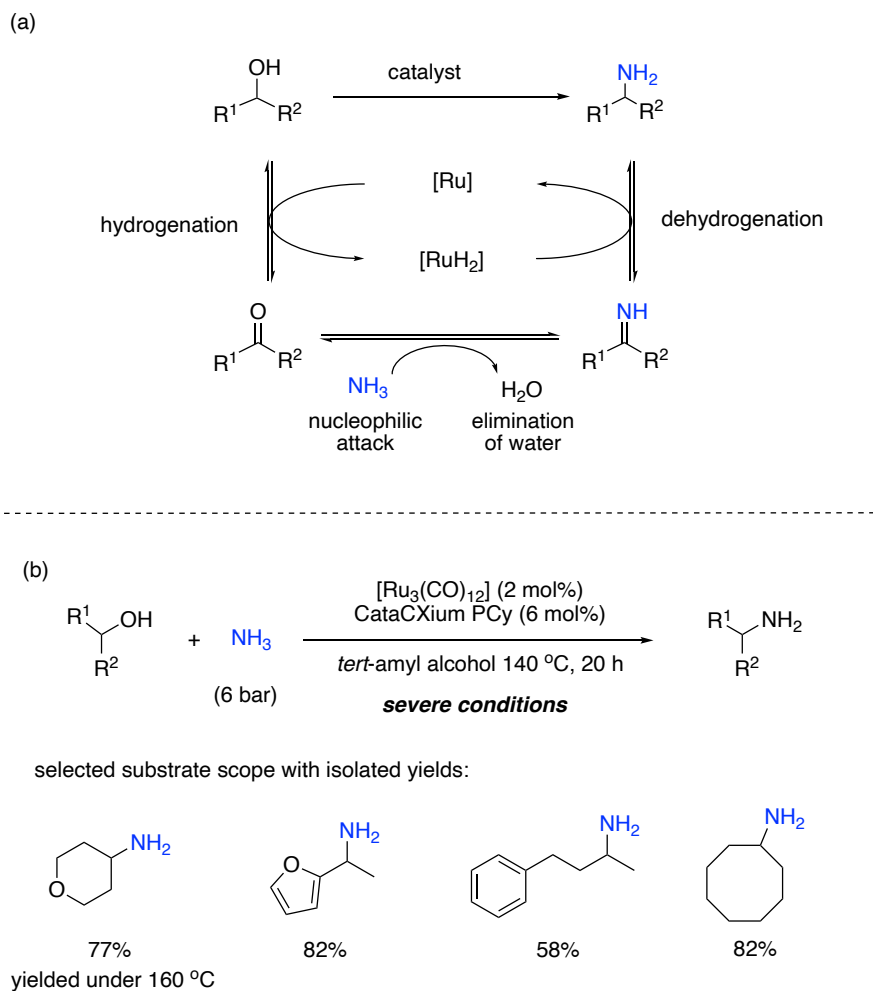


Figure 9. (a) Catalytic borrowing hydrogen process for the amination of alcohols with ammonia; (b) Amination of alcohols using Ru/CataCXiumPcy catalyst from Beller's group.²⁵

Due to biocatalysis's significant enantioselectivity, enzymes are compelling tools to synthesize primary amines. Classically, a kinetic resolution process results in a maximum 50% theoretical yield of the desired enantiomeric product, as only one of the two non-interconverting substrate enantiomers reacts with the chiral catalyst (**Figure 10a**). Conversely, a dynamic kinetic resolution (DKR) occurs if the substrate enantiomers undergo facile racemization, allowing a theoretical conversion of 100% to the desired

enantiopure product (**Figure 10b**). Extensive research has been done to achieve the equivalent reaction outcomes as offered via DKR.²⁶ The standard criteria for these sequences must guarantee that the conditions required for racemate epimerization do not have a detrimental influence on the enzyme's stability, structural integrity, and catalytic activity.

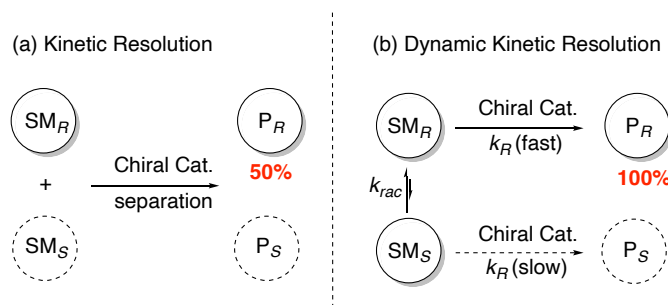


Figure 10. General scenarios for classical and dynamic kinetic resolutions

A dual enzyme-based cascade developed by Turner and coworkers, shown in **Figure 11a**, uses stereocomplementary alcohol dehydrogenases (ADHs) in conjunction with an amine dehydrogenase (AmDH) to convert both Prelog and anti-Prelog alcohols to amines.²⁷ However, only (*R*)-configured amines can be produced using this strategy, despite the time-consuming and challenging protein engineering process to identify the specific enzyme pairs to run concurrently. A more recent protein engineering study was conducted by Zhi *et al*, as shown in **Figure 11b**. An ambidextrous ADH oxidizes both enantiomers of the alcohols to give the prochiral ketone, which was subsequently converted to a (*S*)-amine by an ATA co-expressed in an *E. coli* system.²⁸ The possibility of producing (*R*)-amine was not addressed in the paper. Therefore, to freely generate either configured amine in a simple sequence remains an unfulfilled goal.

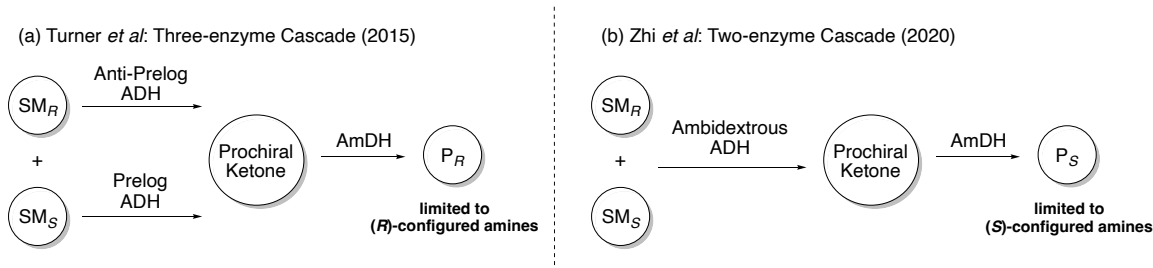
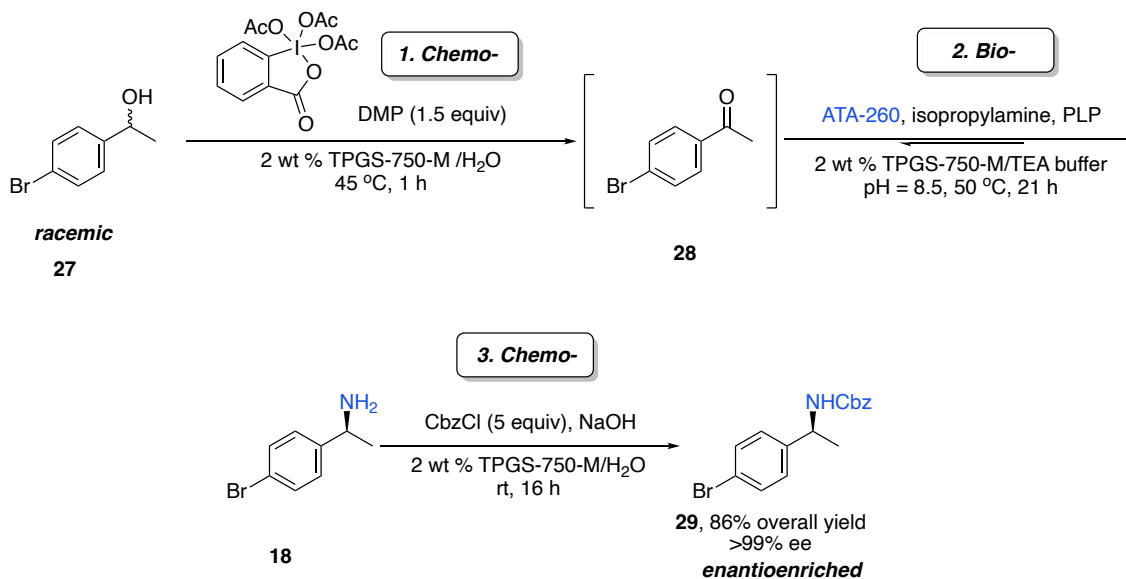


Figure 11. Deracemization of secondary alcohols to nonracemic primary amine in *E. coli* system^{27,28} (SM = secondary alcohol; P = primary amine).

2.3.7. 2-Step, 1-pot chemoenzymatic process to deracemize a secondary alcohol to a nonracemic primary amine

In a first approach to the one-pot deracemization of secondary alcohols, an unprecedented Dess-Martin periodinane (DMP) oxidation of a secondary alcohol to ketone in water was carried out. DMP was chosen over chromium- and DMSO-based oxidants due to its mild and highly chemoselective oxidizing characteristics, as well as its fast reaction rate. The oxidation of 1-(4-bromophenyl)ethanol **27** to the corresponding ketone **28** (**Scheme 1**) with 1.5 equivalent of DMP was accomplished cleanly and rapidly in 1 h. Without isolation, the reaction mixture was treated with transaminase and triethanolamine to afford nonracemic amine, demonstrating that the reduced form of DMP did not impede the biotransformation. After extraction and concentration, the mixture was subsequently converted to its Cbz derivative **29** in 86% overall yield. Depending upon the choice of ATA, either the (*R*) or (*S*) stereocenter can be formed. The use of an organic reagent in conjunction with enzymes allows for not only unprecedented sequential transformations, but also the realization of

hitherto infeasible cascades in a purely biological or chemical process. To the best of our knowledge, no comparable process for secondary alcohol deracemization has been reported.



Scheme 1. Conversion of a racemic alcohol to a nonracemic 1° amine via chemoenzymatic catalysis

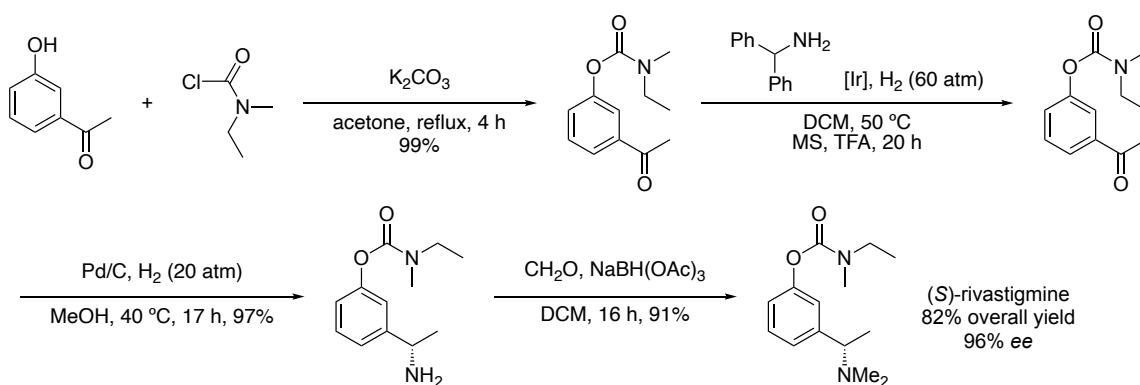
2.3.8. Rivastigmine synthesis

2.3.9. Early work of rivastigmine synthesis

By way of highlighting and illustrating the potential of an ATA to be used as part of streamlined chemoenzymatic catalysis, rivastigmine was chosen as an important target. Rivastigmine is a reversible acetylcholinesterase inhibitor (AChE) for treating dementia associated with mild to moderate Alzheimer's disease (AD), approved by the U.S. Food and Drug Administration in 2000. Traditionally, (*S*)-rivastigmine was resolved from

diastereomeric crystallization with (+)-di-*O,O'*-*p*-toluoyl tartaric acid monohydrate. This method involves three or more recrystallizations to increase enantiomeric excess to an acceptable level. Accordingly, the steps were tedious, and the total yield was low.²⁹

Improved methods demonstrated more practical and efficient syntheses of this drug focused on development of generating the stereocenter enantioselectively; all prior art is summarized in **Table 3**. For example, a reported 4-step synthesis of rivastigmine relies on asymmetric reductive amination of a diphenylmethyl amine using a chiral iridium-based catalyst (1 mol %) at high pressure (60 atm), as shown in step 2 in **Scheme 2**. Subsequent deprotection was conducted with Pd/C at again, high pressure (20 atm) overnight. Ultimately a reductive amination afforded the dimethylamine residue present in the target. While the overall yield is impressive (82%), and the *ee* is 96%, solvents used (acetone, then MeOH, then DCM) lead to considerable organic waste, and the pressurized hydrogenation involved requires special equipment (**Table 3**, entry 1).³⁰



Scheme 2. Chang's synthetic route towards rivastigmine.³⁰

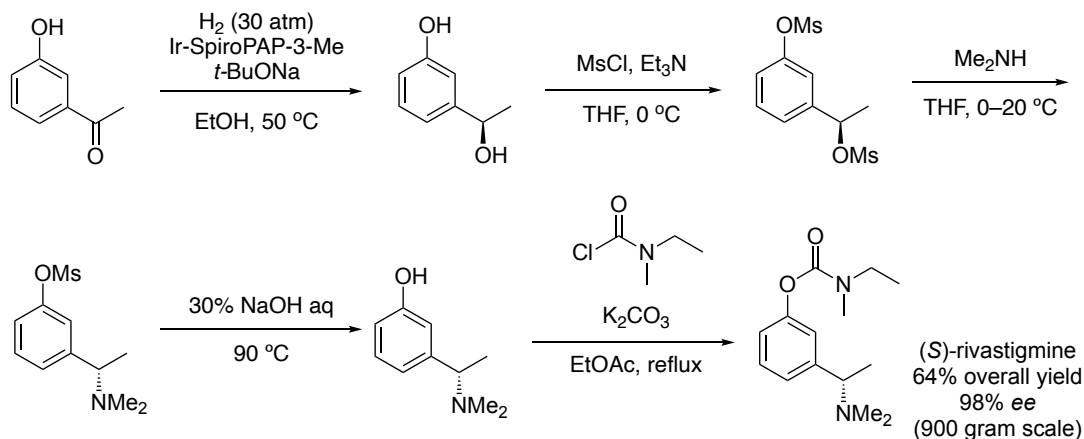
Table 3. Comparison of literature routes to (*S*)-rivastigmine.

Entry	Reference	Cat. to generate chiral center	No. of rxn steps	No. of pots	Time ^a [h]	Overall yield [%]	<i>ee</i> [%] ^b	E Factor ^c
1	Chang et al ³⁰	Ir (1 mol%), H ₂ (60 atm), Pd/C	4	4	49.3	82	96	2779
2	Che et al ³¹	Ir (1 mol%), H ₂ (30 atm)	5	4	29.5	64	98	270
3	List et al ³²	Hantzsch ester, disulfonimide	5	5	177	78	>99	3268
4	Capriati et al ³³	ADHs in DSM 20016 whole cells	4	3	N/A	78	98	N/A
5	Faber et al ³⁴	ATA-114 or ATA-117	5	4	53	61	>99	6125
6	Faber et al ³⁵	PD- ω -TA	3	3	45.5	66	99	3626
7	This work	ATA-256	3	2	35	95	>99	561 ^d

^a Total reaction time; ^b represents the % *ee* of (*S*)-rivastigmine; ^c mass of organic solvents used in the reaction and workup divided by the mass of the product; ^d the high E Factor is attributed to the EtOAc needed to extract ketone **38** from the ATA reaction mixture; recovery and recycling of this solvent were not attempted.

Another example utilizing Ir-catalyzed hydrogenation of the initial 3'-hydroxyacetophenone to an (*R*)-configured alcohol at 30 atmospheres was demonstrated on an industrial scale as part of a 5-step route (**Table 3**, entry 2). Treatment of the alcohol intermediate with mesyl chloride enabled an S_N2 reaction with dimethylamine in THF to invert the stereocenter. The mesylated phenol was then deprotected using 30% aqueous NaOH solutions in a biphasic solution. Finally, an amidoesterification with *N*-ethyl-*N*-

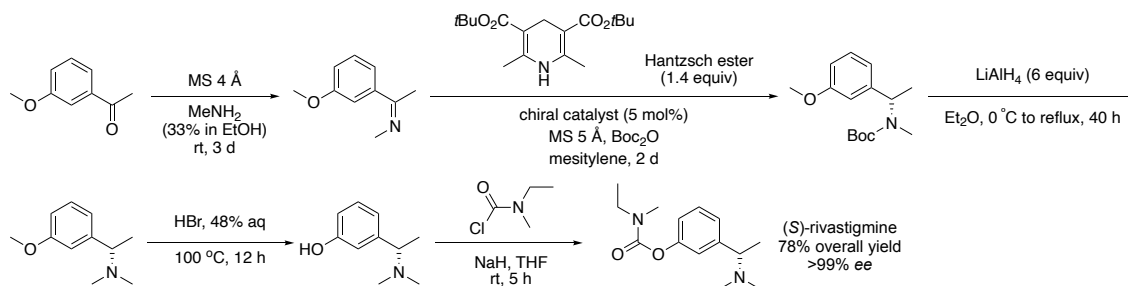
methyl carbamoyl chloride under reflux in ethyl acetate afforded rivastigmine (**Scheme 3**).³¹



Scheme 3. Che's rivastigmine synthetic route at scale³¹

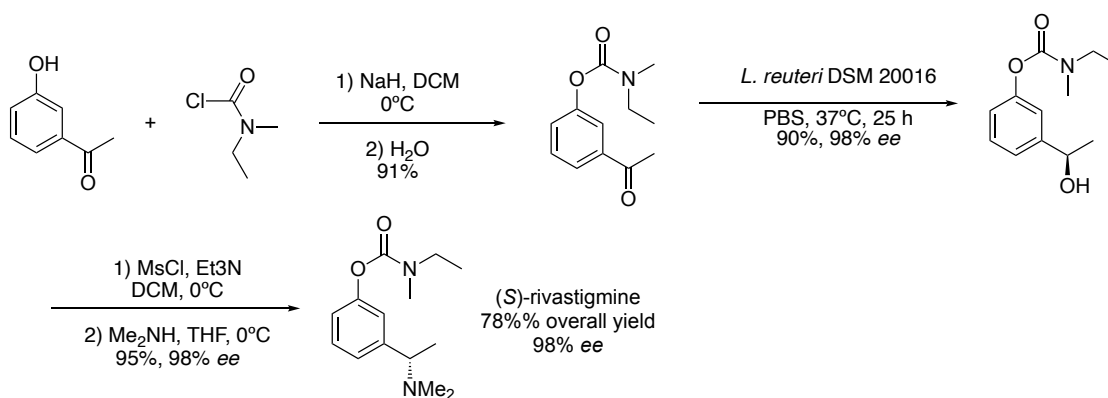
The development of asymmetric organocatalysis and its impact on pharmaceutical research was recognized in 2021 by being awarded the Nobel Prize in Chemistry. Early research done by List and co-workers on a chiral binaphthyl-containing disulfonimide catalyst using a Hantzsch ester as the stoichiometric source of hydride was applied to generate chiral centers for several marketed nitrogen-containing active pharmaceutical ingredients (APIs) including rivastigmine. The asymmetric imine reduction of a methyl imine was performed in dilute mesitylene at 10 °C over two days to afford a Boc-protected nonracemic tertiary amine intermediate (step 2 in **Scheme 4**), after which an exhaustive reduction was conducted in refluxing THF to generate the required methyl residue from the Boc group. Then, demethylation of the methoxy group using HBr aqueous solution was carried out to reveal the phenol moiety. Lastly, the solvent was switched back to THF and a carbamylation was conducted, which led to the target.³² Although the *ee* was satisfying, this route suffers from long reaction times and considerable waste generation from use of

various organic solvents, molecular sieves, and excess amounts of reagents involved (**Table 3**, entry 3).



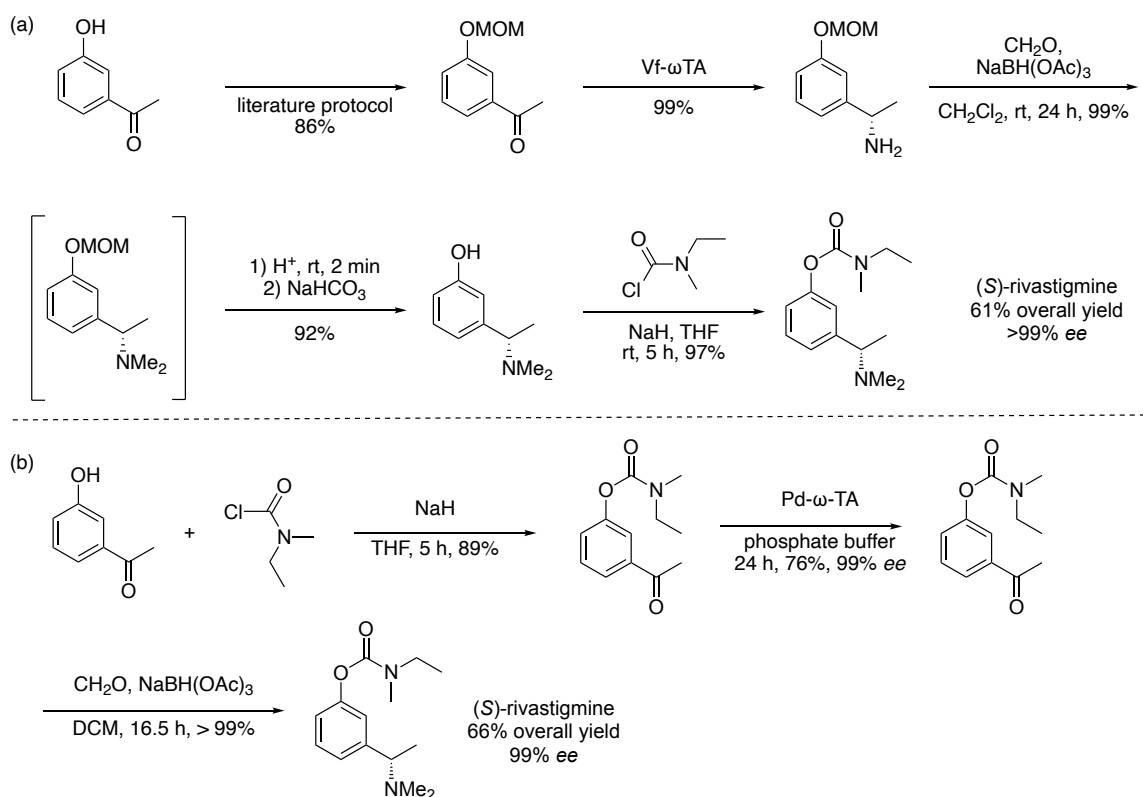
Scheme 4. List's synthetic route towards rivastigmine ³²

On the other hand, biocatalysis, a green and efficient tool, utilized an (*R*)-selective ketoreductase in whole cells to produce the corresponding alcohol in both high yield and *ee*; see step 2 in **Scheme 5**. The alcohol was then treated with mesyl chloride followed by dimethylamine to invert the stereocenter, resulting in a 78% overall yield (**Table 3**, entry 4). This sequence took only four steps in three pots; however, several different unsustainable organic solvents were used and exchanged between steps.



Scheme 5. Capriati's chemoenzymatic method to synthesize rivastigmine.³³

In addition to use of ketoreductase in biocatalysis, applying transaminase to the synthesis of (*S*)-rivastigmine was examined by Faber *et al* (**Table 3**, entry 5). This study discovered that masking the phenolic 3'-hydroxyacetophenone with MOMCl was the key to achieving full conversion for the biotransformation using transaminase (**Scheme 6a**).³⁴ Later, the same group demonstrated a concise synthesis involving only three steps; however, the overall yield was impaired by the inefficiency of introducing the carbamate using a combustible base (NaH), and a lower extent of conversion of transamination of ketone (**Scheme 6b**). Of note, unsustainable solvents (*e.g.* THF and DCM) were used in carbamylation and demethylation steps, respectively (**Table 3**, entry 6).³⁵



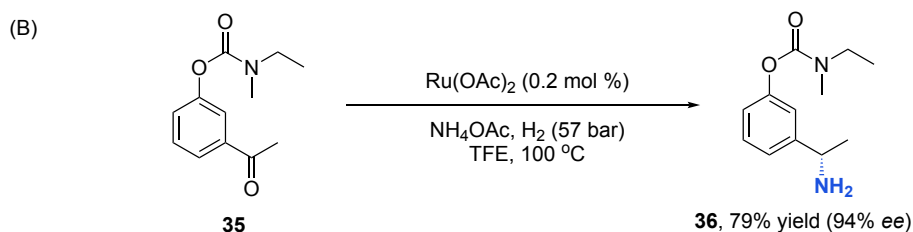
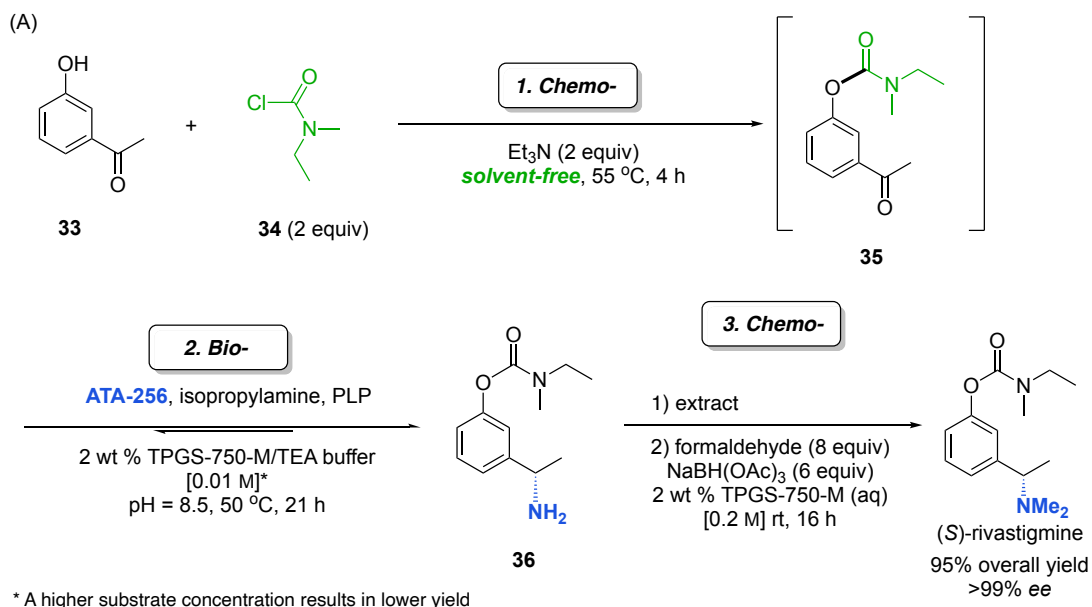
Scheme 6. Faber's chemoenzymatic method to synthesize rivastigmine.^{34, 35}

2.3.10. *A greener route to (S)-rivastigmine*

An alternative route to (S)-rivastigmine was developed in this work. The synthesis started with a clean, solvent-free carbamoylation of 3'-hydroxyacetophenone, previously unknown, which inserted the required carbamate; see step 1 in **Scheme 7A**. Without isolation, TPGS-750-M (2 wt %) in an aqueous buffer solution was added, followed by the ATA (along with the amine and co-factor PLP), leading to primary amine **36**. Newly formed intermediate **36** was then extracted with EtOAc from the aqueous reaction mixture. The crude material (from the evaporation of the solvent) was placed again into an aqueous reaction mixture containing the surfactant, paraformaldehyde, and sodium triacetoxyborohydride to realize dimethylation via reductive diamination. Virtually enantiomerically pure (S)-rivastigmine was ultimately isolated in 95% overall yield (**Scheme 7A**). The protocol involving extraction and re-addition to the same aqueous medium was necessitated due to the low concentration of the ATA-catalyzed process, as subsequent chemocatalysis requires this reaction variable to be far higher than the 0.xx M at which the biocatalysis must be run.

This 3-step, 2-pot synthesis represents not only a very mild and effective chemoenzymatic alternative sequence to known routes that are based solely on traditional chemocatalysis but also, and importantly, an environmentally friendly approach. This route contrasts with the recent report from Zhang *et al.* describing use of a nonracemically ligated Ru/C₃-TunePhos catalyst (0.2 mol %) to affect the desired reductive amination on aryl ketone **35** (**Scheme 7B**). This reaction was run in trifluoroethanol (TFE) at 100 °C at 57 bars with

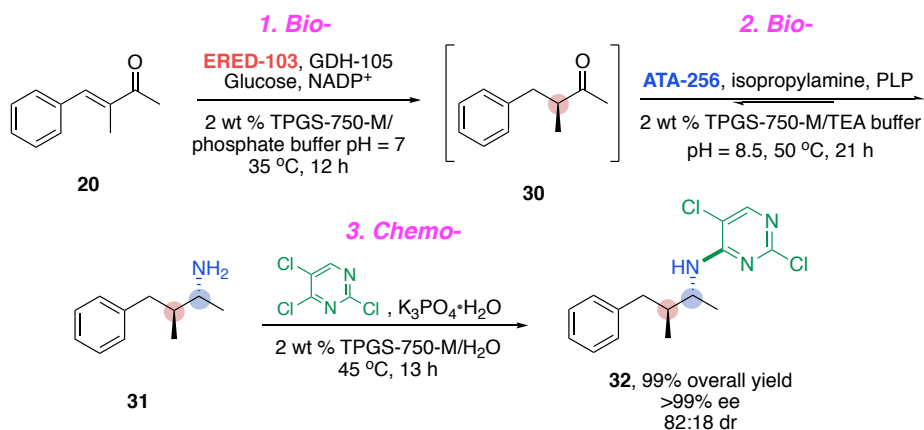
hydrogen over 24 hours in the presence of a source of ammonia to arrive at nonracemic amine **36**, prior to *N,N*-dimethylation to (*S*)-rivastigmine.⁸



Scheme 7. (A) A sustainable and efficient synthesis of (*S*)-rivastigmine using transaminase; (B) representative literature route using ruthenium-catalyzed asymmetric hydrogenation towards (*S*)-rivastigmine.⁸

2.3.11. Tandem ERED and ATA for the construction of amines with vicinal stereocenters

An additional 3-step tandem process that generates vicinal stereocenters was demonstrated. The multi-enzymatic route to generate vicinal stereocenters involving ene-reductase and transaminase was first reported in 2015 by Riva and co-workers.³⁶ In this work, an ene-reductase (ERED-103) was chosen to enantioselectively reduce a double bond present in enone **20**, followed by treatment with a transaminase (ATA-256) to convert the resulting nonracemic ketone **30** to the desired nonracemic amine **31**. After extraction, trichlorinated pyrimidine was introduced, leading to an S_NAr reaction ultimately leading to a very high-yielding sequence to product **32**, the major isomer being virtually enantiopure (Scheme 8).



Scheme 8. Tandem 3-step bio-, bio-, then chemo-catalysis sequence

2.4. Conclusions

In summary, the work described herein presents several advances in the chemoenzymatic catalysis category, including:

- the first study documenting quantitatively the beneficial impact of surfactants on enzymatic inhibition associated with reactions of transaminases in water;
- the first investigation illustrative of the sensitivity of ATAs to the nature of the nanomicelles in the aqueous medium that can be used to extend the levels of conversion to nonracemic primary amines;
- the first examples of mixed chem- and bio-catalytic reactions involving an ATA where *both* types of reactions involve environmentally responsible conditions;
- the first synthesis of the drug (*S*)-rivastigmine for the treatment of dementia is not only the most efficient process to date but is performed in a single reaction vessel in the complete absence of organic solvents as reaction media.

2.5. References

- (1) Development of New Stereoisomeric Drugs <https://www.fda.gov/regulatory-information/search-fda-guidance-documents/development-new-stereoisomeric-drugs> (accessed 2022 -02 -02).
- (2) Peñafiel, I.; Mangas-Sánchez, J.; Claver, C. Asymmetric (Transfer) Hydrogenation of Imines. In *Asymmetric Hydrogenation and Transfer Hydrogenation*; John Wiley & Sons, Ltd, 2021; pp 281–305.
- (3) Zhang, X.; Shao, P.-L. Industrial Applications of Asymmetric (Transfer) Hydrogenation. In *Asymmetric Hydrogenation and Transfer Hydrogenation*; John Wiley & Sons, Ltd, 2021; pp 175–219.
- (4) Bartoszewicz, A.; Ahlsten, N.; Martín-Matute, B. Enantioselective Synthesis of Alcohols and Amines by Iridium-Catalyzed Hydrogenation, Transfer Hydrogenation, and Related Processes. *Chem. Eur. J.* **2013**, *19*, 7274–7302.
- (5) Li, Y.; Lei, M.; Yuan, W.; Meggers, E.; Gong, L. An N-Heterocyclic Carbene Iridium Catalyst with Metal-Centered Chirality for Enantioselective Transfer Hydrogenation of Imines. *Chem. Comm.* **2017**, *53*, 8089–8092.
- (6) Reshi, N. U. D.; Saptal, V. B.; Beller, M.; Bera, J. K. Recent Progress in Transition-Metal-Catalyzed Asymmetric Reductive Amination. *ACS Catal.* **2021**, *11*, 13809–13837.

- (7) Kadyrov, R.; Riermeier, T. H. Highly Enantioselective Hydrogen-Transfer Reductive Amination: Catalytic Asymmetric Synthesis of Primary Amines. *Angew. Chem., Int. Ed.* **2003**, *42*, 5472–5474.
- (8) Yin, Q.; Shi, Y.; Wang, J.; Zhang, X. Direct Catalytic Asymmetric Synthesis of α -Chiral Primary Amines. *Chem. Soc. Rev.* **2020**, *49*, 6141–6153.
- (9) Bornscheuer, U. T.; Huisman, G. W.; Kazlauskas, R. J.; Lutz, S.; Moore, J. C.; Robins, K. Engineering the Third Wave of Biocatalysis. *Nature* **2012**, *485*, 185–194.
- (10) Mangas-Sanchez, J.; Sharma, M.; Cosgrove, S. C.; Ramsden, J. I.; Marshall, J. R.; Thorpe, T. W.; Palmer, R. B.; Grogan, G.; Turner, N. J. Asymmetric Synthesis of Primary Amines Catalyzed by Thermotolerant Fungal Reductive Aminases. *Chem. Sci.* **2020**, *11*, 5052–5057.
- (11) Arnold, F. H. Directed Evolution: Bringing New Chemistry to Life. *Angew. Chem., Int. Ed.* **2018**, *57*, 4143–4148.
- (12) Hansen, K. B.; Hsiao, Y.; Xu, F.; Rivera, N.; Clausen, A.; Kubryk, M.; Krska, S.; Rosner, T.; Simmons, B.; Balsells, J.; Ikemoto, N.; Sun, Y.; Spindler, F.; Malan, C.; Grabowski, E. J. J.; Armstrong, J. D. Highly Efficient Asymmetric Synthesis of Sitagliptin. *J. Am. Chem. Soc.* **2009**, *131*, 8798–8804.
- (13) Wu, S.; Snajdrova, R.; Moore, J. C.; Baldenius, K.; Bornscheuer, U. T. Biocatalysis: Enzymatic Synthesis for Industrial Applications. *Angew. Chem., Int. Ed.* **2021**, *60*, 88–119.
- (14) Cortes-Clerget, M.; Akporji, N.; Zhou, J.; Gao, F.; Guo, P.; Parmentier, M.; Gallou, F.; Berthon, J.-Y.; Lipshutz, B. H. Bridging the Gap between Transition Metal- and Bio-Catalysis via Aqueous Micellar Catalysis. *Nat. Commun.* **2019**, *10*, 2169.
- (15) Akporji, N.; Singhanian, V.; Dussart-Gautheret, J.; Gallou, F.; Lipshutz, B. H. Nanomicelle-Enhanced, Asymmetric ERED-Catalyzed Reductions of Activated Olefins. Applications to 1-Pot Chemo- and Bio-Catalysis Sequences in Water. *Chem. Commun.* **2021**, *57*, 11847–11850.
- (16) Singhanian, V.; Cortes-Clerget, M.; Dussart-Gautheret, J.; Akkachairin, B.; Yu, J.; Akporji, N.; Gallou, F.; Lipshutz, B. H. Lipase-Catalyzed Esterification in Water Enabled by Nanomicelles. Applications to 1-Pot Multi-Step Sequences. *Chem. Sci.* **2022**, *10*, 1039.
- (17) Oliveira, E. F.; Cerqueira, N. M. F. S. A.; Fernandes, P. A.; Ramos, M. J. Mechanism of Formation of the Internal Aldimine in Pyridoxal 5'-Phosphate-Dependent Enzymes. *J. Am. Chem. Soc.* **2011**, *133*, 15496–15505.
- (18) Sayer, C.; Martinez-Torres, R. J.; Richter, N.; Isupov, M. N.; Hailes, H. C.; Littlechild, J. A.; Ward, J. M. The Substrate Specificity, Enantioselectivity and Structure of the (*R*)-Selective Amine: Pyruvate Transaminase from *Nectria Haematococca*. *FEBS J.* **2014**, *281*, 2240–2253.

- (19) A Novel Method for Preventing Non-specific Binding in Equilibrium Dialysis Assays Using Solutol as an Additive | Elsevier Enhanced Reader <https://reader.elsevier.com/reader/sd/pii/S0022354920307474?token=E4A016BAA7133921C85C09607BDB073923D9B798D722AA4ECA6D76BFC1D3AA4A54B19F750949519D06441C041FC2FA13&originRegion=us-east-1&originCreation=20220128184904> (accessed 2022 -01 -26).
- (20) Yamada, M.; Azuma, K.; Yamano, M. Highly Enantioselective Direct Asymmetric Reductive Amination of 2-Acetyl-6-Substituted Pyridines. *Org. Lett.* **2021**, *23*, 3364–3367.
- (21) Cosgrove, S. C.; Thompson, M. P.; Ahmed, S. T.; Parmeggiani, F.; Turner, N. J. One-Pot Synthesis of Chiral N-Arylamines by Combining Biocatalytic Aminations with Buchwald–Hartwig N-Arylation. *Angew. Chem., Int. Ed.* **2020**, *59*, 18156–18160.
- (22) Bering, L.; Craven, E. J.; Sowerby Thomas, S. A.; Shepherd, S. A.; Micklefield, J. Merging Enzymes with Chemocatalysis for Amide Bond Synthesis. *Nat. Commun.* **2022**, *13*, 380.
- (23) Hastings, C. J.; Adams, N. P.; Bushi, J.; Kolb, S. J. One-Pot Chemoenzymatic Reactions in Water Enabled by Micellar Encapsulation. *Green Chem.* **2020**, *22*, 6187–6193.
- (24) Watson, A. J. A.; Williams, J. M. J. The Give and Take of Alcohol Activation. *Science* **2010**, *329*, 635–636.
- (25) Imm, S.; Bähn, S.; Neubert, L.; Neumann, H.; Beller, M. An Efficient and General Synthesis of Primary Amines by Ruthenium-Catalyzed Amination of Secondary Alcohols with Ammonia. *Angew. Chem., Int. Ed.* **2010**, *49*, 8126–8129.
- (26) Yang, L.-C.; Deng, H.; Renata, H. Recent Progress and Developments in Chemoenzymatic and Biocatalytic Dynamic Kinetic Resolution. *Org. Process Res. Dev.* **2022**, Article ASAP. DOI: 10.1021/acs.oprd.1c00463 (accessed 2022-04-25)
- (27) Mutti, F. G.; Knaus, T.; Scrutton, N. S.; Breuer, M.; Turner, N. J. Conversion of Alcohols to Enantiopure Amines through Dual-Enzyme Hydrogen-Borrowing Cascades. *Science* **2015**, *349*, 1525–1529.
- (28) Tian, K.; Li, Z. A Simple Biosystem for the High-Yielding Cascade Conversion of Racemic Alcohols to Enantiopure Amines. *Angew. Chem., Int. Ed.* **2020**, *59*, 21745–21751.
- (29) Hu, M.; Zhang, F.-L.; Xie, M.-H. Novel Convenient Synthesis of Rivastigmine. *Synth. Comm.* **2009**, *39*, 1527–1533.
- (30) Gao, G.; Du, S.; Yang, Y.; Lei, X.; Huang, H.; Chang, M. Direct Asymmetric Reductive Amination for the Synthesis of (S)-Rivastigmine. *Molecules* **2018**, *23*, 2207.

- (31) Yan, P.-C.; Zhu, G.-L.; Xie, J.-H.; Zhang, X.-D.; Zhou, Q.-L.; Li, Y.-Q.; Shen, W.-H.; Che, D.-Q. Industrial Scale-Up of Enantioselective Hydrogenation for the Asymmetric Synthesis of Rivastigmine. *Org. Process Res. Dev.* **2013**, *17*, 307–312.
- (32) Wakchaure, V. N.; Kaib, P. S. J.; Leutzsch, M.; List, B. Disulfonimide-Catalyzed Asymmetric Reduction of N-Alkyl Imines. *Angew. Chem., Int. Ed.* **2015**, *54*, 11852–11856.
- (33) Vitale, P.; Perna, F. M.; Agrimi, G.; Pisano, I.; Mirizzi, F.; Capobianco, R. V.; Capriati, V. Whole-Cell Biocatalyst for Chemoenzymatic Total Synthesis of Rivastigmine. *Catalysts* **2018**, *8*, 55.
- (34) Fuchs, M.; Koszelewski, D.; Tauber, K.; Kroutil, W.; Faber, K. Chemoenzymatic Asymmetric Total Synthesis of (S)-Rivastigmine Using ω -Transaminases. *Chem. Comm.* **2010**, *46*, 5500–5502.
- (35) Fuchs, M.; Koszelewski, D.; Tauber, K.; Sattler, J.; Banko, W.; Holzer, A. K.; Pickl, M.; Kroutil, W.; Faber, K. Improved Chemoenzymatic Asymmetric Synthesis of (S)-Rivastigmine. *Tetrahedron* **2012**, *68*, 7691–7694.
- (36) Monti, D.; Forchin, M. C.; Crotti, M.; Parmeggiani, F.; Gatti, F. G.; Brenna, E.; Riva, S. Cascade Coupling of Ene-Reductases and ω -Transaminases for the Stereoselective Synthesis of Diastereomerically Enriched Amines. *ChemCatChem* **2015**, *7*, 3106–3109.

2.6. General experimental information

a. TLC

Thin layer chromatography (TLC) was performed using Silica Gel 60 F254 plates (Merck, 0.25 mm thick), and visualized with a UV lamp and ninhydrin stain. Flash chromatography was done in glass columns using Silica Gel 60 (EMD, 40-63 μ m).

b. NMR

^1H and ^{13}C NMR spectra were recorded on either a Varian Unity Inova 400 MHz (400 MHz for ^1H , 100 MHz for ^{13}C), a Varian Unity Inova 500 MHz (500 MHz for ^1H , 125 MHz for ^{13}C), a Varian Unity Inova 600 MHz (600 MHz for ^1H), Bruker (400 MHz for ^1H ,

100 MHz for ^{13}C , 376 MHz for ^{19}F), or Bruker (500 MHz for ^1H , 125 MHz for ^{13}C , 471 MHz for ^{19}F).

Deuterated NMR solvents were purchased from Cambridge Isotopes Laboratories. DMSO- d_6 , CD_3OD , and CDCl_3 were used as solvents. Residual peaks for CHCl_3 in CDCl_3 ($^1\text{H} = 7.26$ ppm, $^{13}\text{C} = 77.00$ ppm), $(\text{CH}_3)_2\text{SO}$ in $(\text{CD}_3)_2\text{SO}$ ($^1\text{H} = 2.50$ ppm, $^{13}\text{C} = 39.52$ ppm) or MeOH in MeOD ($^1\text{H} = 3.31$ ppm, $^{13}\text{C} = 49.00$ ppm) have been assigned as internal standards. The chemical shifts are reported in ppm. The coupling constants J value are given in Hz. Data are reported as follows: chemical shift, multiplicity (s = singlet, bs = broad singlet, d = doublet, bd = broad doublet, t = triplet, q = quartet, quin = quintet, m = multiplet), coupling constant (if applicable) and integration.

c. HRMS

Mass spectra were obtained from the UC Santa Barbara and UC Irvine Mass Spectrometry Facility.

LCT-Premier (ESI): Mass spectra were acquired via ESI-MS using a Waters LCT Premier mass spectrometer equipped with an Alliance 2695 Separations module. Samples dissolved in methanol were directly infused into the mass spectrometer with no chromatography performed. Accurate mass data was calibrated using sodiated polyethylene glycol or sodiated polyethylene glycol monomethyl ether as an internal standard for positive ions and clusters of sodium formate as an internal standard for negative ions.

GCT-Premier (GC-EI and GC-CI): Mass spectra were acquired via GC-MS using a Waters GCT Premier mass spectrometer equipped with an Agilent 7890A GC oven and J&W Scientific DB-5ms+DG narrow bore column using helium carrier gas. Samples dissolved

in DCM were injected into the GC injector port which was maintained at 260 °C. The GC oven temperature was maintained at 50 °C for one minute then raised to 290 °C at a rate of 10 °C per minute to elute the sample. Accurate mass data were calibrated using perfluorotriethylamine or 2,4,6-tris(trifluoromethyl)-1,3,5-triazine as a co-injected standard. Where applicable, methane reagent gas was used to perform chemical ionization (CI) experiments.

d. Aminotransferase (ATA) and PLP cofactor

Amine Transaminase (ATA) Screening Kit containing 24 amine transaminase enzymes and PLP were purchased from Codex® and were used as received. The enzyme powder was stored at -18 °C until use. Purchasing website: <https://www.codexis-estore.com/product-page/codex-amine-transaminase-ata-screening-kit>.

e. Reagents

Triethanolamine was purchased from Sigma-Aldrich. Ketone reagents were purchased from Sigma-Aldrich, Combi-Blocks, Alfa Aesar, TCI, or Acros Organics and used without further purification.

2.7. Experimental procedures

a. Surfactant solution preparation

TPGS-750-M was synthesized according to the published procedure and is also commercially available from Sigma-Aldrich (catalog number 733857). The 2 wt % TPGS-

750-M aqueous solution was prepared by mixing TPGS-750-M wax (10.0 g) with HPLC grade water (490.0 g), and stir until dissolved.¹

b. Triethanolamine buffer solution preparation

To a 500 mL beaker equipped with a magnetic stirrer, 2 wt % TPGS-750-M aqueous solution (200.0 mL), triethanolamine (5.0 g), and isopropylamine (18.0 g) were added. Under gentle stirring at rt, concentrated HCl was added dropwise. After pH reached 8.5 (indicated by a pH meter), the total volume was then adjusted to 300.0 mL by adding 2 wt % TPGS-750-M aqueous solution. The buffer solution was stored at 4 °C until use.

c. 2 wt % TPGS-750-M in triethanolamine buffer solution preparation

To a 500 mL beaker equipped with a magnetic stirrer, triethanolamine (5.0 g), 2 wt % TPGS-750-M aqueous solution (200.0 mL), and isopropylamine (18.0 g) were added. Under gentle stirring at rt, concentrated HCl was added dropwise, monitoring the pH by a pH meter. After the pH reached 8.5, the total volume was then adjusted to 300.0 mL by adding 2 wt % TPGS-750-M aqueous solution in a graduate cylinder. The buffer solution was stored under 4 °C until use.

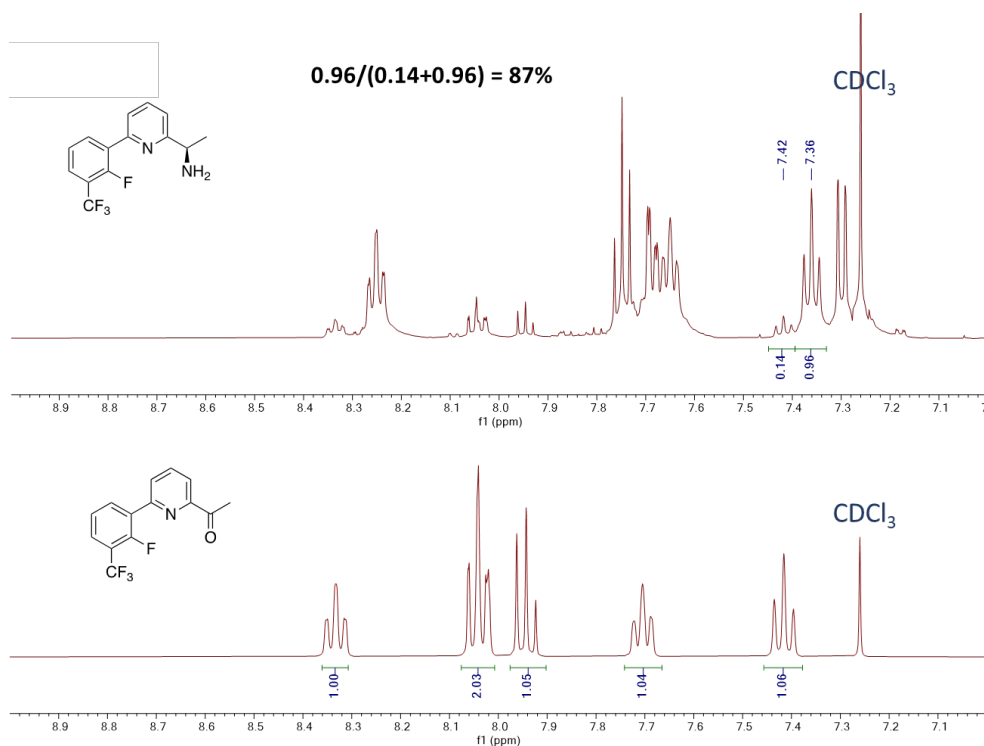
Alternative Method: Desired amount (2 wt %, 4 wt %, or 6 wt %) of nonionic surfactant (TPGS-750-M, solutol, PTS-600, or Brij 35, or Triton X-100) was weighed into a beaker, then stirred in triethanolamine buffer solution (pH 8.5) until surfactant dissolved.

d. Conversion monitoring in buffer and TPGS-750-M/buffer

To evaluate the impact of TPGS-750-M on the conversion of different ketone substrates by transaminase, comparative monitoring has been performed. There is one time

monitoring per vial ($t = 30 \text{ min}, 1 \text{ h}, 3 \text{ h}, 5 \text{ h}, \text{ and } 24 \text{ h}$). To each of the five 5 mL vials equipped with a magnetic stir bar was added the ketone (0.01 mmol). Triethanolamine buffer at $\text{pH} = 8.5$ (1.0 mL; with or without 2 wt % TPGS-750-M) was then added. Each reaction vial was capped by a screw cap and stirred at $50 \text{ }^\circ\text{C}$ for 2 min to afford an emulsified solution. Pyridoxal 5'-phosphate (PLP) (0.266 mg/mL or 1 mM), and transaminase (1.0 mg) were then added sequentially and stirred vigorously (1000 rpm) at $50 \text{ }^\circ\text{C}$. After the desired time is reached, the reaction mixture was basified with 5 N NaOH ($\sim 0.30 \text{ mL}$) to $\text{pH} 12\text{--}13$ (indicated by pH indicator paper). The resulting mixture was extracted with EtOAc (1.0 mL x 5). The organic layer was separated with the aid of a low-speed centrifuge for 5 min. The combined organic phases were collected and washed with distilled water (3.0 mL x 1) and dried over anhydrous MgSO_4 . The conversion was determined by $^1\text{H NMR}$.

Example using the NMR spectrum to determine the extent of conversion of the nonracemic amine **8** after 24 h (7.42 ppm (t) \rightarrow 7.36 ppm (t)).



e. Screening of the aqueous reaction medium involving various surfactants

Ketone substrate (0.01 mmol) was added to a 5 mL vial equipped with a magnetic stir bar. Triethanolamine buffer at pH = 8.5 (1.0 mL; with or without 2, 4, 6 wt % surfactant) was then added and stirred at 50 °C for 2 min to afford an emulsified solution. Pyridoxal 5'-phosphate (PLP; 0.266 mg/mL or 1 mM), and transaminase (1.0 mg) was then added sequentially and stirred vigorously (1000 rpm) at 50 °C. The reaction vial was capped with a screw cap, and after 24 h, the reaction mixture was basified with 5 N NaOH (~0.30 mL) to pH 12–13 (indicated by pH indicator paper). The resulting mixture was extracted with EtOAc (1.0 mL x 5). The organic layer was separated with the aid of a low-speed centrifuge for 5 min. The combined organic phases were collected and washed with distilled water (3.0 mL x 1) and dried over anhydrous MgSO₄. The conversion was determined by ¹H NMR.

f. Synthesis of nonracemic amines by transaminase

Ketone substrate (0.10 mmol) was added to a 20 mL vial equipped with a magnetic stir bar. A solution of 2 wt % TPGS-750-M in a triethanolamine buffer (10 mL, pH = 8.5) was then added and the mixture stirred at 50 °C for 2 min to afford an emulsified solution. Pyridoxal 5'-phosphate (PLP) (0.266 mg/mL or 1 mM), and transaminase (10 mg) were then added sequentially. The reaction vial was capped with a screw cap and stirred vigorously (1000 rpm) at 50 °C.

chemical species	concentration
ketone substrate	10.0 mM
triethanolamine	142.5 mM
isopropylamine	1.3 M
PLP	1.0 mM
ATA	10 mg per 0.1 mmol ketone

Workup: The reaction mixture was basified with 5 N NaOH (~1.5 mL) to pH 12–13 (indicated by pH indicator paper). The resulting mixture was extracted with EtOAc (5.0 mL x 5). The organic layer was separated with the aid of a low-speed centrifuge for 5 min. The combined organic phases were collected and washed with distilled water (30 mL x 1) and dried over anhydrous MgSO₄. Volatiles were evaporated under reduced pressure. The residue was analyzed by NMR, HRMS, and HPLC.

Cbz protection: To a stirred solution of the crude product in DCM (1.0 mL) was added sodium carbonate (12 mg, 0.30 mmol, 3 equiv), and benzyl chloroformate (85.3 mg, 70.5

□L, 0.50 mmol, 5.0 equiv). Upon completion of the reaction, the solvents were evaporated. Purification of the crude material was done via flash chromatography.

Acetyl derivatization: To a stirred solution of the extracted crude product in DCM (1.0 mL) were added triethylamine (30.3 mg, 41.8 μ L, 0.30 mmol, 3 equiv) and Ac₂O (30.6 mg, 20.4 μ L, 0.30 mmol, 3.0 equiv). Upon completion of the reaction, the solvents were evaporated. Purification of the crude material was done via flash chromatography.

g. General procedures for the synthesis of racemic amines

General procedure A was employed for preparation of the corresponding racemic amines 14_{rac} and 36_{rac}. General procedure B was used for the corresponding racemic amines 8_{rac}, 10_{rac}, 12_{rac}, 13_{rac}, 16_{rac}, 17_{rac}, 18_{rac}, 19_{rac}, 20_{rac}, 21_{rac}, 22_{rac}, 23_{rac}, 24_{rac}, 25_{rac}, 26_{rac} and 31_{rac} (rac = racemic). The protecting group installation procedures are the same for both the racemic and nonracemic amines.

- Procedure A

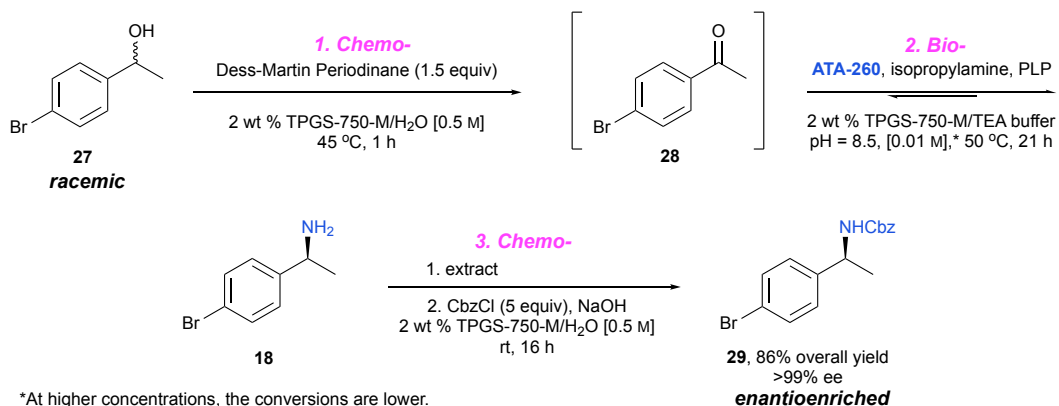
Ammonium formate (5 equiv) and ketone (1.0 mmol, 1.0 equiv) were added to a 4 mL vial equipped with a magnetic stir bar. $[\text{Ir}(\text{COD})\text{Cl}_2]_2$ (1.0 mg, 0.50 mol %) was added in a glove box. Methanol was added via syringe under argon. The vial was sealed and refluxed overnight. Upon completion, the resulting mixture was extracted with EtOAc (1v x 5). The organic layers were separated and washed with 1 N HCl (1v x 3). The aqueous layers were combined, basified with 5 N NaOH to pH 12–13 and extracted with EtOAc (1v x 4). The separated organic layer was dried over anhydrous MgSO_4 , filtered, and concentrated under reduced pressure. Volatiles were evaporated under reduced pressure and analyzed by NMR.

- Procedure B

To a solution of ketone (1.0 mmol, 1.0 equiv) in methanol was added ammonium acetate (0.15 g, 2.0 mmol, 2.0 equiv) and sodium cyanoborohydride (0.31 g, 5.0 mmol, 5.0 equiv). The resulting mixture was stirred at 60 °C. (Caution: gas evolution) After 12 h, the reaction mixture was basified with 5 N NaOH to pH 12–13 (indicated by pH paper). The resulting mixture was extracted with EtOAc (1v x 5). The organic layers were separated and washed with 1 N HCl (1v x 3). The aqueous layers were combined, basified with 5 N NaOH to pH 12–13 and extracted with EtOAc (1v x 4). The separated organic layer was dried over anhydrous MgSO_4 , filtered, and concentrated under reduced pressure. The racemic amine was analyzed by NMR.

note: 1v = the volume of solvent used in the reaction

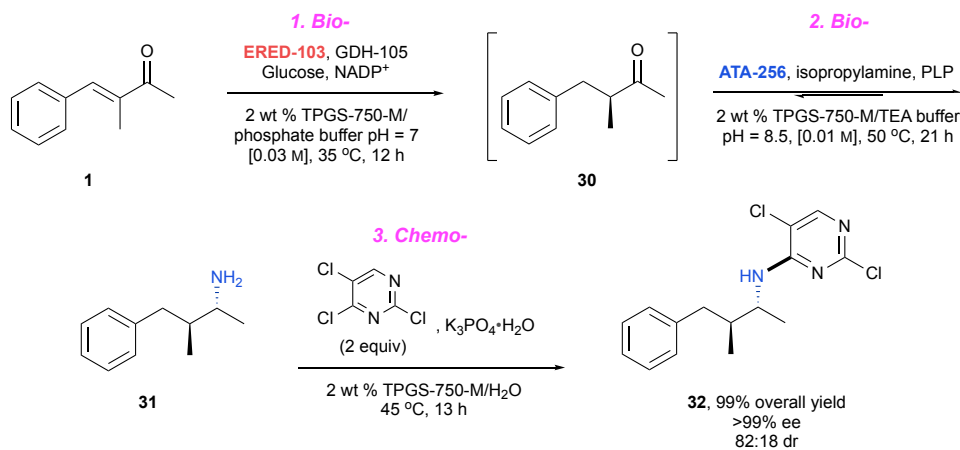
h. Experimental procedures for a 3-step sequence (DMP/ATA/CbzCl)



To a 4 mL vial equipped with a magnetic stirrer, 1-(4-bromophenyl)ethan-1-ol (20 mg, 0.10 mmol, 1 equiv), Dess-Martin periodinane (63.6 mg, 0.15 mmol, 1.5 equiv) and 2 wt % TPGS-750-M (0.2 mL) were added. The reaction vial was capped with a screw cap. The mixture was stirred vigorously at 45 °C until complete consumption of the starting material monitored by TLC. The reaction solution was then transferred to a 20 mL vial equipped with a magnetic stir bar, 2 wt % TPGS-750-M/triethanolamine buffer (9.8 mL, pH = 8.5), PLP (2.6 mg), and ATA-260 (5.0 mg) was added sequentially and stirred (1000 rpm) at 50 °C for 21 h. The reaction mixture was basified with 5 N NaOH (~1.5 mL) to pH 12–13 (indicated by pH indicator paper). The resulting mixture was extracted with EtOAc (5 mL x 5). The organic layer was separated with the aid of a centrifuge (low speed for 5 min). The combined organic phases were collected and dried over anhydrous MgSO₄. Volatiles were evaporated under reduced pressure. To a stirred solution of the crude product in 2 wt % TPGS-750-M (0.2 mL), sodium hydroxide (12.0 mg, 0.30 mmol, 3.0 equiv), and benzyl chloroformate (85.3 mg, 70.5 μ L, 0.50 mmol, 5.0 equiv) were added and stirred at rt. The reaction mixture was then loaded on silica gel and purified by flash column

chromatography to yield (*S*)-benzyl (1-(4-bromophenyl)ethyl)carbamate (28.7 mg, 86% yield, >99% *ee*, $R_f = 0.43$, 10% EtOAc/hexanes) as a white solid.

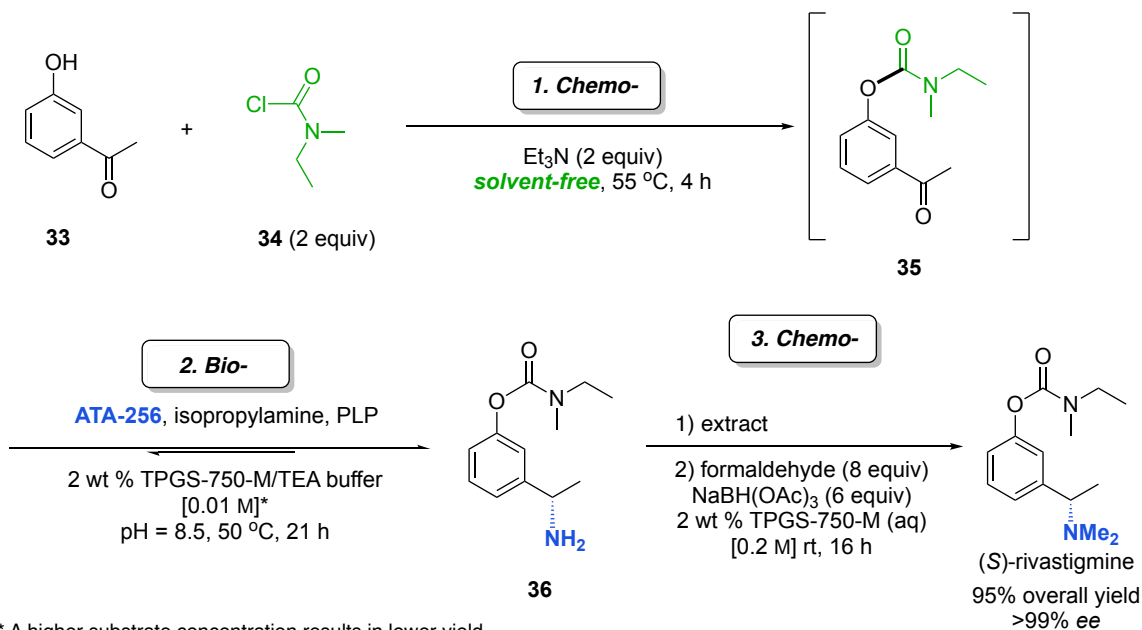
i. Experimental procedures for 1-pot sequence (ERED/ATA/SNAr)



To a 20 mL vial equipped with a magnetic stirrer, (*E*)-3-methyl-4-phenylbut-3-en-2-one (20 mg, 0.127 mmol, 1.0 equiv), ERED-103 (40 mg), GDH-105 (8 mg), glucose (46 mg, 0.26 mmol, 2.0 equiv), and NADP⁺ (2 mg) were suspended in 2 wt % of TPGS-750-M in phosphate buffer (pH = 7, 4 mL). The reaction was stirred at 35 °C for 12 h. The reaction progress was monitored by ¹H NMR. After the reaction reached completion, the substrate concentration was adjusted to 10 mM by adding 8.72 mL of triethanolamine buffer solution (triethanolamine, [118 mM], pH = 8.5). ATA-256 (50 mg) was then added and stirred (1000 rpm) at 50 °C for 21 h. The reaction progress was monitored by ¹H NMR. After completion, potassium phosphate tribasic monohydrate (29 mg, 0.127 mmol, 1 equiv) and 2,4,5-trichloropyrimidine (23 μ L, 0.254 mmol, 2.0 equiv) were added and the mixture was stirred at 45 °C for 21 h. The resulting mixture was extracted with EtOAc (10 mL x 5), and the combined organic extracts were dried over anhydrous MgSO₄. The volatiles were evaporated under reduced pressure and the crude residue was purified by flash column

chromatography (0 to 25% EtOAc/hexane) to yield 2,5-dichloro-*N*-((2*R*,3*S*)-3-methyl-4-phenylbutan-2-yl)pyrimidin-4-amine. (60.5 mg, 99% yield, >99% *ee*, $R_f = 0.36$, 10% EtOAc/hexanes).

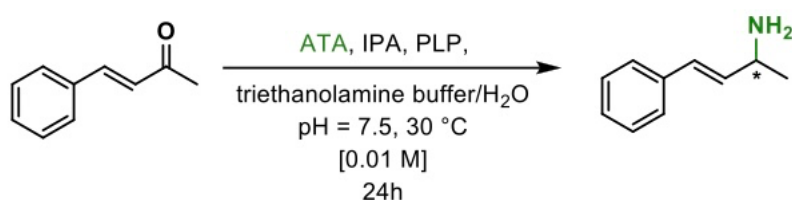
j. Experimental procedures leading to (S)-rivastigmine



To a 5 mL vial equipped with a magnetic stir bar was added 3'-hydroxyacetophenone (0.1 mmol, 1 equiv), triethylamine (0.2 mmol, 2 equiv), and *N*-ethyl-*N*-methylcarbamoyl chloride (0.2 mmol, 2 equiv) was added sequentially. The reaction was stirred at 55 °C for 4 h. After completion of the reaction (monitored by ^1H NMR), 2 wt % TPGS-750-M/triethanolamine buffer (pH 8.5) was added in (3.3 mL x 3) and transferred to a 20 mL vial. To the stirred resulting reaction mixture, PLP (2.6 mg) and ATA-256 (5 mg) were added sequentially and heated to 50 °C and stirred for 21 h. After completion of the reaction, the solution was basified to pH 12-13 and extracted with EtOAc (3 x 4 mL). The combined organic layers were evaporated to provide crude amine intermediate. To the stirred solution

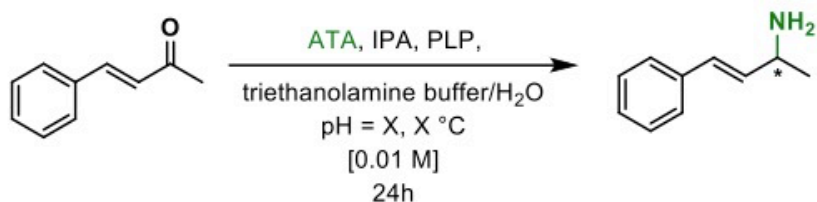
of crude amine intermediate in 2 wt % TPGS-750-M (0.5 mL) was added formaldehyde (37% in water; 0.8 mmol, 8 equiv, 65.0 uL) and NaBH(OAc)₃ (0.6 mmol, 0.6 equiv). The reaction was allowed to stirred at rt for 10 h. After completion, the mixture was loaded on silica gel and purified by flash column chromatography (2 v/v % MeOH in DCM + 1 v/v% Et₃N) to provide (*S*)-rivastigmine (23.7 mg, 95% yield, >99% *ee*) as a colorless oil.

k. Screening of transaminases in aqueous buffer



Ketone substrate (0.01 mmol) was added to a 4 mL vial equipped with a magnetic stir bar. Triethanolamine buffer at pH = 7.5 (1 mL) was then added and stirred at 30 °C for 2 min to afford an emulsified solution. Pyridoxal 5'-phosphate (PLP) (0.266 mg/mL or 1 mM), and transaminase (1.0 mg) was then added sequentially and stirred vigorously (1000 rpm) under 30 °C. The reaction vial was capped with a screw cap, and after 24 h, the reaction mixture was basified with 5 N NaOH (~0.30 mL) to pH 12–13 (indicated by pH indicator paper). The resulting mixture was extracted with EtOAc (1.0 mL x 5). The organic layer was separated with the aid of a low-speed centrifuge for 5 min. The combined organic phases were collected and washed with distilled water (3.0 mL x 1) and dried over anhydrous MgSO₄. The conversion was determined by ¹H NMR.

1. Optimization of temperature and pH for transamination in aqueous buffer



Ketone substrate (0.01 mmol) was added to a 4 mL vial equipped with a magnetic stir bar. Triethanolamine buffer at pH = 7.5 or 8.5 (1 mL) was then added and stirred at 30 °C, 40 °C or 50 °C for 2 min to afford an emulsified solution. Pyridoxal 5'-phosphate (PLP) (0.266 mg/mL or 1 mM), and transaminase (1.0 mg) was then added sequentially and stirred vigorously (1000 rpm) under 30 °C, 40 °C, or 50 °C. The reaction vial was capped with a screw cap, and after 24 h, the reaction mixture was basified with 5 N NaOH (~0.30 mL) to pH 12–13 (indicated by pH indicator paper). The resulting mixture was extracted with EtOAc (1.0 mL x 5). The organic layer was separated with the aid of a low-speed centrifuge for 5 min. The combined organic phases were collected and washed with distilled water (3.0 mL x 1) and dried over anhydrous MgSO₄. The conversion was determined by ¹H NMR.

m. Concentration effect of transamination in aqueous buffer vs. surfactant over 24 h

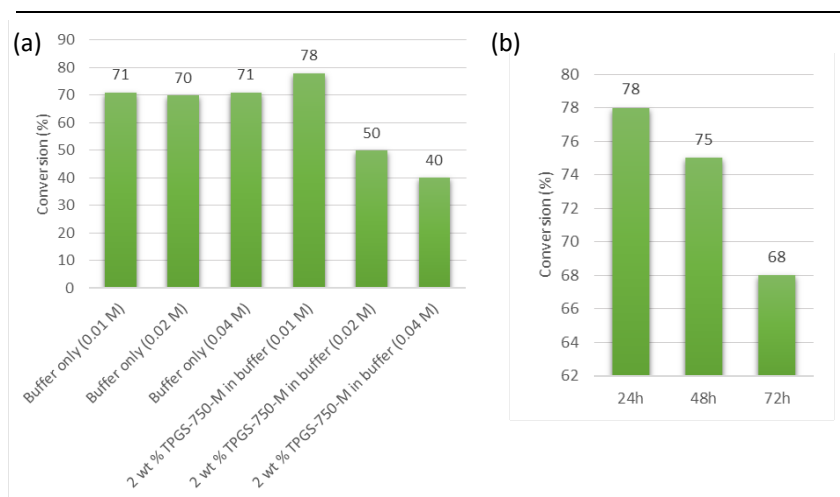
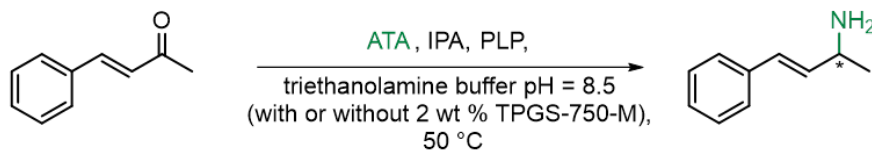


Table S3. (a) Concentration effect of transamination in aqueous buffer vs. surfactant for 24 h; (b) time screening of transamination in 2 wt % TPGS-750-M/buffer (0.01 M)

To evaluate the concentration effect of transamination in aqueous buffer vs. that in surfactant, a triethanolamine buffer solution was prepared for each concentration (0.01 M, 0.02 M, and 0.04 M).

- For a concentration of 0.01 M

To a 50 mL beaker equipped with a magnetic stirrer, triethanolamine (0.5 g), 2 wt % TPGS-750-M aqueous solution or aqueous solution (20.0 mL), and isopropylamine (1.80 g) were added. Concentrated HCl was added dropwise under gentle stirring at rt, monitoring the pH with a pH meter. After the pH reached 8.5, the total volume was then adjusted to 30.0

mL by adding 2 wt % TPGS-750-M aqueous solution or water in a graduated cylinder. The buffer solution was stored at 4 °C until use.

Ketone substrate (0.04 mmol) was added to a 5 mL vial equipped with a magnetic stir bar. Triethanolamine buffer at pH = 8.5 (4 mL) (with or without 2 wt % surfactant) was then added and stirred at 50 °C for 2 min to afford an emulsified solution. Pyridoxal 5'-phosphate (PLP; 0.266 mg/mL), and transaminase (4.0 mg) were then added sequentially and the reaction mixture was stirred vigorously (1000 rpm) under 50 °C. The reaction vial was capped with a screw cap, and after 24 h, the reaction mixture was basified with 5 N NaOH (~0.60 mL) to pH 12–13 (indicated by pH indicator paper). The resulting mixture was extracted with EtOAc (2.0 mL x 5). The organic layer was separated with the aid of a low-speed centrifuge for 5 min. The combined organic phases were collected and washed with distilled water (5.0 mL x 1) and dried over anhydrous MgSO₄. The conversion was determined by ¹H NMR.

- For a concentration of 0.02 M

To a 50 mL beaker equipped with a magnetic stirrer, triethanolamine (0.25 g), 2 wt % TPGS-750-M aqueous solution or aqueous solution (10.0 mL), and isopropylamine (1.80 g) were added. Concentrated HCl was added dropwise under gentle stirring at rt, monitoring the pH with a pH meter. After the pH reached 8.5, the total volume was then adjusted to 15.0 mL by adding 2 wt % TPGS-750-M aqueous solution or water in a graduated cylinder. The buffer solution was stored at 4 °C until use.

Ketone substrate (0.04 mmol) was added to a 5 mL vial equipped with a magnetic stir bar. Triethanolamine buffer at pH = 8.5 (2 mL; with or without 2 wt % surfactant) was then added and the reaction mixture stirred at 50 °C for 2 min to afford an emulsified solution.

Pyridoxal 5'-phosphate (PLP; 0.53 mg/mL) and transaminase (4.0 mg) were then added sequentially and stirred vigorously (1000 rpm) under 50 °C. The reaction vial was capped with a screw cap, and after 24 h, the reaction mixture was basified with 5 N NaOH (~0.60 mL) to pH 12–13 (indicated by pH indicator paper). The resulting mixture was extracted with EtOAc (2.0 mL x 5). The organic layer was separated with the aid of a low-speed centrifuge for 5 min. The combined organic phases were collected and washed with distilled water (5.0 mL x 1) and dried over anhydrous MgSO₄. The conversion was determined by ¹H NMR.

- For a concentration of 0.04 M

To a 25 mL beaker equipped with a magnetic stirrer, triethanolamine (0.125 g), 2 wt % TPGS-750-M aqueous solution or aqueous solution (5.0 mL), and isopropylamine (1.80 g) were added. Concentrated HCl was added dropwise under gentle stirring at rt, monitoring the pH using a pH meter. After the pH reached 8.5, the total volume was then adjusted to 7.5 mL by adding 2 wt % TPGS-750-M aqueous solution or water in a graduated cylinder. The buffer solution was stored at 4 °C until use.

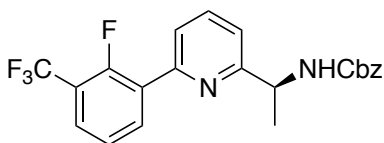
Ketone substrate (0.04 mmol) was added to a 5 mL vial equipped with a magnetic stirrer. Triethanolamine buffer at pH = 8.5 (1 mL) (with or without 2 wt % surfactant) was then added and stirred at 50 °C for 2 min to afford an emulsified solution. Pyridoxal 5'-phosphate (PLP; 1.07 mg/mL), and transaminase (4.0 mg) was then added sequentially and stirred vigorously (1000 rpm) under 50 °C. The reaction vial was capped with a screw cap, and after 24 h, the reaction mixture was basified with 5 N NaOH (~0.60 mL) to pH 12–13 (indicated by a pH indicator paper). The resulting mixture was extracted with EtOAc (2.0 mL x 5). The organic layer was separated with the aid of a low-speed centrifuge for 5

minutes. The combined organic phases were collected and washed with distilled water (5.0 mL x 1) and dried over anhydrous MgSO₄. The conversion was determined by ¹H NMR.

- Time screening of transamination in 2 wt % TPGS-750-M/buffer

Ketone substrate (0.04 mmol) was added to a 5 mL vial equipped with a magnetic stir bar. A solution of 2 wt % TPGS-750-M in a triethanolamine buffer at pH = 8.5 (4 mL) was then added and stirred at 50 °C for 2 min to afford an emulsified solution. Pyridoxal 5'-phosphate (PLP; 0.266 mg/mL or 1 mM), and transaminase (4.0 mg) were then added sequentially and stirred vigorously (1000 rpm) under 50 °C. The reaction vial was capped with a screw cap, and after 24 h, 48 h, or 72 h, the reaction mixture was basified with 5 N NaOH (~0.60 mL) to pH 12–13 (indicated by pH indicator paper). The resulting mixture was extracted with EtOAc (2.0 mL x 5). The organic layer was separated with the aid of a low-speed centrifuge for 5 min. The combined organic phases were collected and washed with distilled water (5.0 mL x 1) and dried over anhydrous MgSO₄. The conversion was determined by ¹H NMR.

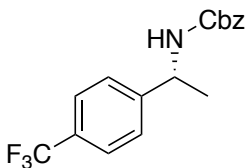
2.8. Product characterization (NMR, HRMS, and chirality assessment)



Benzyl (*S*)-1-(6-(2-fluoro-3-(trifluoromethyl)phenyl)pyridin-2-yl)ethyl carbamate **8**

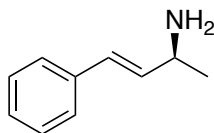
Following the general procedure with enzyme ATA-256, the product **16** was obtained as a white solid, 35.6 mg from a 0.1 mmol batch, 85% yield, 97% *ee*. ¹H NMR (500 MHz, CDCl₃) δ 8.19 (t, *J* = 7.5 Hz, 1H), 7.76 (t, *J* = 7.7 Hz, 1H), 7.72 (ddd, *J* = 7.9, 2.5, 1.2 Hz,

1H), 7.66 (t, $J = 7.2$ Hz, 1H), 7.40 – 7.25 (m, 7H), 5.99 (d, $J = 7.8$ Hz, 1H), 5.18 – 5.08 (m, 2H), 5.01 (t, $J = 7.1$ Hz, 1H), 1.54 (d, $J = 6.8$ Hz, 3H). ^{13}C NMR (126 MHz, CDCl_3) δ 161.4, 158.7, 156.7, 155.7, 151.1, 137.4, 136.5, 135.1, 128.6, 128.5, 128.2, 128.1, 127.5, 127.0, 124.2, 123.3, 123.2, 121.6, 120.5, 66.7, 51.6, 22.9. ^{19}F NMR (471 MHz, CDCl_3) δ -61.26, -119.48. HRMS TOF MS EI+ m/z calcd $\text{C}_{22}\text{H}_{18}\text{F}_4\text{N}_2\text{O}_2$ $[\text{M}]^+$: 418.1304; found 418.1314. The enantioselectivity was determined by HPLC analysis using a Chiralcel® 5 μm OD-H column 150 x 4.6 mm, isopropanol : *n*-hexane = 10:90, flow rate 1.0 mL/min) $t_1 = 6.697$ min (minor) $t_2 = 7.296$ min (major).



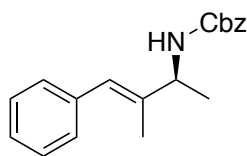
(R)-Benzyl (1-(4-(trifluoromethyl)phenyl)ethyl)carbamate 10

Following the general procedure with enzyme ATA-025, the product was obtained as a yellow oil, 29.1 mg from a 0.1 mmol batch, 88% yield, 79% *ee*. ^1H NMR (400 MHz, CDCl_3) δ 7.50 (d, $J = 8.0$ Hz, 2H), 7.33 (d, $J = 8.1$ Hz, 7H), 5.07 – 4.89 (m, 3H), 4.86 – 4.75 (m, 1H), 1.40 (d, $J = 7.0$ Hz, 3H). ^{13}C NMR (101 MHz, CDCl_3) δ 155.5, 136.2, 129.7, 128.5, 128.2, 126.2, 125.7, 125.6, 125.6, 125.4, 66.9, 50.5, 22.5. ^{19}F NMR (376 MHz, CDCl_3) δ -62.49. HRMS TOF MS EI+ m/z calcd $\text{C}_{17}\text{H}_{16}\text{F}_3\text{NO}_2$ Na $[\text{M}+\text{Na}]^+$: 346.1031; found 346.1031. The enantioselectivity was determined by HPLC analysis (Phenomenex® 3 μm Lux Cellulose-2 column 150 x 2 mm, isopropanol : *n*-hexane = 10:90, flow rate 1.0 mL/min) $t_1 = 0.416$ min (minor) $t_2 = 0.873$ min (major).



(S)-E-4-Phenylbut-3-en-2-amine 12

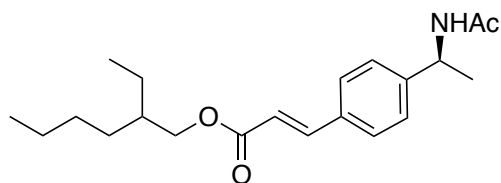
Following the general procedure with enzyme ATA-260, the product was obtained as a yellow oil, 90 mg from a 120 mg batch, 75% yield, >99% *ee*. **¹H NMR** (400 MHz, CDCl₃) δ 8.01 (s, 2H), 7.44 – 7.27 (m, 5H), 6.69 (d, *J* = 16.0, 1H), 6.28 – 6.22 (m, 1H), 3.98 (s, 1H), 1.34 (d, *J* = 6.8 Hz, 3H). **¹³C NMR** (100 MHz, CDCl₃) δ 135.5, 134.7, 128.6, 126.9, 125.4, 50.1, 19.2. The enantioselectivity was determined by HPLC analysis (Chiralcel OD-H 250 mm x 4.6 mm, 5 μ column, *n*-hexane: 0.1% TFA in methanol = 95:5, flow rate 1.0 mL/min) *t*₁ = 18.520 min (major). Spectral data matched those previously reported.⁴



(S)-E-Benzyl-(3-methyl-4-phenylbut-3-en-2-yl)carbamate 13

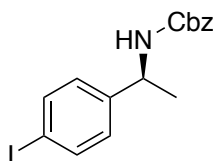
Following the general procedure with enzyme ATA-256, the product was obtained as a white solid, 19.2 mg from a 0.1 mmol batch, 65% yield, >99% *ee*. **¹H NMR** (400 MHz, CDCl₃) δ 7.47 – 7.28 (m, 7H), 7.21 (q, *J* = 7.2 Hz, 3H), 6.46 (s, 1H), 5.25 – 5.04 (m, 2H), 4.84 (s, 1H), 4.35 (s, 1H), 1.85 (s, 3H), 1.34 (d, *J* = 6.9 Hz, 3H). **¹³C NMR** (126 MHz, CDCl₃) δ 155.5, 138.9, 137.6, 136.6, 129.0, 128.5, 128.1, 128.1, 128.0, 126.4, 124.9, 66.7, 53.7, 20.1, 14.8. **HRMS** TOF MS EI⁺ *m/z* calcd C₁₉H₂₁NO₂ [M]⁺: 295.1572; found 295.1564. The enantioselectivity was determined by HPLC analysis (Chiralcel[®] 5 μm OD-

H column 150 x 4.6 mm, isopropanol : *n*-hexane = 10:90, flow rate 1.0 mL/min) $t_1 = 10.611$ min (major).



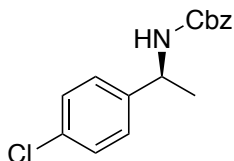
(S)-2-Ethylhexyl (E)-3-(4-(1-((benzyloxy)carbonyl)amino)ethyl)phenyl)acrylate 14

Following the general procedure with enzyme ATA-256, the product was obtained as a colorless oil, 15.5 mg from a 0.1 mmol batch, 45% yield, >99% *ee*. $^1\text{H NMR}$ (500 MHz, CDCl_3) δ 7.65 (d, $J = 16.0$ Hz, 1H), 7.50 (dd, $J = 8.2, 2.4$ Hz, 2H), 7.33 (d, $J = 8.1$ Hz, 2H), 6.42 (d, $J = 16.0$ Hz, 1H), 5.63 (d, $J = 7.9$ Hz, 1H), 5.15 – 5.10 (m, 1H), 4.19 – 4.07 (m, 2H), 2.00 (s, 3H), 1.49 (d, $J = 7.0$ Hz, 3H), 1.41 (m, 3H), 0.95 – 0.82 (m, 12H). $^{13}\text{C NMR}$ (101 MHz, CDCl_3) δ 168.7, 158.7, 145.4, 143.9, 133.7, 128.4, 126.7, 118.4, 67.4, 48.6, 38.9, 30.5, 29.7, 29.0, 23.8, 23.5, 23.0, 21.7, 14.0, 11.0. TOF MS Cl^+ m/z calcd $\text{C}_{21}\text{H}_{32}\text{NO}_3$ $[\text{M}]^+$: 345.2304; found 345.2313. The enantioselectivity of the unprotected primary amine was determined by HPLC analysis (Phenomenex[®] 5 μm Lux Cellulose-1 column 250 x 4.6 mm, isopropanol : *n*-hexane = 10:90, flow rate 1.0 mL/min) $t_1 = 6.333$ min (major).



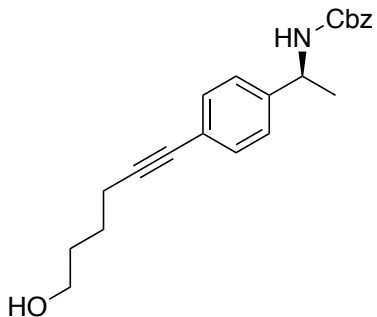
(S)-Benzyloxycarbonyl (1-(4-iodophenyl)ethyl)carbamate 16

Following the general procedure with enzyme ATA-260, the product was obtained as a white solid, 28.6 mg from a 0.1 mmol batch, 75% yield, >99% *ee*. **¹H NMR** (400 MHz, CDCl₃) δ 7.65 (d, *J* = 8.0 Hz, 2H), 7.34 (s, 5H), 7.06 (d, *J* = 7.9 Hz, 2H), 5.15 – 4.99 (m, 3H), 4.86 – 4.71 (m, 1H), 1.44 (d, *J* = 7.0 Hz, 3H). **¹³C NMR** (101 MHz, CDCl₃) δ 155.4, 143.3, 137.7, 136.3, 128.5, 128.2, 127.9, 92.6, 66.8, 50.3, 22.4. **HRMS** TOF MS EI+ *m/z* calcd C₁₆H₁₆INO₂ Na [M+Na]⁺: 404.0124; found 404.0128. The enantioselectivity was determined by HPLC analysis (Phenomenex[®] 5 μm Lux Cellulose-1 column 250 x 4.6 mm, isopropanol: *n*-hexane = 10:90, flow rate 1.0 mL/min) *t*₁ = 13.488 min (major).



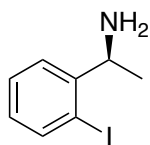
(S)-Benzyl(1-(4-chlorophenyl)ethyl)carbamate 17

Following the general procedure with enzyme ATA-260, the product was obtained as a white solid 24.0 mg from a 0.1 mmol batch, 81% yield, >99% *ee*. **¹H NMR** (400 MHz, CDCl₃) δ 7.38 – 7.19 (m, 9H), 5.15 – 5.02 (m, 2H), 4.98 (s, 1H), 4.88 – 4.75 (m, 1H), 1.45 (d, *J* = 6.9 Hz, 3H). **¹³C NMR** (101 MHz, CDCl₃) δ 156.1, 141.1, 136.3, 133.0, 128.8, 128.5, 128.2, 127.3, 66.8, 50.8, 22.4. **HRMS** TOF MS EI+ *m/z* calcd C₁₆H₁₆ClNO₂ Na [M+Na]⁺: 312.0767; found 312.0767. The enantioselectivity was determined by HPLC analysis (Chiralcel[®] 5 μm OD-H column 150 x 4.6 mm, isopropanol : *n*-hexane = 10:90, flow rate 1.0 mL/min) *t*₁ = 9.987 min (major).



(S)-Benzyl (1-(4-(6-hydroxyhex-1-yn-1-yl)phenyl)ethyl)carbamate 19

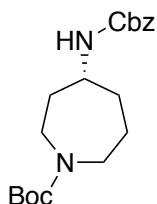
Following the general procedure with enzyme ATA-256, the product was obtained as a white solid, 26.3 mg, 75% yield, >99% *ee*. **¹H NMR** (400 MHz, CDCl₃) δ 7.35 (d, *J* = 8.0 Hz, 7H), 7.21 (d, *J* = 7.8 Hz, 2H), 5.18 – 4.74 (m, 5H), 3.71 (t, *J* = 6.1 Hz, 2H), 2.45 (t, *J* = 6.5 Hz, 2H), 1.72 (dq, *J* = 14.8, 7.8 Hz, 5H), 1.45 (d, *J* = 6.9 Hz, 3H). **¹³C NMR** (101 MHz, CDCl₃) δ 155.5, 142.9, 136.4, 131.8, 128.5, 128.1, 125.8, 122.9, 89.9, 80.6, 66.8, 62.5, 50.5, 31.9, 30.9, 25.0, 19.2, 14.1. **HRMS TOF MS EI⁺ *m/z* calcd C₂₂H₂₅NO₃ Na [M+Na]⁺: 374.1732; found 374.1732.** The enantioselectivity of the unprotected primary amine was determined by HPLC analysis (Agilent® Poroshell 120 2.7 μm chiral-V column 50 x 4.6 mm, NH₄COOH pH = 3.5 (15 mM) : *n*-hexane = 10:90, flow rate 1.0 mL/min) *t*₁ = 3.780 min (major).



(S)-1-(2-Iodophenyl)ethan-1-amine 20

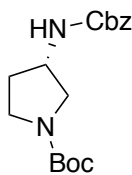
Following the general procedure with enzyme ATA-260, the product was obtained as a clear oil, 100.0 mg from a 190.0 mg batch, 52% yield, >99% *ee*. **¹H NMR** (400 MHz,

CDCl₃) δ 8.33 (s, 1H), 7.87 (q, *J* = 0.8 Hz, 1H), 7.52 (d, *J* = 8.0 Hz, 1H), 7.39 (t, *J* = 8.0 Hz, 1H), 7.27 (s, 1H), 7.07-7.03 (m, 1H), 4.73 (t, *J* = 8 Hz, 1H), 1.59 (d, *J* = 8.0 Hz, 3H). ¹³C NMR (100 MHz, CDCl₃) δ 140.2, 140.0, 130.6, 129.4, 126.1, 98.7, 55.7, 20.0. HRMS TOF MS EI⁺ *m/z* calcd C₈H₁₀IN H[M+H]⁺: 247.993626; found 247.9946. The enantioselectivity was determined by HPLC analysis (Chiralpak[®] AY-H 5 μ column 250 mm x 4.6 mm, *n*-hexane: 0.1% diethylamine in ethanol = 95:5, flow rate 1.0 mL/min) *t*₁ = 12.579 min (major).



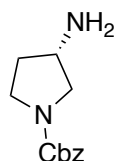
(S)-*t*-Butyl-4-(((benzyloxy)carbonyl)amino)azepane-1-carboxylate 21

Following the general procedure with enzyme ATA-260, the product was obtained as a colorless oil, 21.6 mg from a 0.1 mmol batch, 62% yield, 83% *ee*. ¹H NMR (500 MHz, CDCl₃) δ 7.33 (d, *J* = 3.5 Hz, 5H), 5.06 (s, 2H), 4.77 – 4.65 (m, 1H), 3.67 (s, 1H), 3.52 (d, *J* = 16.9 Hz, 2H), 3.33 (s, 1H), 3.14 – 3.05 (m, 1H), 2.05 – 1.97 (m, 1H), 1.91 – 1.83 (m, 1H), 1.81 (s, 1H), 1.51 (d, *J* = 39.7 Hz, 3H), 1.43 (s, 9H). ¹³C NMR (126 MHz, CDCl₃) δ 155.5, 155.4, 136.5, 128.5, 128.1, 128.1, 79.4, 66.6, 51.5, 51.3, 46.5, 45.4, 42.6, 42.3, 35.3, 35.0, 33.6, 33.3, 28.5, 24.2, 24.2. HRMS TOF MS EI⁺ *m/z* calcd C₁₉H₂₈N₂O₄ Na [M+Na]⁺: 371.1947; found 371.1946. The enantioselectivity was determined by HPLC analysis (Phenomenex[®] 5 μm Lux Cellulose-1 column 250 x 4.6 mm, isopropanol : *n*-hexane = 10:90, flow rate 0.5 mL/min) *t*₁ = 24.767 min (major) *t*₂ = 28.886 min (minor).



(S)-*t*-Butyl 3-(((benzyloxy)carbonyl)amino)pyrrolidine-1-carboxylate 22

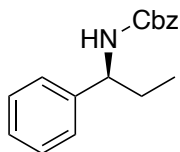
Following the general procedure with enzyme ATA-260, the product was obtained as a white solid, 24.6 mg from a 0.1 mmol batch, 75% yield, >99% *ee*. **¹H NMR** (400 MHz, CDCl₃) δ 7.44 – 7.32 (m, 5H), 5.18 (d, *J* = 13.8 Hz, 3H), 3.56 (dd, *J* = 12.5, 4.6 Hz, 2H), 3.52 – 3.35 (m, 2H), 2.13 – 2.02 (m, 2H), 1.45 (s, 9H). **¹³C NMR** (126 MHz, CDCl₃) δ 154.6, 154.5, 154.4, 154.2, 140.9, 134.9, 128.7, 128.7, 128.6, 128.5, 128.4, 127.7, 127.0, 79.6, 77.7, 69.9, 65.4, 60.4, 51.8, 51.5, 43.9, 43.5, 31.5, 31.0, 30.8, 29.7, 28.5, 21.2, 14.2. (rotamer was observed). The enantioselectivity was determined by HPLC analysis (Chiralcel® 5 μm OD-H column 150 x 4.6 mm, isopropanol : *n*-hexane = 10:90, flow rate 1.0 mL/min) *t*₁ = 1.295 min (major). Spectral data matched those previously reported.²



(S)-Benzyl 3-(((benzyloxy)carbonyl)amino)pyrrolidine-1-carboxylate 23

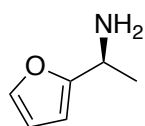
Following the general procedure with enzyme ATA-260, the product was obtained as a black oil, 156.0 mg from a 196.0 mg batch, 80% yield, 98.4% *ee*. **¹H NMR** (400 MHz, d₆-DMSO) 7.96 (s, 3H), 7.37-7.31 (m, 4 H), 5.07 (d, *J* = 1.2 Hz, 2H), 3.81- 3.48 (m, 6H), 3.42-3.34 (m, 2H), 2.16 (d, *J* = 4 Hz, 1H), δ 1.94 (d, *J* = 80 Hz, 1H). **¹³C NMR** (100 MHz, DMSO-d₆) 136.9, 128.0, 66.0, 49.3, 43.5, 40.1, 38.9, 29.0. The enantioselectivity was determined by HPLC analysis (Chiralpak® AD-H 250 mm x 4.6 mm, 5 μ column, *n*-hexane:

0.1% DEA in ethanol = 75:25, flow rate 1.0 mL/min) $t_1 = 12.829$ min (major) $t_2 = 15.665$ min (minor). Spectral data matched those previously reported.³



(S)-Benzyl-(1-phenylpropyl)carbamate 24

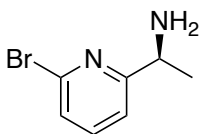
Following the general procedure with enzyme ATA-260, the product was obtained as a white solid, 42.6 mg from a 0.2 mmol scale batch, 79% yield, >99% *ee*. ¹H NMR (400 MHz, CDCl₃) δ 7.19 (dd, $J = 9.0, 5.8$ Hz, 6H), 7.12 (d, $J = 6.4$ Hz, 4H), 5.00 – 4.82 (m, 3H), 4.46 (q, $J = 7.9$ Hz, 1H), 1.65 (hept, $J = 7.0$ Hz, 2H), 0.75 (t, $J = 7.4$ Hz, 3H). ¹³C NMR (101 MHz, CDCl₃) δ 155.7, 142.3, 136.5, 128.7, 128.6, 128.5, 128.1, 127.3, 126.4, 66.7, 56.9, 29.6, 10.6. The enantioselectivity was determined by HPLC analysis (Chiralcel[®] 5 μ m OD-H column 150 x 4.6 mm, isopropanol : *n*-hexane = 10:90, flow rate 1.0 mL/min) $t_1 = 9.777$ min (major). Spectral data matched those previously reported.⁵



(S)-1-(Furan-2-yl)ethan-1-amine 25

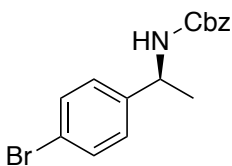
Following the general procedure with enzyme ATA-260, the product was obtained as a yellow oil, 61 mg from an 88 mg batch, 70% yield, 98.9% *ee*. ¹H NMR (400 MHz, CDCl₃) δ 7.37 (d, $J = 1.2$ Hz, 1H), 6.37 – 6.33 (m, 2H), 4.42 (s, $J = 8.0$ Hz, 1H), 1.62 (d, $J = 8.0$ Hz, 3H). ¹³C NMR (100 MHz, CDCl₃) δ 150.3, 143.5, 110.7, 108.5, 44.9, 17.1. The enantioselectivity was determined by HPLC analysis (Chiralpak[®] IG 250 mm x 4.6 mm,

5 μ column, *n*-hexane: 0.1% diethylamine in ethanol = 90:10, flow rate 1.0 mL/min) t_1 = 8.250 min (major) t_2 = 9.016 min (minor). Spectral data matched those previously reported.⁶



(S)-1-(6-Bromopyridin-2-yl)ethan-1-amine 26

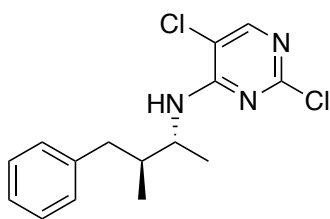
Following the general procedure with enzyme ATA-260, the product was obtained as a brown oil, 110 mg from a 160 mg batch, 69% yield, 95.7% *ee*. **¹H NMR** (400 MHz, DMSO-*d*₆) δ 8.33 (s, 2H), 7.85 (t, J = 7.6 Hz, 1H), 7.689 (d, J = 8 Hz, 1H), 7.56 (d, 7.6 Hz, 1H), 4.52 (d, J = 7.2 Hz, 1H), 1.46 (d, J = 6.8 Hz, 3H). **¹³C NMR** (100 MHz, DMSO-*d*₆) δ 159.3, 158.3, 140.7, 127.8, 121.2, 39.5, 19.6. The enantioselectivity was determined by HPLC analysis (Chiralpak[®] AY-H 250 mm x 4.6 mm, 5 μ column, *n*-hexane: 0.1% diethylamine in isopropanol = 90:10, flow rate 0.8 mL/min) t_1 = 11.630 min (major) t_2 = 12.872 min (minor). Spectral data matched those previously reported.⁷



(S)-Benzyl (1-(4-bromophenyl)ethyl)carbamate 29

Following the general procedure with enzyme ATA-260, the product was obtained as a white solid, 29.4 mg from a 0.1 mmol batch, 88% yield, >99% *ee*. **¹H NMR** (400 MHz, CDCl₃) δ 7.45 (d, J = 8.1 Hz, 2H), 7.34 (s, 5H), 7.18 (d, J = 8.1 Hz, 2H), 5.16 – 4.93 (m, 3H), 4.86 – 4.72 (m, 1H), 1.45 (d, J = 6.9 Hz, 3H). **¹³C NMR** (101 MHz, CDCl₃) δ 155.4,

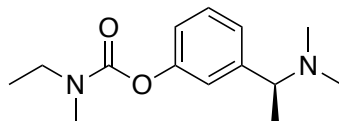
142.6, 136.3, 131.7, 131.5, 128.5, 128.2, 127.7, 121.1, 66.8, 50.2, 22.4. **HRMS** TOF MS EI⁺ *m/z* calcd C₁₆H₁₆BrNO₂ Na [M+Na]⁺: 356.0262; found 356.0273. The enantioselectivity was determined by HPLC analysis (Chiralcel[®] 5 μm OD-H column 150 x 4.6 mm, isopropanol : *n*-hexane = 10:90, flow rate 1.0 mL/min) t₁ = 10.709 min (major).



2,5-Dichloro-*N*-((2*R*,3*S*)-3-methyl-4-phenylbutan-2-yl)pyrimidin-4-amine **32**

Following the experimental procedure used for the 1-pot sequence (ERED/ATA/S_NAr), the product was obtained as a colorless oil, 60.5 mg from a 0.127 mmol batch, 99% yield, >99% *ee*, 82:18 dr. **¹H NMR** (500 MHz, CDCl₃) δ 7.99 (s, 1H), 7.33 – 7.25 (m, 3H), 7.24 – 7.20 (m, 1H), 7.20 – 7.11 (m, 2H), 5.31 (d, *J* = 9.3 Hz, 1H), 4.37 (dqt, *J* = 8.1, 6.5, 4.2 Hz, 1H), 2.76 (dt, *J* = 13.5, 6.5 Hz, 1H), 2.44 (td, *J* = 14.1, 13.6, 8.6 Hz, 1H), 2.16 – 2.02 (m, 1H), 1.31 – 1.21 (m, 4H) (mixed with a diastereomer), 0.93 (dd, *J* = 29.4, 6.9 Hz, 3H). **¹³C NMR** (126 MHz, CDCl₃) δ 158.5, 158.2, 158.1, 158.0, 153.4, 153.4, 153.3, 140.3, 140.1, 129.0, 128.9, 128.5, 128.4, 128.3, 126.2, 126.1, 126.0, 113.0, 113.0, 52.2, 50.6, 50.2, 43.2, 39.9, 39.8, 39.5, 38.9, 36.0, 32.2, 31.9, 29.7, 27.7, 22., 22.5, 17.6, 16.3, 15.3, 14.6, 10.0. **HRMS** TOF MS EI⁺ *m/z* calcd C₁₅H₁₇C₁₂N₃H [M+H]⁺: 310.0878; found 310.0893. The dr was determined by ¹H NMR (4.37 ppm int. = 1.00; 4.26 ppm int. = 0.22); the enantioselectivity was determined by HPLC analysis (Phenomenex[®] 5 μm Lux Cellulose-

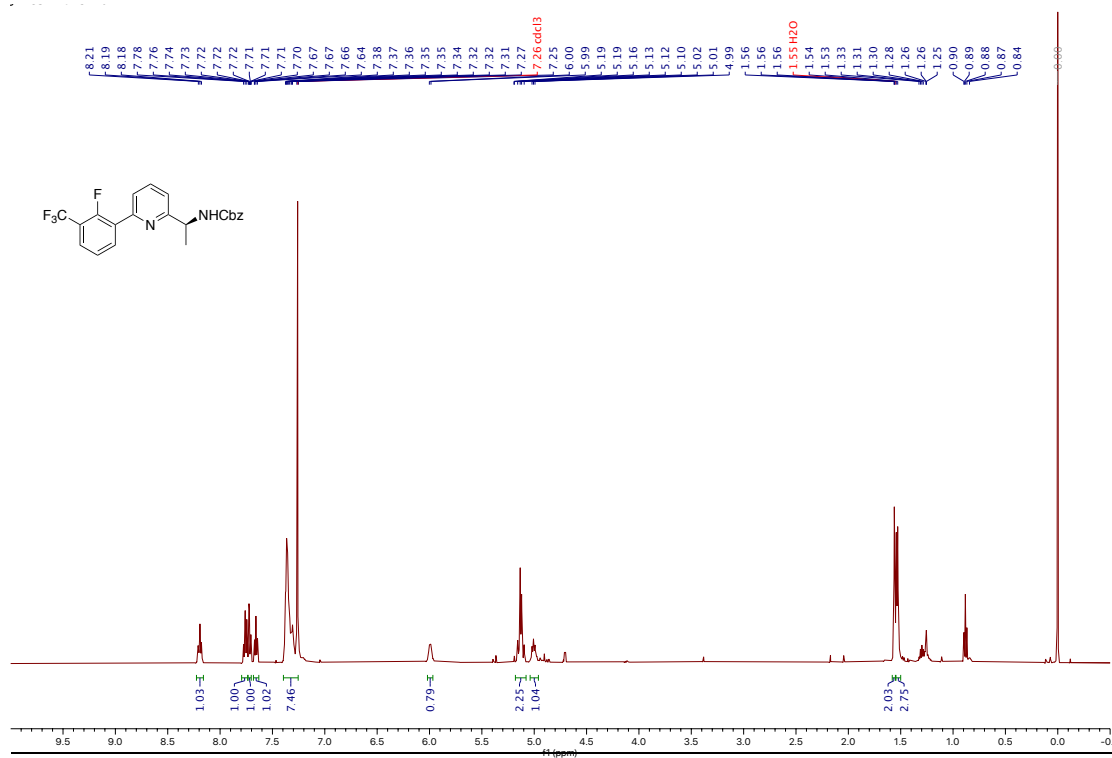
1 column 250 x 4.6 mm, isopropanol : *n*-hexane = 10:90, flow rate 1.0 mL/min) $t_1 = 17.219$ min (minor) $t_2 = 20.928$ (major).



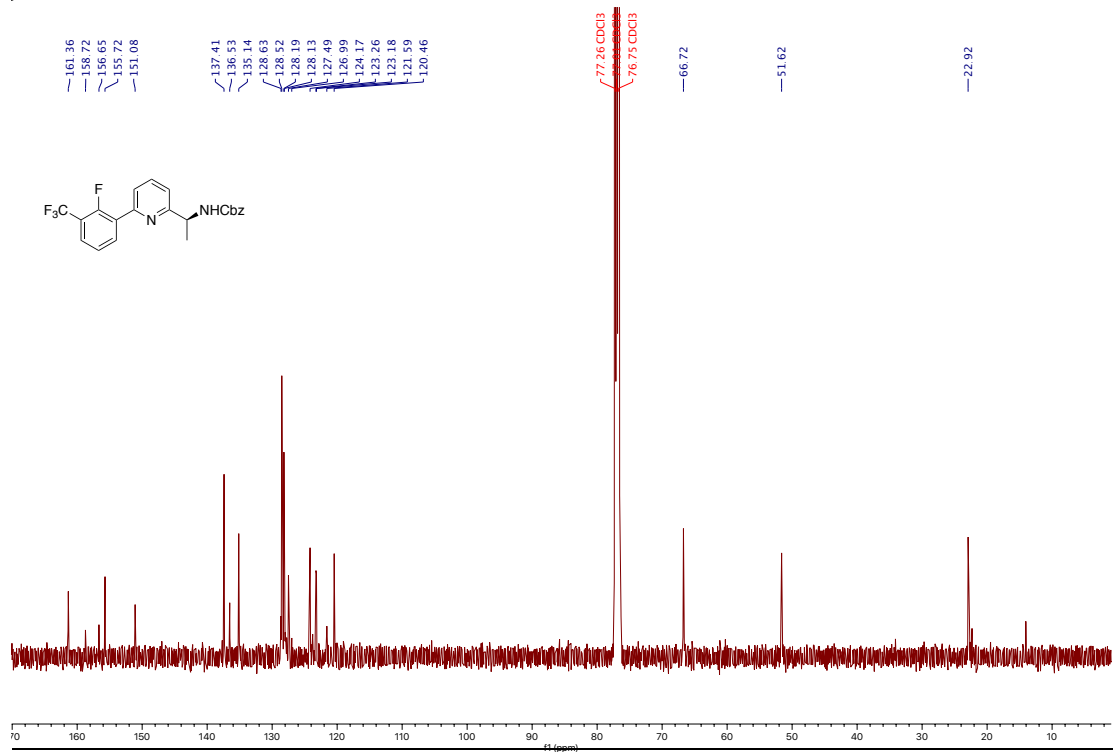
(S)-Rivastigmine

Following the experimental procedure for (*S*)-rivastigmine, the product was obtained as a colorless oil, 23.7 mg from a 0.1 mmol batch, 95% yield, >99% *ee*. **¹H NMR** (500 MHz, CDCl₃) δ 7.28 (t, $J = 7.8$ Hz, 1H), 7.11 (dd, $J = 7.7, 1.4$ Hz, 1H), 7.08 – 7.03 (m, 1H), 7.00 (d, $J = 8.0$ Hz, 1H), 3.44 (dq, $J = 31.3, 7.2$ Hz, 2H), 3.24 (q, $J = 6.7$ Hz, 1H), 3.02 (d, $J = 37.1$ Hz, 3H), 2.20 (d, $J = 0.9$ Hz, 6H), 1.39 – 1.33 (m, 3H), 1.26 – 1.17 (m, 3H). **¹³C NMR** (126 MHz, CDCl₃) δ 154.6, 154.4, 151.5, 145.8, 145.7, 128.9, 124.2, 124.2, 120.7, 120.7, 120.2, 65.6, 44.0, 43.2, 34.2, 33.8, 29.7, 27.1, 20.1, 13.2, 12.5. The enantioselectivity was determined by HPLC analysis Chiralcel® 5 μ m OD-H column 150 x 4.6 mm, isopropanol : *n*-hexane = 10:90, flow rate 1.0 mL/min) $t_1 = 5.565$ min (major). Spectral data matched those previously reported.⁸

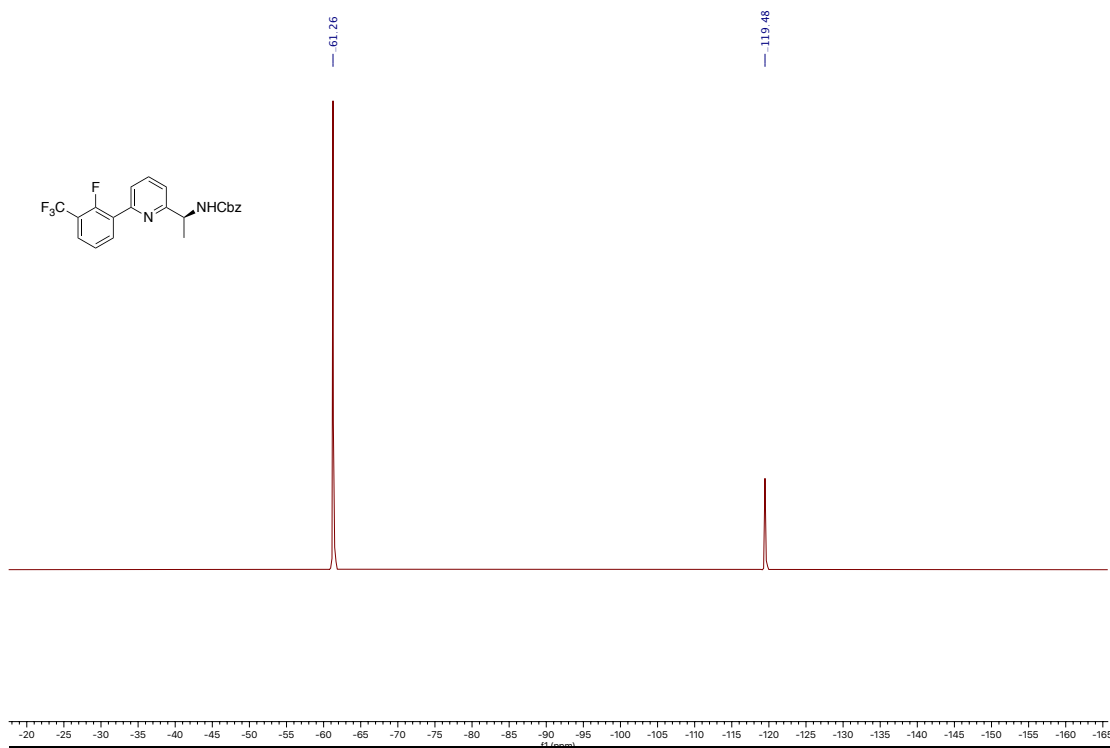
2.9. NMR spectra



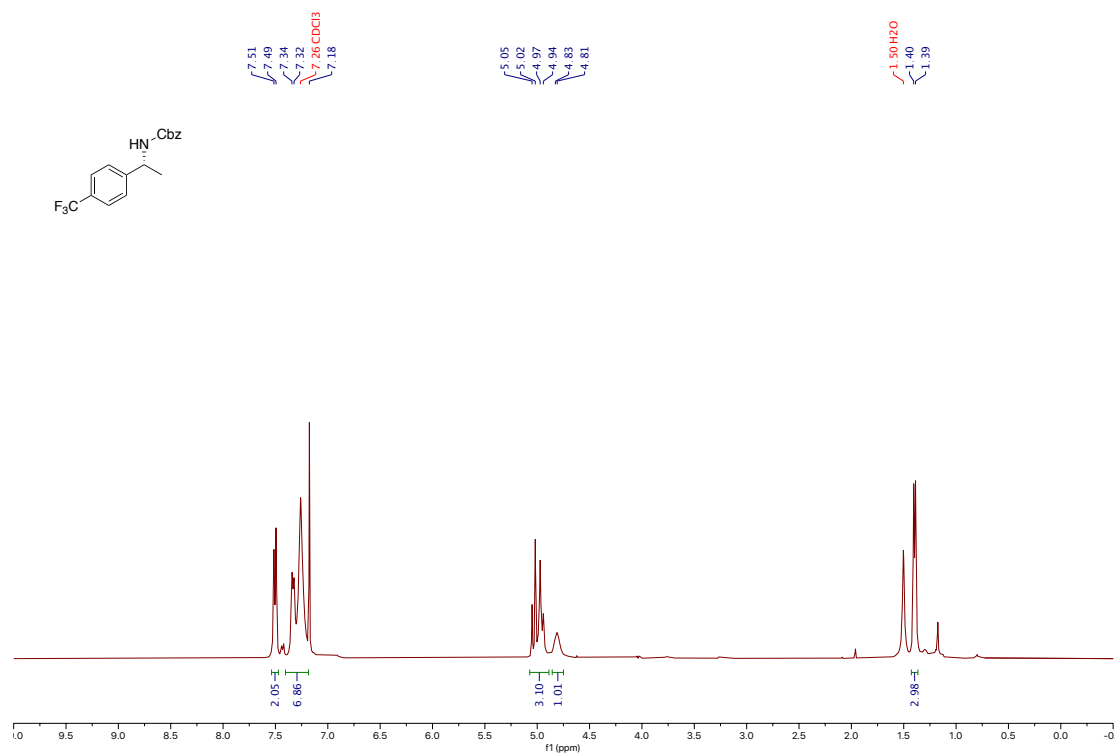
^1H NMR spectrum of benzyl (*S*)-(1-(6-(2-fluoro-3-(trifluoromethyl)phenyl)pyridin-2-yl)ethyl)carbamate 8



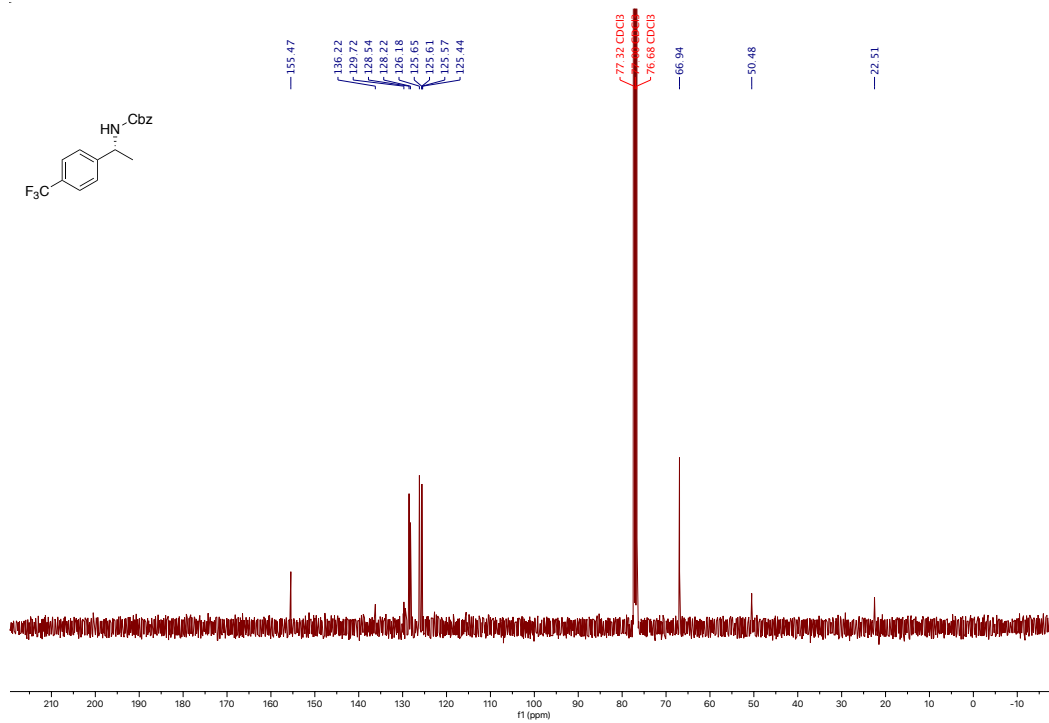
¹³C NMR spectrum of **benzyl (S)-1-(6-(2-fluoro-3-(trifluoromethyl)phenyl)pyridin-2-yl)ethylcarbamate 8**



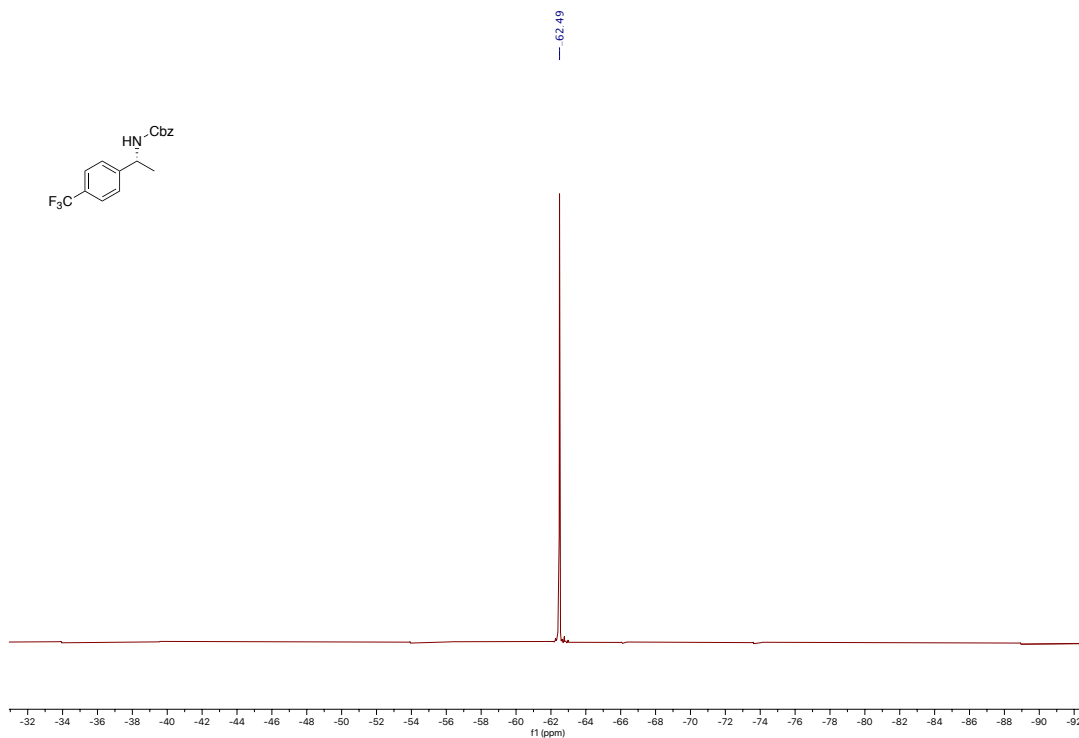
¹⁹F NMR spectrum of **benzyl (*S*)-(1-(6-(2-fluoro-3-(trifluoromethyl)phenyl)pyridin-2-yl)ethyl)carbamate 8**



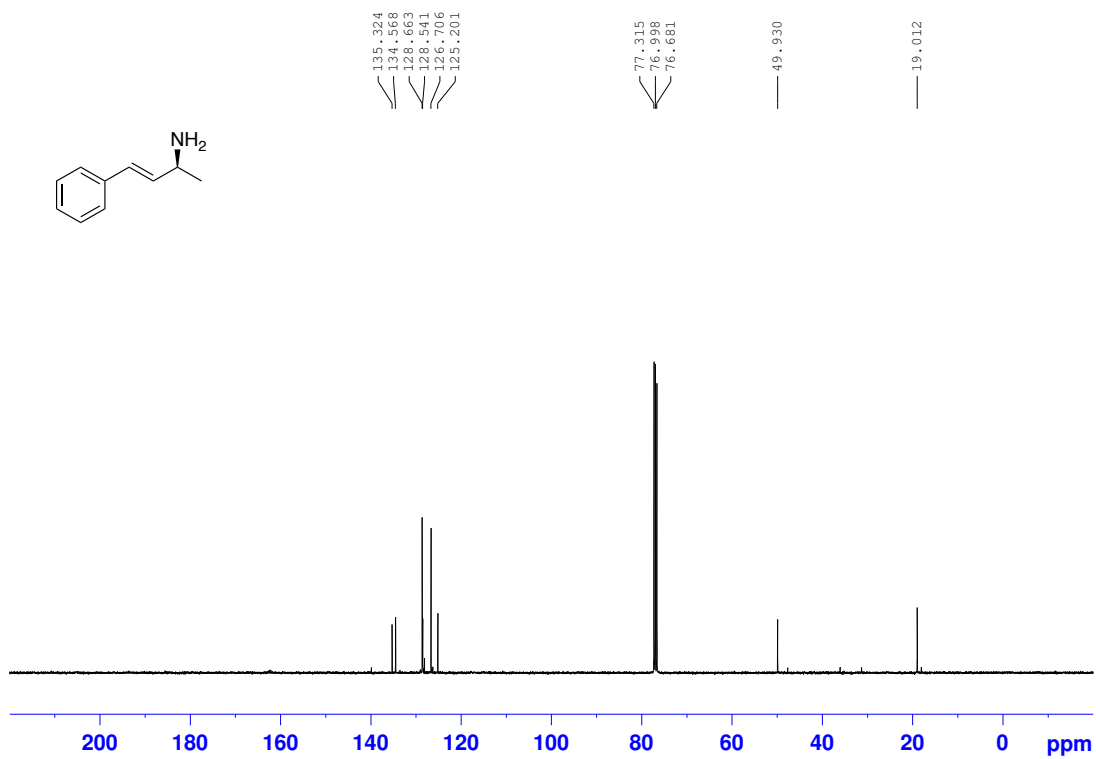
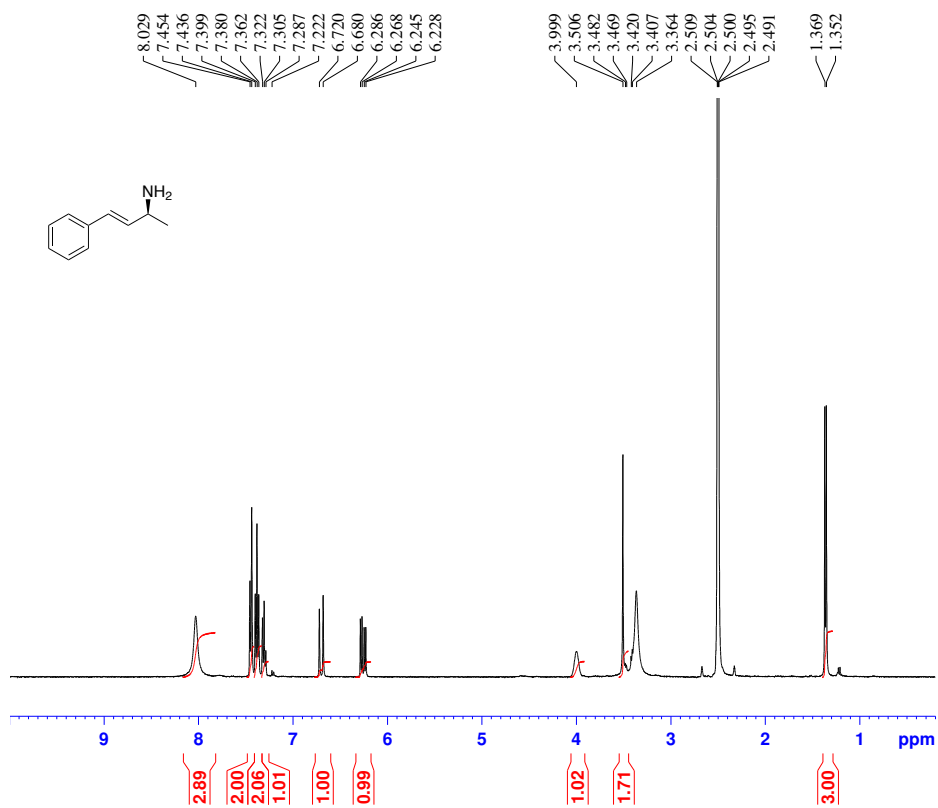
¹H NMR spectrum of **(*R*)-benzyl (1-(4-(trifluoromethyl)phenyl)ethyl)carbamate 10**



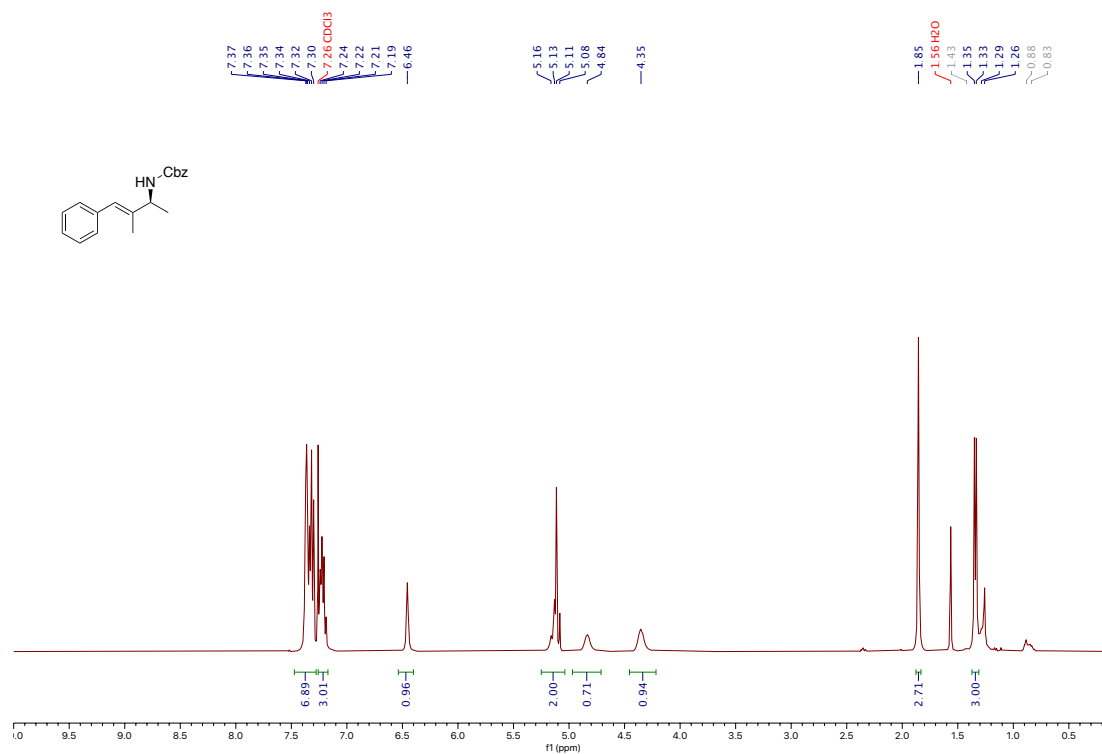
¹³C NMR spectrum of (*R*)-benzyl (1-(4-(trifluoromethyl)phenyl)ethyl)carbamate 10



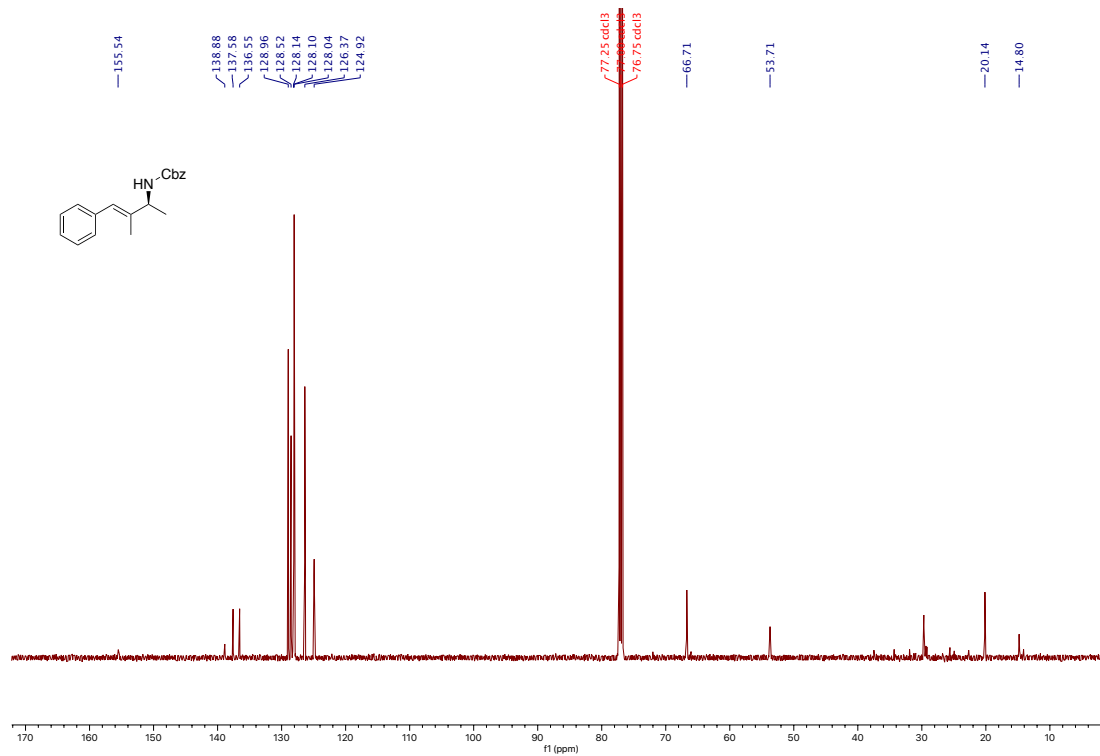
¹⁹F NMR spectrum of (*R*)-benzyl (1-(4-(trifluoromethyl)phenyl)ethyl)carbamate 10



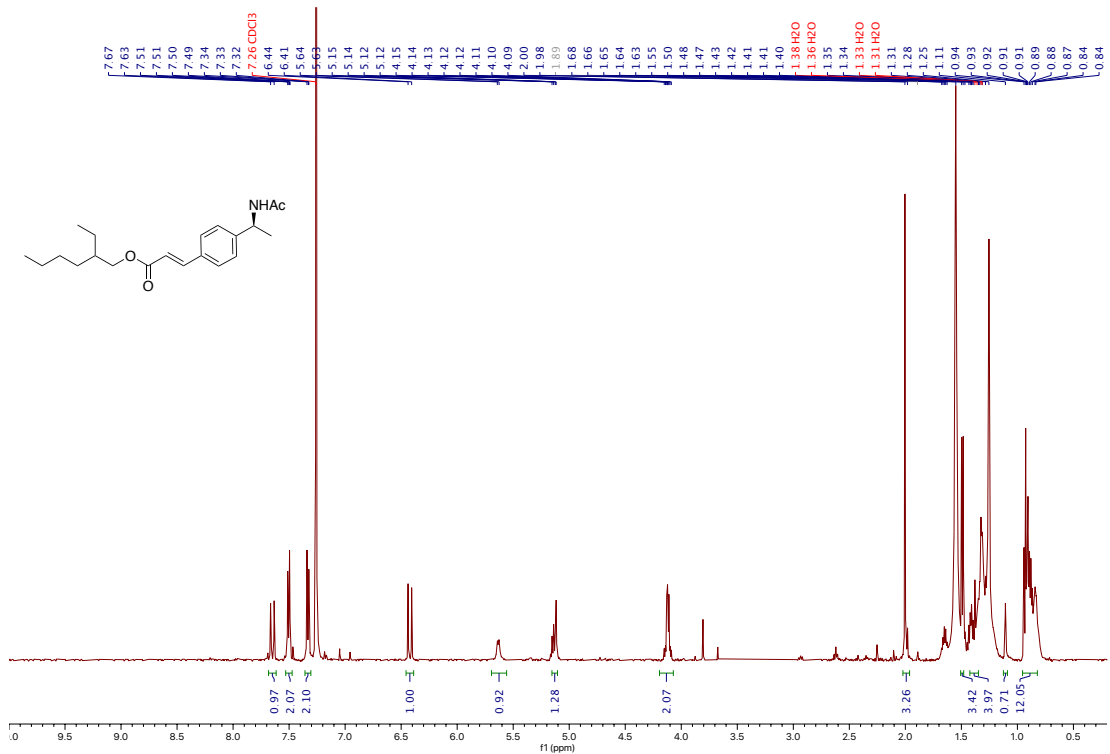
¹³C NMR spectrum of (*S,E*)-4-phenylbut-3-en-2-amine 12



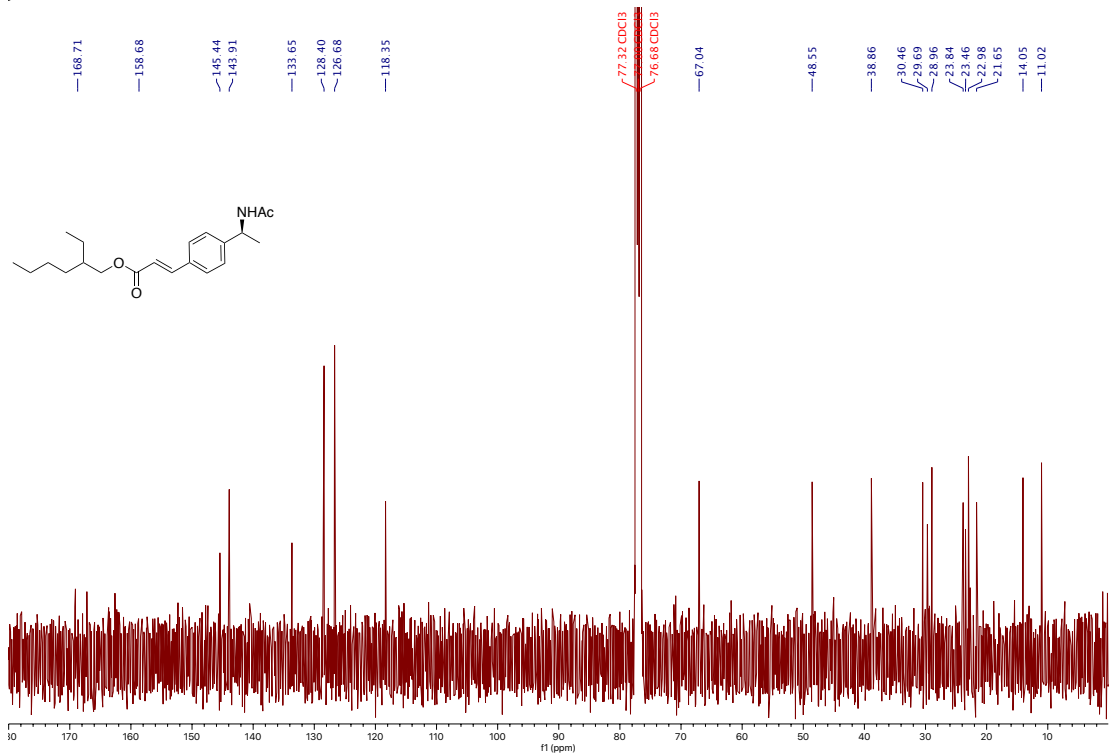
¹H NMR spectrum of (*S,E*)-benzyl-(3-methyl-4-phenylbut-3-en-2-yl)carbamate 13



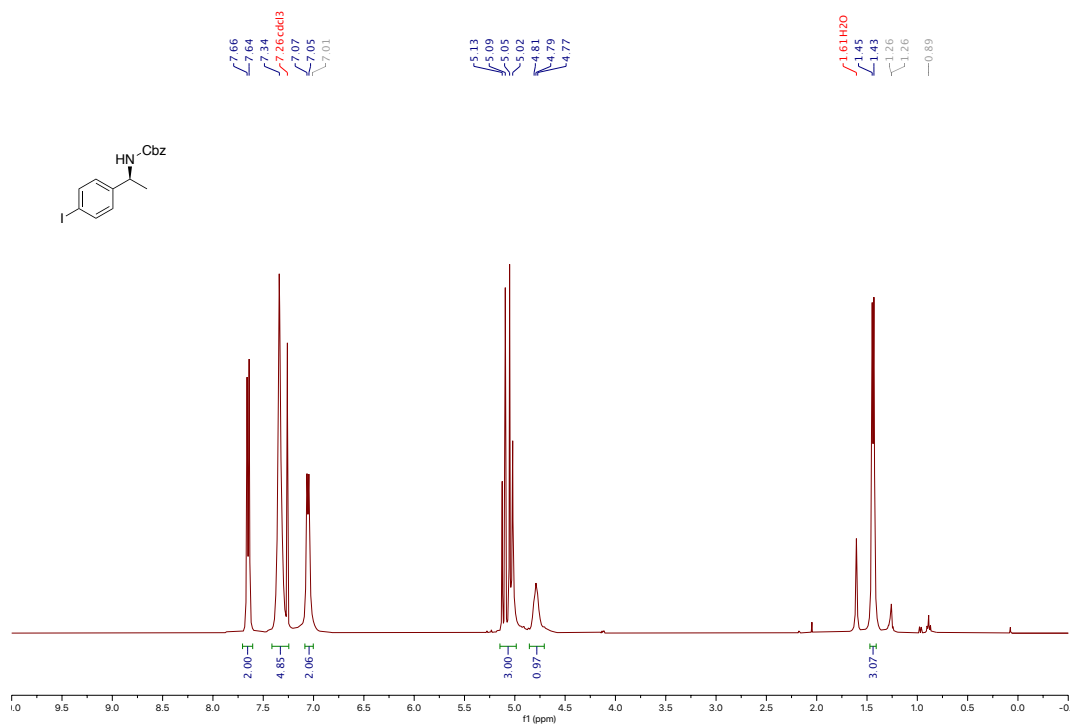
¹³C NMR spectrum of (*S,E*)-benzyl-(3-methyl-4-phenylbut-3-en-2-yl)carbamate 13



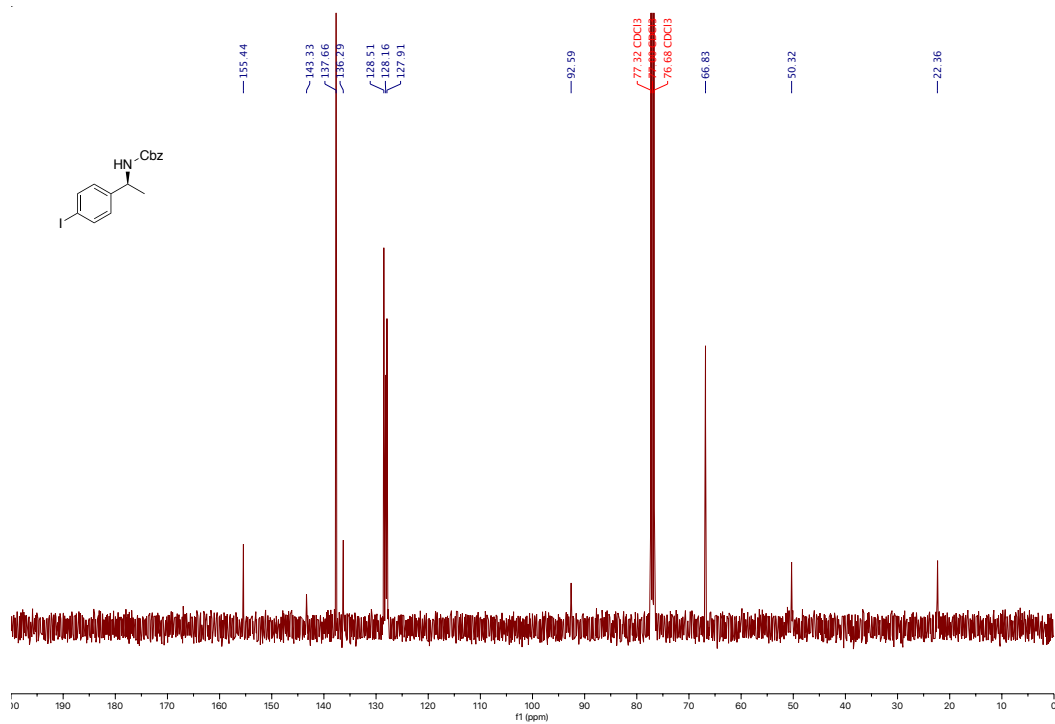
¹H NMR spectrum of 2-ethylhexyl (*E*)-3-(4-(1-((benzyloxy)carbonyl)amino)ethyl)phenyl)acrylate 14



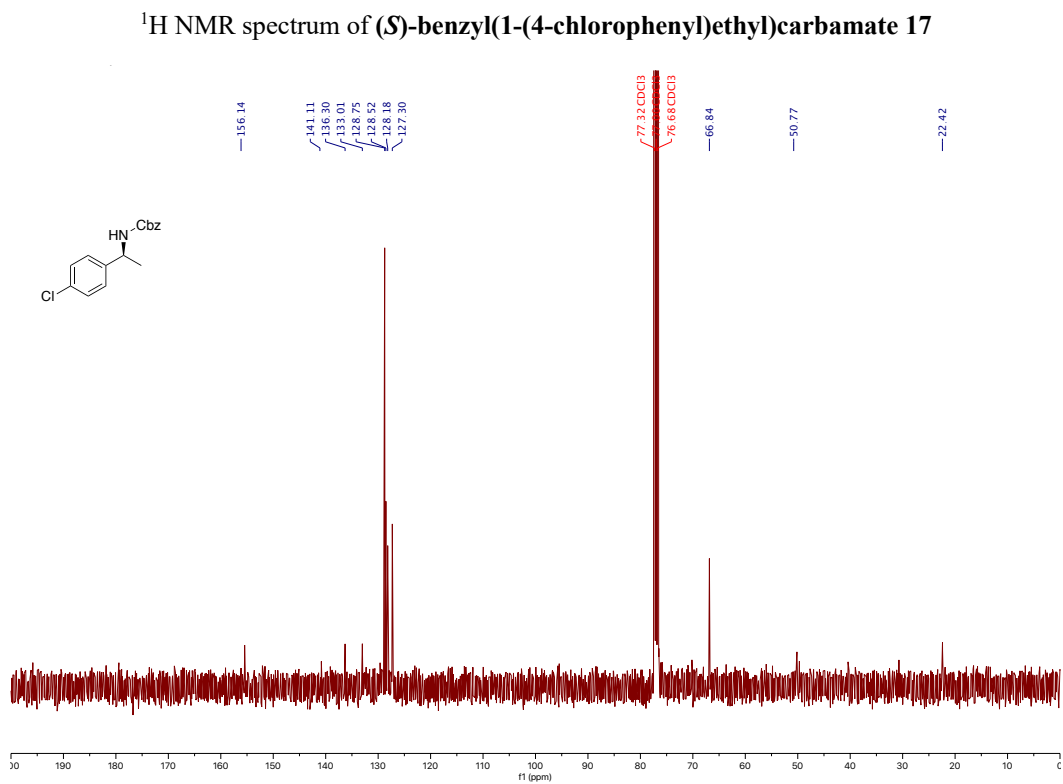
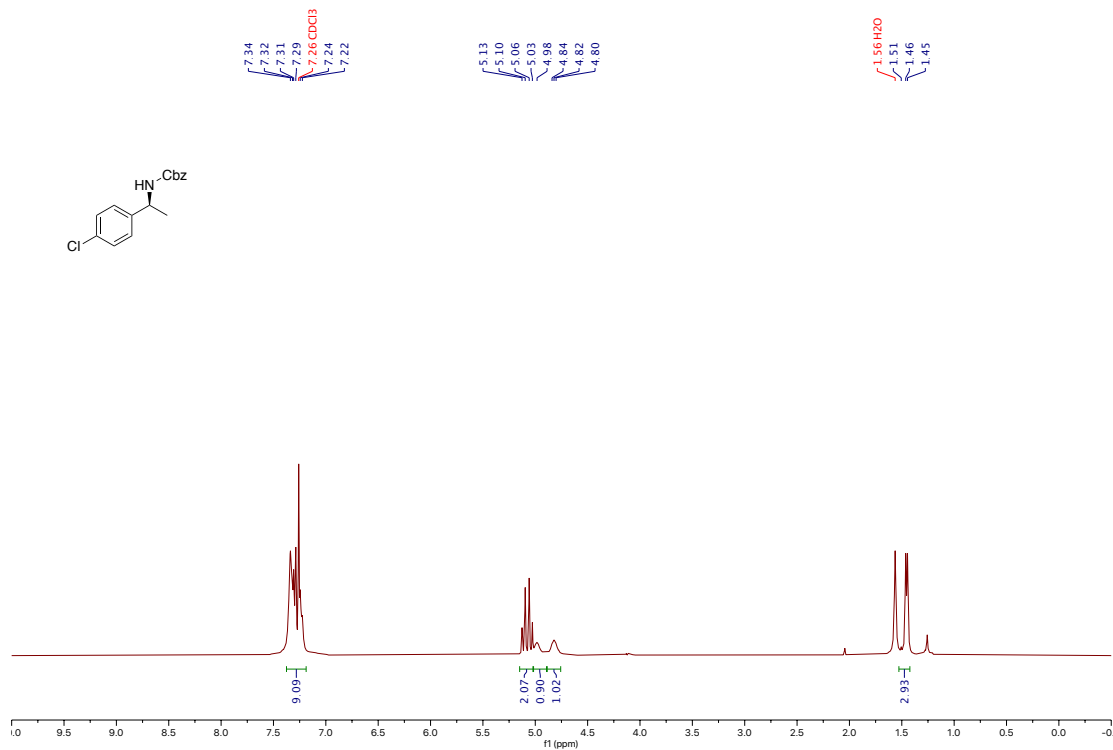
¹³C NMR spectrum of 2-ethylhexyl (*E*)-3-(4-(1-((benzyloxy)carbonyl)amino)ethyl)phenyl)acrylate 14

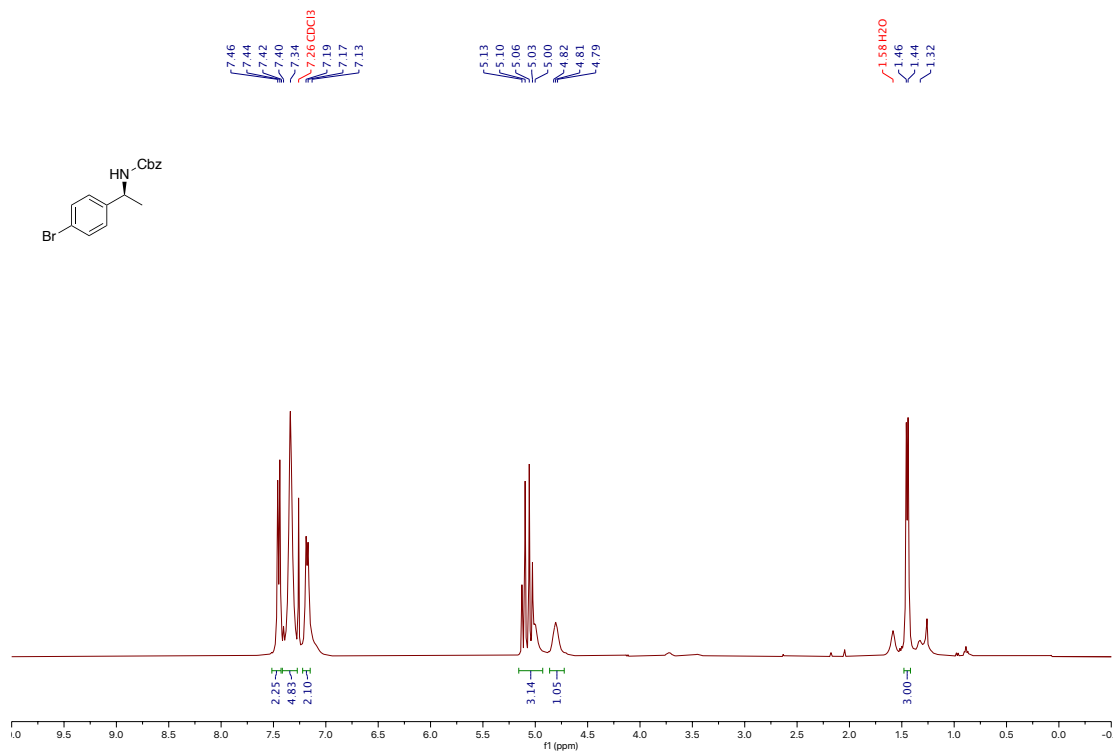


¹H NMR spectrum of (S)-benzyl(1-(4-iodophenyl)ethyl)carbamate 16

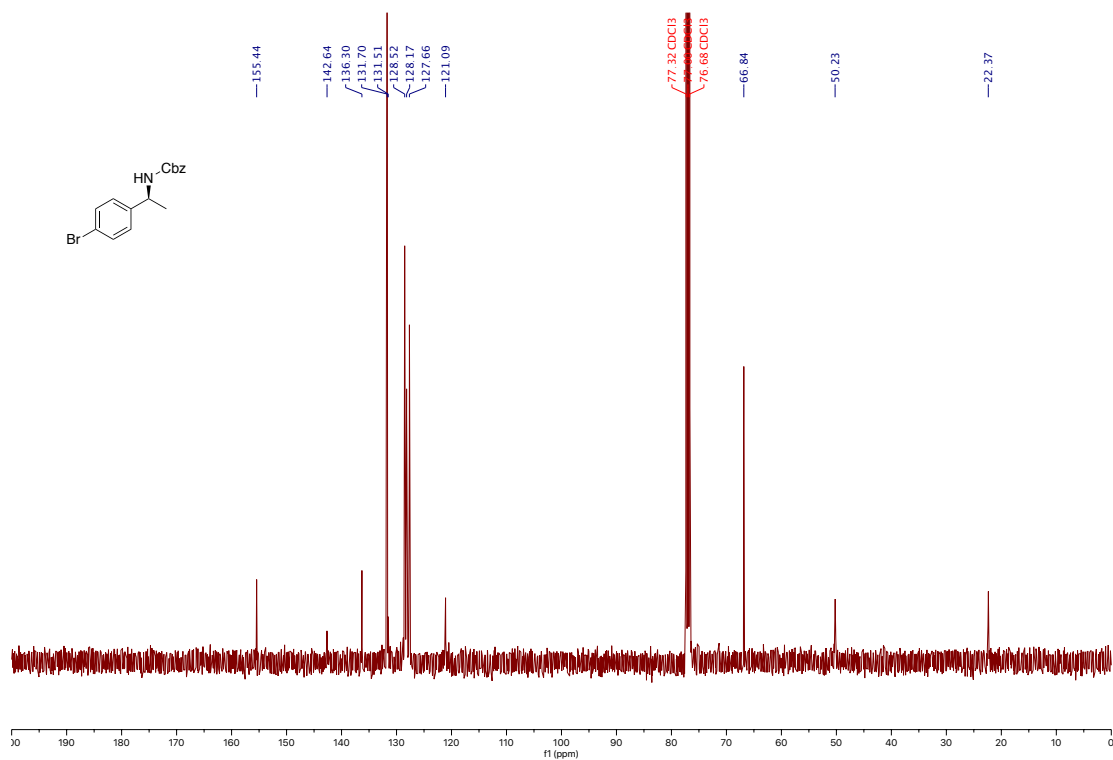


¹³C NMR spectrum of (S)-benzyl(1-(4-iodophenyl)ethyl)carbamate 16

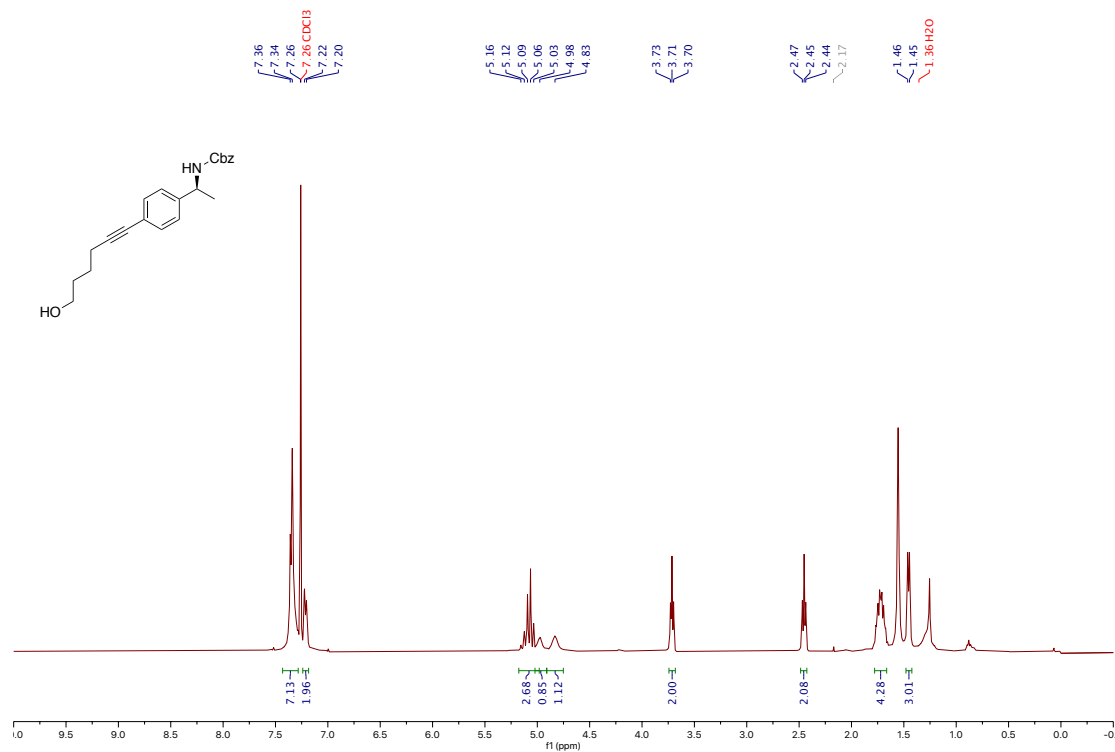




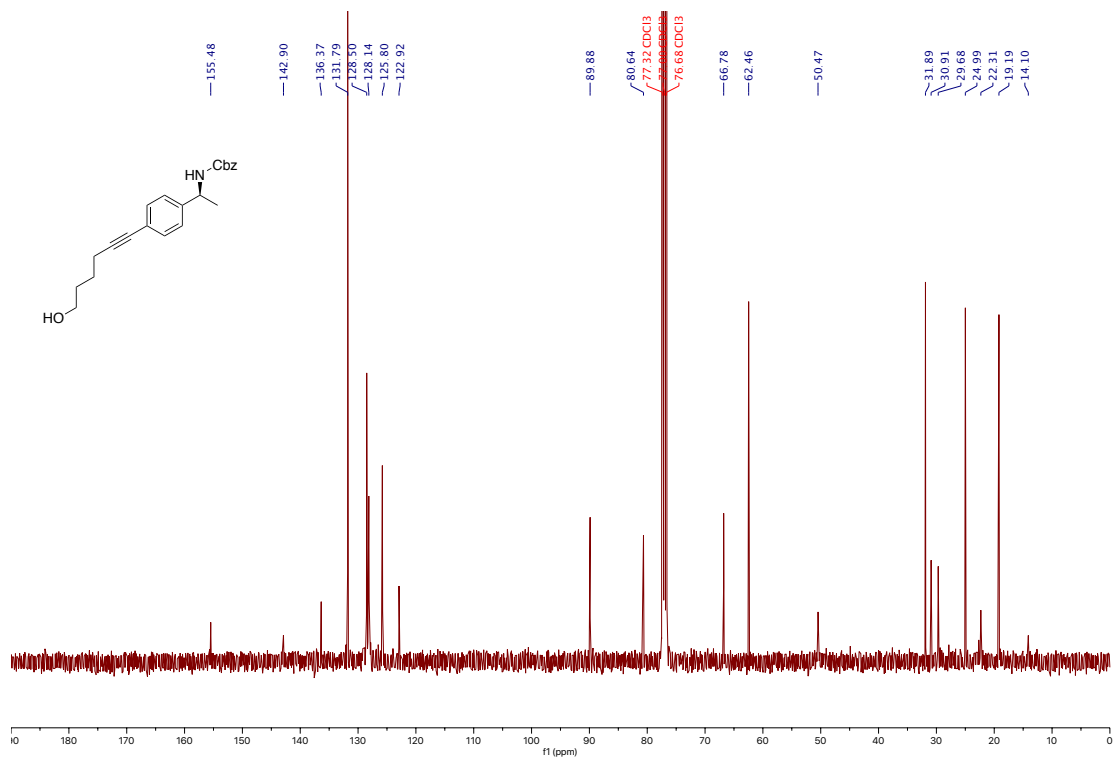
¹H NMR spectrum of (S)-benzyl(1-(4-bromophenyl)ethyl)carbamate 18



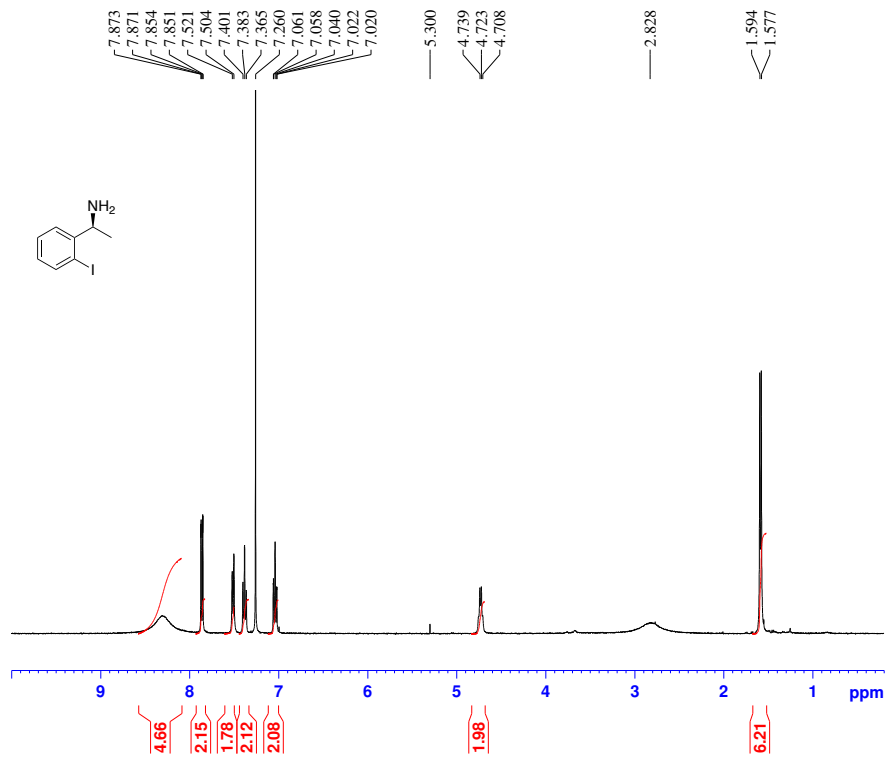
¹³C NMR spectrum of (S)-benzyl(1-(4-bromophenyl)ethyl)carbamate 18



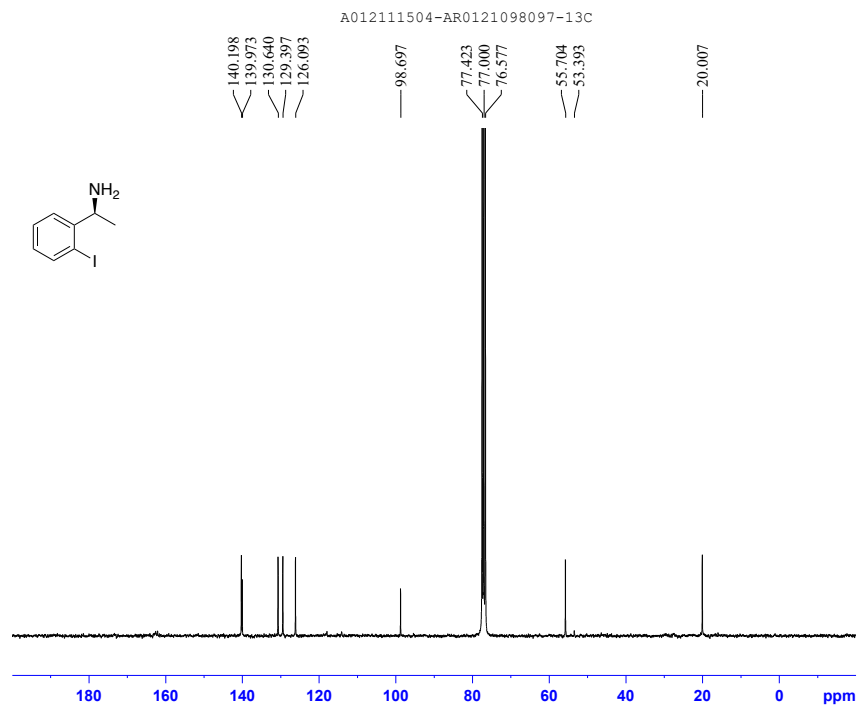
¹H NMR spectrum of (S)-benzyl (1-(4-(6-hydroxyhex-1-yn-1-yl)phenyl)ethyl)carbamate 19



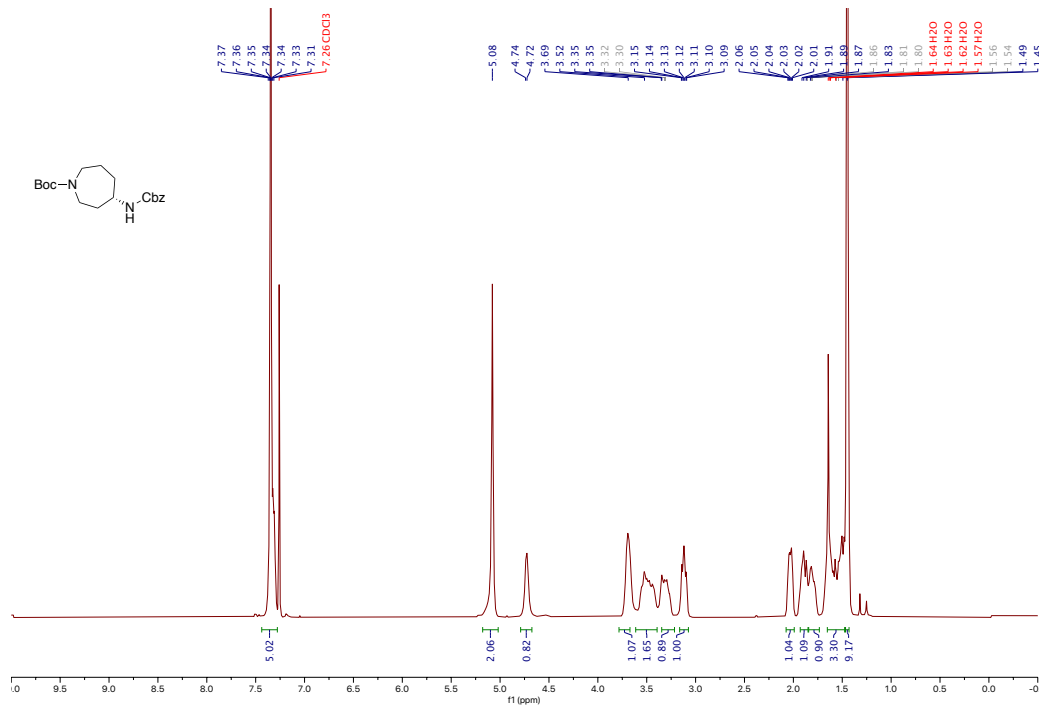
¹³C NMR spectrum of (S)-benzyl (1-(4-(6-hydroxyhex-1-yn-1-yl)phenyl)ethyl)carbamate 19



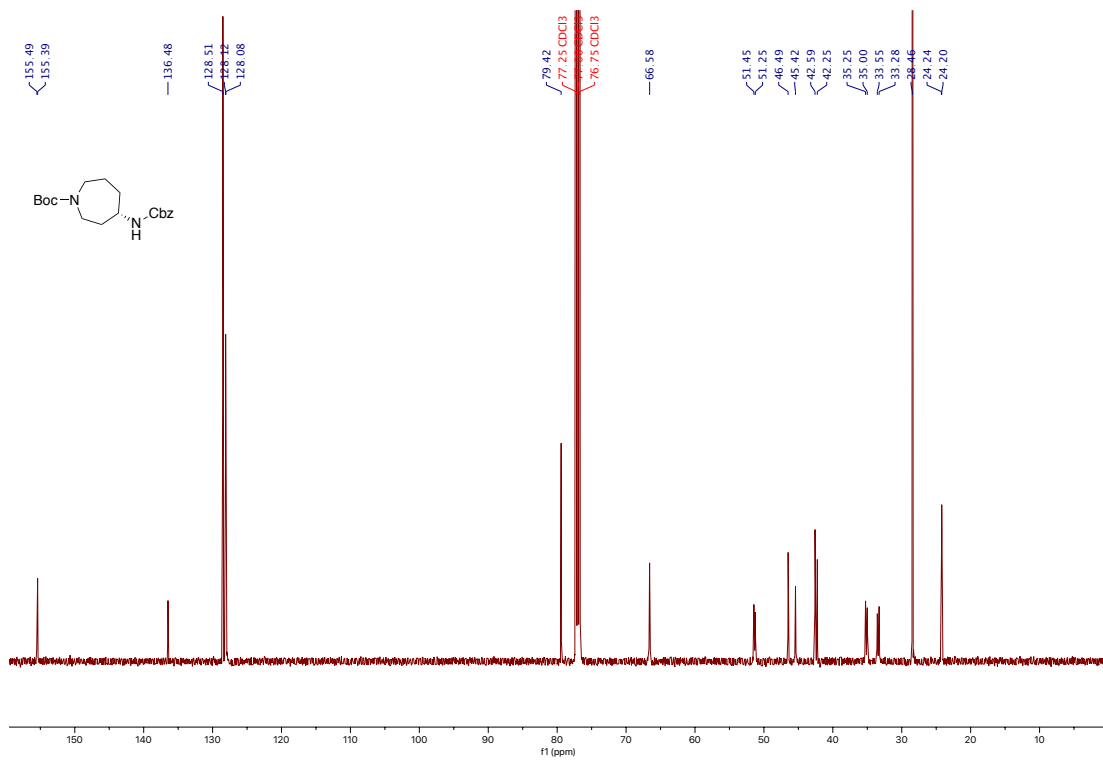
¹H NMR spectrum of (S)-1-(2-iodophenyl)ethan-1-amine 20



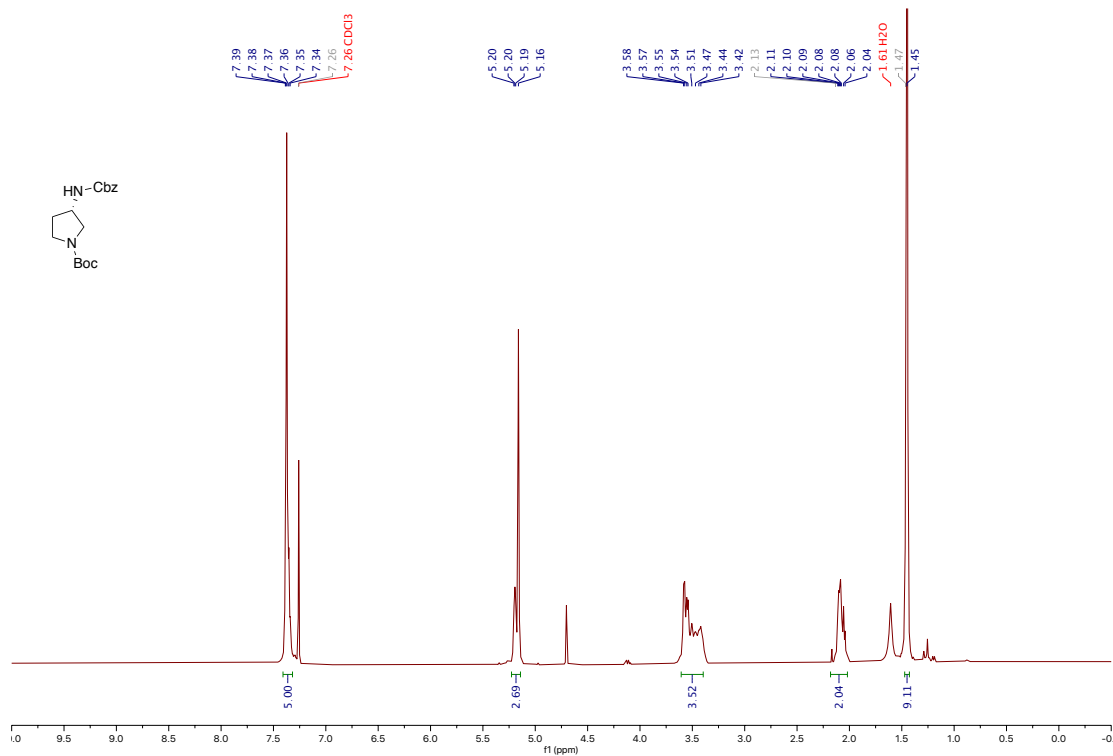
¹³C NMR spectrum of (S)-1-(2-iodophenyl)ethan-1-amine 20



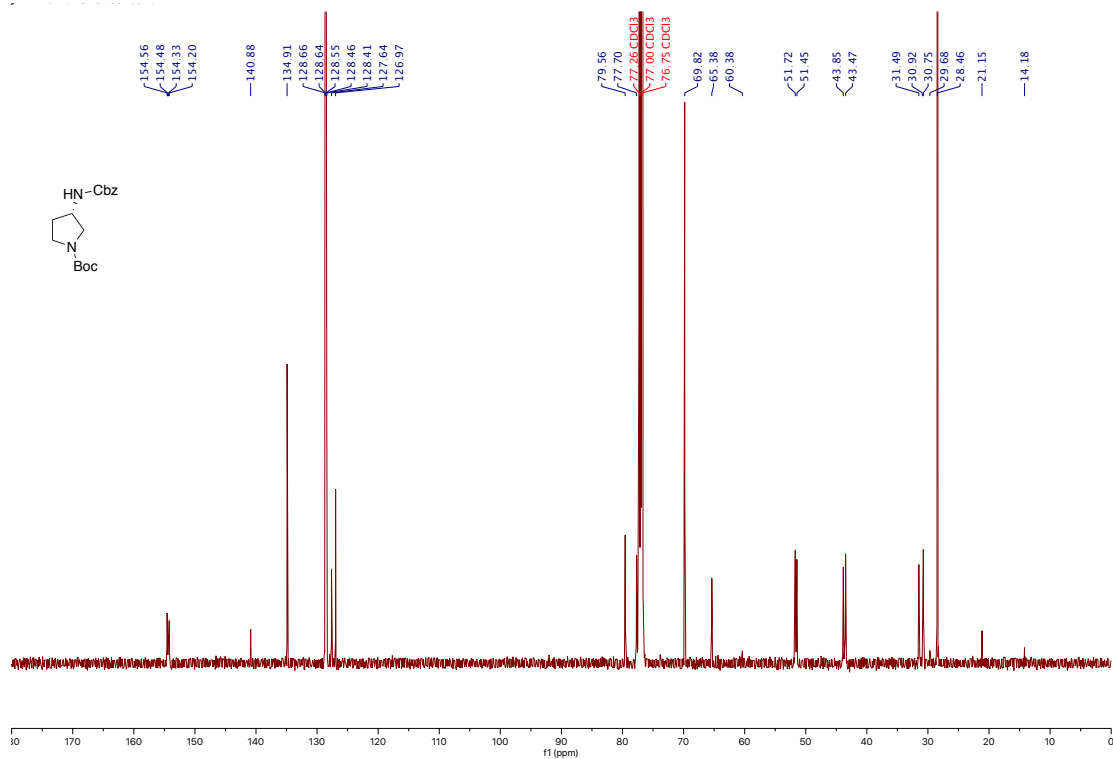
¹H NMR spectrum of **(S)-tert-butyl 4-(((benzyloxy)carbonyl)amino)azepane-1-carboxylate 21**



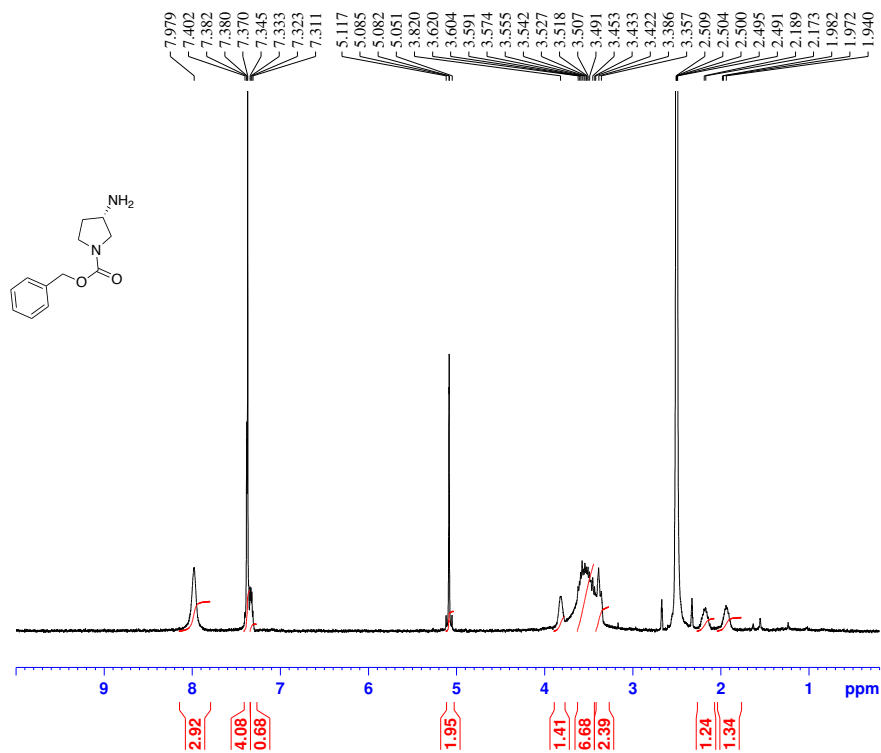
¹³C NMR spectrum of **(S)-tert-butyl 4-(((benzyloxy)carbonyl)amino)azepane-1-carboxylate 21**



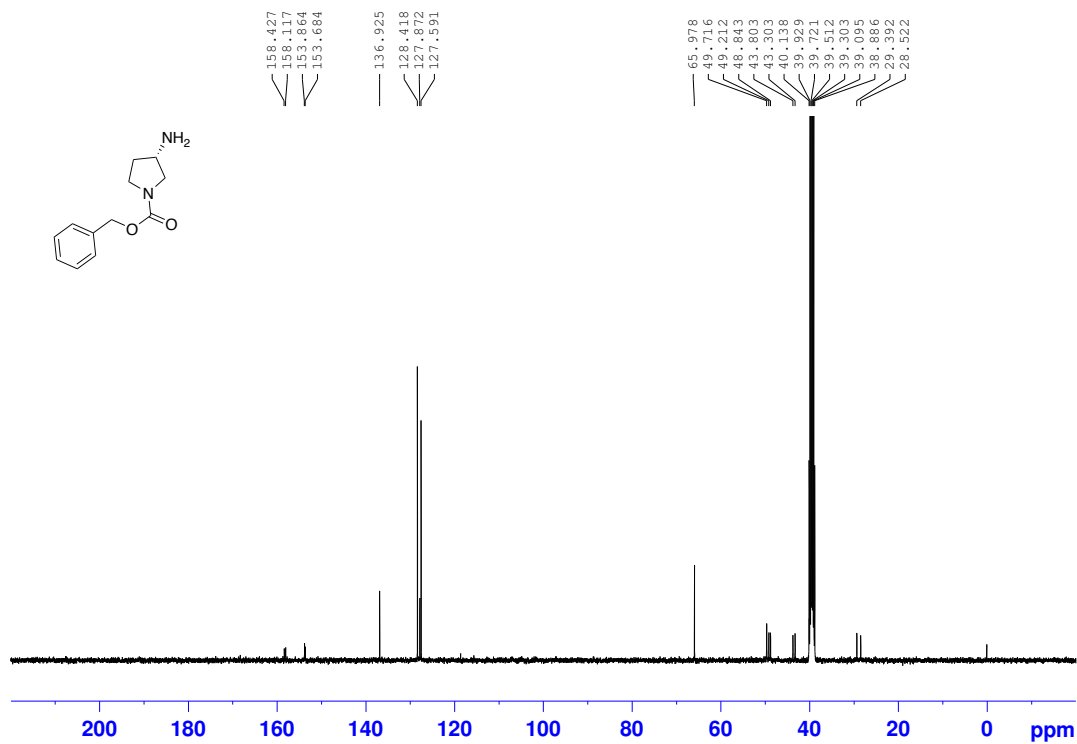
¹H NMR spectrum of (*S*)-*tert*-butyl-3-(((benzyloxy)carbonyl)amino)pyrrolidine-1-carboxylate **22**



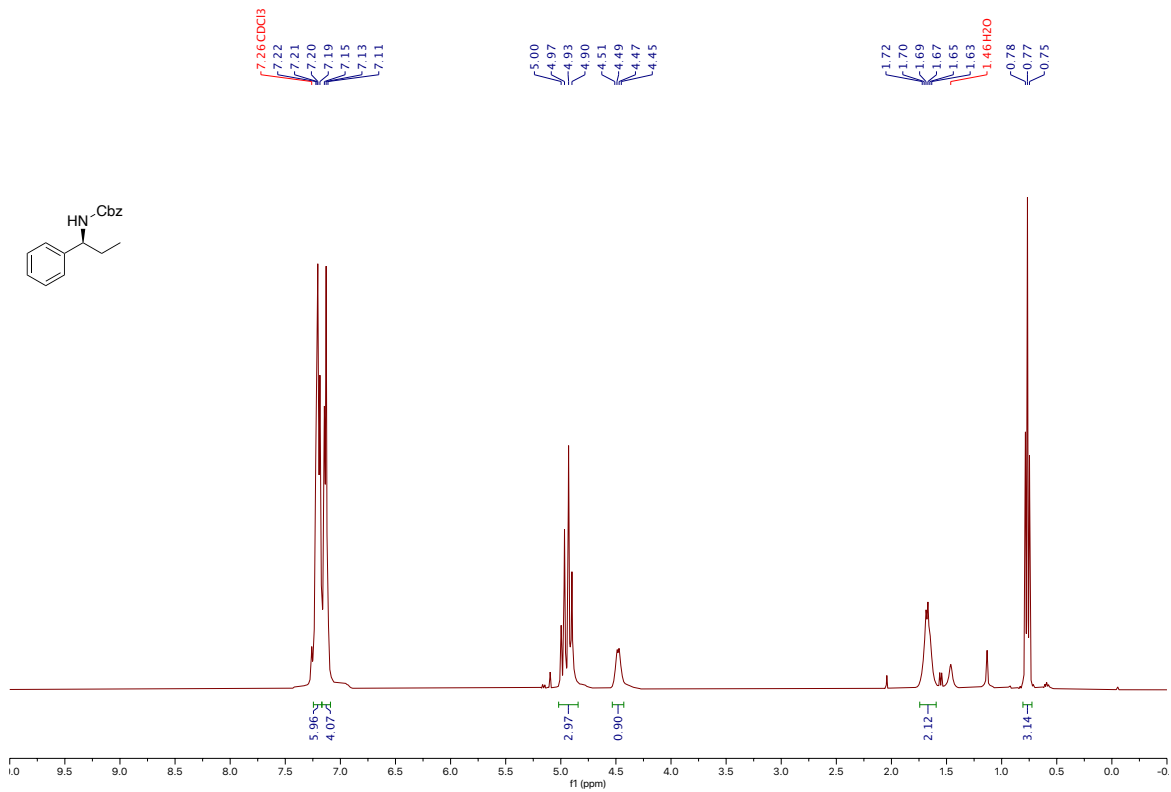
¹³C NMR spectrum of (*S*)-*tert*-butyl-3-(((benzyloxy)carbonyl)amino)pyrrolidine-1-carboxylate **22**



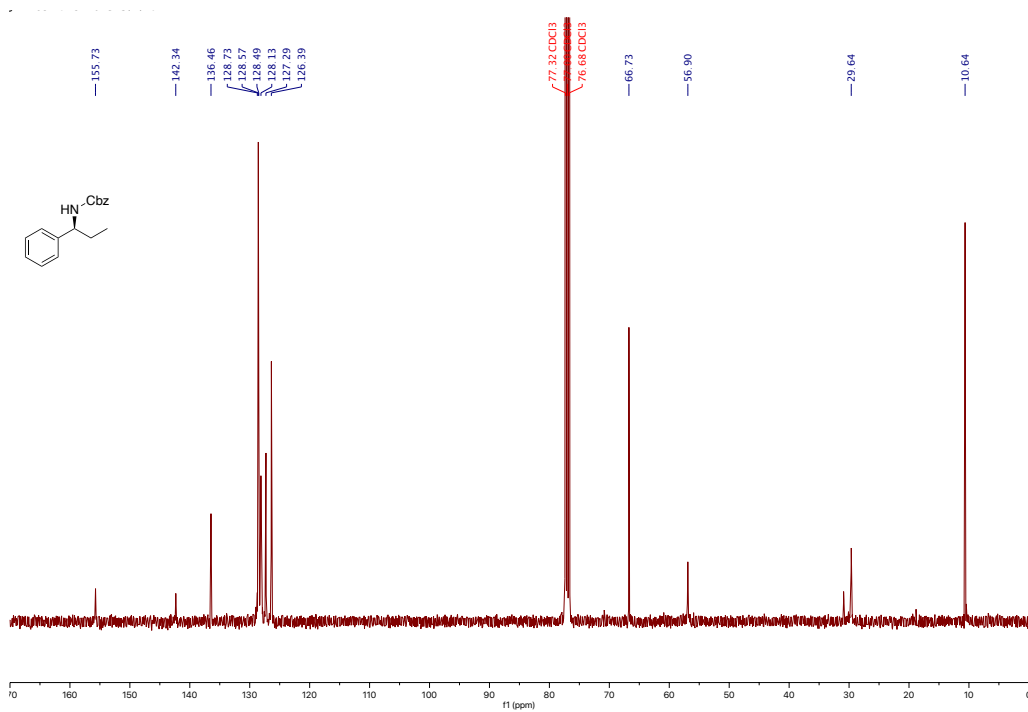
¹H NMR spectrum of (*S*)-benzyl 3-(((benzyloxy)carbonyl)amino)pyrrolidine-1-carboxylate 23



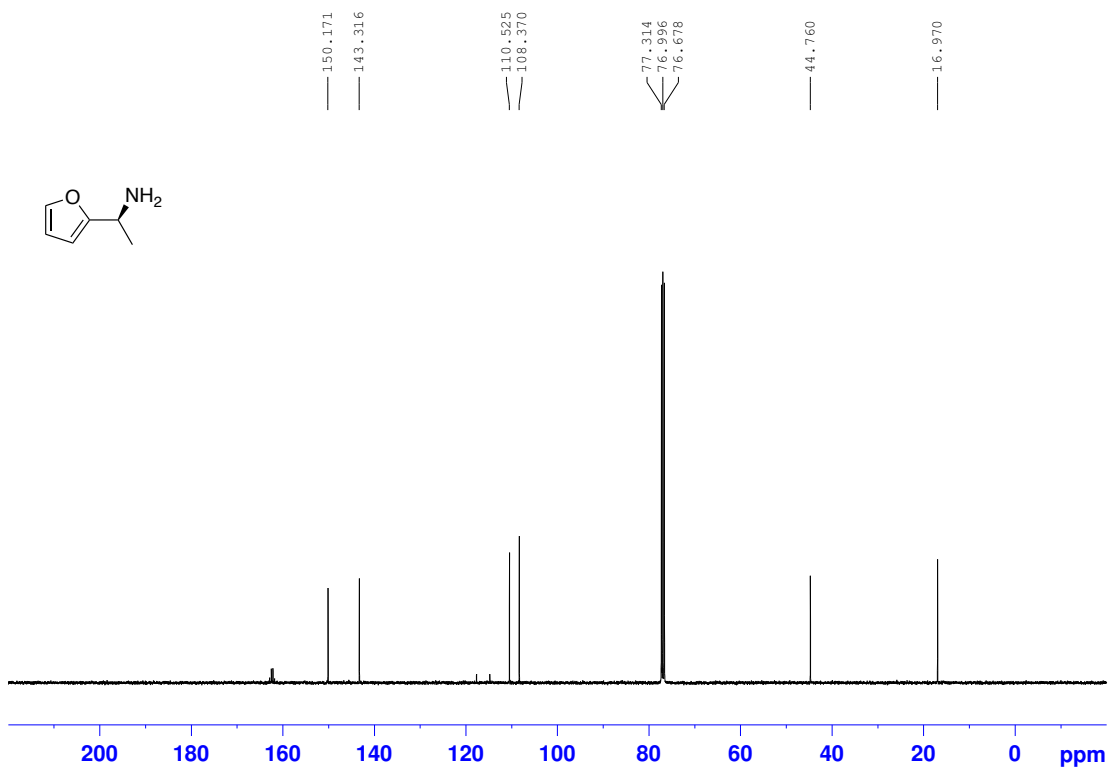
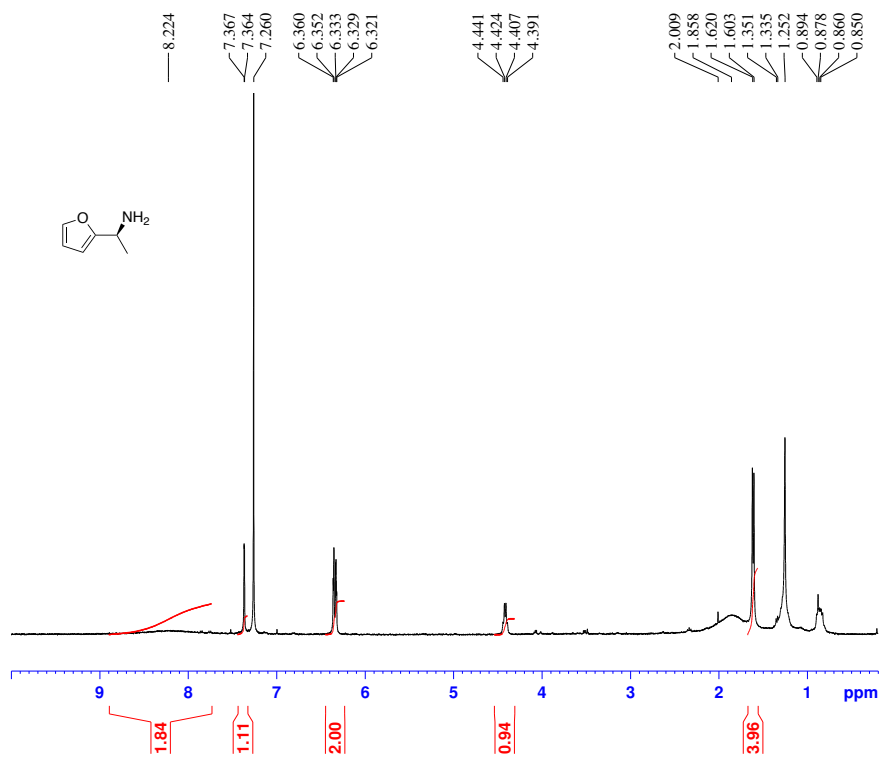
¹³C NMR spectrum of (*S*)-benzyl 3-(((benzyloxy)carbonyl)amino)pyrrolidine-1-carboxylate 23

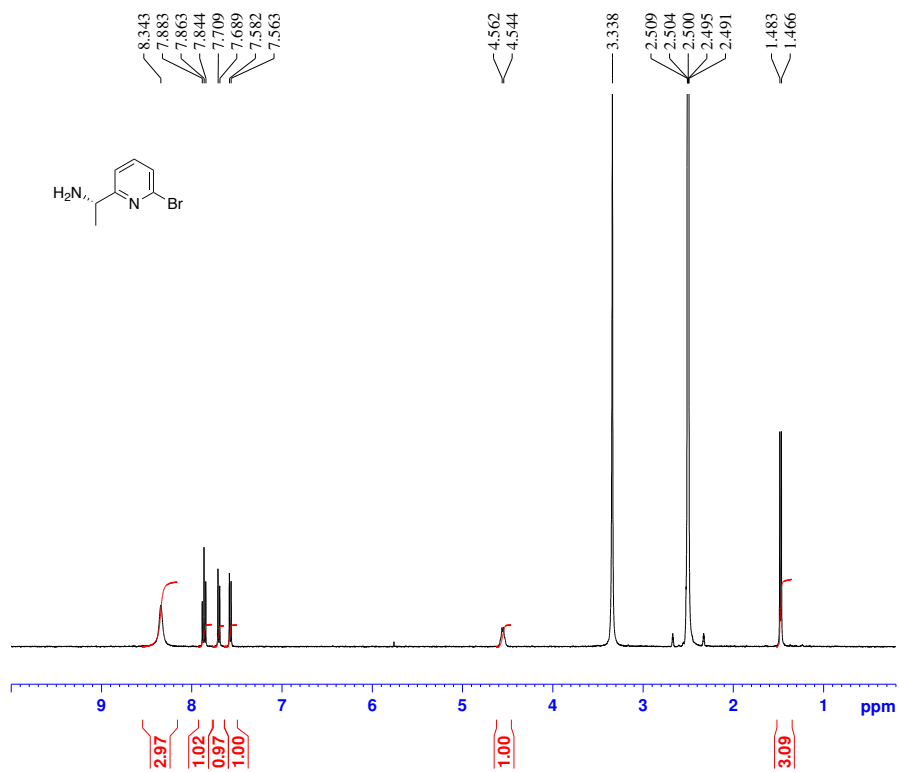


¹H NMR spectrum of benzyl (*S*)-(1-phenylpropyl)carbamate 24

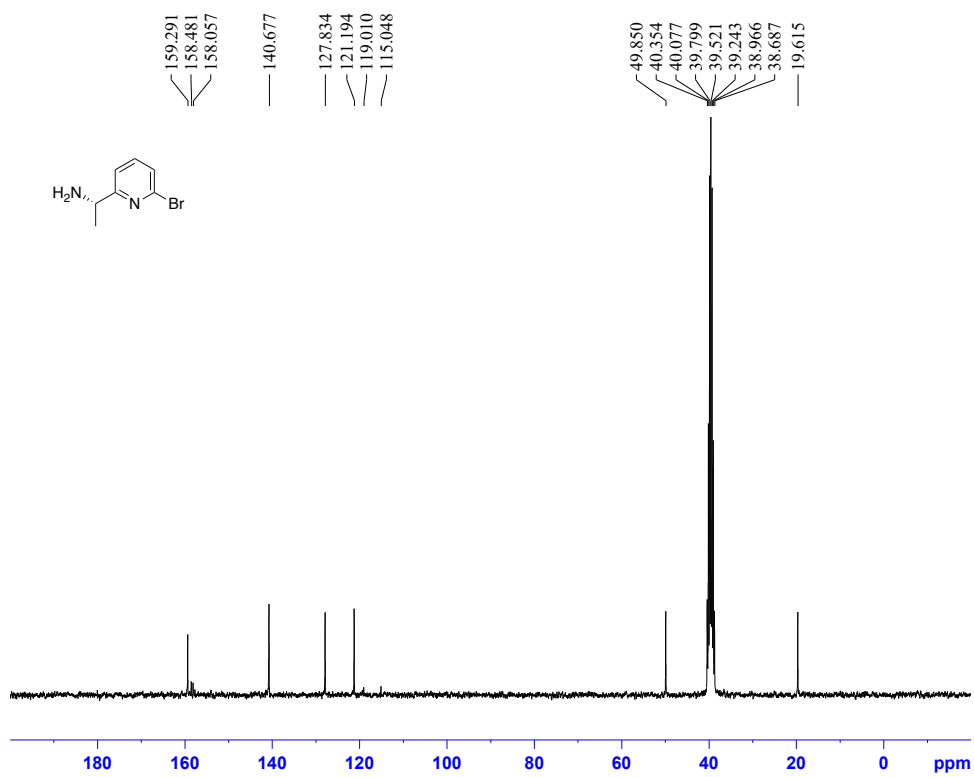


¹³C NMR spectrum of benzyl (*S*)-(1-phenylpropyl)carbamate 24

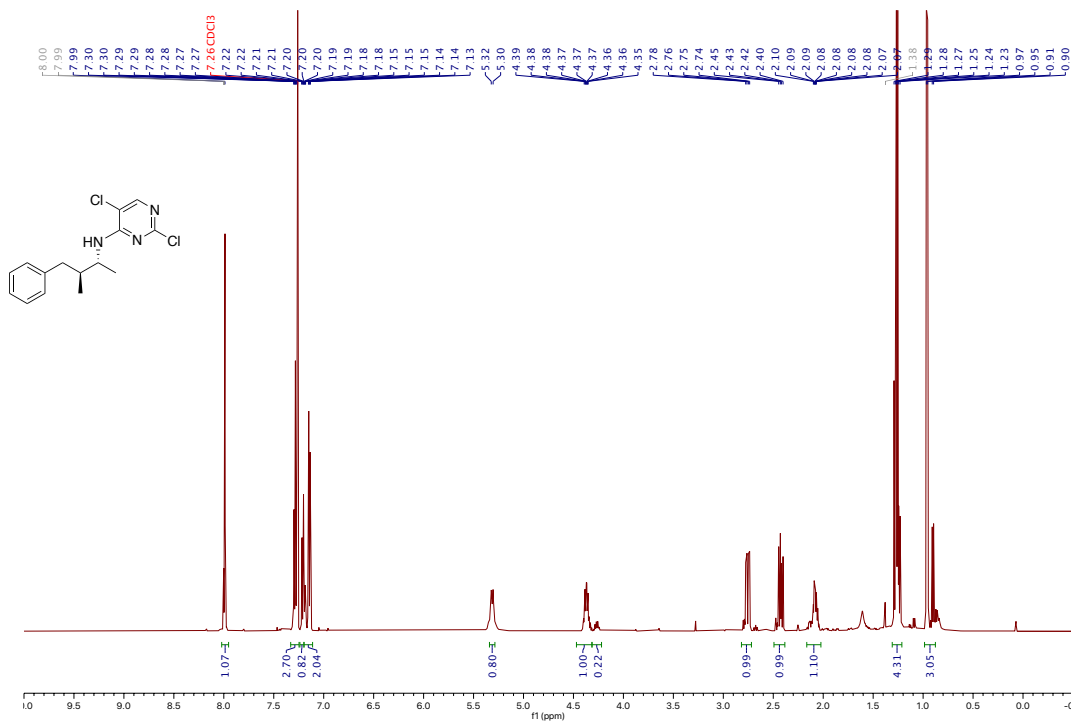




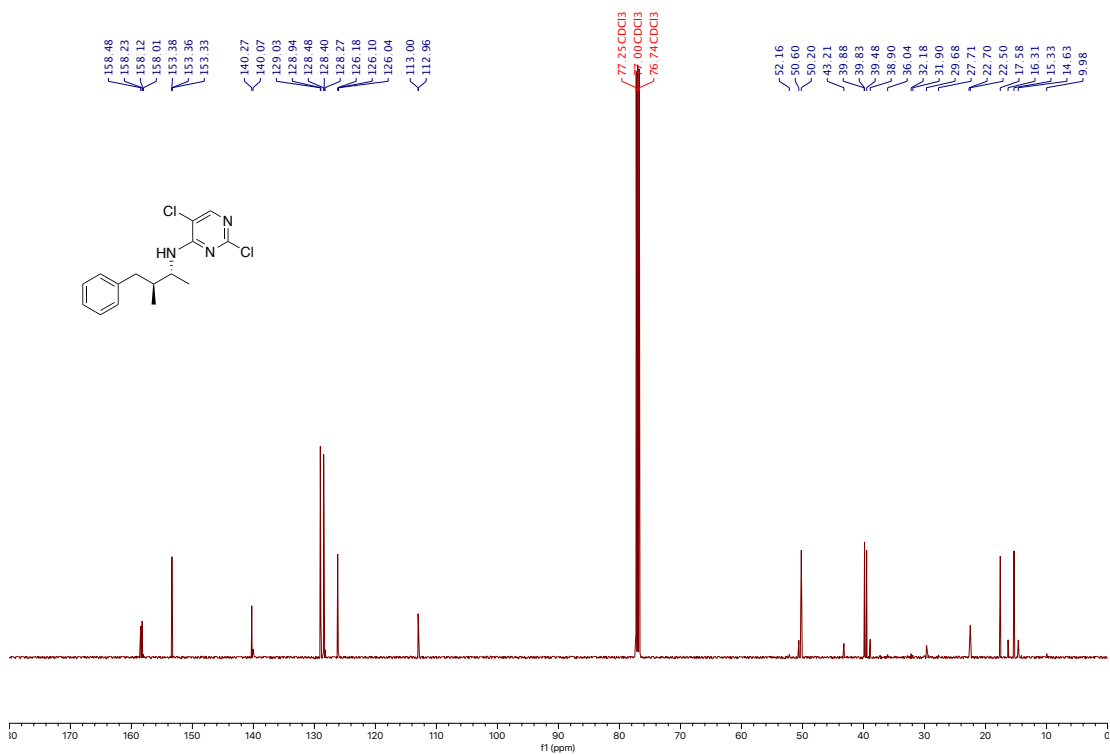
¹H NMR spectrum of (S)-1-(6-bromopyridin-2-yl)ethan-1-amine 26



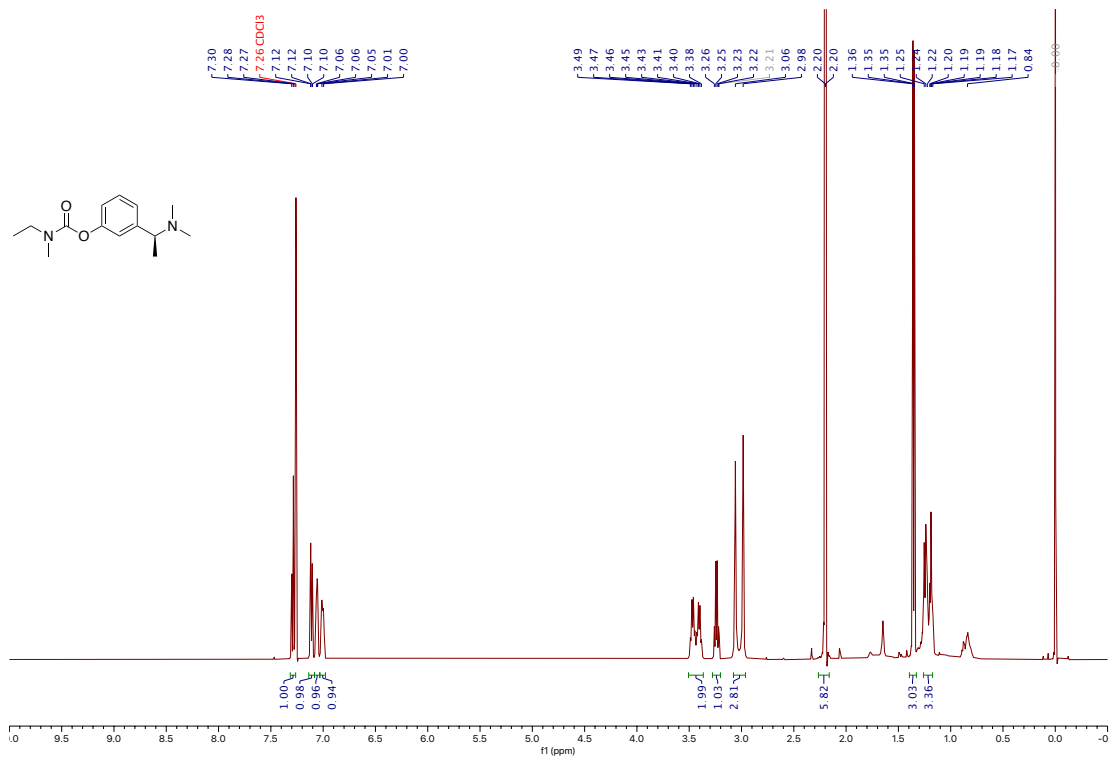
¹³C NMR spectrum of (S)-1-(6-bromopyridin-2-yl)ethan-1-amine 26



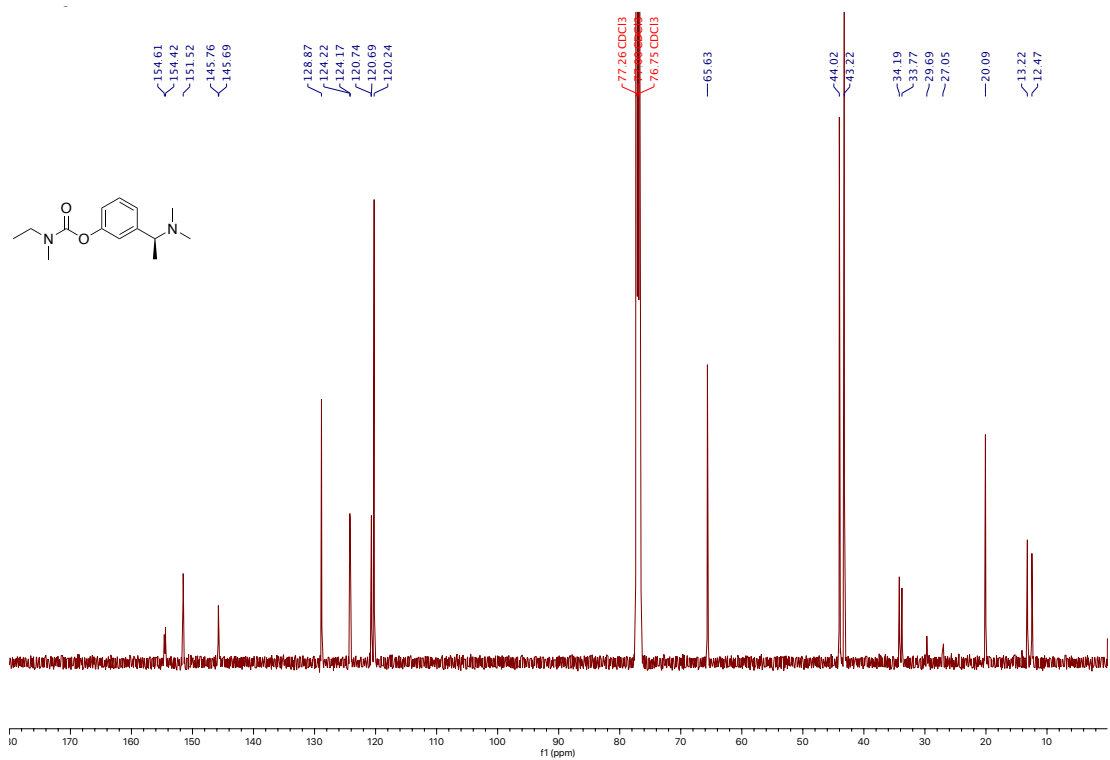
¹H NMR spectrum of 2,5-dichloro-*N*-((2*R*,3*S*)-3-methyl-4-phenylbutan-2-yl)pyrimidin-4-amine 32



¹³C NMR spectrum of 2,5-dichloro-*N*-((2*R*,3*S*)-3-methyl-4-phenylbutan-2-yl)pyrimidin-4-amine 32

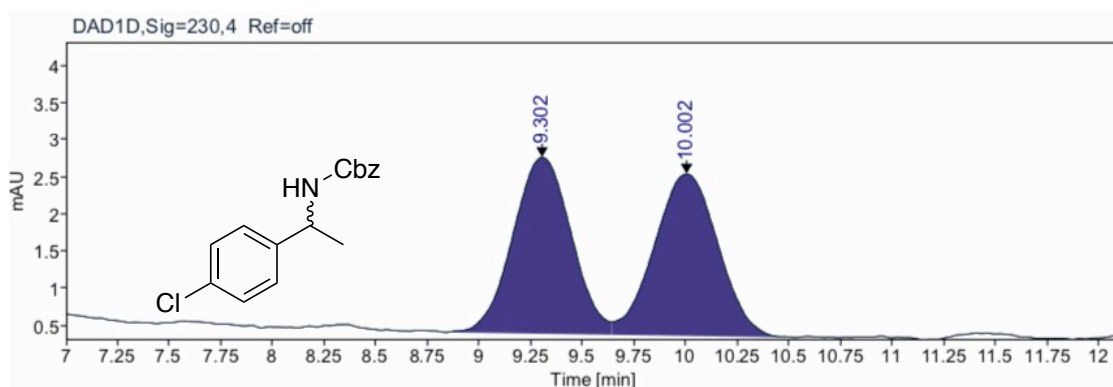


¹H NMR spectrum of (*S*)-rivastigmine

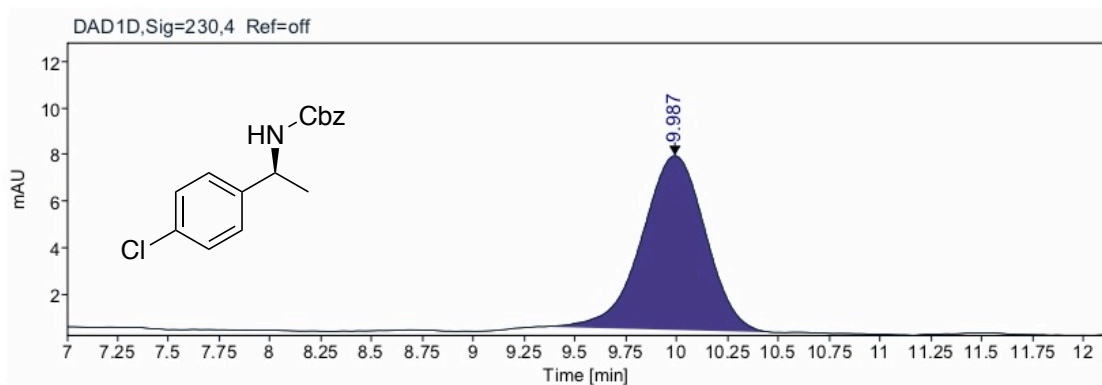


¹³C NMR spectrum of (*S*)-rivastigmine

2.10. HPLC traces

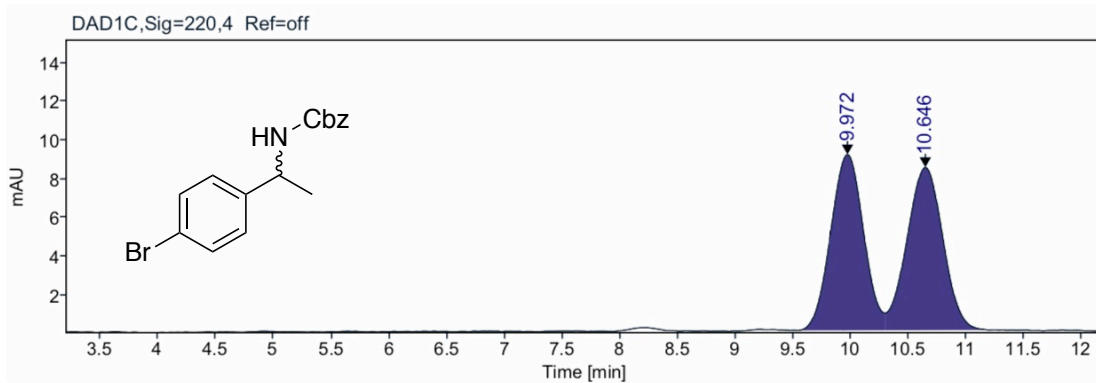


RT [min]	Area	Area%
9.302	46.7580	49.9
10.002	46.8697	50.1
Sum	93.6277	

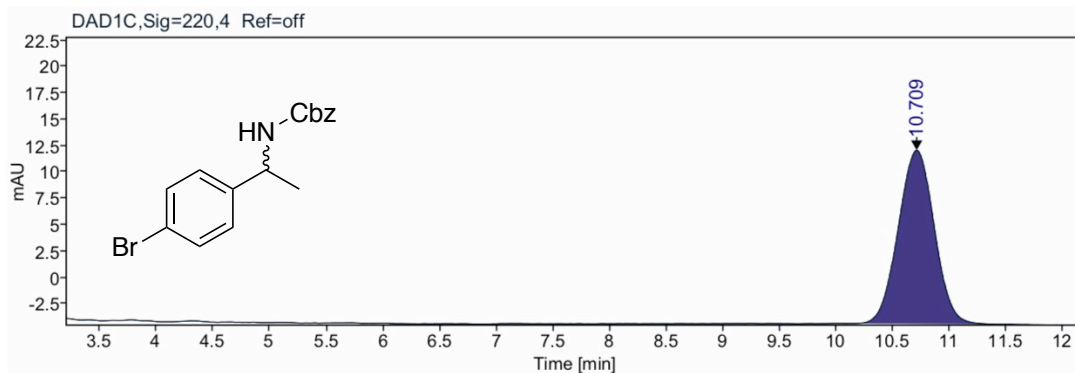


RT [min]	Area	Area%
9.987	163.1647	100.0
Sum	163.1647	

HPLC analysis of (*S*)-benzyl(1-(4-chlorophenyl)ethyl)carbamate

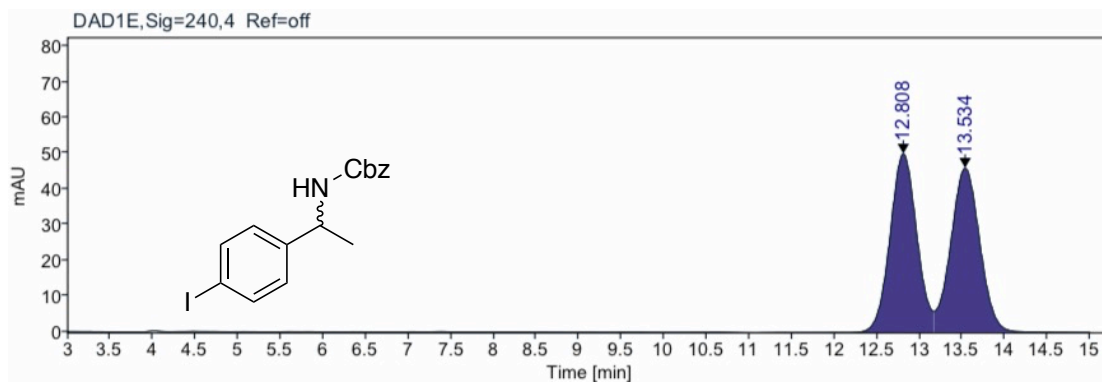


RT [min]	Area	Area%
9.972	180.7430	49.7
10.646	183.1462	50.3
Sum	363.8893	

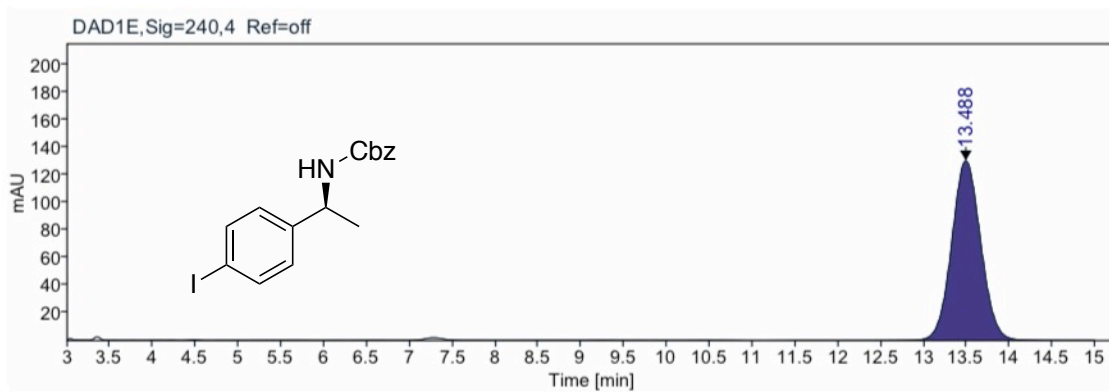


RT [min]	Area	Area%
10.709	363.4214	100.0
Sum	363.4214	

HPLC analysis of (*S*)-benzyl(1-(4-bromophenyl)ethyl)carbamate

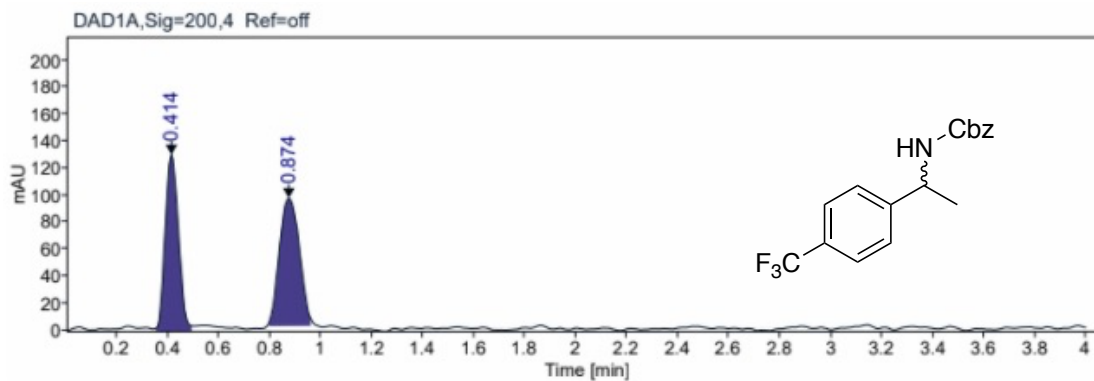


RT [min]	Area	Area%
12.808	1094.1356	50.0
13.534	1096.2754	50.0
Sum	2190.4110	

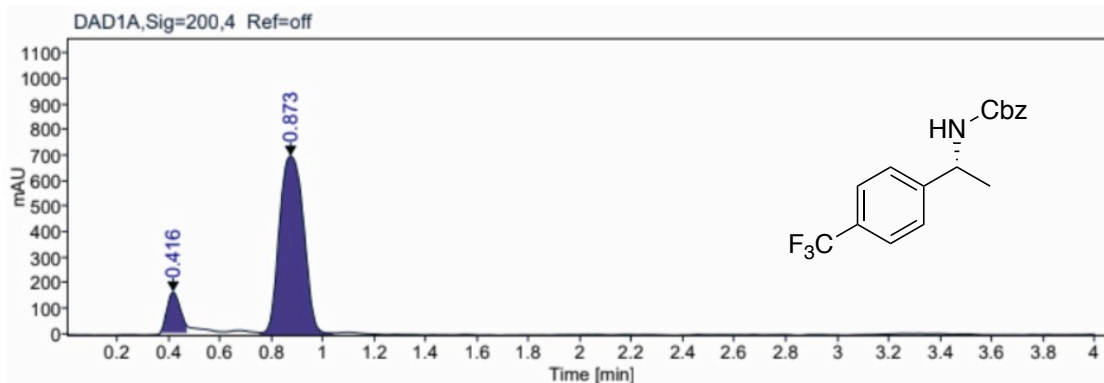


RT [min]	Area	Area%
13.488	3060.1331	100.0
Sum	3060.1331	

HPLC analysis of (*S*)-benzyl(1-(4-iodophenyl)ethyl)carbamate

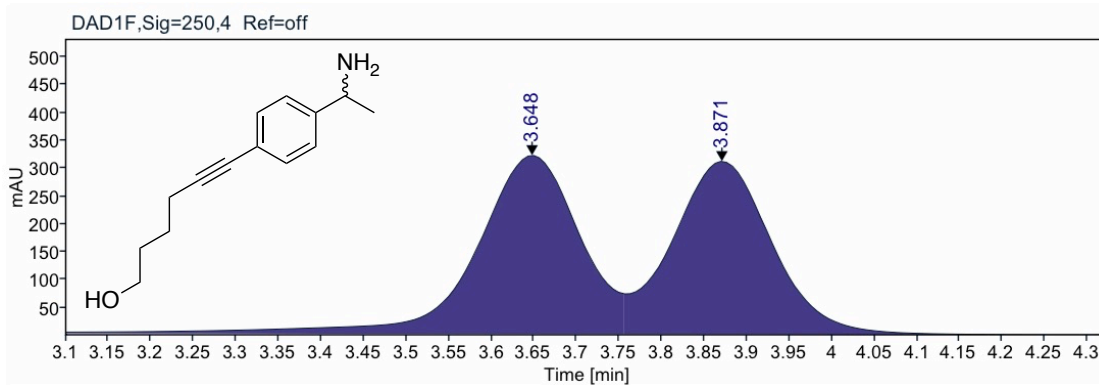


RT [min]	Area	Area%
0.414	509.8059	49.9
0.874	511.3966	50.1
Sum	1021.2025	

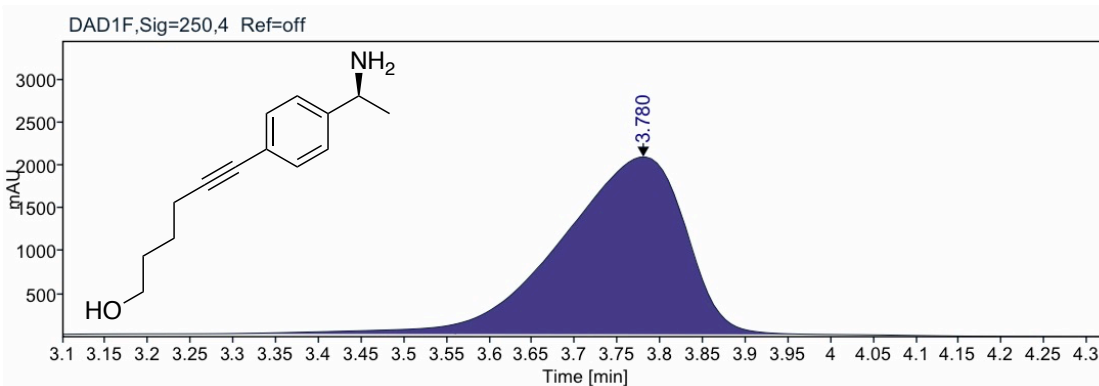


RT [min]	Area	Area%
0.416	564.8058	10.7
0.873	4722.5385	89.3
Sum	5287.3443	

HPLC analysis of (*R*)-benzyl (1-(4-(trifluoromethyl)phenyl)ethyl)carbamate

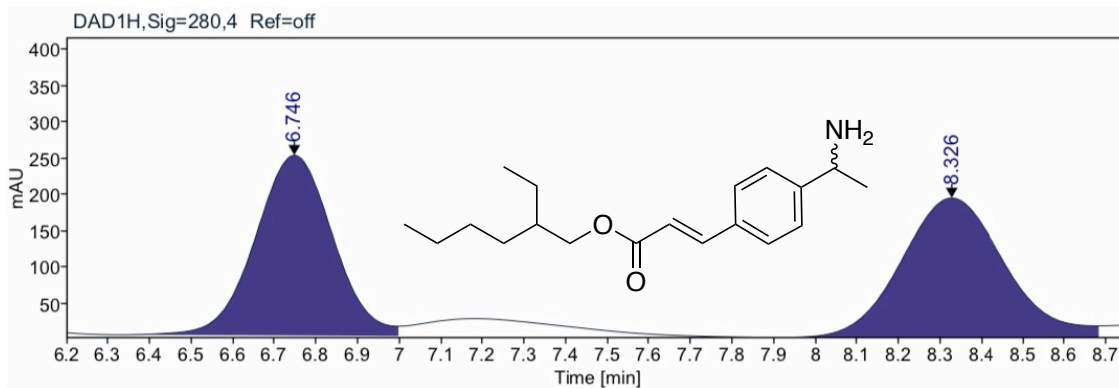


RT [min]	Area	Area%
3.648	2737.5088	51.9
3.871	2535.1423	48.1
Sum	5272.6511	

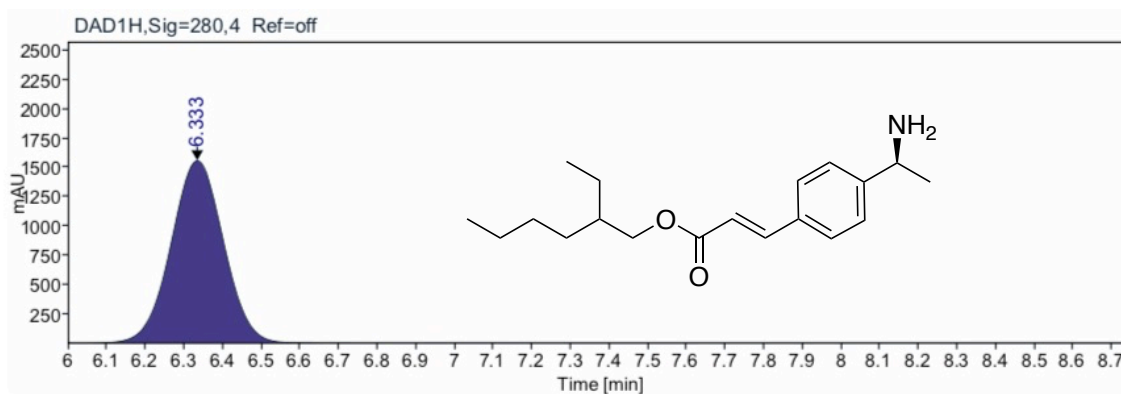


RT [min]	Area	Area%
3.780	21178.1383	100.0
Sum	21178.1383	

HPLC analysis of (*S*)-benzyl (1-(4-(6-hydroxyhex-1-yn-1-yl)phenyl)ethyl)carbamate

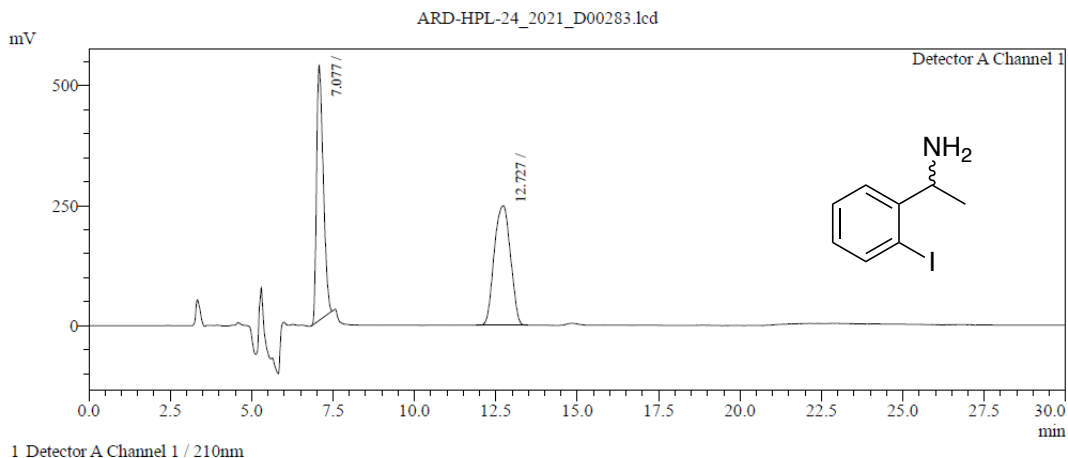


RT [min]	Area	Area%
6.746	3214.7639	49.0
8.326	3340.7536	51.0
Sum	6555.5174	



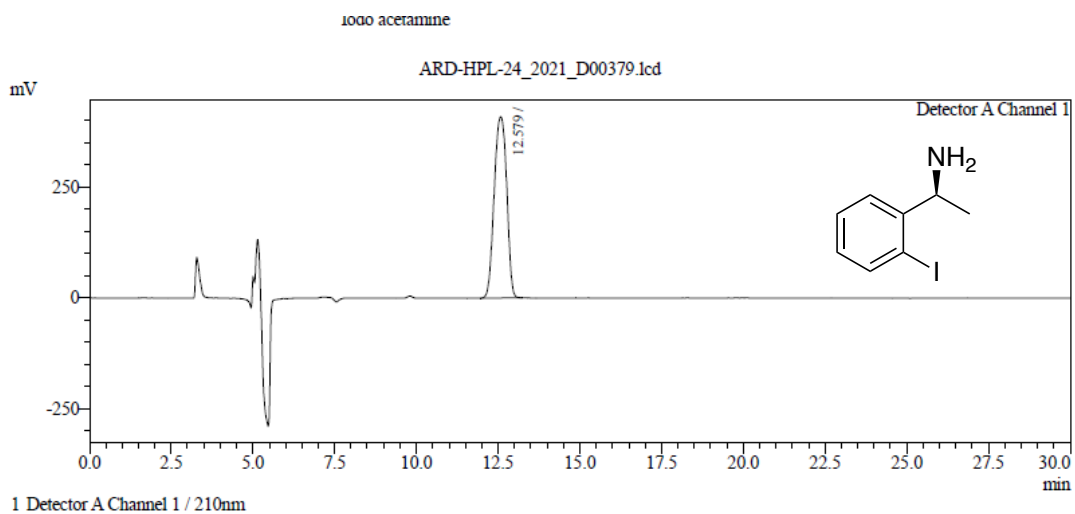
RT [min]	Area	Area%
6.333	14725.0334	100.0
Sum	14725.0334	

HPLC analysis of (S)-2-ethylhexyl (E)-3-(4-(1-((benzyloxy)carbonyl)amino)ethyl)phenyl)acrylate



Peak Table

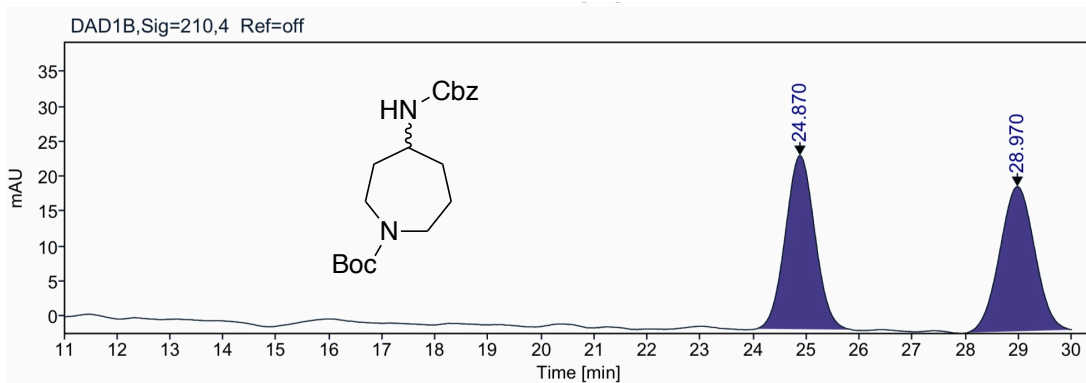
Peak#	Ret. Time (min)	RRT	Height	Area	Area%	Name
1	7.077	1.000	530230	7617644	46.906	
2	12.727	1.798	248954	8622671	53.094	
Total			779184	16240316	100.000	



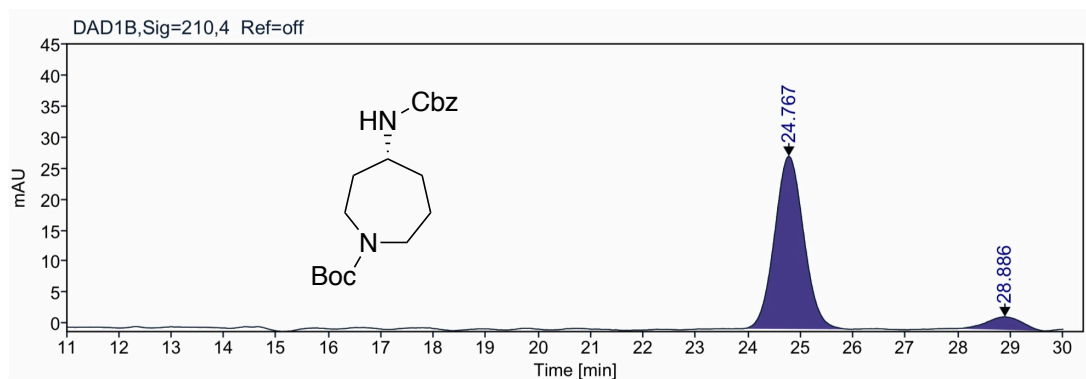
Peak Table

Peak#	Ret. Time (min)	RRT	Height	Area	Area%	Name
1	12.579	1.000	408369	10870539	100.000	
Total			408369	10870539	100.000	

HPLC analysis of (S)-1-(2-iodophenyl)ethan-1-amine

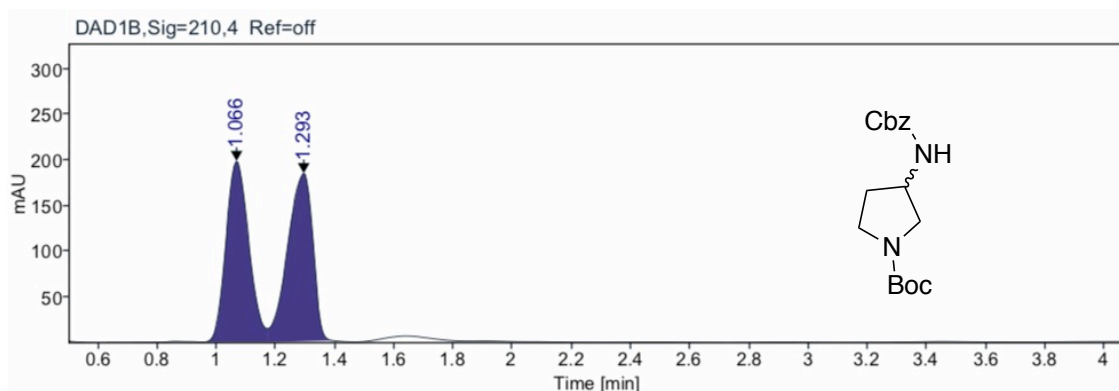


RT [min]	Area	Area%
24.870	962.1121	50.4
28.970	946.8702	49.6
Sum	1908.9823	

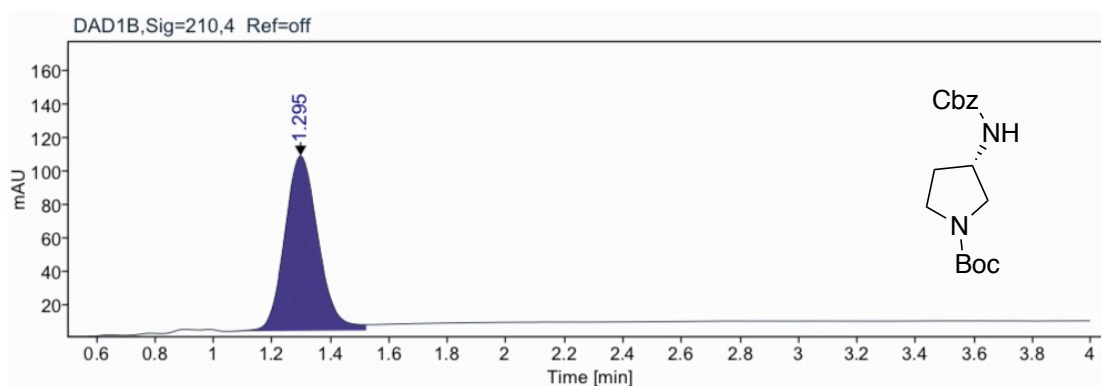


RT [min]	Area	Area%
24.767	1079.8347	91.6
28.886	99.3328	8.4
Sum	1179.1675	

HPLC analysis of (*S*)-*tert*-butyl-4-(((benzyloxy)carbonyl)amino)azepane-1-carboxylate

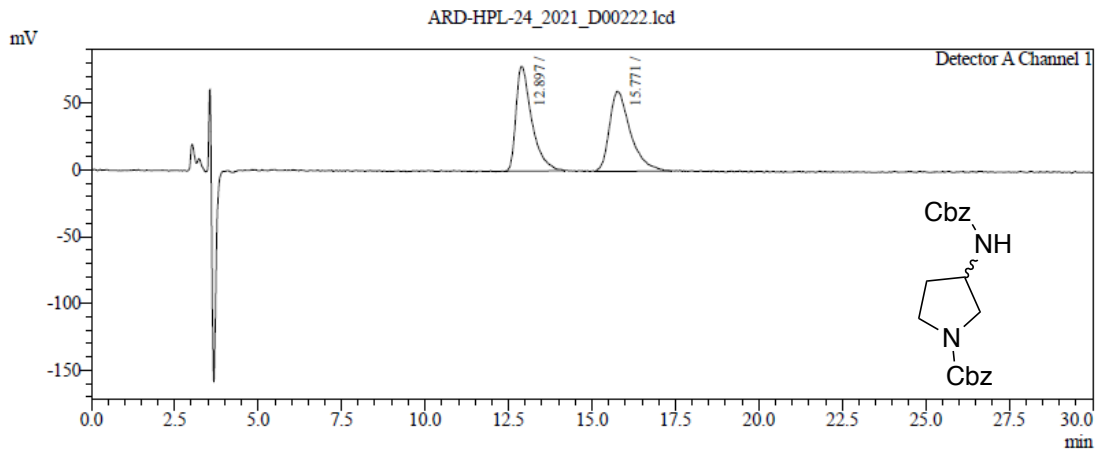


RT [min]	Area	Area%
1.066	1065.6655	49.4
1.293	1091.0728	50.6
Sum	2156.7383	



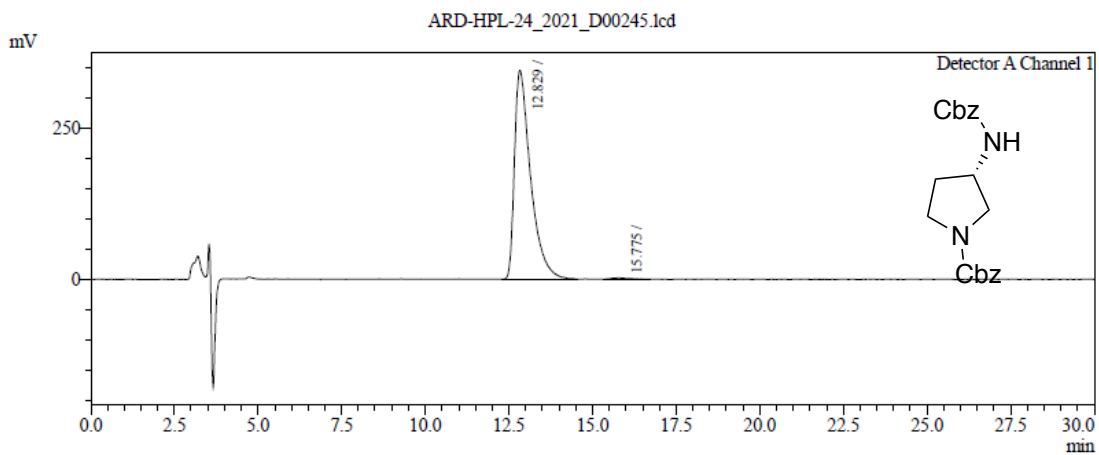
RT [min]	Area	Area%
1.295	832.8978	100.0
Sum	832.8978	

HPLC analysis of (*S*)-*tert*-butyl-3-(((benzyloxy)carbonyl)amino)pyrrolidine-1-carboxylate



Peak Table

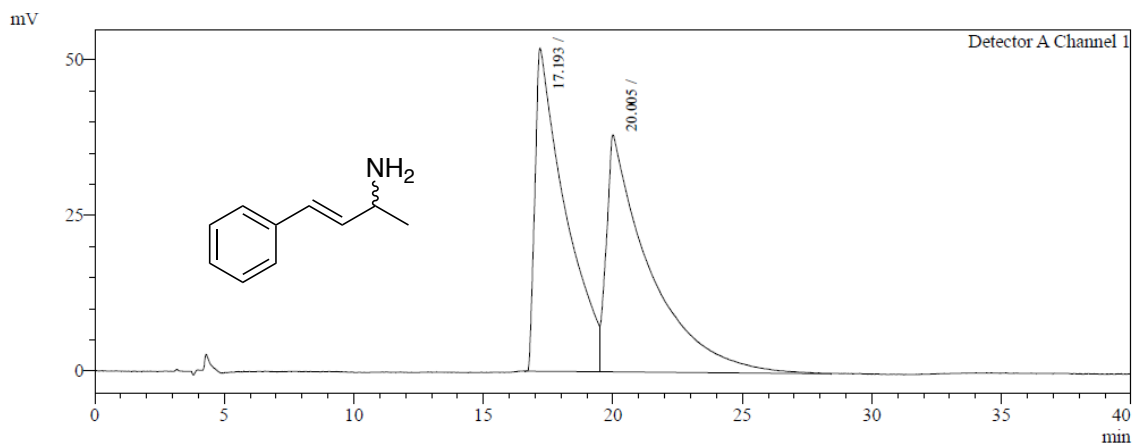
Peak#	Ret. Time (min)	RRT	Height	Area	Area%	Name
1	12.897	1.000	78302	2576513	49.557	
2	15.771	1.223	59836	2622525	50.443	
Total			138138	5199038	100.000	



Peak Table

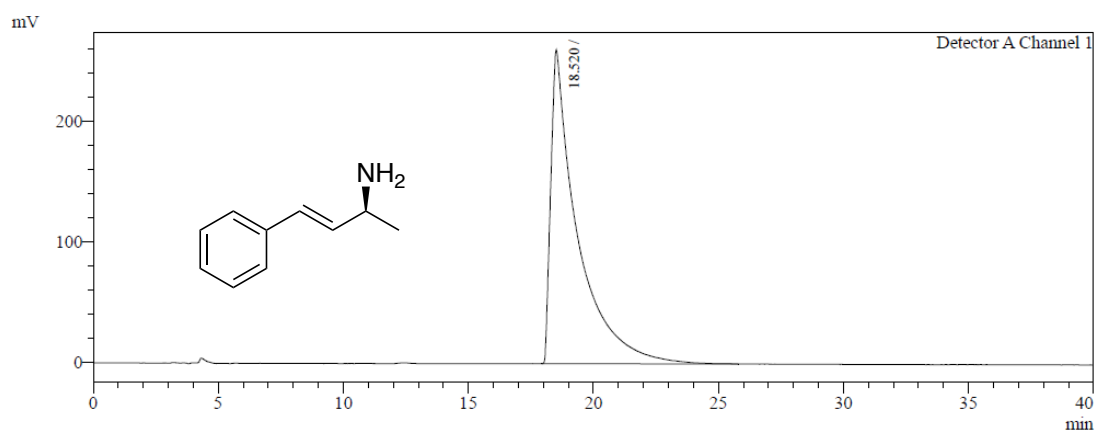
Peak#	Ret. Time (min)	RRT	Height	Area	Area%	Name
1	12.829	1.000	344813	11575460	99.215	
2	15.775	1.230	2474	91581	0.785	
Total			347287	11667041	100.000	

HPLC analysis of (S)-benzyl 3-((benzyloxy)carbonyl)pyrrolidine-1-carboxylate



1 Detector A Channel 1 / 240nm

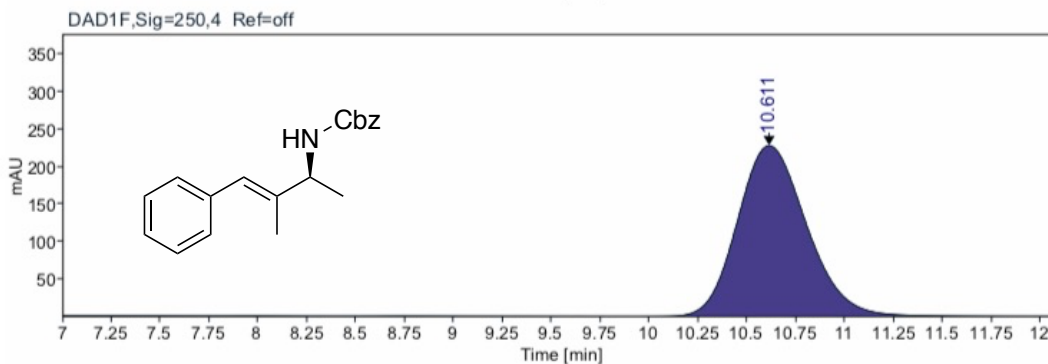
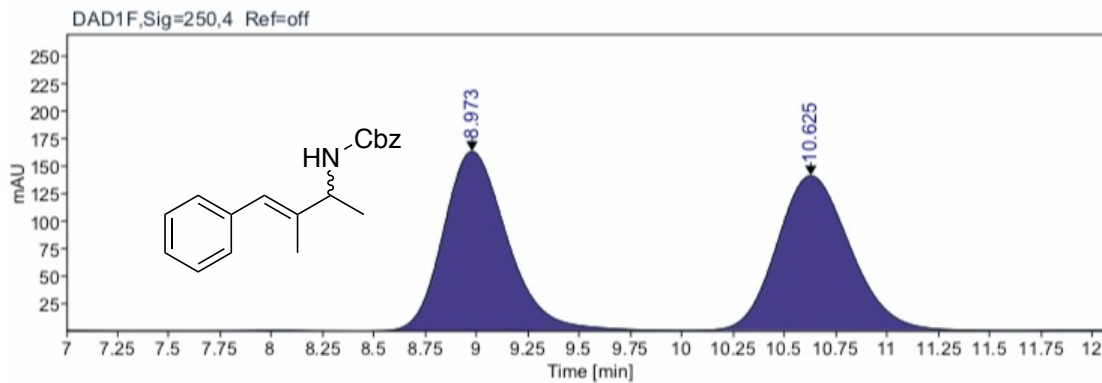
Detector A Channel 1 240nm						Peak Table
Peak#	Ret. Time (min)	RRT	Height	Area	Area%	Name
1	17.193	0.859	51905	4182004	48.855	
2	20.005	1.000	38099	4377981	51.145	
Total			90004	8559985	100.000	



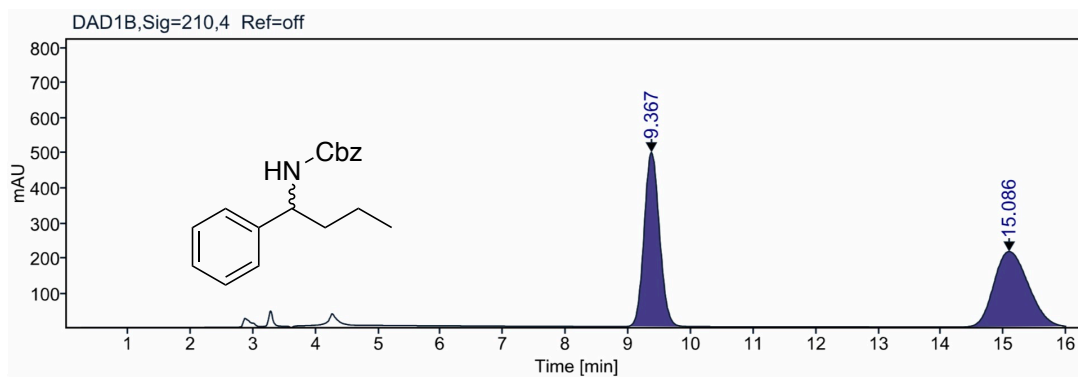
1 Detector A Channel 1 / 240nm

Detector A Channel 1 240nm						Peak Table
Peak#	Ret. Time (min)	RRT	Height	Area	Area%	Name
1	18.520	1.000	259796	19161367	100.000	
Total			259796	19161367	100.000	

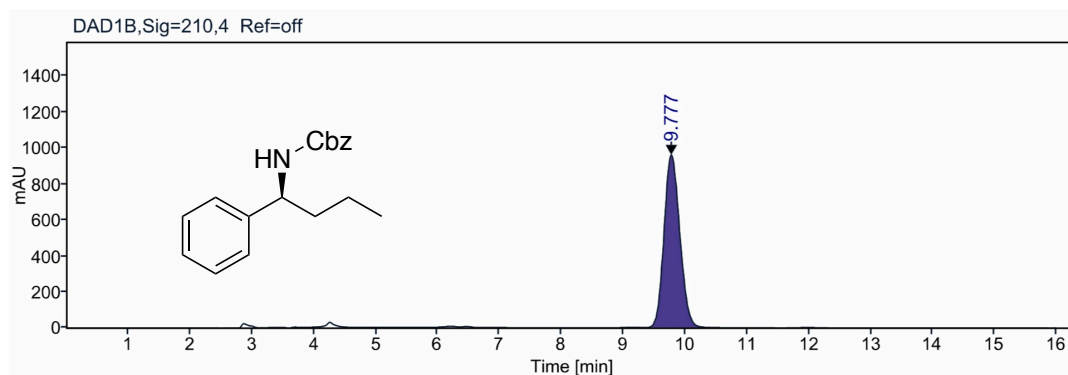
HPLC analysis of (S,E)-4-phenylbut-3-en-2-amine



HPLC analysis of (*S,E*)-benzyl-(3-methyl-4-phenylbut-3-en-2-yl)carbamate

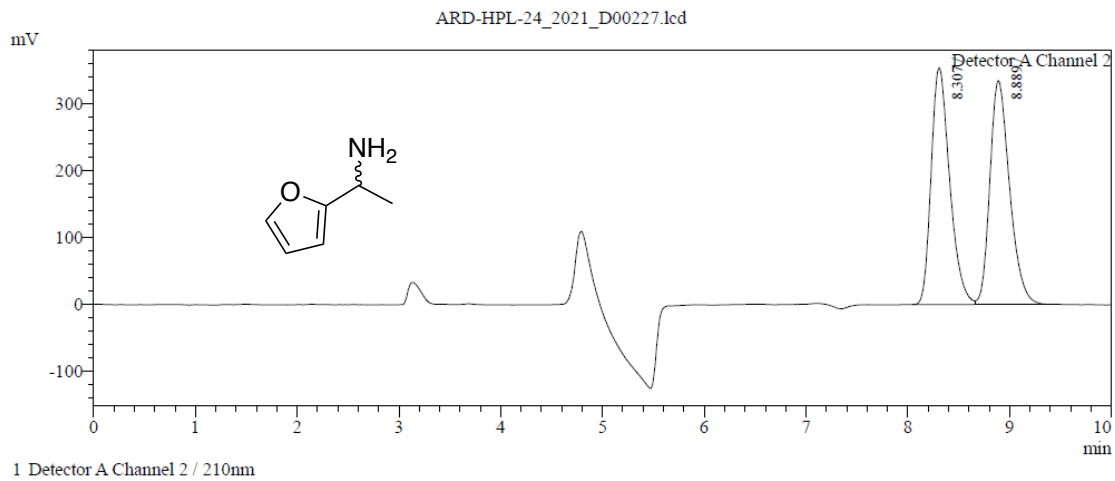


RT [min]	Area	Area%
9.367	8468.2318	50.9
15.086	8167.0223	49.1
Sum	16635.2541	



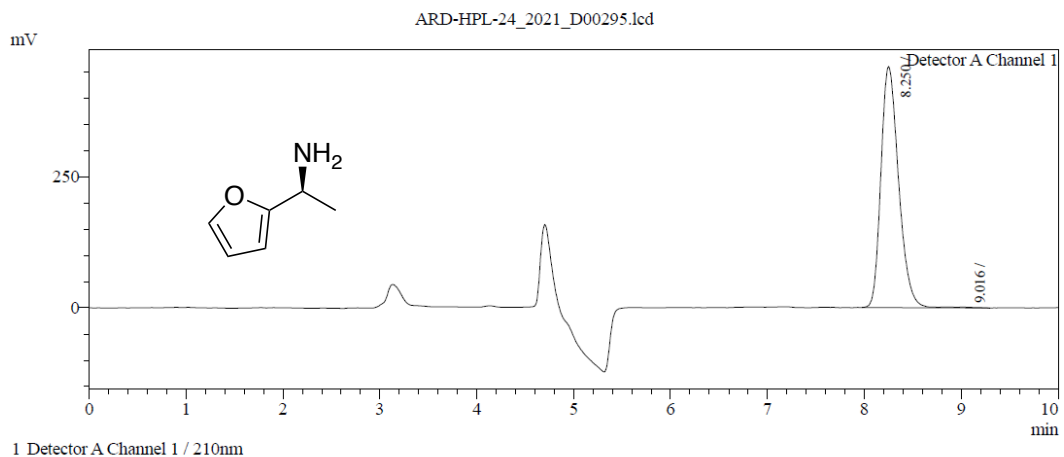
RT [min]	Area	Area%
9.777	17044.5630	100.0
Sum	17044.5630	

HPLC analysis of (*S*)-benzyl-(1-phenylpropyl)carbamate



Peak Table

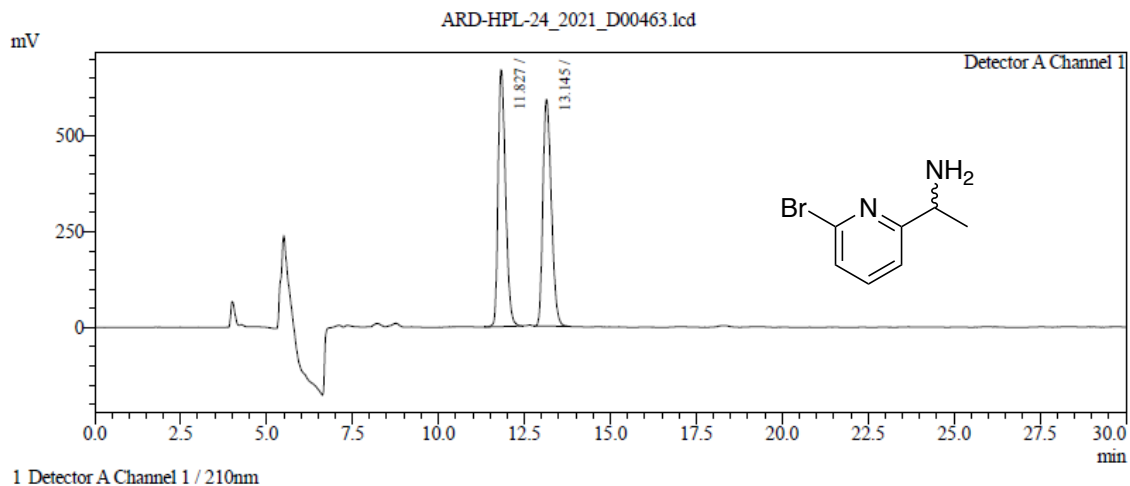
Peak#	Ret. Time (min)	RRT	Height	Area	Area%	Name
1	8.307	1.000	353528	4484166	49.927	
2	8.889	1.070	333989	4497219	50.073	
Total			687517	8981385	100.000	



Peak Table

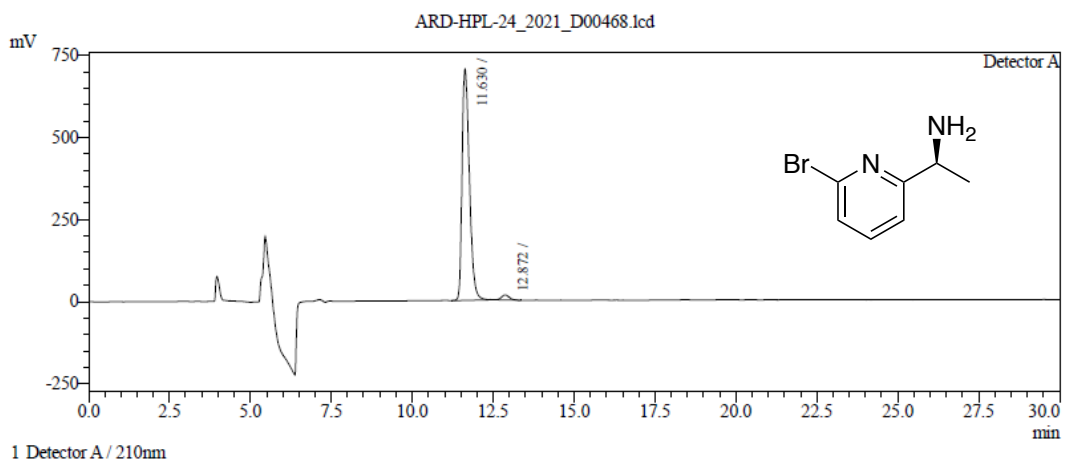
Peak#	Ret. Time (min)	RRT	Height	Area	Area%	Name
1	8.250	1.000	460481	5820238	99.469	
2	9.016	1.093	1563	31051	0.531	
Total			462044	5851289	100.000	

HPLC analysis of (S)-1-(furan-2-yl)ethan-1-amine



Peak Table

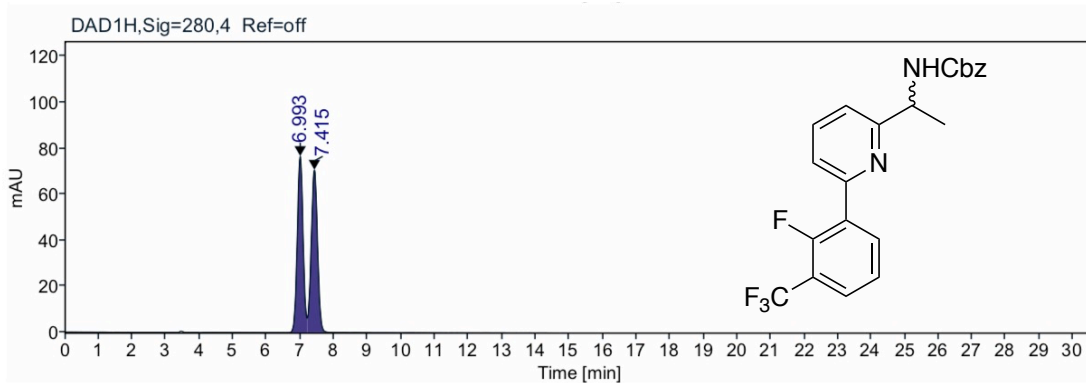
Peak#	Ret. Time (min)	RRT	Height	Area	Area%	Name
1	11.827	1.000	668987	10105539	49.958	
2	13.145	1.111	590566	10122347	50.042	
Total			1259553	20227885	100.000	



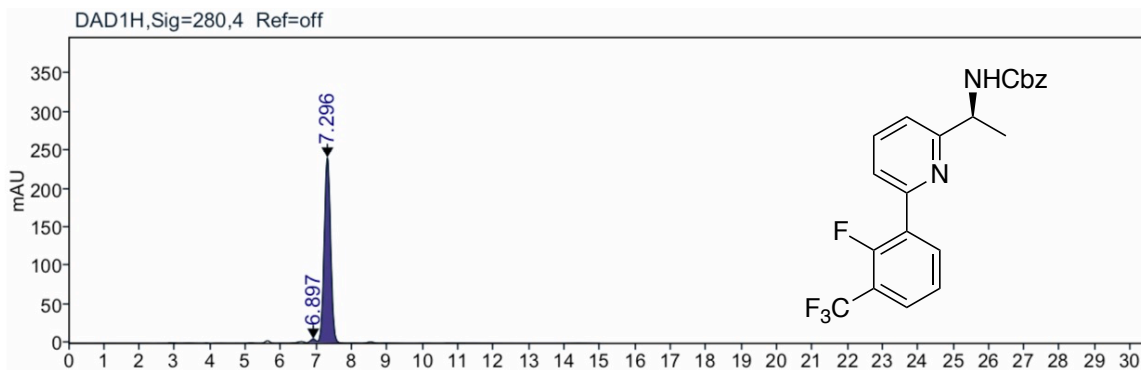
Peak Table

Peak#	Ret. Time (min)	RRT	Height	Area	Area%	Name
1	11.630	1.000	703872	11057601	97.863	
2	12.872	1.107	14700	241500	2.137	
Total			718572	11299101	100.000	

HPLC analysis of (*S*)-1-(6-bromopyridin-2-yl)ethan-1-amine

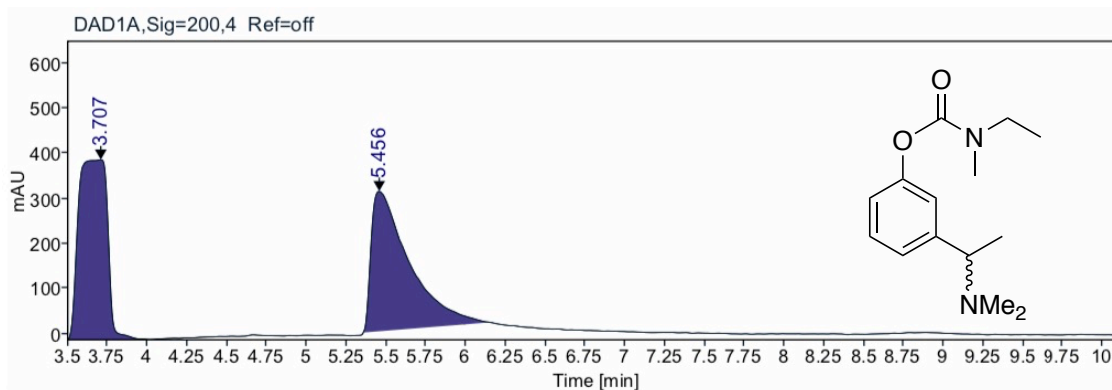


RT [min]	Area	Area%
6.993	912.0047	49.7
7.415	922.0871	50.3
Sum	1834.0918	

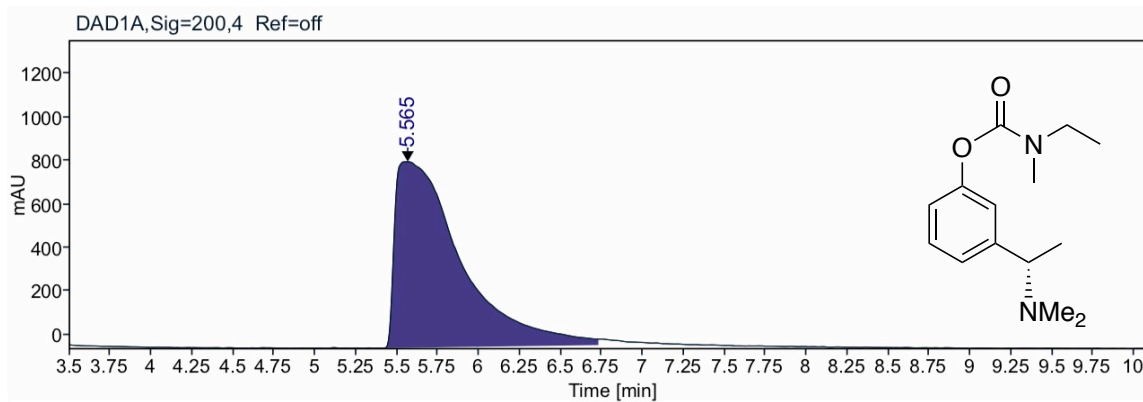


RT [min]	Area	Area%
6.897	44.0198	1.4
7.296	3013.2262	98.6
Sum	3057.2460	

HPLC analysis of benzyl (S)-1-(6-(2-fluoro-3-(trifluoromethyl)phenyl)pyridin-2-yl)ethyl carbamate

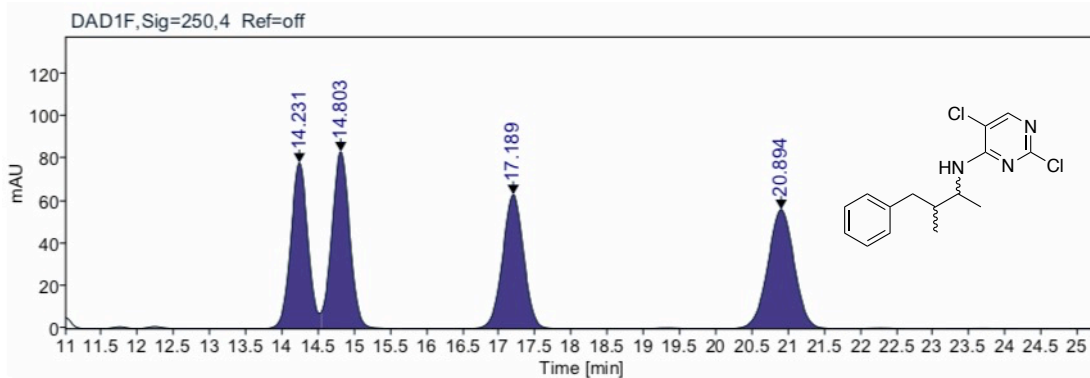


RT [min]	Area	Area%
3.707	5184.0055	50.1
5.456	5169.8312	49.9
Sum	10353.8367	

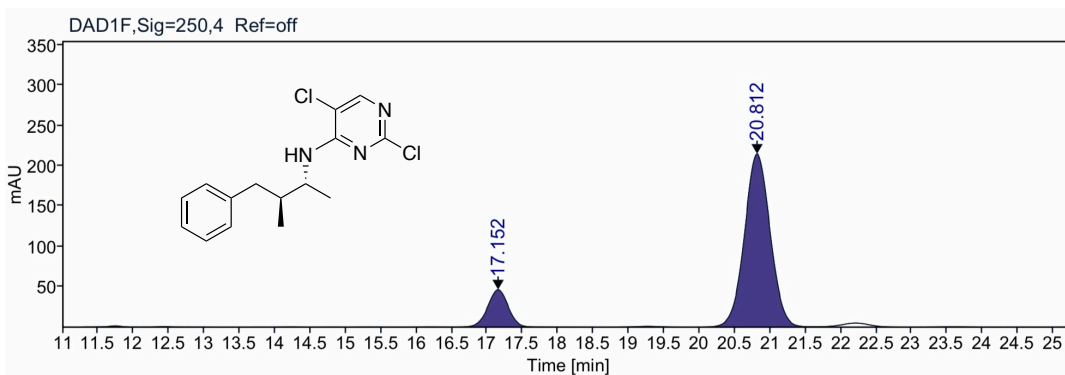


RT [min]	Area	Area%
5.565	24031.3379	100.0
Sum	24031.3379	

HPLC analysis of (*S*)-rivastigmine



RT [min]	Area	Area%
14.231	1285.4020	23.9
14.803	1419.7391	26.4
17.189	1271.6822	23.6
20.894	1406.8956	26.1
Sum	5383.7190	



RT [min]	Area	Area%
17.152	932.9441	14.7
20.812	5420.0159	85.3
Sum	6352.9600	

HPLC analysis of 2,5-dichloro-N-((2R,3S)-3-methyl-4-phenylbutan-2-yl)pyrimidin-4-amine

2.11. *SI References*

- (1) Andersson, M. P., Gallou, F., Klumphu, P., Takale, B. S. & Lipshutz, B. H. Structure of Nanoparticles Derived from Designer Surfactant TPGS-750-M in Water, As Used in Organic Synthesis. *Eur. J. Chem.* **2018**, *24*, 6778–6786.
- (2) Han, Z.-J., Li, Y.-B., Gu, B.-H., Li, Y.-M. & Chen, H. Economical synthesis of *tert*-butyl (*S*)-3-aminopyrrolidine-1-carboxylate from L-aspartic acid. *Synthetic Communications* **2018**, *48*, 2452–2456.
- (3) Ashton, T. D., Aumann, K. M., Baker, S. P., Schiesser, C. H. & Scammells, P. J. Structure–activity relationships of adenosines with heterocyclic N6-substituents. *Bioorg. Med. Chem. Lett.* **2007**, *48*, 6779–6784.
- (4) Albarrán-Velo, J., Lavandera, I. & Gotor-Fernández, V. Sequential Two-Step Stereoselective Amination of Allylic Alcohols through the Combination of Laccases and Amine Transaminases. *ChemBioChem* **2020**, *21*, 200–211.
- (5) Pizzuti, M. G., Minnaard, A. J. & Feringa, B. L. Catalytic Enantioselective Addition of Organometallic Reagents to N-Formylimines Using Monodentate Phosphoramidite Ligands. *J. Org. Chem.* **2008**, *73*, 940–947.
- (6) Tan, X. *et al.* Asymmetric Synthesis of Chiral Primary Amines by Ruthenium-Catalyzed Direct Reductive Amination of Alkyl Aryl Ketones with Ammonium Salts and Molecular H₂. *J. Am. Chem. Soc.* **2018**, *140*, 2024–2027.
- (7) Baratta, W. *et al.* Chiral Pincer Ruthenium and Osmium Complexes for the Fast and Efficient Hydrogen Transfer Reduction of Ketones. *Organometallics*, **2021**, *29*, 3563–3570.
- (8) Fuchs, M., Koszelewski, D., Tauber, K., Kroutil, W. & Faber, K. Chemoenzymatic asymmetric total synthesis of (*S*)-Rivastigmine using ω -transaminases. *ChemCommun*, **2020**, *46*, 5500–5502.

3. An Environmentally Responsible 5-step, 3-pot Synthesis of the Antitumor Agent Lapatinib (Tykerb)

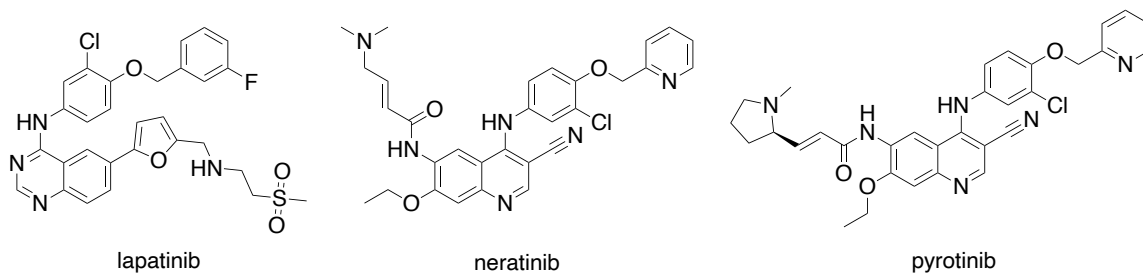
Reproduced with permission from

Yu, J.; Iyer, K. S. Lipshutz, B. H. An environmentally responsible synthesis of the antitumor agent lapatinib (Tykerb). *Green Chem*, **2022**, *24*, 3640–3643

Copyright 2022 Royal Society of Chemistry

3.1. Background and introduction

Breast cancer is the most common cancer in women worldwide, accounting for 25.8 percent of all new cancer cases diagnosed in 2020.¹ Targeted therapeutic drugs have become mainstream cancer treatments.² Tyrosine kinase inhibitors (TKIs), such as lapatinib, neratinib, and pyrotinib, are members of the most important class of anticancer drugs used in treating breast cancer patients; their structures are shown in **Scheme 1**. Lapatinib (Tykerb[®]) was developed by GlaxoSmithKline (GSK) in the early 2000s for targeting overexpressed EGFR (HER-1) and HER-2 receptors in breast cancer cells.³ A number of existing synthetic routes have been developed towards this drug (a representative example is shown in **Section 3.2**). The procedures, however, fall into the category of traditional organic synthesis, as they rely heavily on use of organic solvents and precious metal catalysts. Several environmental laws, such as REACH, the Clean Air Act, and the European Union Solvents Emission Directive, have increased pressure on the fine chemical industry to reduce or, ideally, eliminate organic waste.⁴ As a result, rapid construction of complex molecular scaffolds in an environmentally responsible and cost-effective manner, with built-in step and pot economy, is highly desirable.



Scheme 1. Structures of TKI breast cancer drugs used in the clinic

Sheldon's E (environmental) factor, which is defined as kilos of waste per kilogram of (drug) product, has served as a benchmark indicator of the environmental footprint of production processes across several chemical industries.⁵ One approach for decreasing an E Factor is to strategically combine many synthetic steps into a single pot, hence, minimizing the number of product isolations, purification of intermediates, and material transfer between vessels; this concept is also referred to as "pot economy."⁶ It was proposed by Hayashi and has grown in popularity in the community, as seen by the increasing number of publications featuring 1-pot processes over the last two decades (**Figure 1**).

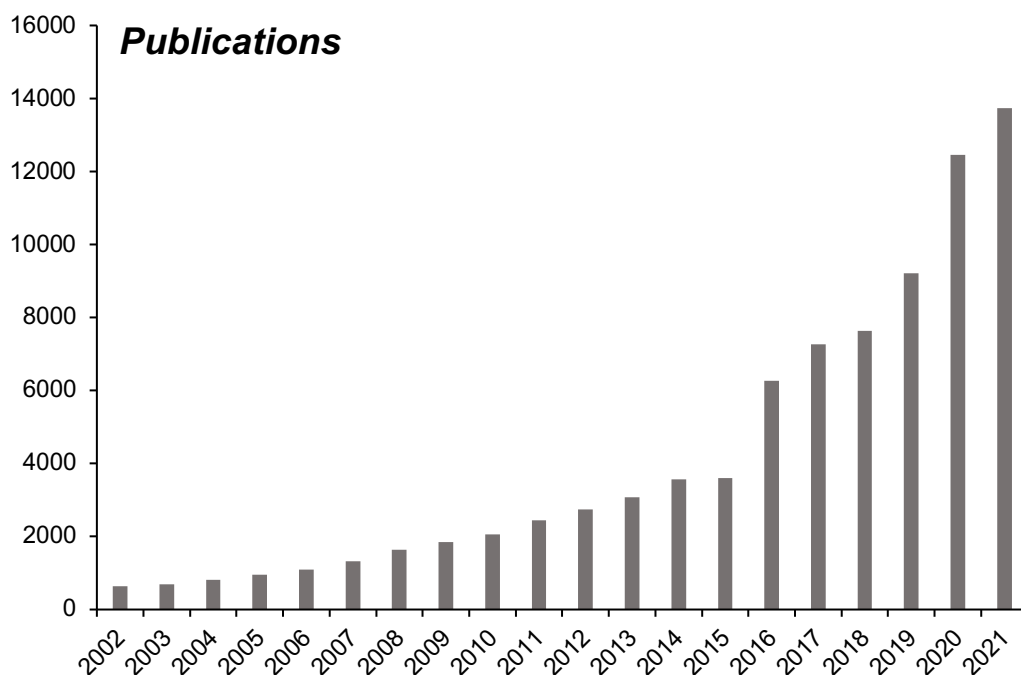


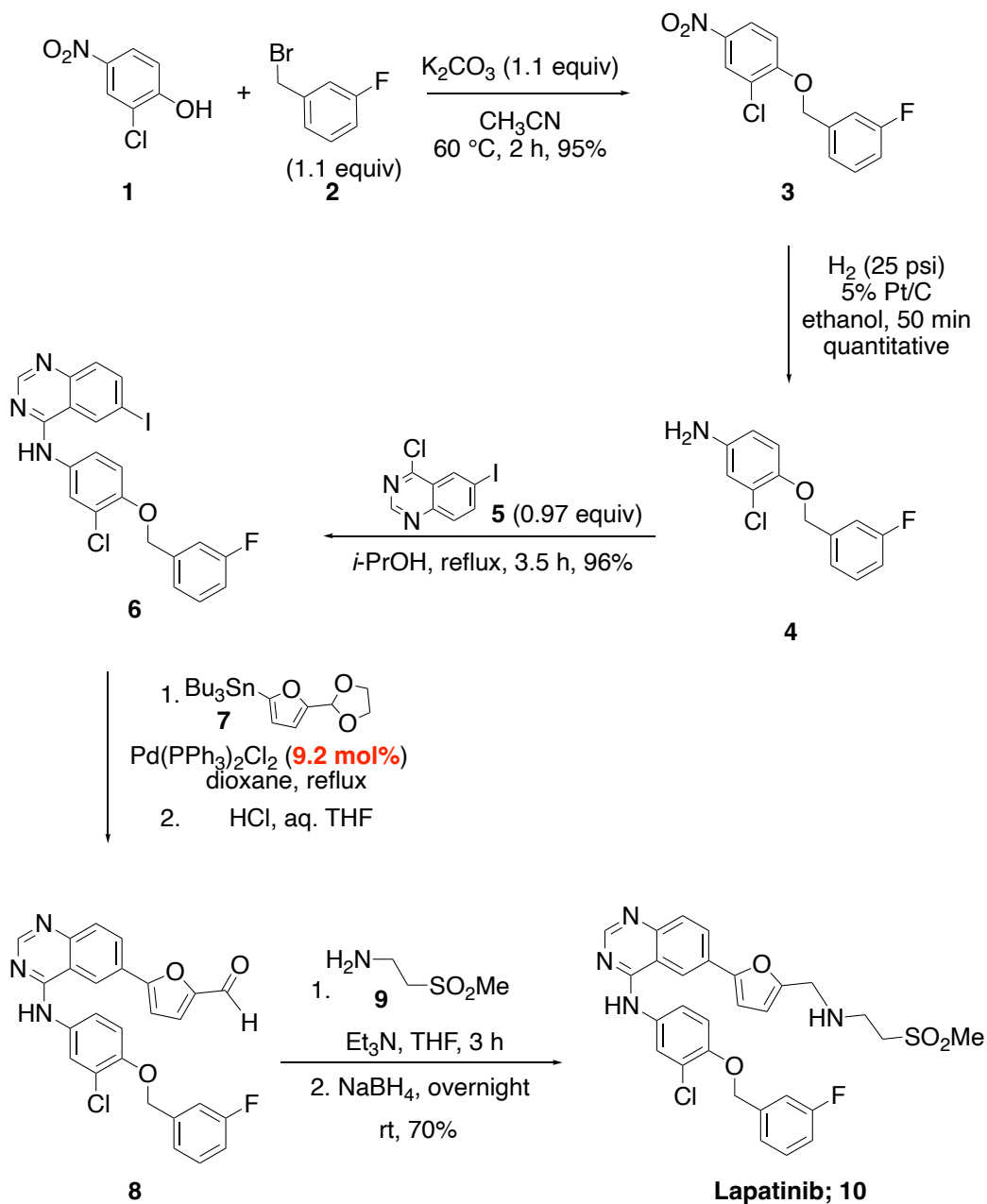
Figure 1. Number of publications of “1-pot reactions” during 2002–2021 (data collected from Reaxys)

3.2. Literature on the synthesis of lapatinib

Scheme 2 below depicts a traditional synthetic route from the literature. The synthesis first required assembly of phenol **1** and benzylic bromide **2** via an S_N2 reaction in acetonitrile to form nitro adduct **3**. Subsequent nitro group reduction using Pt/C under a pressure of 25 psi hydrogen resulted in the synthesis of aniline **4**, which is a very efficient process. However, a significant amount of Pt is invested in this hydrogenation, and specific equipment is required for use under pressure. Once reduction is complete, an S_NAr reaction was performed to install the iodo-substituted quinazoline ring **5** yielding compound **6**. Product **6** is worked up in the typical fashion, which implies that water washings are required given the alcoholic medium used, which results in significant amounts of aqueous waste. The E Factors involved, based on both solvent and water usage, reflect these issues: this literature method results in an E Factor considerably more than 106.⁷

Intermediate **6** was then coupled with furfural derivative **7** using a Stille coupling. This particular choice of C-C bond formation provides an excellent example for direct comparison purposes since every reaction parameter (see **Scheme 2**) fails to meet any of the *12 Principles of Green Chemistry*.⁸ That is: (1) usage of a stannane, by definition, results in the generation of at least an equivalent of potentially poisonous tin waste; (2) the use of an excessive amount of Pd catalyst: 9.2% of Pd(Ph₃P)₂Cl₂, which is 92,000 ppm Pd; (3) dioxane, classified as an “undesirable” solvent, was chosen as the solvent that, given its water miscibility, necessitates extensive water-workup, thereby also leading to large amounts of aqueous waste; (4) use of reflux; indicative of the energy that must be invested to achieve this reaction temperature; and (5) use of an aldehyde protecting group, the acetal

in **7**, mandating an additional step for its aqueous hydrolysis. The yield for this step is conspicuously absent from the published report. Finally, reductive amination is performed to couple aldehyde **8** and amine **9** in THF, necessitating an aqueous workup yet again, yielding the desired drug, **10**, in 70% yield.⁹



Scheme 2. Literature pathway to lapatinib⁹

3.3. Green chemistry: telescoping synthetic sequences

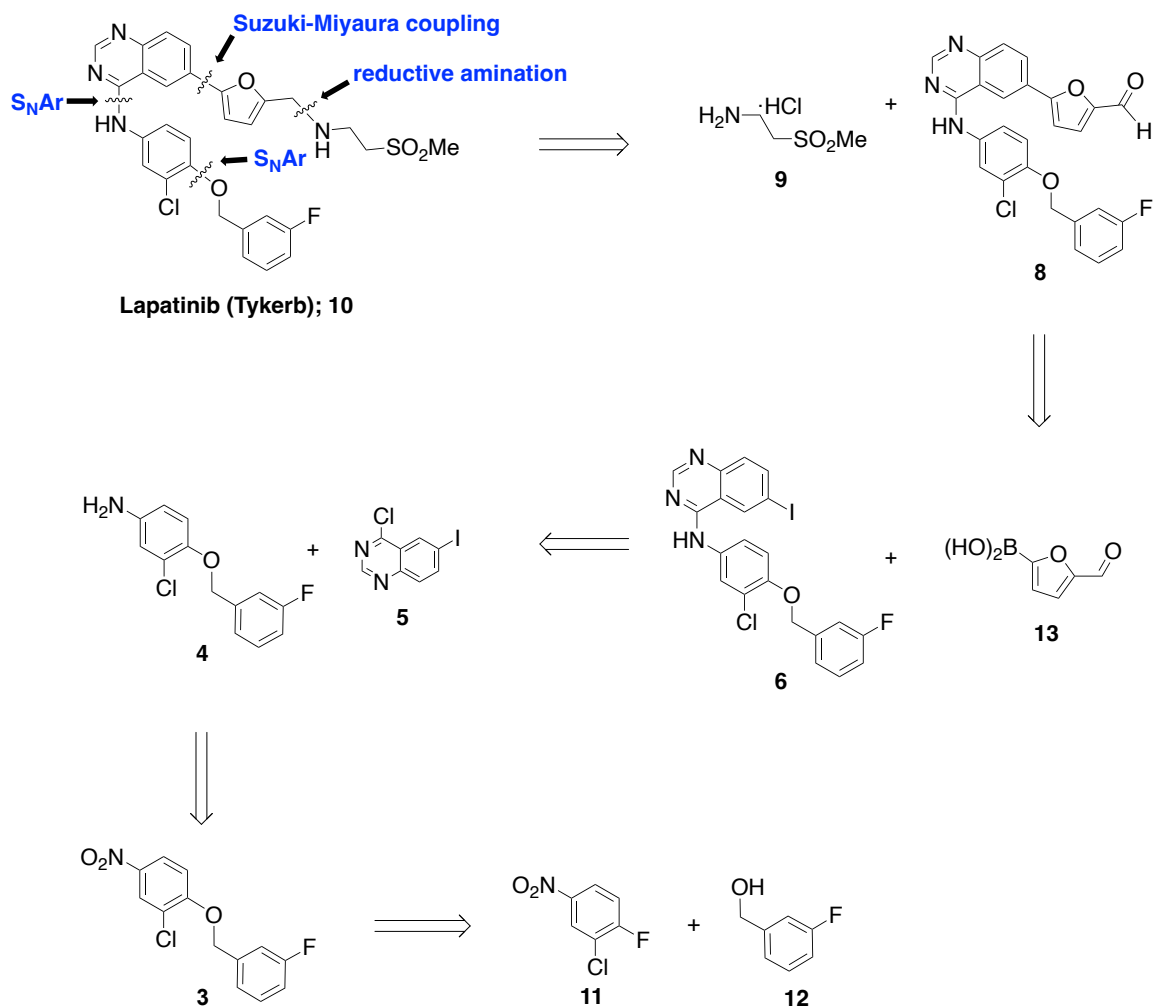
In classical chemistry, it is thought to be advantageous to utilize low-boiling solvents that can be quickly removed under high vacuum when designing an uninterrupted sequence.¹⁰ However, from the perspective of green chemistry, high volatility of solvents inhibits recovery, resulting in undesirable air emissions and the risk of worker exposure.¹¹ Chemistry in water, as opposed to chemistry “on water” or “with water”,¹² enabled by engineered designer surfactants (such as TPGS-750-M¹³) that address substrate solubility issues began with our first reports back in 2008.^{14,15} Since then, the toolbox has grown significantly, now containing procedures that cover many of the most important reactions in synthetic chemistry, including Pd-catalyzed Suzuki-Miyaura,^{16,17} Stille,¹⁸ Heck,^{19,20} and Sonogashira couplings,^{21,22} aminations,²³ S_NAr reactions,²⁴ and amide/peptide bond formations,²⁵ among others that can now be run in most cases completely without organic solvents. These provide opportunities for the community, particularly the pharmaceutical and agrochemical industries, to make targeted molecules under far greener conditions than those that are more traditional and typically rely on waste-generating and unsafe reaction media, unsustainable and expensive levels of precious metal catalysts, and which require an investment of energy (*e.g.*, heating) that often generates reaction by-products that require additional time and effort to obtain purified products.²⁶

Sequences of reactions in the same pot become possible since the medium for all these reactions remains constant, *i.e.*, nanomicelles generated from TPGS-750-M in water that serve as nanoreactors in which the chemistry takes place. This eliminates the need for further workup and handling at each phase.

3.4. Results and discussion

3.4.1. Retrosynthesis

In looking to establish a synthesis of lapatinib using the principles of green chemistry, and as shown in **Scheme 3**, Lapatinib **10** can be envisioned retrosynthetically to arise from a reductive amination of aldehyde **8** and amine **9** using a non-toxic reducing agent 2-picolineborane. Aldehyde **8** can be generated from iodide **6** and boronic acid **13** through a Suzuki-Miyaura coupling reaction using *ppm* levels of a palladium catalyst, which has been previously extensively researched in the micellar catalysis area. Iodide **6** can be readily prepared from an S_N2 reaction involving aniline **4** and chloride **5** in an aqueous surfactant medium. Using carbonyl iron powder (CIP) and ammonium chloride, aniline **4** can be formed via reduction of nitro compound **3** in a practical manner. Nitro compound **3** can be easily traced back to commercially available compounds, fluoride **11** and benzylic alcohol **12**.

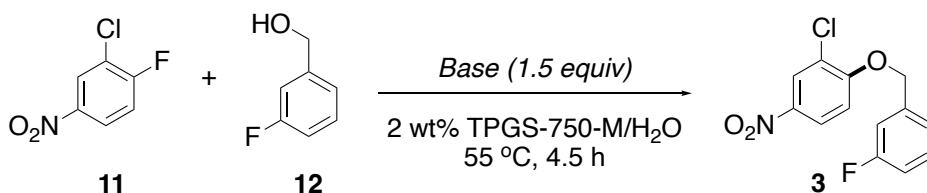


Scheme 3. Retrosynthetic analysis of lapatinib.

3.4.2. Screening of conditions for individual steps

We began by identifying the optimum conditions for each step. Based on prior studies, an initial S_NAr reaction between fluoroaromatic **11** and 3-fluorobenzyl alcohol **12** was anticipated to proceed smoothly under aqueous micellar conditions when standard bases such as K₃PO₄, NaO^tBu, and KOH were used in a 2 wt % TPGS-750-M/H₂O solution (**Table 1**). KOH was used in this case to achieve nearly full conversion to nitro aromatic **3**. The product can be collected through filtration as a pale-yellow solid.

Table 1. Optimization of base for the initial S_NAr reaction en route to lapatinib^a



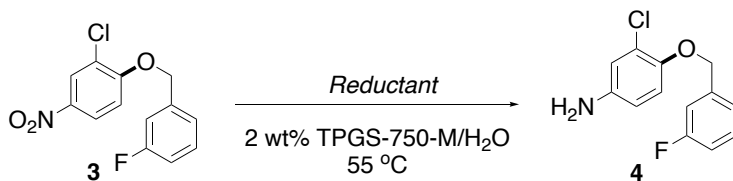
Entry	Base (1.5 equiv)	Conversion to 3 (%) ^b
1	K ₃ PO ₄	97%
2	NaO ^t Bu	98%
3	KOH	>99%

^aReaction conditions: 0.25 mmol **1**, 0.275 mmol **2**, 0.375 mmol base, stirred at 55 °C for 4.5 h; ^b conversion was determined by GC-MS.

Next, common nitro group reduction conditions were evaluated on adduct **3**, as indicated in **Table 2**. When commercially available 1 wt % Pd/C was used in combination with a silane (1.5 equiv), no conversion occurred. When triethylsilane was replaced with atmospheric hydrogen, the extent of conversion increased by around 20%, as shown in **entry 2**. While maintaining the Pd loading constant, utilizing 10 wt % Pd/C instead of 1 wt % Pd/C resulted in enhanced conversion, from *ca.* 20% to *ca.* 90% (**entry 3**).

An alternate approach developed by our laboratory employed carbonyl iron powder (CIP), which enabled complete conversion to the desired product under aqueous micellar conditions (**entry 4**).²⁷ Such nitro group reductions can be very challenging at times,²⁸ although in this case, the CIP produced very clean results. To remove CIP, the reaction can be simply worked up by filtering through cotton or a silica plug.

Table 2. Optimization of nitro reduction in the second step of the synthesis of lapatinib

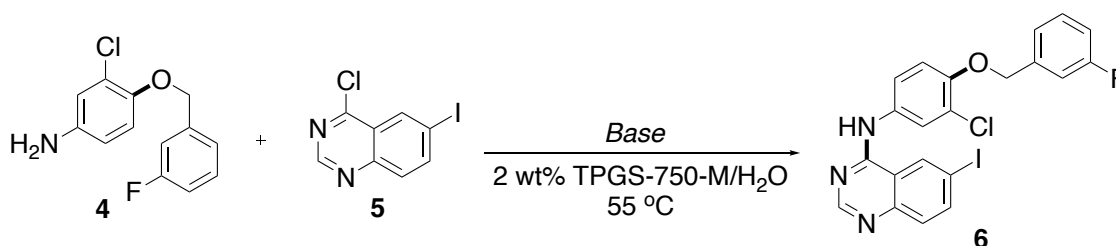


Entry	Conditions	Conversion to 4 (%) ^a
1	1% Pd/C (1 mol %), Et ₃ SiH (1.5 equiv)	0
2	1 wt % Pd/C (1 mol % based on Pd), H ₂ balloon	~20
3	10 wt % Pd/C (1 mol % based on Pd), H ₂ balloon	~90
4	carbonyl iron powder (CIP) (5 equiv), NH₄Cl (3 equiv)	100

^aConversion was determined by NMR.

Following the successful synthesis of aniline **4**, quinazoline **5** smoothly underwent an S_NAr addition in 2 wt % TPGS-750-M aqueous medium in the absence of base. Adding bases like K₃PO₄, Et₃N, and KOH, on the other hand, reduced the extent of conversion by *ca.* 5–15 percent. The product crashed out of the aqueous medium as a yellow solid and was isolated by vacuum filtration.

Table 3. Optimization of base for S_NAr in the third step of the synthesis of lapatinib^a



Entry	Base (1 equiv)	Time	Conversion to 6 (%) ^a
1	No base	1.5 h	100
2	K ₃ PO ₄	1.5 h	~95
3	Et ₃ N	8 h	~75
4	KOH	8 h	~85

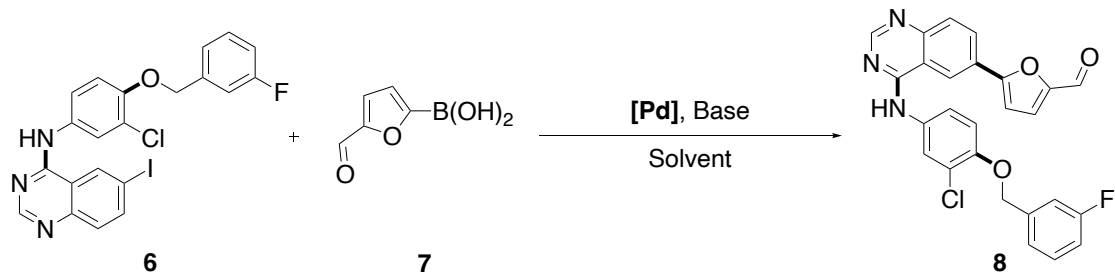
^aReaction conditions: 0.25 mmol **4**, 0.25 mmol **5** and base stirred at 55 °C;

^bConversion was determined by crude NMR.

With access to iodide **6**, a Nobel prize-winning Suzuki-Miyaura (SM) reaction was chosen to effect coupling with boronic acid **7** due to its efficient and robust nature (**Table 4**). According to the literature, a SM coupling involved catalysis with the complex Pd(dtbpf)Cl₂.²⁹ Attempts to conduct this transformation in TPGS-750-M, however, failed to produce good results, whether with or without the DCM as part of the Pd complex (**entries 1–3**), due to the poor solubility of the starting iodide **6**. As a result, 95% ethanol,

a suggested solvent from the Innovative Medicines Initiative (IMI) EU,³⁰ was chosen as a solubility aid due to its low cost, bio-based nature, and environmental friendliness. The reactions were performed in a mix of TPGS-750-M and ethanol at 0%, 20%, and 50% v/v (**entries 4–6**). This reaction proceeded cleanly to conversion in ethanol. The appearance of the solution changed from brown to brilliant yellow once the reaction was complete. When the same reaction conditions were used with Pd(dtbpf)Cl₂ (no DCM complex), the product was not generated (**entry 7**).

Table 4. Screening of Pd catalyst for SM cross-coupling in the fourth step of the synthesis of lapatinib^a



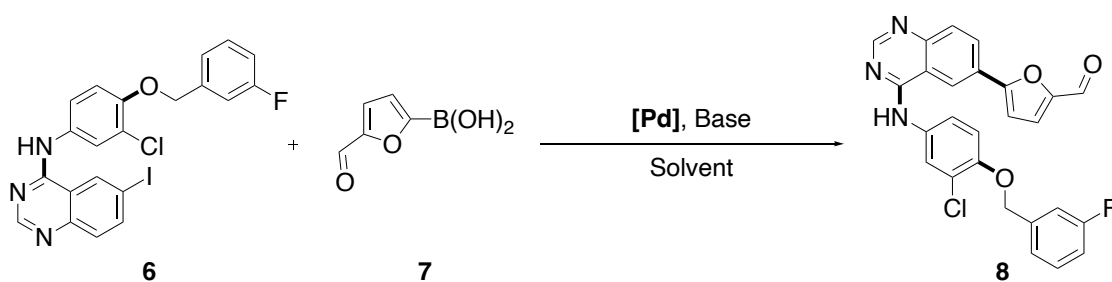
Entry	Catalyst	Base	Solvent	Conversion to 8 (%) ^b
1	Pd(dtbbpf)Cl ₂ (1 mol %)	Et ₃ N (3 equiv)	2 wt % TPGS-750-M	<3
2	Pd(dtbbpf)Cl ₂ (3 mol %)	Et ₃ N (3 equiv)	2 wt % TPGS-750-M	<50
3	Pd(dppf)Cl ₂ :DCM (4 mol %)	Et ₃ N (5 equiv)	2 wt % TPGS-750-M	~50
4 ^c	Pd(dppf)Cl₂:DCM (4 mol %)	Et₃N (5 equiv)	EtOH (reflux)	100
5	Pd(dppf)Cl ₂ :DCM (4 mol %)	Et ₃ N (5 equiv)	2 wt % TPGS-750-M : EtOH = 80 : 20	<40
6	Pd(dppf)Cl ₂ :DCM (4 mol %)	Et ₃ N (5 equiv)	2 wt % TPGS-750-M : EtOH = 50 : 50	<50
7	Pd(dppf)Cl ₂ (4 mol %)	Et ₃ N (5 equiv)	EtOH (reflux)	0

^aReaction conditions: 0.25 mmol **6**, 0.5 mmol **7** and base, stirred at 55 °C (with TPGS-750-M) or under reflux conditions (with EtOH) overnight; ^bConversion was determined by crude NMR or GC-MS. ^cReaction time = 2 h.

In our ongoing efforts to provide new methods based on sustainable chemistry, we varied the amounts of palladium to identify the required loading of the catalyst (**Table 5**). We were pleased to see that reducing the Pd loading by two orders of magnitude to 0.05 mol

% did not diminish the extent of product formation. These results translate into (a) environmental benefits; (b) cost-effectiveness; (c) recognition of the status of Pd as an endangered metal (d) observance of regulatory requirements; and (e) minimization of product contamination in terms of residual metals.

Table 5. Screening of Pd catalyst loading for SM cross-coupling in the fourth step of the synthesis of lapatinib^a



Entry	Pd(dppf)Cl ₂ loading	Base	Conversion to 8 (%) ^b
1	2 mol % (20,000 ppm)	Et ₃ N (3 equiv)	100
2	1 mol % (10,000 ppm)	Et ₃ N (3 equiv)	100
3	0.5 mol % (5000 ppm)	Et ₃ N (5 equiv)	100
4	0.1 mol % (1000 ppm)	Et ₃ N (5 equiv)	100
5	0.05 mol % (500 ppm)	Et ₃ N (5 equiv)	100

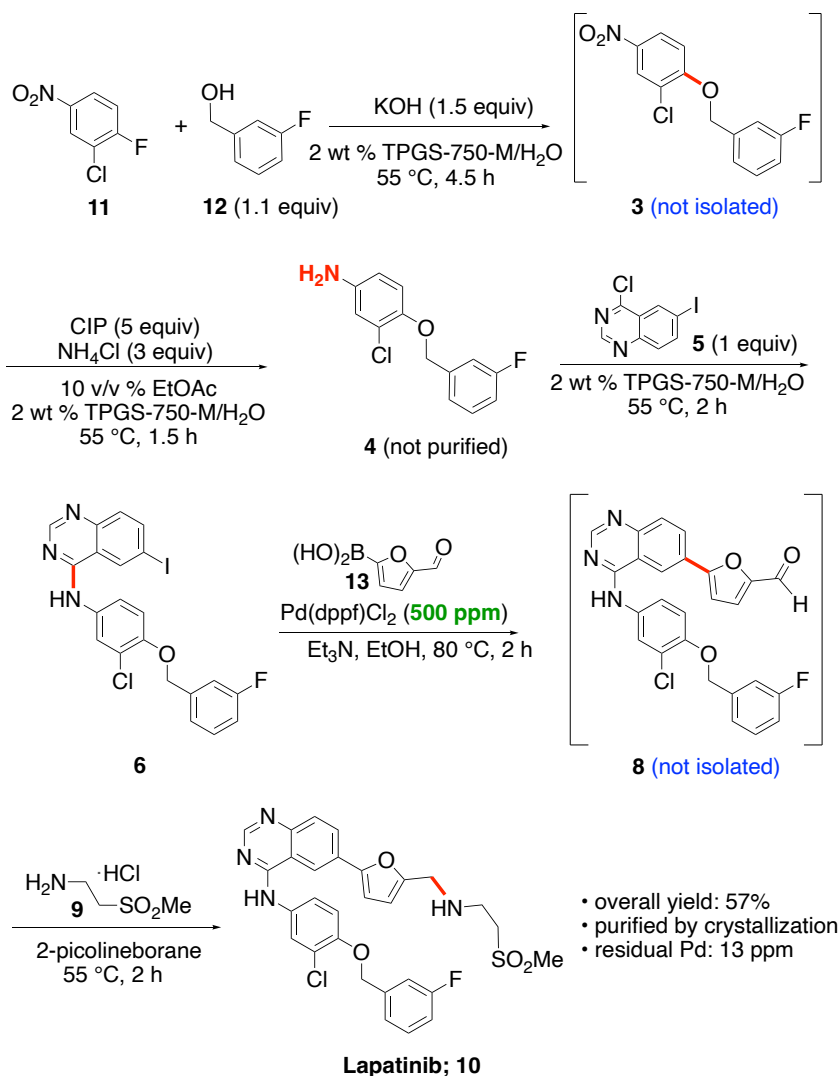
^aReaction conditions: 0.25 mmol **6**, 0.5 mmol **7**, 1.25 mmol Et₃N, stirred at 80 °C for 2 h;

^bDetermined by crude NMR or GC-MS.

3.4.3. 1-Pot sequence

After an exhaustive analysis of the conditions associated with each step toward lapatinib, we attempted to telescope as many of the steps as possible to minimize the number of pots (**Scheme 4**). This revised sequence began with an S_NAr reaction between fluoroaromatic **1** and 3-fluorobenzyl alcohol **2** leading to formation of adduct **3**, as observed with TLC. Without workup, carbonyl iron powder (CIP) was added to the same pot which effectively reduced the nitro group, both steps done in water as previously indicated in **Section 4.2**. The aqueous mixture containing nitroaromatic **3** only required a pH adjustment by addition of NH₄Cl to the water, as the CIP is best used under the resulting slightly acidic conditions. A modest amount (10% v/v) of EtOAc was also added as co-solvent to ensure proper mixing and substrate solubility.³¹ Following formation of product aniline **4** (confirmed using TLC; EtOAc:hexanes = 1:4), the mixture was filtered to remove the CIP, and the aqueous filtrate (containing **4**) was used directly for the second S_NAr reaction with quinazoline **5** leading to heteroaryl iodide **6**. This substance has major solubility issues in the micellar medium, which were best handled by isolating it (as crude material) via simple filtration, followed by dissolution using 95% EtOH. Into this reaction vessel was then added the furanylboronic acid **7**, along with commercially available catalyst Pd(dppf)Cl₂ as its DCM complex. Heating the resulting mixture to 80 °C for two hours led to the expected biaryl coupling product **8**. Noteworthy was that no protection of the formyl group was needed. Without isolation, reductive amination on **8** was accomplished by introducing amine **9** (as its hydrochloride salt) and subsequently 2-picolineborane, as described in a recent disclosed procedure developed collaboratively with Bailey *et al.* (Takeda Pharmaceuticals).³² This reaction was done in two hours, whereas overnight stirring was

usually involved using conventional protocols.^{9,29} Lapatinib (**10**) was formed as a yellow solid precipitate and purified by crystallization in EtOAc, with an overall yield of 57% for all five reactions (or 89% yield/step). Removal of residual surfactant when such reactions in water are done at scale using this amphiphile has been fully addressed by Novartis.³³ HPLC analysis of the crystallized material indicated an initial purity of 97.5%. Lapatinib, bearing a secondary amine, is typically further purified to raise the level of purity, after which it is delivered as its tosylate salt.



Scheme 4. Greener route to lapatinib; 5-step, 3-pot

In total, this approach involves 5-steps, but only 3-pots. This results from avoidance of isolation of intermediates **3** and **8**, given the reliance on an aqueous micellar medium *en route* to **10**, and partial use of 95% EtOH as a common reaction medium. These choices enable both the Suzuki-Miyaura coupling (**6** to **8**) and reductive amination (**8** to **10**) steps to take place in a telescoped fashion. Also, especially noteworthy in the cross-coupling is the dependence on only 500 ppm of the Pd catalyst, or 0.05 mol %, which is cost effective and respectful of the endangered status of the platinoids.¹⁴ Pleasingly, without any column chromatography, ICP-MS analysis of **10** indicated only 13 ppm Pd is presented in lapatinib isolated following this route, as shown in **Table 1**. A simple recrystallization would surely remove enough of this palladium to reduce the levels to below the FDA allowed limit of 10 ppm. Quite a different result is to be expected, and was found, had the existing literature procedure relied on a Suzuki-Miyaura coupling (*vide infra*), which typically uses 1-5 mol %, resulting in 1853 ppm Pd residue after recrystallization.

Table 1. Residual Pd level determination by ICP-MS^a

	Pd loading in SM coupling	Residual Pd level (ppm)
This work	0.05 mol % (500 ppm)	13.554 ± 0.318
Literature ²⁹	4 mol % (40,000 ppm)	1853.888 ± 10.950

^aEach sample was measured in triplicate with background correction.

3.5. Conclusions

In summary, using a purely chemistry-based approach for the synthesis of lapatinib is representative of the opportunities currently available to the fine chemical arena to (a) begin to move away from a dependence on petroleum-based solvents and chemicals that, ultimately, lead to the majority (>80%) of organic waste created, *e.g.*, by the pharmaceutical industry; (b) utilize far less precious metal-containing catalysts, and yet, realize the same outcomes with oftentimes more excellent selectivity, higher yields, and in less time; (c) carry our reactions under milder conditions that in most cases will lead to far better impurity profiles, thereby streamlining and simplifying product purifications. And while the example of lapatinib synthesis in no way is suggestive that existing routes to pharmaceuticals currently on the market should be redone, notwithstanding the apparent benefits in terms of both environmental and economic factors, it does highlight the favorable options available today to medicinal and process chemists, especially now that the merging of chemo- and bio-catalysis into 1-pot sequences has been amply demonstrated, all in Nature's "solvent": water.

3.6. References

- (1) Worldwide Cancer Data | World Cancer Research Fund International. *WCRF International*, <https://www.wcrf.org/cancer-trends/worldwide-cancer-data/> (access 2022-05-02)
- (2) Zhong, L.; Li, Y.; Xiong, L.; Wang, W.; Wu, M.; Yuan, T.; Yang, W.; Tian, C.; Miao, Z.; Wang, T.; Yang, S. Small Molecules in Targeted Cancer Therapy: Advances, Challenges, and Future Perspectives. *Sig Transduct. Target. Ther.* **2021**, *6*, 1–48.
- (3) Lin, N. U.; Carey, L. A.; Liu, M. C.; Younger, J.; Come, S. E.; Bullitt, E.; Van Den Abbeele, A. D.; Li, X.; Hochberg, F. H.; Winer, E. P. Phase II Trial of Lapatinib for Brain Metastases in Patients with HER2+ Breast Cancer. *J. Clin. Oncol.* **2006**, *24*, 503–503.
- (4) Clarke, C. J.; Tu, W.-C.; Levers, O.; Bröhl, A.; Hallett, J. P. Green and Sustainable Solvents in Chemical Processes. *Chem. Rev.* **2018**, *118*, 747–800.
- (5) Sheldon, R. A. The E Factor 25 Years on: The Rise of Green Chemistry and Sustainability. *Green Chem.* **2017**, *19*, 18–43.
- (6) Hayashi, Y. Pot Economy and One-Pot Synthesis. *Chem. Sci.* **2016**, *7*, 866–880.
- (7) The E Factor could be much higher, as the exact amounts of water used in each workup was not specified, and hence, not included in this calculation.
- (8) Burns, M.; Bi, W.; Kim, H.; Lall, M. S.; Li, C.; O'Neill, B. T. Ketoreductase/Transaminase, One-Pot, Multikilogram Biocatalytic Cascade Reaction. *Org. Process Res. Dev.* **2021**, *25*, 941–946.
- (9) M. C. Carter, G. S. Cockerill, S. B. Guntrip, K. E. Lackey and K. J. Smith, Glaxo Wellcome Inc., WO1999035146A1, 1999.
- (10) Vaxelaire, C.; Winter, P.; Christmann, M. One-Pot Reactions Accelerate the Synthesis of Active Pharmaceutical Ingredients. *Angew. Chem., Int. Ed.* **2011**, *50*, 3605–3607.
- (11) Byrne, F. P.; Jin, S.; Paggiola, G.; Petchey, T. H. M.; Clark, J. H.; Farmer, T. J.; Hunt, A. J.; Robert McElroy, C.; Sherwood, J. Tools and Techniques for Solvent Selection: Green Solvent Selection Guides. *Sustain. Chem. Process* **2016**, *4*, 7–33.
- (12) Cortes-Clerget, M.; Yu, J.; A. Kincaid, J. R.; Walde, P.; Gallou, F.; H. Lipshutz, B. Water as the Reaction Medium in Organic Chemistry: From Our Worst Enemy to Our Best Friend. *Chem. Sci.* **2021**, *12*, 4237–4266.
- (13) Lipshutz, B. H.; Ghorai, S.; Abela, A. R.; Moser, R.; Nishikata, T.; Duplais, C.; Krasovskiy, A.; Gaston, R. D.; Gadwood, R. C. TPGS-750-M: A Second-

- Generation Amphiphile for Metal-Catalyzed Cross-Couplings in Water at Room Temperature. *J. Org. Chem.* **2011**, *76*, 4379–4391.
- (14) Lipshutz, B. H.; Aguinado, G. T.; Ghorai, S.; Voigtritter, K. Olefin Cross-Metathesis Reactions at Room Temperature Using the Nonionic Amphiphile “PTS”: Just Add Water. *Org. Lett.* **2008**, *10*, 1325–1328.
- (15) Lipshutz, B. H.; Ghorai, S.; Leong, W. W. Y.; Taft, B. R.; Krogstad, D. V. Manipulating Micellar Environments for Enhancing Transition Metal-Catalyzed Cross-Couplings in Water at Room Temperature. *J. Org. Chem.* **2011**, *76*, 5061–5073.
- (16) Akporji, N.; Thakore, R. R.; Cortes-Clerget, M.; Andersen, J.; Landstrom, E.; Aue, D. H.; Gallou, F.; Lipshutz, B. H. N₂Phos – an Easily Made, Highly Effective Ligand Designed for Ppm Level Pd-Catalyzed Suzuki–Miyaura Cross Couplings in Water. *Chem. Sci.* **2020**, *11*, 5205–5212.
- (17) Takale, B. S.; Thakore, R. R.; Handa, S.; Gallou, F.; Reilly, J.; Lipshutz, B. H. A New, Substituted Palladacycle for Ppm Level Pd-Catalyzed Suzuki–Miyaura Cross Couplings in Water. *Chem. Sci.* **2019**, *10*, 8825–8831.
- (18) Takale, B. S.; Thakore, R. R.; Casotti, G.; Li, X.; Gallou, F.; Lipshutz, B. H. Mild and Robust Stille Reactions in Water Using Parts Per Million Levels of a Triphenylphosphine-Based Palladacycle. *Angew. Chem., Int. Ed.* **2021**, *60*, 4158–4163.
- (19) Lipshutz, B. H.; Taft, B. R. Heck Couplings at Room Temperature in Nanometer Aqueous Micelles †. *Org. Lett.* **2008**, *10*, 1329–1332.
- (20) Pang, H.; Hu, Y.; Yu, J.; Gallou, F.; Lipshutz, B. H. Water-Sculpting of a Heterogeneous Nanoparticle Precatalyst for Mizoroki–Heck Couplings under Aqueous Micellar Catalysis Conditions. *J. Am. Chem. Soc.* **2021**, *143*, 3373–3382.
- (21) Handa, S.; Jin, B.; Bora, P. P.; Wang, Y.; Zhang, X.; Gallou, F.; Reilly, J.; Lipshutz, B. H. Sonogashira Couplings Catalyzed by Fe Nanoparticles Containing Ppm Levels of Reusable Pd, under Mild Aqueous Micellar Conditions. *ACS Catal.* **2019**, *9*, 2423–2431.
- (22) Jin, B. Ppm Pd-Catalyzed, Cu-Free Sonogashira Couplings in Water Using Commercially Available Catalyst Precursors. *Chem. Sci.* **2019**, 3481–3485.
- (23) Zhang, Y.; Takale, B. S.; Gallou, F.; Reilly, J.; Lipshutz, B. H. Sustainable Ppm Level Palladium-Catalyzed Aminations in Nanoreactors under Mild, Aqueous Conditions. *Chem. Sci.* **2019**, *10*, 10556–10561.
- (24) Isley, N. A.; Linstadt, R. T. H.; Kelly, S. M.; Gallou, F.; Lipshutz, B. H. Nucleophilic Aromatic Substitution Reactions in Water Enabled by Micellar Catalysis. *Org. Lett.* **2015**, *17*, 4734–4737.

- (25) Cortes-Clerget, M.; Berthon, J.-Y.; Krolkiewicz-Renimel, I.; Chaisemartin, L.; Lipshutz, B. H. Tandem Deprotection/Coupling for Peptide Synthesis in Water at Room Temperature. *Green Chem.* **2017**, *19*, 4263–4267.
- (26) Lipshutz, B. H.; Ghorai, S.; Cortes-Clerget, M. The Hydrophobic Effect Applied to Organic Synthesis: Recent Synthetic Chemistry “in Water.” *Eur. J. Chem.* **2018**, *24*, 6672–6695.
- (27) Lee, N. R.; Bikovtseva, A. A.; Cortes-Clerget, M.; Gallou, F.; Lipshutz, B. H. Carbonyl Iron Powder: A Reagent for Nitro Group Reductions under Aqueous Micellar Catalysis Conditions. *Org. Lett.* **2017**, *19*, 6518–6521.
- (28) Massolo, E.; Pirola, M.; Puglisi, A.; Rossi, S.; Benaglia, M. A One Pot Protocol to Convert Nitro-Arenes into *N*-Aryl Amides. *RSC Adv.* **2020**, *10*, 4040–4044.
- (29) R. Tung US2008024439A3, **2008**.
- (30) Prat, D.; Wells, A.; Hayler, J.; Sneddon, H.; McElroy, C. R.; Abou-Shehada, S.; Dunn, P. J. CHEM21 Selection Guide of Classical- and Less Classical-Solvents. *Green Chem.* **2016**, *18*, 288–296.
- (31) Gabriel, C. M.; Lee, N. R.; Bigorne, F.; Klumphu, P.; Parmentier, M.; Gallou, F.; Lipshutz, B. H. Effects of Co-Solvents on Reactions Run under Micellar Catalysis Conditions. *Org. Lett.* **2017**, *19*, 194–197.
- (32) Li, X.; Iyer, K. S.; Thakore, R. R.; Leahy, D. K.; Bailey, J. D.; Lipshutz, B. H. Bisulfite Addition Compounds as Substrates for Reductive Aminations in Water. *Org. Lett.* **2021**, *23*, 7205–7208.
- (33) Krell, C.; Schreiber, R.; Hueber, L.; Sciascera, L.; Zheng, X.; Clarke, A.; Haenggi, R.; Parmentier, M.; Baguia, H.; Rodde, S.; Gallou, F. Strategies to Tackle the Waste Water from α -Tocopherol-Derived Surfactant Chemistry. *Org. Process Res. Dev.* **2021**, *25*, 900–915.

3.7. General experimental information

a. TLC

Thin layer chromatography (TLC) was performed using Silica Gel 60 F254 plates (Merck, 0.25 mm thick), and visualized with a UV lamp and ninhydrin stain. Flash chromatography was done in glass columns using Silica Gel 60 (EMD, 40-63 μm).

b. NMR

^1H and ^{13}C NMR spectra were recorded on either a Varian Unity Inova 400 MHz (400 MHz for ^1H , 100 MHz for ^{13}C), a Varian Unity Inova 500 MHz (500 MHz for ^1H , 125 MHz for ^{13}C), a Varian Unity Inova 600 MHz (600 MHz for ^1H), Bruker (400 MHz for ^1H , 100 MHz for ^{13}C , 376 MHz for ^{19}F), or Bruker (500 MHz for ^1H , 125 MHz for ^{13}C , 471 MHz for ^{19}F).

Deuterated NMR solvents were purchased from Cambridge Isotopes Laboratories. DMSO- d_6 , CD_3OD , and CDCl_3 were used as solvents. Residual peaks for CHCl_3 in CDCl_3 (^1H = 7.26 ppm, ^{13}C = 77.00 ppm), $(\text{CH}_3)_2\text{SO}$ in $(\text{CD}_3)_2\text{SO}$ (^1H = 2.50 ppm, ^{13}C = 39.52 ppm) or MeOH in MeOD (^1H = 3.31 ppm, ^{13}C = 49.00 ppm) have been assigned as internal standards. The chemical shifts are reported in ppm. The coupling constants J value are given in Hz. Data are reported as follows: chemical shift, multiplicity (s = singlet, bs = broad singlet, d = doublet, bd = broad doublet, t = triplet, q = quartet, quin = quintet, m = multiplet), coupling constant (if applicable) and integration.

c. HRMS

Mass spectra were obtained from UC Irvine Mass Spectrometry Facility.

d. Reagents

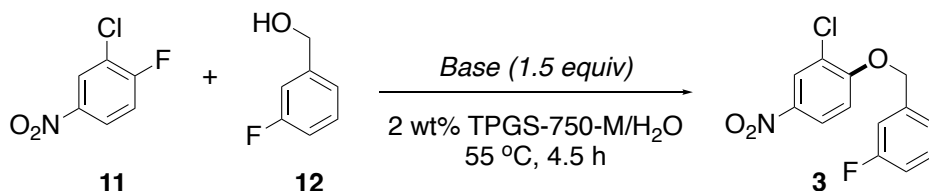
Reagents and chemicals were purchased from Sigma-Aldrich, Combi-Blocks, Alfa Aesar, Acros Organics, or TCI Chemicals and used without further purification. Carbonyl iron powder (CIP) used for reductions was 99.9% purity, R10 grade, with an average particle size of 2.5-3.5 μm . This material was stored in air with no special precautions.

TPGS-750-M is either prepared or supplied by PHT International (also available from Sigma-Aldrich catalog #733857). The desired 2 wt % of surfactant solution in HPLC water was prepared by dissolving 2 g of surfactant to 98 g of HPLC water (degassed with argon before use) and stored under argon. Thin-layer chromatography (TLC) was performed using Silica Gel 60 F254 plates (Merck, 0.25 mm thick). Flash chromatography is performed manually or in an automated Biotage system using Silica Gel 60 (Silicycle, 40-63 nm). GCMS data were recorded on a 5975C Mass Selective Detector, coupled with a 7890A Gas Chromatograph (Agilent Technologies). ^1H , ^{13}C , and ^{19}F NMR spectra were recorded on either a Bruker Avance III HD 400 MHz (400 MHz for ^1H , 100 MHz for ^{13}C), a Bruker Avance NEO 500 MHz (500 MHz for ^1H , 125 MHz for ^{13}C , 470 MHz for ^{19}F) or on a Varian Unity Inova 500 MHz (500 MHz for ^1H , 125 MHz for ^{13}C); DMSO- d_6 , CDCl_3 , or CD_3OD was used as NMR solvent. Residual peaks for DMSO in DMSO- d_6 (^1H = 2.50 ppm, ^{13}C = 39.51 ppm), CHCl_3 in CDCl_3 (^1H = 7.26 ppm, ^{13}C = 77.00 ppm), CH_3OH in CD_3OD (^1H = 3.31 ppm, ^{13}C = 49.00 ppm) have been assigned. The chemical shifts are reported in parts per million (ppm), and the coupling constants J values are given in Hertz (Hz). The peak patterns are indicated as follows: bs, broad singlet; s, singlet; d, doublet; t, triplet; q, quartet; p, pentet; m, multiplet.

3.8. Procedures for the synthesis of lapatinib

a. S_NAr reaction

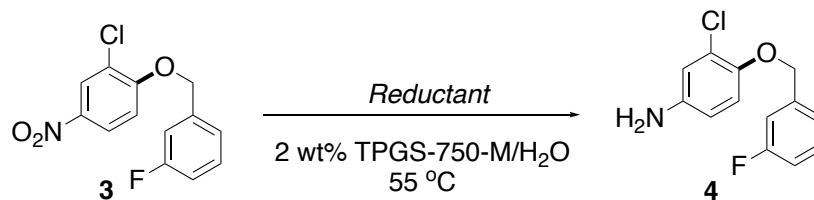
- Screening of base



Reaction conditions: 0.25 mmol **11**, 0.275 mmol of **12**, 0.375 mmol of base, stirred at 55 °C for 4.5 h; conversion was determined by GC-MS.

In a 1 dram vial equipped with a magnetic stir bar, 2-chloro-1-fluoro-4-nitrobenzene **11** (0.25 mmol), (3-fluorophenyl)methanol **12** (0.275 mmol), and base (0.375 mmol) were added. Aqueous 2 wt % TPGS-750-M solution (0.5 mL) was then added. The resulting mixture was stirred at 55 °C until completion (as monitored by TLC or GC-MS). The desired product was isolated by filtration and dried under vacuum to give a light-yellow powder in 98% yield.

b. Nitro reduction

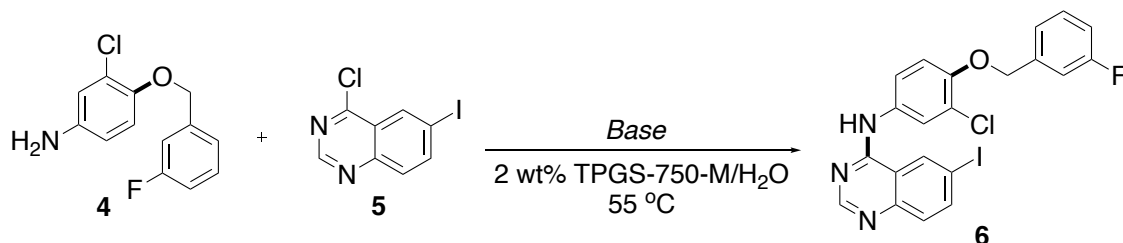


Entry	Conditions	Conversion to 4 (%) ^c
1	1% Pd/C (1 mol %), Et ₃ SiH (1.5 equiv)	0
2	1 wt % Pd/C (1 mol % based on Pd), H ₂ balloon	~20
3	10 wt % Pd/C (1 mol % based on Pd), H ₂ balloon	~90
4	CIP (5 equiv),^d NH₄Cl (3 equiv)	100

In a 1 dram vial equipped with a magnetic stir bar, 2-chloro-1-((3-fluorobenzyl)oxy)-4-nitrobenzene **3** (0.25 mmol) and the reducing agents were added. Aqueous 2 wt % TPGS-750-M (0.5 mL) solution was added, and the vial was stirred at 55 °C until completion (as monitored by TLC or GC-MS). The reaction mixture was filtered through cotton and washed with EtOAc or Et₂O (3 x 1 mL). The combined organic layers were evaporated to give the crude product as a brown-colored oil, which was analyzed by GC-MS or crude NMR and used subsequently without further purification.

c. S_NAr reaction

• Screening of base

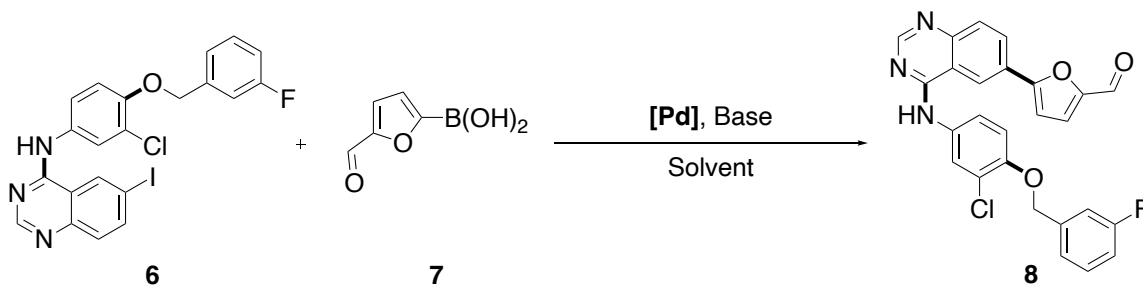


Reaction conditions: 0.25 mmol **4**, 0.25 mmol **5** and base stirred at 55 °C; °Conversion was determined by crude NMR.

In a 1 dram vial with a magnetic stir bar, the crude product from the previous step (**4**; 0.25 mmol) was used along with 0.25 mmol **5**. Aqueous 2 wt % TPGS-750-M (0.5 mL) solution was then added, and the reaction was stirred at 55 °C until completion (as monitored by TLC or GC-MS). The product was then separated by vacuum filtration to give a light-yellow powder, **6**.

d. Suzuki-Miyaura coupling reaction

- Screening of palladium catalysts

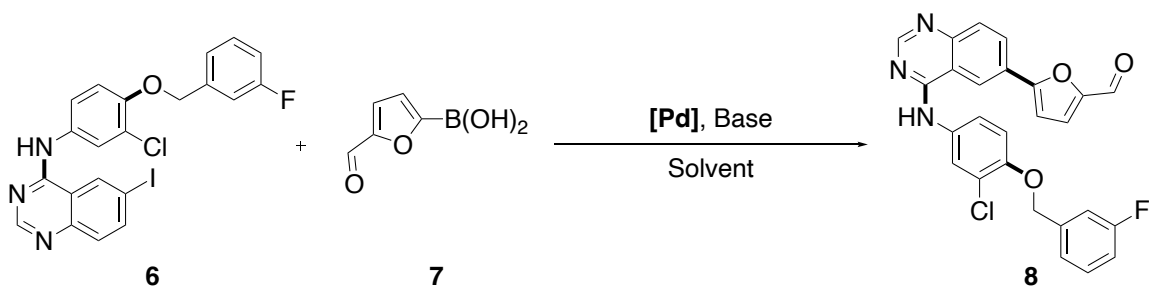


Entry	Catalyst	Base	Solvent	Conversion to 8 (%) ^f
1	Pd(dtbpf)Cl ₂ (1 mol %)	Et ₃ N (3 equiv)	2 wt % TPGS-750-M	<3
2	Pd(dtbpf)Cl ₂ (3 mol %)	Et ₃ N (3 equiv)	2 wt % TPGS-750-M	<50
3	Pd(dppf)Cl ₂ ·DCM (4 mol %)	Et ₃ N (5 equiv)	2 wt % TPGS-750-M	~50
4 ^g	Pd(dppf)Cl ₂ ·DCM (4 mol %)	Et ₃ N (5 equiv)	EtOH (reflux)	100
5	Pd(dppf)Cl ₂ ·DCM (4 mol %)	Et ₃ N (5 equiv)	2 wt % TPGS-750-M, 20 v/v% EtOH	<40
6	Pd(dppf)Cl ₂ ·DCM (4 mol %)	Et ₃ N (5 equiv)	50:50 2 wt % TPGS- 750-M: EtOH	<50
7	10 wt% Pd/C (3 mol %)	Et ₃ N (5 equiv)	EtOH (reflux)	>90

Reaction conditions: 0.25 mmol **6**, 0.5 mmol **7** and base, stirred at 55 °C (with TPGS-750-M) or under reflux conditions (with EtOH) overnight. ^fConversion was determined by crude NMR or GC-MS. ^gReaction time = 2 h

In a 2 dram vial with a magnetic stir bar, 0.25 mmol **6**, 0.5 mmol **7**, Pd catalyst and base (1.25 mmol) were added. Aqueous 2 wt % TPGS-750-M solution (0.5 mL) or EtOH (2.5 mL) was subsequently added, and the reaction was allowed to stir at 55 °C (TPGS-750-M) or at 80 °C (EtOH) until completion (as monitored by TLC or GC-MS). The crude product was used for the subsequent reaction without further purification.

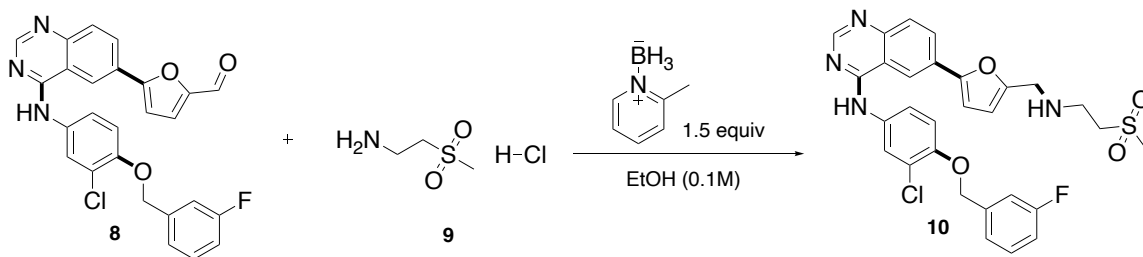
- Screening of catalyst loading



In a 2 dram vial with a magnetic stir bar, 0.25 mmol **6**, 0.5 mmol **7**, Pd(dppf)Cl₂•DCM and base (1.25 mmol) were added. Aqueous 2 wt % TPGS-750-M solution (0.5 mL) or EtOH (2.5 mL) was subsequently added, and the reaction was allowed to stir at 55 °C (TPGS) or at 80 °C (EtOH) until completion (as monitored by TLC or GC-MS).

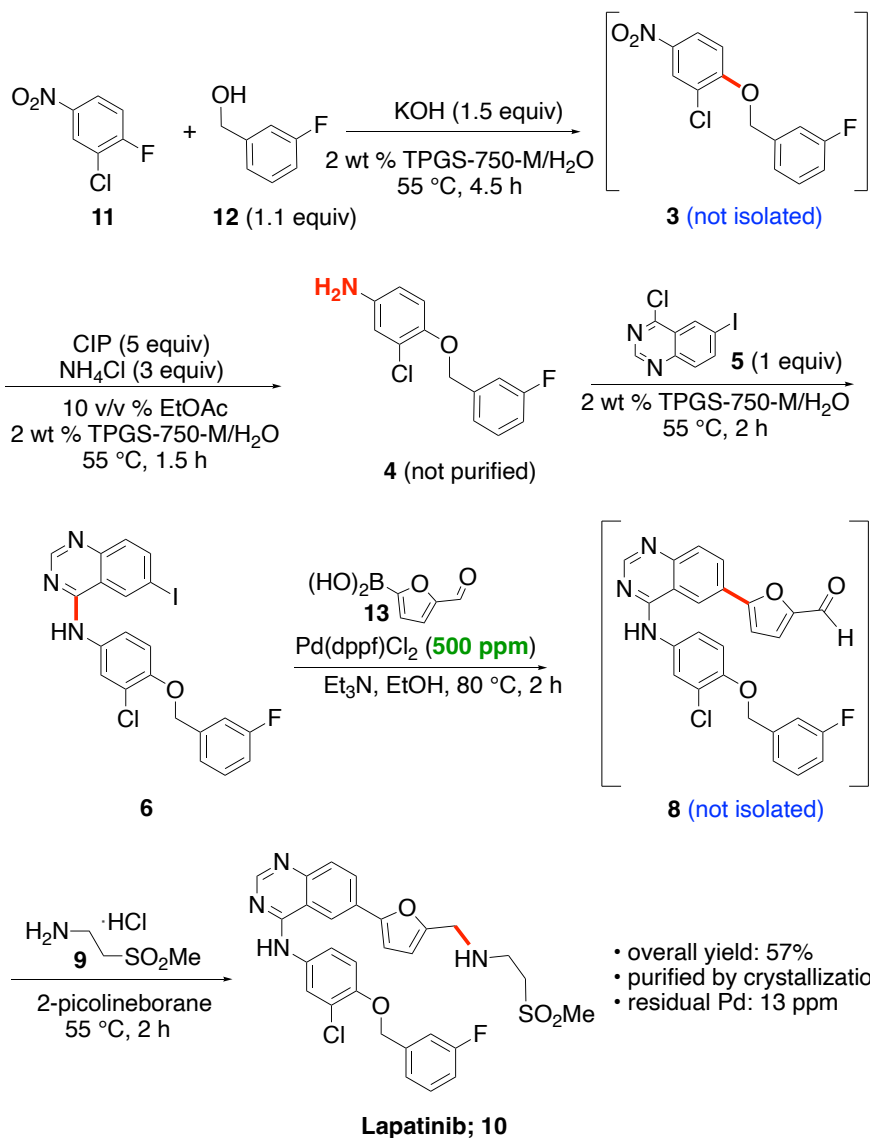
Entry	Pd(dppf)Cl ₂ loading	Base	Conversion to 8 (%) ^b
1	2 mol % (20,000 ppm)	Et ₃ N (3 equiv)	100
2	1 mol % (10,000 ppm)	Et ₃ N (3 equiv)	100
3	0.5 mol % (5000 ppm)	Et ₃ N (5 equiv)	100
4	0.1 mol % (1000 ppm)	Et ₃ N (5 equiv)	100
5	0.05 mol % (500 ppm)	Et ₃ N (5 equiv)	100

e. Reductive amination



In the same 2 dram vial from the previous reaction was added 2-(methylsulfonyl)ethan-1-amine hydrochloride **9** (1.2 equiv) and 2-picolineborane (1.5 equiv) and the reaction mixture was allowed to stir at 55 °C until completion (as monitored by crude NMR or GC-MS). The resulting product was purified by column chromatography using DCM : EtOAc (3:1) + 2% MeOH + 1% Et₃N as the mobile phase to yield lapatinib free base **10** as a light brown oil.

f. Procedures for the 5-step, 3-pot synthesis of lapatinib



Step 1: S_NAr reaction

In a 1 dram vial with a magnetic stir bar, 2-chloro-1-fluoro-4-nitrobenzene **1** (0.15 mmol, 1 equiv), (3-fluorophenyl)methanol **2** (1.1 equiv) and KOH (1.5 equiv) were added. Aqueous 2 wt % TPGS-750-M solution (0.5 M global concentration) was then added. The reaction was stirred at 55 °C until completion (as monitored by TLC or GC-MS).

Step 2: Reduction of nitro group

Once step 1 (S_NAr) was completed, CIP (carbonyl iron powder; 5 equiv) and NH_4Cl (3 equiv) were added. 20 v/v% EtOAc (0.1 mL) was added to enhance solubility and stirring. The pH of the system was adjusted to neutral or slightly acidic (pH 6 – 7) by adding a few drops of concentrated HCl if needed. Subsequently, the resulting mixture was allowed to stir at 55 °C until completion (as monitored by TLC or GC-MS). The reaction mixture was filtered through a silica plug and washed with EtOAc (~3 mL). The solvents were evaporated to give the crude product as a brown colored oil, which was analyzed by GC-MS or crude NMR and used subsequently without further purification.

Step 3: S_NAr reaction

In a 1 dram vial with a magnetic stir bar, the crude product from step 2 was used along with 4-chloro-6-iodoquinazoline **5** (1 equiv). Aqueous 2 wt % TPGS-750-M (0.5 M global concentration) solution was then added, and the reaction was stirred at 55 °C until completion (as monitored by TLC or GC-MS). The product was then separated by vacuum filtration to give a light-yellow powder **6**.

Note: The presence of >50% water in the reaction mixture is detrimental for the subsequent Suzuki-Miyaura coupling (see section 3.8.d). Water can be removed by vacuum filtration. Alternatively, the Suzuki-Miyaura coupling can also be carried out in the same pot if the water is dried by placing the resulting reaction vial from step 3 in an oven at 120 °C for 2 h, or by placing it in a hot plate at 60 °C and attaching a high vacuum line overnight.

Step 4: Suzuki-Miyaura reaction

The product from step 3, **6** (1 equiv), was transferred to a 2 dram vial equipped with a magnetic stir bar. To the vial, 5-formyl furan-2-boronic acid **7** (2 equiv), Pd(dppf)Cl₂•DCM (500 ppm) and Et₃N (5 equiv) were added, followed by 95% ethanol (1.5 mL or 0.1 M global concentration). The reaction was allowed to stir at 80 °C until completion (as monitored by taking a crude NMR, TLC, or GC-MS). The crude product was analyzed by NMR (in DMSO-d₆) and was used in the subsequent step without further purification.

*Note: Pd(dppf)Cl₂•DCM (500 ppm) was added by preparing a stock solution of Pd(dppf)Cl₂•DCM in ethanol.

*Pd(dppf)Cl₂ (with no DCM complex) failed to give the product under the same reaction conditions.

Step 5: Reductive amination

To the same 2 dram vial from the previous step was added 2-(methylsulfonyl)ethan-1-amine hydrochloride **9** (1.2 equiv) and 2-picolineborane (1.5 equiv). The reaction mixture was allowed to stir until completion (as monitored by NMR, TLC, or GC-MS). The resulting mixture was purified by recrystallization in EtOAc to yield lapatinib free base **10** as light-yellow solid, (49.7 mg, 0.086 mmol, 57% yield).

Alternatively, the resulting product was purified by column chromatography using DCM : EtOAc (3:1) + 2% MeOH + 1% Et₃N as the mobile phase to yield lapatinib free base **10** as a light brown oil (48.8 mg, 0.084 mmol, 56% yield).

3.9. E Factor calculations

$$E \text{ Factor} = \frac{\text{grams of wastes}}{\text{grams of product}}$$

- **This work:**

waste:

$$\begin{aligned} &0.5 \text{ ml TPGS-750-M (aq)} * 1 \text{ g/mL} + 0.1 \text{ ml EtOAc} * 0.902 \text{ g/mL} + 3.0 \text{ ml EtOAc} * 0.902 \\ &\text{g/mL} + 0.5 \text{ ml TPGS-750-M (aq)} * 1 \text{ g/mL} + 2.5 \text{ ml EtOH} * 0.789 \text{ g/mL} \\ &= 5.77 \text{ g wastes} \end{aligned}$$

(density of EtOAc = 0.902 kg/m³; density of EtOH = 0.789 kg/m³)

$$E \text{ Factor} = \frac{5.77 \text{ grams of wastes}}{0.808 \text{ grams of product}} = \mathbf{7.1}$$

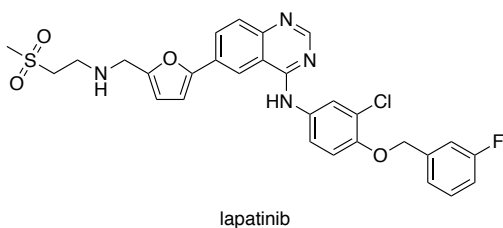
- **Literature:** (US 8444988 B2) GSK, 2013

waste:

$$\begin{aligned} &90.0 \text{ mL CH}_3\text{CN (aq)} * 0.786 \text{ g/mL} + 180.0 \text{ mL EtOH} * 0.789 \text{ g/mL} + 250.0 \text{ mL } i\text{-PrOH} \\ &* 0.786 \text{ g/mL} + 740.5 \text{ mL} * 0.888 \text{ g/mL THF} + x \text{ mL (unstated volume) dioxane and THF} \\ &= 1066.8 \text{ g} + x \text{ waste} \end{aligned}$$

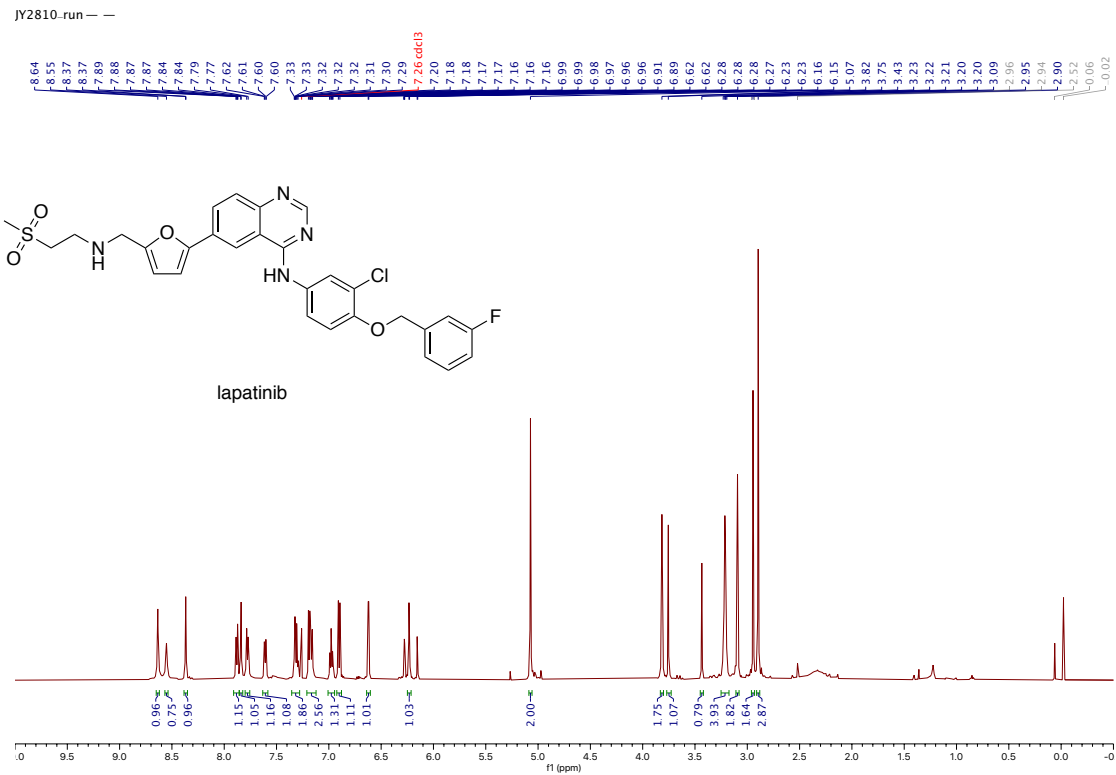
$$E \text{ Factor} = \frac{1066.82 \text{ grams of wastes}}{10.0 \text{ grams of product}} > \mathbf{106.7}$$

3.10. Compound characterization data and spectra

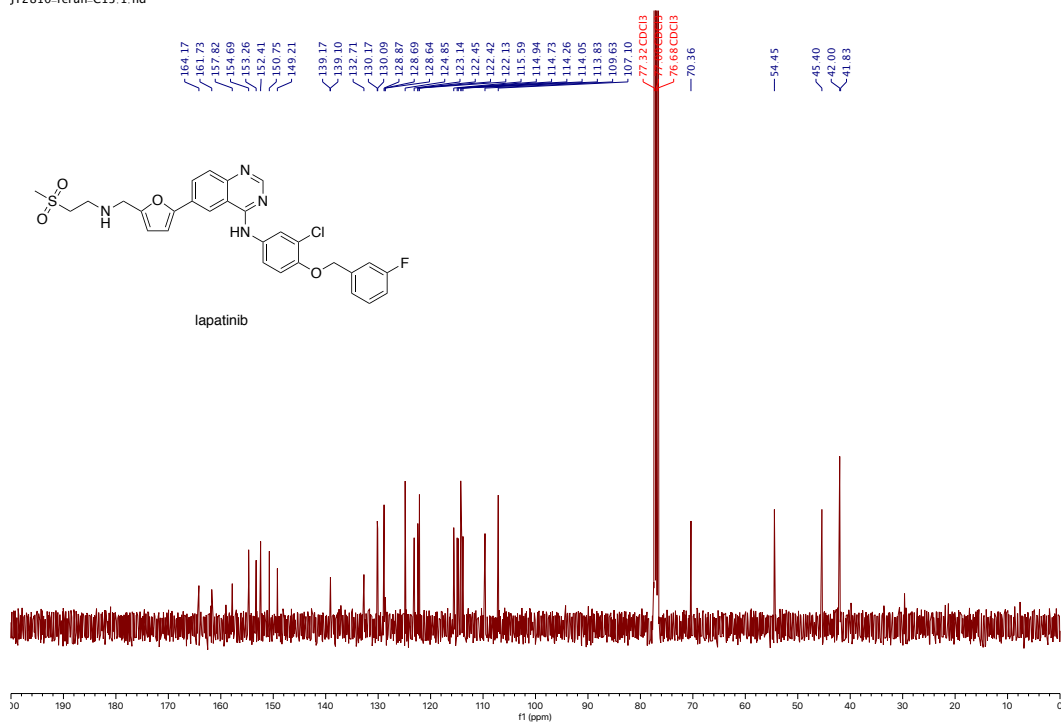


¹H NMR (600 MHz, CD₃OD) δ 8.75 (s, 1H), 8.51 (s, 1H), 8.23 (d, *J* = 8.5 Hz, 1H), 7.91 (dd, *J* = 2.7, 1.2 Hz, 1H), 7.80 (d, *J* = 8.6 Hz, 1H), 7.66 – 7.61 (m, 1H), 7.42 – 7.36 (m, 1H), 7.30 (d, *J* = 7.7 Hz, 1H), 7.24 (dd, *J* = 9.9, 2.4 Hz, 1H), 7.17 (dd, *J* = 8.9, 1.1 Hz, 1H), 7.07 – 7.00 (m, 2H), 6.68 (s, 1H), 5.22 (s, 2H), 4.23 (s, 2H), 3.49 (d, *J* = 7.0 Hz, 2H), 3.43 (d, *J* = 8.2 Hz, 2H), 3.06 (s, 3H). **¹³C NMR** (101 MHz, CDCl₃) δ 162.95 (d, *J*_{C-F} = 246.4), 157.82, 154.69, 153.26, 152.41, 150.75, 149.21, 139.14 (d, *J*_{C-F} = 7.1) 132.71, 130.1 (d, *J*_{C-F} = 8.1) 128.87, 128.69, 128.64, 124.85, 123.14, 122.44 (d, *J*_{C-F} = 3.0), 122.13, 115.59, 114.83 (d, *J*_{C-F} = 21.2), 114.26, 113.94 (d, *J*_{C-F} = 22.2), 109.63, 107.10, 70.36, 54.45, 45.40, 42.00, 41.83. **¹⁹F NMR** (376 MHz, CDCl₃) δ -112.66 (td, *J*_{F-H} = 9.1, 5.6 Hz). **HRMS TOF MS EI+** *m/z* calcd C₂₉H₂₆ClFN₄O₄S H [M+H]⁺: 581.1426; found 581.1405.

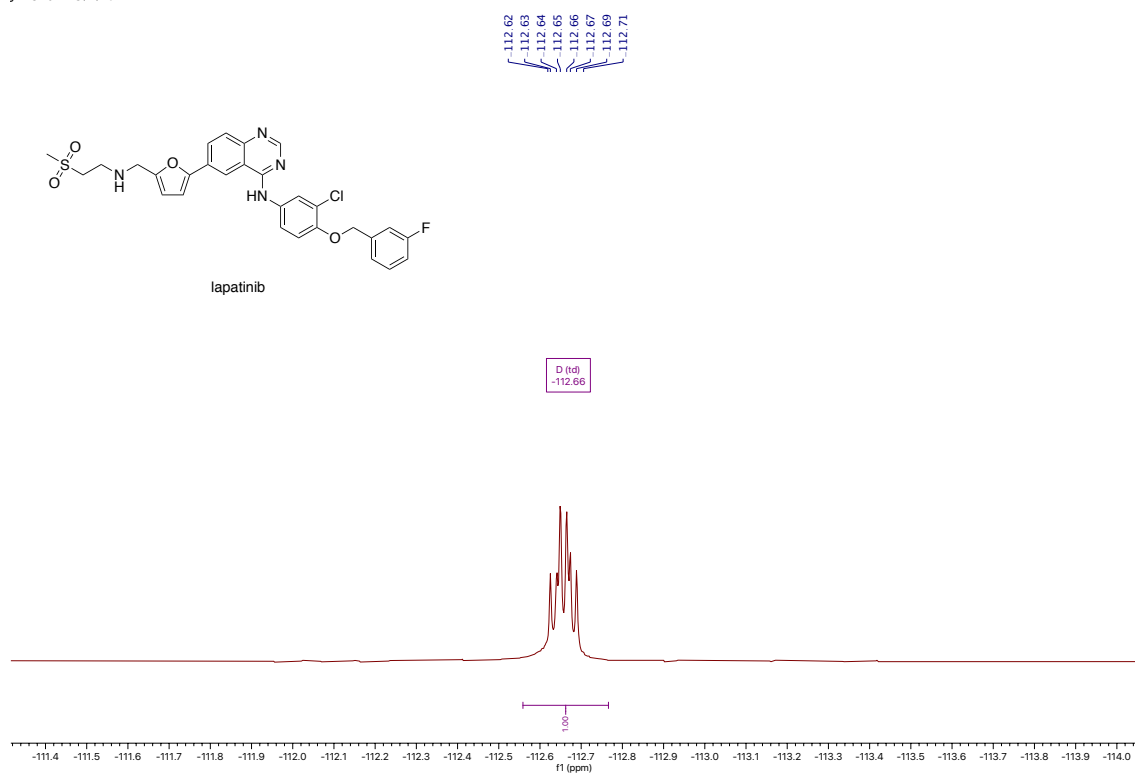
- NMR spectra: ^1H , ^{13}C , and ^{19}F NMR of lapatinib



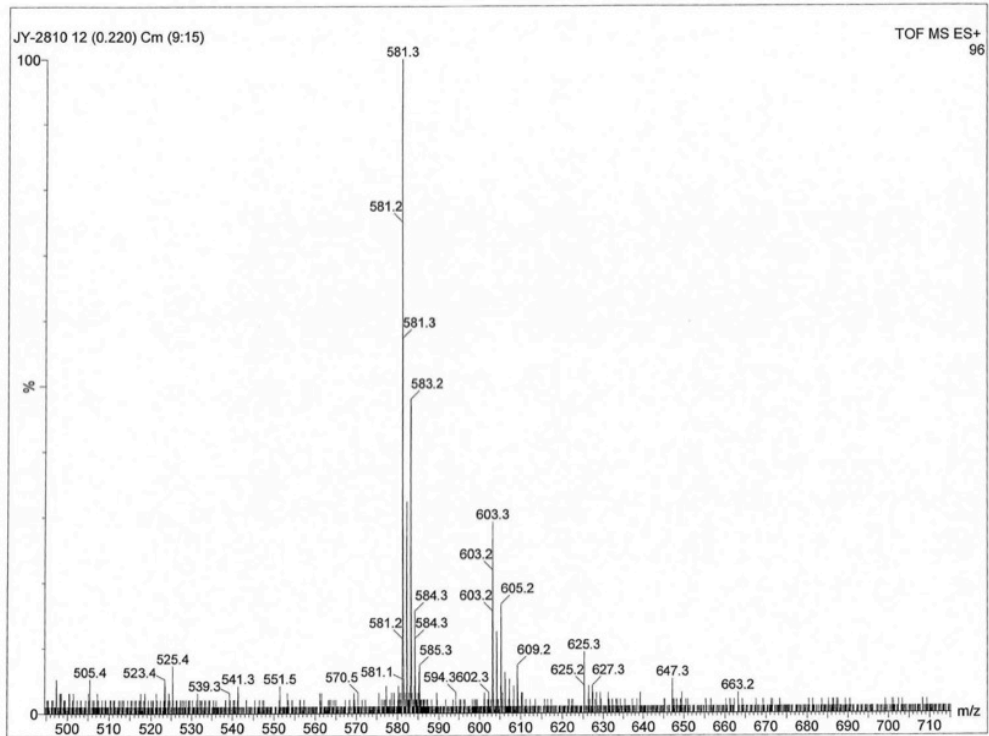
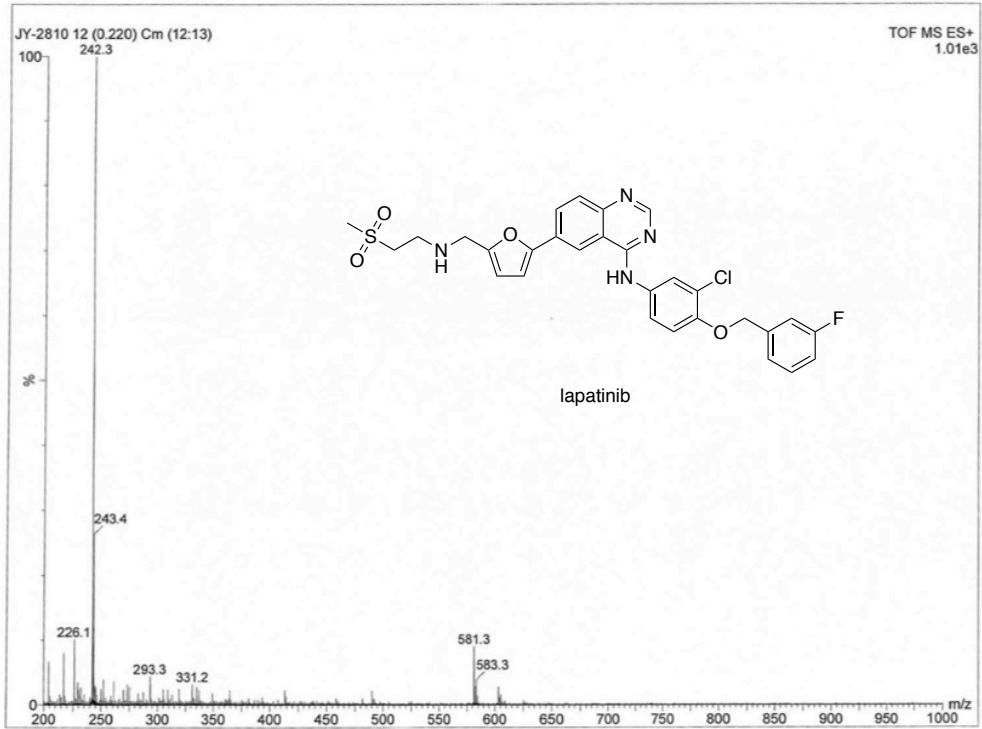
JY2810_rerun_C13.1.fid

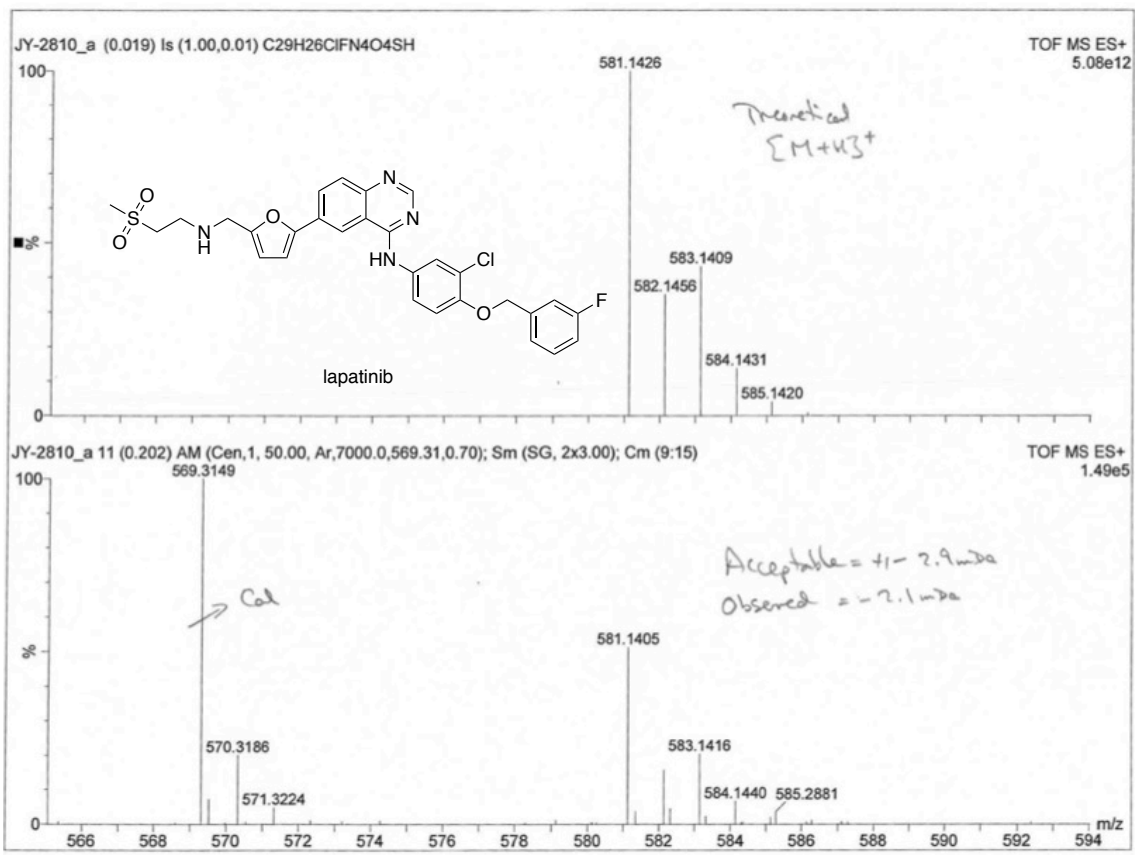


JY2810-F19.1.fid



- HRMS





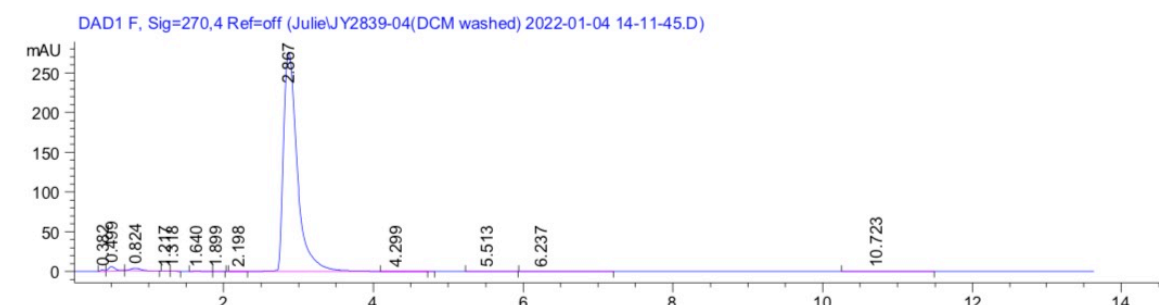
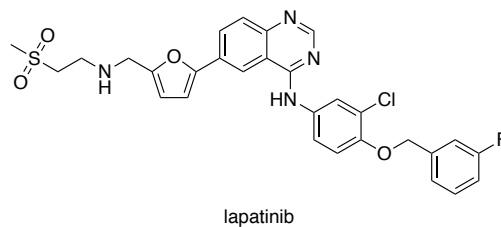
- Purity analysis by HPLC

Column: InfinityLab Poroshell HPH-C18, 2.7 micron, 4.6 x 50 mm

Eluent: hexane/ *i*-PrOH = 90/10

Flow rate: 1 mL/min

Column temperature: 20 °C



Signal 6: DAD1 F, Sig=270, 4 Ref=of f

Peak #	Ret Time [min]	Type	Width [min]	Area [mAU s]	Height [mAU]	Area %
1	0.382	BV	0.0545	5.91052	1.70355	0.1655
2	0.499	W R	0.0932	34.15775	5.44683	0.9564
3	0.824	BB	0.1479	30.27498	3.15671	0.8477
4	1.217	BV	0.0648	3.24298e-1	8.08731e-2	9.080e-3
5	1.318	VB	0.0856	2.81078e-1	5.32584e-2	7.870e-3
6	1.640	BV	0.1532	1.94257	1.83929e-1	0.0544
7	1.899	VB	0.0874	3.13159e-1	5.58503e-2	8.769e-3
8	2.198	BV E	0.1127	7.74780e-1	1.09258e-1	0.0217
9	2.867	W R	0.1953	3483.06519	275.81552	97.5268
10	4.299	VB E	0.2295	2.02840	1.18630e-1	0.0568
11	5.513	BB	0.2504	4.36215	2.61799e-1	0.1221
12	6.237	BB	0.3664	4.30216	1.47452e-1	0.1205
13	10.723	BB	0.3784	3.65734	1.16457e-1	0.1024

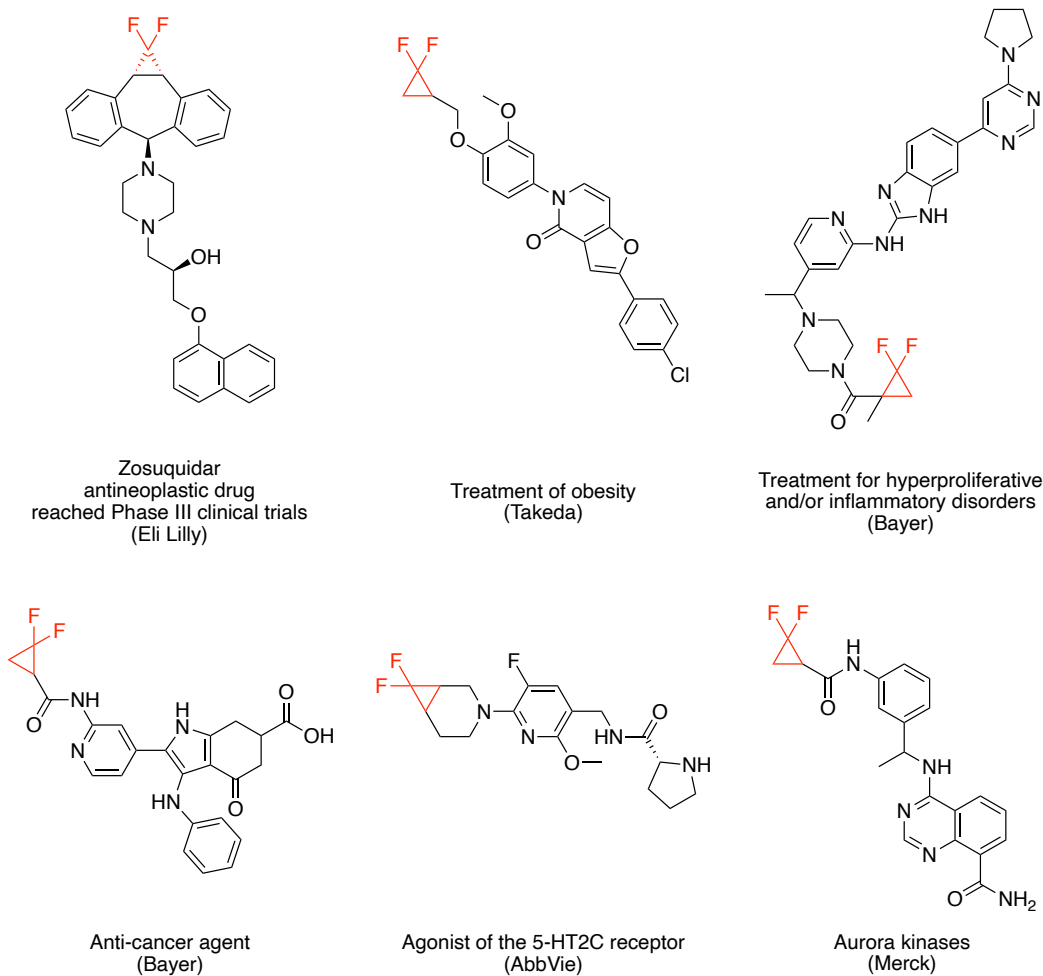
Total s : 3571.39438 287.25012

4. Difluorocarbene addition to alkenes and alkynes using TMSCF₂Br under neat conditions

4.1. Background and introduction

In medicinal chemistry, the introduction of fluorine atoms at specified places on a target pharmaceutical has attracted attention and been widely applied to modern drug designs due to its beneficial effects on physicochemical properties. More specifically, fluorine's compact size and strong electronegativity (3.98) make it an excellent tool for lowering the pKa of proximal functional groups. Changes in pKa influence the pH-dependent features of drug candidates, such as solubility, lipophilicity, permeability, and protein binding, which affect potency, selectivity, toxicity, and pharmacokinetic (PK) properties such as adsorption, distribution, metabolism, and excretion (ADME).¹ Fluorinated organic compounds account for more than 30% of medicines and 60% of agrochemicals registered in the last five years. However, 80% of these fluorinated drugs are monofluorinated (R-F) or trifluoromethylated (R-CF₃) compounds, indicating that access to diverse fluoro-functional groups remains limited. Additionally, small aliphatic rings have proven in studies to be a beneficial strategy for regulating overall lipophilicity, shielding sites from undesired metabolism, or improving key interactions via hydrophobic and space-filling effects.² Therefore, numerous contemporary biologically active compounds containing a difluorinated cyclopropane functional group have been reported; selected examples are shown in **Scheme 1**. According to Pfizer's most recent publication, a *gem*-difluorocyclopropane building block on a multikilogram scale is in high demand.³ As a

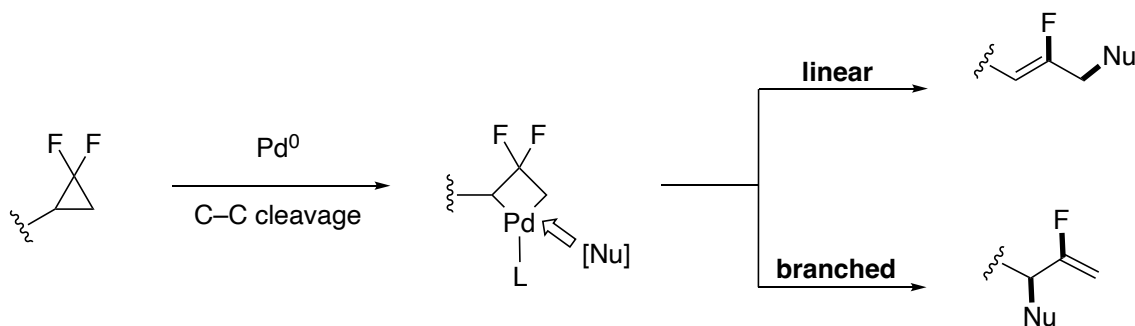
result, simple methods to access novel fluorinated motifs are becoming increasingly popular within synthetic chemistry research.



Scheme 1. Bioactive compounds containing a difluorocyclopropane^{4,5}

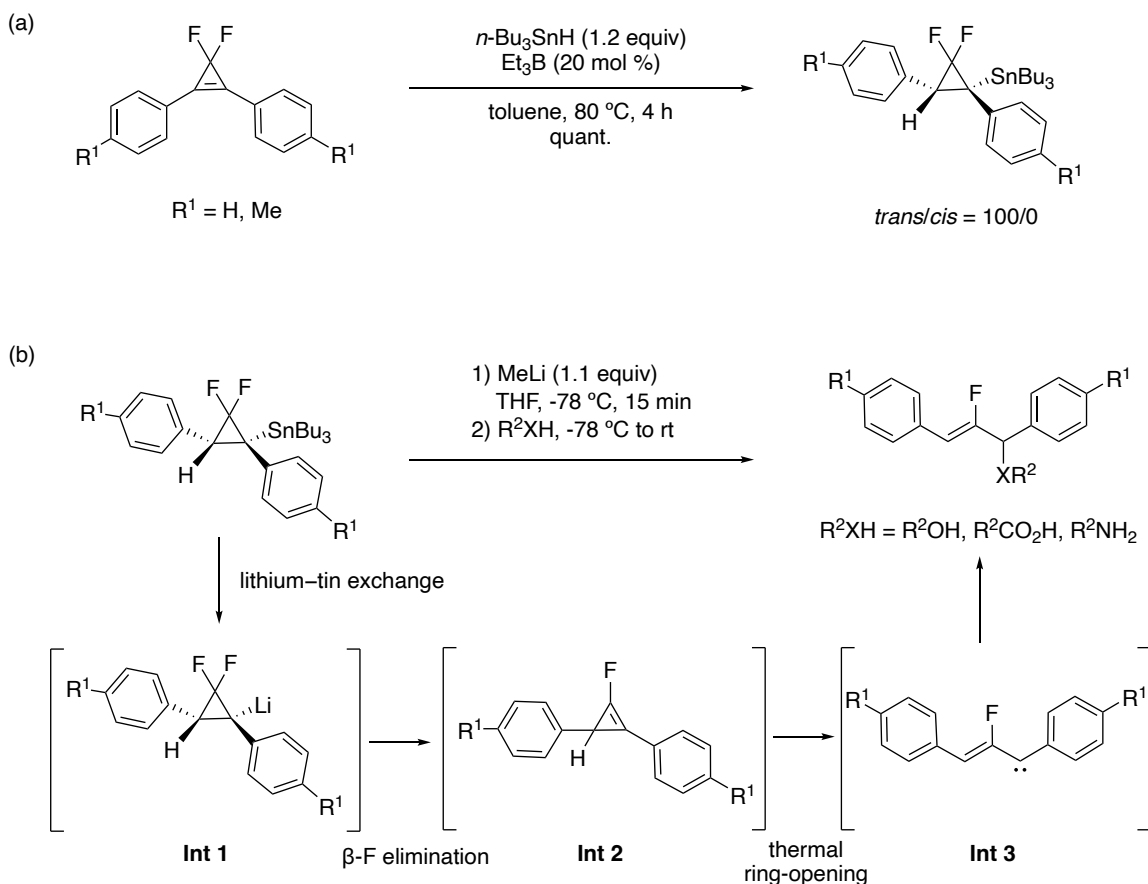
On the other hand, because the strongly polarized C–C bond is easily converted into structurally distinct types of organic compounds using a transition-metal-catalyzed ring-opening approach, the structurally distinct *gem*-difluorocyclopropane unit has been recognized as a versatile building block in synthetic organic chemistry. As shown in

Scheme 2, Fu and co-workers reported the first Pd-catalyzed C–C bond cleavage of such rings, which involved β -F elimination followed by attack of N, O, and C nucleophiles providing valuable 2-fluorinated allylic amines, ethers, esters, and alkylation products with high regioselectivity (linear product) and stereoselectivity (*Z*-configuration), which are valuable synthetic building blocks for further transformations.⁶



Scheme 2. Derivatization of *gem*-difluorocyclopropanes with Pd-catalyzed ring-openings.^{6,7}

Konno and co-workers further extended this ring-opening strategy to the structurally similar *gem*-difluorocyclopropenes by treating them with *n*-Bu₃SnH in the presence of 20 mol % of Et₃B, as shown in **Scheme 3a**. After a lithium–tin exchange with methyllithium (**Int 1**, **Scheme 3b**), β -fluoride elimination occurred resulting in **Int 2**, which then underwent a thermal ring-opening to produce **Int 3**, followed by exposure of **Int-3** to a quenching agent (R₂XH) to yield the corresponding β -fluoroallylic alcohols, ethers, and amides.⁸

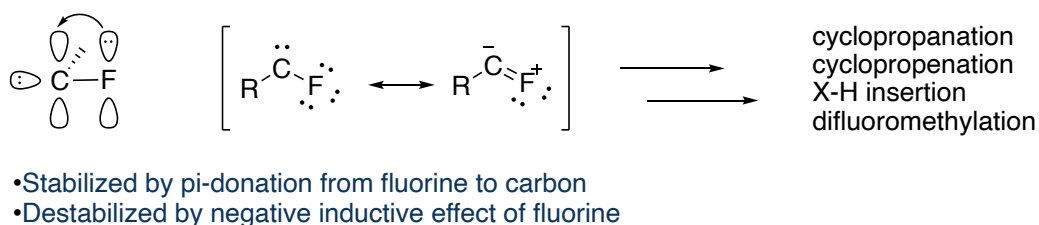


Scheme 3. (a) Preparation of *gem*-difluorocyclopropylstannanes; (b) Ring-opening with R^2XH , and proposed intermediates.⁸

4.2. Literature on the synthesis of difluorocyclopanes and difluorocyclopropenes

The synthesis of difluorocyclopanes and difluorocyclopropenes can be achieved in various ways. Not surprisingly, direct [2 + 1] addition of difluorocarbene to an alkene or an alkyne represents the most efficient method. Difluorocarbene in its singlet ground state is stabilized by π -donation from the fluorine to carbon, while the strong electron-withdrawing inductive effect contributes to the moderate electrophilicity to the carbene,

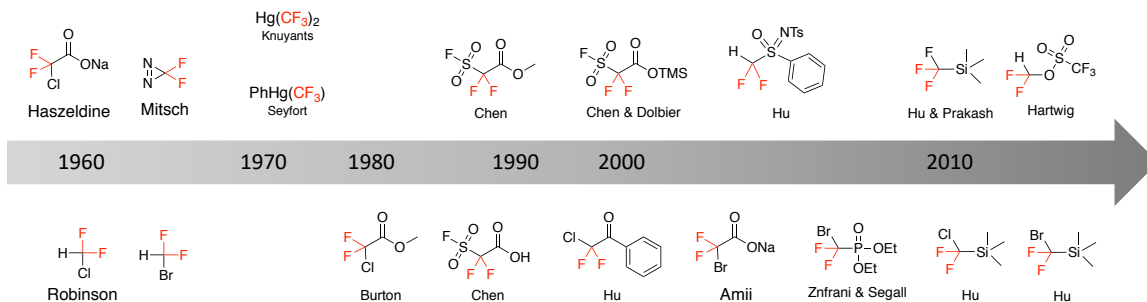
making it react more easily with electron-rich rather than electron-poor substrates.⁹ Studies have shown that the reactions of difluorocarbene with negatively charged heteroatom nucleophiles, such as phenolates and thiolates, can be carried out at ambient temperatures, while reactions with both alkenes and alkynes required heating to overcome the substantial activation barrier for addition to all but the most reactive of alkenes.^{10,11}



Scheme 4. Resonance stabilization of singlet difluorocarbene by p-donation.

A variety of methods for the generation of difluorocarbene has appeared, as shown in **Scheme 5**. However, many precursors were unavailable on a multikilogram scale, and some of the precursors such as difluorohalomethanes (or “halons”) that were previously used due to their low cost are now known to be ozone-depleting substances (ODS) and have been phased out by the US Environmental Protection Agency (EPA).¹² Difluorodiazirine is one of the few compounds that can be activated photochemically when heated over 165 °C. Major limitations of this reagent include its potentially explosive nature and the requirement of an elemental fluorination step during preparation.¹³ Another reagent that gives good results with alkenes over a broad reactivity range is Seyferth’s reagent, PhHgCF_3 , albeit restricted because of its toxicity and lack of commercial

availability. It decomposes in the presence of NaI in refluxing benzene to form a reactive $:CF_2$ species.¹⁴

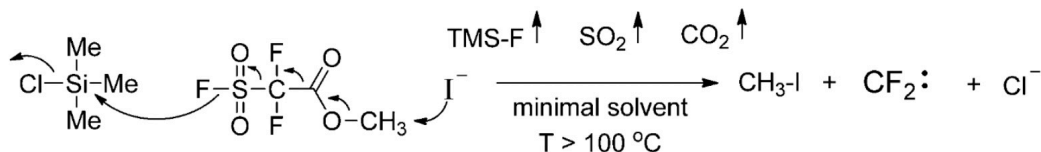


Scheme 5. The evolution of difluorocarbene sources over time.

Thermal decarboxylation of sodium halodifluoroacetate has proven to be a reliable method of producing difluorocyclopropanes from a broad range of olefins, leading to good conversions of even the most unreactive alkenes.¹⁵ While effective, this method suffers from the high temperatures required for carbene formation (in refluxing diglyme; 150–190 °C) and the need for a considerable (10–27-fold) excess of the precursor.^{16,17}

A similar thermal decomposition of trimethylsilyl fluorosulfonyldifluoroacetate (TFDA)¹⁸ has the advantage of generating carbenes that are more reactive toward electron-poor alkenes.^{19,20,21,22} However, the reaction conditions remain harsh, and TFDA has hydrolytic stability issues resulting in a poor shelf life. Another effective source of difluorocarbene has been recently reported by Dolbier and co-workers. As shown in **Scheme 6**, methyl 2,2-difluoro-2-(fluorosulfonyl)acetate (MDFA) was first demethylated with iodide ion, which led to decarbonylation and the release of difluorocarbene and TMSF, the former adding efficiently to even the most unreactive alkenes, such as acrylate esters. However,

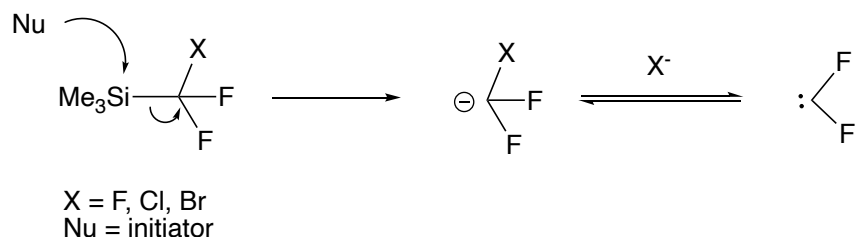
this procedure raised several environmental concerns, including the release of CO₂ and the use of dipolar solvents such as dioxane and diglyme.



Scheme 6. Generation of difluorocarbene from MDFA from Dolbier *et al.*¹⁹

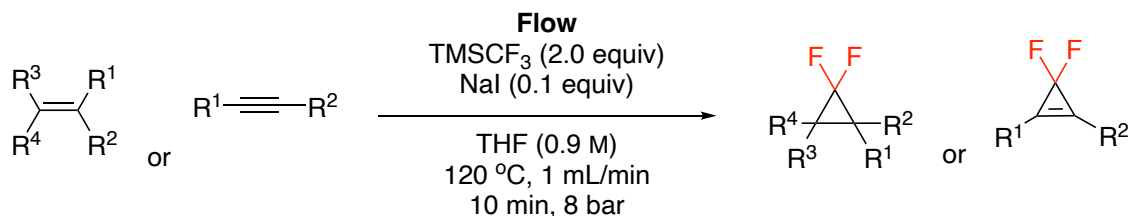
To circumvent some drawbacks of the reagents in these previous reports, a new method has been developed for the generation of difluorocarbene from trifluoromethyltrimethylsilane (TMSCF₃, Ruppert-Prakash reagent) or its chlorinated and brominated derivatives (TMSCF₂Cl, TMSCF₂Br) which are more effective owing to the better leaving ability of bromide ion through α -fluoride elimination, as shown in **Scheme 7**. It was found useful to yield *gem*-difluorocyclopropane at (-50 °C) by using TBAT (terabutylammonium triphenyldifluorosilicate) as initiator.⁹ NaI can be used as an alternative initiator for this same reagent at 65 °C in THF.⁹ This particular TMSCF₃/NaI method has been found practical and applied to various recent developments; for example, a continuous flow technology with high back pressure (8 bar) was applied to the system to achieve rapid transformations (**Scheme 8a**).²³ Mykhailiuk and co-workers attempted to perform difluorocyclopropanation using this TMSCF₃/NaI system on various drug syntheses-related building blocks, including nitrogen-containing rings, amines, sulfonyl chlorides, and sulfonamides (**Scheme 8b**). Notably, other reagents, such as CF₂ClCO₂Na,²⁴ CF₂BrCO₂Na,¹⁷ (CF₃)₂Hg, or FSO₂CF₂CO₂TMS/LiF failed to undergo this same transformation.¹ This method is also compatible with electron-deficient substrates, which are challenging due to the inherent electrophilic nature of difluorocarbene. The

transformation of a pyridinyl tetrafluorosulfanyl alkyne to a highly lipophilic and polarized, fully fluorinated novel motif, which was previously unknown, was done under superheated THF (110 °C) conditions, (**Scheme 8c**).

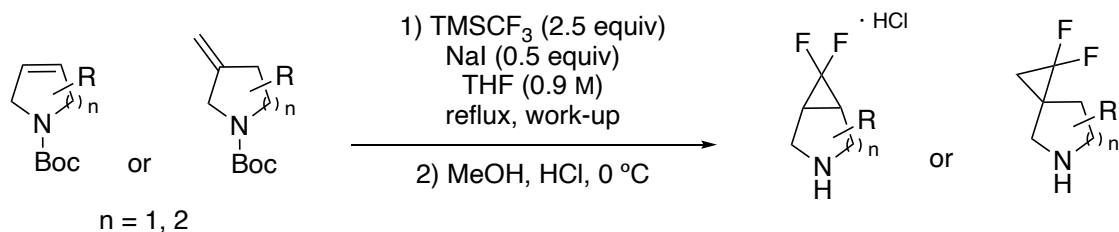


Scheme 7. Mechanism of difluorocarbene formation from trimethylsilane reagents

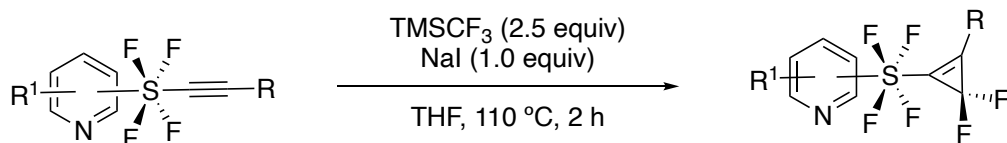
(a) Charette *et al*



(b) Mykhailiuk *et al*



(c) Shibata *et al*



Scheme 8. (a) Difluorocarbene addition to alkenes and alkynes in continuous flow²³ (b) Synthesis of building blocks for drug discovery⁵ (c) Synthesis of an electron-deficient difluorinated product.²⁵

However, toxic and non-biobased solvents (e.g., THF, anisole, biphenyl, diphenyl ether, and 1,2-chlorobenzene) were usually involved in these reactions and workup processes, which, in most cases, are high-boiling in order to be compatible with the heat requirements. Use of these high boiling point solvents has been found to be problematic, as it decreased the isolated yields when removed from the reaction mixture due to product losses in inseparable fractions during the distillation process. Hence, an opportunity remains for new technology which takes these important issues into account, providing a solution that is operationally simple, highly efficient, and environmentally responsible. Herein, we developed a convenient and environmentally attractive method for synthesizing difluorocyclopropanes and difluorocyclopropenes with commercially available TMSCF₂Br utilizing a solvent-free strategy.

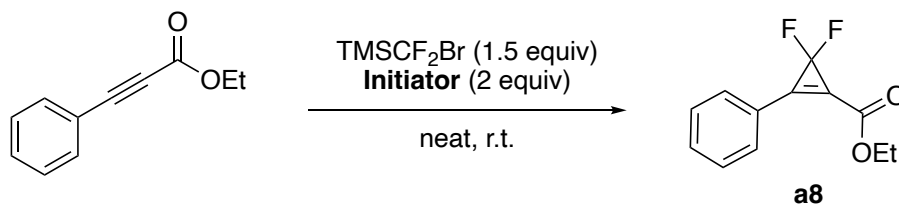
4.3. Results and discussion

4.3.1. Optimization and substrate scope of [2 + 1] cycloadditions of difluorocarbene to alkynes

Ethyl phenylpropiolate was chosen as the model substrate to initiate our studies (**Table 1**). All reactions were run in the complete absence of any solvents. An initial screening of potential initiators that had been used in the literature and related salts, including KOH,^{26,27}

K_2CO_3 ,²⁷ NaI,^{23,28} CsF, TBAF,²⁹ TBAB,²⁶ TBAI, KF, KH_2F ,³⁰ revealed that fluorine salts KF and KH_2F promoted the reaction at room temperature when no solvent was involved, yielding the cycloaddition product in 15% and 20%, respectively (**Table 1**).

Table 1. Screening of initiators^a

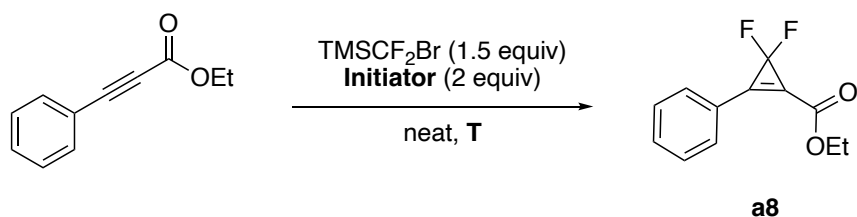


entry	initiator	conversion (%) ^a
1	KOH	0
2	K_2CO_3	0
3	NaI	0
4	CsF	0
5	TBAF	100% (no desired product)
6	TBAB	trace product observed
7	TBAI	0
8	KF	15%
9	KH_2F	20%

^a By crude NMR.

Soon thereafter it was found that by varying the temperature the extent of conversion was improved to 49% at 60 °C when using KF (**Table 2**, entries 1–4), but only 27% when using KH₂F (entry 5). Other similar fluorine salts, such as NaF and LiF, were screened at 60 °C but failed to produce useful yields (**Table 2**, entries 6 and 7). Surprisingly, TBAI, which failed to catalyze the reaction at room temperature, gave 53% conversion at this temperature (**Table 2**, entry 8); when the temperature was increased to 80 °C, the extent of conversion was improved to 84% (**Table 2**, entry 9).

Table 2. Initiator and temperature screening^a

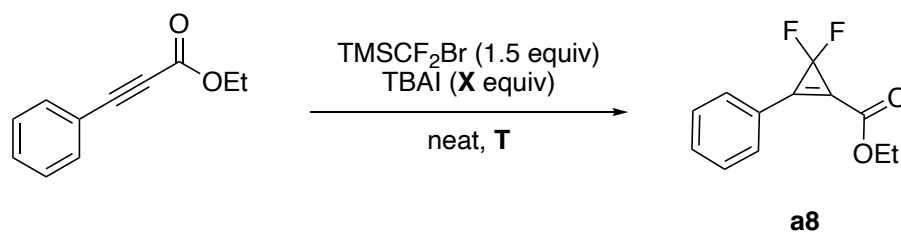


entry	initiator	temperature	conversion (%) ^a
1	KF	rt (18 °C)	15
2	KF	45 °C	27
3	KF	60 °C	49
4	KF	80 °C	46
5	KH ₂ F	60 °C	27
6	NaF	60 °C	10
7	LiF	60 °C	0
8	TBAI	60 °C	53
9	TBAI	80 °C	84

^a By crude NMR.

After identifying a suitable initiator, the number of equivalents of TBAI was screened. The extent of conversion was found to be unaffected in the range 0.5–2.0 equivalents (entries 1–4). The use of 0.5 equivalents is optimal, as a decreased yield from *ca.* 85% to 68% was observed when 0.2 equivalents was employed (entry 5). Increasing the temperature to 90 °C improved the yield marginally but increasing to 100 °C resulted in a reduced yield (70%, entry 7), which might be caused by side reactions, such as dimerization of difluorocarbene to form tetrafluoroethylene, or the thermolysis of TBAI via Hofmann elimination.³¹

Table 3. Screening of equivalents and temperature using TBAI^a



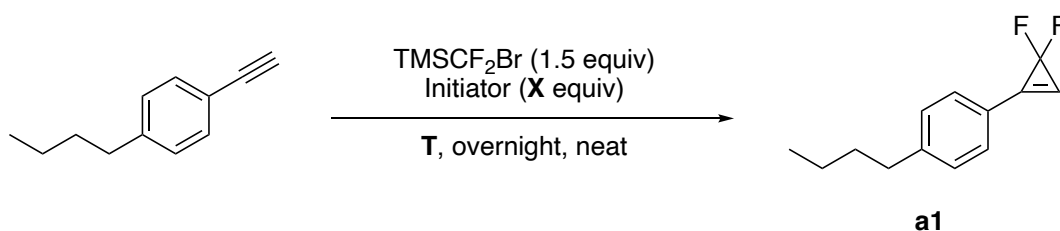
entry	equivalent	temperature	conversion (%) ^a
1	2.0	80 °C	84
2	1.5	80 °C	85
3	1.0	80 °C	84
4	0.5	80 °C	83
5	0.2	80 °C	68
6	0.5	90 °C	87
7	0.5	100 °C	70

^a By crude NMR.

Subsequently, *para-n*-butylphenylacetylene was chosen as a representative terminal alkyne and evaluated under the optimized conditions: TBAI (0.5 equiv) at 90 °C. The results showed that the desired cycloaddition product **a1** was not observed (by NMR) while the

starting material was fully consumed (**Table 4**, entry 1). Unfortunately, substantial improvement was not observed when the temperature was reduced from 90 °C to 60 °C, the equivalents of TBAB was increased, or TBAI was changed to TBAB or TBAF (**Table 4**, entries 2–6). Interestingly, when the inferior conditions found with the previous substrate were used (**Table 2**, entry 3: KF, 2.0 equiv), the reaction produced the desired product exclusively, albeit in a yield of 35% at 60 °C, which increased to 100% at 90 °C (**Table 4**, entries **8 vs. 9**).

Table 4. Optimization of conditions for a terminal alkyne^a

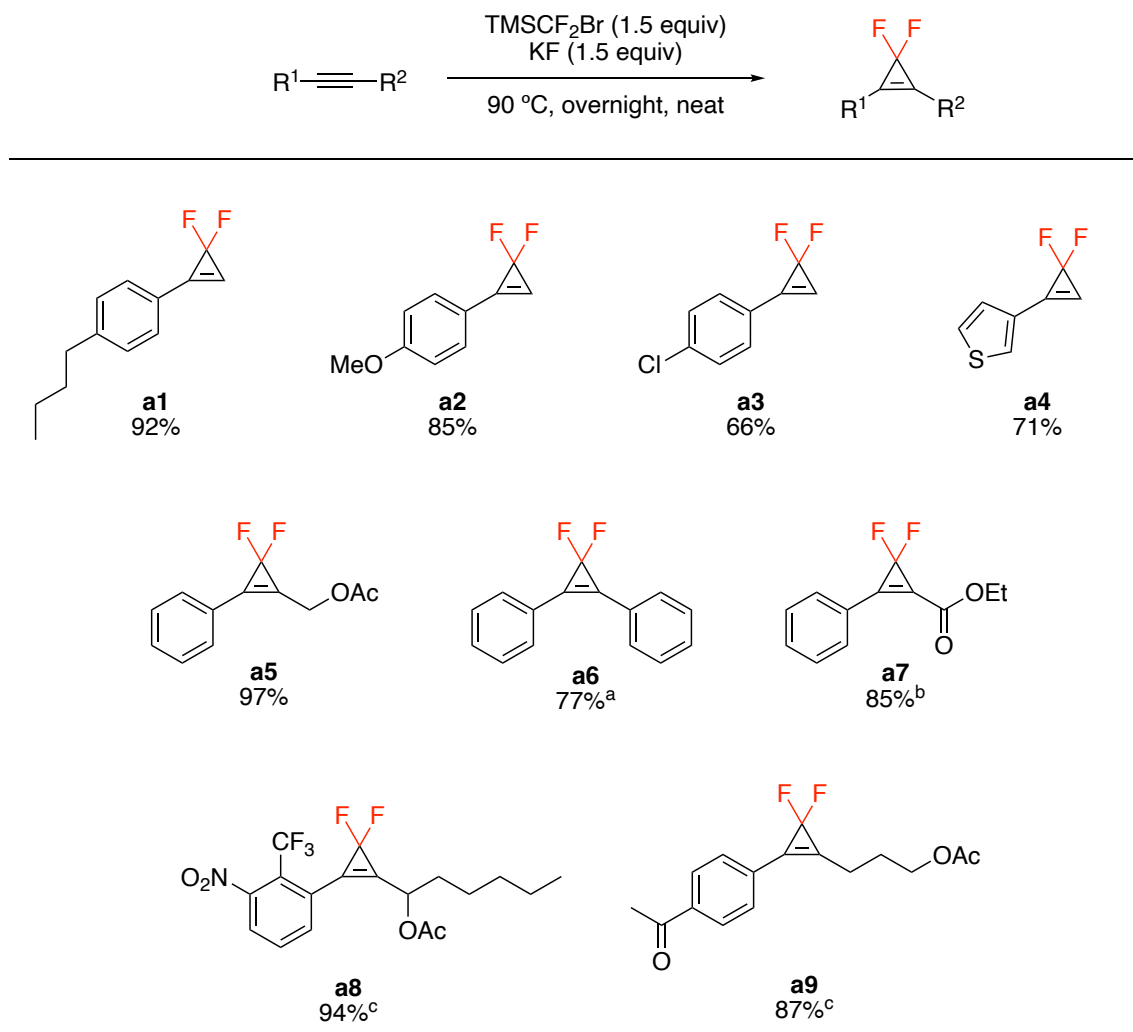


entry	initiator	equivalent	temperature	conversion (%) ^a
1	TBAI	0.5	90 °C	100 (messy)
2	TBAI	0.5	60 °C	64 (messy)
3	TBAI	1.0	60 °C	56 (messy)
4	TBAB	1.0	90 °C	100 (messy)
5	TBAB	1.0	60 °C	76 (messy)
6	TBAB	0.5	60 °C	61 (messy)
7	TBAF	0.1	60 °C	0
8	KF	2.0	60 °C	35
9	KF	2.0	90 °C	100

^a By crude NMR.

With the newly optimized reaction parameters in hand, the efficacy of different alkynes was then explored using TMSCF_2Br (1.5 equiv), and KF (2 equiv) as the initiator at 90 °C. This cycloaddition protocol accommodated a range of terminal alkynes as well as internal alkynes, as shown in **Table 5**. Electron rich *para*-substituents, such as *n*-butyl (**a1**) and a methoxy group (**a2**) were isolated in 92% and 85% yields, respectively. An electron-deficient *para*-chloro-substituent gave product **a3** in 66% yield. Heterocyclic scaffolds such as thiophene yielded **a4** in 71% yield. Several internal alkynes were also investigated, such as acetyl-protected butynol (**a5**), diphenylacetylene (**a6**), and the ester-containing acetylene (**a7**), affording the anticipated products in 77–97% yields. Strong electron-withdrawing groups such as NO_2 , CF_3 , or acetyl in various positions on the ring were also readily accommodated, leading to products **a8** and **a9** in 94% and 87% yields, respectively.

Table 5. Substrate scope for cycloadditions of alkynes



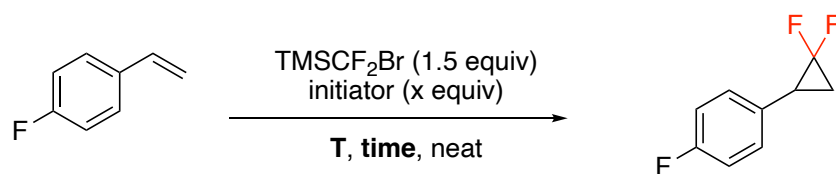
Isolated yields were reported. ^a 60 °C instead of 90 °C. ^b 0.5 equiv TBAI instead of KF.

^cAdditional 1.5 equiv TMSCF₂Br was added after 12 h; total reaction time: 2 days.

4.3.2. Optimization and substrate scope of [2 + 1] cycloadditions of difluorocarbene to alkenes

Encouraged by the above results, the conditions needed for *para*-fluorostyrene (**Table 6**) were next examined. However, different results were observed from those previously found for alkynes. For example, with *para*-fluorostyrene, when KF (2 equiv) was used, the desired difluorocyclopropane product was formed in only 2% yield, along with formation of unrecognizable side products (entry 1). When switching to KI (2 equiv), the reaction was unproductive, with most of the starting styrene remaining unreacted (entry 2). Applying TBAB (0.5 equiv) as a more soluble salt, the desired product was formed exclusively at 60 °C in one hour with 45% conversion (entry 3). The extent of conversion was increased with a longer reaction time, up to 95% at 24 h (entries 4–6). When a higher temperature was used, the reaction went to completion (entry 7).

Table 6. Optimization of cycloaddition of alkenes



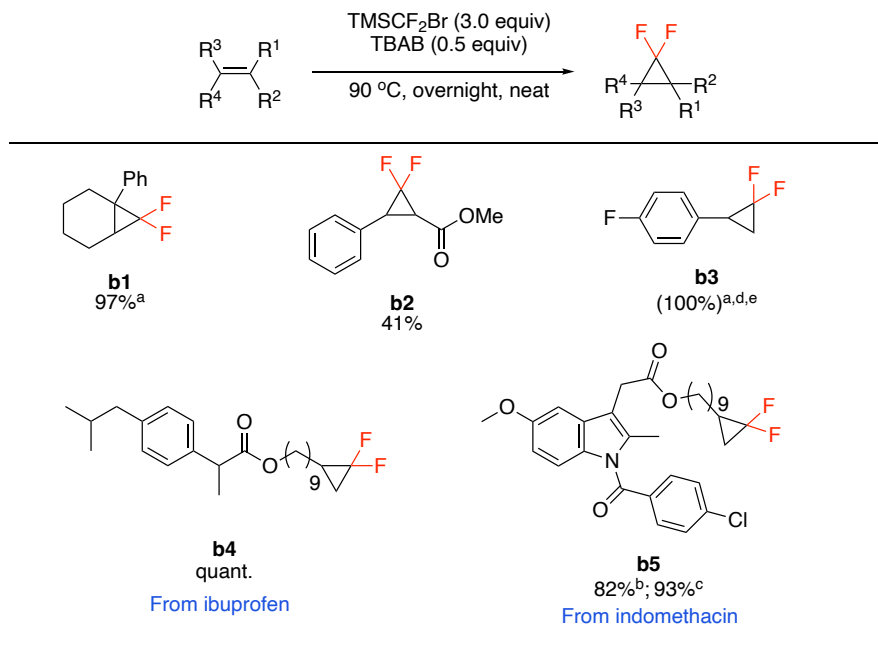
entry	initiator	equivalent	temperature	Time	NMR yield (%) ^a
1	KF	2.0	90 °C	24 h	2% (messy)
2	KI	2.0	90 °C	24 h	<1% (S.M. was left)
3	TBAB	0.5	60 °C	1 h	45%
4	TBAB	0.5	60 °C	2 h	60%

5	TBAB	0.5	60 °C	5 h	68%
6	TBAB	0.5	60 °C	24 h	95%
7	TBAB	0.5	90 °C	24 h	100%

^a α,α,α -Trifluorotoluene was used as the internal standard.

When these conditions were applied to various alkenes, *ca.* 5% of the starting material remained in some batches. Therefore, three equivalents of TMSCF_2Br were employed to ensure full conversion and reduce batch inconsistency. A trisubstituted alkene was cyclized to give product **b1** in high isolated yield (97%). An α,β -unsaturated ester was used to obtain product **b2** in 41% yield. Benzylic product **b3** formed exclusively with exceptional conversion, but the isolated yield is unavailable due to its instability to column chromatography or aqueous extractive workup. Furthermore, the reaction was applied to more structurally complex scaffolds including that in ibuprofen **b4**, furnishing the desired cyclized in quantitative isolated yield. The E Factor associated with these neat conditions was calculated to be only 1.4, indicative of the limited amounts of waste to be expected when no solvent is used. Indomethacin adduct **b5** was obtained in 82% yield under the standard protocol; however, demethylation of the aryl methoxy group occurred in the presence of bromide due to the heat applied. This side reaction can be avoided by replacing TBAB with TBAI to afford the desired product in high yield (93%). Similarly, the E Factor was calculated to be only 0.9.

Table 7. Substrate scope of cycloadditions with alkenes



Isolated yields were reported.

^a 1.5 equiv TMSCF₂Br was used.

^b Demethylated side product was observed when using TBAB.

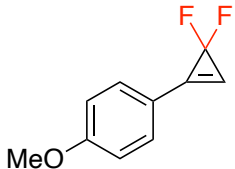
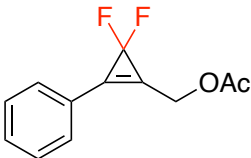
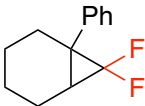
^c TBAI was used instead of TBAB.

^d 60 °C.

^e Number in the parenthesis were ¹H NMR conversion.

To demonstrate the greenness of these solvent-free conditions, the calculated environmental factors or E Factors for the reaction performed under solvent-free conditions can be compared with the literature reaction performed in organic solvents, as listed in **Table 8**. The values for the known conditions, run in various organic solvents such as THF, toluene, dioxane, and diglyme, are 2.0 to ca. 14 times higher than those using neat chemistry.

Table 8. Direct comparisons between literature conditions and those using neat ^a

Compound	Literature conditions	This work
	NaI (0.35 equiv) TMSCF ₃ (0.5 equiv) ^b THF, 4 h E Factor = 9.8	KF (2.0 equiv) TMSCF ₂ Br (0.5 equiv) ^b 16 h E Factor = 1.4
	TBAC (2.0 equiv) TMSCF ₂ Br (0.5 equiv) ^b Toluene, 4 h E Factor = 13.9	KF (2.0 equiv) TMSCF ₂ Br (0.5 equiv) ^b 16 h E Factor = 1.0
	KI (2.25 equiv) MDFA (0.5 equiv) _{b,c} TMSCl (2 equiv) Dioxane/diglyme mixture, 2 d E Factor = 5.6	TBAB (0.5 equiv) TMSCF ₂ Br (2.0 equiv) ^b 16 h E Factor = 2.8

^aCalculations are shown in the SI. ^bExcess amounts of the source of difluorocarbene were used in the reaction. ^cMDFA: methyl 2,2-difluoro-2-(fluorosulfonyl)acetate.

4.4. Conclusions and future work

In summary, a new method has been developed for the synthesis of difluorocyclopropenes and difluorocyclopropanes using commercially available TMSCF_2Br together with simple salts such as KF or TBAB under neat conditions. Notable features include exceptionally low E Factors, as well as applicability to complex structures which are unprecedented in the difluorination literature. Furthermore, the neat conditions were also found to have promising results in X-H insertions (X = O and S) to construct difluoromethylated alcohols and thiols, which are important functionalities serving as lipophilic hydrogen-bond donors and bioisosteres for both the OH and SH units.³² Future developments are now underway to expand the scope of *O*- and *S*-difluoromethylation and investigate the possibility of tandem, 1-pot sequences that include these neat difluorocyclopropanations with other reactions in the area of green chemistry.

4.5. References

- (1) Gillis, E. P.; Eastman, K. J.; Hill, M. D.; Donnelly, D. J.; Meanwell, N. A. Applications of Fluorine in Medicinal Chemistry. *J. Med. Chem.* **2015**, *58*, 8315–8359.
- (2) Talele, T. T. The “Cyclopropyl Fragment” Is a Versatile Player That Frequently Appears in Preclinical/Clinical Drug Molecules. *J. Med. Chem.* **2016**, *59*, 8712–8756.
- (3) Goetz, A. E.; Becirovic, H.; Blasberg, F.; Chen, B.; Clarke, H. J.; Colombo, M.; Daddario, P.; Damon, D. B.; Depretz, C.; Dumond, Y. R.; Grilli, M. D.; Han, L.; Houck, T. L.; Johnson, A. M.; Jones, K. N.; Jung, J.; Leeman, M.; Liu, F.; Lu, C. V.; Mangual, E. J.; Nelson, J. D.; Puchlopek-Dermenci, A. L. A.; Ruggeri, S. G.; Simonds, P. A.; Sitter, B.; Virtue, D. E.; Wang, S.; Yu, L.; Yu, T. Large-Scale Cyclopropanation of Butyl Acrylate with Difluorocarbene and Classical Resolution of a Key Fluorinated Building Block. *Org. Process Res. Dev.* **2022**, *26*, 683–697.
- (4) Nosik, P. S.; Ryabukhin, S. V.; Grygorenko, O. O.; Volochnyuk, D. M. Transition Metal-Free Gem-Difluorocyclopropanation of Alkenes with $\text{CF}_3\text{SiMe}_3\text{-NaI}$

- System: A Recipe for Electron-Deficient Substrates. *Adv. Synth. Catal.* **2018**, *360*, 4104–4114.
- (5) Bychek, R. M.; Levterov, V. V.; Sadkova, I. V.; Tolmachev, A. A.; Mykhailiuk, P. K. Synthesis of Functionalized Difluorocyclopropanes: Unique Building Blocks for Drug Discovery. *Chem. Eur. J.* **2018**, *24*, 12291–12297.
 - (6) Xu, J.; Ahmed, E.-A.; Xiao, B.; Lu, Q.-Q.; Wang, Y.-L.; Yu, C.-G.; Fu, Y. Pd-Catalyzed Regioselective Activation of Gem-Difluorinated Cyclopropanes: A Highly Efficient Approach to 2-Fluorinated Allylic Scaffolds. *Angew. Chem., Int. Ed.* **2015**, *54*, 8231–8235.
 - (7) Lv, L.; Li, C.-J. Palladium-Catalyzed Defluorinative Alkylation of Gem-Difluorocyclopropanes: Switching Regioselectivity via Simple Hydrazones. *Angew. Chem., Int. Ed.* **2021**, *60*, 13098–13104.
 - (8) Nihei, T.; Hoshino, T.; Konno, T. Unusual Reaction Behavior of Gem - Difluorocyclopropane Derivatives: Stereoselective Synthesis of β -Monofluoroallylic Alcohols, Ethers, Esters, and Amide. *Org. Lett.* **2014**, *16*, 4170–4173.
 - (9) Wang, X.; Wang, X.; Wang, J. Application of Carbene Chemistry in the Synthesis of Organofluorine Compounds. *Tetrahedron* **2019**, *75*, 949–964.
 - (10) Dolbier, W. R.; Battiste, M. A. Structure, Synthesis, and Chemical Reactions of Fluorinated Cyclopropanes and Cyclopropenes. *Chem. Rev.* **2003**, *103*, 1071–1098.
 - (11) Ni, C.; Hu, J. Recent Advances in the Synthetic Application of Difluorocarbene. *Synthesis* **2014**, *46*, 842–863.
 - (12) Volchkov, N. V.; Lipkind, M. B.; Nefedov, O. M. One-Step Synthesis of 2,3-Difluoronaphthalene by the Gas-Phase Co-Pyrolysis of Styrene with Chlorodifluoromethane. *Russ. Chem. Bull.* **2019**, *68*, 7.
 - (13) Brahms, D. L. S.; Dailey, W. P. Fluorinated Carbenes. *Chem. Rev.* **1996**, *96*, 1585–1632.
 - (14) Seyferth, D.; Hopper, S. P. Halomethyl Metal Compounds. LX. Phenyl(Trifluoromethyl)Mercury. Useful Difluorocarbene Transfer Agent. *J. Org. Chem.* **1972**, *37*, 4070–4075.
 - (15) Fujioka, Y.; Amii, H. Boron-Substituted Difluorocyclopropanes: New Building Blocks of gem-Difluorocyclopropanes. *Org. Lett.* **2008**, *10*, 769–772.
 - (16) Kubyshkin, V. S.; Mykhailiuk, P. K.; Afonin, S.; Ulrich, A. S.; Komarov, I. V. Incorporation of Cis- and Trans-4,5-Difluoromethanoprolines into Polypeptides. *Org. Lett.* **2012**, *14*, 5254–5257.

- (17) Oshiro, K.; Morimoto, Y.; Amii, H. Sodium Bromodifluoroacetate: A Difluorocarbene Source for the Synthesis of Gem-Difluorocyclopropanes. *Synthesis* **2010**, *2010*, 2080–2084.
- (18) Dolbier, W. R.; Tian, F.; Duan, J.-X.; Li, A.-R.; Ait-Mohand, S.; Bautista, O.; Buathong, S.; Marshall Baker, J.; Crawford, J.; Anselme, P.; Cai, X. H.; Modzelewska, A.; Koroniak, H.; Battiste, M. A.; Chen, Q.-Y. Trimethylsilyl Fluorosulfonyldifluoroacetate (TFDA): A New, Highly Efficient Difluorocarbene Reagent. *J. of Fluor. Chem.* **2004**, *125*, 459–469.
- (19) Eusterwiemann, S.; Martinez, H.; Dolbier, W. R. Methyl 2,2-Difluoro-2-(Fluorosulfonyl)Acetate, a Difluorocarbene Reagent with Reactivity Comparable to That of Trimethylsilyl 2,2-Difluoro-2-(Fluorosulfonyl)Acetate (TFDA). *J. Org. Chem.* **2012**, *77*, 5461–5464.
- (20) Tian, F.; Kruger, V.; Bautista, O.; Duan, J.-X.; Li, A.-R.; Dolbier, William R.; Chen, Q.-Y. A Novel and Highly Efficient Synthesis of Gem-Difluorocyclopropanes. *Org. Lett.* **2000**, *2*, 563–564.
- (21) Tran, G.; Gomez Pardo, D.; Tsuchiya, T.; Hillebrand, S.; Vors, J.-P.; Cossy, J. Modular, Concise, and Efficient Synthesis of Highly Functionalized 5-Fluoropyridazines by a [2 + 1]/[3 + 2]-Cycloaddition Sequence. *Org. Lett.* **2015**, *17*, 3414–3417.
- (22) Aono, T.; Sasagawa, H.; Fuchibe, K.; Ichikawa, J. Regioselective Synthesis of α,α -Difluorocyclopentanone Derivatives: Domino Nickel-Catalyzed Difluorocyclopropanation/Ring-Expansion Sequence of Silyl Dienol Ethers. *Org. Lett.* **2015**, *17*, 5736–5739.
- (23) Rullière, P.; Cyr, P.; Charette, A. B. Difluorocarbene Addition to Alkenes and Alkynes in Continuous Flow. *Org. Lett.* **2016**, *18*, 1988–1991.
- (24) Gill, D. M.; McLay, N. An Improved Method for Difluorocyclopropanation of Alkenes. *Synlett* **2014**, *25*, 1756–1758.
- (25) Maruno, K.; Niina, K.; Nagata, O.; Shibata, N. Synthesis of an Eccentric Electron-Deficient Fluorinated Motif, Tetrafluoro- λ^6 -Sulfanyl Gem -Difluorocyclopropenes. *Org. Lett.* **2022**, *24*, 1722–1726.
- (26) Li, L.; Wang, F.; Ni, C.; Hu, J. Synthesis of Gem-Difluorocyclopropa(e)nes and O-, S-, N-, and P-Difluoromethylated Compounds with TMSCF₂Br. *Angew. Chem., Int. Ed.* **2013**, *52*, 12390–12394.
- (27) Zhang, L.; Zheng, J.; Hu, J. 2-Chloro-2,2-Difluoroacetophenone: A Non-ODS-Based Difluorocarbene Precursor and Its Use in the Difluoromethylation of Phenol Derivatives. *J. Org. Chem.* **2006**, *71*, 9845–9848.
- (28) García-Domínguez, A.; West, T. H.; Primožic, J. J.; Grant, K. M.; Johnston, C. P.; Cumming, G. G.; Leach, A. G.; Lloyd-Jones, G. C. Difluorocarbene Generation

from TMSCF₃ : Kinetics and Mechanism of NaI-Mediated and Si-Induced Anionic Chain Reactions. *J. Am. Chem. Soc.* **2020**, *142*, 14649–14663.

- (29) Wang, F.; Zhang, W.; Zhu, J.; Li, H.; Huang, K.-W.; Hu, J. Chloride Ion-Catalyzed Generation of Difluorocarbene for Efficient Preparation of Gem-Difluorinated Cyclopropenes and Cyclopropanes. *Chem. Commun.* **2011**, *47*, 2411–2413.
- (30) Zhang, R.; Ni, C.; Xie, Q.; Hu, J. Difluoromethylation of Alcohols with TMSCF₂Br in Water: A New Insight into the Generation and Reactions of Difluorocarbene in a Two-Phase System. *Tetrahedron* **2020**, *76*, 131676.
- (31) Lopez, A. F.; de Ariza, M. T. P.; Orío, O. A. Rapid Method for Quantitative Determination of Tetrabutylammonium Bromide in Aqueous Solution by Gas Chromatography. *J. High Resolut. Chromatogr.* **1989**, *12*, 503–504.
- (32) Synopsis of Some Recent Tactical Application of Bioisosteres in Drug Design | Journal of Medicinal Chemistry <https://pubs.acs.org/doi/full/10.1021/jm1013693> (accessed 2022 -05 -24).
- (33) Lipshutz, B. H.; Ghorai, S.; Abela, A. R.; Moser, R.; Nishikata, T.; Duplais, C.; Krasovskiy, A.; Gaston, R. D.; Gadwood, R. C. TPGS-750-M: A Second-Generation Amphiphile for Metal-Catalyzed Cross-Couplings in Water at Room Temperature. *J. Org. Chem.* **2011**, *76*, 4379–4391.
- (34) Wang, F.; Luo, T.; Hu, J.; Wang, Y.; Krishnan, H. S.; Jog, P. V.; Ganesh, S. K.; Prakash, G. K. S.; Olah, G. A. Synthesis of Gem-Difluorinated Cyclopropanes and Cyclopropenes: Trifluoromethyltrimethylsilane as a Difluorocarbene Source. *Angew. Chem., Int. Ed.* **2011**, *50*, 7153–7157.

4.6. General experimental information

a. Reagents

Bromodifluoromethyl)trimethylsilane (TMSCF₂Br) was purchased from Gute Chemie abcr (catalog number: AB359713; CAS: 115262-01-6; bp = 112 °C) and used without further purification. Commercially available reagents were purchased from Sigma-Aldrich, Combi-Blocks, Alfa Aeser, TCI, or Acros Organics and used without further purification.

b. Surfactant solution preparation

TPGS-750-M was synthesized according to the published procedure and is also commercially available from Sigma-Aldrich (catalog number: 733857). HPLC grade water was purged by argon before use to prepare surfactant solution. The 2 wt % TPGS-750-M aqueous solution was prepared by dissolving 2 g of TPGS-750-M solid into 98 g of HPLC water and stored under argon.³³

g. TLC

Thin layer chromatography (TLC) was performed using Silica Gel 60 F254 plates (Merck, 0.25 mm thick). Flash chromatography was done in glass columns using Silica Gel 60 (EMD, 40–63 μm).

h. NMR

^1H , ^{13}C NMR, and ^{19}F NMR spectra were recorded on either a Varian Unity Inova 400 MHz, a Bruker Avance III HD 400 MHz (400 MHz for ^1H , 100 MHz for ^{13}C , 376 MHz for ^{19}F NMR), a Varian Unity Inova 500 MHz, or a Bruker Avance NEO 500 MHz (500 MHz for ^1H , 125 MHz for ^{13}C , 470 MHz for ^{19}F NMR). Deuterated NMR solvents were purchased from Cambridge Isotopes Laboratories. $\text{DMSO-}d_6$, CD_3OD , and CDCl_3 were used as solvents. Residual peaks for CHCl_3 in CDCl_3 ($^1\text{H} = 7.26$ ppm, $^{13}\text{C} = 77.00$ ppm), $(\text{CH}_3)_2\text{SO}$ in $(\text{CD}_3)_2\text{SO}$ ($^1\text{H} = 2.50$ ppm, $^{13}\text{C} = 39.52$ ppm) or MeOH in MeOD ($^1\text{H} = 3.31$ ppm, $^{13}\text{C} = 49.00$ ppm) have been assigned as internal standards. The chemical shifts are reported in ppm. The coupling constants J value are given in Hz. Data are reported as follows: chemical shift, multiplicity (s = singlet, bs = broad singlet, d = doublet, bd = broad doublet, t = triplet, q = quartet, quin = quintet, m = multiplet), coupling constant (if applicable) and integration.

i. HRMS

Mass spectra were obtained from the UC Irvine or Scripps Research mass spectrometry facility.

4.7. General procedures

a. Procedure A (for compounds a1–a7)

To a 1 dram vial equipped with a PTFE-coated magnetic stirrer was added alkyne (0.25 mmol, 1 equiv) and potassium fluoride (29.1 mg, 0.5 mmol, 2 equiv). TMSCF₂Br (58.32 μL, 0.375 mmol, 1.5 equiv) was then added via syringe. The vial was closed with a screw cap and heated at 90 °C (or 60 °C for compound **a6**) and stirred vigorously in an aluminum block placed over IKA hot plate overnight. After the reaction, the mixture was purified by flash chromatography over silica gel using Et₃N/hexanes/Et₂O as eluent.

Note: Products **a1–a6** are sensitive to acid; the column must be pretreated with 5% Et₃N/hexanes.

Notes for product a7: (1) TBAI (46.2 mg, 0.125 mmol 0.5 equiv) was added instead of KF (2 equiv); (2) this product is sensitive to base; the column *cannot* be pretreated with 5% Et₃N/hexanes.

b. Procedure B (for compounds a8 and a9)

To a 0.5 dram vial charged with a PTFE-coated magnetic stir bar was added alkyne (0.1 mmol, 1 equiv), KF (0.2 mmol, 2 equiv, 11.6 mg) and TMSCF₂Br (26.6 μL, 0.15 mmol, 1.5 equiv). The vial was closed with a screw cap and heated at 90 °C and stirred vigorously

in an aluminum block placed over IKA hot plate for 12 h. After cooled to rt, the cap was opened and another portion of TMSCF_2Br (26.6 μL , 0.15 mmol, 1.5 equiv) was added. The vial was again heated to 90 °C and stirred overnight. After the reaction, the mixture was purified by flash chromatography over silica gel using Et_3N /hexanes/ Et_2O as eluent.

Note: Products **a8** and **a9** are sensitive to acid; the column must be pretreated with 5% Et_3N /hexanes.

c. Procedure C (for compounds b1–b5)

To a 0.5 dram vial equipped a PTFE-coated magnetic stirrer was added alkene (0.1 mmol, 1 equiv) and TBAB (46.2 mg, 0.5 equiv, 0.125 mmol). TMSCF_2Br (58.32 μL , 0.375 mmol, 1.5 equiv) was then added via syringe. The vial was closed with a screw cap and heated at 90 °C and stirred vigorously in an aluminum block placed over IKA hot plate overnight. After the reaction, unless specified, the mixture was purified by flash chromatography over silica gel using Et_3N /hexanes/EA as eluent.

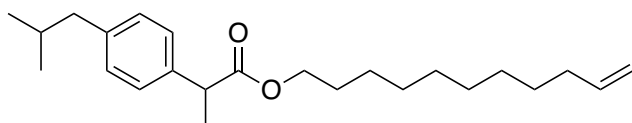
Note: Substrate **b1** and **b3** were done on a 0.2 mmol scale.

Note for methoxy group containing product b5: the demethylated side product was observed when using TBAB; therefore, TBAI (46.2 mg, 0.5 equiv, 0.125 mmol) was used instead of TBAB.

Note: The reaction is usually very clean; the impurities that need to be removed after the reaction are mainly TBAB and unreacted starting material, if any.

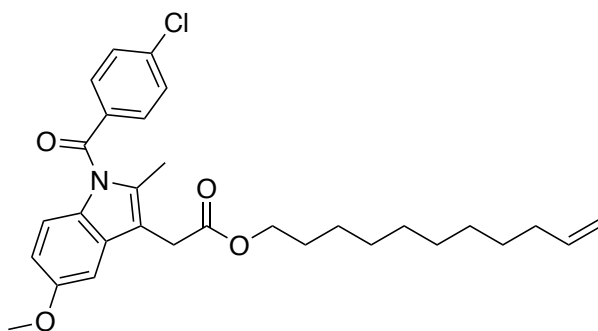
d. General procedure for preparing unreported substrates

To a solution of alcohol (1.1 equiv, 1.1 mmol), carboxylic acid (1 equiv, 1 mmol) and DMAP (0.1 equiv, 0.1 mmol) in DCM (3 mL) was added DCC (1.2 equiv, 1.2 mmol). The resulting mixture was stirred at 30 °C for 16 h. The precipitate was removed by filtration. The filtrate was concentrated. The residue was purified by column chromatography on silica gel.



9-(2,2-Difluorocyclopropyl)nonyl 2-(4-isobutylphenyl)propanoate

Colorless oil, flash chromatography using 0% to 10% EtOAc/hexanes ($R_f = 0.81$), 324.8 mg from a 1.0 mmol scale, 91% yield.

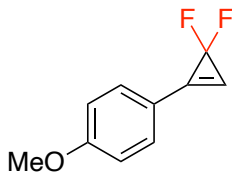


Undec-10-en-1-yl 2-(1-(4-chlorobenzoyl)-5-methoxy-2-methyl-1H-indol-3-yl)acetate

Yellow oil, flash chromatography using 10% EtOAc/hexanes ($R_f = 0.33$), 467.4 mg from a 1.0 mmol scale, 92% yield.

4.8. E Factor calculations

1-(3,3-Difluorocycloprop-1-en-1-yl)-4-methoxybenzene (a2)



Our method:

- Mass of product: **38.4 mg** (from a 0.25 mmol scale)

- Mass of waste:

KF (MW = 58.10 g/mol, 2.0 equiv, 0.5 mmol) + TMSCF₂Br (MW = 203.10 g/mol,

0.5 equiv excess, 0.125 mmol)

$$= 0.5 \text{ mmol} * 58.10 \text{ g/mol} + 0.125 \text{ mmol} * 203.10 \text{ g/mol}$$

$$= \mathbf{54.4 \text{ mg}}$$

- E Factor = mass of waste/mass of product = 54.4 mg/38.4mg = **1.4**

Literature method: [*Eur. J. Org. Chem.* **2021**, 47, 6604-6625]

- Mass of product: 0.1 mol*97%*182.0 g/mol = **17.7 g**

- Mass of waste:

NaI (MW = 149.9 g/mol, 0.35 equiv, 0.035 mol) + TMSCF₃ (MW = 142.2 g/mol,

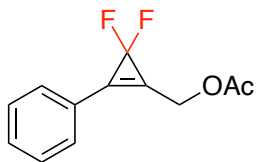
2.5 equiv excess, 0.25 mmol) + THF (150 mL, d = 0.889 g/mL)

$$= 0.035 \text{ mmol} * 149.9 \text{ g/mol} + 0.25 \text{ mmol} * 142.2 \text{ g/mol} + 150 \text{ mL} * 0.889 \text{ g/mL}$$

$$= \mathbf{174.1 \text{ g}}$$

- E Factor = mass of waste/mass of product = 54.4 mg/38.4 mg = **9.8**

(3,3-Difluoro-2-phenylcycloprop-1-en-1-yl)methyl acetate (a5)



Our method:

- Mass of product: **54.2 mg** (from a 0.25 mmol scale)
- Mass of waste:

KF (MW = 58.10 g/mol, 2.0 equiv, 0.5 mmol) + TMSCF₂Br (MW = 203.10 g/mol, 0.5 equiv excess, 0.125 mmol)

$$= 0.5 \text{ mmol} \cdot 58.10 \text{ g/mol} + 0.125 \text{ mmol} \cdot 203.10 \text{ g/mol} = \mathbf{54.4 \text{ mg}}$$

- E Factor = mass of waste/mass of product = 54.4 mg/54.2 mg = **1.0**

Literature method: [*Chem. Commun.* **2011**, 47, 2411-2413]

- Mass of product: 1 mmol*89%*224.2 g/mol = **199.5 mg**
- Mass of waste:

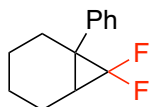
TBAC (MW = 277.90 g/mol, 0.04 equiv, 0.04 mol) + TMSCF₂Cl (MW = 158.65 g/mol, 1.0 equiv excess, 1 mmol) + toluene (3 mL, d = 0.867 g/mL)

$$= 0.04 \text{ mmol} \cdot 277.90 \text{ g/mol} + 1 \text{ mmol} \cdot 158.65 \text{ g/mol} + 3 \text{ mL} \cdot 0.867 \text{ g/mL} \cdot 1000 \text{ mg/g}$$

$$= \mathbf{2770.6 \text{ mg}}$$

- E Factor = mass of waste/mass of product = 54.4 mg/54.2 mg = **13.9**

7,7-Difluoro-1-phenylbicyclo[4.1.0]heptanes (b1)



Our method:

- Mass of product: **40.40 mg** (from a 0.2 mmol scale)
- Mass of waste:

TBAB (MW = 322.37 g/mol, 0.5 equiv, 0.1 mmol) + TMSCF₂Br (MW = 203.10 g/mol, 2.0 equiv excess, 0.4 mmol)

$$= 0.1 \text{ mmol} \cdot 322.37 \text{ g/mol} + 0.4 \text{ mmol} \cdot 203.10 \text{ g/mol} = \mathbf{113.5 \text{ mg}}$$

- E Factor = mass of waste/mass of product = 113.5 mg/40.40 mg = **2.8**

Literature method: [*J. Org. Chem.* **2012**, 77, 5461–5464]¹⁹

- Mass of product: 10.4 mmol*98% yield*208.25 g/mol = 2122.48 mg = **2.12 g**
- Mass of waste:

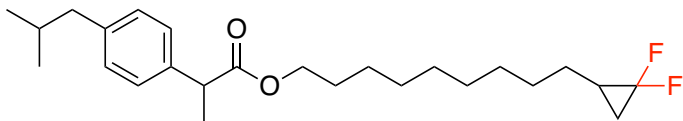
KI (MW = 166.00 g/mol, 2.25 equiv, 23.4 mmol) + 1.5 mL dioxane (MW = 88.11 g/mol, 1.7 equiv, 17.6 mmol) + diglyme (MW = 134.18 g/mol, 0.1 equiv, 1.0 mmol) + TMSCl (MW = 108.64 g/mol, 2 equiv, 20.8 mmol) + MDFA[†] (MW = 192.11 g/mol, 2 equiv, 20.8 mmol)

$$= 23.4 \text{ mmol} \cdot 166.00 \text{ g/mol} + 17.6 \text{ mmol} \cdot 88.11 \text{ g/mol} + 1.0 \text{ mmol} \cdot 134.18 \text{ g/mol} + 20.8 \text{ mmol} \cdot 108.64 \text{ g/mol} + 20.8 \text{ mmol} \cdot 192.11 = 11824.92 \text{ mg} = \mathbf{11.82 \text{ g}}$$

- E Factor = mass of waste/mass of product = **5.6**

†MDFA: methyl 2,2-difluoro-2-(fluorosulfonyl)acetate

9-(2,2-Difluorocyclopropyl)nonyl 2-(4-isobutylphenyl)propanoate (b4)



(work up by washing with brine and aq. NaHCO₃)

Our method:

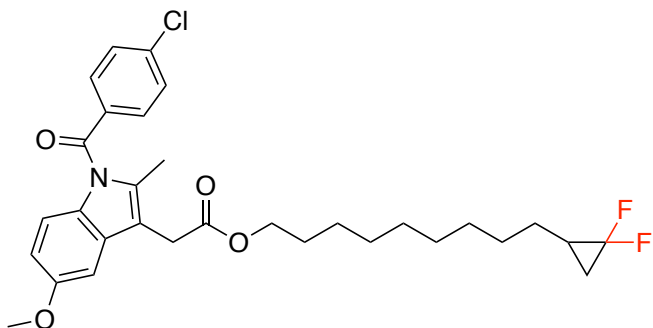
- Mass of product: **40.8 mg** (from a 0.1 mmol scale)
- Mass of waste:

TBAB (MW = 322.37 g/mol, 0.5 equiv, 0.05 mmol) + TMSCF₂Br (MW = 203.10 g/mol, 2.0 equiv excess, 0.2 mmol)

$$= 0.05 \text{ mmol} * 322.37 \text{ g/mol} + 0.2 \text{ mmol} * 203.10 \text{ g/mol} = \mathbf{56.7 \text{ mg}}$$

- E Factor = mass of waste/mass of product = 113.5 mg/40.40 mg = **1.4**

9-(2,2-Difluorocyclopropyl)nonyl 2-(1-(4-chlorobenzoyl)-5-methoxy-2-methyl-1H-indol-3-yl)acetate (b5)



(work up by column chromatography)

Our method:

- Mass of product: **52.1 mg** (from a 0.1 mmol scale)

- Mass of waste:

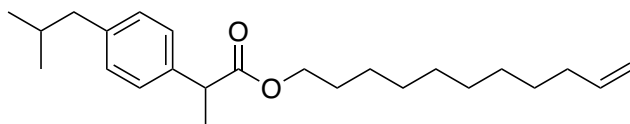
TBAB (MW = 322.37 g/mol, 0.5 equiv, 0.05 mmol) + TMSCF₂Br (MW = 203.10 g/mol, 2.0 equiv excess, 0.2 mmol)

$$= 0.05 \text{ mmol} \times 322.37 \text{ g/mol} + 0.2 \text{ mmol} \times 203.10 \text{ g/mol} = \mathbf{56.7 \text{ mg}}$$

- E Factor = mass of waste/mass of product = 56.7 mg/52.1 mg = **0.9**

4.9. Compound characterization data

9-(2,2-Difluorocyclopropyl)nonyl 2-(4-isobutylphenyl)propanoate

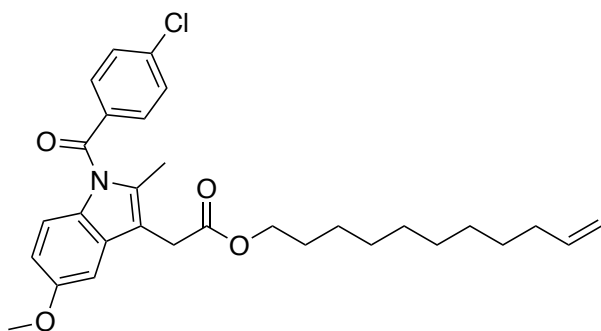


Colorless oil, flash chromatography using 0% to 10% EtOAc/hexanes ($R_f = 0.81$), 324.8 mg from a 1.0 mmol scale, 91% yield.

¹H NMR (400 MHz, CDCl₃) δ 7.24 – 7.17 (m, 2H), 7.12 – 7.02 (m, 2H), 5.82 (ddt, $J = 16.9, 10.2, 6.6$ Hz, 1H), 5.00 (dq, $J = 17.1, 1.8$ Hz, 1H), 4.94 (ddd, $J = 10.2, 2.3, 1.2$ Hz, 1H), 4.05 (t, $J = 6.6$ Hz, 2H), 3.68 (q, $J = 7.2$ Hz, 1H), 2.45 (d, $J = 7.2$ Hz, 2H), 2.04 (tdd, $J = 8.1, 6.1, 1.4$ Hz, 2H), 1.85 (dp, $J = 13.6, 6.8$ Hz, 1H), 1.56 (d, $J = 13.7$ Hz, 2H), 1.49 (d, $J = 7.1$ Hz, 3H), 1.37 (p, $J = 7.1$ Hz, 2H), 1.24 (d, $J = 6.8$ Hz, 10H), 0.91 (s, 3H), 0.89

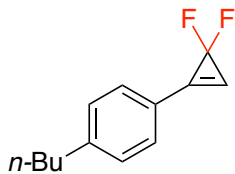
(s, 3H). ^{13}C NMR (126 MHz, CDCl_3) δ 174.79, 140.39, 139.16, 137.89, 129.23, 127.12, 114.12, 77.25, 77.00, 76.75, 64.73, 45.19, 45.02, 33.79, 30.16, 29.40, 29.36, 29.13, 29.08, 28.90, 28.51, 25.74, 22.36, 18.44. HRMS (ESI-TOF) m/z : $[\text{M}+\text{Na}]^+$ calcd for $\text{C}_{24}\text{H}_{38}\text{O}_2\text{Na}$: 381.2769; found 381.2770.

Undec-10-en-1-yl 2-(1-(4-chlorobenzoyl)-5-methoxy-2-methyl-1*H*-indol-3-yl)acetate



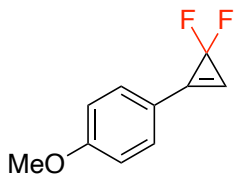
Yellow oil, flash chromatography using 10% EtOAc/hexanes ($R_f = 0.33$), 467.4 mg from a 1.0 mmol scale, 92% yield. ^1H NMR (400 MHz, CDCl_3) δ 7.71 – 7.62 (m, 2H), 7.52 – 7.43 (m, 2H), 6.97 (d, $J = 2.5$ Hz, 1H), 6.87 (d, $J = 9.0$ Hz, 1H), 6.67 (dd, $J = 9.0, 2.5$ Hz, 1H), 5.81 (ddt, $J = 16.9, 10.2, 6.7$ Hz, 1H), 5.04 – 4.96 (m, 1H), 4.96 – 4.89 (m, 1H), 4.09 (t, $J = 6.7$ Hz, 2H), 3.83 (s, 3H), 3.65 (s, 2H), 2.39 (s, 3H), 2.08 – 1.98 (m, 2H), 1.61 (t, $J = 7.0$ Hz, 2H), 1.35 (d, $J = 7.2$ Hz, 2H), 1.28 – 1.23 (m, 8H), 0.88 (t, $J = 7.0$ Hz, 2H). ^{13}C NMR (126 MHz, CDCl_3) δ 170.93, 168.26, 156.01, 139.22, 139.16, 135.84, 133.93, 131.15, 130.78, 130.66, 129.09, 114.91, 114.13, 112.74, 111.64, 101.28, 65.17, 55.66, 33.78, 30.43, 29.43, 29.37, 29.18, 29.07, 28.88, 28.59, 25.86, 13.34. HRMS (ESI-TOF) m/z : $[\text{M}+\text{Na}]^+$ calcd for $\text{C}_{30}\text{H}_{36}\text{ClNO}_4\text{Na}$: 532.2231; found 532.2237.

1-*n*-Butyl-4-(3,3-difluorocycloprop-1-en-1-yl)benzene (a1)



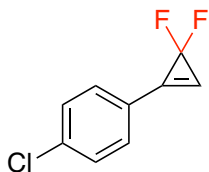
Pale yellow solid, flash chromatography using 5% Et₃N/ hexanes ($R_f = 0.25$). 47.8 mg from 0.25 mmol scale, 92% yield. **¹H NMR** (400 MHz, CDCl₃) δ 7.62 – 7.54 (m, 2H), 7.38 (t, $J = 1.8$ Hz, 1H), 7.33 – 7.27 (m, 2H), 2.70 – 2.64 (m, 2H), 1.62 (ddt, $J = 9.2, 7.7, 3.6$ Hz, 2H), 1.41 – 1.34 (m, 2H), 0.95 (t, $J = 7.3$ Hz, 3H). **¹³C NMR** (101 MHz, CDCl₃) δ 147.26, 133.81 (t, $^2J_{CF} = 10.4$ Hz), 130.17, 129.18, 120.79, 112.15 (t, $^2J_{CF} = 12.4$ Hz), 101.91 (t, $^1J_{CF} = 269.7$ Hz), 35.76, 33.35, 22.30, 13.90. **¹⁹F NMR** (376 MHz, CDCl₃) δ -106.37.

1-(3,3-Difluorocycloprop-1-en-1-yl)-4-methoxybenzene (a2)



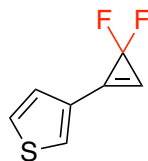
Colorless oil, flash chromatography using 5% Et₃N/ hexanes ($R_f = 0.20$). 38.7 mg from 0.25 mmol scale, 85% yield. **¹H NMR** (400 MHz, CDCl₃) δ 7.64 – 7.56 (m, 2H), 7.28 (t, $J = 2.0$ Hz, 1H), 7.01 – 6.95 (m, 2H), 3.87 (s, 3H). **¹³C NMR** (126 MHz, CDCl₃) δ 162.20, 133.20 (t, $^2J_{CF} = 10.3$ Hz), 132.01, 115.96, 114.54, 110.34 (t, $^2J_{CF} = 12.6$ Hz), 102.00 (t, $^1J_{CF} = 269.4$ Hz), 55.47. **¹⁹F NMR** (376 MHz, CDCl₃) δ -106.42. The spectral data were in record with those in literature. [*Chem. Commun.* **2015**, 51, 8805]

1-Chloro-4-(3,3-difluorocycloprop-1-en-1-yl)benzene (a3)



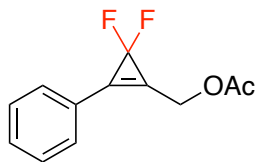
Yellow oil, flash chromatography using 5% Et₃N/ hexanes ($R_f = 0.30$). 30.6 mg from 0.25 mmol scale, 66% yield. **¹H NMR** (400 MHz, CDCl₃) δ 7.61 – 7.57 (m, 2H), 7.50 – 7.47 (m, 2H), 7.46 (d, $J = 1.9$ Hz, 1H). **¹³C NMR** (126 MHz, CDCl₃) δ 137.95, 132.98 (t, $^2J_{CF} = 10.7$ Hz), 131.35, 129.52, 121.84, 114.09 (t, $^2J_{CF} = 12.4$ Hz), 101.28 (t, $^1J_{CF} = 270.4$ Hz). **¹⁹F NMR** (376 MHz, CDCl₃) δ -106.54. The spectral data were in accord with those in the literature. [*J. Org. Chem.* **2020**, *85*, 7916–7924]

3-(3,3-Difluorocycloprop-1-en-1-yl)thiophene (a4)



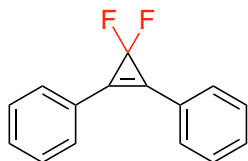
Pale yellow oil, flash chromatography using 2% Et₃N/ hexanes ($R_f = 0.20$). 28.0 mg from 0.25 mmol scale, 71% yield. **¹H NMR** (500 MHz, CDCl₃) δ 7.84 (dd, $J = 3.0, 1.2$ Hz, 1H), 7.46 (dd, $J = 5.0, 2.9$ Hz, 1H), 7.37 (dd, $J = 5.0, 1.2$ Hz, 1H), 7.31 (t, $J = 1.9$ Hz, 1H). **¹³C NMR** (126 MHz, CDCl₃) δ 130.87, 128.32 (t, $^2J_{CF} = 10.6$ Hz), 127.72, 127.18, 124.40, 110.88 (t, $^2J_{CF} = 12.4$ Hz), 100.82 (t, $^1J_{CF} = 270.1$ Hz). **¹⁹F NMR** (376 MHz, CDCl₃) δ -106.23. The spectral data were in accord with those in the literature. [*Chem. Commun.* **2015**, *51*, 8805–8808]

(3,3-Difluoro-2-phenylcycloprop-1-en-1-yl)methyl acetate (a5)



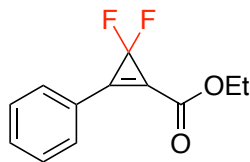
Pale yellow oil, flash chromatography using 5% Et₃N/ hexanes ($R_f = 0.30$). 54.2 mg from 0.25 mmol scale, 97% yield. ¹H NMR (400 MHz, CDCl₃) δ 7.63 (dd, $J = 6.7, 3.0$ Hz, 2H), 7.47 (dd, $J = 5.0, 1.9$ Hz, 3H), 5.18 (t, $J = 2.7$ Hz, 2H), 2.21 (s, 3H). ¹³C NMR (126 MHz, CDCl₃) δ 170.15, 131.33, 130.40, 129.12, 129.09, 128.21 (t, $^2J_{CF} = 10.8$ Hz), 123.20, 121.82 (t, $^2J_{CF} = 11.9$ Hz), 101.94 (t, $^1J_{CF} = 272.2$ Hz), 56.81, 20.66. ¹⁹F NMR (376 MHz, CDCl₃) δ -108.00. The spectral data were in accord with those in the literature. [*Angew. Chem. Int. Ed.* **2013**, *52*, 12390–12394]

(3,3-Difluorocycloprop-1-ene-1,2-diyl)dibenzene (a6)



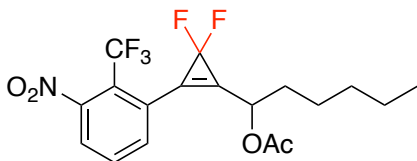
White solid, flash chromatography using 5% Et₃N/ hexanes ($R_f = 0.30$). 43.9 mg from 0.25 mmol scale, 77% yield. ¹H NMR (400 MHz, CDCl₃) δ 7.83 – 7.76 (m, 4H), 7.57 – 7.47 (m, 6H). ¹³C NMR (126 MHz, CDCl₃) δ 131.00, 130.38, 129.20, 124.62, 123.20 (t, $^2J_{CF} = 10.8$ Hz), 102.29 (t, $^1J_{CF} = 271.3$ Hz). ¹⁹F NMR (376 MHz, CDCl₃) δ -112.17. The spectral data were in accord with those in the literature. [*Chem. Commun.*, **2015**, *51*, 8805–8808]

Ethyl 3,3-difluoro-2-phenylcycloprop-1-ene-1-carboxylate (a7)



White solid, flash chromatography using 5% Et₃N/ 5% Et₂O/ 90% hexanes ($R_f = 0.30$). 48.8 mg from 0.25 mmol scale, 87% yield. ¹H NMR (400 MHz, CDCl₃) δ 7.94 – 7.84 (m, 2H), 7.63 – 7.56 (m, 1H), 7.53 (dd, $J = 8.1, 6.4$ Hz, 2H), 4.41 (q, $J = 7.1$ Hz, 2H), 1.42 (t, $J = 7.1$ Hz, 3H). ¹³C NMR (126 MHz, CDCl₃) δ 156.60, 138.18 (t, $^2J_{CF} = 10.3$ Hz), 133.37, 132.23, 129.30, 122.77, 115.77 (t, $^2J_{CF} = 13.4$ Hz), 98.98 (t, $^1J_{CF} = 276.2$ Hz), 62.35, 14.14. ¹⁹F NMR (376 MHz, CDCl₃) δ -107.57.

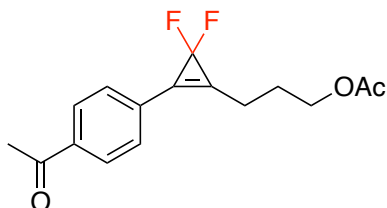
1-(3,3-Difluoro-2-(3-nitro-2-(trifluoromethyl)phenyl)cycloprop-1-en-1-yl)hexyl acetate (a8)



Yellow oil, flash chromatography using 5% Et₃N/ 10% Et₂O/ 85% hexanes ($R_f = 0.30$). 38.1 mg from 0.10 mmol scale, 94% yield. ¹H NMR (400 MHz, CDCl₃) δ 8.09 (d, $J = 1.7$ Hz, 1H), 8.00 (d, $J = 8.3$ Hz, 1H), 7.94 (dd, $J = 8.3, 1.7$ Hz, 1H), 5.93 (td, $J = 6.6, 2.7$ Hz, 1H), 2.19 (s, 3H), 1.93 (dq, $J = 8.9, 6.5$ Hz, 2H), 1.46 (ddp, $J = 15.6, 5.5, 2.9$ Hz, 2H), 1.38 – 1.30 (m, $J = 3.5, 3.0$ Hz, 4H), 0.90 (td, $J = 5.7, 4.5, 2.4$ Hz, 3H). ¹³C NMR (126 MHz, CDCl₃) δ 169.76, 148.76, 134.29, 131.79 (t, $^2J_{CF} = 11.5$ Hz), 129.72 (q, $^3J_{CF} = 5.1$ Hz), 127.86, 126.04, 121.46 (q, $^1J_{CF} = 268.4$ Hz), 124.71 (q, $^2J_{CF} = 35.3$ Hz), 124.71 (t, $^2J_{CF} =$

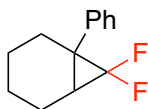
11.34 Hz), 100.55 (t, $^1J_{CF} = 274.7$ Hz), 68.77, 32.71, 31.26, 24.25, 22.34, 20.74, 13.88. ^{19}F NMR (376 MHz, CDCl_3) δ -60.23, -106.19, -106.52, -107.56, -107.89.

3-(2-(4-Acetylphenyl)-3,3-difluorocycloprop-1-en-1-yl)propyl acetate (a9)



Pale yellow solid, flash chromatography using 5% Et_3N / 25% Et_2O /70% hexanes ($R_f = 0.20$). 25.5 mg from 0.10 mmol scale, 87% yield. ^1H NMR (400 MHz, CDCl_3) δ /8.03 (d, $J = 8.0$ Hz, 2H), 7.65 (d, $J = 8.0$ Hz, 2H), 4.19 (t, $J = 6.3$ Hz, 2H), 2.79 (td, $J = 7.2, 3.7$ Hz, 2H), 2.63 (s, 3H), 2.11 (q, $J = 6.8$ Hz, 2H), 2.05 (s, 3H). ^{13}C NMR (126 MHz, CDCl_3) δ 197.18, 170.97, 138.30, 129.99, 128.95, 128.91(t, $^2J_{CF} = 10.7$ Hz), 128.12, 125.74 (t, $^2J_{CF} = 11.2$ Hz), 102.77 (t, $^1J_{CF} = 272.3$ Hz), 63.19, 26.74, 26.29, 20.86, 20.72. ^{19}F NMR (376 MHz, CDCl_3) δ -109.05.

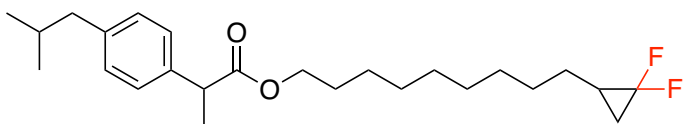
7,7-Difluoro-1-phenylbicyclo[4.1.0]heptanes (b1)



Colorless oil, flash chromatography using 0–10% EtOAc /hexanes ($R_f = 0.81$), 40.4 mg from a 2.0 mmol scale, 97% yield. ^1H NMR (500 MHz, CDCl_3) δ 7.38 – 7.26 (m, 5H), 7.26 – 7.21 (m, 1H), 2.21 – 2.13 (m, 1H), 2.05 – 1.95 (m, 1H), 1.88 – 1.73 (m, 3H), 1.51 –

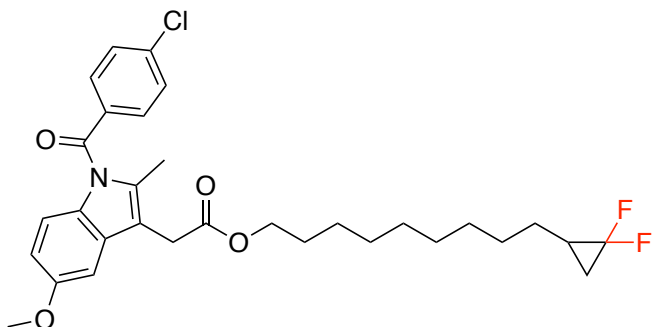
1.30 (m, 4H). ^{13}C NMR (126 MHz, CDCl_3) δ 141.83, 128.50, 128.30, 128.28, 126.82, 115.69 (t, $J_{\text{CF}} = 293.2$ Hz), 31.01 (t, $J_{\text{CF}} = 9.6$), 27.31 (t, $J_{\text{CF}} = 2.6$), 26.91, 23.33 (t, $J_{\text{CF}} = 2.6$), 21.09 (t, $J_{\text{CF}} = 2.6$), 20.73, 16.93. ^{19}F NMR (471 MHz, CDCl_3) δ -127.78 (ddd, $J = 149.7, 15.9, 2.9$ Hz), -143.02 (dd, $J = 149.9, 2.9$ Hz). The spectral data were in accord with those in the literature.^{19,34}

9-(2,2-Difluorocyclopropyl)nonyl 2-(4-isobutylphenyl)propanoate (b4)



Yellow oil, flash chromatography using 5% Et_3N /hexanes ($R_f = 0.26$) and increase to 10% EtOAc /hexanes + 5% Et_3N , or workup by washing with brine and NaHCO_3 aq. 40.8 mg from a 0.10 mmol scale, quantitative yield. ^1H NMR (400 MHz, CDCl_3) δ 7.23 – 7.17 (m, 2H), 7.12 – 7.05 (m, 2H), 4.05 (t, $J = 6.7$ Hz, 2H), 3.68 (q, $J = 7.1$ Hz, 1H), 2.44 (d, $J = 7.2$ Hz, 2H), 1.84 (dt, $J = 13.5, 6.8$ Hz, 1H), 1.56 (t, $J = 6.7$ Hz, 2H), 1.48 (d, m, 3H), 1.47 – 1.38 (m, 4H), 1.25 (d, $J = 9.6$ Hz, 11H), 0.89 (d, $J = 6.6$ Hz, 8H). ^{13}C NMR (101 MHz, CDCl_3) δ 174.81, 140.40, 137.89, 129.23, 127.13, 114.78 (t, $^1J_{\text{CF}} = 352.5$, CF_2), 64.73, 45.19, 45.02, 30.17, 29.69, 29.37, 29.35, 29.11, 29.04, 28.86, 28.84, 28.50, 26.84, 26.81, 25.73, 22.61 (t, $^2J_{\text{CF}} = 13.8$, CH_2CF_2), 22.50, 22.36, 18.44, 16.04 (t, $^2J_{\text{CF}} = 13.8$, CHCF_2). ^{19}F NMR (376 MHz, CDCl_3) δ -127.58 – -128.43 (m), -144.61 (ddd, $J = 155.1, 12.8, 3.8$ Hz). HRMS (ESI-TOF) m/z : $[\text{M}+\text{Na}]^+$ calcd for $\text{C}_{25}\text{H}_{38}\text{F}_2\text{O}_2\text{Na}$: 431.2737; found 431.2743.

9-(2,2-Difluorocyclopropyl)nonyl 2-(1-(4-chlorobenzoyl)-5-methoxy-2-methyl-1H-indol-3-yl)acetate (b5)

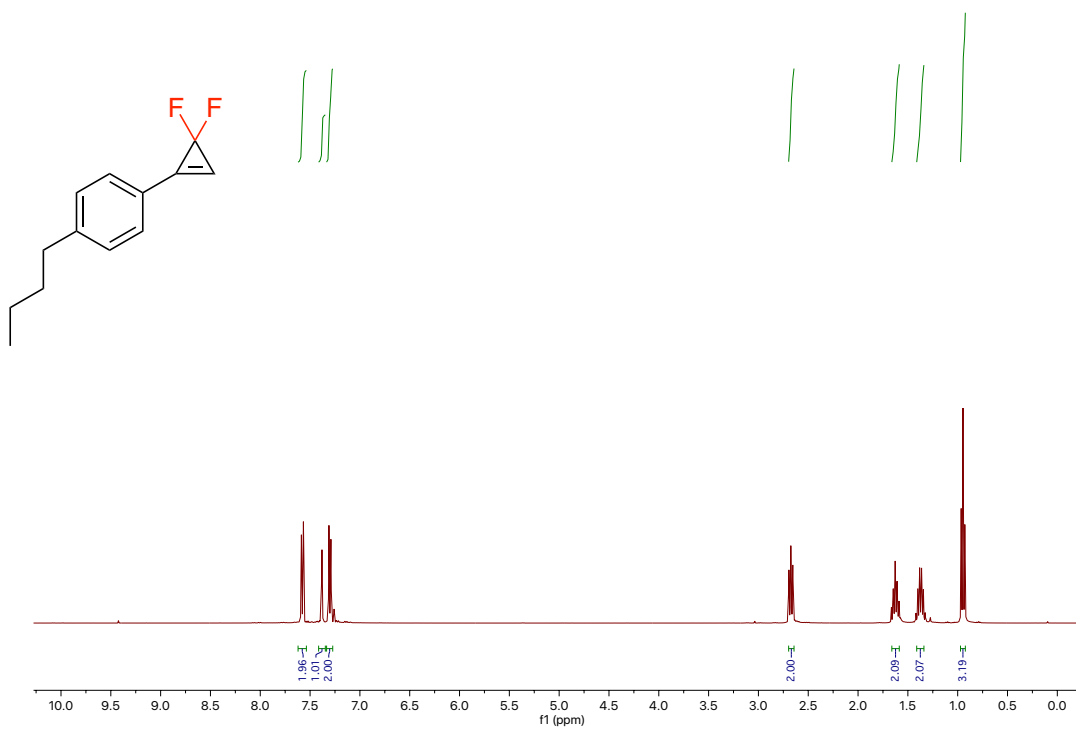


Yellow oil, flash chromatography using 5% Et₃N/hexanes ($R_f = 0.26$) and increase to 10% EtOAc/hexanes + 5% Et₃N. 52.1 mg from a 0.10 mmol scale, 93% yield. ¹H NMR (500 MHz, CDCl₃) δ 7.69 – 7.63 (m, 2H), 7.50 – 7.44 (m, 2H), 6.97 (d, $J = 2.5$ Hz, 1H), 6.87 (d, $J = 9.0$ Hz, 1H), 6.67 (dd, $J = 9.0, 2.6$ Hz, 1H), 4.09 (t, $J = 6.7$ Hz, 2H), 3.83 (s, 3H), 3.65 (s, 2H), 2.39 (s, 3H), 1.61 (t, $J = 7.1$ Hz, 2H), 1.47 – 1.35 (m, 5H), 1.26 (q, $J = 7.6, 4.2$ Hz, 10H), 0.91 – 0.81 (m, 2H). ¹³C NMR (126 MHz, CDCl₃) δ 170.95, 168.28, 156.02, 139.24, 135.86, 133.92, 131.16, 130.79, 130.67, 130.25, 129.10, 128.50, 114.92, 114.80 (t, $^1J_{CF} = 281.3$, CF₂), 114.13, 112.74, 111.63, 101.30, 65.16, 55.67, 31.57, 30.43, 29.69, 29.40, 29.35, 29.17, 29.03, 28.85, 28.84, 28.59, 26.84, 26.81, 25.85, 22.60 (t, $^2J_{CF} = 10.0$, CH₂CF₂), 16.05 (t, $^2J_{CF} = 10.0$, CHCF₂), 13.34. ¹⁹F NMR (471 MHz, CDCl₃) δ -127.96 (dt, $J = 154.4, 14.1$ Hz), -144.59 (dd, $J = 155.0, 13.1$ Hz). HRMS (ESI-TOF) m/z : [M+Na]⁺ calcd for C₃₁H₃₆ClF₂NO₄Na: 582.2198; found 582.2193.

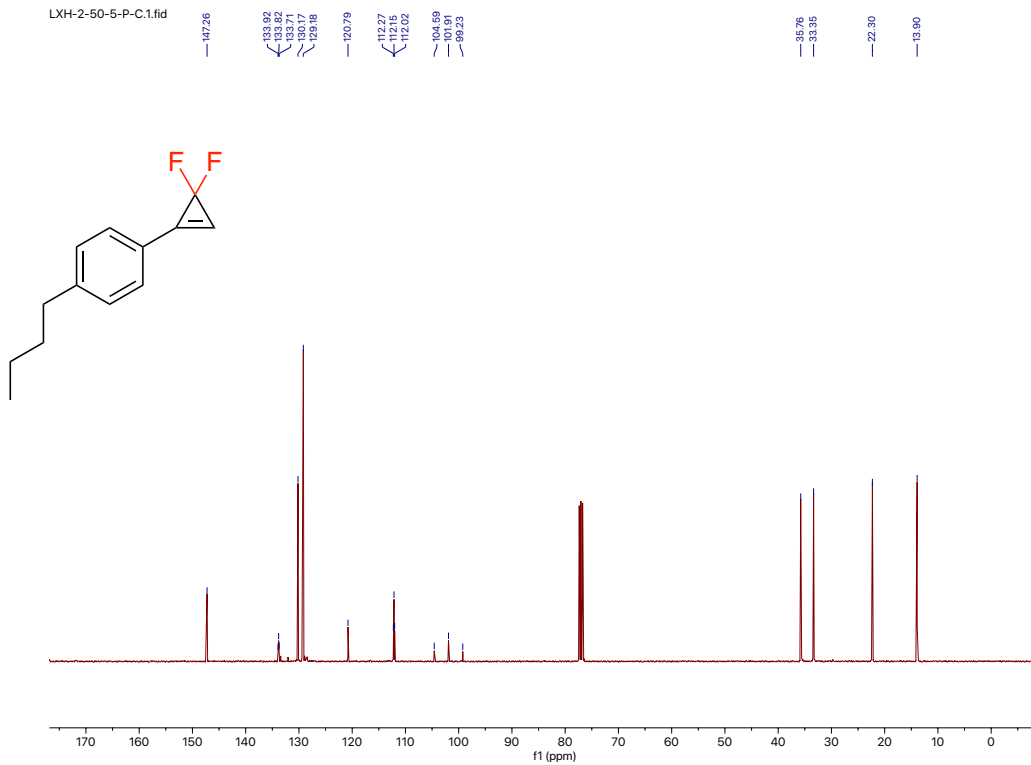
4.10. NMR spectra

^1H , ^{13}C , and ^{19}F NMR of 1-butyl-4-(3,3-difluorocycloprop-1-en-1-yl)benzene (**a1**)

LXH-2-50-5-P.3.fid

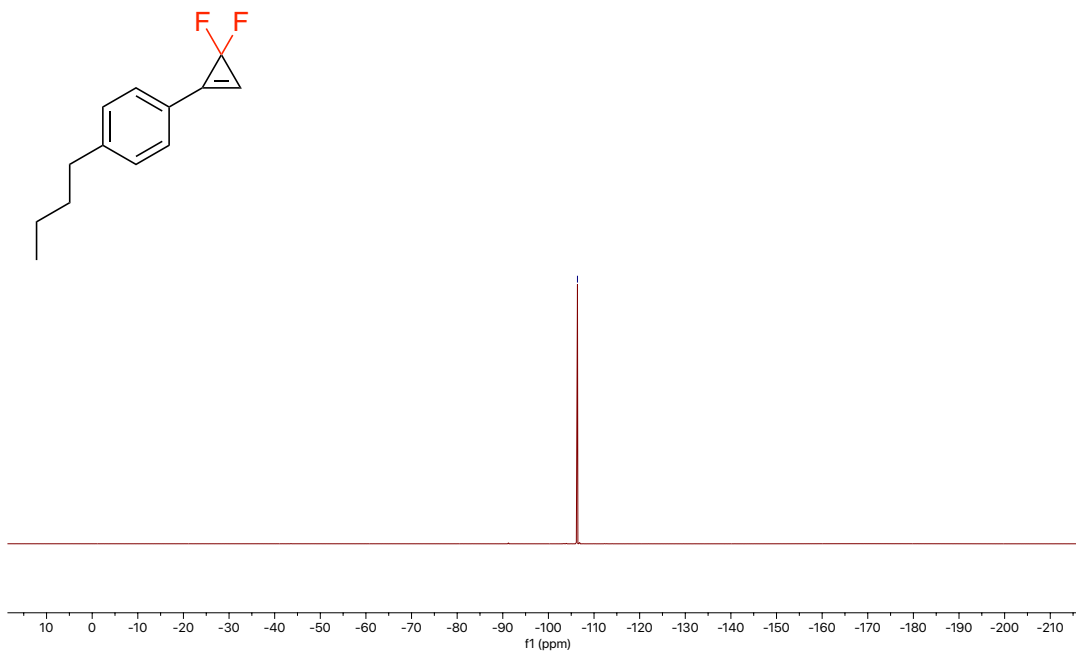


LXH-2-50-5-P-C.1.fid



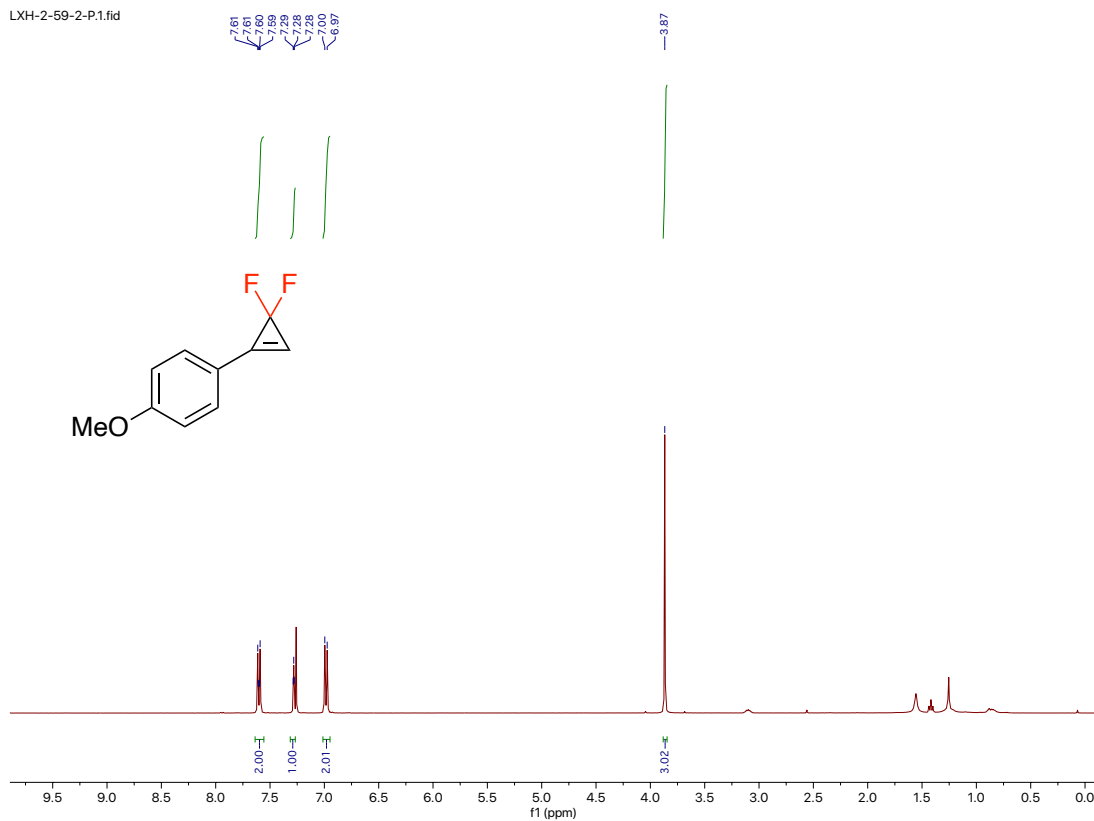
LXH-2-50-5-P.2.fid

—106.37

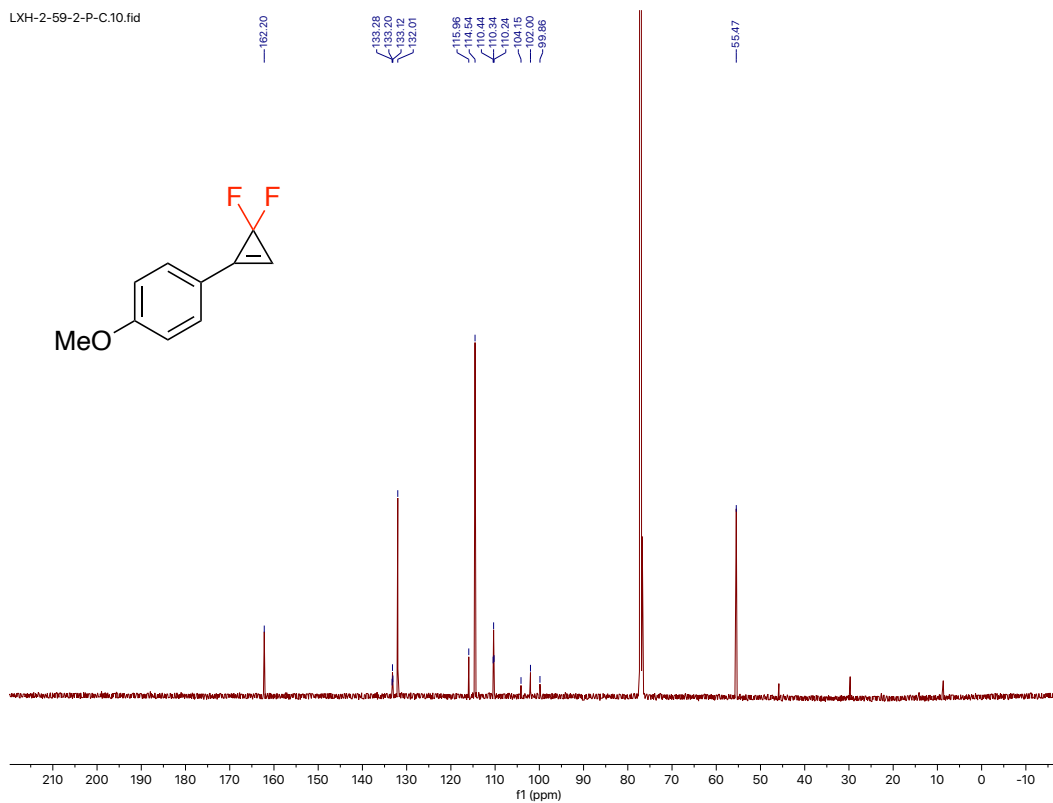


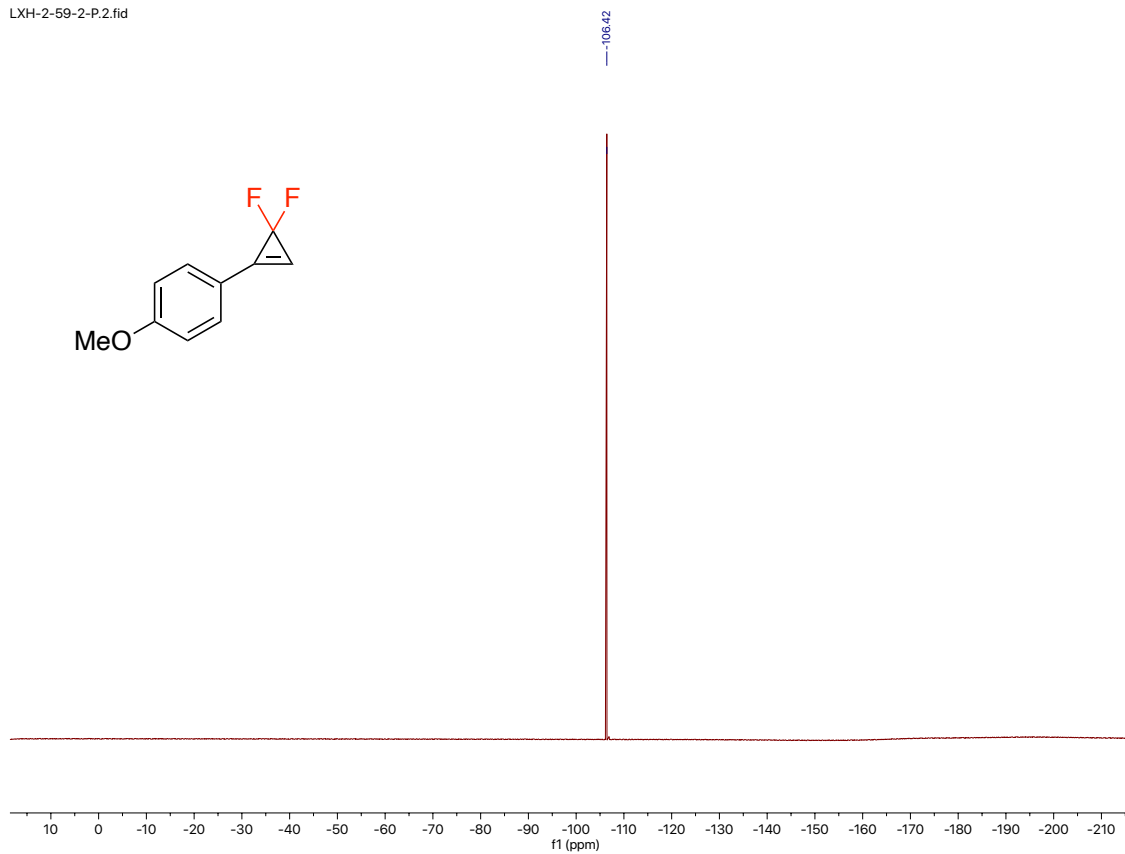
^1H , ^{13}C , and ^{19}F NMR of 1-(3,3-difluorocycloprop-1-en-1-yl)-4-methoxybenzene (**a2**)

LXH-2-59-2-P.1.fid



LXH-2-59-2-P-C.10.fid

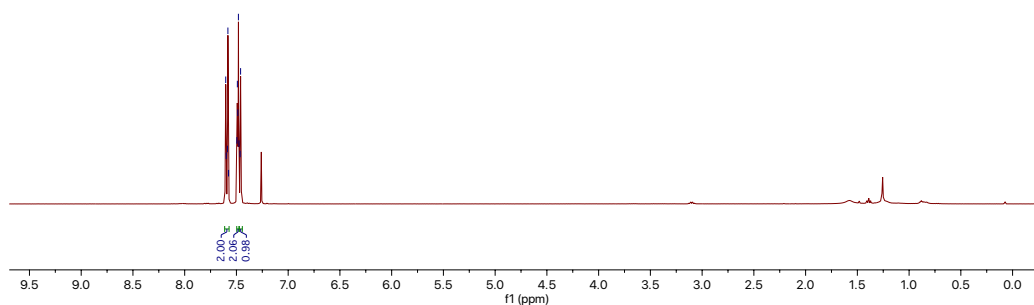
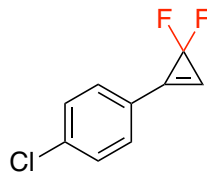




^1H , ^{13}C , and ^{19}F NMR of 1-chloro-4-(3,3-difluorocycloprop-1-en-1-yl)benzene (**a3**)

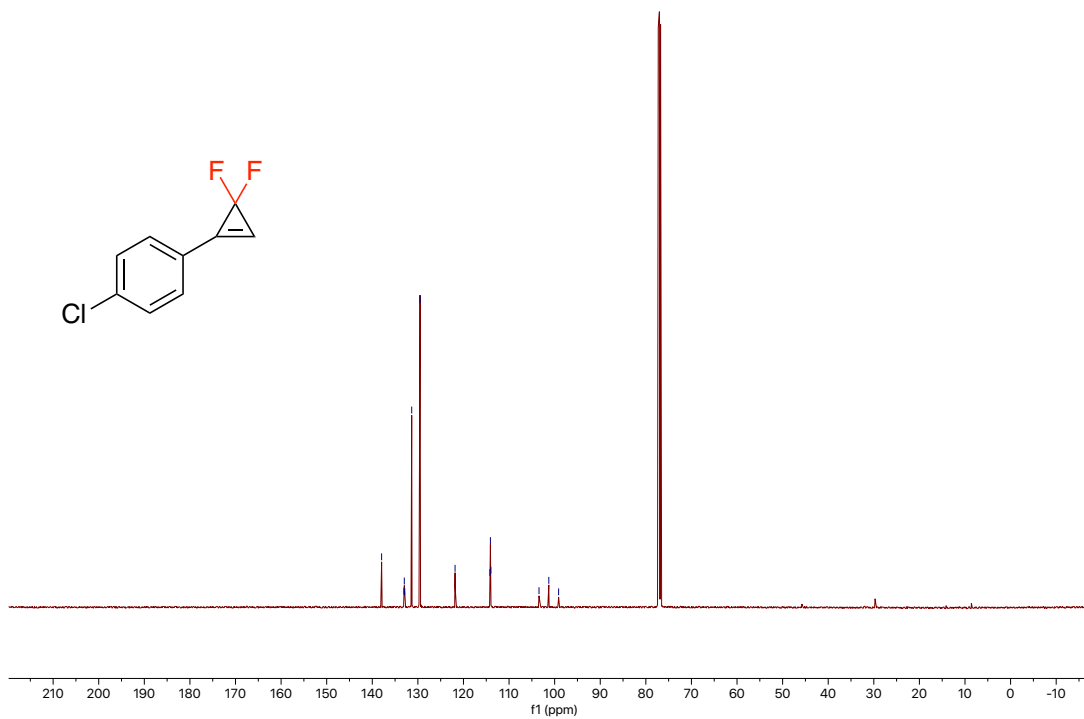
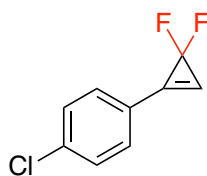
LXH-2-63-1-P1.fid

7.60
7.59
7.58
7.50
7.49
7.48
7.46



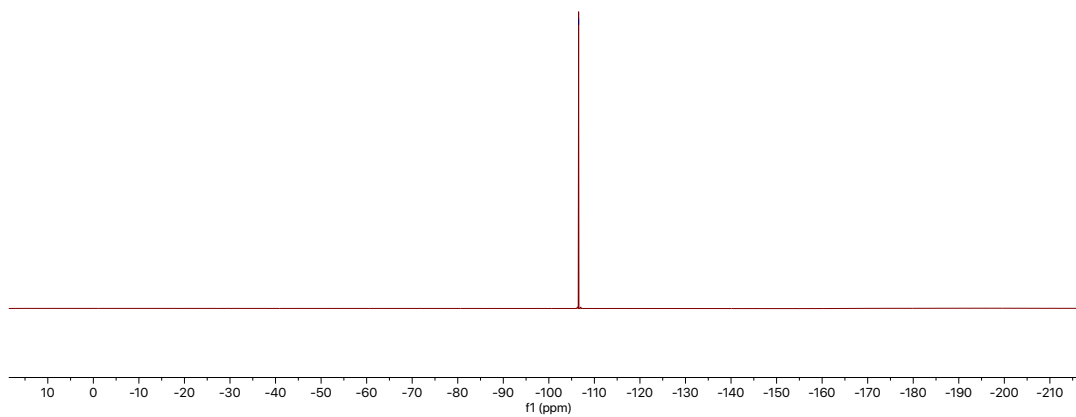
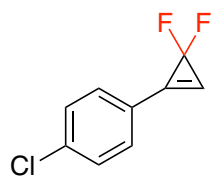
LXH-2-63-1-P-C.10.fid

137.95
133.06
132.89
132.89
131.35
129.52
121.84
114.19
113.09
103.43
101.28
99.13



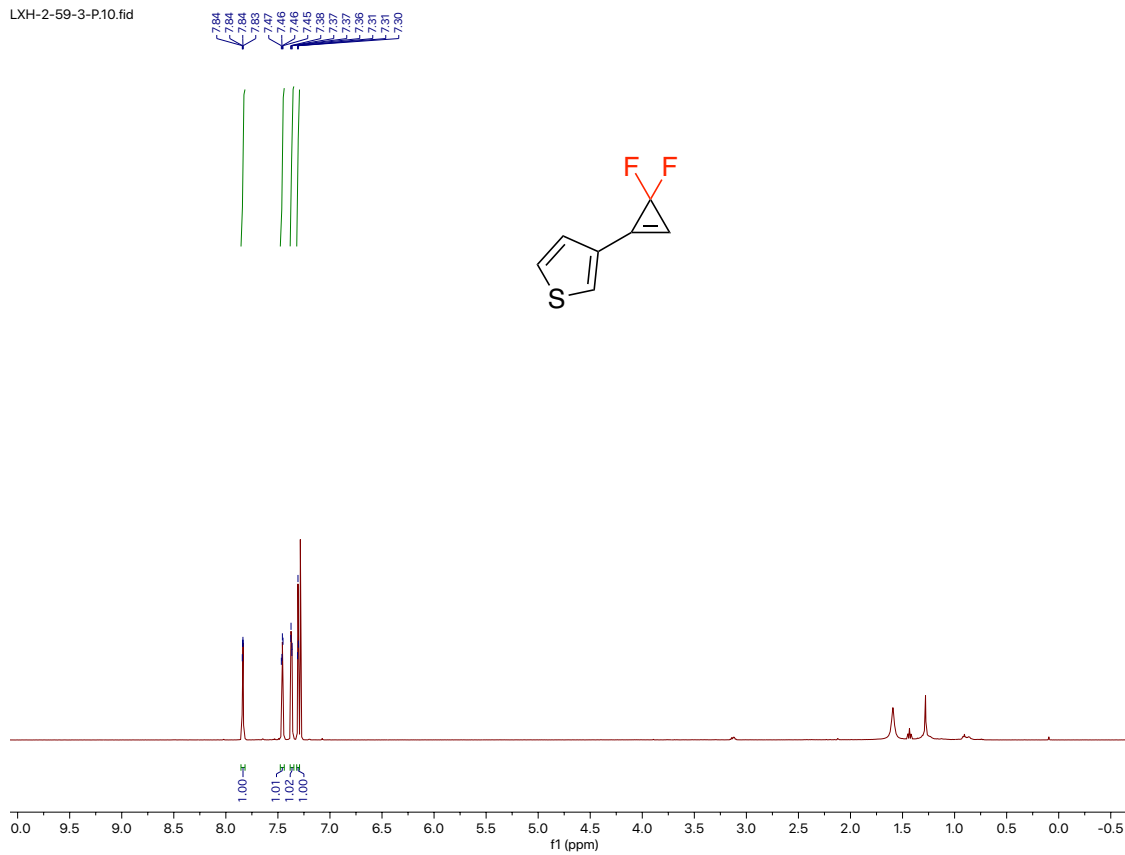
LXH-2-63-1-P.2.fid

—106.54

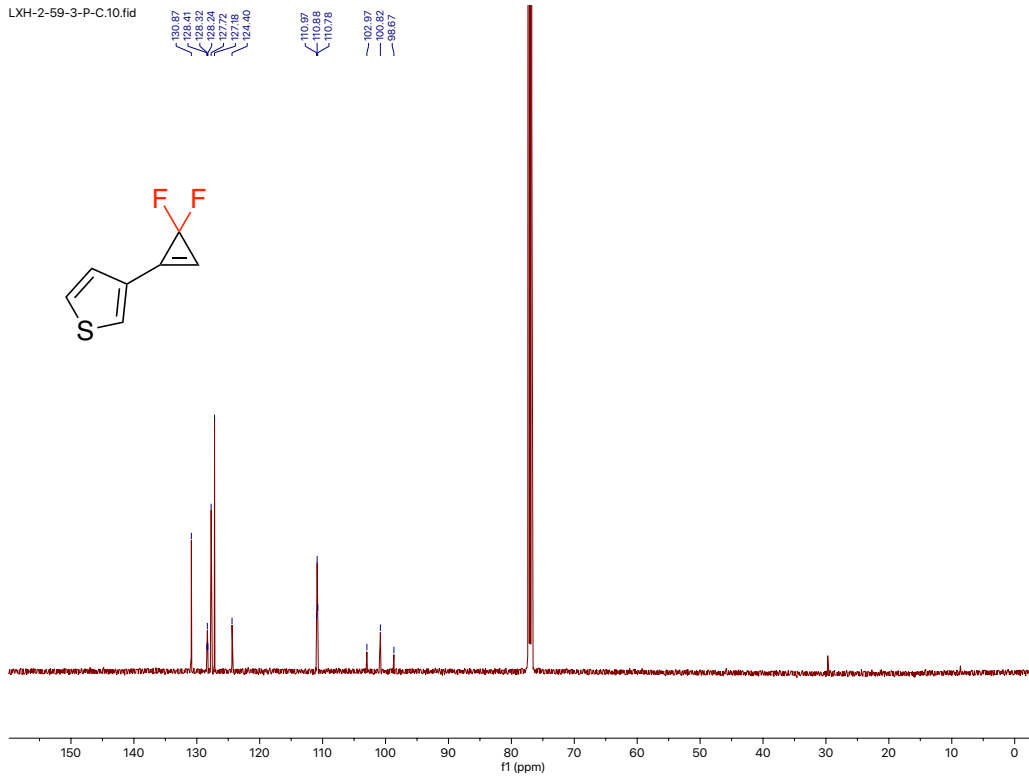


^1H , ^{13}C , and ^{19}F NMR of 3-(3,3-difluorocycloprop-1-en-1-yl)thiophene (**a4**)

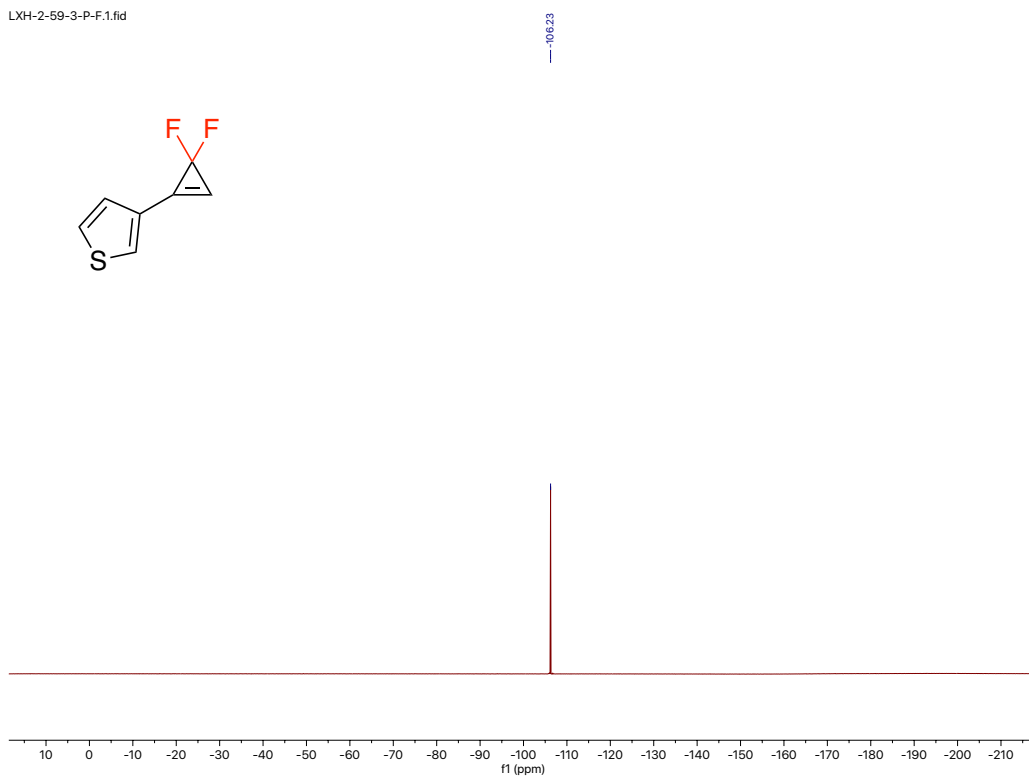
LXH-2-59-3-P10.fid



LXH-2-59-3-P-C.10.fid

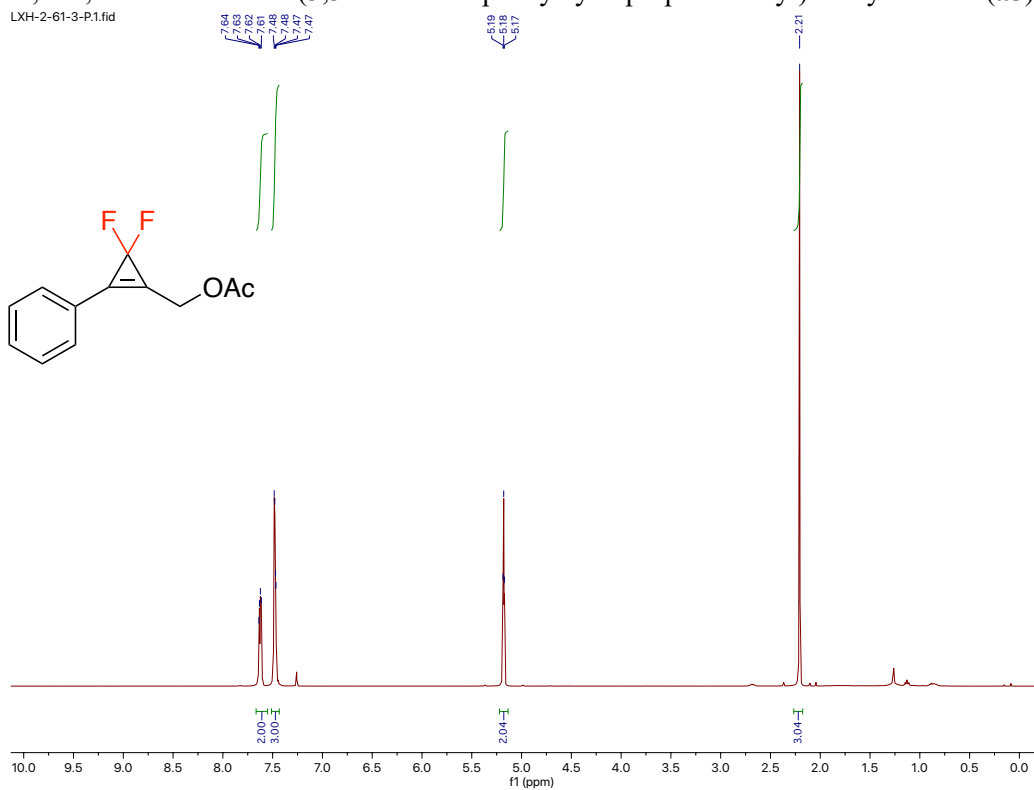


LXH-2-59-3-P-F.1.fid

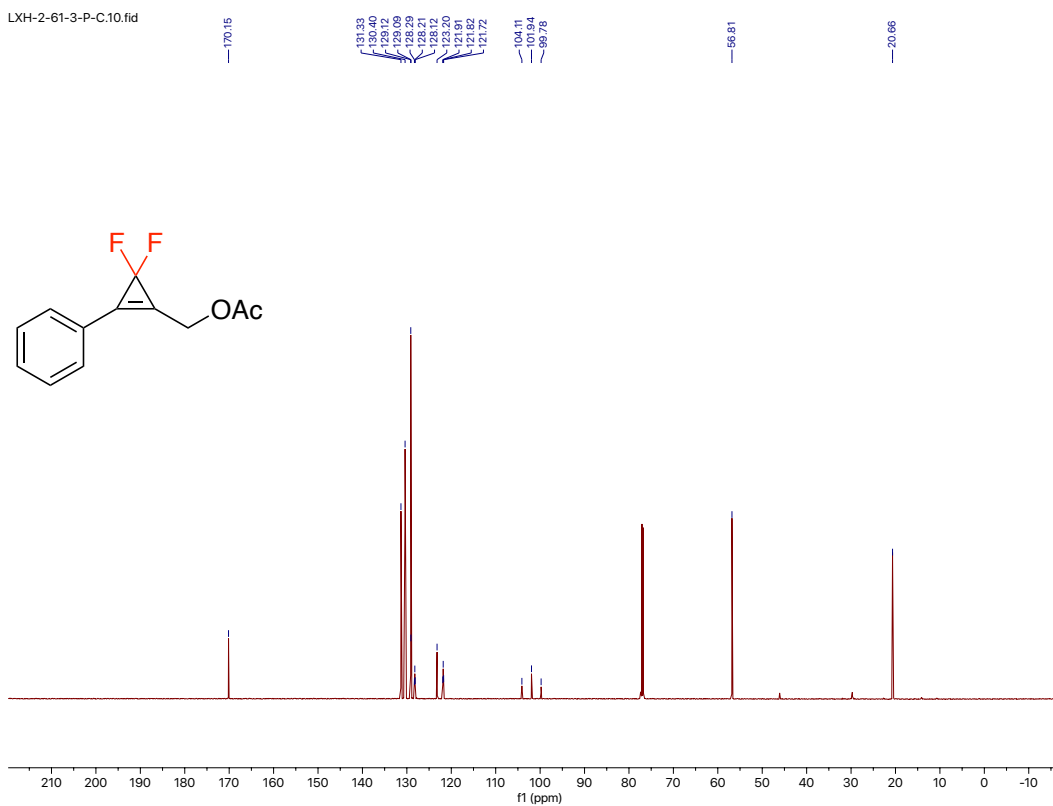


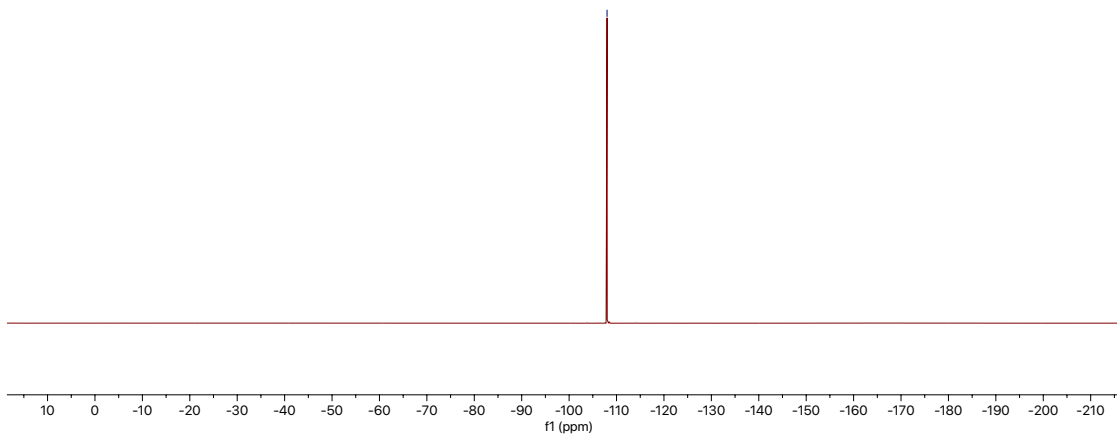
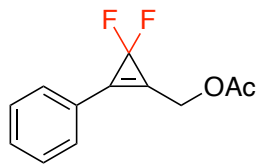
^1H , ^{13}C , and ^{19}F NMR of (3,3-difluoro-2-phenylcycloprop-1-en-1-yl)methyl acetate (**a5**)

LXH-2-61-3-P.1.fid



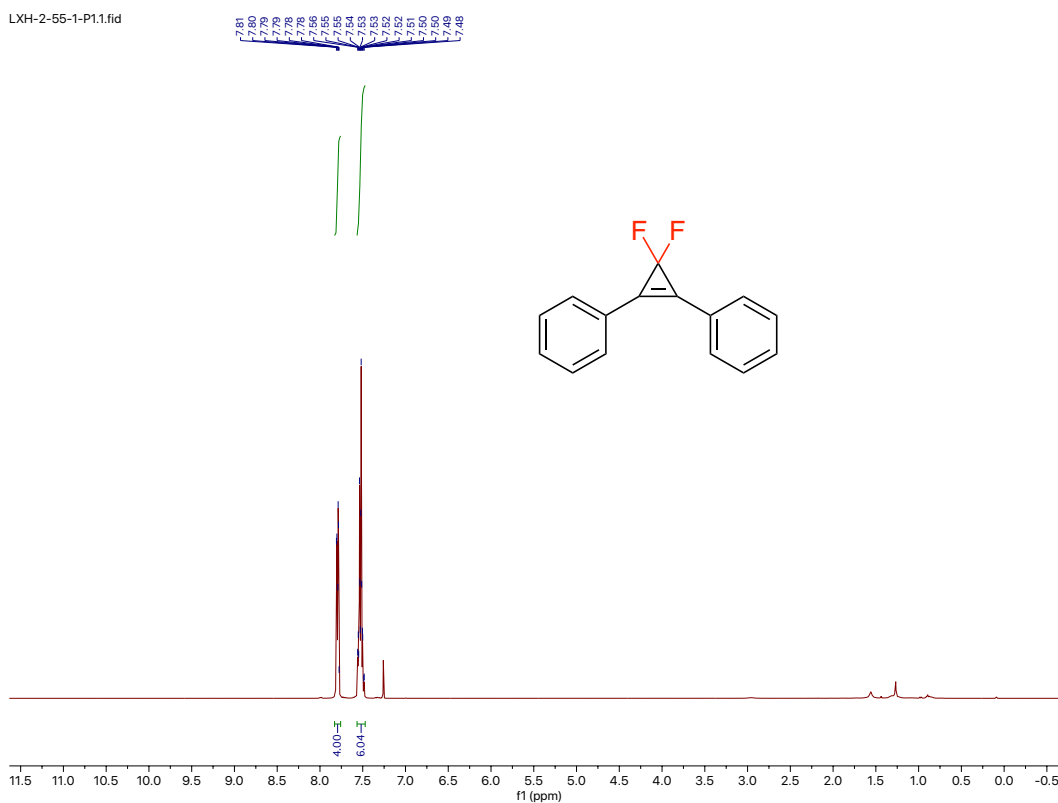
LXH-2-61-3-P-C.10.fid



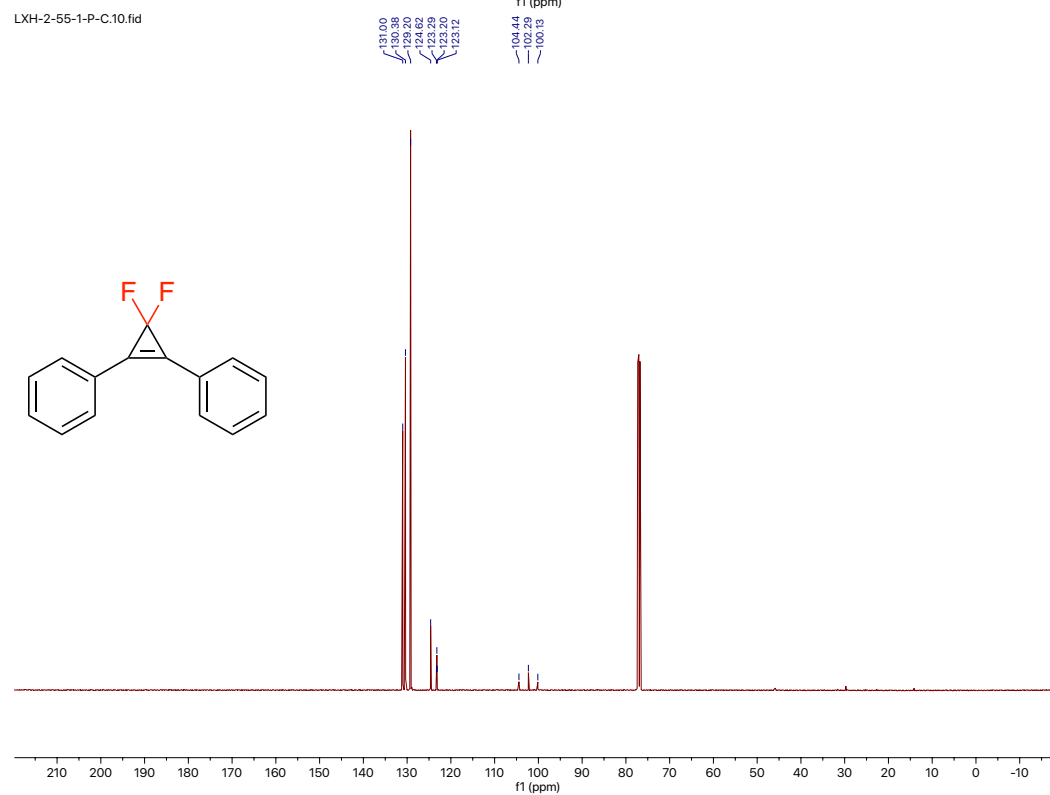


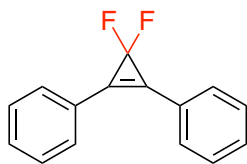
^1H , ^{13}C , and ^{19}F NMR of (3,3-difluorocycloprop-1-ene-1,2-diyl)dibenzene (**a6**)

LXH-2-55-1-P1.1.fid

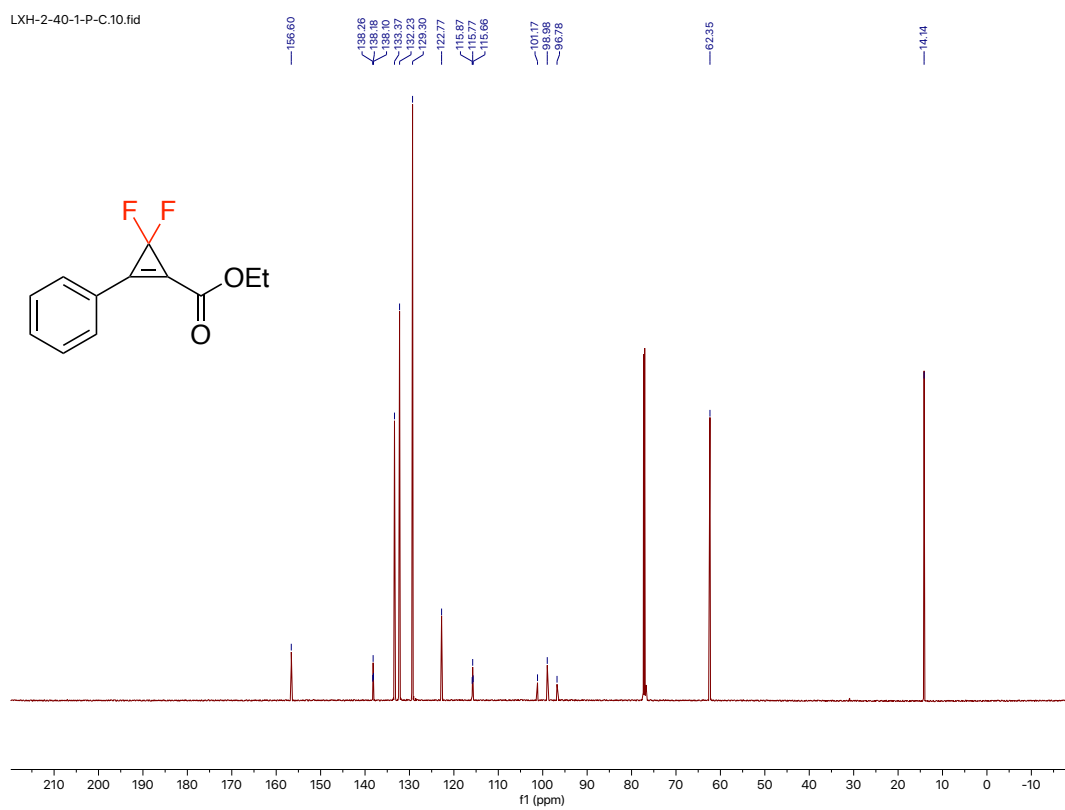
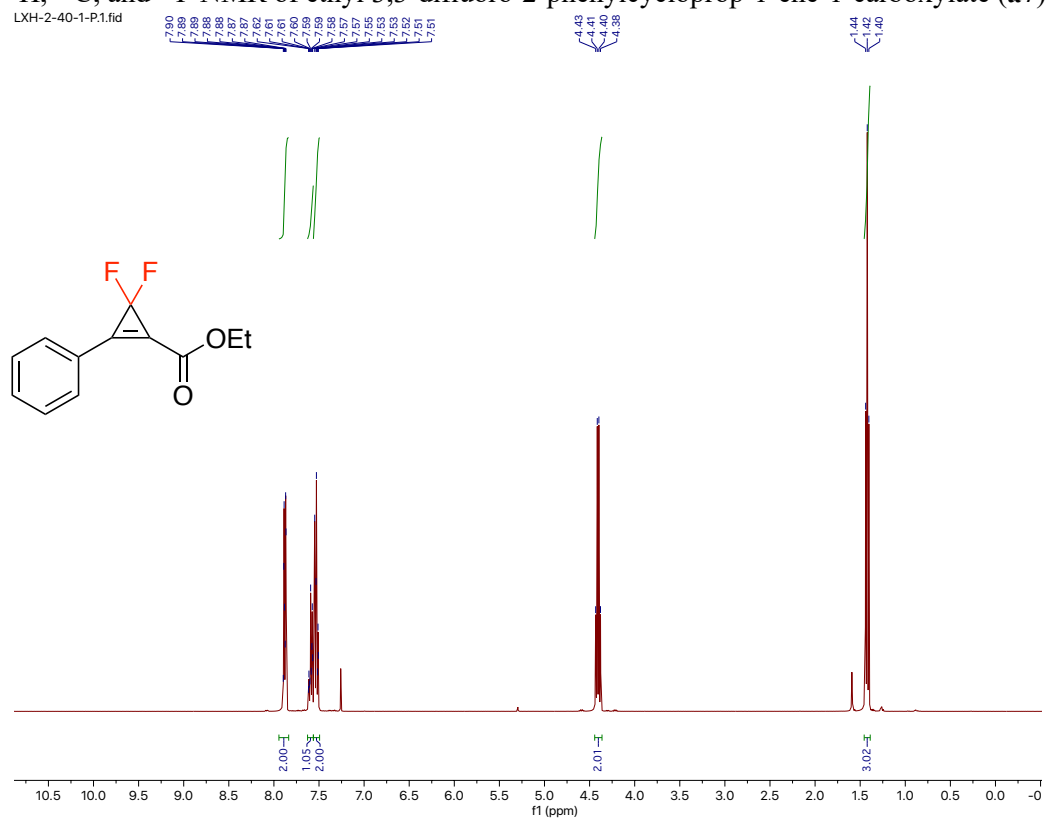


LXH-2-55-1-P-C.10.fid



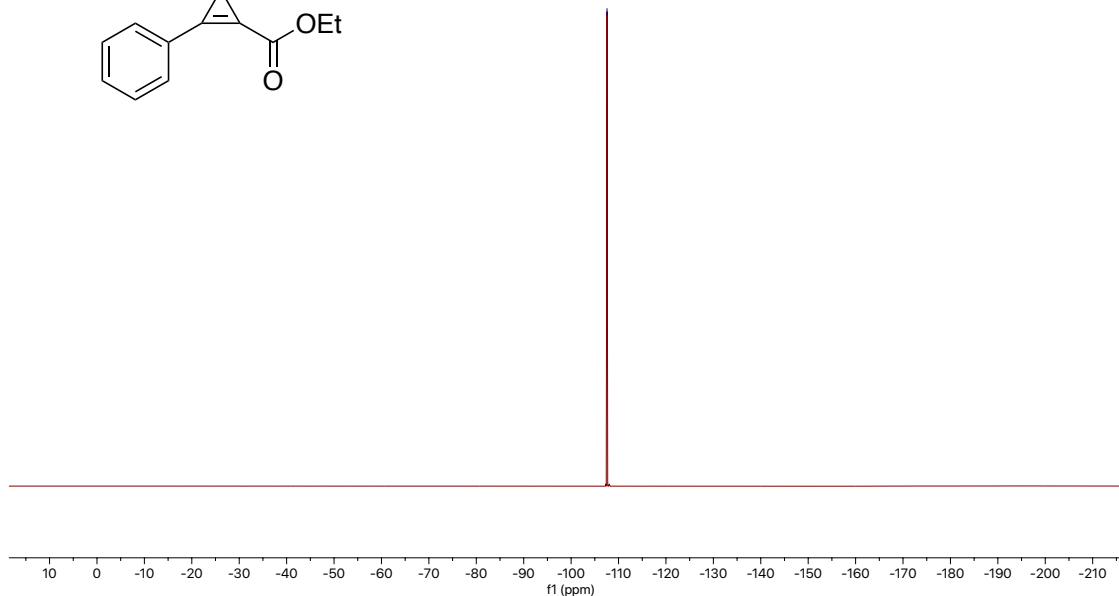
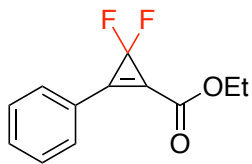


^1H , ^{13}C , and ^{19}F NMR of ethyl 3,3-difluoro-2-phenylcycloprop-1-ene-1-carboxylate (**a7**)



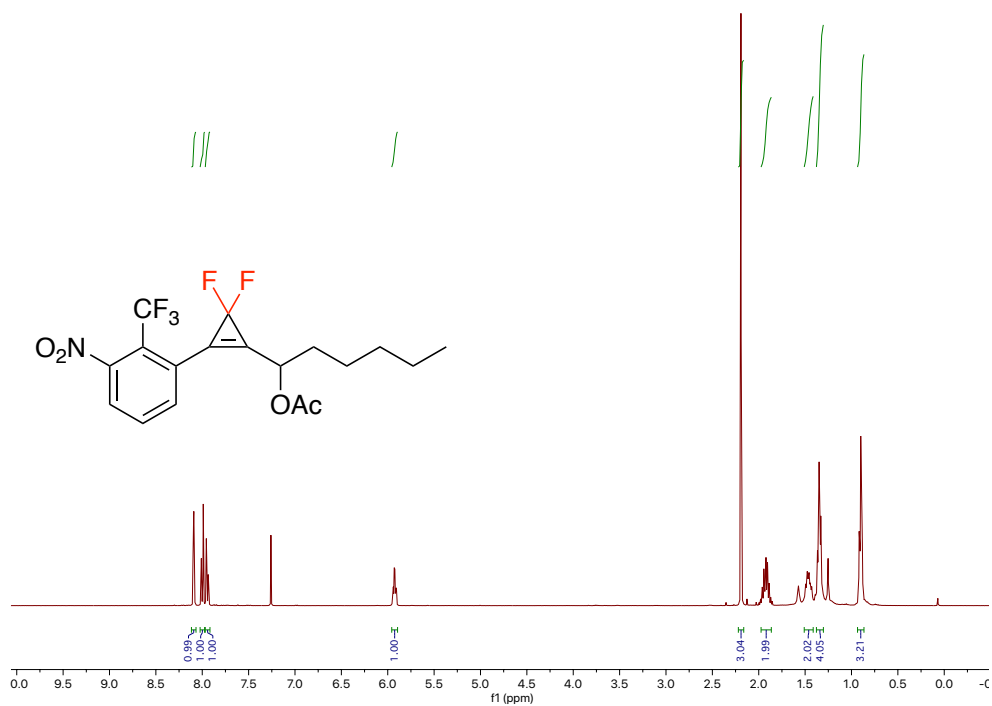
LXH-2-40-1-P/F

-107.57

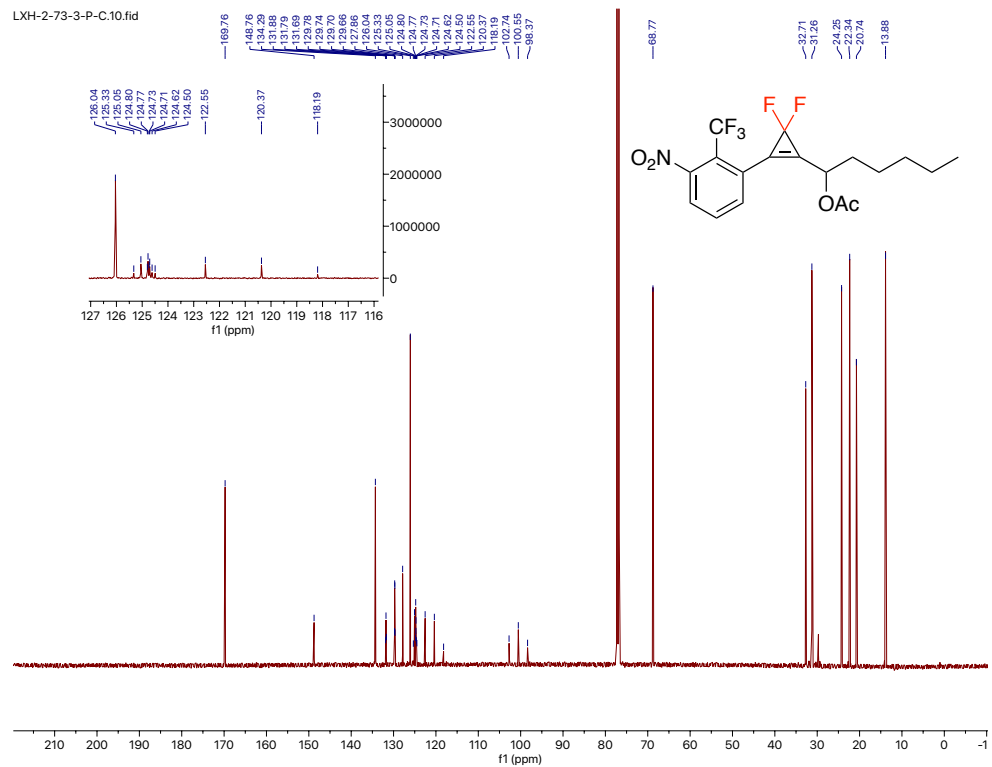


^1H , ^{13}C , and ^{19}F NMR of 1-(3,3-difluoro-2-(3-nitro-2-(trifluoromethyl)phenyl)cycloprop-1-en-1-yl)hexyl acetate (**a8**)

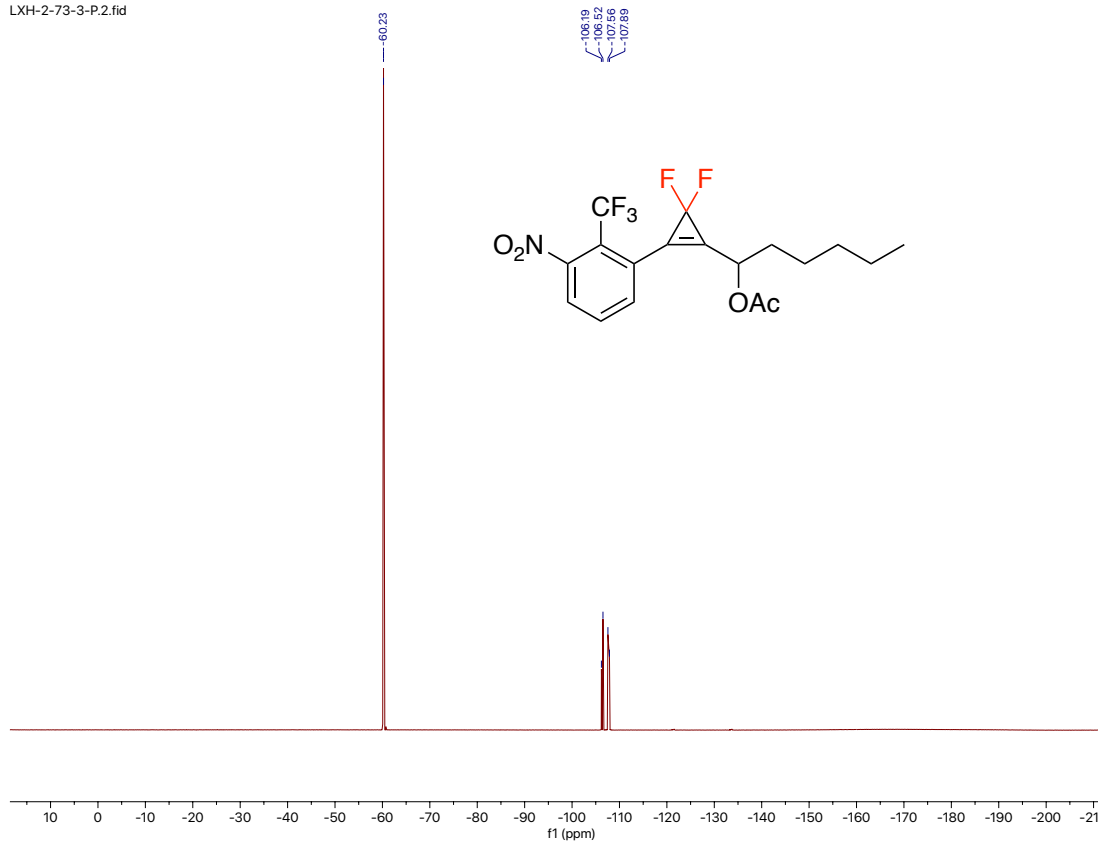
LXH-2-73-3-P1.fid



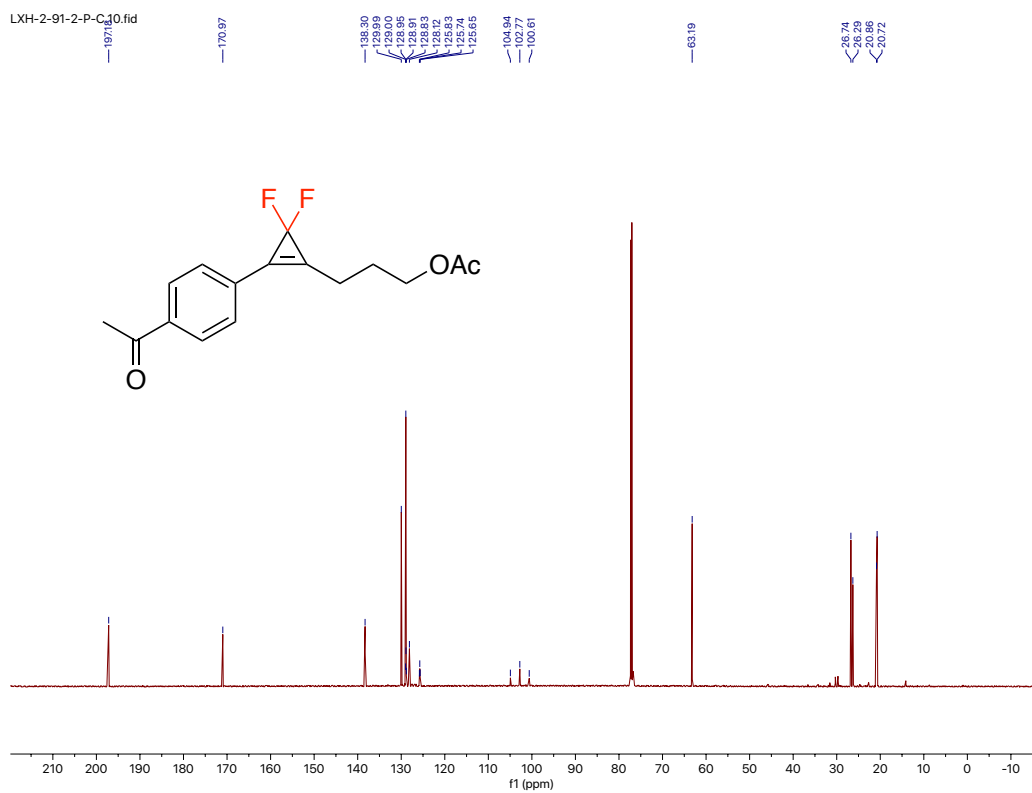
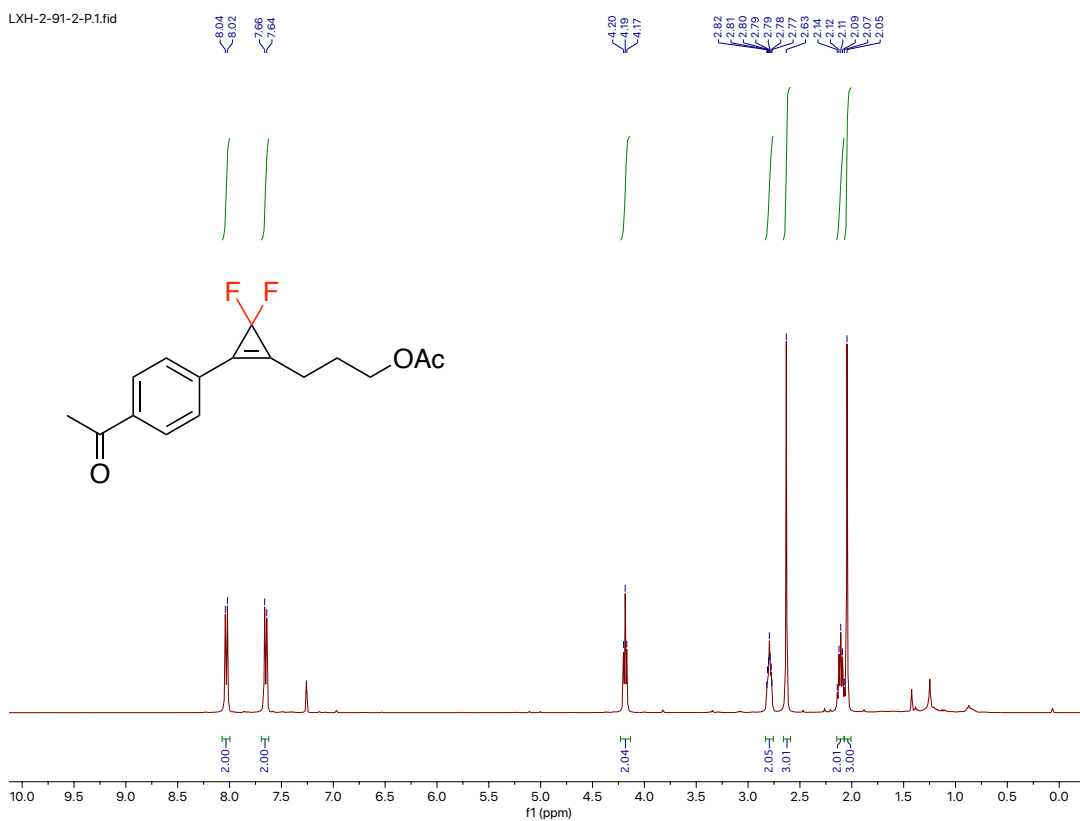
LXH-2-73-3-P-C.10.fid



LXH-2-73-3-P.2.fid

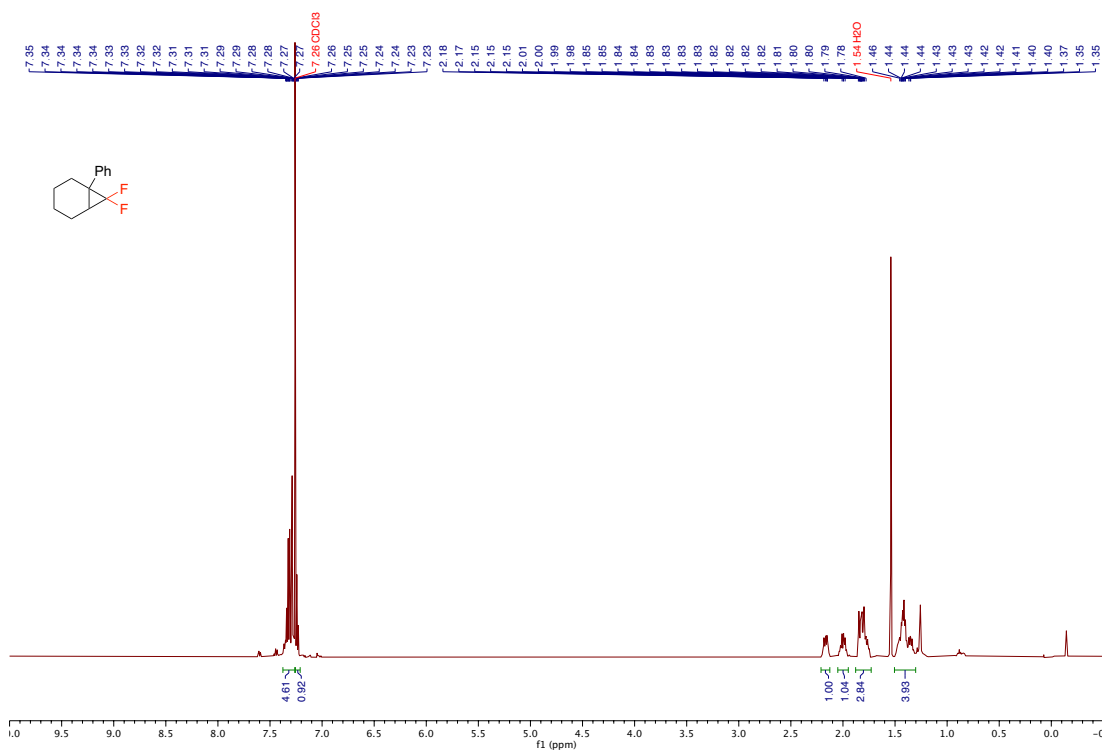


^1H , ^{13}C , and ^{19}F NMR of 3-(2-(4-acetylphenyl)-3,3-difluorocycloprop-1-en-1-yl)propyl acetate (**a9**)

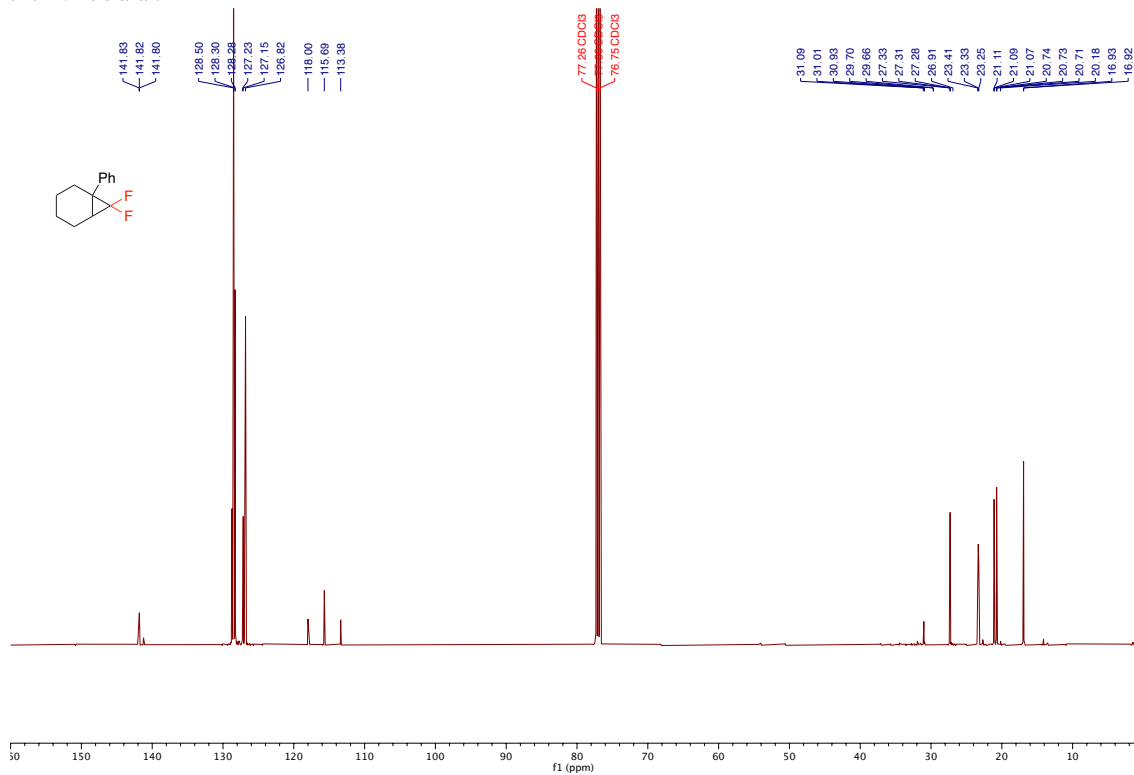


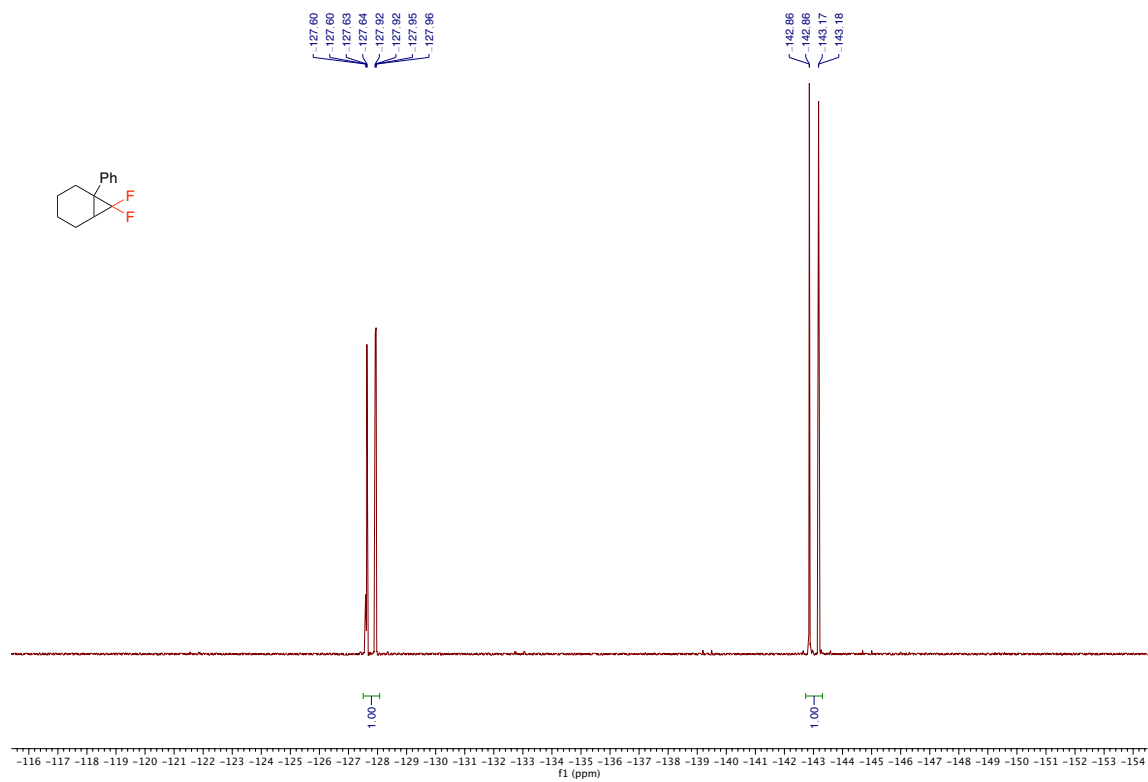
^1H , ^{13}C , and ^{19}F NMR of 7,7-Difluoro-1-phenylbicyclo[4.1.0]heptanes (**b1**)

JY2917-run4-5.10.fid —



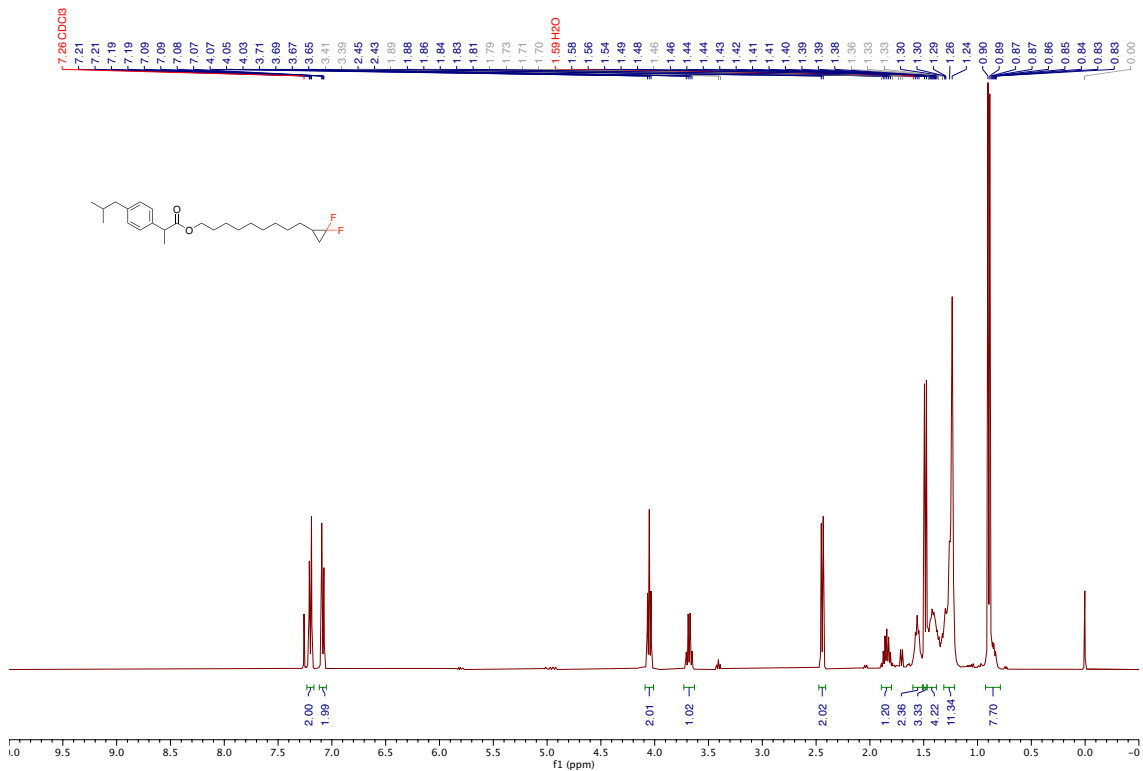
JY2917-run2-8-C13.10.fid —



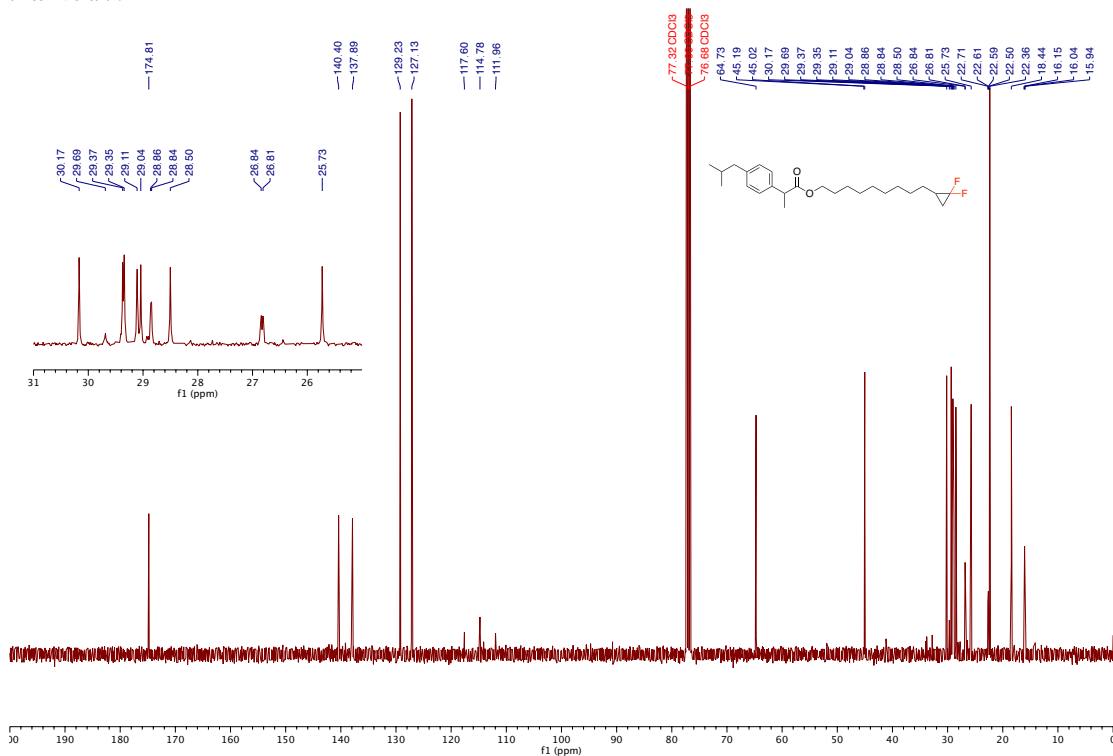


¹H, ¹³C, and ¹⁹F NMR of 9-(2,2-difluorocyclopropyl)nonyl 2-(4-isobutylphenyl)propanoate (**b4**)

JY2882_x1.1.fid —



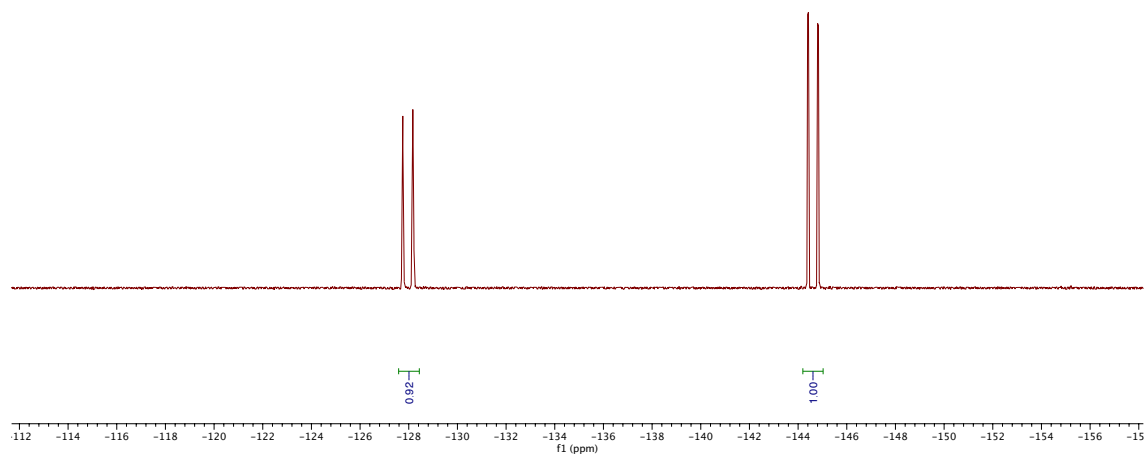
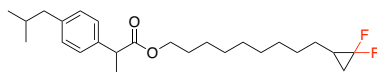
JY2882_x1.C13.1.fid —



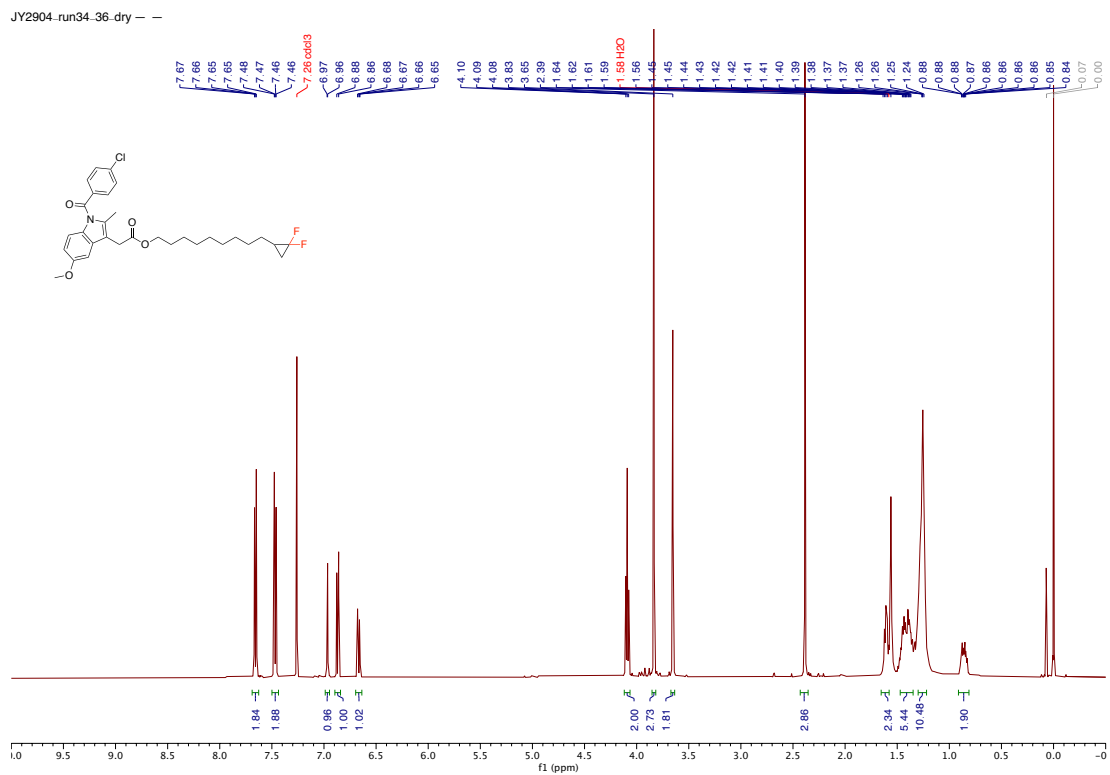
JY2882_xt_F19.3 fid -

127.71
127.75
127.76
127.77
128.12
128.13
128.15
128.16
128.17
128.18

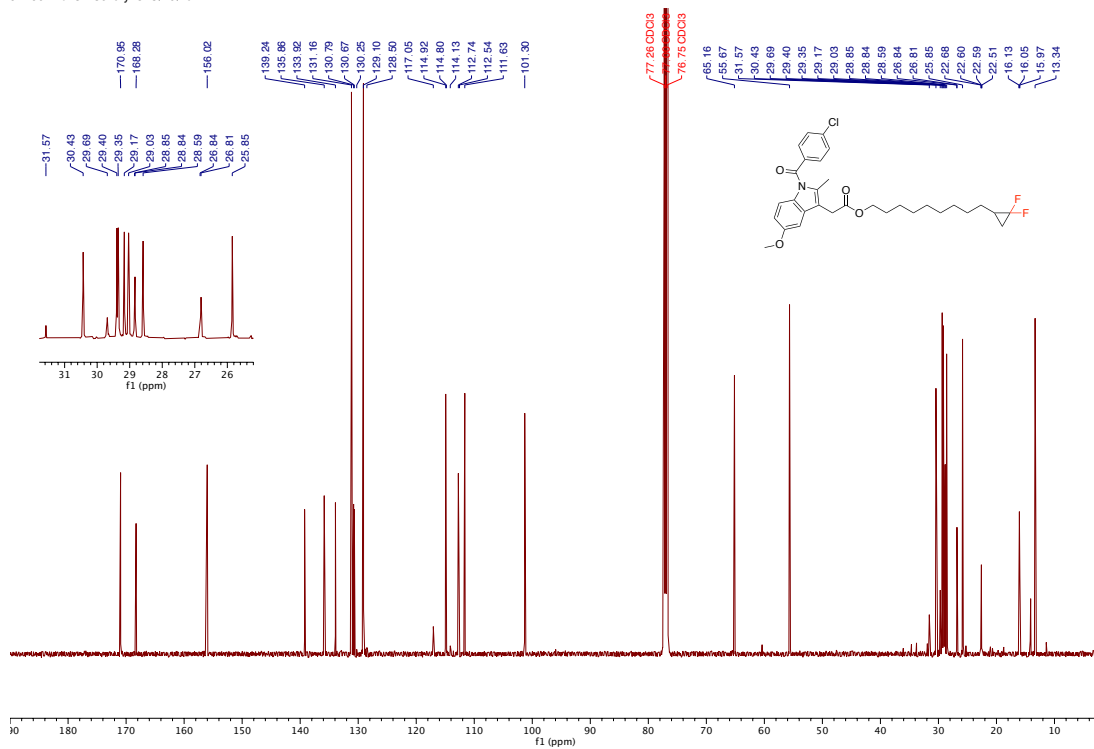
144.38
144.39
144.41
144.43
144.79
144.80
144.83
144.84



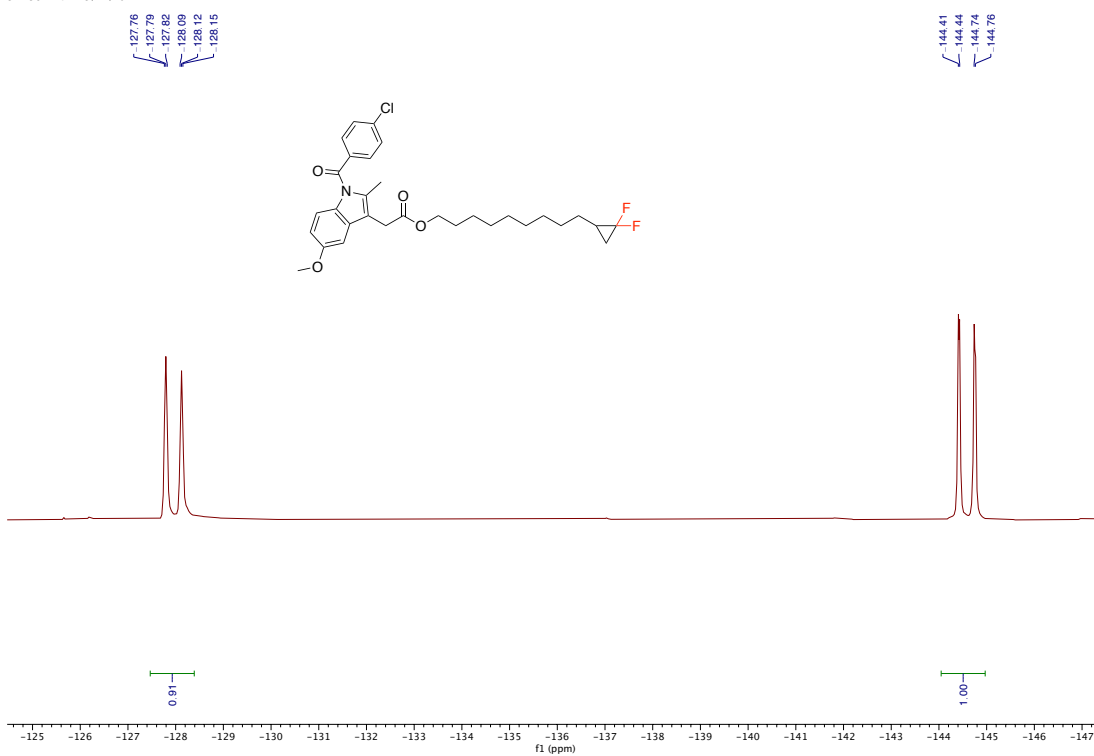
^1H , ^{13}C , and ^{19}F NMR of
9-(2,2-difluorocyclopropyl)nonyl 2-(1-(4-chlorobenzoyl)-5-methoxy-2-methyl-1*H*-indol-3-yl)acetate (**b5**)



JY2904_run34-36-dry_C13.10.fid -



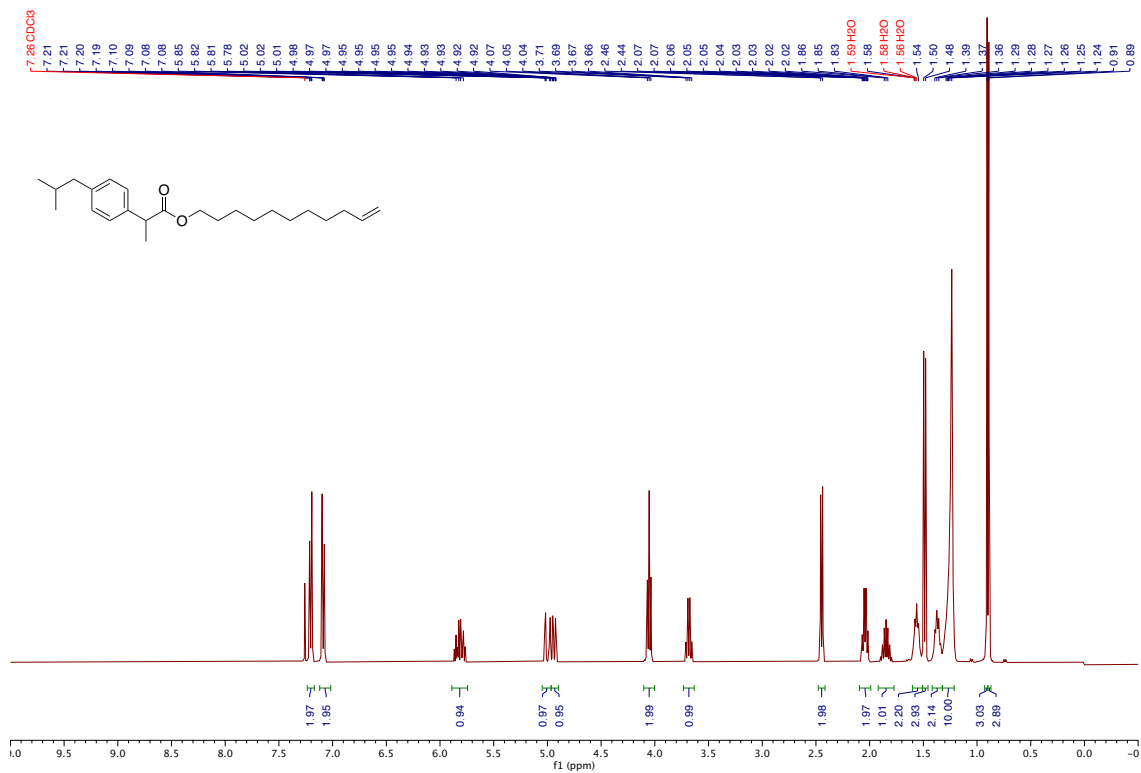
JY2904-xt-F19.12.fid -



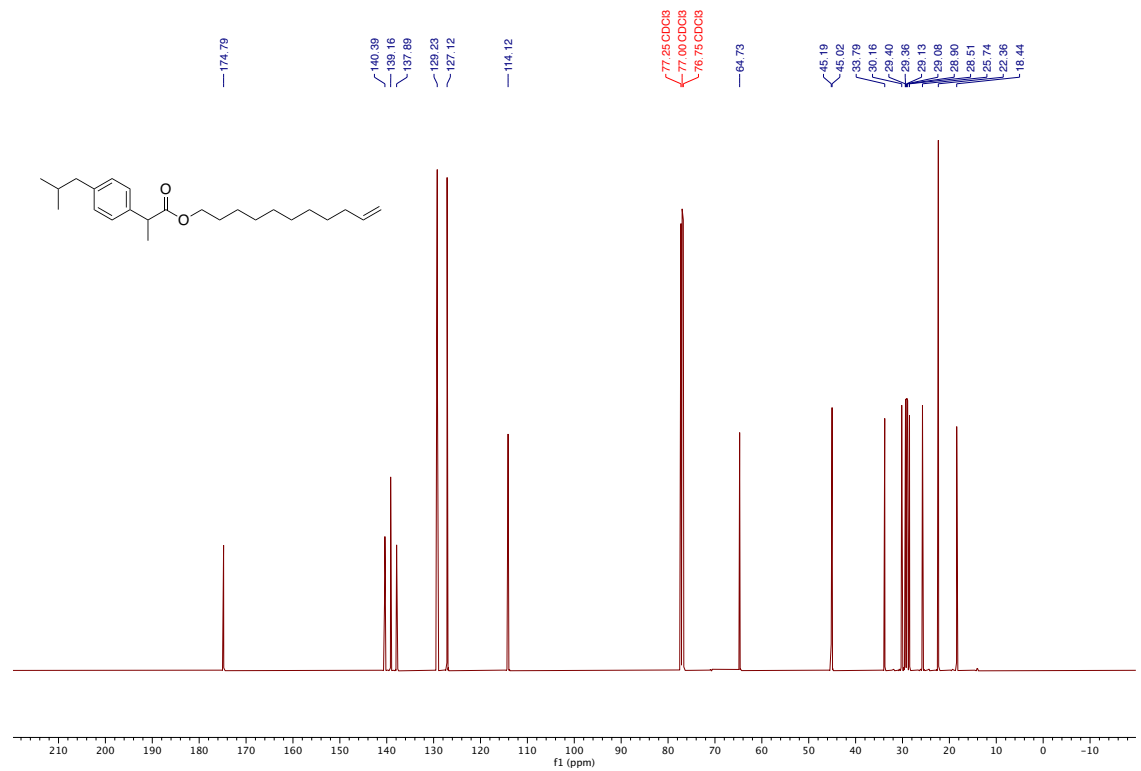
^1H and ^{13}C NMR of

9-(2,2-difluorocyclopropyl)nonyl 2-(4-isobutylphenyl)propanoate

JY2879-run-check.1.fid —



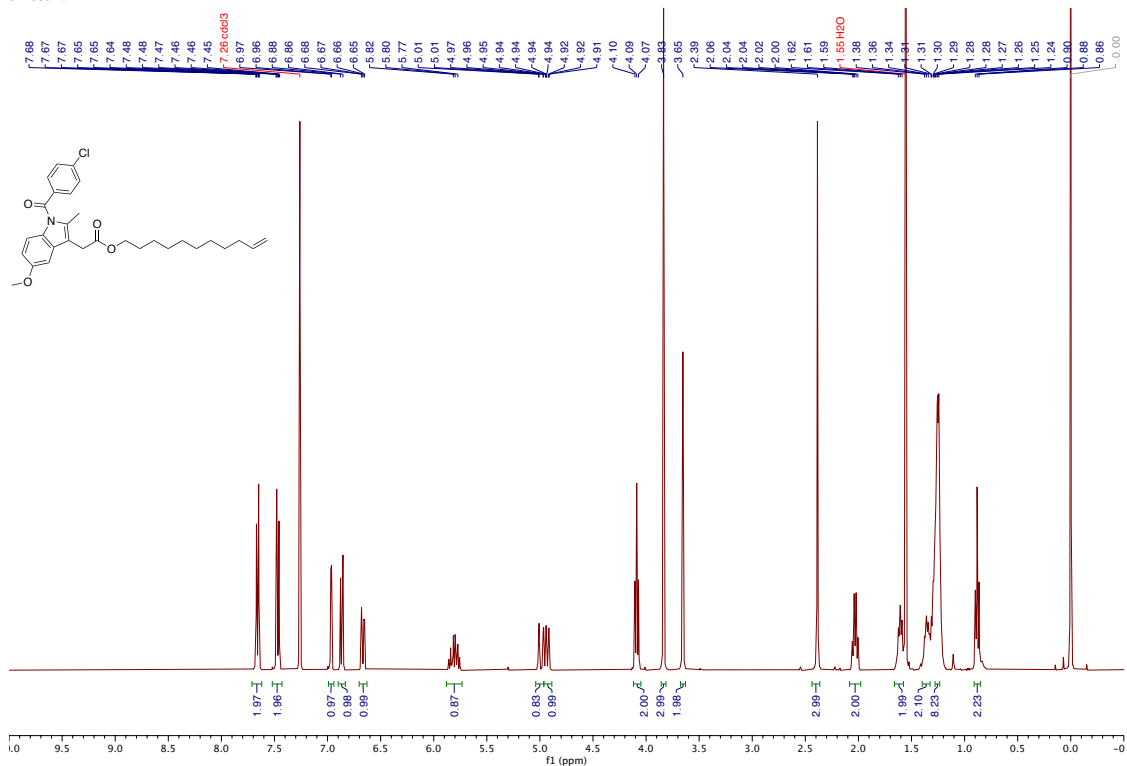
JY2879-C13.10.fid —



^1H and ^{13}C NMR of

undec-10-en-1-yl 2-(1-(4-chlorobenzoyl)-5-methoxy-2-methyl-1H-indol-3-yl)acetate

JY2880.run --



JY2880.run.C13.10.fid --

